PROCEEDINGS OF THE IRE®

Published Monthly by
The Institute of Radio Engineers, Inc.

VOLUME 44 — *October, 1956* — NUMBER 10

CONTENTS

Joseph J. Gershon, Director, 1956–1957 1231

Poles and Zeros ..... *The Editor* 1232

5830. Introduction to the Ferrites Issue ..... *C. Lester Hogan* 1233

5831. A Survey of the Properties and Applications of Ferrites Below Microwave Frequencies ..... *C. Dale Owens* 1234

5832. Fundamental Theory of Ferro- and Ferri-Magnetism ..... *J. H. Van Vleck* 1248

5833. Magnetic Resonance in Ferrites ..... *N. Bloembergen* 1259

5834. The Nonlinear Behavior of Ferrites at High Microwave Signal Levels ..... *Harry Suhl* 1270

5835. Microwave Resonance Relations in Anisotropic Single Crystal Ferrites ..... *Joseph O. Artman* 1284

5836. Dielectric Properties of and Conductivity in Ferrites ..... *LeGrand G. Van Uitert* 1294

5837. Methods of Preparation and Crystal Chemistry of Ferrites ..... *Donald L. Fresh* 1303

5838. Intrinsic Tensor Permeabilities on Ferrite Rods, Spheres, and Disks ..... *E. G. Spencer, L. A. Ault, and R. C. LeCraw* 1311

5839. Permeability Tensor Values from Waveguide Measurements ..... *E. B. Mullen and E. R. Carlson* 1318

5840. Resonance Loss Properties of Ferrites in 9 KMC Region ..... *Samuel Sensiper* 1323

5841. Anisotropy of Cobalt-Substituted Mn Ferrite Single Crystals ..... *P. E. Tannenwald and M. H. Seavey* 1343

5842. The Elements of Nonreciprocal Microwave Devices ..... *C. Lester Hogan* 1345

5843. Frequency and Loss Characteristics of Microwave Ferrite Devices ..... *Benjamin Lax* 1368

5844. Ferrites as Microwave Circuit Elements ..... *Gerald S. Heller* 1386

5845. Network Properties of Circulators Based on the Scattering Concept ..... *Milton A. Treuhaft* 1394

5846. Topics in Guided-Wave Propagation in Magnetized Ferrites ..... *Morris L. Kales* 1403

5847. Anomalous Propagation in Ferrite-Loaded Waveguide ..... *Harold Seidel* 1410

5848. Birefringence of Ferrites in Circular Waveguide ..... *N. Karayianis and J. C. Cacheris* 1414

5849. A New Ferrite Isolator ..... *Bengt N. Enander* 1421

5850. Magnetic Tuning of Resonant Cavities and Wideband Frequency Modulation of Klystrons ..... *G. R. Jones, J. C. Cacheris, and C. A. Morrison* 1431

5851. Ferrite Directional Couplers ..... *A. D. Berk and E. Strumwasser* 1439

5852. Ferrite-Tuned Resonant Cavities ..... *Clifford E. Fay* 1446

Contents continued on following page

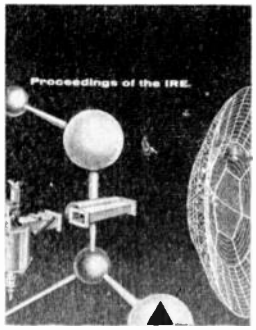

THE COVER—Connecting the klystron oscillator on the left and the antenna on the right is an isolator, one of a new family of microwave devices which utilize the magnetic properties of ferrites. The isolator consists of a slab of ferrite mounted inside a waveguide which has a permanent magnet strapped to the outside. The magnetized ferrite exhibits nonreciprocal properties at microwave frequencies, permitting transmitted waves to travel freely to the antenna but absorbing waves reflected back from the antenna. Ferrites derive their unusual properties from the spinning of electrons around axes which are oriented in a common direction, as depicted in the background. As the cover suggests, this special issue is concerned with both the fundamentals and the applications of ferrites.

PROCEEDINGS OF THE IRE

Published Monthly by

The Institute of Radio Engineers, Inc.

Change of address (with 15 days advance notice) and letters regarding subscriptions and payments should be mailed to the Secretary of the IRE, 1 East 79 Street, New York 21, N. Y.

(*Continued*)

5853. Ferrite-Tunable Microwave Cavities and the Introduction of a New Reflectionless, Tunable Microwave Filter ..... *Conrad E. Nelson* 1449

5854. Three New Ferrite Phase Shifters ..... *Howard Scharfman* 1456

5855. Ferrite-Tunable Filter for Use in S Band ..... *James H. Burgess* 1460

5856. Radiation from Ferrite-Filled Apertures ..... *D. J. Angelakos and M. M. Korman* 1463

5857. Correction to "Some Aspects of Mixer Crystal Performance" ..... *Peter D. Strum* 1468

Correspondence:

5858. The Radiation Patterns and Conductances of Slots Cut on Rectangular Metal Plates ..... *J. R. Wait and D. G. Frood* 1469

5859. Standard Frequencies and Time Signals WWV and WWVH ..... *National Bureau of Standards* 1470

5860. Analog Computer Amplifier Circuits ..... *Hiroshi Amemiya* 1473

5861. Spurious Modulation in Q-Band Magnetrons ..... *T. M. Goss and P. A. Lindsay* 1474

5862. Inductive AC Admittance of Junction Transistor ..... *M. Onoe and A. Ushirokawa* 1475

5863. Note on "The Variation of Junction Transistor Current Amplification Factor with Emitter Current" ..... *N. H. Fletcher* 1475

Contributors 1476

IRE News and Radio Notes:

Final Call for IRE National Convention Papers 1481

Miscellaneous Publications of the IRE 1483

Obituaries 1484

Technical Committee Notes 1485

Books:

5864. "Electronics and Electron Devices," by A. L. Albert ..... *Reviewed by Samuel Seely* 1486

5865. "A Study of the Double Modulated FM Radar," by Mohamed Ismail ..... *Reviewed by R. M. Page* 1486

5866. "Electronic Computers and Management Control," by George Kozmetsky and Paul Kircher ..... *Reviewed by J. R. Weiner* 1486

5867. "Random Processes in Automatic Control," by J. H. Laning, Jr. and R. H. Battin ..... *Reviewed by W. R. Bennett* 1487

5868. "Transistors I," by RCA Laboratories ..... *Reviewed by A. P. Stern* 1487

5869. "Electronic Engineering," by Samuel Seely ..... *Reviewed by J. G. Brainerd* 1488

5870. "Radio Electronics," by Samuel Seely ..... *Reviewed by A. V. Eastman* 1488

5871. "Solid State Physics, Vol. I," ed. by Frederick Seitz and David Turnbull ..... *Reviewed by G. C. Dacey* 1489

5872. Recent Books 1489

Programs 1489

5873. Abstracts of IRE Transactions 1491

IRE Committees—1956 1493

IRE Representatives on Other Bodies 1499

IRE Representatives in Colleges 1500

5874. Abstracts and References 1502

ADVERTISING SECTION

Meetings with Exhibits	6A	Meetings	100A	Membership	126A
News—New Products	20A	Section Meetings	106A	Positions Wanted	146A
IRE People	52A	Industrial Engineering Notes	108A	Positions Open	164A
Professional Group				Advertising Index	221A

Joseph J. Gershon

DIRECTOR, 1956–1957

Joseph J. Gershon received the B.S. degree in electrical engineering from Illinois Institute of Technology. From 1944 to 1945 he was with Ilg Electric Ventilating Company as electrical engineer in research and development. He entered DeVry Technical Institute in 1945 as instructor. Three months later he was given the assignment of developing a program in engineering mathematics and communications. Upon completion he organized a technology and design curriculum intended to follow the earlier courses, which later developed into a television design program.

In January of 1954 he was placed in charge of the resident school. At the present time he is revising the curriculum to more closely fit the changing needs of industry by expanding the circuit analysis and mathematics in conjunction with new servomechanism and computer networks in the technology and design program.

Mr. Gershon has been an active member of the executive committee of the Chicago Section since 1948. He served on most of the section committees and in several instances was chairman. He became Secretary of the Chicago Section in 1952 and in 1954–55 he was Section Chairman. His activity extended to the circuit theory symposiums held at the National Electronics Conferences.

Mr. Gershon also served as Sections Committee Chairman of the Professional Group on Circuit Theory for the past four years, and on its administrative committee, and on the Professional Groups Committee. He is now a member of the Nominations and Appointments Committees.

He is a registered professional engineer in the state of Illinois, and a member of Eta Kappa Nu, Tau Beta Pi, American Society for Engineering Education and the Armed Forces Communications and Electronic Association.

Poles and Zeros

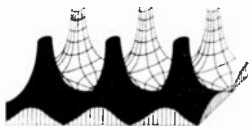

Conference in Print. Lester Hogan describes the contents of this issue (p. 1233) so well that we have decided to omit *Scanning the Issue.* But it would be wrong to let the occasion pass without comment from the editorial chair, for this issue is special in more ways than Professor Hogan, in his modesty, is likely to admit. We have the opinion of an expert when Managing Editor Gannett says "This issue will stand up to any special issue we have ever published." Up to now there has been no place in the literature where an engineer can get a starting point on ferrites and their use at microwave frequencies. In this issue we are privileged to publish 26 papers in this area, ten of them of a tutorial nature—in essence the first textbook on the subject and no doubt the principal reference for years to come.

Compilations of this sort don't just happen; they require the most exacting preparation. In this case, it took three organizations to float the issue: the Air Force Cambridge Research Center, the IRE Professional Group on Microwave Theory and Techniques, and Harvard University. Last April these not-so-strange bedfellows sponsored a Conference on the Properties and Applications of Ferrites at Microwave Frequencies at Cambridge. Ten invited papers, plus a larger number of contributed papers, were presented. By good management and a little luck, they covered the subject in masterful fashion. It had been planned to publish the papers in the TRANSACTIONS of the PGMTT, but the Editorial Board requested the sponsors to make the papers available to the PROCEEDINGS, arguing that the subject matter was of such timeliness, fundamental importance and widespread utility that it should be presented to the profession at large.

This proposal having been accepted, the editorial work began. Professor Hogan agreed to organize the issue and to review the papers in detail. In this he was assisted by Howard Scharfman, Benjamin Lax, G. S. Heller and John Rowen. John Rowen made the further contribution of the ideas underlying the cover of this issue and checked the artist's sketches. These men, no less than the authors of the papers and the sponsor bodies, made possible this issue, for which every IRE member can be thankful.

An especially valuable aspect of the organization of the issue is the arrangement of the ten tutorial papers in such a way that, as Professor Hogan points out, the reader with no previous knowledge of the field should be able to prepare himself for intelligent research in this field.

New? The technology reported in this issue is new, as close to the frontier of solid-state physics as the semiconductors treated in the special issue of December, 1955. But the novelty is of a special sort, residing in the combination of properties of materials which were identified in the earliest stages of electrical science. The ferrites, as we know them today, combine high magnetic permeability with such high resistivity that eddy currents cannot interfere with their utility as concentrators and manipulators of high-frequency magnetic energy. The implications and second-order consequences of this basic concept occupy the two hundred-odd pages that follow.

The widespread amazement at the growing importance of solid-state materials in electronics cannot be supported by a sober view of the past. Far from being upstarts, the solid-state materials have always been the backbone of our art and the desire to understand them better has existed for fifty years. Omitting ordinary conductors and insulators, the historical sequence of solid-state technology in telephony and electronics runs approximately as follows: high retentivity magnets in the telephone receiver; surface states of carbon grains in the telephone transmitter; low-purity semiconductors in crystal detectors; tungsten and thoriated tungsten cathodes; the oxide cathode; phosphors; the photosensitive cathode; secondary emissive surfaces; high-purity semiconductors in crystal diodes; ferrites for megacycles; highest-purity semiconductors in transistors; ferrites for kilomegacycles.

Viewed in this perspective, the vacuum in the vacuum tube is almost an interloper. So viewed also, the solid-state materials are seen to be new only in the sophistication with which they are currently handled. Future progress would appear to be well indicated by the recent history of the development of ferrites for microwaves. These have been produced by bringing together traditionally separate properties, by the utmost patience in their preparation and refinement, and by more accurate and comprehensive knowledge of the internal processes which underly their external properties.
—D.G.F.

Introduction to the Ferrites Issue

C. LESTER HOGAN

During the past decade we have witnessed a tremendous advance in the field of radio electronics through novel applications of solid-state materials. The most outstanding contributions have probably come from the class of materials known as semiconductors. However, within the past few years an increasing interest in the properties and applications of ferromagnetic materials has led to a whole new family of communications' devices which utilize the magnetic properties of matter. The rapid progress is due to many reasons. Probably the foremost is the development of a new class of ferromagnetic materials that have become known as ferrites. An important reason for this progress is the fact that a growing group of radio engineers have learned that a thorough understanding of the basic concepts of solid-state physics is essential to them if they are to be creative engineers in this new "solid-state electronics era."

Actually, it has been difficult for the communications engineer to obtain the background that he needs on the properties of ferromagnetic materials. To be sure, the information is in the literature (along with many concepts, theories, and experiments which are misleading or incorrect), but it has never been organized for the engineer in the way that information on semiconductors has been organized.

It was in appreciation of this need that this particular issue was conceived. Ten leading authorities have been invited to prepare review papers concerning various aspects of ferromagnetic materials and their applications. All have been prepared with the needs of the radio engineer in mind.

The issue starts with a general survey of the properties and applications of ferrites by C. Dale Owens. This article summarizes the basic properties of ferrites which have given them a unique position in the field of ferromagnetic materials. In addition, it discusses the major uses that engineers have found for these materials so far.

Following this general survey paper are four papers dealing specifically with various phases of the theory of ferromagnetism and ferromagnetic resonance that the engineer needs to know in order to understand the operation of the various devices which he uses. The first of these (Van Vleck) summarizes the present status of the physical theory of ferro- and ferri-magnetism. Then, there are three papers (Bloembergen, Suhl, Artman) dealing with various aspects of the theory of ferromagnetic resonance, which, of course, is the phenomenon upon which all microwave ferrite devices depend. Bloembergen is a tutorial review covering the linear theory, while Suhl is a tutorial paper on the nonlinear theory, which constitutes for the most part original work not previously published in any such extensive form.

The next six papers (Van Uitert; Fresh; Spencer, Ault, and Le Craw; Mullen; Sensiper; Tannenwald and Seavey) discuss the chemistry and general physical properties of ferrites along with the unique measuring techniques which have been found useful for measuring these properties.

The final fifteen papers deal with the theory and art of microwave ferrite devices. Those by Hogan, Lax, Heller, and Kales are tutorial reviews on various phases of the subject, while the remainder of the issue deals with original contributions either to the theory, or art, of microwave ferrite devices. These papers should give the reader an appreciation of the tremendous activity which is now taking place.

Only the serious student who is devoting a major share of his time to this field will find it worthwhile to attempt to digest all the material here. The less serious reader should be able to pick those fields of greatest interest to him by the titles of the articles. The ten tutorial review papers (Owens, Van Vleck, Bloembergen, Suhl, Van Uitert, Fresh, Hogan, Lax, Heller, and Kales) were selected and arranged so that a reader with no previous knowledge would be able to prepare himself for intelligent research in this ever-expanding field.

A Survey of the Properties and Applications of Ferrites Below Microwave Frequencies*

C. DALE OWENS†, SENIOR MEMBER, IRE

Summary—**A review of the properties, applications, and engineering significance of ferrites below microwave frequencies is presented. The survey includes a discussion of the nature of ferrites, their magnetic and electrical properties, the use of the μQ product as a design index of efficiency, core losses, and the effects of air gaps. This is followed by a discussion of the use of ferrites in a wide variety of applications. A Bibliography is also included.**

Introduction

THE PRACTICAL achievement of modern magnetic ferrites was announced just 10 years ago. They are ceramic-like materials, with permeabilities ranging up to several thousand combined with specific electrical resistivities over a million times those of metals. Laminating or powdering is not necessary, as it is with metals, in order to limit eddy currents to permissible values. The impact of this development on both engineering applications and on the basic understanding of magnetism has been very great. This paper will review the properties, applications, and engineering significance of ferrites below microwave frequencies.

Today, large numbers of persons are engaged in the study, manufacture, improvement, and use of ferrites. These include research scientists, students, technicians, and engineers working directly with ferrites. In addition others are working to improve the basic oxide materials, to design and build processing equipment, such as furnaces or grinding machines, and to develop new test equipment to meet the specific requirements for the controlled manufacture and application of ferrites. Ferrites now are in everyday use in inductors and transformers for carrier telephony, in flyback transformers, deflection coils, and inductance adjustment slugs in tv sets, and in antennas and IF transformers in radio sets. They are uniquely suitable for miniaturized inductors and pulse transformers demanded for transistorized circuits. The rapid development of ferrites for the new fields of computer circuits and microwave components promises an even greater effect on the daily lives of engineers and the public in the near future.

The work on ferrites comprises a very extensive activity in the field of magnetism, and is the subject of many symposia and large numbers of articles. It is an integral part of the advance in solid state and atomic physics. Ferrite is a member of the semiconductor family, which includes diodes, transistors, and solar cells. It is intriguing to consider this modern ferrite as a rebuilt version of lodestone, the first magnetic material discovered by man, and a possible forerunner of future new magnetic materials synthesized directly from performance specifications prepared by design engineers. Fig. 1 outlines on a time scale some of the major steps in the development of magnetic materials.

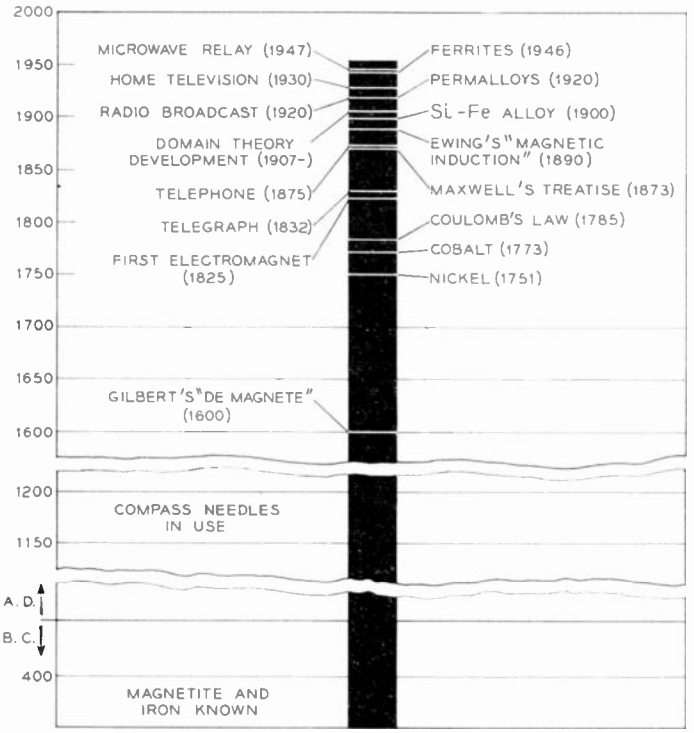

Fig. 1—Time scales of some magnetic discoveries and fields of use.

The modern ferrite development is timely. The emphasis on carrier, radio, and tv frequencies and on miniaturization has brought increasing demands for reduction of core losses. A point of diminishing return for effort and cost in further laminating and powdering metals appears to have been reached. Although sporadic efforts to develop ferromagnetic nonmetals have gone on for 50 years, the stimulating need has developed only in recent years. The advantages of the combined high permeability and high resistivity announced by Phillips in 1946 were apparent immediately to engineers designing inductors and transformers for communication use.

* Original manuscript received by the IRE, July 25, 1956.
† Merrimack Valley Lab., Bell Telephone Labs., Inc., North Andover, Mass.

An unexpected increase in core losses accompanied by a decrease in permeability was discovered in ferrites at frequencies far below those calculated to produce troublesome eddy currents. This led to intensive investigations of magnetic mechanisms and to new insight into magnetic theory. Domain wall movement, dimensional resonance, and ferromagnetic resonance were studied as mechanisms contributing to core loss. Very high "apparent" dielectric constants were measured on some of the ferrites in connection with dimensional resonance studies. The investigation of ferromagnetic resonance led to the discovery that ferrites were transparent to microwaves under proper conditions and produced Faraday rotation of the microwaves with very low losses. This is the phenomenon on which the gyrator and revolutionary new components for waveguides are based.

In turn, the studies of magnesium-manganese compositions most suitable for microwaves showed tendencies of some of the materials to have rectangular loops, that is, a high ratio of remanence to saturation. Development studies have provided cores suitable for memories and magnetic switches in computers and data processing circuits.

A study of why the saturation magnetization of ferrites is lower than that calculated from the simple addition of all the atomic moments led to the new concept of *ferrimagnetism*. The saturation moment of ferrites is explained as the resultant of two interplacing lattices of metal atoms with opposing magnetic moments.

The story of ferrites is one of mutual teamwork and stimulation in research, engineering applications, theory manufacture, and measurements.

The Nature of Ferrites

As a simple explanation, the modern ferrite may be described as a material derived from lodestone, or magnetite ($Fe^{++}O.Fe_2^{+++}O_3$) by substituting other metal atoms in place of the divalent iron (Fe^{++}). If these atoms are divalent and about the same diameter as iron atoms, the basic spinel type crystal structure of magnetite can be preserved, and greatly increased values of permeability and resistivity can be obtained. The properties of the ferrite are dependent upon the kinds of metal atoms and their proportions and geometric arrangement among the interstices of the close packed cubic array of oxygen atoms in the spinel structure. Suitable atoms to replace iron include manganese, magnesium, nickel, copper, cobalt, zinc, and cadmium. If the divalent iron is entirely replaced by zinc or cadmium alone, a nonmagnetic material is obtained. If it is replaced by one of the other atoms, the resulting material is magnetic, but the permeability seldom exceeds 100 and the hysteresis losses are high. These types of materials have been known for many years.

However, if the divalent iron in magnetite is partially replaced by zinc and partially by manganese, for example, the requirements for high permeability (and low hysteresis loss) are met. These are that the crystal be easy to magnetize in all directions (*i.e.*, have low crystal anisotropy) and that the change in dimensions with magnetization (magnetostriction) be small.[1]

The ferrites most commonly are manufactured from finely divided metal oxide powders, which are intimately mixed, pressed to shape, and then sintered. The process is similar to that for producing ceramics. As with ceramics, alternate processes are adaptable to ferrites. Ferrite compositions may be prepared by coprecipitation of the constituents from solution. For long rods or shapes which do not lend themselves to pressing from powder, casting or extrusion from a slip can be employed. Ferrite parts shrink some 10 to 20 per cent during firing. Fig. 2 illustrates some of the shapes and sizes of parts which have been produced. The final magnetic and electrical properties are highly dependent upon many factors which affect the arrangement of metal atoms in the crystal structure and the chemical homogeneity of the sintered compact. This includes the purity and "activity" of the constituent oxides, the heat treatment, and the atmosphere in which the parts are sintered and cooled. Ferrites of higher quality and new and more uniform properties are being achieved commercially as these factors are brought under better control.

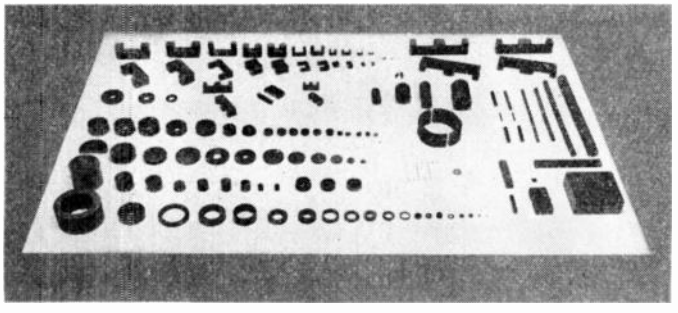

Fig. 2—Various shapes and sizes of ferrite cores.

The Magnetic and Electrical Properties of Ferrites

The magnetic properties of a material are defined by the way the flux density B is related to the applied magnetic field H (see Fig. 3), and by the losses resulting from changing magnetic fields. There are almost unlimited variations in composition and heat treatment possible among the ferrites giving rise to a large and

[1] Crystals containing metal atoms substantially larger in diameter than iron atoms, as when the divalent iron is replaced by barium, are found to be hexagonal in structure. They exhibit high crystal anisotropy and high coercive force, up to 3000 oersteds intrinsic value. This is the basis of the development of ferrite type permanent magnets with high resistivity, suitable for use in high frequency fields. The high coercive force makes it particularly useful for disk magnets.

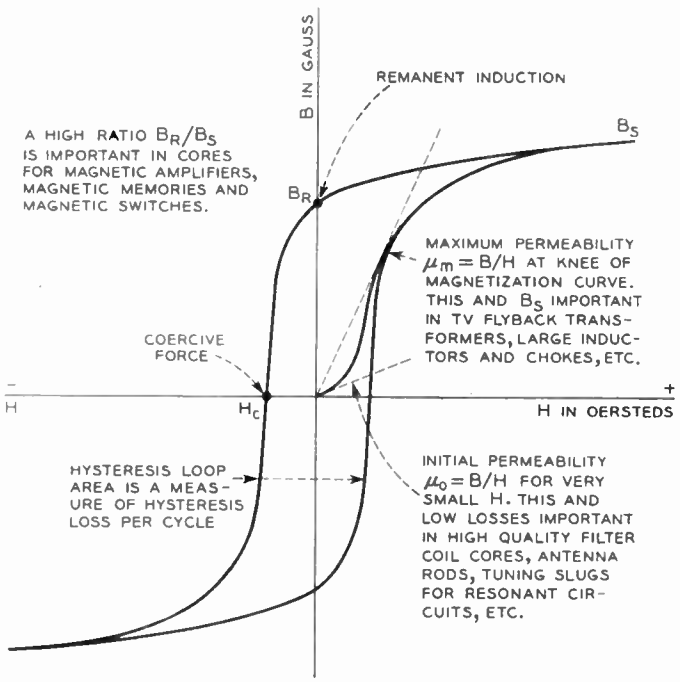

THE PLOT OF INDUCTION B VERSUS MAGNETIZING FORCE H GIVES THE CHARACTERISTIC HYSTERESIS LOOP FOR A MAGNETIC MATERIAL. WHEN THE MAGNETIZING FIELD H IS RAPIDLY CHANGED AS IN AC APPLICATIONS, THE CHANGING FLUX DENSITY B GENERATES A VOLTAGE WHICH PRODUCES CURRENTS, AND ENERGY LOSSES, IN CONDUCTING AND DIELECTRIC PATHS.

Fig 3

versatile family of materials. The ranges of values obtained for several characteristics are shown in Fig. 4, and compared to those of iron and other magnetic materials. Certain typical combinations of properties are indicated by letter designations. It will be observed that many of the characteristics such as Curie temperature T_c, coercive force H_c, maximum permeability μ_m and resistivity ρ show a general correlation, direct or inverse, with the initial permeability μ_0.

The initial permeability μ_0 of ferrites varies from around 5 for magnetite to over 6000 for a nickel zinc ferrite of the type designated *A* in Fig. 4. While these values are not particularly impressive compared to those which can be obtained in metals, the significant factor is that they are combined with resistivities many orders of magnitude greater. The dc resistivities of ferrites, except for magnetite with 0.01 ohm-centimeter, range from 10 ohm-centimeters to values as high as 10^8 ohm-centimeters. These compare with values of 10×10^{-6} ohm-centimeters for iron to around 100×10^{-6} ohm-centimeters for some of the metal alloys.

A comparison of the hysteresis loops of iron, molybdenum permalloy, and a ferrite are shown in Fig. 5. The ferrite corresponds to type *B* in Fig. 4. The saturation flux density B_s is relatively low for all the ferrites, ranging from about 1500 to less than 5000. This imposes

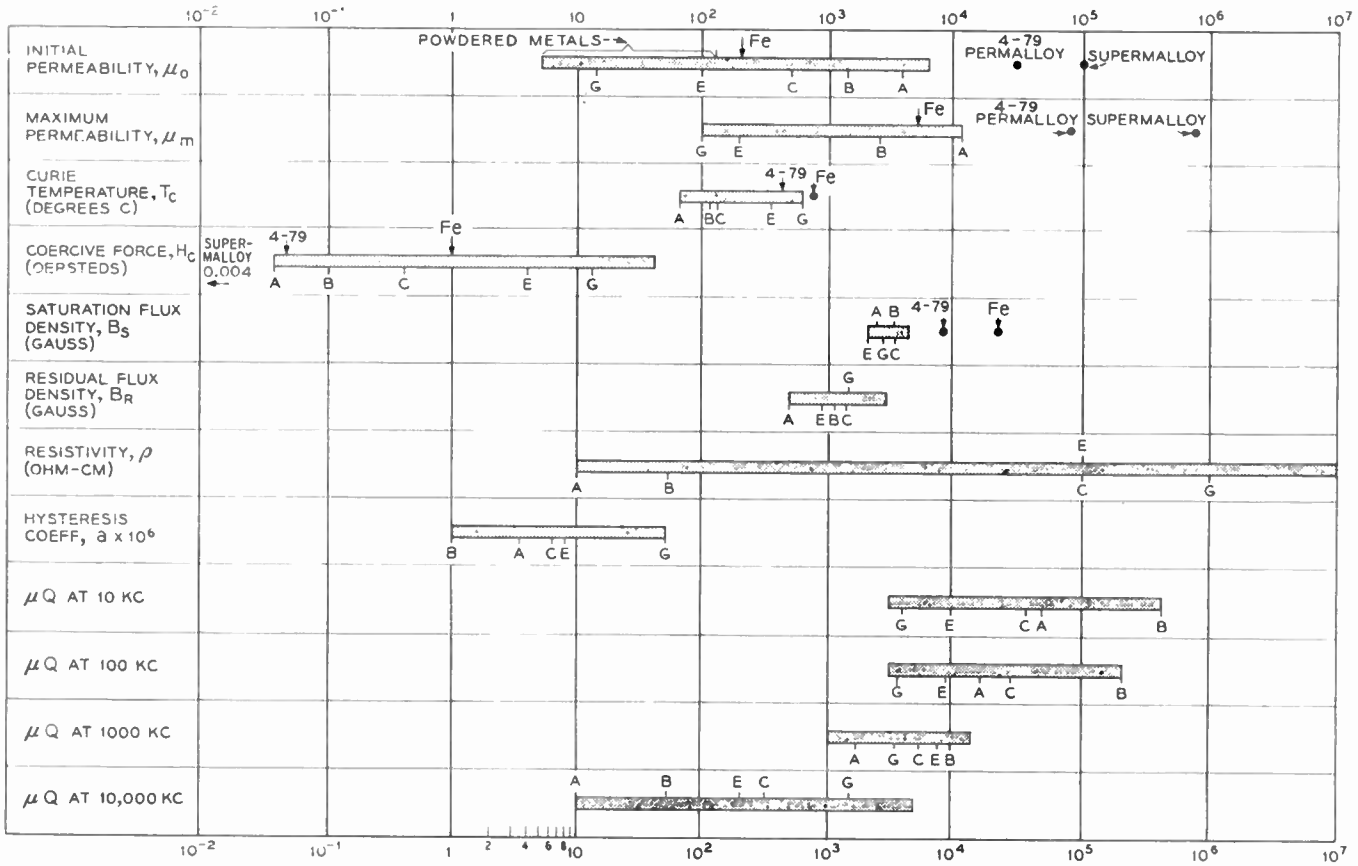

Fig. 4—Ranges of properties obtained in ferrites compared to properties of iron and permalloys. Letters designate certain typical ferrites. A) NiZn. B) MnZn. C), E) NiZn, often with additional elements Mg, Mn, Co, or Cu. G) Ni.

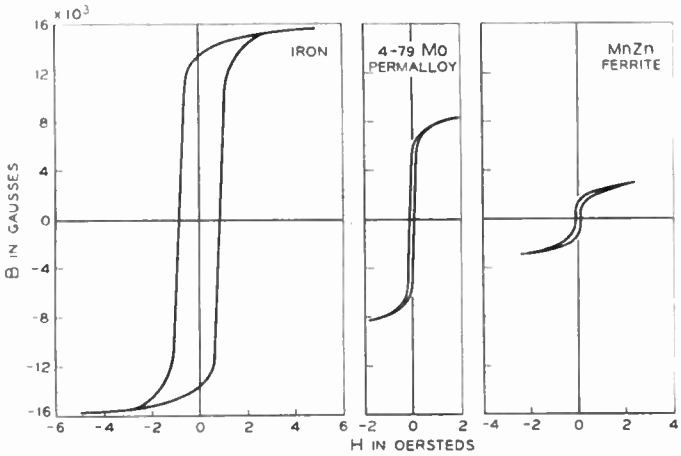

Fig. 5—Hysteresis loops of iron, 4-79 molybdenum permalloy and a MnZn ferrite.

a limitation on their use in power transformers or devices operating at high flux levels. A large variety of loop shapes are obtained with the ferrites, including those which are highly rectangular.

Another of the significant characteristics of ferrite is the low Curie temperature found in the high permeability materials. The Curie temperature is the temperature above which thermal agitation overcomes the alignment of magnetic moments and causes the material to become paramagnetic. It is typical of most magnetic materials that the initial permeability increases with rising temperature to a peak value just below the Curie temperature. This is shown in Fig. 6 for iron and

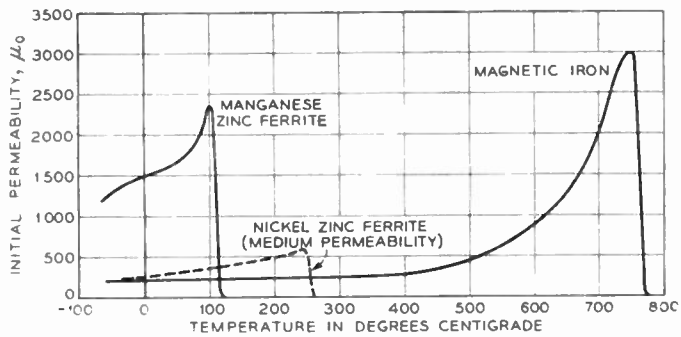

Fig. 6—Change of permeability with temperature for magnetic iron, a MnZn and a NiZn ferrite.

ferrite. The high permeability realized in some of the ferrites is due largely to the fact that they have Curie temperatures near room temperature and are used near the peak permeability. This condition tends to produce high sensitivity of permeability and other properties to temperature variations. The effect of temperature on the hysteresis loop of a nickel zinc ferrite with a permeability of 800 is shown in Fig. 7.

Material μQ Product as a Useful Index

In the appraisal of magnetic materials for design applications, especially for precision inductors, low

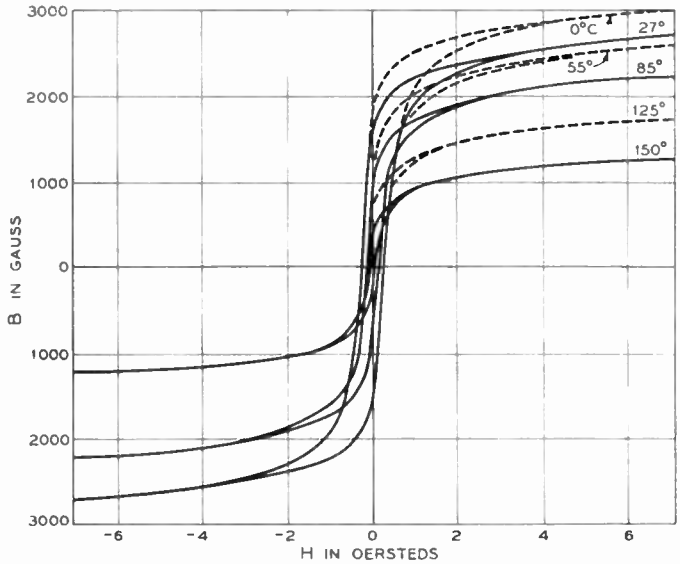

Fig. 7—Effect of temperature on the hysteresis loop of a NiZn ferrite with a permeability of 800.

losses and small changes of permeability and losses with frequency, flux density, temperature, and time are often of more importance than the actual value of permeability. The μQ product of a material, sometimes written $\mu_m Q_m$, has been found to be a useful index of efficiency for design applications. In this product, μ is the permeability and the material $Q(=2\pi fL/R_m)$ represents the reactance of a winding on a core per unit of core loss, as indicated in Fig. 8. The term R_m is the effective series resistance arising from core loss in the material. It is easy to see that a high value of μQ is desired. A higher value of μ will produce a larger amount of inductance L per turn, which can be used to provide a more efficient coil or a smaller coil of the same efficiency. A high value of μ also reduces leakage flux and improves the shielding when the core material surrounds the winding. A higher value of material Q means less loss per cycle per henry.

Fig. 8—Representation of core loss R_m as a series resistance. R_c = winding resistance; R_m = effective series resistance due to magnetic core; L_s = series inductance; $R_s = R_c + R_m$ = effective resistance of inductor;

$$\text{inductor } Q = \frac{2\pi fL_s}{R_c + R_m} = \frac{2\pi fL_s}{R_s};$$

material $Q = 2\pi fL_s/R_m$

where f = frequency in cps.

In a practical inductor design, the inductor $Q(=2\pi fL/R_s)$ which can be obtained is proportional to $\sqrt{\mu Q}$ of the material. In a transformer, a core material with a higher μQ results in a proportionally smaller shunt loss across the transformer windings. Fig. 9 shows the improvement of the μQ product over the years, reaching a peak in the recent ferrites.

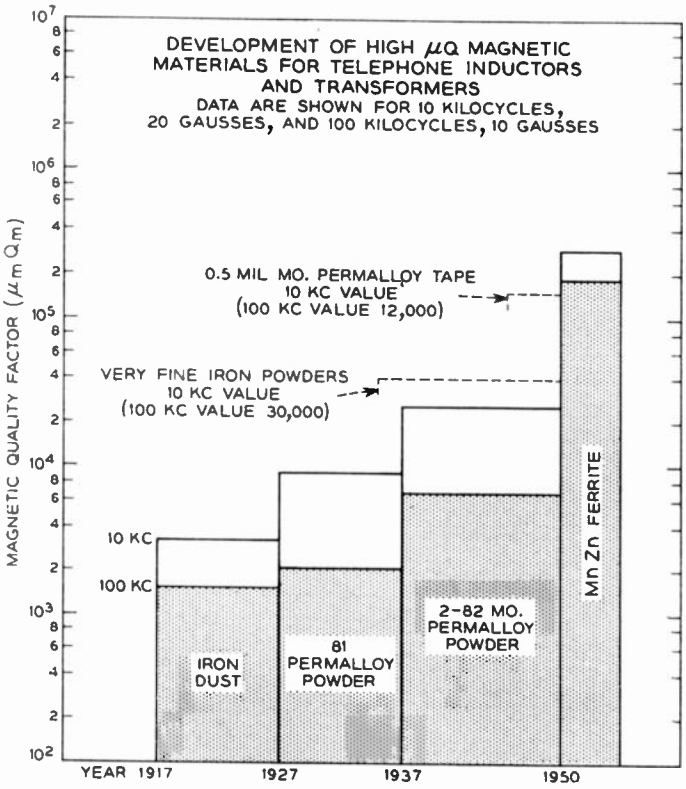

Fig. 9—Improvements in the μQ product over the years.

The μQ product of a material may be determined on a solid core but will remain practically unchanged if an air gap is cut in the core to reduce μ. In a design with an assembled core structure containing air gaps, when the air gap is correctly chosen, the core loss per henry can be made equal to the dc resistance per henry and the inductor Q can be optimized. It is found that the optimum value of permeability as well as the optimum inductor Q is proportional to the $\sqrt{\mu Q}$ of the core material.

The variation of μ and μQ with frequency, temperature, and flux density are shown in Figs. 10–12 to illustrate the behavior of typical ferrites. The μ and μQ begin to decline very rapidly above a certain "critical" frequency which depends on the permeability. Because of the high resistivities of ferrites this cannot be attributed to bulk eddy current effects. The values of the μQ products will be observed to drop off with increasing temperatures and flux densities and to "disappear" at the Curie temperature and at the saturation flux density.

Core Loss in Ferrites

Core loss data on metal laminations and powders can be expressed in terms of an eddy current coefficient e, hysteresis coefficient a, and residual coefficient c related by the Legg equation:

$$R_m = e\mu f^2 L + a\mu B_m f L + c\mu f L$$

where R_m is the effective series resistance in ohms, f is in cycles, the inductance L is in henrys, and B_m is the peak flux density in gausses. This equation is inadequate for use with ferrites except at frequencies well below the

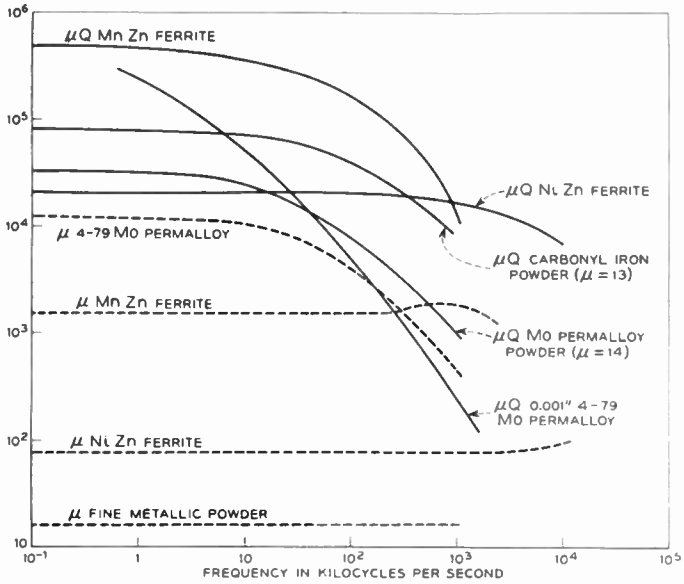

Fig. 10—Change of μQ with frequency for ferrites and other materials.

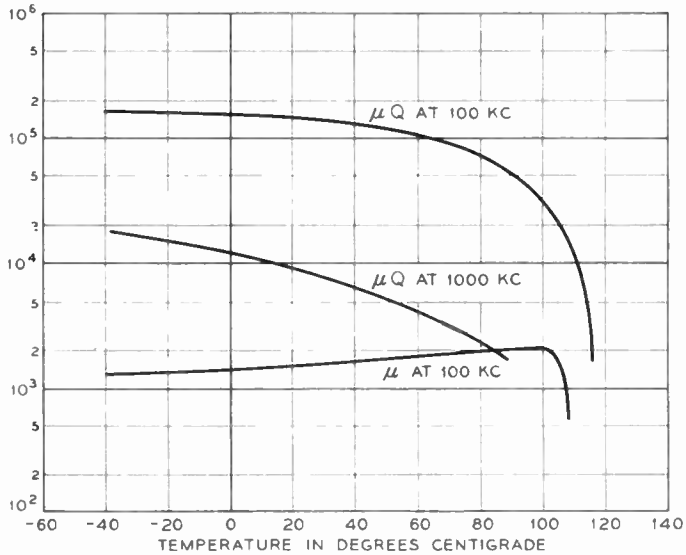

Fig. 11—Change of μ and μQ with temperature for a MnZn ferrite.

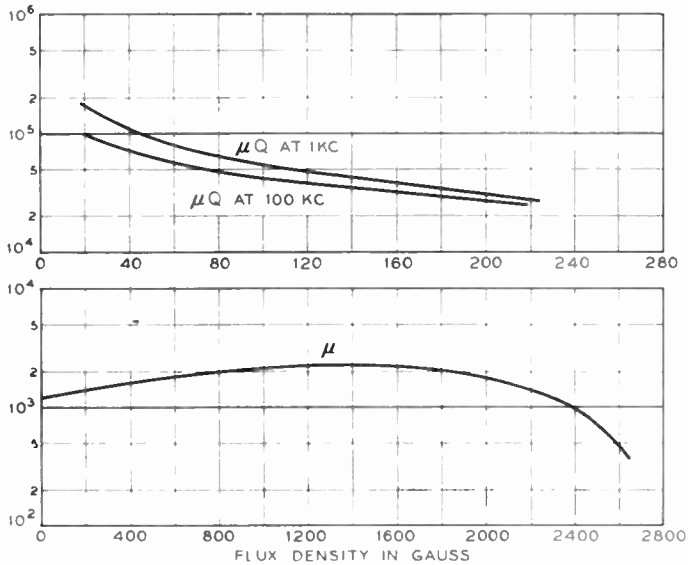

Fig. 12—Change of μ and μQ with flux density for a MnZn ferrite.

critical frequency at which μQ begins to decrease rapidly. This is often arbitrarily taken as the frequency at which Q decreases to 10. Above this frequency in ferrites the residual term increases faster than the first power of frequency and becomes predominant. The coefficient c then becomes frequency dependent.[2]

The theoretical physicist has been challenged by the frequency characteristics of ferrites and has vigorously hunted the mechanisms responsible for the residual losses, no longer masked by eddy currents. He has been almost too successful in that there are several plausible mechanisms, possibly with overlapping effects. The explanations are largely an extension of the theory of domain behavior in magnetic bodies. They deal with the basic response of the magnetic moments of spinning electrons when applied fields are superimposed upon their natural crystal environment. The high frequency losses in ferrites are attributed to domain wall resonance or relaxation, ferromagnetic resonance, and dimensional resonance. Briefly, these are described as follows.

Domain Wall Resonance or Relaxation

The domain wall is the region between domains in which the direction of the magnetic moments of the electron spins is in a state of transition from the direction of one domain to that of the other. Because of the angular momentum of the spinning electrons (inertia), crystal forces (elasticity), and damping factors (loss), the domain wall can exhibit resonance like an RLC circuit at certain critical frequencies or will "relax" if the damping is critical.

Ferromagnetic Resonance

This occurs when the frequency of the applied ac field and the precession frequency of the spinning electrons correspond. The precession frequency is a function of the steady field aligning the electron spins. This phenomenon is usually observed at 4000–24,000 megacycles when the material is saturated by a strong applied dc field. The effect is a sharp peak in the absorption loss curve and a resonance in the permeability curve. However several investigators have pointed out that ferromagnetic resonance could occur under the influence of a self-contained crystal anisotropy field even at frequencies as low as a few megacycles, in a ferrite in which permeability depends upon rotations of the spins as a whole instead of by growth of domains through wall movement. The resonance effects would be expected to be very broad under these conditions and could account for the type of dispersion of permeability and μQ observed at frequencies of one to one hundred megacycles.

[2] When the complex notation is used for permeability, $\mu=\mu'-j\mu''$, a loss angle $\tan\delta=\mu''/\mu'$ is commonly used. Here μ' is the usual permeability and μ'' is the loss per cycle. The following relationships exist:

$$\mu Q=\frac{\mu'}{\tan\delta}=\frac{(\mu')^2}{\mu''}=\frac{2\pi}{ef+aB_m+c}.$$

Dimensional Resonance

This is a cavity-type electromagnetic resonance which can occur in cores in which a dimension of the core corresponds to a half wavelength of an electromagnetic wave propagated through the material. The "apparent" dielectric constant k of manganese zinc ferrite with a permeability of 1000 may be as high as 100,000 at 100 kc. This value drops with frequency to a constant value of the order of 10 at a few megacycles. This suggests that the high measured values of dielectric constant may arise from a granular structure of ferrite, of more conducting regions separated by high resistance films. The apparent dielectric constants in most nickel zinc ferrites are of the order of 1000 at low frequencies, except for very low permeability types, in which the dielectric constant may be less than 100. The dielectric Q is low, of the order of 1. Since the velocity of propagation of an electromagnetic wave is equal to $3\times10^{10}/\sqrt{\mu k}$ centimeters per second, the velocity will be 1×10^7 centimeters per second for $\mu=1000$ and $k=9000$. A half wavelength would be 5 centimeters at one megacycle, or 1 centimeter at 5 megacycles.

Effects of Air Gaps

An air gap in a magnetic circuit reduces the instability of permeability due to mechanical or magnetic shock or temperature changes below that experienced on a continuous ring core. In ferrite cores for precision, high quality components, air gaps are used for improving stability as well as for obtaining optimum values of Q, previously discussed. The following equation relates the effective permeability μ_c of the core containing an air gap to the intrinsic permeability μ of the ferrite parts neglecting leakage.

$$\mu_c=\frac{\mu}{r(\mu-1)+1}$$

where r is the ratio of the air gap length l_a to the total mean length l_t of magnetic flux in the core assembly. The differential of the above equation can be written in the following form relating the percentage change in μ_c to the percentage change in μ:

$$\frac{d\mu_c}{\mu_c}=\frac{d\mu}{\mu}\,\frac{\mu_c}{\mu}(1-r).$$

If the value of μ is 1000 and the air gap is 1 per cent of the total flux path, then the value of μ_c will be 91 and the percentage change in μ_c will be only 9 per cent that of μ.

In some structures it is desired to assemble the core from parts but to retain a high permeability. It can be determined from the above relationship that the air gap ratio cannot exceed 0.01 per cent if the core permeability is to be greater than 90 per cent of the intrinsic ferrite permeability (of around 1000). If the flux path is 2.0 inches the total air gap would need to be less than 0.2 mil, or 0.1 mil each for two air gaps. This type of accuracy can be achieved through grinding and polishing the ferrite mating surfaces.

Other Characteristics

Like magnetic materials in general, ferrites show a decrease in permeability with increasing values of superimposed dc fields, and show a residual change after removal of the steady field. These effects are reduced by the use of an air gap. Some ferrites undergo shifts in permeability after ac demagnetization at high flux levels or after the materials are heated just through the Curie temperature and recooled to room temperature. Other ferrites, particularly extruded rod, have been found to be sensitive to vibration. This effect may be enhanced after the material has been subjected to a strong ac or dc magnetic field. Since these latter phenomena probably are functions of impurities, porosity, imperfections, and domain structure, ferrites can exhibit widely varying properties and representative samples should be checked carefully prior to application in designs requiring the highest stability.

Ferrites have about the hardness of quartz and are machined to size or provided with flat mating surfaces when required, by grinding operations under a water coolant. Diamond tools are often used. Cutting and machining also can be done satisfactorily with a supersonic machine tool. Mechanical polishing and lapping can be done in conventional ways when a smooth surface is needed.

Magnetostriction in the common polycrystalline ferrites is negative. The change in length when magnetized to saturation ranges from -0.5 parts per million to -22 parts per million. Because of the high resistivities, they are of interest for delay lines and magnetostrictive oscillators. It is a matter of interest that the highest value of magnetostriction so far measured on a magnetic material, 800×10^{-6}, was on a single crystal of cobalt ferrite in the [100] direction, after a magnetic anneal.

A number of investigators have grown single crystals of ferrites. These have been useful for studying domain wall motion and loss mechanisms. Initial permeabilities as high as 5000 have been measured on single crystals of Fe_3O_4, as compared to less than 10 in the polycrystalline form. No commercial applications involving single crystals are known to the author.

Applications of Ferrites

Ferrites have a large and increasing number of applications because component and circuit engineers have found them advantageous in accomplishing specific objectives. In some cases, ferrites yield higher efficiency, smaller volume, lower costs, greater uniformity, or easier manufacture than can be obtained with other materials. In others, including the microwave field, the unique properties of ferrites permit accomplishments not feasible with any other known material. Table I (opposite) summarizes the principal design applications, the most important component characteristics, and the properties of ferrites on which they depend. The applications fall roughly into categories determined by the material properties used:

1) *Linear B-H*, low flux level, high stability.
2) *Nonlinear B-H*, medium to high flux levels.
3) *Highly nonlinear B-H*, rectangular loop.
4) *Microwave properties*, ferromagnetic resonance, Faraday rotation.
5) *Magnetostriction.*

The microwave applications are included in the table for completeness but will not be covered in the discussion which follows on several typical ferrite designs. A recent article by Duncan and Stone [66] surveys ferrite applications in inductor design rather comprehensively, particularly those in the linear *B-H* region. Various methods of inductance adjustment are discussed, including wide range methods for tuners.

Filter Inductors

The high μQ product of ferrites over the frequency range of 50 kc to 150 kc has led to their extensive use in filter inductors for band-pass filters in carrier telephone circuits. Precise inductance adjustment, high inductor Q, and good stability are necessary for the function of separating channels. Such coils are normally of the pot type construction in which the cores are assembled using a center post, two end plates, and an outside ring. An alternate assembly uses two cups either with integral posts or a separate post. The principal air gap is provided by shortening the posts. With a proper magnitude of air gap built in, the permeability can be made correct for an optimum value of Q. Movable magnetic details which shorten or shunt the air gap have been incorporated for inductance adjustment. This eliminates the need for close factory adjustment, permits alignment of equipment after assembly, and eliminates trimmers. In the pot type cores described, the ferrite material provides an effective shield around the form winding. Permeabilities ranging from 35 to 100 are used most commonly to obtain the desired Q and required stability.

A completed filter coil is shown in Fig. 13 (p. 1242). Here, with a volume of 1.5 cubic inches, a Q of 500 is obtained at 100 kc. The core consists of manganese zinc ferrite with an intrinsic permeability of 1500. A coil wound on a molybdenum permalloy powder ring and previously used for a similar purpose had more than six times the volume but only one-half the Q. Furthermore, it could not be adjusted after final assembly. The ferrite coil can be adjusted over a range of plus or minus fifteen per cent by means of a movable cylindrical core shown in Fig. 13.

In experimental models on this structure, inductor Q's in excess of 1000 at 100 kc have been obtained. The manner in which distributed capacitance tends to reduce Q becomes an important consideration under these conditions.

TABLE I

A Summary of Ferrite Applications

Type of component	Typical frequency	Characteristic sought	Favorable ferrite properties	Typical ferrite μ_0	Desired improvements
A. Linear B-H, low flux density					
Filter inductors	100 kc	High Q, precision, stability low modulation	High μQ, low hysteresis, convenient core shapes	MnZn 1000–2500	Higher μQ, lower temperature coefficient
IF transformers	465 kc	High Q, stability, adjustability	High μQ, shapes	NiZn* 100– 200	Higher μQ to higher frequencies better stability to temperature and to magnetic and mechanical shock
Antenna cores	1000 kc	Moderate Q, stability	High μQ, rod shapes		
Wide band transformers	to 15 mc	Reproducability of transmission characteristics	High μ, low losses, assembled core structures	Mn Zn 1000–2500 NiZn* >500	Very uniform magnetic and mechanical properties
Adjustable inductors	Various	Adjustment ±20 per cent	High μ, shapes	MnZn NiZn*	
Tuners	Various	Adjustment >10/1	Various mechanical structures, μ variation in dc field		
Miniature inductors	Various	Moderate Q, small size	Cup shapes	MnZn >1000 Ni Zn* >1000	Higher saturation, less loss at moderate Bm
Loading coils	Voice	Stability, low modulations, low leakage flux	High μQ		Lower sensitivity to dc fields Lower hysteresis loss
B. Nonlinear B-H, medium to high flux densities					
Flyback transformers	15–100 kc	Low loss, moderate size		MnZn >750 NiZn* >750	Higher saturation, lower losses Higher curie temperatures
Deflection yokes					
Miniature transformers	Pulse	Small size, easy mounting	High μ, cup shapes	NiZn 4000	Higher saturation
Carrier power transformers	Various				
Choke coils					
Suppression beads		High resistive impedance	High loss above critical frequency	MnZn >500 NiZn* >500	
Recording heads			Mechanical rigidity, low loss	NiZn, MnZn	Higher saturation, nonabrasive surface
C. Highly nonlinear, rectangular loop					
Memory cores	Pulse	Two identifiable stable states, fast flux reversal	Small rings practical reasonable rectangularity	MgMn	Higher degree of rectangularity, stability, uniformity, low cost
Switching cores	Pulse	Fast flux reversal, high output	Reasonable rectangularity	MgMn	High saturation for high output
Multiaperture cores					
Magnetic amplifiers					
D. Microwave properties					
Isolators, attenuators, circulators, switches, modulators			Faraday rotation Ferromagnetic resonance	MgMn*	
E. Magnetostriction and other properties					
Delay lines					
Filters and oscillators					
Temperature controls		Sensitivity to temperature	Low curie temperature Temperature sensitivity		

* May contain additional elements such as Mg, Mn, Co, Cu, Al.

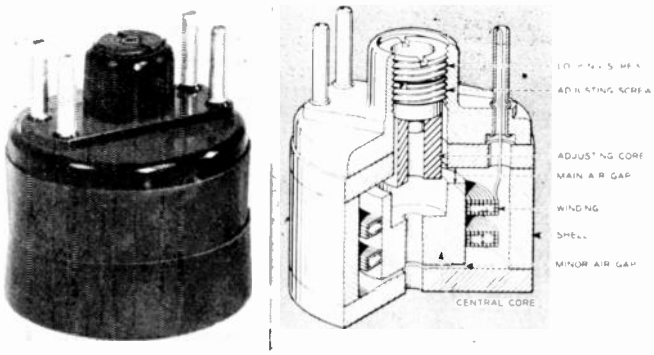

Fig. 13—A high-Q adjustable filter inductor.

Wide-Band Transformers

High permeability ferrites, in core assemblies made up of C's or E's, are being used in wide-band high frequency transformers. A precision transformer of this type (Fig. 14) is used in line amplifiers in the L-3 coaxial

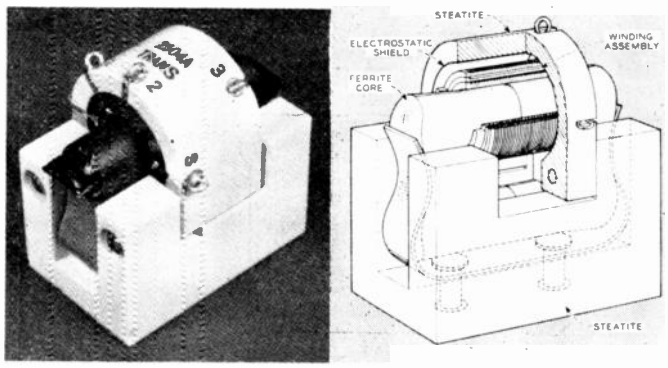

Fig. 14—A wide-band transmission transformer.

cable system in which the video band extends up to 8.4 megacycles. Here two C-shaped cores are assembled into two precise windings plated on optical quartz forms. The assembly is held to very close dimensions in order to control leakage inductance and parasitic capacitances and thereby the over-all transmission characteristics. Such close mechanical and electrical tolerances would not be possible with windings on toroidal cores. The permeability of the ferrite is high enough to provide the inductance necessary for transmission at low frequencies with the relatively small number of turns required to provide good high frequency response. With carefully ground mating surfaces, the loss in permeability due to air gaps is only about ten per cent.

Antenna Cores

Extruded rods of ferrite are utilized for antenna cores for broadcast radio receivers. These are usually one quarter to three quarter inch in diameter, in lengths ranging from two to eight inches. A winding is applied, normally distributed over the length of the core, to form an inductive antenna. The number of flux linkages is increased through the effective permeability of the core. The length to diameter ratio of the rod needs to be large in order to reduce demagnetizing effects and thus realize as much as possible of the intrinsic permeability of the ferrite. This generally has led to the extrusion of rods. For a given ratio of length to diameter, the sensitivity of the antenna is increased by enlarging both length and diameter. Sizes of portable radio cabinets and costs of the core material have influenced the production of cores toward the sizes noted above. The ferrite material should have moderately high Q over the broadcast frequency band to provide needed selectivity. It should be stable with respect to temperature changes, residual magnetic shock from high ac or dc magnetization, or mechanical vibration to prevent inductance changes large enough to cause detuning. Improvements in these respects have been achieved recently by new compositions and manufacturing techniques.

Miniature Components

The ferrites are finding more and more applications in a growing field for miniature inductors and transformers. The pot type structure is well suited for the efficient utilization of space. Two cups are commonly used and assembled around a winding. Terminal plates or pigtail leads are attached and the assembly is molded in plastic. Fig. 15 shows such an inductor assembly. The

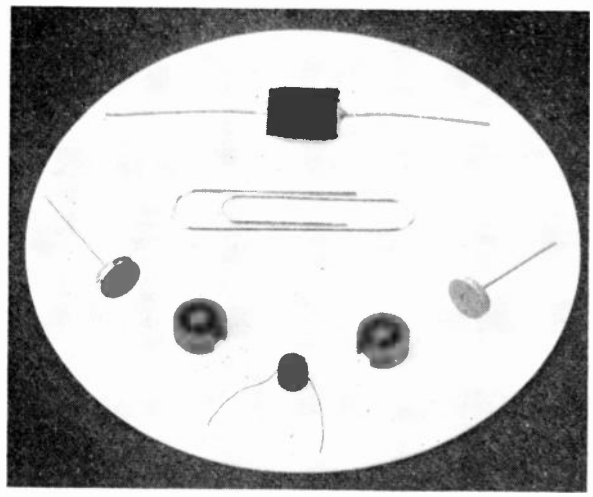

Fig. 15—A miniature inductor.

low power levels common with transistorized circuits are favorable to the use of ferrites in a similar structure in pulse transformers. In this case, high permeability materials, such as nickel zinc ferrite with 4000 permeability, or a manganese zinc ferrite with a permeability greater than 1000 are most suitable. The temperature rise in transistor circuits usually is low enough to permit the use of high permeability materials having low Curie temperatures.

Flyback Transformers and Deflection Yokes

Undoubtedly the largest use of ferrite measured in terms of pounds of material has been in flyback trans-

formers for television circuits. They were first used in 1948. *C*-shaped cores are used in practically all designs, with a small air gap for reducing the variability caused by the presence of dc fields. Fig. 16 shows a flyback transformer assembled on ferrite cores with legs of square cross section. An evolution in the design of cores from square legs to hexagonal legs to round legs has been taking place. The round leg is helpful in reducing high voltage corona and has been made desirable by the progressive increase in flyback voltages from 10 kv up to 25 kv as larger picture tubes have been used. The manufacture has been made practical through the development of new die structures and pressing techniques.

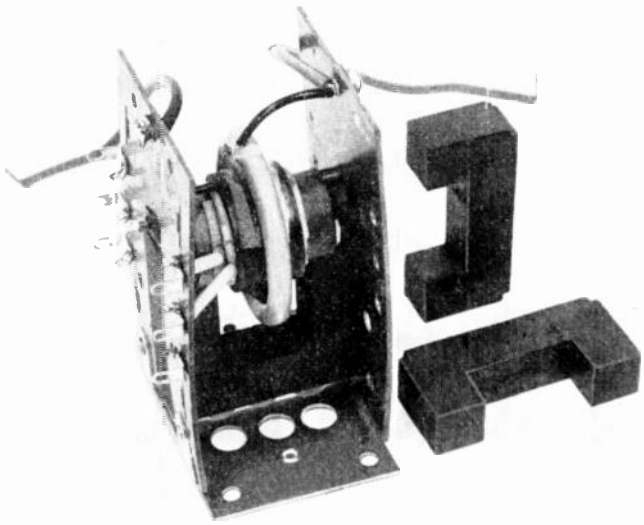

Fig. 16—A television flyback transformer.

These cores must have low losses at operating flux levels up to as high as 1500 gausses at the 15.75 kc scanning frequency and at flyback frequencies up to 100 kc. Low losses are not only important from the standpoint of reducing size and cost of the transformer itself but also to permit reductions in the size of the power supply. The Curie temperature must be high enough so that losses do not rise excessively at operating temperatures. Increased permeabilities combined with higher saturation have been obtained in manganese zinc ferrites fired to high density and have contributed to reductions in size and cost.

Cores for deflection yokes in tv sets quite generally are made of ferrite materials. They are pressed as halves or quadrants of a circular ring for assembly around the neck of the picture tube. The material properties are less critical in yoke applications than in flyback transformers.

Magnetic Memories and Switches

One of the fastest growing and potentially large applications for ferrite cores is for memory and switching uses in digital computers and data processing circuits. This application involves the use of microsecond pulses for transmitting, storing, and reading information expressed in a binary code.

Rectangular hysteresis loop properties are required to provide two identifiable stable states of remanent magnetization and to provide a highly nonlinear *B-H* relationship so the state of magnetization can be definitely and quickly changed. The degree of rectangularity and the uniformity and stability of characteristics have a direct bearing upon the number of cores which can be used reliably in a memory, and hence upon the storage capacity of the memory. The values of coercive force determine how rapidly the information can be handled.

Cores of magnesium manganese ferrite now are being produced with a good degree of rectangularity. Uniformity is being sought through control of composition and processing and by an elaborate selection procedure. Ferrite cores have several inherent advantages. They can be formed into tiny rings down to 0.050 inch diameter in automatic presses. The cost of the raw materials is low. Ferrite cores are chemically and mechanically stable and are practically indestructible, except for actual mechanical breakage. In common with other magnetic cores, once triggered to a stable state, they will retain their magnetization indefinitely without further power consumption.

The properties of rectangular loop ferrite cores in relation to certain circuit operations may be understood by reference to Fig. 17.

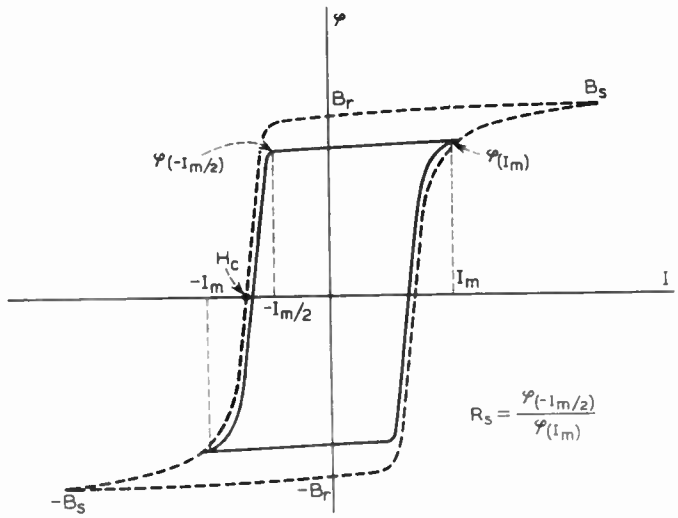

Fig. 17—Hysteresis loops of MgMn ferrite. Dashed line—loop at saturation. Solid line—Loop for optimum I_m for double coincident memory use.

When the material is magnetized by an applied field in the plus direction, it will retain the larger part of its magnetization when the applied field is removed. It is said to be "set" at plus B_r. If the rectangularity were perfect, B_r would be equal to the saturation flux density B_s. There would be no further change in the state of magnetization due to additional plus fields of any magnitude or to any negative field smaller in magnitude

than minus H_c. However, if a negative pulse larger than minus H_c is applied the magnetization will be reversed and the core will remain set at minus B_r when the field is removed. For the latter case, the total flux change occurring in the core during reversal will be 2 B_r. The changing flux will induce a voltage in a "read-out" winding on the core and thus provide a method of detecting when the state of magnetization is changed by a current pulse.

If an array of cores is wired as shown in Fig. 18 any core in the group can be magnetized independently of the others by dividing the total magnetizing current equally between two windings. If the current is properly chosen, the one half current in either winding alone will be insufficient to magnetize or reverse a core, but the two half currents will be large enough to magnetize or switch the one core located at the intersection of the two wires. This provides the basis for setting each core in the array in a plus or minus state of magnetization to correspond to a binary code. The information can be read out by scanning the array with unidirectional half current pulses applied to the horizontal and vertical wires in a proper time sequence and noting which cores give a flux reversal when subjected to both currents simultaneously. The flux change is detected through the read-out winding which can be common to all cores. This action is indicated in Fig. 18.

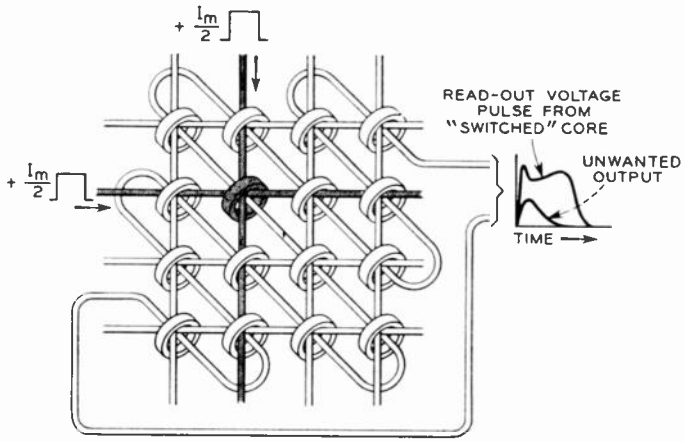

Fig. 18—An array of ferrite cores wired for double coincident memory use.

The above describes a single plane double coincident current memory in which the elements of each "word" are read out in sequence. Many planes may be operated in parallel, in which case whole words can be read out at once by locating each element of the word in a different plane. Each plane would have its own read-out winding. Also it is possible to divide the current into more than two parts and operate the array as a multiple coincident system by threading the appropriate number of driving windings in each core. Practical difficulties multiply due to departure of available materials from true rectangularity.

Magnetic cores also have important uses in the logic and switching circuits which direct and control the flow of information in and out of the memories and through the various processing operations. Fast operation is desired, which requires rapid switching and the generation of voltage pulses large enough to actuate succeeding cores.

Two highly important characteristics in a rectangular loop core are a large flux reversal and a short switching time t_w for a low applied drive. The latter indicates a low coercive force H_c, since a core will not switch until the applied pulse drive NI exceeds the coercive force. We may write

$$NI_0 = CH_c$$

where NI_0 is the minimum pulse drive required to switch the core and C is a constant (between 1 and 2) which depends upon the "inertia" of the magnetic domains to change direction and hence upon the characteristics of the core material. The switching time is related to the drive by the following expression:

$$t_w = \frac{k}{NI - NI_0}$$

where k is a constant applicable over a certain range of $(NI - NI_0)$ and is related to the damping or loss mechanisms in the core material. Much study is in progress on the magnetic mechanisms involved in switching behavior, but not all phenomena have been correlated as yet.

Departure from rectangularity causes unwanted output voltages to be generated when cores are subjected to pulses not intended to set or switch the core. This is due to some change in flux as the magnetization is driven from remanence to saturation of the same sign, or by a half pulse in the opposite direction from remanence. The latter condition can produce demagnetization of the core if the minor loop runs down onto the rounded corner of the major loop. Demagnetization effects are minimized by improving the rectangularity of the loop, by careful selection of the optimum current and associated one half current drives, as well as by arranging to have each half pulse followed by a pulse in the opposite direction to prevent progressive demagnetization steps. The temperature coefficient of the material and changes in ambient temperature must be such that the optimum point of operation is not shifted appreciably.

In memory planes, the noise or unwanted voltage pulses can be caused to cancel by wiring the series pickup winding so that outputs from one half of the cores will oppose the others. This solution requires that all the cores have exactly the same characteristics.

Since ideal rectangularity has not been obtained and since a high degree of uniformity is needed to compensate for nonrectangularity, a heavy responsibility is placed upon manufacturing control and testing. This

is leading toward automation in processing and test inspection. Several automatic testers are now in operation for checking and sorting cores. These apply a prescribed program of pulses to the test core and compare the response to that of a standard core.

The performance of a ferrite core used in computer applications is a function of the circuit as well as the intrinsic properties of the core. Or conversely, the circuitry is dictated largely by the characteristics of available cores. In this stage of intensive development in both circuits and cores, standards for core characteristics and core test procedures have not yet been established. In general, cores are characterized by the coercive force H_c and the B_r/B_s ratio obtained from static loops. Then for double coincident memory, the optimum pulse drive which will produce switching with the minimum disturbance from the one half pulse is specified. The dynamic squareness ratio R_s is expressed as the flux density associated with the reverse half pulse to the flux density for the full pulse. The switching time t_w for the optimum drive also is important. For switching functions, the variation of switching time with the amplitude of the driving pulse is determined as well as the magnitude of the flux switched. The latter indicates the output voltage which can be obtained.

Table II lists properties of two types of magnesium manganese cores now in general use. A further reduction in H_c will improve the operation of ferrite cores for switching purposes in logic circuits. The present magnesium manganese ferrites develop reasonably good rectangular loop properties and have a Curie temperature high enough so that they are not critically sensitive to temperature variations. Rings of high permeability nickel zinc ferrites with nonrectangular loops have had the loops squared effectively by being cast in a disk of plastic, or other material such as glass, to produce a radial stress. Some compositions of high density manganese ferrite have been made with square loops but the Curie temperature is so low that they are too sensitive to temperature variations to be practical.

ties of ferrite materials. The basic principle is that a second aperture is located within the flux path of a primary aperture and is controlled by the flux bias from the primary aperture. Fig. 19(a) shows such a device.

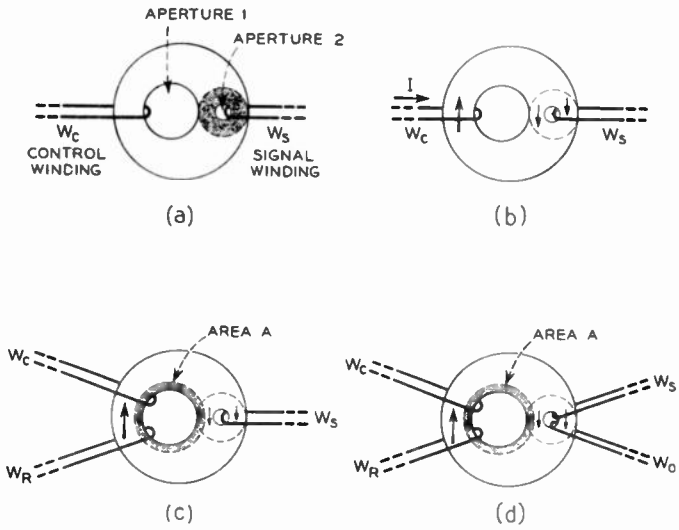

Fig. 19—Conditions in a two-aperture ferrite core. (a) Two-aperture core. (b) Blocked condition around aperture 2. (c) Partially blocked condition around aperture 2. (d) Variable transformer action on aperture 2.

If the core consists of nonrectangular ferrite, the device becomes a simple saturable reactor. If the bias from the dc control winding W_c is made large enough it will saturate the flux path surrounding the second aperture containing the signal winding W_s as indicated in Fig. 19(b). The path around aperture 2 is then said to be blocked, since no additional flux can be made to flow in either a clockwise or counterclockwise direction by a signal current in winding W_s. The inductance of W_s varies from a maximum when there is no bias to a minimum when the bias flux from W_c is increased to saturation.

If ferrite material with a high degree of rectangularity

TABLE II

Typical Characteristics of Rectangular-Loop Ferrite Cores

Material	μ_0	μ_m	T_c	H_c	B_r	B_s	B_r/B_s	R_s	T_w NI Drive	Reference
			−°C	(Oersteds)	(Gausses)	(Gausses)			(μs) (Oersteds)	
MgMn	40	515	>150	1.4	1600	1750	0.9	0.8	1 @ 2*	[43]
MgMn	45	1,800	>150	0.65	1920	2000	0.96	0.95	5 @ 0.8*	[43]
NiZn (stressed)	2500	37,000	70	0.03	1460	1870	0.78	—	1 @ 1.2	[39]

* Optimum drive for double coincident memory use.

Multiaperture Ferrite Core Devices

Some interesting devices have been produced using one-piece ferrite cores with two or more apertures, and will be discussed in some detail to show the potentiali-

is used in the same arrangement it will continue to provide a saturating bias on W_s after the dc has been removed, due to its high remanence. However, if a reverse dc field is applied by a "set" winding W_r, the magnetiza-

tion of the ferrite path around the primary aperture can be reversed progressively from the inside circumference to the outside. This is because the path length is shorter around the inside and the field reaches the value necessary to reverse the magnetization before it has been reached further out along the radius. The reversed flux area grows outward from the primary aperture. The reversal of flux can be stopped at any degree desired as indicated in Fig. 19(c), leaving the leg common to apertures 1 and 2 only partially blocked. Suppose that a current pulse is applied to the winding W_s to produce an electromotive force in a counterclockwise direction. For small pulses the path immediately surrounding aperture 2 is blocked and no flux can be reversed. But as the counterclockwise current pulse in W_s is made larger it will produce a magnetomotive force overlapping the area A and large enough to reverse the flux in the overlapped area of A. Hence a counterclockwise flux will be caused to flow around aperture 2. If this is followed by a clockwise pulse the flux will be again reversed. Hence, the setting of area A around aperture 1 determines the amount of flux which can be controlled by pulses applied to winding W_s. When the outer circumference of area A reaches the center of aperture 2, the available flux will be a maximum.

If an additional winding W_0 is provided in the secondary aperture, as shown in Fig. 19(d), there will be a coupling between the signal winding W_s and the output winding W_0 except when the core is blocked by complete saturation. A continuously variable output level is provided through the degree of magnetization set up by the control and set windings, and the device operates as a variable pulse transformer. The coupling between the control and signal windings is very small.

Such a device has possibilities as an operate-nonoperate control on a circuit containing W_s, depending on whether the core is in a blocked or unblocked state. It also has been suggested as a nondestructive read-out since the state of the core can be determined without altering the setting and hence has potentialities in random access memories.

With the use of additional apertures various combinations of interflux linkages can be set up so that a change in flux will be transmitted from one aperture to another, providing sequential steps of operation.

Other Applications

The applications described above are typical of how the properties of ferrites enter into component design and circuit operations. The high μQ product of ferrites has made them particularly useful in IF transformers in radio circuits and in slug tuned inductors. Many of the IF transformer designs utilize small cup cores. The slug cores are made as cylinders with or without coaxial holes and can be threaded by grinding or can be provided with threaded studs cemented into a hole in the end of the core.

The rapid increase in core losses above a critical frequency has proved advantageous for suppressing high frequency resonances in inductors and transformers. The high core losses cause a large resistive impedance and damp out resonances from leakage inductance and distributed capacitance. Beads or washers of ferrite used on lead wires can be used for suppressing high frequencies, or to produce resistive decoupling of components.

The square loop properties of ferrites make them useful for high frequency magnetic amplifiers and other saturable reactor devices. One interesting application is the magnetic counter. If a pulse of proper magnitude and length is applied to a ring core, it will partially magnetize the core. Successive pulses will produce progressive degrees of magnetization until saturation is reached. At that point the impedance of a winding on the core will become very low and can be arranged to cause a circuit response. Cores have been made to operate reliably with as many as 100 steps. The core will retain partial magnetization indefinitely so the full number of steps required to produce saturation may be spread over any period of time.

The ferrites have found some degree of interest for magnetostrictive delay lines and magnetostriction resonators.

The high resistivity of ferrites has made them useful as pole pieces for concentrating flux in high frequency induction heaters.

The final application to be considered in this paper is the suitability of ferrites in loading coils. The ferrites have found some use in both voice and carrier frequency loading coils in Europe, where circuit requirements and restricted availability of raw materials have combined to make them advantageous in these applications. In the United States, work on the development of ferrite for loading coils is being carried on, but has not progressed to the point where it can be substituted satisfactorily for molybdenum permalloy powder. The latter cores, used as toroids, were developed specifically to withstand superimposed currents up to 100 milliamperes dc, to have low residual magnetization, low modulation, and low crosstalk. Most voice frequency loading circuits have been based upon the capabilities of the loading coils.

The ferrite-cored loading coils used in Europe mostly employ pot type structures with special mechanisms for obtaining circuit balances by shifting the positions of the windings.

Conclusion

Modern magnetic ferrites have achieved a position of economic and engineering importance within the ten-year period they have been available. They are widely used in inductors and transformers because of their high μQ and mechanical design capabilities, including miniature components, and in computers because of square loop properties. They have produced quite revolutionary contributions to microwave circuitry,

the discussion of which is outside the scope of this paper. The ferrites are a stimulating and powerful research tool in magnetics. Ferrite manufacture and design applications embrace the cooperative efforts of persons engaged in the development and manufacture of oxide materials, processing equipment, and test apparatus. The future holds promise of many new advances in the properties and applications of the modern ferrite materials.

Bibliography

A very large volume of literature has appeared on ferrites over the past ten years. The following references have been selected primarily to cover properties and applications of ferrites below the microwave frequency range, and include some pertinent material on applicable theory. Except in one or two instances, references have not been included in the text. The titles generally will identify the subject matter of the articles.

1946–1950

[1] Snoek, J. L., "Non-Metallic Magnetic Materials for High Frequencies." *Philips Technical Review*, Vol. 8 (December, 1946), pp. 353–360.
[2] Snoek, J. L., *New Developments in Ferromagnetic Materials*. Amsterdam-New York: Elsevier Publishing Co., 1947.
[3] Snoek, J. L., "Dispersion and Absorption in Magnetic Ferrites at Frequencies Above One mc/s." *Physica*, Vol. 14 (May, 1948), pp. 207–222.
[4] Néel, L., "Magnetic Properties of Ferrites; Ferrimagnetism and Antiferromagnetism." (in French), *Annales de Physique*, Vol. 3 (1948), p. 137.
[5] Landon, V. D., "Use of Ferrite Cored Coils as Converters, Amplifiers and Oscillators." *RCA Review*, Vol. 10 (September, 1949) pp. 387–396.
[6] Snyder, C. L., Albers-Schoenberg, E., and Goldsmith, H. A. "Core Materials for High Frequencies." *Electrical Manfacturing*, Vol. 44 (December, 1949), pp. 86–91.
[7] Brockman, F. G., Dowling, P. H., and Steneck, W. G., "Dimensional Effects Resulting from a High Dielectric Constant Found in Ferromagnetic Ferrite." *Physical Review*, Vol. 7 (January 1, 1950), pp. 85–93.
[8] Polder, D., "Ferrite Materials." *Proceedings of the IEE*, Vol. 97 (April, 1950), p. 246.
[9] Latimer, K. E., and MacDonald, H. B. "A Survey of the Possible Applications of Ferrites." *Proceedings of the IEE*, Vol. 97 (April, 1950), pp. 257–267.
[10] Harvey, R. L., Hegyi, I. J., and Leverenz, H. W., "Ferromagnetic Spinels for Radio Frequencies." *RCA Review*, Vol. 11 (September, 1950), pp. 321–363.
[11] Strutt, M. J. O., "Ferromagnetic Materials and Ferrites." *Wireless Engineer*, Vol. 27 (December, 1950), pp. 277–284.
[12] Guillaud, C., and Barbazet, A., "Magnetic Properties of a Manganese Ferrite in Weak Fields." (in French), *Journal des Recherches*, (1950), pp. 83–100.

1951

[13] Kittel, C., "Ferromagnetic Resonance." *Journal de Physique et le Radium*, Vol. 12 (March, 1951), pp. 291–302.
[14] Collection of Papers Presented at the Conference on Ferromagnetism and Antiferromagnetism at Grenoble, France, July 4, 1950. *Journal de Physique et le Radium*, Vol. 12 (March, 1951), pp. 153–506.
[15] Rajchman, J. A., "Static Magnetic Matrix Memory and Switching Circuits," *RCA Review*, Vol. 13 (June, 1951), p. 183.
[16] Both, E., "Ferrite Materials Permit Improved Designs of Magnetic Devices." *Materials and Methods*, Vol. 34 (July, 1951), pp. 76–79.

1952

[17] Went, J. J., Rathenau, G. W., Gorter, E. W., and Oosterhout, G. W. "Ferroxdure, A Class of New Permanent Magnet Materials." *Philips Technical Review*, Vol. 13 (January, 1952), pp. 194–208.
[18] Hogan, C. L., "The Ferromagnetic Faraday Effect at Microwave Frequencies and Its Applications—The Microwave Gyrator." *Bell System Technical Journal*, Vol. 31 (January, 1952), pp. 1–31.
[19] Went, J. J., and Gorter, E. W., "Magnetic and Electrical Properties of Ferroxcube." *Philips Technical Review*, Vol. 13 (January, 1952), pp. 181–193.
[20] Vonderschmitt, V. B., Albert, M. J., and Stott, H. B., "Ferrite Applications in Electronic Components." *Electronics*, Vol. 25 (March, 1952), pp. 138–139.
[21] Both, E., "Development and Utilization of Magnetic Ferrites." *Ceramic Age*, Vol. 59 (April, 1952), pp. 39–45.
[22] Emmerick, E., and Klaus, S. C., "Evaluating Electrical Properties of Ferrite Materials for Specific Applications." *Ceramic Age*, Vol. 50 (May, 1952), pp. 26–29.
[23] Six, W., "Some Applications of Ferroxcube." *Philips Technical Review*, Vol. 13 (May, 1952), pp. 301–311.
[24] Gelbard, E., "Magnetic Properties of Ferrite Materials." *Tele-Tech*. Vol. 11 (May, 1952), p. 50.
[25] Galt, J. K., "Initial Permeability and Related Losses in Ferrites." *Ceramic Age*, Vol 60 (August, 1952), pp. 29–33.
[26] Newhall, E., Gomard, P., and Ainlay, A., "Saturable Reactors as r-f Tuning Elements." Vol. 25 (September, 1952), pp. 112–115.
[27] Fairweather, A., Roberts, F. F., and Welch, A. J. E., "Ferrites." *Reports on Progress in Physics*, Physical Society, London, Vol 15 (1952), pp. 142–172.
[28] Bozorth, R. M., and Walker, J. G., "Magnetostriction of Single Crystals of Cobalt and Nickel Ferrites." *Physical Review*, Vol. 88 (December 1, 1952), p. 1209.

1953

[29] Galt, J. K., Andrus, J., and Hopper, H. G., "Motion of Domain Walls in Ferrite Crystals." *Reviews of Modern Physics*, Vol. 25 (January, 1953), pp. 93–97.
[30] Owens, C. D., "Analysis of Measurements on Magnetic Ferrites." Proceedings of the IRE, Vol. 41 (March, 1953), pp. 359–365.
[31] Stone, H. A., Jr., "Ferrite Core Inductors." *Bell System Technical Journal*, Vol. 32 (March, 1953), pp. 265–291.
[32] van der Burgt, C. M., Gevers, M., and Wijn, H. P. J., "Measuring Methods for Some Properties of Ferroxcube Materials." *Philips Technical Review*, Vol. 14 (March, 1953), pp. 245–256.
[33] Van Roberts, W., "Some Applications of Permanently Magnetized Ferrite Resonators." *RCA Review*, Vol. 14 (March, 1953), pp. 3–16.
[34] Brown, D. R., and Albers-Schoenberg, E., "Ferrites Speed Digital Computers." *Electronics*, Vol. 26 (April, 1953), pp. 146–149.
[35] van der Burgt, C. M., "Dynamical Parameters in the Magnetostrictive Excitation of Extensional and Torsional Vibrations in Ferrites." *Philips Research Reports*, Vol. 8 (April, 1953), pp. 91–132.
[36] Hering, H., and Leichseuring, F., "Morden Loading Coils with Siferrit Pot-Cores." (German), Siemens-Zeitschrift, Vol. 27 (September, 1953), p. 124.
[37] Alley, R. E., Jr., "A Review of New Magnetic Phenomena." *Bell System Technical Journal*, Vol. 32 (September, 1953), pp. 1155–1172.
[38] Rajchman J. A., "A Myriabit Magnetic Core Matrix Memory." Proceedings of the IRE, Vol. 41 (October, 1953), pp. 1407–1421.
[39] Williams, H. J., Sherwood, R. C., Goertz, Matilda, Schnettler, F. J., "Stressed Ferrites Having Rectangular Hysteresis Loops." *AIEE Communications and Electronics* (November, 1953), pp. 531–536.
[40] Hoh, S. R., "Evaluation of High Performance Magnetic Core Materials." *Tele-Tech*, Vol. 12 (October, 1953), and p. 86; (November, 1953), p. 92.
[41] Lennartz, H., "Ferrites. Properties and Applications." (in German), *Funk und Ton*, Vol. 7 (December, 1953), pp. 613–627.
[42] Richards, E. E., and Lynch, A. C., (ed.). *Soft Magnetic Materials for Telecommunications*. New York: Interscience Publishers, Inc., London: Pergamm Press, Ltd., 1953. Symposium held at the Post Office Research Station in April, 1952.

1954

[43] Albers-Schoenberg, E., "Ferrites for Microwave Circuits and Digital Computers." *Journal of Applied Physics*, Vol. 25 (February, 1954), pp. 152–154.
[44] Saltpeter, J. L., "Developments in Sintered Magnetic Materials." *Proceedings of the IRE (Australia)*, Vol. 14 (May, 1953), p. 105; and Proceedings of the IRE, Vol. 42 (March, 1954), p. 514.
[45] Geroulo, M., Peck, D. B., and Cushman, N., "Improved Components Based on Ferrite Materials." Electronic Components Symposium Proceedings, (May 4–6, 1954), pp. 141–146.
[46] Wijn, H. P. J., Gorter, E. W., Esveldt, C. J., and Geldermans, P., "Conditions for Square Hysteresis Loops in Ferrites." *Philips Technical Review*, Vol. 16 (August, 1954), pp. 49–58.

[47] Legg, V. E., and Owens, C. D., "Magnetic Ferrites—New Materials for Modern Applications." *Electrical Engineering*, Vol. 73 (August, 1954), pp. 726–729.
[48] Brown, D. R., Buch, D. A., and Menyuk, N., "A Comparison of Metals and Ferrites for High Speed Pulse Operation." *Transactions of the AIEE*, Vol. 73 (1954), p. 631.
[49] Goodenough, J. B., "A Theory of Domain Creation and Coercive Force in Polycrystalline Ferromagnetics." *Physical Review*, Vol. 95 (1954), p. 917.
[50] Gelbard, E., and Olander, W., "Ferrite Memory Devices." *Computers and Automation*, Vol. 3 (1954), p. 6.
[51] Say, M. G. (ed.). *Magnetic Alloys and Ferrites*, London: Geo. Newnes, Ltd., 1954.

1955

[52] Block, H., and Rietveld, J. J., "Inductive Aerials in Modern Broadcast Receivers." *Philips Technical Review*. Vol. 16 (January, 1955), pp. 181–194.
[53] Grimmet, C. A., "Improving Ferrite Cored Antennas." *Tele-Tech and Electronic Industries*, Vol. 14 (February, 1955), p. 84.
[54] Vonderschmitt, B. V., and Barkow, W. H., "Application of Ferrites to Deflection Components." Proceedings of the Eleventh Annual Meeting, Metal Powder Association, Vol. II (May, 1955), pp. 189–199.
[55] Torsch, Charles E., "Trends in Ferrite Core Design for TV Yokes and Flybacks." Proceedings of the Eleventh Annual Meeting, Metal Powder Association, Vol. II (May, 1955), pp. 175–182.
[56] Papian, W. N., "Application of Ferrites to Memory Systems." Proceedings of the Eleventh Annual Meeting, Metal Powder Association, Vol. II (May, 1955), pp. 183–186.
[57] Katz, H. W., "High Impedance Ferrite Delay Lines." Proceedings of the AIEE-IRE Electronic and Materials Symposium, Philadelphia, June 2–3, 1955.
[58] Aden, A. L., Ayres, W. P., and Melchor, J. L., "Ferrites—Part I. Fundamentals." *The Sylvania Technologist*, Vol. 8 (July, 1955), pp. 76–83.
[59] Blackman, L. C. F., "A Review of the Structure and Some Magnetic Properties of Ferrites." *Journal of Electronics*, Vol. 1 (July, 1955), pp. 64–77.
[60] Synder, R. L., "Magnistor Circuits." *Electronics Design*, Vol. 3 (August, 1955).
[61] Hanaoka, Yukiaki, "Very Wide Band Radio Frequency Transformer Using Ferrite Core and Permalloy Tape Wound Cores." *Electrical Communication*, (Tokyo), Vol. 3 (September, 1955), p. 7.
[62] Bozorth, R. M., Tilden, E. F., and Williams, A. F., "Anisotropy and Magnetostriction of Some Ferrites." *Physical Review*, Vol. 99 (September 15, 1955), pp. 1788–1798.
[63] Wilson, V. C., "Applications of Ferrites." AIEE Publication T-78, Conference on Magnetism and Magnetic Materials, October, 1955.
[64] Rathemau, G. W., and Fast, J. W., "Initial Permeabilities of Sintered Ferrites." *Physica*, Vol. 21 (1955), pp. 964–970.
[65] Menyuk, N., and Goodenough, J. B., "Magnetic Materials for Digital Computer Components I. A Theory of Flux Reversals in Polycrystalline Ferromagnetics." *Journal of Applied Physics*, Vol. 26 (1955), p. 8.

1956

[66] Duncan, R. S., and Stone, H. A., Jr., "A Survey of the Application of Ferrites to Inductor Design." PROCEEDINGS OF THE IRE, Vol. 44 (January, 1956), pp. 4–13.
[67] Bozorth, R. M., "The Physics of Magnetic Materials." *Electrical Engineering*, Vol. 75 (Feburary, 1956), pp. 134–140.
[68] Brailsford, F., "Ferromagnetism in Relation to Engineering Materials." *Proceedings of the IEE* (London), Part A, Vol. 103 (February, 1956), pp. 39–51.
[69] Rajchman, J. A., and Lo, A. W., "The Transfluxor." PROCEEDINGS OF THE IRE, Vol. 44 (March, 1956), p. 321.
[70] Schlicke, H. M., "Cascaded Feedthrough Capacitors." PROCEEDINGS OF THE IRE, Vol. 44 (May, 1956), pp. 686–691.

Fundamental Theory of Ferro- and Ferri-Magnetism*

J. H. VAN VLECK†

Summary—**The presentation is centered around the four important forms of magnetic energy in ferromagnetic media: (I) the Zeeman energy of the elementary magnets in the applied magnetic field, (II) the classical electromagnetic interaction between dipoles, (III) the Heisenberg exchange energy, and (IV) the energy of anisotropy which is pseudodipolar or pseudoquadrupolar in structure but is attributable ultimately to rather recondite quantum-mechanical spin-orbit interaction. The primary cause of ferromagnetism is (III), and anisotropy arises from (IV). Domain structure and the concomitant hysteresis phenomena owe their existence to (II). The magnetic theory of the ferrites is in many ways simpler and less ambiguous than that for conducting ferromagnetic media, as there are no complications due to electron migrations. Néel's theory of ferrimagnetism explains the saturation magnetization and other properties of the ferrites.**

MONOGRAPHS or articles on fundamentals of the theory of magnetism are today so common that the subject is becoming rather hackneyed. Hence any paper such as the present one is, of necessity, rather stereotyped, because the broad outlines of a successful theory have been pretty well stabilized. It is true that exciting developments are still taking place on the frontiers of the theory, as witnessed, for instance, by Clogston's [1] recent work on the linebreadths of ferromagnetic resonance lines. These improvements take place mostly in rather recondite technical areas beyond the scope of any elementary talk. To vary things a little from the standard presentations, I am going to center most of the discussion on the various forms of energy which are encountered in analyzing the behavior of a ferromagnetic body. After all, energy plays a very fundamental role in all modern physics and engineering. I will examine energy from the atomic rather than macroscopic viewpoint, inasmuch as stating that the macroscopic energy is $1/4\pi \int H d\beta$ etc., does not help one particularly in understanding what is going on physically.

The story of ferro- or ferri-magnetism is essentially that of four kinds of energy. There is, to be sure, a fifth kind, associated with diamagnetic induction, but those

* Original manuscript received by the IRE, June 13, 1956. Presented at Symposium on the Microwave Properties and Applications of Ferrites, Harvard Univ., Cambridge, Mass., April 2–4, 1956.
† Harvard University, Cambridge, Mass.

interested in the phenomena of ferro- or ferri-magnetism are such big operators energetically speaking, that the work done in creating a Larmor precession is a bagatelle which can be disregarded for their purposes.

I. The Zeeman Energy

The first form of magnetic energy is that of the elementary magnets in the applied field $\boldsymbol{H}$, often called the Zeeman energy.

$$-2\beta \sum_i (\boldsymbol{H}\cdot\boldsymbol{S}_i). \tag{I}$$

Here β is the Bohr magneton, $he/4\pi mc$, associated fundamentally with the quantization of angular momentum. $\boldsymbol{H}$ is the applied field, *i.e.*, the field in the absence of the magnetic body. In this connection $\boldsymbol{H}$ is to be considered as exclusive of any demagnetizing corrections, and of any of the Weiss molecular field. If we try to modify the definition of $\boldsymbol{H}$ to include any of these other effects (as is, however, conveniently done for some purposes), we immediately run into involved questions of redundancy or double-entry bookkeeping as far as energy storage is concerned. $\boldsymbol{S}_i$ is the spin angular momentum vector of atom i, measured in multiples of the quantum unit $h/2\pi$. The factor 2 in (I) is the well-known gyromagnetic anomaly connected with the spin. It is also well known that most of the magnetism in ferro or ferrimagnetic materials arises from the spin of the d electrons. Actually there are secondary contributions arising from the orbital angular momentum, which should be added to (I). A perturbation calculation shows that the corrections for the effects of orbital angular momentum are, in first approximation, equivalent to replacing the factor 2 in (I) by a factor g which is nearly, but not exactly 2. Then (I) is replaced by

$$-g\beta \sum_i (\boldsymbol{H}\cdot\boldsymbol{S}_i). \tag{I'}$$

The factor g thus inserted is called the spectroscopic splitting factor, and is not the same as the gyromagnetic ratio, which, following Kittel we shall denote by the letter g' to distinguish it from g. Experiments on magnetization by rotation, or rotation by magnetization, are concerned with g', and those in ferromagnetic resonance measure g. Kittel [2] and the writer [3] showed that according to fairly simple perturbation theory, the deviations of g and g' from 2 should be equal and opposite. It was indeed found experimentally that whereas g' was less than 2, and g greater, the deviations of g from 2 were quite appreciably greater than those of g'. However, workers at the University of California have found that when the wavelength in ferromagnetic resonance is reduced sufficiently, as in say the $K/2$ band, the quantities $2-g'$ and $g-2$ approach equality. Kittel [4] has shown that the failure of the relation $g-2=2-g'$ to hold at longer wavelengths is to be ascribed to a rather complicated blending effect between the g factors of the $4s$ conduction and the more tightly bound $3d$ electrons.

II. Classical Electromagnetic Dipolar Energy

The next energy I will write down is the usual electromagnetic energy of interaction between elementary magnets, which is a purely classical effect and dates back to the 19th century. It is the mutual potential of dipoles, which all textbooks on electromagnetism show to be (in our quantum-mechanical notation)

$$\sum_{j>i} \frac{g^2\beta^2}{r_{ij}^3}\left[\boldsymbol{S}_i\cdot\boldsymbol{S}_j - 3\frac{(\boldsymbol{r}_{ij}\cdot\boldsymbol{S}_i)(\boldsymbol{r}_{ij}\cdot\boldsymbol{S}_j)}{r_{ij}^2}\right]. \tag{II}$$

For many years physicists thought or hoped that this interaction energy would supply the coupling which makes elementary magnets tend to be parallel in a ferromagnetic material. However, the resulting coupling is too small by a factor 10,000 or so. What is more, the total energy is dependent on the shape of the specimen, *i.e.*, on how it is cut. The reason for this is easy to see. The potential (II) varies as the inverse cube of the distance, and so is a long-range force. In fact, one at first is apt to conclude that the dipolar energy per atom, *i.e.*,

$$\frac{1}{2}\sum_j \frac{g^2\beta^2}{r_{ij}^3}\left[\boldsymbol{S}_i\cdot\boldsymbol{S}_j - 3\frac{(\boldsymbol{r}_{ij}\cdot\boldsymbol{S}_i)(\boldsymbol{r}_{ij}\cdot\boldsymbol{S}_j)}{r_{ij}^2}\right]$$

involves a radial integral of the form $\int r_{ij}^{-1}dr_{ij}$ when one replaces the sum $\sum_j$ by an integral $\iiint \cdots r_{ij}^2 \sin\theta\, dr d\theta d\phi$. Such an integral clearly diverges as r goes to infinity. Those who jump at snap conclusions might decide that the energy per unit volume in a ferromagnetic material would increase without limit if the size is made arbitrarily large—a behavior somewhat reminiscent of critical size phenomena in atomic bombs. Actually, one must consider rather carefully the effect of the angular or bracketed factor in (II), which is essentially $1-3\cos^2\theta$ for parallel magnets. This factor averages to zero for a sphere, and as a result the catastrophe at infinity is avoided, but shape dependence still remains. Even if the elementary magnets are parallel, the total energy of interaction, which involves calculating the boundary-dependent double sum in (II), explicitly, cannot be expressed in any tractable form except for ellipsoidally cut specimens. For simplicity we will consider ellipsoids of revolution magnetized parallel to the axis of symmetry. Then the classical dipolar energy per unit volume takes the form

$$\frac{1}{2}\left(D=\frac{4\pi}{3}\right)M^2 \tag{II'}$$

where M is the intensity of magnetization per unit volume, and D is the so-called demagnetizing factor, which is 0 for a very long or cigar shaped ellipsoid, $4\pi/3$ for a sphere, and 4π for a very flat ellipsoid or disk. The addi-

tive constant $-4\pi/3$ in (II′) is a manifestation of the well-known Lorentz local or cavity field. The fact that (II′) is independent of volume shows that there is no critical size phenomenon, but the D factor gives a dependence on shape. This dependence has a simple physical explanation. From the standpoint of classical electromagnetic theory, elementary magnets like to be parallel when they are arranged *end-on*, but not when they are placed sidewise. Hence the energy is most negative, most favorable, for an elongated specimen, magnetized longitudinally, whereas it is positive, or unfavorable, when all magnets are constrained to be in the same direction perpendicular to the surface of a disk. Another way of saying the same thing is that parallel elementary magnets like to set themselves parallel rather than perpendicular to a surface (*cf.* Fig. 1) for then on the whole one magnet sees fewer magnets sidewise than end-on. The more conventional way of explaining why the energy is then low is that there are no poles on the surface out of which lines of force, associated with positive energy, can emanate, but the microscopic picture in terms of the interaction potential between elementary dipoles is, in my opinion, even more physical.

Fig. 1—Unfavorable dipolar energy. Favorable dipolar energy.

III. Exchange Energy

Since the classical electromagnetic coupling between elementary magnets is far too small to be adequate, the origin of ferromagnetism was shrouded in mystery until well along in the twentieth century. Finally, in 1928, Heisenberg [5] showed that the exchange effect provided the requisite interaction between the atomic spins. Unfortunately, exchange coupling is a purely quantum-mechanical phenomenon which has no classical analog, and so cannot be explained in elementary or intuitive terms. Heisenberg, in his original paper, used the language of group theory, but Dirac a year or two later showed that the exchange coupling could be expressed analytically in terms of his vector model. Dirac [6] proved that, with certain simplifying assumptions, the exchange effects are equivalent to a potential of the form

$$-2\sum_{j>i} J_{ij}(\mathbf{S}_i\cdot\mathbf{S}_j) \qquad \text{(III)}$$

insofar as the dependence of energy on spin-alignment is concerned. This is our third form of magnetic energy —I should really say effectively magnetic, for this interaction is not really magnetic in origin; it is rather an electrostatic effect associated with the dependence of the overlapping of orbital wave functions on the type of symmetry in the representation of the permutation group. The spin is involved only because it enters as essentially an *indicator* of the type of orbital symmetry, but, be this as it may, the result is the long-sought-for interaction between spins. The coupling (III) is the most relevant, in fact the predominant interaction for all problems of ferromagnetism. The factor J_{ij} involved in (III) is the quantum mechanical exchange integral connecting atoms i and j, which we need not discuss in detail, and which we can here regard as a constant produced rather magically by quantum mechanics. For simplicity we disregard the complications associated with the degeneracy of d electrons, and assume that the exchange integral is the same for all electrons in a given atom not in closed shells.

The Heisenberg exchange mechanism gives us the desired ferromagnetic coupling provided that the exchange integral J_{ij} is positive and sufficiently large, a subject to which we will return later.

The exchange integral usually decreases quite rapidly with distance, and to give further analytical simplicity, it is customary to assume that the exchange integral has a nonvanishing value only between nearest neighbors, in which case (III) simplifies further to

$$-2J\sum_{\text{neighbors}} \mathbf{S}_i\cdot\mathbf{S}_j. \qquad \text{(III′)}$$

There is one property of the exchange interaction (III) or (III′) which we cannot emphasize too strongly, namely that it is a purely isotropic interaction, *i.e.*, depends only on the relative angle between the two spins. This is obviously true, since the scalar product $\mathbf{S}_i\cdot\mathbf{S}_j$ of two vectors is invariant under a rotation. On the other hand, the classical dipolar interaction (II) involves the angles between the spin vectors $\mathbf{S}_i$, $\mathbf{S}_j$ and a given direction $\mathbf{r}_{ij}$, and so is not spatially invariant.

The conventional Heisenberg exchange effect, though robbing ferromagnetism of its main mystery, is hence incapable of explaining the phenomenon of ferromagnetic anisotropy, *i.e.*, the fact that most ferromagnetic materials are more easily magnetized along certain directions than others. Furthermore, the classical interaction (II) is inadequate, as we have already seen, being both too small and shape dependent.

IV. Anisotropic Exchange —Pseudodipolar and Pseudoquadrupolar Energy

It is now generally recognized that the explanation of ferromagnetic anisotropy is to be found in what is called *anisotropic exchange*. The statement that the coupling between spins has the scalar invariant form (III) is true only as long as the spin-orbit interaction is neglected. Actually, spin-orbit effects cause appreciable deviations from (III). It is not appropriate for us here to describe the rather involved perturbation calculations that lead to this conclusion. [7]. The essential physical reason that anisotropy results is that orbital wave functions are not spherically symmetric, especially in virtual excited states, and at the same time, the spin-orbit coupling makes the spin feel the anisotropy of

the orbital charge distribution. Expressed differently, the effective angular momentum vector is not 100 per cent spin, but rather arises to a small extent from asymmetrical orbital whirling charge distributions.

The anisotropic exchange of lowest order has what is usually called a pseudodipolar structure, *i.e.*, a dependence on angle similar to (II), but with a different constant of proportionality, so that one has coupling of the form

$$\sum_{j>i} C_{ij}(r_{ij})\left[\mathbf{S}_i\cdot\mathbf{S}_j - 3\frac{(\mathbf{S}_i\cdot\mathbf{r}_{ij})(\mathbf{S}_j\cdot\mathbf{r}_{ij})}{r_{ij}^2}\right]. \qquad \text{(IV)}$$

The factor of proportionality C_{ij} in (IV) differs from that of $g^2\beta^2/r_{ij}^3$ involved in (II) in two notable respects: (1) it is larger at small interatomic distance; (2) it dies out rapidly, essentially exponentially with distance. Thus anisotropic exchange, unlike classical electromagnetic coupling, is a short-range affair.

If the material is noncubic, the pseudodipolar coupling (IV) undoubtedly is the origin of most of the energy of anisotropy. In fact, in a crystal not of cubic symmetry, the most important part of the energy of anisotropy has macroscopically the form

$$A\alpha_1^2 + B\alpha_2^2 + C\alpha_3^2, \qquad (\text{IV}_{\text{noncubic}})$$

with $A = B$ if there is axial symmetry. Here α_1, α_2, α_3 are the direction cosines connecting the directions of magnetization with the principal crystal axes. This is just the type of angular dependence furnished by (IV) in the first approximation of a perturbation calculation in which (IV) is regarded as small compared with (III). On the other hand, in a cubic crystal, the anisotropy energy of lowest order is of the form

$$D(\alpha_1^2\alpha_3^2 + \alpha_1^2\alpha_2^2 + \alpha_2^2\alpha_3^2). \qquad (\text{IV}_{\text{cubic}})$$

In the first approximation, the pseudodipolar potential (IV) is incapable of giving this kind of anisotropy, for it is a quadratic affair as regards the way the direction cosines are involved, and any quadratic form becomes spherically symmetric when cubic symmetry is imposed. However, cubic anisotropy creeps in when one makes a perturbation development in the ratio C_{ij}/J_{ij} and considers the second order effect of (IV), because a quadratic form raised to the second power becomes essentially biquadratic in structure. Another way of obtaining cubic anisotropy is to include pseudoquadrupolar interaction of the type

$$\sum_{j>i} D_{ij}(r_{ij})(\mathbf{S}_i\cdot\mathbf{r}_{ij})^2(\mathbf{S}_j\mathbf{r}_{ij})^2 \qquad \text{(IV}')$$

which results if the effects of spin-orbit interaction are carried to a higher stage of perturbation calculation than in obtaining (IV). Either the first order effect of (IV′), or the second order effect of (IV) is capable of yielding anisotropy of the structure (IV_{cubic}) in a cubic crystal. However, it should be noted that quadrupolar forces are possible only if the spin of each atom is greater than $\frac{1}{2}$, and it is not at all clear that this condition is fulfilled in ferromagnetic materials with rather low atomic spin such as nickel.

Orders of Magnitude

The whole problem of ferro- or ferri-magnetism is simply to determine which spin configuration gives the lowest free energy, in the thermodynamic sense, when one includes simultaneously the four energies I, II, III, and IV (or IV′). Before we discuss this program in detail, it is instructive to compare the different orders of magnitude of the various types of energy I, II, III, and IV. If, following spectroscopists we take the cm^{-1} as the unit of energy, and normalize results so that they relate to energy per ferromagnetic atom, the various energies have roughly the following orders of magnitude

$$\text{I} \sim 10^{-4}H, \quad \text{II} \sim 0.1, \quad \text{III} \sim 10^3, \quad \text{IV} \sim 10\ \text{cm}^{-1}.$$

In estimating (II), it is assumed that the material has approximately its maximum saturation achieved at low temperatures. The estimate (IV) applies only to noncubic crystals. With cubic symmetry the relevant estimate in place of (IV) is

$$\text{IV}' \sim 0.1 \quad \text{to} \quad 1\ \text{cm}^{-1}.$$

In this connection, (IV′) is to be interpreted rather symbolically as expressing the first order effect of the true pseudoquadrupolar interaction (IV′), or the second order effect of the pseudodipolar coupling (IV), as it is not always known which of the two effects is the more important.

The reader may ask whether the estimates in the preceding paragraph are obtained empirically from experiment or from pure theory. As regards (I) and (II), the constants are known theoretically, so that the estimate is straightforward. The unequivocal determination of (III), (IV), or (IV′) from theory would involve calculation of prohibitively difficult integrals, and detailed knowledge of atomic wave functions in the solid state. The estimates (III), (IV), (IV′) are therefore based on the empirical determination from experiment of the sizes of constants which are required to give the observed behavior. However, the magnitudes thus obtained are also in accord with the best theoretical estimates that one can make.

The Molecular Field and Other Approximations to the Exchange Energy

The next question is, of course, to what extent the theory can describe, qualitatively or quantitatively, the observed magnetic phenomena, helping us to understand what goes on, and perhaps even to predict certain experimental facts before they are observed. It is immediately clear that since one is dealing with an eigenvalue problem or secular equation of degree 10^{23} or so, one cannot hope to solve the quantum-mechanical wave equations exactly, and must instead resort to approximations. The first simplification is pretty clearly to

consider the largest interaction without the others, or in other words to study the energetic and alignment behavior which results when exchange coupling alone is present, assuming that the exchange integral is positive and so favorable to ferromagnetic alignment. For this problem, the most straightforward and intuitive approach is that which was developed by Weiss some fifty years ago [8], almost two decades before the advent of quantum mechanics. The theoretical physicist with an engineering intuition approaching any coupling problem is apt to inquire whether the action of the other atoms on a given atom i can perchance be represented at least approximately by an effective field. Under such circumstances (III′) is replaced by an expression of the form

$$-g\beta \sum_i (\boldsymbol{S}_i \cdot \boldsymbol{H}_{eff})$$

in obvious analogy to (I) or (I′). Weiss assumed that the effective field was linear in the magnetization M. This was an *ad hoc* assumption in Weiss' day, which was inserted to make ferromagnetism a cooperative alignment phenomenon. Quantum mechanics, however, furnishes a real foundation for this assumption of linearity, since (III) or (III′) shows that the mean exchange potential coupling a spin i to its surroundings is proportional to the expectation value of the spin angular momentum of neighboring atoms.

It is well to elaborate this point a little as follows. The instantaneous exchange potential acting on a given spin $\boldsymbol{S}_i$ is by (III′)

$$V = -2J\boldsymbol{S}_i \cdot \sum_i \boldsymbol{S}_j \tag{1}$$

the sum being over the neighbors of i. The various spins $\boldsymbol{S}_j$ involved in this equation will fluctuate in their orientations with time, but one is tempted to neglect the fluctuations, and replace the instantaneous positions of the nearby magnets by their average positions. If it is assumed that on the average all atoms are alike in their behavior, we then have

$$V = -2zJ\boldsymbol{S}_i \cdot \langle \boldsymbol{S}_j \rangle_{AV} \tag{2}$$

where z is the number of neighbors possessed by a given atom. If the material is magnetized along the z direction, one can write

$$\langle S_{jx} \rangle_{AV} = \langle S_{jy} \rangle_{AV} = 0, \qquad \langle S_{jz} \rangle_{AV} = M/Ng\beta$$

where M is the magnetization per unit volume, and N is the number of atoms/cc. If μ_i denotes the magnetic moment $g\beta\boldsymbol{S}_i$ of atom i, the expression (2) then acquires precisely the form

$$-\mu_i qM$$

assumed by Weiss. The constant q of this so-called molecular field, which to Weiss was a purely *ad hoc* affair, is now seen to have the significance $q = 2Jz/Ng^2\beta^2$ in terms of the exchange integral J.

The mean alignment of an atom is obtained by assuming that the various quantum allowed orientations $S_{z_j} = -S, -(S-1), \cdots, S$ are weighted statistically according to their Boltzmann factors. Hence we obtain

$$M = Ng\beta\langle S_{z_i} \rangle_{AV} = Ng\beta S_S\left(\frac{g\beta qM}{kT} S\right) \tag{3}$$

where B_s is the so-called Brillouin function given by

$$B_S(xS) = \frac{1}{S} \frac{Se^{Sx} + (S-1)e^{(S-1)x} + \cdots + (-S)e^{-Sx}}{e^{Sx} + e^{(S-1)x} + \cdots + e^{-Sx}}.$$

Weiss, living in a classical era, of course had a continuous rather than discrete distribution of orientations, and so a Langevin rather than a Brillouin function, but except for this difference he obtained a formula of the structure (3). It is indeed a tribute to the genius of Weiss that he was thus able to develop so fine a phenomenological theory. The first derivation of (3) on the basis of the exchange mechanism of quantum mechanics was given by Heisenberg [5] in 1928. He did not use the device of effective fields, as we have done following Stoner [9]. Rather he obtained (3) in a more abstruse but rigorous fashion by assuming that all quantum-mechanical states with the same absolute magnitude for the resultant spin of the entire crystal have the same energy. Actually this assumption is not really true, but most attempts to correct this error make matters worse rather than better.

The relation (3) is a transcendental equation which must be solved for M. The resulting graphs of the magnetization as a function of temperature are shown in Fig. 2, along with experimental points for a variety of materials. This is a rather old figure, going back over twenty years, but not much has changed in the meantime as regards the comparison between theory and experiment for the basic ferromagnetic elements Fe, Ni, Co. Since that time of course a wealth of data has been amassed on other compounds, such as the ferrites, but no new basic light as to the degree of validity of the molecular field model is shed by including them. In comparing the theory and experiment, it is tacitly assumed that the magnetization is parallel to the applied field, in other words that the latter is large enough for so-called saturation, a question to which we will return later. It is seen that on the whole, the simple molecular field theory reproduces remarkably well the trend of the saturation magnetization with temperature. A word should be said as to the scale of ordinates and abscissa in Fig. 2—so-called reduced units are used—*i.e.*, the magnetization is measured relative to its ideal maximum M_0 achieved at $T = 0$, and the temperature in terms of the Curie point as the unit. With such units there is a law of corresponding states that for given spin quantum number S per atom, the curve should be the same for all materials. The values of the spin which work best are rather low, as is to be expected since the atomic configurations involved are almost complete shells.

In one respect there is, however, a discrepancy between theory and experiment; when the temperature is near to the absolute zero the deviations of the magnetization from the absolute value are considerably larger than given by the molecular field theory. The latter predicts that these deviations should have a temperature dependence of the exponential form $Ae^{-B/T}$ in this region whereas actually a power law AT^C with $C\sim 3/2$ works much better.

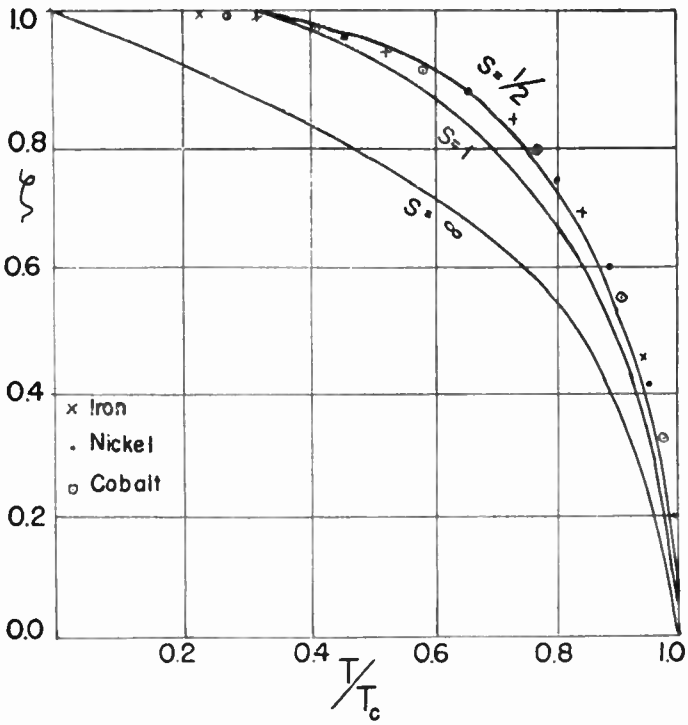

Fig. 2—Reduced saturation magnetization as a function of reduced temperature.

At very low temperatures, however, there is a better way of calculating the magnetization than that provided by the quantum mechanical version of the Weiss molecular field. This better method is the so-called spin wave theory, first devised by Bloch. We shall not go into the details of this theory, but simply mention that for very low temperatures, the relevant eigenvalues of the energy can be calculated almost exactly.

The most famous and important result of the spin wave theory is that the magnetization should approach its maximum value M_0 achieved at $T=0$ in the fashion

$$M_0 - M = AT^{3/2}$$

where a is a constant depending on the lattice-geometry (simple cubic, body-centered cubic, etc.). This prediction is confirmed pretty well by experiment, but the data are not accurate enough to settle definitely that the exponent is 3/2, rather than say 7/4 or 2. The experimental difficulties are not primarily cryogenic in character. For purposes of magnetic experimentation the unit of temperature is essentially the Curie point, which is quite high ($\sim 10^3\,°K$) in most magnetic materials, including the ferrites. Thus temperatures which we class as very low are not exceedingly small by ordinary standards. If measurements are available down to liquid air temperatures, the extrapolation to $T=0$ is relatively short.

There is another temperature region besides that near the absolute zero where there is a better method of calculation than that provided by the molecular field model. This other region is that above the Curie point. Here the improved method of approximation is the so-called Bethe-Peirls-Weiss one [10], which is essentially a scheme wherein the interactions inside a cluster are treated rigorously, and those with atoms outside of it by means of a molecular field scheme. The B-P-W theory predicts that the reciprocal of the susceptibility should be approximately a linear function of the temperature, but with rather different constants than furnished by the simple molecular field theory. In my opinion, the formula $1/\chi = a + bT$ of the molecular field theory for the susceptibility χ above the Curie point is usually taken more literally than it should be, and attempts to deduce information concerning magneton numbers, etc. from this formula should be discounted, inasmuch as higher approximations will cause curvature in the graphs of $1/\chi$ vs T. The straight line which gives the best approximation to the actual curve may be quite different from the first term of the development.

Theoretical Calculation of the Energy of Anisotropy IV

After these attempts, in one way or another, to calculate the effect of the main, or exchange part of the energy, the next thing is, of course, to include the energy of anisotropy. This part of the problem we shall not discuss in any detail. As we have already indicated, the anisotropic exchange mechanisms of quantum mechanics give the proper directional dependence of the energy of anisotropy—not too surprising, for agreement is more or less dictated by the crystal structure. A more crucial test of the theory is whether it gives the proper dependence of the anisotropy on temperature. The theory has been fairly successful for iron. Here the pseudoquadrupolar model gives under certain conditions an anisotropy varying as the 10th power of the ratio of the magnetization to that at $T=0$, in fairly good accord with experiment [11]. In the case of nickel, no explanation has yet been found for the more rapid variation, approximately as the 20th power of this ratio.

Domain Structure Caused by the Classical Dipolar Interaction II

The interactions which we have included so far are able to explain the existence of preferential directions of magnetization, but they are completely inadequate to describe the hysteresis and other phenomena associated with aligning the magnetization parallel to the applied field. All processes would be reversible until the elementary magnets are all rotated past a common

shoulder associated with the direction of hardest magnetization, and this would require a large field whose Zeeman energy was comparable with the energy of anisotropy, whereas actually irreversible processes are found even in very weak fields. The difficulty is that with the mechanisms III and IV alone present, (along with the energy due to the applied field) there is no reason why the average positions of all the elementary magnets should not be parallel throughout the entire crystal. Actually we need some mechanism which will provide small domains of magnetization; the clicks in the Barkhausen effect are, for instance, signals that a small domain is turning over—if we had one big magnetic domain for the entire crystal, the Barkhausen effect would not be a succession of clicks, but rather one big bang wherein the entire crystal goes *over the top* into the direction of easy magnetization. The requisite mechanism is, however, provided by the old-fashioned nineteenth century electromagnetic interaction between dipoles. We have already pointed out that this is a long range coupling, and that as a result it is energetically unfavorable for dipoles to be aligned perpendicularly to the bounding surfaces of the specimen. In consequence, a lower energy is achieved when the direction of magnetization is different in different small regions, called domains.

We shall not go into the question of the particular domain sizes and geometries which lead to the lowest energies. This subject was first properly investigated by Landau and Lifshitz [12]. A typical domain structure for a uniaxial crystal is shown in Fig. 3. Notice that the magnets near the surface are parallel to it.

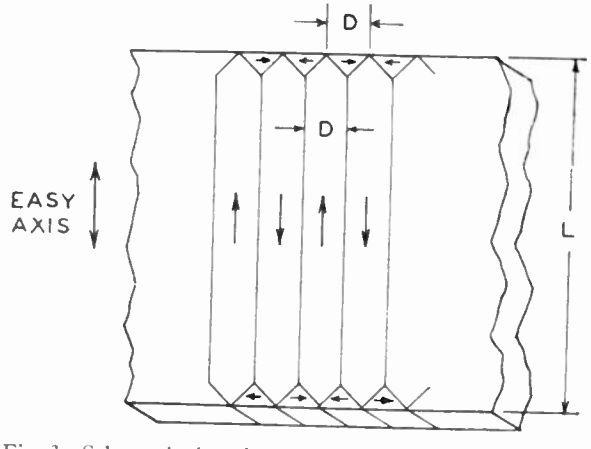

Fig. 3—Schematic domain structure for a uniaxial crystal.

The whole point of the argument is that an arrangement such as that shown in Fig. 3 gives a lower energy for the sum of the three energies II, III, and IV than does one of completely parallel alignment, for the improvement in the classical electromagnetic energy more than offsets the less favorable exchange energy III.

Most readers are, I am sure, familiar with the powder patterns obtained by Bitter, Elmore, and Williams which provide photographic evidence of the existence

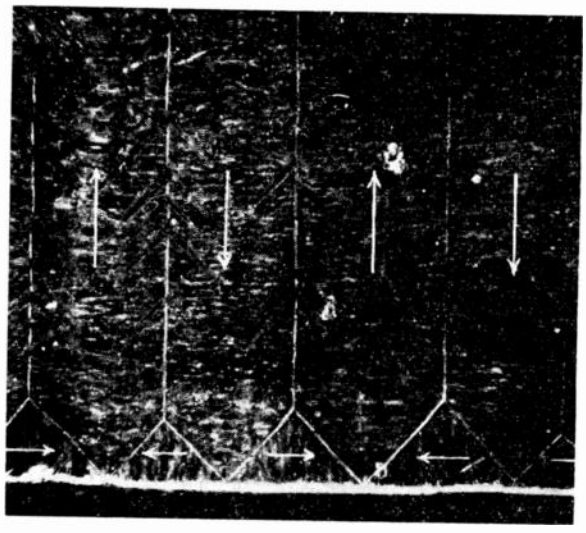

Fig. 4—Powder pattern (retouched) obtained by Williams in Si-Fe crystals, corresponding to the situation sketched schematically in Fig. 3.

of the elementary domains. Fig. 4 shows the observed pattern corresponding to the prediction sketched in Fig. 3. The trick used to obtain the powder patterns is to place a colloidal suspension of finely divided ferromagnetic material on the surface of the ferromagnetic specimen under study. The colloidal particles settle on and so delineate the domain boundaries, where they are attracted by the very strong local magnetic fields.

It may at first sight seem that the domain structure should disappear if the specimen is large enough, for it only takes place in order to reduce the dipolar energy associated with the bounding surfaces. However, because the dipolar interaction dies down only as $1/r^3$, its repercussions even at the center cannot be eliminated by increasing the size of the sample.

The domain structure seems to account quite well for the various phenomena of hysteresis, remanence, etc. [13]. When an applied field shifts the direction of magnetization, this readjustment can be achieved in either of the two ways shown in Fig. 5—by rotation

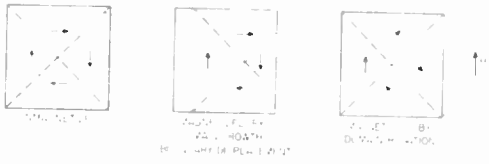

Fig. 5—Fundamental magnetization processes.

of the magnetization in a domain of given size, or by expansion of the domains wherein the magnets happen to be situated favorably, *i.e.*, more or less parallel to the field, and contraction of those domains in which the magnets are unfavorably situated. The second of these processes is usually the more important, and of course involves migration of the domain boundaries. Some readers may even have seen the Bell Telephone Laboratories' motion pictures of the migrations of these Bloch

walls. The speed of migration observed in these movies, incidentally, agrees very well with theoretical estimates [14]. The pictures, both still and moving, of the domain structure provided by the powder pattern photographs are undoubtedly one of the most spectacular developments in magnetism in the past quarter century, but it should not be forgotten that half a century ago Weiss predicted the existence of microdomains, at least in a qualitative way, from his molecular field theory. The domain properties have great technological importance. High coercivity is obtained by suppressing the possibility of boundary displacements. The suppression may be achieved by using fine powders, or as in Alnico V, by making the material heterogeneous by precipitating a second metallurgical phase. High permeability, on the other hand, is obtained by using very pure and homogeneous substances.

Except for distortions by the applied field, the magnets in each of the elementary domains are on the average aligned parallel to one of the directions of easy magnetization. There may, for example, be two such directions (inclusive of sense) in a uniaxial crystal, and six or eight in a cubic one. So far we have given the impression that the walls separating these different domains are infinitely thin. The energy of anisotropy would indeed be a minimum if the boundaries between them were infinitely sharp. However, the exchange energy is more favorable if the transition is gradual, as shown in Fig. 6. The reason for this is essentially

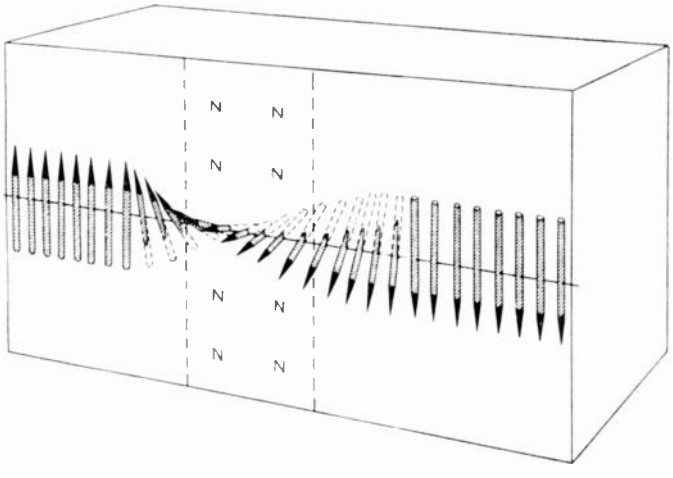

Fig. 6—The Bloch wall.

that the exchange energy H of two adjacent spins differing in orientation by a small angle $\delta\theta$ is, proportional to $-\cos\delta\theta$ and hence to $-1+\frac{1}{2}(\delta\theta)^2$ if $\delta\theta \ll 1$. If only the coupling between neighbors is important, the price paid in increased exchange energy for changing the direction of magnetization by a finite amount θ can be made as small as we please by distributing the transition over a sufficiently thick layer, for if there are n atoms in this layer the price is of the order $J\sum(\theta/n)^2 \sim J\theta^2/n$. On the other hand, in the region of transition, there will be spins, especially those near the middle of this region, for which the energy of anisotropy is unfavorable, corresponding to directions of hard magnetization. The thicker the transition layers, the greater, therefore, will be the price paid in the way of unfavorable energy of anisotropy. There is evidently an optimum thickness for the transition region, or Bloch wall, which is the best compromise between minimizing the exchange energy and that of anisotropy. We shall not discuss the details of the theoretical estimates of the thickness of the Bloch wall, and simply mention that they are in accord with experiment [13].

Difficulties in the Theory of Ferromagnetism

At this stage the reader has probably been given a quite optimistic impression that everything connected with the theory of ferromagnetism is in order. This is, however, not really the case, and the cynic can find much to deprecate. In the first place, it is not proved that the exchange integrals are positive, as assumed by Heisenberg. Instead the usual valence rules of chemistry correspond to negative exchange integrals, wherein the configuration of lowest energy is one of antiparallel rather than parallel alignment.

Another objection to the calculations of exchange energy which we have outlined is that they are based on the so-called Heisenberg model. Actually this model does not correspond to the physical situation which exists in a ferromagnetic conductor. It assumes that all atoms have the same spin, and, if we disregard the deviations of the g factor from 2, the saturation magnetization at $T=0$ should be an integral number of Bohr magnetons. (The spin quantum number can, to be sure, be either a half or whole integer, but becomes an integer in any case when multiplied by $g=2$.) In fact the saturation magnetization in nickel, for example, is about 0.6 of a Bohr magneton. This indicates that, on the average, 60 per cent of the nickel atoms have lost one of their d electrons from the closed shell d^{10} to s conduction bands. Some of the nickel atoms are thus in the configuration d^{10}, and others in d^9 or perhaps d^8, d^7. The atoms are thus not all alike in their spin quantum number, contrary to the tenets of the simple forms of the Heisenberg model. What is more, the process of electron conduction, to the extent that the d electrons participate in it, makes the various lattice sites continuously change their configuration. The actual situation is thus far more complex than contemplated in the Heisenberg model, and almost impossible to grapple with mathematically in any rigorous way. One limiting type of approximation has been introduced by Stoner [15]—the so-called collective electron model. Here the d electrons are treated as essentially completely free and in a conduction band. This model at least has the merit of something which can be calculated definitively. One of its predictions is that the saturation magnetization should approach its limiting value at $T=0$ in the fashion $M_0(1-bT^2)$

rather than $M_0(1-aT^{3/2})$ as with the Heisenberg model; the latter seems to agree rather better with experiment in this respect, though the measurements are not unequivocably decisive. In my opinion [16], however, the approximations made in the Stoner model of neglecting inter-electronic repulsions, or the energy of ionization, so that even configurations like d^8, d^7, are allowed to occur, are even more unrealistic than those of the Heisenberg model. The truth undoubtedly falls between the two, and is too difficult to calculate with very much success. Almost every theoretical solid-state physicist has his own particular dogma regarding which type of approximation is best; it is not appropriate for us here to enter into these controversies.

Néel's Theory of Ferrimagnetism

If we were to stop here, we would be ending on a note of partial defeatism, but at this juncture we can happily recall that this is a conference on ferrites rather than ferromagnetic materials in general. This limitation is most fortunate. Engineers will tell you that the good thing about ferrites is that they are nonconducting, though ferromagnetic. This is precisely the same property that makes ferrites attractive materials to the theoretical physicist. Of course from a practical standpoint, the advantage of the nonconductivity is that it reduces eddy current losses, but to the theoretical physicist the boon is that one does not have to worry about electron transport from one ion to another, and the Heisenberg model is really relevant provided one generalizes it to allow different types of lattice sites to have different spin quantum numbers. The difficulty of nonintegral Bohr magneton numbers does not arise, and what is more, the worry about the sign of the exchange integral does not enter. So far I have doubtless given the impression that a positive exchange integral is a necessary condition for ferromagnetism. This stipulation, however, is only essential as long as all atoms have the same spin. If two atoms of unlike spin are antiparallel, there can be a resultant magnetic moment, and an exchange coupling which favors an antiparallel short-range order can lead to an outstanding magnetic moment, as shown symbolically in Fig. 7. Néel [17] first proposed this type of

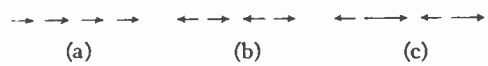

Fig. 7—(a) Ferromagnetism, (b) antiferromagnetism, and (c) ferrimagnetism.

mechanism, wherein ferromagnetism can occur even when the exchange integral has the normal negative sign associated with chemical valence rules. He also suggested the name ferrimagnetism for it, a happy suggestion as the ferrites are the prototype case, though there are doubltess other materials of this character. Ferrimagnetism is thus a special kind of ferromagnetism and differs from antiferromagnetism in that the oppositely aligned moments are of different magnitude and so do not compensate. It may seem that so far in discussing ferromagnetism in general rather than ferrimagnetism, I have been rather too general in the scope of this paper. However, the various general energetic considerations, etc., which I have presented apply perfectly well to ferrites. Also the various mathematical methods of approximation, such as the molecular field, etc., are even more appropriate in ferrites than in conventional ferromagnetic materials with positive exchange integrals. In an issue of the *Physical Review* only a few months ago, Smart [18] has extended the Bethe-Peirls-Weiss approximation to ferrites. The spin-wave theory can also be employed at low temperatures [19], with more assurance as to the physical correctness of the model used than in most ferromagnetics (but somewhat greater mathematical complexity and less numerical accuracy because of the high degree of degeneracy associated with a given value of the resultant crystalline magnetic quantum number). In particular, the saturation magnetization should still approach its maximum at $T=0$ in the characteristic spin-wave fashion $M_0(1-aT^{3/2})$. The experimental evidence on this point is not too conclusive, but a better test of the theory is that the exchange specific heat obeys the $T^{3/2}$ law also predicted by theory. This has been confirmed experimentally by Kouvel [20] in certain ferrites. The prediction cannot be tested in conductors, as there the specific heat arising from exchange coupling is masked by the much larger so-called electronic specific heat associated with conduction bands.

Some relatively simple considerations suffice to predict the effective magneton numbers or saturation magnetization at $T=0$, for the ferrites. These materials have the so-called spinel structure, wherein for the cations there is one so-called A site, and two so-called B sites per ferrite molecule Fe_3O_4. (The molecule does not really exist as a separate entity, and instead the fundamental unit is the unit cell containing eight such molecules; the factor 8, however, is irrelevant for our discussion.) In this molecule there are two ferric ions and one ferrous, and the natural assumption one would make is that the ferrous ion is located on the single A site, and the two ferric ions on the B sites. Néel, however, proposed the so-called inverse structure, wherein the A site has a ferric ion, and the B sites contain a ferric and a ferrous ion. This hypothesis is unequivocably required to explain the magnetic properties, and is not so bold as it seems, for as far back as 1931 Barth and Posnjak [21] showed from X-ray data that the inverse rather than normal structure was possessed by $MgFe_2O_4$; hence better written $Fe(MgFe)O_4$. No X-ray measurements on Fe_3O_4 regarding this point are possible, as there is no appreciable difference in scattering power between Fe^{++} and Fe^{+++}. Néel furthermore assumed that the A-B exchange interactions (*i.e.*, the coupling between atoms on A and B lattice sites) are stronger than those of the A-A or

B-B category. Furthermore, an *A* atom is surrounded by many of the *B* variety, and the geometry of the lattice is such that the spins of the atoms on the *A* sites cannot be antiparallel to those of the neighboring atoms on the *B* sites unless the *A* atoms are all mutually parallel, pointing say N., and those of the *B* atoms all pointing in the opposite direction, *e.g.*, S. The situation is illustrated schematically in Fig. 8, which also includes the antiferromagnetic ferrite $ZnFe_2O_4$ to be discussed later as an illustration of the normal spinel structure. Actually the lattices have a complicated three-dimensional geometry rather than the linear structure sketched in Fig. 8, but the division into two categories of lattice sites is preserved.

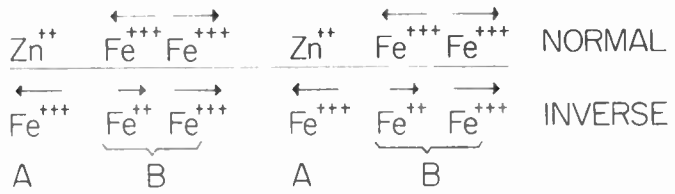

Fig. 8—Schematic illustration of magnetic alignment in normal and inverse spinels.

The spins of the Fe^{++} and Fe^{+++} ions are respectively 2 and 5/2. According to the Néel model shown in Fig. 8, the saturation magnetization per molecule of Fe_3O_4 at $T=0$ should hence be

$$g\left[\left(2+\frac{5}{2}\right)-\frac{5}{2}\right]\sim 4 \text{ Bohr magnetons.}$$

The observed value is 4.2.

The ferrites $Fe(MnFe)O_4$ and $Fe(NiFe)O_4$ differ from Fe_3O_4 in that the ferrous ion is replaced by Mn^{++} or Ni^{++}. The spin quantum numbers of the Mn^{++} and Ni^{++} ions are respectively 5/2 and 1. If in each case the inverted structure is assumed, the saturation moment at $T=0$ should be

$$g\left[\left(\frac{5}{2}+\frac{5}{2}\right)-\frac{5}{2}\right]\sim 5 \text{ Bohr magnetons for } Fe(MnFe)O_4$$

$$g\left[\left(\frac{5}{2}+1\right)-\frac{5}{2}\right]\sim 2 \text{ Bohr magnetons for } Fe(NiFe)O_4$$

The observed values are respectively 5.0 and 2.3. The discrepancies between theory and experiment, here and in Fe_3O_4, are seen to be small, and furthermore, practically disappear when allowance is made for the fact that the *g* factor of the divalent ion is slightly greater than 2.

Experiments in which varying amounts of zinc are substituted for iron in Fe_3O_4 are most interesting. The Zn^{++} ion is in an *S* state, and has no magnetic moment. It is known from *X*-ray data that $ZnFe_2O_4$ has the normal spinel structure (divalent Zn on *A* sites; trivalent Fe all on *B* sites). Hence it is natural to suppose that when a Zn ion is substituted for a Fe^{++} ion, the Fe^{+++} ion takes the place of a Fe^{++} in the *B* site, and the Zn ion occupies the *A* site. In a sample in which on the average there are *t* Zn atoms per molecule, one would expect—according to this picture—the saturation moment to be

$$g[2(1-t)+5t]\sim 4+6t.$$

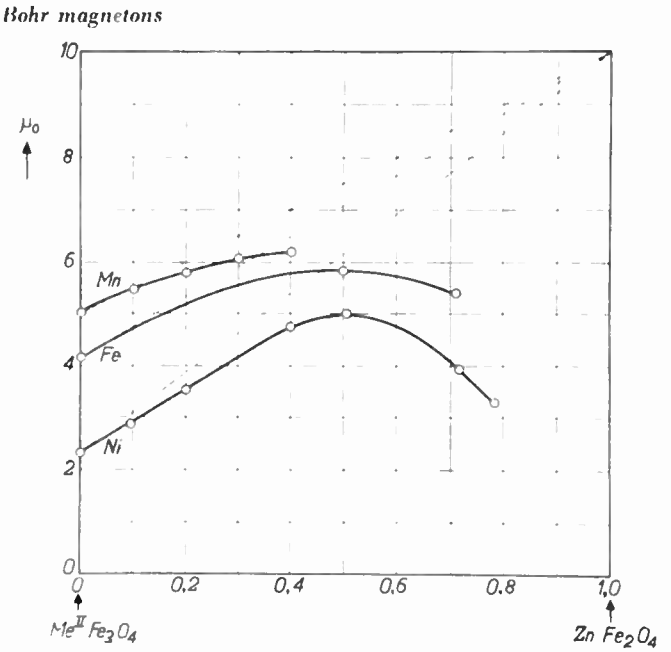

Fig. 9—Dependence of saturation moment per molecule for various ferrites on concentration of substituted zinc ions.

Fig. 9 [21] shows that this prediction is confirmed for small values of *t*. Here the dashed line gives the moment to be expected from this formula, including allowance for the deviation of the *g* factor from 2. The analogous experiments in which Zn is substituted for the divalent ion in $Fe(MnFe)O_4$ and $Fe(NiFe)O_4$ are also included. The formulas for the dashed lines are respectively $5+5t$ and $2+8t$ if $g=2$. The failure of the saturation moments to follow the theoretical straight lines except at low values of the mixture parameter *t* is readily understood. If we assume that the normal sign of the exchange integral holds throughout, the various atoms on the *B* sites would like to be antiparallel to their neighboring *B* atoms, but are constrained to take up an unfavorable parallel *B-B* alignment in order to have the predominating *A-B* bonds antiparallel. The overwhelming importance of the *A-B* bonds, however, ceases to be a factor when many of the *A* sites become filled with nonmagnetic Zn atoms, which give no exchange coupling. Ultimately, if the value of *t* is sufficiently large, a situation is reached wherein the *B* atoms prefer to be mutually antiparallel, and so antiferromagnetic, rather than parallel, in order to minimize the *B-B* rather than the weakened *A-B* exchange interaction. The zero magnetization observed experimentally when all the divalent ions are replaced by Zn is explained.

Experiments have been made by Maxwell and Pickert [23] in which ferric ions are replaced by Al^{+++} or Ga^{+++} ions (both in nonmagnetic S states). The results are shown in Fig. 10. They indicate conclusively that the

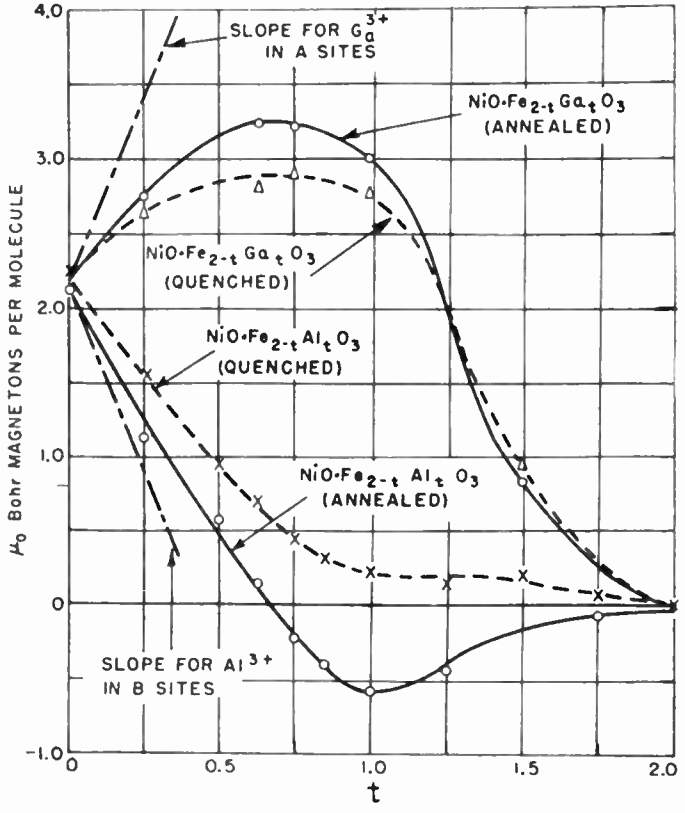

Fig. 10—Variation of μ_0 with composition for $NiO \cdot Fe_{2-t}Al_tO_3$ and $NiO \cdot Fe_{2-t}Ga_tO_3$ annealed at 1°/min, quenching carried out from 1410° C.

Al^{+++} atoms go primarily into the B sites, thus lowering the magnetization, and the Ga^{+++} into the A sites, hence raising it. The crossover from a positive to negative ordinate for a critical value of t in the case of $Fe(Al_tFe_{2-t})O_4$ is to be ascribed to the fact that for small values of t, the magnetic moment of the B sites is greater than that of the A sites, whereas for values of t greater than the critical crossover value, the reverse is true. The atoms on the A sites go over from a mutually parallel to a mutually antiparallel arrangement when most of the B sites are magnetically vacant, and so the saturation moment of $FeAl_2O_4$ is 0 rather than $(5/2)g$. The reason that the annealed specimens conform more closely to theory than do the quenched is that slow cooling is necessary in order to insure the proper equilibrium distribution between the A and B sites.

All told, the saturation moments of the various ferrites, and the analogous compounds with varying amounts of magnetically inert substituents conform very well to the predictions of theory. To the engineer, the ferrites appeal because of their combination of ferromagnetism and electric insulation. In closing I should like to stress that the ferrites are also most satisfactory and agreeable materials to the theoretical physicist as well, because they provide such a beautiful confirmation of Néel's simple and elegant concept of ferrimagnetism.

Bibliography

[1] Clogston, A. M., Suhl, H., Walker, L. R., and Anderson, P. W., "Possible Source of Line Width in Ferromagnetic Resonance." *Physical Review*, Vol. 101 (January 15, 1956), p. 903.

[2] Kittel, C. "On the Gyromagnetic Ratio and Spectroscopic Splitting Factor of Ferromagnetic Substances." *Physical Review*, Vol. 76 (September, 1949), p. 743.

[3] Van Vleck, J. H., "Concerning the Theory of Ferromagnetic Resonance Absorption." *Physical Review*, Vol. 78 (May 1, 1950), p. 272.

[4] Kittel, C., and Mitchell, A. H., "Ferromagnetic Relaxation and Gyromagnetic Anomalies in Metals." *Physical Review*, Vol. 101 (March, 1956), p. 1611.

[5] Heisenberg, W., "Zur Theorie des Ferromagnetismus." *Zeitschrift für Physik*, Vol. 49 (July, 1928), p. 619.

[6] Dirac, P. A. M., *The Principles of Quantum Mechanics*. 2d ed. Oxford, Clarendon Press, 1935, Chap. X.
Van Vleck, J. H., "The Theory of Electric and Magnetic Susceptibilities." Oxford, Clarendon Press, 1932, Chap. XII.

[7] Van Vleck, J. H., "On the Anistropy of Cubic Ferromagnetic Crystals." *Physical Review*, Vol., 52 (December, 1937), p. 1178.

[8] Weiss, P., "L'Hypothèse du Champ Moléculaire et la Propriété Ferromagnétique." *J. de Phys.* Vol. 6 (September, 1907), p. 661.

[9] Stoner, E. C. *Magnetism and Matter*. London, Methuen and Co., 1934, p. 358.

[10] Weiss, P. R., "The Application of the Bethe-Peierls Method to Ferromagnetism." *Physical Review*, Vol. 74 (November, 1948), p. 1493.

[11] Keffer, F., "Temperature Dependence of Ferromagnetic Anisotropy in Cubic Crystals." *Physical Review*, Vol. 100 (December 15, 1955), p. 1692.

[12] Landau, L., and Lifshitz, E. "On the Theory of the Dispersion of Magnetic Permeability in Ferromagnetic Bodies." *Physikalische Zeitschrift Sowjetunion*, Vol. 8 (March, 1935), p. 153.

[13] For an excellent review of domain structure and copious references on the related topics, see Kittel, C., "Physical Theory of Ferromagnetic Domains." *Reviews of Modern Physics*, Vol. 21 (October, 1949), p. 541.

[14] Akulov, N. S., and Krinchik, G. S., "Theory of Displacement of Domain Boundaries." *Doklady Akademii Nauk SSSR*, Vol. 89 (1953), NSF-tr-106, pp. 809–812.

[15] Stoner, E. C., "Collective Electron Ferromagnetism." *Proceedings of the Royal Society*, Series A, Vol. 165 (1938), p. 372. Part II, "Energy and Specific Heat." vol. 169 (1939), p. 339.

[16] Van Vleck, J. H., "The Coupling of Angular Momentum Vectors in Molecules." *Reviews of Modern Physics*, Vol. 23 (July, 1951), p. 213.

[17] Néel, L., "Propriétés Magnétiques des Ferrites; Ferrimagnétisme et Antiferromagnétisme." *Annales de Physique*, Vol. 3 (March, 1948), p. 137.

[18] Smart, J. S., "Application of the Bethe-Weiss Method to Ferrimagnetism." *Physical Review*, Vol. 101 (January 15, 1956), p. 585.

[19] Wangsness, R. K., "Sublattice Effects in Magnetic Resonance," "Magnetic Resonance in Ferrimagnetics." *Physical Review*, Vol. 91 (September, 1953), p. 1085. *Physical Review*, Vol. 93 (January, 1954), p. 68.

[20] Kouvel, J. S., and Brooks, H., *Some Spin Wave Properties of Ferrimagnetic and Antiferromagnetic Simple Cubic Crystals*. Harvard University, Cruft Laboratory, Cambridge, Mass., Technical Report No. 198 (May 20, 1954).
Kouvel, J. S., *A Spin Wave Analysis of the Magnetite Structure*. Harvard University, Cruft Laboratory, Cambridge, Mass., Technical Report No. 210 (February, 1955).
Kouvel, J. S., "Specific Heat of a Magnetite Crystal at Liquid Helium Temperatures." *Physical Review*, Vol. 102 (June 15, 1956), pp. 1489–1490.

[21] Barth, T. F., and Posnjak, E., "Spinel Structures; with and without Variate Atom Equipoints." *Zeitschrift für Kristallographie*, Vol. 82 (June, 1932), p. 325.

[22] Went, J. J., and Gorter, E. W., "The Magnetic and Electrical Properties of Ferroxcube Materials." *Phillips Technical Review*, Vol. 13 (January, 1952), p. 181.

[23] Maxwell, L. R., and Pickart, S. J., "Magnetization in Nickel Ferrite-Aluminates and Nickel Ferrite-Gallates," *Physical Review*, Vol. 92 (December, 1953), p. 1120.

Magnetic Resonance in Ferrites*

NICOLAAS BLOEMBERGEN†

Summary—**Ferromagnetic resonance in ferrites is reviewed. The concept of tensor permeability, the influence of magnetic anisotropy, demagnetizing fields, and damping mechanisms are discussed. Special consideration is given to coupled magnetic systems and the behavior in ferrites with compensation points. The general theoretical results are compared with a few illustrative examples. The behavior in polycrystalline material, *g*-value, line width, and anisotropy as a function of temperature and external magnetic field are outlined.**

Introduction

THE EQUATION of motion of a system with angular momentum J and magnetic moment M in a magnetic field H_{eff} is given by the condition that the rate of change in angular momentum is equal to the torque acting on the system.

$$\dot{J} = M \times H_{\text{eff}} \tag{1}$$

M and J are proportional to each other

$$M = \gamma J = -\frac{ge}{2mc} J \tag{2}$$

where g is called the gyromagnetic ratio. If H_{eff} consists only of a constant field which may be taken in the z-direction, a solution of (1) is a uniform precession of M around the direction of H with an angular frequency

$$\omega_0 = \gamma H_{z,\text{eff}} \tag{3}$$

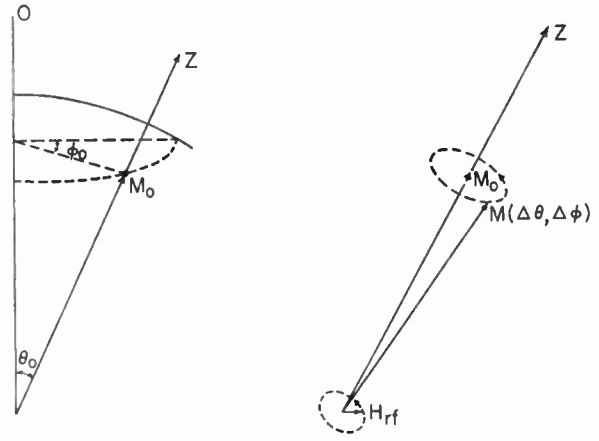

Fig. 1—Precession of a magnetic gyroscope in a static field and a small rotating magnetic field. The direction of the effective static field in general does not coincide in direction and magnitude with an applied field. The torque produced by the rotating magnetic field balances the damping torque.

This is illustrated in Fig. 1. For a free electron the numerical value of γ is 1.76×10^7 sec. oersted^{-1}. The spin precesses with a frequency 28,000 mc in a field of 10^4 oersted. In the absence of damping the magnetization would precess indefinitely with the apex angle $\Delta\theta$ which it happened to have at $t=0$. Damping will tend to align the magnetization vector with $H_{z,\text{eff}}$. The damping torque may be counteracted by a torque exerted by time-dependent magnetic field components. Consider, *e.g.*, a field which rotates with the same frequency (3) as the free precession of the magnetization. This produces a torque which is in resonance with the motion. The problem has a close resemblance to that of a driven harmonic oscillator. Two phenomenological forms of damping have been used, each having some merits.

$$\dot{M} = \gamma(M \times H) - \frac{a\gamma}{|M|} M \times (M \times H) \quad \text{(L-L)} \tag{4a}$$

$$\dot{M} = \gamma(M \times H) - \frac{M - M_0}{\tau} + \frac{|M|}{|H|} \frac{H}{\tau} \quad \text{(B)} \tag{5}$$

The L-L type damping was introduced by Landau and Lifshitz [1]. Sometimes $\lambda|M|^2$ is written instead of $\alpha\gamma/|M|$. The B-type damping was introduced by Bloch [2] and applied to ferromagnetic resonance by Bloembergen [3]. For convenience the same relaxation time τ is used in all three component equations. The x- and y-components of the last term were omitted in early work, but are of no consequence near resonance. These components take account of the physical fact that the magnetization relaxes exponentially to the equilibrium orientation given by the instantaneous magnetic field, rather than to the static direction $H_{z,\text{eff}}$. This fact has been recognized by various authors [4] and should not be overlooked when working far away from resonance or in small static fields. Otherwise negative absorption would result for magnetic fields rotating in a sense opposite to the free precession. M_0 is the magnitude of magnetization in thermal equilibrium with the lattice in the presence of the field H. For L-L damping $|M|$ is a constant of the motion and must retain the magnitude it had at the beginning of the experiment.

Take the z-axis in the direction of the static effective field. In addition to the component $H_{z,\text{eff}}$ there are three time dependent components $h_x e^{i\omega t}$ and $h_y e^{i\omega t}$ and $h_z e^{i\omega t}$. A steady state solution can be obtained in the form

$$b = \|T\| \cdot h = h + 4\pi m = \|1 + 4\pi\chi\| \cdot h \tag{6}$$

expressing a linear tensor relationship between the time varying components of magnetic induction and magnetic field. To obtain this relationship, terms quadratic in the time varying components (m_x^2, $m_x h_y$, etc.) have been neglected. This is permissible if the time varying components are small compared to the static components $h_x, h_y, h_z \ll H_{z,\text{eff}}$, and $m_x, m_y, m_z \ll M_{0z}$. In this approximation the L-L damping and B-damping become equivalent, provided one takes

* Original manuscript received by the IRE, May 21, 1956. Presented at Symposium on the Microwave Properties and Applications of Ferrites, Harvard Univ., Cambridge, Mass., April 2–4, 1956.

† Harvard Univ., Cambridge, Mass.

$$\lambda \frac{|H_z|}{|M_z|} = \alpha\gamma |H_z| = \frac{1}{\tau}.$$

Perhaps the relaxation time τ is more nearly independent of frequency and external magnetic field than the damping parameter α (or λ).[1] The complex permeability tensor is given by

$$\|T\| = \begin{Vmatrix} \mu' - j\mu'' & -j(k' - jk'') & 0 \\ +j(k' - jk'') & \mu' - j\mu'' & 0 \\ 0 & 0 & 1 \end{Vmatrix} \quad (7)$$

with

$$\mu' = 1 + 2\pi \frac{M_z}{H_z}\left[\frac{(-\omega+\omega_0)\omega_0\tau^2+1}{(-\omega_0+\omega_0)^2\tau^2+1} + \frac{(\omega+\omega_0)\omega_0\tau^2+1}{(\omega+\omega_0)^2\tau^2+1}\right] \quad (8a)$$

$$\mu'' = 2\pi \frac{M_z}{H_z}\left[\frac{\omega\tau}{(-\omega+\omega_0)^2\tau^2+1} + \frac{\omega\tau}{(\omega+\omega_0)^2\tau^2+1}\right] \quad (8b)$$

$$\kappa' = 2\pi \frac{M_z}{H_z}\left[\frac{(-\omega+\omega_0)\omega_0\tau^2+1}{(-\omega+\omega_0)^2\tau^2+1} - \frac{(\omega+\omega_0)\omega_0\tau^2+1}{(\omega+\omega_0)^2\tau^2+1}\right] \quad (8c)$$

$$\kappa'' = 2\pi \frac{M_z}{H_z}\left[\frac{\omega\tau}{-(\omega+\omega_0)^2\tau^2+1} - \frac{\omega\tau}{(\omega+\omega_0)^2\tau^2+1}\right] \quad (8d)$$

with

$$\omega_0 = \gamma H_{z,\text{eff}}. \quad (8e)$$

It can readily be verified that these equations are equivalent to complex expressions given previously by various authors [6, 7]. In the form (8) the contributions from the two normal modes of polarization (left- and right-handed circular) are clearly separated. For these circularly polarized normal modes the susceptibility tensor becomes diagonal with diagonal elements $\mu \pm \kappa$. Considerable care should be exercised in determining the sign of μ'' in the complex notation. With $\mu = \mu' - j\mu''$ and time factors $+j\omega t$ in the exponentials a positive μ'' corresponds to positive absorption. This convention is adhered to in this paper. If a negative time factor $-j\omega t$ is introduced for a mode circulating in the opposite direction, the sign of μ'' should be inverted correspondingly in that mode. Phase differences in time and in space (x- and y-direction) should be clearly distinguished at all times. Errors can be avoided by using the less elegant, but real notation of sines and cosines. In Figs. 2 and 3 the typical resonance behavior of the permeability is illustrated. The quantity μ' corresponding to dispersion and μ'' corresponding to absorption are plotted as a function of magnetic field for nickel ferrite at 24,000 mc. The off-diagonal elements are responsible for the fact that the propagation constant of the electromagnetic wave will depend on its mode of polarization. This fact has been exploited by Hogan [6] in gyrator applications. The measurement of all components of the susceptibility tensor is discussed by Artman and

[1] This damping constant λ should not be confused with the constant for the exchange field λ used later in this paper.

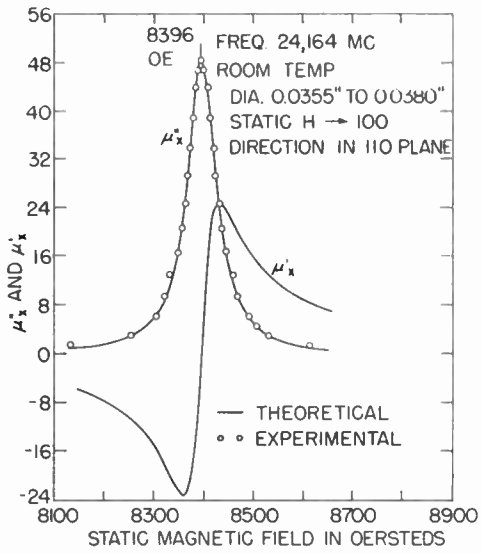

Fig. 2—The complex diagonal element of the susceptibility tensor near resonance at 24,164 mc in a small sphere of nickel ferrite. (Yager, Galt, Merritt, and Wood, [59]).

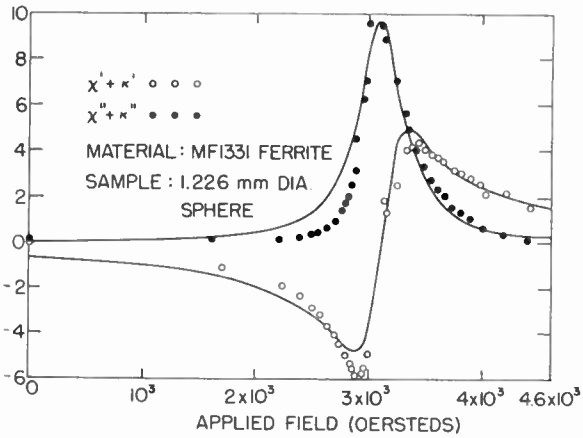

Fig. 3—The real and imaginary part of ($\mu'+\kappa'$, $\mu''+\kappa''$) of one component of the diagonalized premeability tensor near resonance. The deviations from the drawn theoretical curves are probably due to the polycrystalline nature and size of the material used (Artman and Tannenwald, [9]). The other diagonal component, for a circular polarization in the opposite sense, $\mu'-\kappa'-j(\mu''-\kappa'')$, is small and nearly constant as a function of applied field.

Tannenwald [8]. The linear relationship between $\boldsymbol{b}$ and $\boldsymbol{h}$ given by (6), (7), and (8) should be combined with Maxwell's equations and the appropriate boundary conditions for electromagnetic waves to obtain solutions in a ferromagnetic medium. The propagation constant of an infinite plane wave will depend on the direction of propagation with respect to $H_{z,\text{eff}}$, and on the mode of polarization. The method outlined above is due to Polder [5]. Numerous applications [6–10] of this procedure have been made to engineering problems involving microwaves in ferrites and ferromagnetic metals.

It is the purpose of this review to analyze which conditions are necessary for the phenomenological susceptibility tensor description to be valid, and what factors determine the magnitude of the phenomenological constants γ, $H_{z,\text{eff}}$, M_0, τ or α.

Shortly after the experimental discovery of ferromagnetic resonance by Griffiths [11], Kittel [12] pointed out that $H_{z,eff}$ in ferromagnetics may be very much different from the externally applied dc magnetic field H_0. The effective field contains contributions from demagnetizing fields, magnetic anisotropy, magnetostriction, spin exchange interactions. The situation at the end of 1950 is well described in the review papers of Kittel [13] and Van Vleck [14]. A later review stressing the experimental situation has been written by Reich [15]. In the present paper emphasis will be placed on the developments since 1950.

A basic assumption in this introduction has been that the ferromagnetic system can be described by a single macroscopic magnetization vector. This is frequently not warranted. In ferrites ferrimagnetism occurs, and it seems appropriate to introduce at least two magnetic subsystems in each domain as has been done in a description of their static magnetic properties by Néel [16]. If the external field is not high enough to wipe out a magnetic domain structure, clearly magnetization vectors should be introduced for each domain separately. The motions of magnetization of all domains are coupled together by their demagnetizing fields.

Outline of General Theory

The problem of ferromagnetic resonance consists of two separate parts. First the configuration of static equilibrium of magnetization must be determined. Then the problem of small oscillations, or rather gyrations, around this equilibrium must be considered. The static problem can already present insurmountable difficulties. In zero applied field, *e.g.*, it is equivalent to solving the complete domain structure. To make a start we shall assume that the specimen is so small or the external field so high that we can consider the single crystal as one domain. The complete Hamiltonian would consist of the interaction of all electron spins and orbits with the externally applied field H_0, the dipolar and exchange interaction between electron spins, the spin orbit coupling, and the interaction of the orbits with the crystalline field. Fortunately it can be shown [17] that for our purposes this quantum-mechanical Hamiltonian can be replaced by a classical one which should be identified with the free energy of the magnetic system. The time-averaged part of the spin-orbit coupling and crystalline fields is incorporated in the anisotropy term and by replacing the gyromagnetic ratio of a free electron spin by an effective g-value. The time-averaged dipolar interaction is incorporated in a demagnetizing field and sometimes contributes to the anisotropy. For one magnetic system the free energy can be written [18–20] in the case of cubic symmetry,[2]

$$\begin{aligned} F = &-\boldsymbol{M}\cdot\boldsymbol{H}_0 - \tfrac{1}{2}\boldsymbol{M}\cdot\|N\|\cdot\boldsymbol{M} + K_1(\alpha_1^2\alpha_2^2+\alpha_2^2\alpha_3^2+\alpha_1^2\alpha_3^2) \\ &+ K_2\alpha_1^2\alpha_2^2\alpha_3^2 + B_1(\alpha_1^2 e_{xx}+\alpha_2^2 e_{yy}+\alpha_3^2 e_{zz}) \\ &+ B_2(\alpha_1\alpha_2 e_{xy}+\alpha_2\alpha_3 e_{yz}+\alpha_1\alpha_3 e_{zz}) \\ &+ \lambda a^2\boldsymbol{M}\cdot\nabla^2\boldsymbol{M} - \lambda\boldsymbol{M}\cdot\boldsymbol{M}. \end{aligned} \tag{9}$$

The first term is the magnetic interaction with the external field, proportional to the cosine of the angle between magnetization and field. The second term is the energy of demagnetization, containing the square of the cosine of the angles between the magnetization and the principal axes of the ellipsoidal specimen. The third and fourth term are the first order and second order anisotropy; α_1, α_2 and α_3 are the direction cosines of the angle between the magnetization and the crystallographic cubic axes of the crystal. The fifth term is the magnetostrictive energy, a function of the direction of magnetization and the strain. The constants B_1 and B_2 are related to the magnetostrictive constants [20]. The last two terms represent the exchange energy. In the Weiss approximation the exchange can be represented by an effective field $\lambda\boldsymbol{M}$. The last term is very large and is responsible for the existence of ferromagnetism. Curiously enough it is of no importance in our present problem of finding the equilibrium direction of magnetization, since it does not depend on the orientation.

The free energy (9) must be minimized. In general this problem is equivalent to solving the domain structure [20]. In case of a single domain $\boldsymbol{M}$ may be assumed uniform throughout the sample, $\nabla^2\boldsymbol{M}=0$. Polar angles θ and ϕ defining the direction of $\boldsymbol{M}$ with respect to a fixed coordinate system are introduced, as illustrated in Fig. 1. All angles occurring in (9) should be expressed in terms of θ and ϕ. The equilibrium position is found by putting $\partial F/\partial\theta = \partial F/\partial\phi = 0$. Often several solutions are found and one should take one corresponding to a stable equilibrium, where F is a minimum. It is not always necessary to take the position corresponding to the absolute minimum.

After the solution to the static problem has been found, the motion of the homogeneous magnetization with small deviations $\Delta\theta$ and $\Delta\phi$ from the equilibrium position is investigated. The equations of motion become

$$j\omega\gamma^{-1}M_0\sin\theta\Delta\theta = \frac{\partial^2 F}{\partial\phi^2}\Delta\phi + \frac{\partial^2 F}{\partial\phi\partial\theta}\Delta\theta \tag{10a}$$

$$-j\omega\gamma^{-1}M_0\sin\theta\Delta\phi = \frac{\partial^2 F}{\partial\phi\partial\theta}\Delta\phi + \frac{\partial^2 F}{\partial\theta^2}\Delta\theta. \tag{10b}$$

The exponential time factor $\exp(j\omega t)$ has been dropped. The derivatives must be evaluated at the point of stable equilibrium θ_0, ϕ_0. The set of homogeneous equations for $\Delta\theta$ and $\Delta\phi$ has a solution if

$$\omega = \omega_0 = \gamma(M_0\sin\theta)^{-1}\left[\frac{\partial^2 F}{\partial\theta^2}\frac{\partial^2 F}{\partial\phi^2} - \left(\frac{\partial^2 F}{\partial\theta\partial\phi}\right)^2\right]^{1/2} \tag{11}$$

For the special case $\theta = 0$ one may need to re-examine this

[2] Most ferrites have cubic symmetry. Although the individual magnetic ions are in positions with lower symmetry, the average magnetization of a magnetic subsystem is in a crystalline field with cubic symmetry. Certain oxides (*e.g. ferroxdures* with very high anisotropy) have axial symmetry. The dominant anisotropy terms are then $K_1\alpha_3^2+K_2\alpha_3^4$.

procedure. The other sign of the square root does not give a new solution. Inspection of the solution reveals that the relative sign of $\Delta\theta$ and $\Delta\phi$ is inverted, when the sign of ω_0 is changed. The magnetization precesses always in the direction determined by the sign of γ. Looking in the direction of the effective field the spin will rotate clockwise when γ is negative. This is the case for electron spins. Eq. (11) gives the proper or resonant frequency of the system. The resonant mode is in general elliptically polarized.

The procedure outlined above was found independently by Smit [19], Suhl [21], and Zeiger [22]. It can readily be extended to two or more coupled magnetic systems. Express the free energy as a function of the orientations θ_n, ϕ_n of the nth magnetic subsystem. Find the equilibrium position by putting the first derivatives equal to zero. Set up a system of $2N$ simultaneous homogeneous equations of the $\Delta\theta_n$, $\Delta\phi_n$ of the N subsystems. The N proper frequencies, corresponding to N resonant modes are given by the roots of the equation of degree N in ω^2, formed by the characteristic determinant of the problem. Applications of this procedure will be described below.

As in the introductory section, damping terms and the radio-frequency driving field must be added to calculate the permeability tensor. The addition of the driving field to (10) will lead to inhomogeneous equations, and M_θ and M_ϕ can be solved in terms of $h_x = h_\theta$ and $h_y = h_\phi$. Since the problem in general has no longer axial symmetry around the direction of M_0, the permeability tensor will not in general have the symmetrical form (7). If the z-axis is chosen in the direction of the magnetization, the last row and column will still be the same as in (7). For two or more magnetic subsystems, with different orientations of M_0 the susceptibility tensors should be referred to one coordinate system and then added. This will give rise to a permeability tensor of the most general form. In a polycrystalline material one should take an appropriate average over all domains occurring in the specimen. An effective permeability tensor for the polycrystalline specimen can be defined which has of course the symmetry properties of (7). Such averaging procedures have been carried out theoretically by Park [23].

The combination of the susceptibility tensor relation, Maxwell's equation, and the boundary conditions determine the solution of the electromagnetic waves in the material. When the shape of the specimen is ellipsoidal and its size small compared to the wavelength in the interior, the problem is reduced to a magnetostatic one. The rf field inside the body $\boldsymbol{h}_{rf}$ may be replaced by $\boldsymbol{H}_{rf} - \|N\| \cdot \boldsymbol{m}$ where $\boldsymbol{H}_{rf}$ is the exterior rf field and $\|N\|$ the demagnetization tensor. The over-all resonant frequency of the specimen depends sensitively on its shape through the demagnetizing factors. The field acting on the magnetic moment is strictly not the same as the interior field $\boldsymbol{h}$ occurring in Maxwell's equations. One should make a spherical Lorentz cavity around the spin in question and add a Lorentz field $-(4\pi/3)\boldsymbol{M}$. The addition of this field does not change the static problem, as the static torque $4\pi/3\boldsymbol{M}\times\boldsymbol{M}=0$. The equilibrium direction of M_0 is the same. The dynamical problem of gyrations around this equilibrium is not changed either. Using $\boldsymbol{m}$ for the components of the rf magnetization one has an additional torque $-(4\pi/3)(\boldsymbol{m}+\boldsymbol{M})\times(\boldsymbol{m}+\boldsymbol{M})=0$.

It also follows that for a small sphere the relation between the magnetization and the external field is the same as the relation between the magnetization and the internal field in a body of arbitrary shape [8], [24]. It is useful to introduce an effective permeability tensor to denote the linear relationship between the magnetization and the externally applied rf field $\boldsymbol{H}_{rf}$ outside the small ellipsoid. The effective permeability may be obtained from the intrinsic permeability given by (6), (7) and (8), by the relation

$$\boldsymbol{H}_{rf} = \boldsymbol{h} - \|N\| \cdot \boldsymbol{m}$$

For a small sphere the intrinsic and effective permeability are the same.

Considerable simplification of the general theory results further, if the direction of magnetization (the z-axis) coincides with a principal axis of a small ellipsoidal specimen and lies with the external magnetic dc field in a plane of crystal symmetry, $\partial^2 F/\partial\theta\partial\phi = 0$. The influence of the magnetic anisotropy can then be described by effective demagnetization factors N_x', N_y', N_z' which should then be added to the geometrical factors N_x, N_y, N_z. The effective resonance frequency under these conditions becomes [12]

$$\omega_0 = [\{H_{0z} + (N_x + N_x' - N_z - N_z')M_{0z}\} \cdot \{H_{0z} + (N_y' + N_z + - N_z - N_z')M_{0z}\}]^{1/2}. \quad (13)$$

For a cubic crystal with the magnetization in the (011) plane and making an angle θ with the 100 cubic axis the anisotropy demagnetizing factors are [25, 26]

$$N_x' = (2 - \sin^2\theta - 3\sin^2 2\theta)\frac{K_1}{M_0^2} + \frac{1}{2}\sin^2\theta(6\cos^4\theta - 11\sin^2\theta\cos^2\theta + \sin^4\theta)\frac{K_2}{M_0^2} \quad (14a)$$

$$N_y' = 2\left(1 - 2\sin^2\theta - \frac{3}{8}\sin^2 2\theta\right)\frac{K_1}{M_0^2} - \frac{1}{2}\sin^2\theta\cos^2\theta(3\cos^2\theta + 2)\frac{K_2}{M_0^2} \quad (14b)$$

$$N_z' = 0.$$

In noncubic crystals the Lorentz field inside the cavity is not $-(4\pi/3)M$. The effect of this Lorentz field is incorporated in the term of the magnetic anisotropy. Fig. 4 shows the variation of resonant absorption with orientation in a single crystal of MnZn-ferrite.

In should be mentioned that all solutions given here correspond to a uniform magnetization of the specimen, both dc and rf-wise. Many other modes with a non-

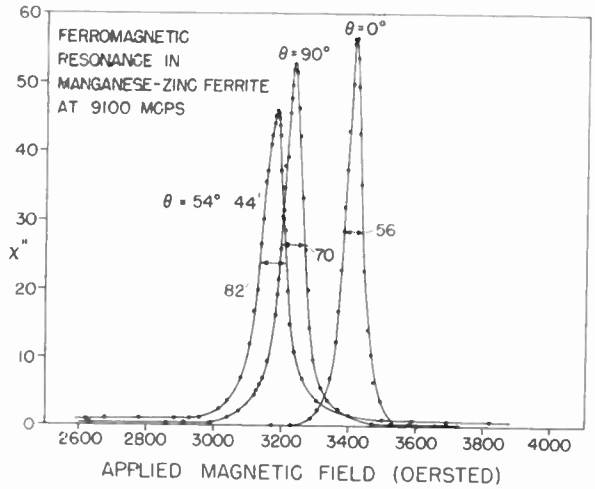

Fig. 4—Variation of resonant absorption with crystallographic orientation in MnZn-ferrite at room temperature at 9100 mc. (P. E. Tannenwald, [60]).

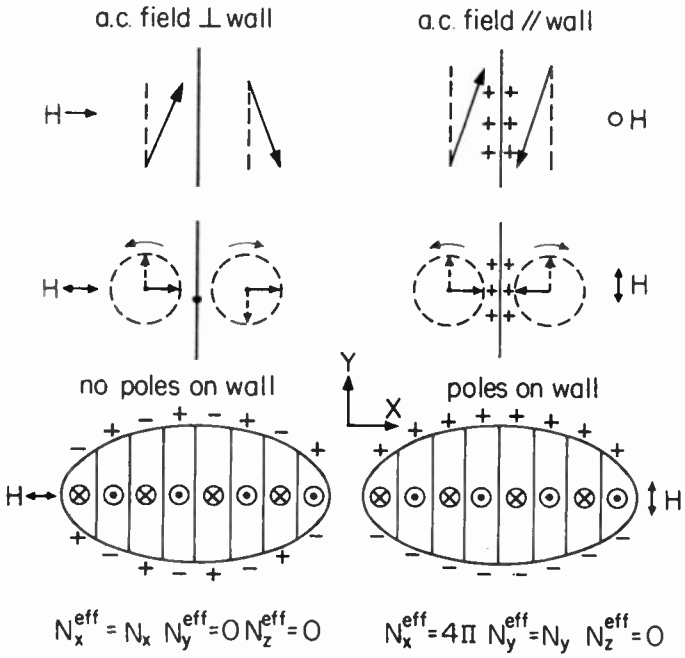

Fig. 5—Effect of Weiss domain structure on ferromagnetic resonance conditions. Two resonance modes occur. The upper figures are parallel to the magnetization and perpendicular to the wall. The figures in the middle are perpendicular to both the magnetizations and the wall. The figures at the bottom are in the same position, but drawn for the entire ellipsoid (J. Smit and H. P. J. Wijn, [61]).

uniform magnetization are possible. These will, however, usually not be excited by a uniform rf driving field of a small magnitude. We shall return briefly to this question at the end of this paper. Here only the case of non-uniform magnetization due to the existence of domains will be discussed. This situation will always occur in small external fields, which are not sufficient to align the individual domains.

For the determination of the domain structure the term in $\nabla^2 M$ which is nonvanishing in the domain wall is of importance. For our purposes we shall assume the static domain problem solved and then consider the motions of the magnetization which is homogeneous in each individual domain. The motions of the various domain magnetizations are coupled through the demagnetizing fields. Smit [19] has given a lucid illustration of the procedure to solve the coupled equations of motion in a hexagonal crystal. The *ferroxdure* $BaFe_{12}O_{19}$ has high crystalline anisotropy with the easy axis parallel to the crystallographic hexagonal axis. The domain structure consists of plane-parallel regions, separated by 180° Bloch walls parallel to the hexagonal axis. The situation is schematized in Fig. 5.

Smit assumed that the specimen has a spheroidal shape of small size, with its axis parallel to the hexagonal axis. The demagnetizing factors are N, N and $4\pi - 2N$. The equations of motion for the coupled magnetizations of the two kinds of domains were then solved. The two resonant frequencies for the two modes of magnetization are plotted in Fig. 6 as a function of the magnitude of the dc field, for various orientations of the dc and rf magnetic fields. For high values of the dc field

$$H_0 > \frac{2K}{M} - (4\pi - 3N)M$$

only one resonance occurs. The domain structure is then lost, as the total magnetization is aligned with the applied field.

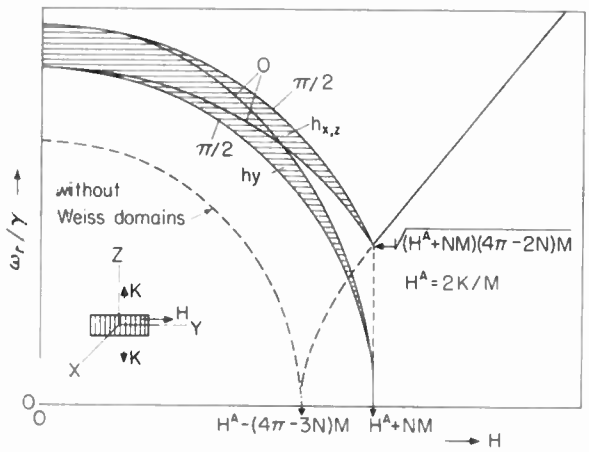

Fig. 6—Dependence of the resonance frequency on the strength of the applied magnetic field H, perpendicular to the hexagonal axis of $Ba\ F_{12}O_{19}$ at room temperature for various orientations of the microwave field and of the Bloch walls with respect to the static field. The values of the angle α between the Bloch walls and H are indicated (O, $\pi/2$). For $H > H_A + NM$ the specimen is saturated in the y-direction (J. Smit and H. G. Beljers, [19]).

To determine the shape and intensity of the two resonances the driving terms of the external rf field and the damping terms have to be inserted. Fig. 5 illustrates the case that the rf field is perpendicular to the magnetization. If the rf field is also perpendicular to the wall, the magnetization normal to the wall is continuous and no demagnetizing effect of the wall occurs. If the rf field is parallel to the wall, the normal components of rf magnetization of the two domains are out of phase.

For rf fields at an oblique angle with the wall, both modes would be excited.

When the specimen is inserted in a microwave cavity, the magnetization modes are coupled with the dominant cavity mode through the electromagnetic field. The combined coupled system of magnetization and cavity oscillator should then in principle be considered. Artman and Tannenwald [8] discuss the removal of the degeneracy of modes in a cylindrical cavity by a ferrite, whereas Bloembergen and Pound [27] discuss the damping associated with the coupling between ferrite and cavity in more detail.

Artman [28] has solved the normal mode problem for simple domain configurations in crystals with cubic symmetry. The method used is the same as Smit's, but the algebra is considerably more complicated in this case.

Ferromagnetic Resonance

In the case of ferrimagnetism the two (or more) magnetic subsystems are coupled strongly by their mutual exchange interaction. They are not separated in space as in the domain problems but are interspersed throughout the ferrite crystal. Since the exchange coupling between the two subsystems is so strong, it may be expected that in many respects it will behave as one single system. This expectation is borne out by experiment and for many applications the discussion in terms of a single net magnetization is adequate. Under certain conditions the ferrimagnetic, rather than ferromagnetic character becomes evident. It is therefore proper to introduce two magnetizations, with different g-factors, anisotropy fields, etc., and write down the equations of motion, following Nagamiya [29], Kittel, and others [30].

$$\frac{d\boldsymbol{M}_i}{dt} = \gamma_i(\boldsymbol{M}_i \times \boldsymbol{H}_i). \tag{15a}$$

Where the effective field acting the i^{th} subsystem is,

$$\boldsymbol{H}_i = H_0\boldsymbol{z} + \sum_j \lambda_{ij}\boldsymbol{M}_j - N_x\hat{\boldsymbol{x}}\sum_j M_{jx} - N_y\hat{\boldsymbol{y}}\sum_j M_{jy} - N_z\hat{\boldsymbol{z}}\sum_j M_{jz} - N_x'\hat{\boldsymbol{x}}M_{ix} - N_y'\hat{\boldsymbol{y}}M_{iy} - N_z'\hat{\boldsymbol{z}}M_{iz} \tag{15b}$$

λ_{ij} describes the strength of the exchange coupling between system i and j. N_x, N_y, N_z are the geometric demagnetization factors. The N_j' describe the anisotropy of system i. For two magnetic subsystems the four homogeneous equations for x- and y-components lead to a determinantal problem for the proper frequencies, the solution of which has been given by Wangsness. Since the algebraic complexity of this solution tends to hide the physical principles, further simplification of (15) will be made by assuming all demagnetizing fields to be zero, except for effective anisotropy fields in the z-direction $+H_A$ acting on M_1 and $-H_A$ acting on the nearly antiparallel magnetization M_2. Then the two normal frequencies of the system are given by

$$\omega = \gamma H_0 + \delta H_A + \tfrac{1}{2}\lambda_{12}(\gamma_2 M_1 + \gamma_1 M_2) \pm \left[\{\gamma H_A + \delta H_0\}\{\gamma H_A + \delta H_0 - \lambda_{12}(\gamma_2 M_1 - \gamma_1 M_2)\} + \tfrac{1}{4}\lambda_{12}^2(\gamma_2 M_1 + \gamma_1 M_2)^2\right]^{1/2}. \tag{16}$$

Here $\gamma = \frac{1}{2}(\gamma_1+\gamma_2)$, $\delta = \frac{1}{2}(\gamma_1-\gamma_2)$. The constant λ_{12} is a measure of the strength of the exchange field between the two systems. For reasons stated earlier [12], the exchange fields within each subsystem do not occur in (16). Since a Curie temperature of 600°K corresponds roughly to an exchange field of 10^7 oersted, it is proper to expand the square in terms of H_A/λ_{12} and H_0/λ_{12}. It is seen that there is one low frequency mode, neglecting small terms in λ_{12}^{-1} etc.

$$\omega = \gamma_{\text{eff}}\{H + (M_1 - M_2)(M_1 + M_2)^{-1}H_A\} \tag{17a}$$

with

$$\gamma_{\text{eff}} = (M_1 + M_2)\{(M_1/\gamma_1) + (M_2/\gamma_2)\}^{-1}. \tag{17b}$$

In this mode the angle between the two magnetizations does not change. The ferrite behaves apparently as a simple ferromagnetic system with an effective γ which is an appropriate average of the γ of the two subsystems. The g-factor may therefore be a sensitive function of the composition. The other proper mode is at the exchange frequency.

$$\omega \approx \gamma_1\gamma_2\lambda_{12}\left(\frac{M_1}{\gamma_1} + \frac{M_2}{\gamma_2}\right). \tag{18}$$

Usually this frequency is very high. For a Curie temperature of 600°K the corresponding wave length is 0.0023 cm, in the infrared.

Special situations arise near compensation points. In Fig. 7 the schematic behavior of the magnetization in a ferrite as a function of temperature is sketched. In ferrites with appropriate composition the magnetization may vanish at a certain temperature. At this point $\gamma_{\text{eff}} = 0$. At a fixed frequency the resonance would seem to occur at infinite field. Actually the field strength required for resonance remains finite since the next term in the expansion in λ^{-1} should be taken into account.

Similarly when the angular momentum vanishes

$$S = \frac{M_1}{\gamma_1} + \frac{M_2}{\gamma_2} = 0$$

the exchange-frequency mode (18) approaches zero, and the low-frequency mode moves up. Again the next term in the expansions should then be retained, but the frequency of the *exchanging mode* may become low enough to become observable at the usual microwave frequencies. Fig. 8 shows the moving down of the exchange mode and the rise in g-factor of the low frequency mode in lithium chromium ferrite around 57°C., found by McGuire [31]. An example of the behavior of the low-frequency mode near the compensation points was obtained earlier by van Wieringen [32] in the same material.

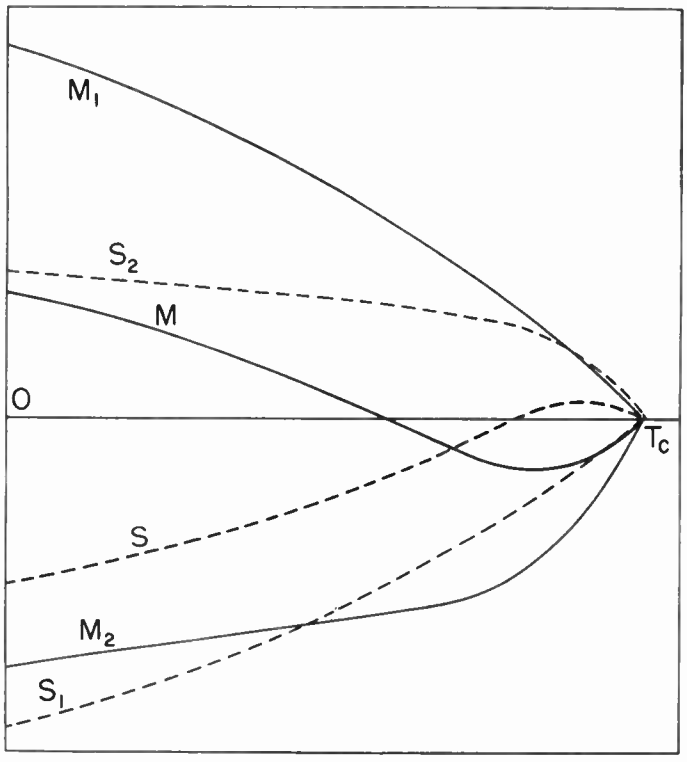

Fig. 7—Magnetizations and angular momenta vs temperature for a two-sublattice ferrimagnetic which has a compensation point (R. K. Wangsness, [62]).

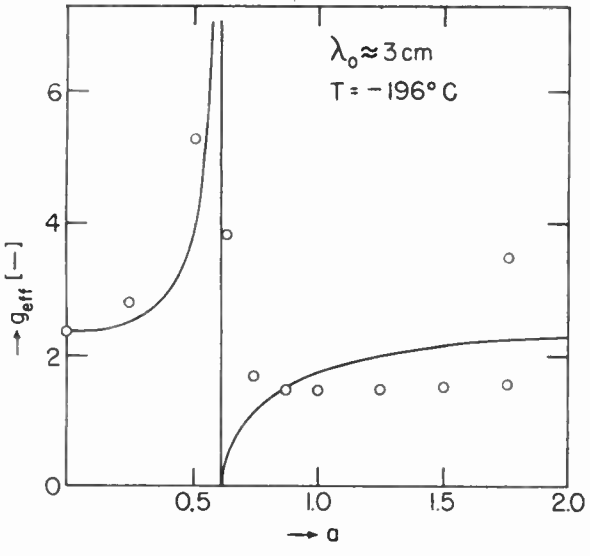

Fig. 8—Effective g-values in Ni Fe_{2-a} Al_aO_4 as a function of a composition (T. R. McGuire, [63]).

The discussion should again be made complete by considering the damping and excitation of the modes. The exchange mode at high frequencies can only be weakly excited. If $\gamma_1=\gamma_2$, the torque exerted by the rf field would tend to turn the two systems through the same angle in each time interval. The relative angle between the magnetizations, and therefore the exchange energy, would not change. Detailed calculation confirms that the intensity of the pure exchange mode is proportional to $(\gamma_1-\gamma_2)^2$. Near the compensation points $S=0$, the modes become mixed and the excitation conditions change correspondingly.

Since it is more convenient to find the resonance experimentally by changing the magnetic field rather than the resonant frequency, Dreyfus [33] has solved the determinantal problem as a characteristic equation in H_0 rather than ω. Such a procedure, however, is not recommended, as the static equilibrium problem changes with varying H_0. It is unrealistic to assume the magnetizations to remain in a fixed orientation. Some spurious solutions without physical meaning (negative absorption) resulted, in which the dc magnetization was in a direction opposite to the applied field.

The condition of static equilibrium should also be considered with care near the compensation points. This is all the more true in the case of antiferromagnetism, where the magnetization and angular momentum are always at the compensation point. A detailed analysis of antiferromagnetic resonance, which can be treated by the same general theory, may be found in an excellent review article by Nagamiya [34].

The Magnetization, g-value and Anisotropy Constants in Ferrites

The attention will now be restricted to the common situation in which the resonance mode is given by the single effective g-value of (17). The g-value would be equal to the free electron value $g=2.0023$ in the absence of spin-orbit coupling. In manganese ferrite g is very close to this value, since both Mn^{++} and Fe^{+++} have virtually no orbital angular momentum. The same appears to be true for *ferroxdure* $BaFe_{12}O_{19}$ which has only Fe^{+++} magnetic ions. In nickel ferrites the g-value is as high as 2.23. In mixed ferrites it will depend upon composition and it may also depend upon temperature according to (17b). An illustration was given in Figs. 8 and 9. The g-value should usually be independent of the external field. Nevertheless measurements at different frequencies have led to different results, which could

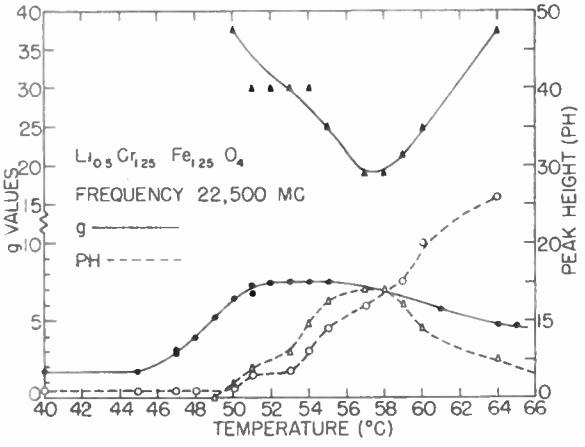

Fig. 9—Temperature dependence of the peak heights and effective g-values for the two modes found near the compensation point in lithium chromium ferrite (T. R. McGuire, [31]).

only be reconciled by the *ad hoc* introduction of an internal field [35]. Proper frequency-independent results are obtained if single crystals of sufficiently small size are used so that the sample is indeed small compared to the internal wave length. Corrections due to finite size have been suggested by Miles and Artman.

The largest spurious effects occur in polycrystalline material of relatively low density [36]. Internal demagnetizing fields and perhaps magnetostriction then cause an apparent frequency dependence of g. A true frequency dependence of the g-factor may occur in ferrites containing excess iron. The g-value may depend on distribution of Fe^{++} and Fe^{+++} ions over available lattice sites. This distribution depends on the magnetization, but at very high frequencies or low temperatures the distribution may not be established rapidly enough to follow the precessing magnetization [44, 45].

In order to measure g, it is best to use a single crystal in an external field large enough to make a single domain out of the specimen. The resonance field at a fixed frequency ω should then be determined in a number of independent crystallographic orientations, *e.g.*, with the magnetization parallel to the [100], [110], and [111] direction in a cubic crystal.

If the magnetization is also unknown, experiments should be carried out for two or more different geometries, *e.g.*, a sphere and a plane, or a plane specimen magnetized parallel or perpendicular to the surface. Using the resonance condition (13) in an appropriate number of ways, g, M_0, K_1, and K_2 may be determined. Care should be taken that the sample is really small compared to the internal wavelength, is unstrained, is far enough from the walls of the cavity, and is indeed magnetized in the direction of the external field H_0. Otherwise appropriate corrections should be made. Table I gives some magnetic constants for representative ferrites at room temperature. Wide variations in these constants may be achieved by varying concentration in mixed ferrites and by temperature variation.

TABLE I

THE CURIE TEMPERATURE, SATURATION MAGNETIZATION, G-VALUE, ANISOTROPY AND MAGNETOSTRICTION CONSTANTS AT ROOM TEMPERATURE FOR FERRITES

Ferrite	T_c(°C)	$4\pi M_s$ (gauss)	g_{eff}	K_1 (erg cm^{-3})	λ_{110}
$MnFe_2O_4$	300	5200	2.00	-2×10^3	
$Fe\,Fe_2O_4$	585	6000	2.06	-1.1×10^5	80×10^{-6}
$CoFe_2O_4$	520	5000		-1.7×10^6	45×10^{-6}
$NiFe_2O_4$	585	3400	2.23	-6.2×10^4	
$CuFe_2O_4$	455	1700	2.05		
$MgFe_2O_4$	440	1400	2.08		
$Li_{0.5}Fe_{2.5}O_4$	670	3900	1.80		

The anisotropy constants are very small near the Curie temperature, but increase rapidly, about as M_0^{10}, with decreasing temperature. There may be reversals of sign. A typical example is illustrated in Fig. 10. The anisotropy constants are extremely sensitive to structure, chemical composition and crystalline imperfection. It is hard to reproduce their values, unless crystals are grown from the same batch. The magnetic anisotropy constants determined from (13) and (14) usually agree rather well with those from static measurements. Sometimes discrepancies exist which may have a physical origin, as the anisotropy may have a frequency dependence [36].

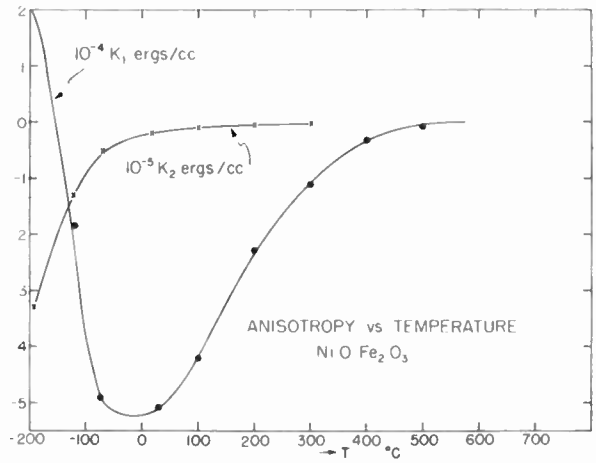

Fig. 10—Anisotropy constants K_1 and K_2 in nickel ferrite as a function of temperature (D. W. Healy, [26]).

In some oxides the crystalline anisotropy is very large, with anisotropy fields $2K/M$ larger than 20,000 Gauss. Such materials, called *ferroxdures*, have desirable properties for permanent magnet material [37].

In zero magnetic field there is still a finite resonant frequency due to precession of the magnetization around anisotropy and demagnetizing fields. In early papers [38] this was called *natural* ferromagnetic resonance. In polycrystalline materials there will be a distribution of resonant frequencies, giving rise to a broad absorption spectrum. The susceptibility tensor in polycrystalline aggregates, like sintered ferrite materials, should, of course, be calculated as the weighed average of the susceptibility tensor for the individual domains. Due to the fields which couple the domains together, an exact solution is in general not possible. Park [23] has made rather extensive calculations to obtain average values for polycrystalline aggregates. These should be compared with measurements by Brown [39] and Duncan [40] on technical ferrites.

The *natural* resonances set a lower frequency limit to the application of ferrites in nonreciprocal devices. The differential phase shift devices are based on the difference in propagation constant for the two modes of polarization of electromagnetic waves in a medium with tensor permeability. The difference in the real part of the complex permeability of the two normal modes of polarization should be large, but the imaginary parts corresponding to electromagnetic absorption should be small to keep the insertion loss of the device low.

One should therefore operate in the wing of the ferromagnetic resonance, where the dispersion is still large

but the absorption small. Preferably one should operate on the low-field (high-frequency) side of the resonance to make the difference in propagation constants large. This was clearly pointed out by Hogan [6]. One therefore requires $\omega > \gamma H_{\text{eff}} + (1/\tau)$. In polycrystalline material the effective field will take on values up to

$$\gamma H_{\text{eff}} = \gamma\left(\frac{2K_1}{M} + 4\pi M\right).$$

This follows from Smit's analysis of resonance in domain structure [19]. The *natural resonances* therefore set a low frequency limit on the operation of the nonreciprocal device given by

$$\omega > \gamma\left(\frac{2K}{M} + 2\pi M\right) + \frac{1}{\tau}.$$

Consequently materials with low magnetization, low anisotropy and small damping are desirable. The aluminum-manganese-magnesium system combines these properties to a large extent [41, 42]. (Compare Fig. 11.)

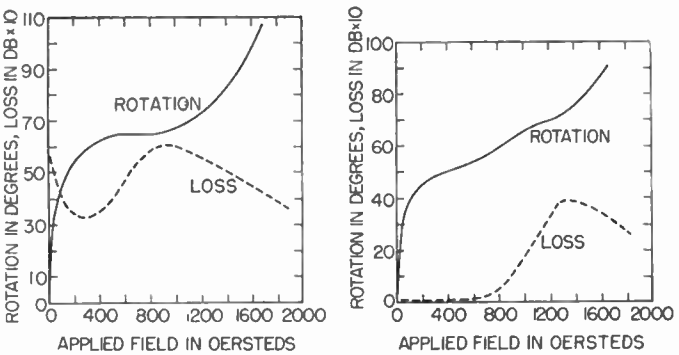

Fig. 11—Loss and rotatory power in a polycrystalline sintered ferrite for two different values of the magnetization at 4000 mc. At the lower value of the magnetization, no resonant absorption in the demagnetizing fields occur. (van Uitert, Schafer, and Hogan, [41]).

Another way to reduce the low-frequency losses is to apply a large external magnetic field and operate on the high-field side of the resonance, although this will reduce the rotatory power of the device. The figure of merit for this case has been analyzed by Fox [43].

Large single domain ferrite crystals where the losses due to the natural resonance mode are limited to a narrow frequency band, would of course be the best solution, but such crystals are not yet available.

Line Width

Nonreciprocal devices based on selective absorption of the electromagnetic mode polarized in the direction to produce resonance will be more effective the higher the imaginary part of the permeability near resonance. In this device, as for the differential phase shifters, the figure of merit is determined by $\omega\tau$, where ω is the frequency and τ the relaxation time. A long relaxation or a small damping is therefore desirable for ferrite application. The phenomenological damping terms have already been introduced in (4) and (5). If only terms linear in H_{rf} are considered, as has been done consistently in this paper, there is no difference between the two types of damping. The L-L term (4a) would always leave the magnitude of the magnetization invariant, even for very large H_{rf}. The Bloch type damping allows for a variation of the temperature of the magnetic system, which changes the value of $|M|$. Dipolar coupling between the elementary spins can in principle produce this type of relaxation.

The atomic mechanism for the damping is imperfectly understood although much theoretical and experimental work has been done. Here only one type of damping mechanism will be discussed which has been well established. In ferrites with an excess of oxygen, where Fe^{++} ions are present, an increase in damping has been observed by Galt [44] with a maximum near 150°K. A satisfactory theory has been given by Clogston [45]. For each orientation of the magnetization vector there is an equilibrium configuration for the $Fe^{++} - Fe^{+++}$ ions on the octahedral sites. This is well known for magnetite. As the magnetization precesses, a reordering of the ions takes place through thermally activated electron jumps from the Fe^{++} to the Fe^{+++} ions. If the magnetization precesses too fast, the electron jumps cannot follow. If the magnetization precesses very slowly, the electron distribution is always in phase. In the intermediate region absorption (damping) occurs, which depends both on frequency and crystallographic orientation. (Compare Fig. 12.)

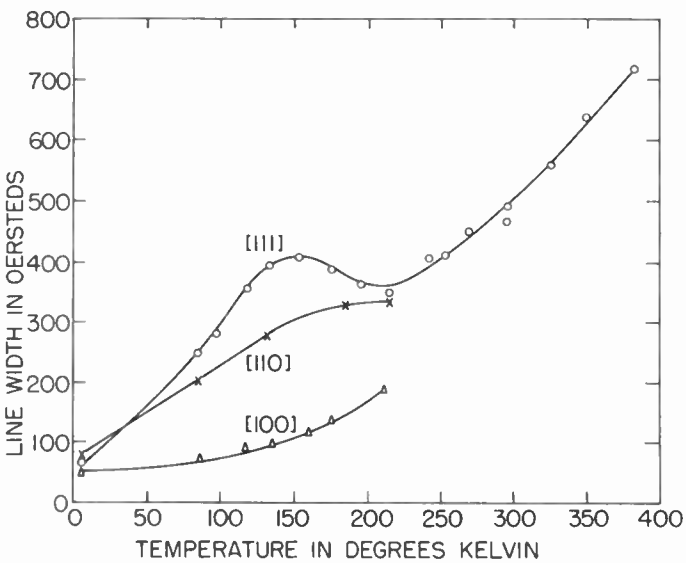

Fig. 12—Damping of ferromagnetic resonance in nickel iron ferrite, $(Ni\ O)_{0.75}\ (FeO)_{0.25}Fe_2O_3$ as a function of temperature for three directions of the magnetization. (Yager, Galt, and Merritt, [44]).

The electron jumps between the Fe-ions are also responsible for higher conductivity of the oxygen rich ferrites. The highest conductivity losses occur again in *ferrous ferrite* or magnetite, Fe_3O_4. For many applications the presence of Fe^{++} ions should be avoided.

It should be emphasized that this type of damping through electron redistribution is superimposed on

another damping mechanism, the nature of which is still not clear despite large efforts of various authors.

The observed line-width in single crystals of ferrites ranges from 13 oersted in manganese ferrite [55] to several hundred oersteds [46]. It should be regarded as a phenomenological property of the material, which cannot be accurately predicted. In polycrystalline materials spurious broadening due to a dispersion of resonant frequencies is superimposed on the true line width. This may produce figures of merit lower than the theoretical limit.

Tannenwald [46] has recently found a pronounced maximum in the damping of the resonance in Mn-Zn ferrite at 15°K. Zeiger and Heller have proposed an acoustical damping mechanism through magnetostriction. This would explain the dependence of this damping on shape and crystallographic orientation.

Finally a remarkable case of ferromagnetic damping should be mentioned, although it has only been found in one metallic specimen, iron-nickel alloy of zero anisotropy, by Rado and Weertman [47]. Suppose that no explicit extraneous damping is introduced ($\tau = \infty$). Then the magnetic permeability as given by (8) would go to infinity. This would mean that the skin depth would go to zero and correspondingly the radio-frequency part of the magnetization would become very inhomogeneous. Consequently there is no justification for dropping the term $\nabla^2 M$ which was one step in deriving (1) from (9) and (10). The proper procedure under these circumstances is to use the differential (10) connecting M or b and h rather than the permeability relation. This differential equation in combination with Maxwell's equations should then be solved subject to the usual boundary conditions plus the additional condition that the net exchange torque on the specimen is zero. Ament and Rado [48] have shown that in general three waves propagate into the medium and they have calculated the corresponding losses. In ferrites this complicated situation fortunately does not seem to arise and the $\nabla^2 M$ term can be neglected.

High Power Level and Relaxation Effects; Higher Modes and Spin Waves

An effort to clarify the basic damping mechanism led to an experiment at high microwave power level [49, 50] in order to study the dissipation of absorbed magnetic energy. A number of interesting effects were discovered, which pointed out that some essential features are missing from the theory developed above.

First it should be borne in mind that the theory presented so far has neglected terms nonlinear in H_{rf}. The equations of motion (1) or (10) are essentially nonlinear in H_{rf} and can be solved by successive approximations for higher harmonies. Terms in H_{rf}^2 give rise to a decrease in M_z, called saturation, and to frequency components at twice the fundamental frequency. Frequency doubling from a ferrite at high microwave power level has recently been obtained by Vartanian [51].

Another important assumption has been that the magnetization of each subsystem is homogeneous. One may well ask, why a further division into subsystems would not be in order. In last analysis each of the N elementary magnetic spins constitutes a degree of freedom and N proper modes may be expected. Such higher modes in which the magnetization varies periodically in space and time exist and are generally called spin waves [52]. They can be derived from (10), if the $\nabla^2 M$ is retained. The frequency of such a mode, representing a spin wave with a wave vector k, making an angle θ_k with respect to the magnetization of a body of finite dimensions is given by

$$\omega = [\eta^2 k^4 + (2\eta\zeta + \xi\eta \sin^2 \theta_k) k^2 + \zeta^2 + \xi\zeta \sin^2 \theta_k]^{1/2}$$

with

$$\xi = 4\pi\gamma M_0, \qquad \eta = \lambda\gamma M_0 a^2, \qquad \zeta = \gamma H_{eff}.$$

This formula breaks down if the wavelength of the spin wave becomes comparable to the linear dimension of the sample. Very recently, Walker [53] has given an analysis of the low-lying nodes with nonuniform magnetization in a spheroidal specimen.

In this paper so far only one mode, corresponding to uniform magnetization, has been considered. This was justified, inasmuch as a uniform radiofrequency field will not excite the other modes. However, if the driving magnetic field varies appreciably over the region of the sample, other modes are excited. A large number of these other modes has been observed recently by White [54] and by Dillon [55]. These modes depend sensitively on the geometry and may occur both above and below the *ordinary* resonance corresponding to uniform magnetization. Previously, additional side maxima in the absorption curve had been observed when the sample size was not sufficiently small. In that case the rf field is again not uniform throughout the specimen. In principle all modes, including the short-wave length spin waves which are not directly excited, are coupled together through magnetic dipolar interaction. The strength of this coupling of the *uniform mode* with other modes depends on the amount of its excitation by the rf field. The question, how energy is transferred from low-lying modes to modes with more rapid spatial variation of the magnetization and eventually to the lattice vibrations of the ferrite crystal where it appears as heat, is extremely interesting both from the theoretical and experimental point of view. Much current research is devoted to these questions which will be discussed in detail in Dr. Suhl's paper.

Bibliography

[1] Landau, L., and Lifshitz, L., "On the Theory of the Dispersion of Magnetic Permeability in Ferromagnetic Bodies." *Physik. Zeitschrift Sowjetunion*, vol. 8 (1935), p. 153.
[2] Bloch, F., "Nuclear Induction." *Physical Review*, Vol. 70 (1946), p. 460.
[3] Bloembergen, N., "On the Ferromagnetic Resonance in Nickel and Supermalloy." *Physical Review*, Vol. 78 (1950), p. 572.

[4] Garstens, M. A., "Paramagnetic Resonance in Gases at Low Fields." *Physical Review*, Vol. 93 (1954), p. 1228.
Garstens, M. A., Codrington, R., Olds, M. A., and Torrey, H. C., "Paramagnetic Resonance in Organic Free Radicals at Low Fields." *Physical Review*, Vol. 95 (1954), p. 607.
Garstens, M. A., Wangsness, R. K., "Magnetic Resonance for Arbitrary Field Strengths." *Physical Review*, Vol. 98 (1955), p. 927.

[5] Polder, D., "On the Theory of Ferromagnetic Resonance." *Philosophical Magazine*, Vol. 40 (1949), p. 99.

[6] Hogan, C. L., "The Ferromagnetic Faraday Effect at Microwave Frequencies and its Applications." *Review of Modern Physics*, Vol. 25 (1953), p. 253.
Hogan, C. L., "The Microwave Gyrator." *Bell System Technical Journal*, Vol. 31 (1952), p. 1.

[7] Young, J. A., and Uehling, E. A., "The Tensor Formulation of Ferromagnetic Resonance." *Physical Review*, Vol. 94 (1954), p. 544.

[8] M van Trier, A. A. Th., "Experiments on the Faraday Rotation of Guided Waves." *Applied Scientific Research*, Vol. B3 (1953), p. 142.

[9] Artman, J. O., and Tannenwald, P. E., "Measurement of Susceptibility Tensor in Ferrites." *Journal of Applied Physics*, Vol. 26 (1955), p. 1124.

[10] Epstein, P. S., "Theory of Wave Propagation in a Gyromagnetic Medium." *Review of Modern Physics*, Vol. 28 (1956), p. 3. This review article contains further references to the literature.

[11] Griffiths, J. H. E., "Anomalous High-Frequency Resistance of Ferromagnetic Metals." *Nature*, Vol. 158 (1946), p. 670.

[12] Kittel, C. "On the Theory of Ferromagnetic Resonance Absorption." *Physical Review*, Vol. 73 (1948), p. 155.

[13] Kittel, C., "Ferromagnetic Resonance." *Journal de physique, Le, et Le radium*, Vol. 12 (1951), p. 291.

[14] Van Vleck, J. H., "Ferromagnetic Resonance." *Physica*, Vol. 17 (1951), p. 234.

[15] Reich, K. H., "Die Theorie der Ferromagnetischen Resonanz und die Ergebnisse ihrer experimentallen Untersuchung." *Zeitschrift für Angewandte Physik*, Vol. 6 (1954), p. 326.

[16] Néel, L., "Proprietes Magnetiques des Ferrites; Ferrimagnetisme et Antiferromagnetisme." *Annales de Physique*, Vol. 3 (1948), p. 137.

[17] Van Vleck, J. H., "Concerning the Theory of Ferromagnetic Resonance Absorption." *Physical Review*, Vol. 78 (1950), p. 266.

[18] MacDonald, J. R., "Ferromagnetic Resonance and the Internal Field in Ferromagnetic Materials." *Proceedings of the Physical Society*, Vol. A 64 (1951), p. 968.

[19] Smit, J., and Beljers, H. G., "Ferromagnetic Resonance Absorption in $BaFe_{11}O_{19}$, A Highly Anisotropic Crystal." *Philosophical Research Report*, Vol. 10 (1955) p. 113.

[20] Kittel, C., "Physical Theory of Ferromagnetic Domains." *Review of Modern Physics*, Vol. 21 (1949), p. 541.

[21] Suhl, H., "Ferromagnetic Resonance in Nickel Ferrite Between One and Two Kilomegacycle." *Physical Review*, Vol. 97 (1955), p. 553.

[22] Zeiger, H. (unpublished).

[23] Park, D., "Magnetic Rotation Phenomena in a Polycrystalline Ferrite." *Physical Review*, Vol. 97 (1955), p. 60.
Park, D., "Magnetic Rotation Phenomena in a Polycrystalline Ferrite, II." *Physical Review*, Vol. 98 (1955), p. 438.

[24] Rowen, J. H., and von Aulock, W., "Measurement of the Complex Tensor Permeability of Ferrites." *Physical Review*, Vol. 96 (1954), p. 1151.

[25] Bickford, L. R., "Ferromagnetic Resonance Absorption in Magnetite." *Physical Review*, Vol. 76 (1949), p. 137.
Bickford, L. R., "Ferromagnetic Resonance Absorption in Magnetite Single Crystals." *Physical Review*, Vol. 78 (1949), p. 449.

[26] Healy, D. W., "Ferromagnetic Resonance in Nickel Ferrite as a Function of Temperature." *Physical Review*, Vol. 86 (1952), p. 1009.

[27] Bloembergen, N., and Pound, R. V., "Radiation Damping in Magnetic Resonance Experiments." *Physical Review*, Vol. 95 (1954), p. 8.

[28] Nagamiya, T., "Theory of Antiferromagnetism and Antiferromagnetic Resonance Absorption, I." *Progress of Theoretical Physics*, Vol. 6 (1951), p. 342.

[29] Keffer, F., and Kittel, C., "Theory of Antiferromagnetic Resonance." *Physical Review*, Vol. 85 (1952), p. 329.

[30] Wangsness, R. K., "Sublattice Effects in Magnetic Resonance." *Physical Review*, Vol. 91 (1953), p. 1085.

[31] McGuire, T. R., "Observation of Exchange Resonance Near a Ferrimagnetic Compensation Point." *Physical Review*, Vol. 97 (1955), p. 831.

[32] van Wieringen, J. S., "Anomalous Behavior of the g Factor of LiFeCr Spinels as a Function of Temperature." *Physical Review*, Vol. 90 (1953), p. 488.

[33] Dreyfus, B., "Champs de Resonance d'un Systeme de Sousreseaux Magnetiques (Resonance ferrimagnetique)." *Comptes Rendus*, Vol. 241 (1955), pp. 552 and 1270.

[34] Nagamiya, T., Yosida, K., and Kubo, R., "Antiferromagnetism." Adv. in Phys. (*Quarterly Supplement of Philosophical Magazine*), Vol. 4 (1955), p. 1.

[35] Okamura, T., Torizuka, Y., and Kojima, Y., "The g Factor of Ferrites." *Physical Review*, Vol. 88 (1952), p. 1425.
Okamura, T., Kojima, Y., *The g-Factor of Ferromagnetic Spinels*. Scientific Report RITU, Vol. A6(1954), p. 614.

[36] Bozorth, R. M., Cetlin, C., Galt, Merritt, F. R., and Yager, W. A., "Frequency Dependence of Magnetocrystalline Anisotropy." *Physical Review*, Vol. 99 (1955), p. 1898.

[37] Went, J., Rathenau, J., Gorter, E. W., and Oosterhout, M., "Ferroxdure, A Class of New Permanent Magnet Materials." *Philips Technical Review*, Vol. 13 (1951), p. 194.

[38] Snoek, J. L., "Dispersion and Absorption in Magnetic Ferrites at Frequencies Above One Mc/S." *Physica*, Vol. 14 (1948), p. 207.

[39] Brown, F., and Gravel, C. L., "Direct Observation of Domain Rotation in Ferrites." *Physical Review*, Vol. 98 (1955), p. 442.

[40] Duncan, B. J., and Swern, L., "Temperature Behavior of Ferrimagnetic Resonance in Ferrites Located in Wave Guides." *Journal of Applied Physics*, Vol. 27 (1956), p. 209.

[41] van Uitert, L. G., Schafer, J. P., and Hogan, C. L., "Low-Loss Ferrites for Applications at 4000 Millicycles per Second." *Journal of Applied Physics*, Vol. 25 (1954), p. 925.

[42] Suhl, H., van Uitert, L. G., and Davis, J. L., "Ferromagnetic Resonance in Magnesium-Manganese Aluminum Ferrite between 160 and 1900 Mc." *Journal of Applied Physics*, Vol. 26 (1955), p. 1180.

[43] Fox, R. H., "Extension of Nonreciprocal Ferrite Devices to the 500-300 Megacycles Frequency Range." *Journal of Applied Physics*, Vol. 26 (1955), p. 128.
Fox, R. H., Lax, B., "Figure of Merit for Microwave Ferrites at Low and High Frequencies." *Journal of Applied Physics*, Vol. 26 (1955), p. 919.

[44] Yager, W. A., Galt, J. K., and Merritt, F. R., "Ferromagnetic Resonance in Two Nickel-Iron Ferrites." *Physical Review*, Vol. 99 (1955), p. 1203.

[45] Clogston, A. M., "Relaxation Phenomena in Ferrites." *Bell System Technical Journal*, Vol. 34 (1955), p. 739.

[46] Tannenwald, P. E., "Line Width in Nm Ferrite Crystals." *Bulletin of the American Physical Society*, Vol. II (1956), p. 126.

[47] Rado, G. T., and Weertman, J., "Observation of Exchange Interaction Effects in Ferromagnetics by Spin Wave Resonance." *Physical Review*, Vol. 94 (1954), p. 1386.

[48] Ament, T. S., and Rado, G. T., "Electromagnetic Effects of Spin Wave Resonance in Ferromagnetic Metals." *Physical Review*, Vol. 97 (1955), p. 1558.

[49] Bloembergen, N., and Wang, S., "Relaxation Effects in Para- and Ferromagnetic Resonance." *Physical Review*, Vol. 93 (1954), p. 72.

[50] Damon, R. W., "Relaxation Effects in the Ferromagnetic Resonance." *Review of Modern Physics*, Vol. 25 (1953), p. 239.

[51] Ayres, W. P., Vartanian, P. H., and Melchor, J. L., "Frequency Doubling in Ferrites." *Journal of Applied Physics*, Vol. 27 (1956), p. 188.

[52] Herring, C., and Kittel, C., "On the Theory of Spin Waves in Ferromagnetic Media." *Physical Review*, Vol. 81 (1951), p. 869.

[53] Walker, H., *Resonant Modes of Ferromagnetic Spheroids*, Bulletin APS, Vol. II (1956), p. 125.

[54] White, Solt and Mercereau, *Multiple Ferromagnetic Resonance Absorption in Manganese and Manganese-Zinc Ferrite*. Bulletin APS, Vol. II (1956) p. 12.

[55] Dillon, J. F., *Ferromagnetic Resonance in Thin Disks of Manganese Ferrite*. Bulletin APS, Vol. II (1956), p. 125.

[56] Anderson, P. W., and Suhl, H., "Instability in the Motion of Ferromagnets at High Microwave Power Levels." *Physical Review*, Vol. 100 (1955), p. 1789.

[57] Clogston, B. A., Suhl, H., Walker, H., and Anderson, P. W., "Possible Source of Line Width in Ferromagnetic Resonance." *Physical Review*, Vol. 101 (1956), p. 903.

[58] Suhl, H., "Subsidiary Absorption Peaks in Ferromagnetic Resonance at High Signal Levels." *Physical Review*, Vol. 101 (1956), p. 1437.

[59] Yager, W. A., Gatt, J. K., Merritt, F. R., and Wood, J., "Ferromagnetic Resonance in Nickel Ferrite," *Physical Review*, Vol. 80 (1950), p. 744.

[60] Tannenwald, P. E., "Ferromagnetic Resonance in Manganese Ferrite Single Crystal," *Physical Review*, Vol. 100 (1955), p. 1713.

[61] Smit, J., and Wijn, H. P. J., "Physical Properties of Ferrites," *Advances in Electronics*, Vol. 6 (1954), p. 69.

[62] Wangsness, R. K., "Ferromagnetic Resonance and Some Related Effects," *American Journal of Physics*, Vol. 24 (1956), p. 60.

[63] McGuire, T. R., "Microwave Absorption in Nickel Ferrite Aluminate," *Physical Review*, Vol. 93 (1954), p. 206.

The Nonlinear Behavior of Ferrites at High Microwave Signal Levels

HARRY SUHL†

Summary—**Above a certain microwave signal level, ferrites show various kinds of anomalies in their power absorption. The conditions under which these anomalies are observed are shown to coincide with the conditions under which certain "spin wave" disturbances in the medium grow to abnormally high levels. This growth is caused by the coupling of the spin waves to the uniform precession through the demagnetizing and exchange fields that accompany the disturbances. In the first part of the paper it is shown that the coupling causes certain spin wave amplitudes to "run away" exponentially with time when the signal field exceeds a threshold value. This will happen most readily exactly at resonance and under suitable conditions in a range of dc biasing fields confined to the low side of resonance.**

In the second part, the steady state of the magnetization beyond the threshold signal is evaluated for one type of anomalous absorption. It is found that the uniform precession "saturates" at a value corresponding to the threshold signal, and that further increases in applied power are diverted into a narrow range of spin waves. The susceptibilities are computed in the new state. Agreement with experiment is found to be good throughout. Since the paper is intended to be tutorial in character, the analysis is kept to a minimum. The full analysis will be the subject of a later publication.

I. Introduction

ENGINEERS concerned with ferrite microwave devices have known for some time that certain structures which perform well and quite according to theory at low signal levels do not always operate satisfactorily at high signal powers. From a practical, as well as from a theoretical viewpoint, the most distressing feature of this deviant behavior is that it sets in at signal powers which, though already in the magnetron range, are still very far below the limit at which the simple linearized theory of the motion of the magnetization should first begin to break down. This appearance of nonlinear effects at a seemingly too low power level is not confined to device structures alone. It has been observed particularly clearly in the cavity resonance experiments undertaken from a fundamental viewpoint, first by Damon,[1] and then, more extensively, by Bloembergen and Wang.[2] These investigators observed two new effects: First of all, the main resonance line appeared to weaken and broaden steadily as the signal power was increased beyond a rather sharply defined threshold value only about one-hundredth to one-fiftieth of the signal level required for observation of any appreciable nonlinear effects according to the simple theory. Secondly, they found that, at similar powers, an additional rather broad absorption peak appeared, always a few hundred oersteds below the field required for the main resonance. It is this second effect which is especially troublesome in those applications that rely on a ferrite element as a field-controlled phase-shifting or tuning device. Usually such structures are intended to operate on the low-field side of resonance, and any additional loss due to the extra absorption that arises at high signal levels is unwelcome.

In the following discussion we shall outline a fairly complete theory[3,4] which satisfactorily accounts for both the phenomena observed by Bloembergen and Wang (hereafter referred to as B.W.) and by Damon (D). Some of its further predictions have been verified in unpublished measurements by Dr. H. E. D. Scovil of Bell Telephone Laboratories, and by the author.

It is perhaps worth noting in advance that the basic reasons for these strange effects are really the very same that make ferrites so useful in microwave applications: it is the tendency of the electron spins to line up parallel to one another as the result of exchange forces and to move as a single unit in the applied signal field which makes a ferrite device useful or indeed feasible. And, as we shall see, it is the same tendency to move as a single, large magnetic moment, which leads to strong demagnetizing and exchange fields when the uniformity of the motion is disturbed slightly, as it must be through thermal agitation. These local nonuniform demagnetizing and exchange fields interact with the motion of the magnetization as a whole in such a way that for large enough signals the disturbances can grow to large values at the expense of the uniform motion.

The motion of the magnetization vector $\vec{M}(\vec{r}, t)$ at time t, and at a point $\vec{r}$ in the sample is governed by an equation of the form

$$\frac{d\vec{M}}{dt} = -\gamma[\vec{M} \times \vec{H}] + \text{a dissipative term} \qquad (1)$$

where γ is the absolute value of the gyromagnetic ratio and $\vec{H}$ the total magnetic field at the point $\vec{r}$ and at time t. $\vec{H}$ must include all forces capable of exerting

† Bell Telephone Laboratories, Murray Hill N.J.

[1] R. W. Damon, "Relaxation effects in ferromagnetic resonance," *Rev. Mod. Phys.*, vol. 25, pp. 239–245; January, 1953.

[2] N. Bloembergen and S. Wang, "Relaxation effects in para- and ferromagnetic resonance," *Phys. Rev.*, vol. 93, pp. 72–83; January, 1954.

[3] P. W. Anderson and H. Suhl, "Instability in the motion of ferromagnets at high microwave power levels," *Phys. Rev.*, vol. 100, pp 1788–1789; December, 1955.

[4] H. Suhl, "Subsidiary absorption peaks in ferromagnetic resonance at high signal levels," *Phys. Rev.*, vol. 101, pp. 1437–1438; February, 1956.

a torque on $\vec{M}$, not only the applied fields (steady and high frequency) but also any demagnetizing field existing at $\vec{r}$, the crystalline anisotropy field (hereafter neglected), and, if $\vec{M}$ varies sufficiently rapidly through the material, a field representing the exchange force between neighboring misaligned spins. The torque $\vec{M}\times\vec{H}$ is such that once $\vec{M}$ is set in motion, this motion would never die out. To account for the relaxation actually observed it is necessary to supplement (1) with a term representing dissipation. Since the microscopic mechanism of this dissipation is not entirely settled, the form of the required term is likewise in doubt. According to taste, some authors take it in the form first proposed by Landau and Lifshitz:[5]

$$+\frac{\alpha}{M}\left[\vec{M}\times\frac{d\vec{M}}{dt}\right]^{6} \tag{2}$$

which specifies the losses in terms of a single parameter α, and which leaves the magnitude of the magnetization, M, unchanged. Others prefer the Bloch-Bloembergen form of the damping term,[2] which has two adjustable parameters, but does not conserve M. We shall assume throughout this discussion that M, defined in a sufficiently small volume element, is conserved. This still does not force us to take the damping in the form (2), some other much more general forms will also leave M unchanged. However, we shall use the form (2), merely for the sake of definiteness, since it is possible to make any desired generalizations at a later point in the calculations, and, in fact, in the final results.

The usual resonance experiment on a ferrite is carefully arranged in such a way that $\vec{M}$ is independent of position. A single crystal sample of ellipsoidal, usually spherical, shape is placed into dc and rf fields that are as uniform as possible. In that case the demagnetizing and crystalline anisotropy fields are also uniform, and no exchange torque is set up, since the magnetization can precess uniformly, as a single unit. Then (1) has a well-known small signal solution: If the dc field H_0 is applied along a principal axis of the ellipsoid, the z-axis, say, and if the rf field is circularly polarized in the x-y plane, with components ($h\cos\omega t$, $h\sin\omega t$, 0), the solution is conveniently summarized in the form

$$M_x + jM_y = \frac{M\gamma h e^{j\omega t}}{\omega_{res} - \omega + j\gamma\Delta H}; \qquad j=\sqrt{-1}. \tag{3}$$

Here $\Delta H=\alpha\omega/\gamma$ is the frequency-linewidth expressed in terms of its field equivalent ΔH, and ω_{res} is the Kittel frequency. If anisotropy is neglected

$$\omega_{res}^2 = \gamma^2(H_0 - 4\pi(N_z - N_x)M)(H_0 - 4\pi(N_z - N_y)M) \tag{4}$$

where N_x, N_y, N_z are the demagnetizing factors along x, y, z, defined so that $N_x+N_y+N_z=1$. Eq. (3) is derived from (1) by assuming H_0 to be sufficiently large to line up $\vec{M}$ along the z-axis, so that in the absence of a signal $M_z=M$.[7] The signal induces small x and y components of M, whose squares and products are neglected in deriving (3). It will be found convenient to use the following reduced variables:

$$\omega_s = \gamma h; \quad \omega_H = \gamma H_0; \quad \omega_M = 4\pi\gamma M; \quad \vec{m} = \vec{M}/M$$
$$m^+ = m_x + jm_y; \quad m^- = (m^+)^* = m_x - jm_y. \tag{4a}$$

In terms of these, (3) and (4) become

$$m^+ = \frac{\omega_s e^{j\omega t}}{\omega_{res} - \omega + j\alpha\omega} = m_0^+ e^{j\omega t} \tag{5}$$

$$\omega_{res}^2 = [\omega_H - (N_z - N_x)\omega_M][\omega_H - (N_z - N_y)\omega_M]. \tag{6}$$

The linewidth ΔH, usually one of the objectives of the experiment, is determined through a measurement of the imaginary part of the susceptibility

$$\chi'' = \frac{\gamma M\gamma\Delta H}{(\omega-\omega_{res})^2+\gamma^2\Delta H^2} = \frac{\frac{1}{4\pi}\omega_M(\alpha\omega)}{(\omega-\omega_{res})^2+\alpha^2\omega^2} \tag{7}$$

which is, of course, signal independent within the range of the linearized theory.

In the case of a sphere it is also quite easy to find the large signal solution of (1), removing all restrictions on the magnitude of m^+. This solution predicts that χ'', at resonance, will essentially retain its signal independent value $M/\Delta H$ given by (7), until the signal field becomes of order ΔH. Thereafter χ'' declines steadily with increasing signal power, a condition known as *saturation*.

On the other hand the experimenters found that χ'' began to decline at only 1/100 to 1/50 of the signal power corresponding to an rf field of ΔH oersteds. A clue to the origin of this discrepancy, which is clearly beyond experimental error, comes from the large signal behavior, not of spheres, but of normally magnetized thin discs.

In the case of a very thin disc magnetized normal to its plane, the small signal theory gives (since $N_x=N_y=0$, $N_z=1$),

$$\omega_{res} = \gamma(H_0 - 4\pi M) = \omega_H - \omega_M.$$

When the signal is moderately large (3), though derived from small signal theory, is still approximately correct, provided we replace ω_{res} by

$$\omega_{res}' = \gamma(H_0 - 4\pi M_z) = \omega_H - \omega_M m_z$$

[5] L. Landau and E. Lifshitz, "On the theory of the dispersion of magnetic permeability in ferromagnetic bodies," *Physik. Zeits. Sowjetunion*, vol. 8, p. 153, 1935.

[6] This form is actually not quite that of Landau and Lifshitz, *ibid.*, but differs from it only to order α^2.

[7] Eq. (3) is strictly true only for a spheroid of revolution about OZ. Nevertheless we shall use this expression in a few isolated cases that do not involve a spheroid. The error incurred is of the order of a factor $\sqrt{2}$ in m_x or m_y.

in the denominator of (3) or (5). From (5), we then obtain

$$m_z = \sqrt{1 - |m^+|^2} \doteq 1 - \frac{1}{2}|m^+|^2$$

$$= 1 - \frac{\frac{1}{2}\omega_s^2}{[\omega - (\omega_H - \omega_M m_z)]^2 + \alpha^2\omega^2}. \quad (7)$$

This equation can be solved for m_z, which is as good a measure of the response as χ''. But without actually solving it we can see an important feature of the response: Suppose that ω_H has been adjusted to a value somewhat below the resonant position $\omega+\omega_M m_z$ and that by some accident, the precession angle is opened slightly beyond its appropriate value. This causes a slight reduction in m_z, and hence a slight increase in $\omega_H-\omega_M m_z$. The denominator in (7) is thus brought closer to its minimum, and therefore a further reduction in m_z results. If the new increment in m_z exceeds the initial one, a runaway condition will result in which the precession angle grows indefinitely until some new steady state is established. Mathematically, the runaway condition is obtained simply by differentiation of the right hand side of (7) with respect to M_z. The differential coefficient is in fact $(\delta M_z)_{\text{new}}/(\delta M_z)_{\text{old}}$, and must exceed unity if instability is to ensue. It is then found that ω_s must exceed a certain threshold; this threshold is least when the dc field is below resonance by an amount of order of the linewidth, and is then given by

$$\omega_{s\text{crit}} = \alpha\omega\sqrt{\frac{3.08\alpha\omega}{\omega_M}}$$

or, in terms of fields, by

$$h_{\text{crit}} = \Delta H\sqrt{\frac{3.08\Delta H}{4\pi M}}. \quad (8)$$

This result can also be derived by solving (7) for M_z, and plotting the solution vs H (as in Fig. 1). When

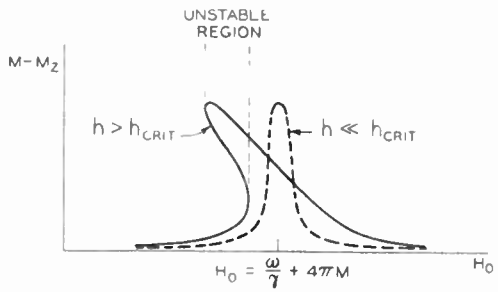

Fig. 1—Anharmonic response of a thin normally magnetized disc due to the dependence of resonant frequency on amplitude. Above the threshold signal, the response curve folds over creating a range of dc fields in which the conventional motion is unstable.

h exceeds h_{crit} it is found that the small signal response is distorted in such a way that M_z is a triple value function of H_0 in a certain region below resonance. Instability may be expected in two of the three possible states. In practice ΔH is, of course, much smaller than $4\pi M$. Therefore (8) predicts that instability can occur at signal powers far below the threshold required for saturation of a sphere. For the conditions of the B.W.-D. experiments, (8) is, in fact, of the order of the signal field at which onset of the premature saturation was noted. The question therefore arises if these observations are in some way related to the instability just discussed. However, most of the experiments were done, not on discs, but on spheres which simply do not show instabilities like discs. It is true that the nonlinear terms arising from the crystalline anisotropy can lead to much the same behavior as predicted for the disc, but for anisotropy fields well below $4\pi M$, the threshold field is much greater than (8), though it may still be less than ΔH. Yet one possibility remains: suppose that the uniform precession of the magnetization of the sphere is perturbed, not uniformly throughout the whole sphere, but only over a thin disc-like stratum normal to the dc field. Such a perturbation is accompanied by a local demagnetizing field, and one may raise the question if the thin stratum might not go unstable just like a real disc. The answer is in the negative unless the stratum is made so thin that exchange effects between it and the remainder of the magnetization are called into play. Crudely, the reason for this is that the stratum is immersed, not in a dc field H_0, but rather into the demagnetized dc field $H_0-4/3\pi M$ prevailing inside the sphere. Our experience with the real disc shows that its instability was confined to dc fields near its resonance field $(\omega/\gamma)+4\pi M$. Hence, by analogy, if the deviation in the stratum is to go unstable it should do so near a field $(\omega/\gamma)+4/3\pi M$, whereas in fact the early onset of saturation was observed at the resonant field of the sphere as a whole, *i.e.*, at ω/γ. However, it will turn out in the next section that a certain disturbance always present in the sphere due to thermal agitation, suffers exchange fields which are just such as to cancel the offending term $4/3\pi M$ in the resonant frequency of the disturbance, and instability can then occur.

II. The Early Onset of Saturation at the Main Resonance

For simplicity it is desirable to consider that the unit vector $\vec{m}_{\text{total}}$ along the total magnetization $\vec{M}$ is disturbed from its "normal" value given by (5), not merely through a thin stratum normal to H_0, but rather throughout the sample, in such a way that the surfaces over which the disturbance $\vec{\delta m}$ has a constant value are planes normal to H_0. Our objective is to write down the equation of motion of the total normalized magnetization $\vec{m}+\vec{\delta m}$ using the equation of motion (1). $\vec{m}$ is to be interpreted as the spatial average through the sample, and $\vec{\delta m}(r)$ the local deviation from the average. The z-component of (1) is redundant, since

$$m_{z\text{total}} = \sqrt{1 - (m_x^2 + m_y^2)_{\text{total}}}.$$

Further, the onset of saturation was observed in a signal range in which it is legitimate to write

$$(m_z)_{\text{total}} = 1 - \tfrac{1}{2}(m_x^2 + m_y^2)_{\text{total}} = 1 - \tfrac{1}{2}(m^+m^-)_{\text{total}}$$

so that

$$\delta m_z = -\tfrac{1}{2}(m^+\delta m^- + m^-\delta m^+).$$

Thus we can restrict ourselves to the x and y components of (1), and must now determine the effective field acting on $\vec{m}+\vec{\delta m}$. Taking the sample to have the shape of a spheroid of revolution about H_0, the effective dc field on the sample is 0, 0, $H_0-4\pi\overline{M}_zN_z$), where $\overline{M}_z$ is the spatial average. Similarly the effective ac field is ($h\cos\omega t-4\pi\overline{M}_xN_T$, $h\sin\omega t-4\pi\overline{M}_yN_T$, 0).[8] The local demagnetizing field caused by the deviation $\vec{\delta m}$ is

$$(0, 0, -4\pi M\delta m_z)$$

provided the spatial variation of δm is sufficiently rapid so that demagnetizing effects due to the poles at the "ends" of the planes of equal δm can be neglected. Finally the exchange effect will make a contribution to the field. If the rate of variation of $\vec{\delta m}$ through the sample is slow compared with the reciprocal lattice spacing this field may be taken in the form[9]

$$H_{ex}\frac{l^2\nabla^2\vec{M}}{M} = H_{\text{ex}}l^2\nabla^2(\vec{m}+\vec{\delta m}) = H_{\text{ex}}l^2\nabla^2\vec{\delta m}$$

where l is the lattice spacing and H_{ex} is an effective "exchange field" given in terms of the exchange integral J, and the ionic spin S by the formula

$$H_{\text{ex}} = \frac{4JS^2}{Ml^3}$$

in the case of a simple cubic lattice. ∇^2 is the Laplacian operator, in the present case simply $\partial^2/\partial z^2$. We also define an exchange frequency

$$\omega_{\text{ex}} = \gamma H_{\text{ex}}.$$

In writing down the equation of motion it is convenient to add j times the y-component-equation of (1) to the x-component equation. Recalling that $\overline{M}_z = Mm_z$ etc., using the reduced notation introduced in (4a), and combining the fields just enumerated, we find, to first order in δm,

$$\begin{aligned}(1 - j\alpha)(\dot{m}^+ + \dot{\delta m}^+) &= j(\omega_H - N_z\omega_M m_z - \omega_{\text{ex}}m_z l^2\nabla^2)(m^+ + \delta m^+) \\ &\quad + j(m_z + \delta m_z)N_T\omega_M m^+ - j\omega_M m^+\delta m_z \\ &\quad - j\omega_s e^{j\omega t} + jm^+\omega_{\text{ex}}l^2\nabla^2\delta m_z. \qquad (9)\end{aligned}$$

[8] Here $N_x = N_y = N_t$.

[9] C. Herring and C. Kittell, "On the theory of spin waves in ferromagnetic media," *Phys. Rev.* vol. 81, pp. 869–881; March, 1951.

Here all nonlinear terms involving the signal, and the loss parameter have been neglected.

Let us now take δm^+ in the form of a standing spin wave:[10]

$$\delta m^+ \sim \cos kz.$$

Then, if in (9), we equate the spatially varying terms we find, since $\delta m_z = -\frac{1}{2}(m^+\delta m^- + m^-\delta m^+)$ also varies as $\cos kz$,

$$\begin{aligned}(1 - j\alpha)\dot{\delta m}^+ &= j(\omega_H - N_z\omega_M m_z + \omega_{\text{ex}}l^2m_zk^2)\delta m^+ \\ &\quad - jm^+(\omega_{\text{ex}}l^2k^2 + \omega_M - N_T\omega_M)\delta m_z\end{aligned}$$

or

$$\begin{aligned}(1 - j\alpha)\dot{\delta m}^+ &= j(\omega_H - N_z\omega_M m_z + \omega_{\text{ex}}l^2m_zk^2)\delta m^+ \\ &\quad + \frac{j}{2}(\omega_{\text{ex}}l^2k^2 + \omega_M - N_T\omega_M) \\ &\quad \cdot [\,|m^+|^2\delta m^+ + (m^+)^2\delta m^-\,]. \qquad (10)\end{aligned}$$

Eq. (10) shows that δm^+ behaves like a damped harmonic oscillator, coupled to a similar oscillator δm^-, and to the uniform precession through the second term on the right-hand side of (10). Leaving aside the small change in frequency due to the term varying as $|m^+|^2\delta m^+$, the natural frequency of the oscillator δm^+ is

$$\omega_k = \omega_H - N_z\omega_M m_z + \omega_{\text{ex}}l^2k^2m_z.$$

In the absence of the coupling term and the loss, δm^+ and δm^- would vary as $e^{j\omega_k t}$, $e^{-j\omega_k t}$ respectively, and their amplitudes would be constants. The coupling term will cause these amplitudes to change. Without further analysis we can say that this change will be substantial, and might even amount to an exponential increase, if the time variation of the coupling term is close to the natural frequency ω_k of δm^+. Now the time variation of $(m^+)^2\delta m^-$ is as $e^{j(2\omega-\omega_k)t}$ and the other coupling term merely detunes δm^+ slightly and can be neglected. Hence a substantial change in the amplitude of δm^+ can be expected when $\omega_k \doteq 2\omega-\omega_k$, *i.e.*, when

$$\omega_k \doteq \omega.$$

But this condition alone is not enough; we further require that the coupling term is large enough to overcome the exponential decay due to the α in (10), and the coupling term will be entirely negligible except close to resonance ($\omega = \omega_{\text{res}} = \omega_H - N_z\omega_M + N_T\omega_M$). Thus we require

$$\omega_k \doteq \omega_H - N_z\omega_M + N_T\omega_M.$$

Replacing m_z by its approximate value, unity, this requires that

$$\omega_{\text{ex}}l^2k^2 \doteq N_T\omega_M. \qquad (11)$$

[10] The use of a standing rather than a traveling wave simplifies the analysis. In general one expands the magnetization in a Fourier series of spin waves, and does not restrict oneself in this way. However, the results are the same.

Setting

$$\delta m^+ = \delta m_0{}^+ e^{j\omega t - \alpha\omega_k t}; \qquad \delta m^- = \delta m_0{}^- e^{-j\omega t - \alpha\omega_k t}$$

$$m^+ = m_0 + e^{j\omega t}$$

in (10), and allowing $\delta m_0{}^+$, $\delta m_0{}^-$ to vary with time, we find

$$\delta \dot{m}_0{}^+ = \frac{j}{2}(\omega_{ex} l^2 k^2 + \omega_M - N_T \omega_M)(m_0{}^+)^2 \delta m_0{}^- e^{2j(\omega-\omega_k)t}$$

terms of order α^2 having been neglected. The exact value of k is critical only in the exponent of the term on the right, in the coefficient we may substitute (11) as if it were true exactly. Then

$$\delta \dot{m}_0 = j\frac{\omega_M}{2}(m_0{}^+)^2 \delta m_0{}^- e^{2j(\omega-\omega_k)t}. \tag{12}$$

Finally, if

$$\delta m_0{}^+ = y e^{j(\omega-\omega_k)t} \qquad \delta m_0{}^- = y^* e^{-j(\omega-\omega_k t)}$$

we obtain

$$\dot{y} + j(\omega - \omega_k)y = j\frac{\omega_m}{2} y^* (m_0{}^+)^2.$$

Eliminating y^* from this, and the complex conjugate equation, we find

$$\left(\frac{d^2}{dt^2} + (\omega - \omega_k)^2 - \frac{\omega_M{}^2}{4}\left| m_0{}^+ \right|^4\right) y = 0.$$

One solution of this equation will increase exponentially with time if $R^2 = (\omega_M{}^2/4)\left| m_0{}^+ \right|^4 - (\omega-\omega_k)^2 > 0$. But this alone is not enough. If the corresponding δm^+ is also to increase exponentially, R must exceed $\alpha\omega_k$. This requires that

$$\left| m_0{}^+ \right|^2 > \frac{2}{\omega_M}\sqrt{(\omega - \omega_k)^2 + \alpha^2\omega_k{}^2}$$

which establishes the instability threshold for $\left| m^+ \right|^2$. Since $\alpha\omega_k$ varies only slowly with k, the threshold is lowest when k is such that $\omega_k = \omega$, and is then $2\alpha\omega_k/\omega_M$. Since $\left| m_0{}^+ \right|^2 = \omega_s{}^2/[\omega - \omega_{res})^2 + \alpha^2\omega^2]$, the threshold signal is given by

$$\sqrt{\frac{2\alpha\omega_k}{\omega_M}[(\omega - \omega_{res})^2 + \alpha^2\omega^2]}$$

which, in turn, is least when $\omega_{res} = \omega$ (at resonance) and is then

$$\omega_{crit} = \alpha\omega\sqrt{\frac{2\alpha\omega_k}{\omega_M}}$$

or, in terms of fields:

$$h_{crit} = \Delta H\sqrt{\frac{2\Delta H_k}{(4\pi M)}} \tag{13}$$

where $\Delta H_k = \alpha\omega_k/\gamma$ is the "linewidth" of the spin wave whose k is given by (11). It is at this point that we can discard the high specialized Landau-Lifshitz term, which forces the loss parameter of the spin wave to have the specific form $\alpha\omega_k$, in favor of a more general form in which

$$a\omega_k \text{ is replaced by } \lambda_k,$$

a yet unknown function of k. The measurements of the threshold field might eventually be used to determine λ_k, as a function of wave number, although for purposes of comparison with existing experiments we are forced to make a guess at λ_k or at $\Delta H_k = \lambda_k/\gamma$. In Table I, the B.W.-D. data of the onset of satura

TABLE I*

$\Delta H = \frac{1}{\gamma T_1}$ (oe.)	RF Threshold field (oe.)		
	Theory	Experimental	
		Bloembergen and Wang	Damon "Sample 7"
51	8.0	9.0	
46	7.0	5.5	
36	5.0	4.0	
23	2.5	1.0	
7	0.45	0.55	≈ 2.0

* Computed and measured threshold signals on the main resonance (when it is distinct from the subsidiary resonance). For definiteness it has been assumed that $\Delta H_k = \Delta H = 1/\gamma T_1$. Agreement is actually not as good as it seems, since the theory assumes circular polarization of the signal, while the measurement referred to linear polarization. The resulting discrepancy is probably due to the uncertainty in ΔH_k, ΔH.

tion are compared with the threshold signal (13), on the assumption that $\Delta H_k = \Delta H$, and that both these quantities are equal to $1/\gamma T_1$. Here T_1 is the relaxation time determined, not from the profile of the absorption line, but from the plot of the observed change in $\overline{M}_z$ with actually dissipated power. ($\delta\overline{M}_z$ must be proportional to the dissipated power, the factor of proportionality depending on T_1.) This method of selecting ΔH was chosen since the line-profile might be complicated by large-scale nonuniformities in the material. Agreement seems rather good. However, the above threshold refers to a circularly polarized signal, whereas the measured signals were linearly polarized. The resulting discrepancy of a factor two might be due to our ignorance concerning the correct value of ΔH_k. Perhaps it is also partly due to uncertainties in the measurement of the precise threshold field.

For an infinitely thin, normally magnetized disc, $N_T = 0$ so that (11) gives $k = 0$. Such a disc therefore goes unstable *as a whole*, in agreement with our earlier observations. However, the threshold (13) differs from the value (8) calculated previously by a numerical factor $\sqrt{2/3.08}$. The reason is to be found in the neglect of the "detuning" term $\sim \left| m^+ \right|^2 \delta m^+$ in (10). If $N_T \neq 0$ so that $k \neq 0$, this detuning can be absorbed by a slight adjustment of k. When $N_T = 0$, such an adjustment is impossible, so that the detuning cannot be neglected.

Analysis shows that it is, indeed, responsible for the change in the numerical factor, as well as for the fact that the minimum threshold (8) applies just below, rather than exactly at, resonance, as in other geometries. This point is, of course, purely academic; for all practicable geometries, the threshold (13) is correct, since (11) always gives a wavelength $2\pi/k$ much less than the practicable sample dimensions. (For the sphere $2\pi/k$ is of the order of about thirty lattice spacings.)

III. The Degenerate Spin Wave Spectrum

We have found that a small-amplitude, z-directed-spin wave of wave number k has a natural frequency

$$\omega_k = \omega_H - N_z\omega_M + \omega_{ex}l^2k^2. \tag{14}$$

The reader familiar with spin-wave theory will note that (14) differs from the conventional formula for ω_k, which is

$$\omega_k = \omega_H + \omega_{ex}l^2k^2 \tag{15}$$

for z-directed spin waves.[9] However, examination of the literature shows that (15) was derived for the infinite medium. The extra term $-N_z\omega_M$ occurring in (14) is simply due to the fact that the spin waves move, not simply in the dc field H_0, but rather in a field $H_0 - 4\pi N_zM$ reduced by the pole distribution on the surface due to the mean magnetization. (14) has a very important implication that we have already used in the preceding section: it tells us that the natural frequency of the uniform precession, $\omega_H-(N_z-N_T)\omega_M$ is always synchronous with the natural frequency ω_k of a z-directed spin wave with wave number given by (11). This means that the transfer of energy from the uniform precession to the spin wave (11) is easy, given a suitable coupling mechanism. In the preceding section the coupling term arose from the essential nonlinearity of the motion of the total $\vec{M}$, and increased with increasing signal, until it became "catastrophic." Below the threshold there is still a transfer of energy, but it then only gives a very small signal-dependent contribution to the loss-parameter of the uniform precession. However, other coupling effects, such as arise, for example, from the random irregularities inherent in the inverted spinel structure, can couple the uniform precession to the spin wave in question and will lead to a signal-independent (and only indirectly temperature dependent) line-width.[11] Actually, not only z-directed spin waves are degenerate with the uniform precession. The generalization of (14) to spin waves whose $\vec{k}$-vector makes an angle θ with the z direction is (refer to Fig. 2)

$$\omega_k^2 = (\omega_H - N_z\omega_M + \omega_{ex}l^2k^2)(\omega_M - N_z\omega_M + \omega_{ex}l^2k^2 + \omega_M\sin^2\theta). \tag{16}$$

[11] A. M. Clogston, H. Suhl, L. R. Walker, and P. W. Anderson, "A possible source of line width in ferromagnetic resonance," *Phys. Rev.* vol. 101, pp. 903–904; 1956.

The equality

$$\omega_{res} = \omega_k$$

therefore is true over a whole surface of revolution in $\vec{k}$-space, and in the calculation of linewidth due to irregularities, the energy removed from the uniform precession distributes itself over the whole degenerate manifold.[12] From thereon it is presumably dissipated by interaction with other spin waves and, perhaps to a lesser extent, by direct interaction with the lattice. Similarly the question arises if degenerate spin waves along directions other than $0z$ could go unstable, perhaps at a lower threshold signal than (13). However, it can be shown that, at resonance, z-directed spin waves do indeed have the lowest threshold, and the indications are (see Section VI) that only spin waves close to the z-direction play any significant part even beyond the threshold signal.

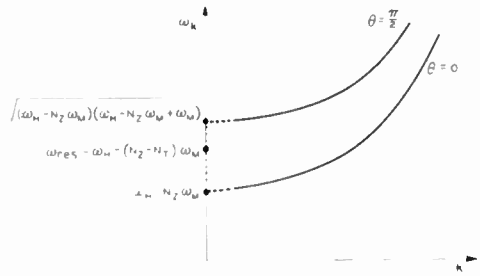

Fig. 2—The spin-wave spectrum. The usual resonant frequency will always be degenerate with spin waves of many wavelengths and propagation directions except for the infinitely thin, normally magnetized disc. In the cross-hatched region, spin waves are not strictly correct modes of the system.

Finally we must draw attention to a difficulty we have so far ignored. We have presupposed that a small, free disturbance in the sample will have the form of a spin wave. But this is not strictly correct. Leaving aside losses, exchange fields, and any coupling to the uniform precession, the actual "natural modes" in the linear approximation are found by solving the linearized form of (1)

$$\dot{\vec{\delta M}} = -\gamma\{(H_0 - 4\pi N_zM)[\vec{\delta M}\times\vec{i_z}] - M[i_z\times\vec{h_d}]\} \tag{17}$$

where $\vec{i_z}$ is a unit vector in the z-direction, and $\vec{h_d}$ is the demagnetizing field, $\vec{h_d}$, due to $\vec{\delta M}$. This is found from the requirement that the divergence of the flux due to $\vec{\delta M}$ should vanish

$$\operatorname{div}\vec{b} = \operatorname{div}(\vec{h_d} + 4\pi\vec{\delta M}) = 0. \tag{18}$$

Since electromagnetic propagation effects are usually negligible in sufficiently small samples, $\vec{h_d}$ will be the gradient of a scalar potential ϕ:

[12] The case of the normally magnetized infinitely thin disc is an exception. Its resonance frequency $\omega_H-\omega_M$ is situated at the lowest point ($k=0$, $\theta=0$) of the spin wave spectrum. The degenerate manifold then shrinks to a point.

$$\vec{h}_d = \nabla\phi$$

since curl $\vec{h}_d = 0$. Hence (18) gives

$$\nabla^2\phi = -4\pi \operatorname{div} \delta\vec{M}. \tag{19}$$

For small disturbances we may write $\delta\dot{\vec{M}} = j\omega\delta\vec{M}$, and then (17) and (19), subject to the boundary conditions that the tangential component of $\vec{h}_d$ and the normal component of $\vec{b}$ should be continuous at the boundary of the sample, determine the correct normal modes of the system and their corresponding eigenvalues ω. This problem has been solved only recently by Dr. L. R. Walker.[13] The correct modes turn out to be superpositions of spherical harmonics and are specified by three numbers (in place of the three components of $\vec{k}$). The eigenvalues ω have certain features in common with ω_k. For example, no ω is less than the least possible value of ω_k,

$$\omega_k(\min) = \omega_H - N_z\omega_M.$$

The failure of spin waves to represent the true modes of the medium need not trouble us however, as long as their wavelength is short compared with the sample dimensions. Their failure to satisfy the boundary conditions could be remedied by placing at the intersections of the surfaces of equal phase with the sample boundaries a suitable distribution of small poles of alternating sign. Since the sign of these poles will vary over the surface with essentially the rate $|k|$, their field will not propagate any appreciable distance into the medium if k is large enough. Therefore they can be omitted altogether without appreciably upsetting the spin waves well inside the material. In Section II, k was of order $(1/l)\sqrt{4\pi M/H_{ex}}$, which for $H_{ex}\sim 3\times 10^7$ oe, $4\pi M\sim 3000$ oe, $l\sim 10$ Å, corresponds to a wavelength of about 1000 Å. This is much smaller than the linear dimensions of any practicable sample, and the spin-wave view is therefore quite justified. On the other hand, in the next section we shall encounter instabilities of spin waves with very long wavelengths, so that the true modes ought to be used there. The problem discussed in the next section can, in fact, be solved formally in terms of these modes, but progress beyond the formal solution is difficult since knowledge of certain necessary integrals involving them is still lacking. Hence we have to rely on the rather good agreement between observation and the spin-wave hypothesis to indicate that the picture does not change greatly, no matter what modes are used.

IV. The Subsidiary Absorption

So far we have presented strong evidence that the early decline of χ'' for the main resonance is due to unstable growth of a certain z-directed spin wave due to coupling to the uniform precession. This suggests that the appearance of the subsidiary absorption peak might be explained by some other form of instability. It turns out that such an instability is found among spin waves that are not z-directed.

Let us again consider a spheroid and single out a disturbance $\delta\vec{M}$ whose components vary with position as $\delta\vec{M}_k \cos(\vec{k}\cdot\vec{r})$ where now $\vec{k}$ is some vector not necessarily directed along $0z$. Just like the deviation considered in Section II, the total magnetization $\vec{M}+\delta\vec{M}$ finds itself immersed in an average field ($h\cos\omega t - N_T\overline{M}_x$, $h\sin\omega t - N_T\overline{M}_y$, $H_0 - N_z\overline{M}_z$), in the exchange field, and in the demagnetizing field due to the deviation $\delta\vec{M}$ from the spatial mean $\vec{M}$. The last-mentioned field is of course no longer $-4\pi\delta M_z$, since the planes of equal δM are no longer normal to the z-direction. But it can easily be calculated from (19), if the boundary conditions are disregarded (see end of Section III), (19) immediately gives

$$\phi = 4\pi \frac{(\delta\vec{M}_k\cdot\vec{k})\sin\vec{k}\cdot\vec{r}}{k^2}$$

so that the demagnetizing field is

$$\vec{h}_d = -4\pi \frac{\vec{k}(\delta\vec{M}_k\cdot\vec{k})\cos\vec{k}\cdot\vec{r}}{k^2} = -4\pi\vec{k}\frac{(\delta\vec{M}\cdot\vec{k})}{k^2} \tag{20}$$

where $k^2 = k_x^2 + k_y^2 + k_z^2$. $\vec{h}_d$ is thus directed along $\vec{k}$. The demagnetizing field $(0, 0, -4\pi\delta M_z)$ previously discussed is, of course, the special case of (20) in which $\vec{k}$ is z-directed. In our reduced notation (4a), $\delta M_z \sim m^+\delta m^- + m^-\delta m^+$, and hence in Section II, the coupling of δm to the uniform precession varied as $m^+(m^+\delta m^- + m^-\delta m^+)$, that is to say, *quadratically* in the uniform precession. In the more general case (20), the coupling still varies as m^+h_{dz}, which is now proportional to

$$m^+k_z\frac{\frac{1}{2}(k^+\delta m^- + k^-\delta m^+) + k_z\delta m_z^-}{k^2}$$

where $k^+ = k_x + jk_y$, $k^- = (k^+)^*$, so that we now also have coupling terms, like $m^+\delta m^-$, which are *linear* in the uniform precession. For the moderate signal amplitudes at which the strange effects of the B.W.-D paper are observed, m^+ is larger by an order of magnitude than $(m^+)^2$, so that at any given dc field the generally directed spin waves are inherently more tightly coupled to the uniform precession than are z-directed waves. However, the coupling terms linear in m^+ cannot, except under special conditions, be synchronous with the natural frequency, ω_k, of δm^+ when the dc field is adjusted for resonance and cannot lead to instability there (see, however, section V). In the more usual experiment such

[13] L. R. Walker, "Resonant modes of a ferromagnetic spheroid," *Bull. Amer. Phys. Soc.*, Pittsburgh Meeting, p. 125; March, 1956.

synchronism will occur only at dc fields some hundreds of oersteds below resonance. These relationships are made evident by the analysis, which is simplified by the fact that the exchange field will produce only coupling terms that are second order in m^+, m^-. Substitution of the fields in the equations of section I now leads to

$$(1-j\alpha)\delta\dot{m}^+ = jA_k\delta m^+ + jB_k\delta m^- - j\frac{\omega_M k_z}{2k^2}(km^+ + k^+m^-)\delta m^+ - j\omega_M\frac{k_z k^+}{k^2}m^+\delta m^- + \text{terms quadratic in } m^+, m^- \quad (21)$$

where the real number A_k is given by

$$A_k = \left(\omega_H - \omega_M N_z + \omega_{ex}l^2k^2 + \omega_M\frac{|k^+|^2}{2k^2}\right) \quad (22)$$

and the complex number B_k by

$$B_k = \frac{\omega_M(k^+)^2}{2k^2}. \quad (23)$$

Nonlinear terms involving α and h have been neglected in deriving (21). Terms quadratic in m^+, m^-, arising from δm_z, and from the exchange will now also be discarded.

In contrast with z-directed spin waves, for which $A_k=\omega_k$ and $B_k=0$, the oscillator δm^+ is connected with δm^- even if the coupling to m^+ and m^- is neglected. Therefore δm^+ will no longer vary as $e^{j\omega_k t}$ even in the absence of the latter coupling. This corresponds to the fact that spin waves other than z-directed ones cannot be circularly polarized. Before proceeding with the analysis of (21) it will be found convenient to change first to circularly polarized variables by means of the transformation

$$\delta m^+ = a_k\delta n^+ - b_k\delta n^- \quad (24)$$

where, in terms of an auxiliary parameter ψ_k,

$$a_k = \cosh\frac{\psi_k}{2}; \quad b_k = \sinh\frac{\psi_k}{2}e^{2j\phi_k}(1+j\alpha)$$

with

$$\cosh\psi_k = \frac{A_k}{\omega_k}; \quad \sinh\psi_k = \frac{|B_k|}{\omega_k}; \quad \tan\phi_k = \frac{k_y}{k_x}$$

$$\omega_k^2 = A_k^2 - |B_k|^2 = \left((\omega_H - \omega_M N_z + \omega_{ex}l^2k^2)(\omega_H - \omega_M N_z + \omega_{ex}l^2k^2 + \omega_M\frac{|k_+|^2}{k^2})\right). \quad (25)$$

Substituting (24) in (21) we readily find that, to order α, and in the absence of the coupling terms to m,

$$\delta\dot{n}^+ = (j\omega_k - \alpha A_k)\delta n^+$$
$$\delta\dot{n}^- = (-j\omega_k - \alpha A_k)\delta n^-.$$

Thus δn^+ varies as $\delta n_0{}^+e^{(j\omega_k-\alpha A_k)t}$ and δn^- as its complex conjugate, where $\delta n_0{}^+$ is a complex constant. In the presence of the coupling, the solution can still be taken in this form, but now $\delta n_0{}^+$ will no longer be constant. Substituting (24) in (21), and eliminating $\delta\dot{n}_0{}^-$ from it and the complex conjugate equation, we find

$$\delta\dot{n}_0{}^+ = -j\frac{\omega_M k_z}{2k^2}\left[(k^-m^+ + k^+m^-)\cosh\psi_k - (k^+m^+e^{-2j\phi_k} + k^-m^-e^{2j\phi_k})\right]\delta n_0{}^+ - j\frac{\omega_M k_z}{k^2}\left[k^+m^+a_k^2 - a_k|b_k|e^{2j\phi_k}(k^-m^+ + k^+m^-)\right]\delta n_0{}^-e^{-2j\omega_k t} \quad (26)$$

In deriving (26) all terms of order α have been neglected. This is legitimate, since the really significant decay constant $-\alpha A_k$ is already included in the expression for δn^+ in terms of δn_0. Hence even if terms of order α in (26) should give additional losses, these will be unimportant.

The general solution of (26), even if it could be written down must of necessity be very complicated. Further progress must therefore involve an intuitive guess at the sort of time-variation δn_0 will undergo as the result of the coupling terms. One such guess is that δn_0 will oscillate only slightly about some mean value which changes slowly compared with $e^{j\omega t}$, $e^{j\omega_k t}$ etc. Then it will be legitimate to neglect those terms on the right-hand side of (26) that have coefficients varying rapidly with time (at rates ω, ω_k etc.). The solution $\delta n_0(t)$ is then an average over a time interval about t which is long compared $1/\omega$, $1/\omega_k$, but still short on the time scale on which the amplitude variation is being studied. The various coefficients on the right-hand side of (26) vary as $e^{j\omega t}$, $e^{-j\omega t}$, $e^{-j(\omega+2\omega_k)t}$, $e^{j(\omega-2\omega_k)t}$. Of these only the last term can vary slowly, and then only if k is such that

$$2\omega_k \doteq \omega.$$

Omitting all other terms in (26), we arrive at

$$\delta\dot{n}_0{}^+ = -j\frac{\omega_M k_z|k^+|e^{j\phi_k}}{k^2}a_k(a_k - |b_k|)m_0{}^+\delta n_0{}^-e^{-j(2\omega_k-\omega)t} = -j\frac{\omega_M k_z|k^+|}{k^2}e^{j\phi_k}\left(\cosh\frac{\psi_k}{2}\right)\cdot e^{-\psi_k/2}m_0{}^+\delta n_0{}^-e^{-j(2\omega_k-\omega)t} \quad (27)$$

Setting

$$\rho_k = -j\omega_M\frac{k_z|k_+|}{k^2}e^{j\phi_k}\left[\cosh\frac{\psi_k}{2}\right]e^{-\psi_k/2}$$

and

$$\delta n_0{}^+ = Ue^{i((\omega/2)-\omega_k)t}; \qquad \delta n_0{}^- = U^*e^{-i((\omega/2)-\omega_k)t}$$

we obtain

$$\left[\frac{\partial^2}{\partial t^2}+\left(\frac{\omega}{2}-\omega_k\right)^2-\rho_k\rho_k^*\left|m_0^+\right|^2\right]U=0. \quad (27a)$$

Returning to the original variable

$$\delta n^+ = Ue^{j(\omega/2-\omega k)t+j\omega kt-\alpha Akt} = Ue^{((\omega/2)-\alpha Ak)t},$$

we see that an exponentially increasing n^+ becomes possible when

$$\left|m_0^+\right|^2 > \frac{\left(\frac{\omega}{2}-\omega_k\right)^2+\alpha^2A_k^2}{\rho_k\rho_k^*} \quad (28)$$

The threshold on the right-hand side can now be minimized with respect to k. Since αA_k, and in all probability also any more general loss-parameter λ_k replacing it, varies only slowly with k, (28) will be very nearly smallest when k is such that

$$\omega_k=\frac{\omega}{2}. \quad (29)$$

This equation defines a surface in k space, on which αA_k and $\rho_k\rho_k^*$ will vary in some manner, so that the threshold can be further reduced by minimizing the remaining expression

$$\frac{\alpha^2A_k^2}{\rho_k\rho_k^*} \quad (30)$$

further with respect to k, subject to the restriction (29). But the actual state of affairs is not as simple as that. Let us trace the variation of the threshold (30) as the applied dc field, and hence ω_H, is increased from zreo towards resonance. For small ω_H, (29) always determines a positive value of k^2, that is, a real spin wave, for any value of the angle θ between $\vec{k}$ and the z-direction. In fact, using (16), we find that (29) reduces to

$$\omega_{ex}l^2k^2 = N_z\omega_M-\frac{\omega_M}{2}\sin^2\theta+\frac{1}{2}\sqrt{\omega_M^2\sin^4\theta+\omega^2}-\omega_H \quad (31)$$

which gives a real value of k for all θ if ω_H is small enough. Hence we can minimize (30) with respect to θ after expressing k, wherever it occurs, in terms of θ from (31). Let θ_1 denote the value of θ which minimizes (30). Since the longitude ϕ_k of $\vec{k}$ does not enter (30), or (31), it follows that the spin waves that first go unstable have k vectors that lie on a cone of angle θ_1. Their wavelength is given by (31), with $\theta=\theta_1$, and their threshold signal is given by

$$\omega_s(\text{crit}) = \left(\frac{\alpha A_k}{\sqrt{\rho_k\rho_k^*}}\right)_{\theta=\theta_1}\sqrt{(\omega-\omega_{res})^2+\alpha^2\omega^2}. \quad (32)$$

Eq. (32) continues to hold as ω_H is increased until it reaches a value at which (31), with $\theta=\theta_1$, gives $k^2=0$. For the typical situation (nickel or manganese ferrite spheres at 10 kmc or higher frequencies) this value is below reasonance by some hundreds of Gauss. Further increases of ω_H then would yield imaginary k's. From that point onwards, the threshold is found by solving (31), for θ in terms of ω_H, with k^2 equated to zero. It then becomes

$$\omega_s(\text{crit}) = \left(\frac{\alpha A_k}{\sqrt{\rho_k\rho_k^*}}\right)_{\substack{\theta=\theta(H)\\k=0}}\sqrt{(\omega-\omega_{res})^2+\alpha^2\omega^2}. \quad (33)$$

This equation represents the threshold until (31) with $k^2=0$, ceases to yield a real value of θ. This first happens when $\theta=0$ and

$$\omega_H=\tfrac{1}{2}\omega+N_z\omega_M. \quad (34)$$

But then $\rho_k\rho_k^*=0$ so that the threshold has become infinitely large. For the usual situation just referred to, (34) is still somewhat below resonance. Fig. 3 shows the

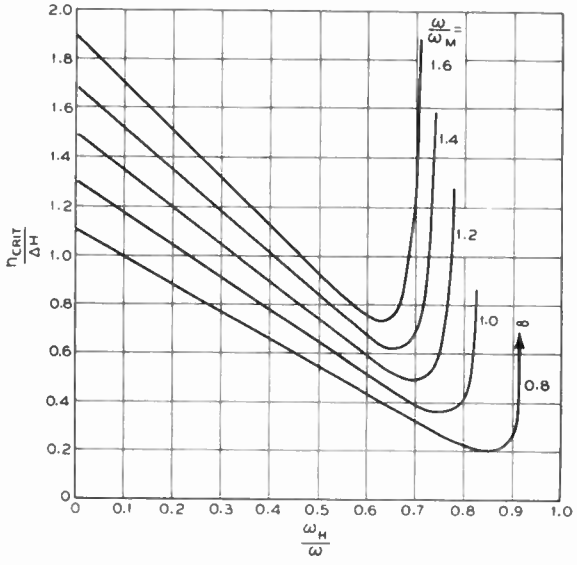

Fig. 3—Threshold signal for instability associated with the subsidiary absorption in a sphere. For definiteness, the loss-term has been taken in the Landau-Lifshitz form here. The straight portion of each curve corresponds to the threshold given by (32), the remainder corresponds to (33).

course of the threshold field from $\omega_H=0$ to ω_H given by (34), on the assumption that the Landau-Lifshitz loss term (2) is actually correct so that the loss parameter of the $\vec{k}$th spin wave is literally taken to be αA_K. Of course the curves of Fig. 3 will not be reliable for values of H_0 less than the minimum required for saturation.

One obtains, as a by-product, the dc field at which the threshold is least, and at which the subsidiary absorption will therefore first appear as the signal is raised. The curves shown in a previous publication[14] show this critical dc field for some common situations. The comparison of the calculated dc fields at the subsidiary peak

[14] Suhl, *op. cit.*, Fig. 1.

with the observations is shown in Table II. In all these cases, the critical field is always in the range for which $k=0$, so that the critical spin waves are very long. Therefore the "true" modes should really have been used in the analysis (see the remarks at end of Section III).

TABLE II*

	Theory	Cavity experiments of Bloembergen and Wang
Ni—ferrite sphere $4\pi M \approx 3320$ oe	0.83	0.73
Mn—ferrite disc $4\pi M \approx 3880$ oe		
$H\parallel$ disc	0.78	0.66
$H\perp$ disc	0.72	0.72
$4\pi M$	Theory	Waveguide experiments of M. T. Weiss (unpublished) at 9 kmc on various ferrites
$H\parallel$ slab 1100	0.51	0.42
$H\parallel$ slab 1600	0.55	0.50
$H\parallel$ slab 2900	0.69	0.65
$H\perp$ slab 1600	0.65	0.62

* Comparison of predicted and measured ratio of field at subsidiary resonance to the field required for the main resonance.

Strictly speaking, since the Landau-Lifshitz loss term is probably not correct αA_k should be replaced by an unknown function λ_k, of $\vec{k}$, and the minimization procedures should then determine λ_k by comparison with experiment. No such measurements are available as yet. Hence it is desirable to restate the threshold in an approximate form, for practical estimates. In terms of fields we may write

$$h_{crit} \doteq \frac{\Delta H_k}{4\pi\gamma M}\, g(\theta)\sqrt{(\omega-\omega_{res})^2+\gamma^2\Delta H^2}$$

where $g(\theta)$ is a function of θ that decreases from $+\infty$ at $\theta=0$ to a minimum of order unity, then rises again to $+\infty$ as θ approaches $\pi/2$. ΔH_k may be replaced by ΔH, the linewidth of the uniform procession, for order of magnitude estimates. ω_H may be assessed by writing $k=0$ and $\theta=45°$ in the formula

$$\omega_k = \frac{\omega}{2}.$$

V. Coincidence of Subsidiary and Main Resonance

For certain favorable experimental arrangements, and certain relative values of ω, ω_M, the range in which the subsidiary instability can occur extends through the main resonance. Then the instability discussed in Section II becomes unimportant compared with that of the last section, since the former involves terms quadratic, rather than linear, in the uniform precession. For a spheroid at resonance

$$\omega = \omega_{res} = \omega_H - N_x\omega_M + N_T\omega_M$$

The upper limit (34) of the relation $\omega_k=\omega/2$ will therefore be above resonance if

$$N_T\omega_M > \frac{\omega}{2}. \tag{35}$$

Should this condition hold, the threshold is least very nearly at resonance, unless (35) is "only just" satisfied. The reason is that the radicand in (33) reaches a rather sharp minimum at $\omega_{res}=\omega$, whereas the coefficient of the square root varies only slowly with ω_H. The same applies if conditions are such that (32) holds at resonance. The threshold signal is thus particularly low, of order $\Delta H_k\Delta H/4\pi M$.

Since no such experiment was found in the literature, a measurement was made to check this prediction. The sample was a thin disc, magnetized in its own plane. This geometry is not spheroidal about the z axis, but it is easily established (by using $\omega_{res}=\sqrt{\omega_H(\omega_H+\omega_M)}$ that the condition for coincidence becomes

$$\omega_M > \frac{3}{2}\,\omega \tag{36}$$

instead of (35). In a manganese ferrite disc ($4\pi M\sim 3300$) this condition holds up to about 7 kmc. The frequency used in the experiment was 4 kmc, and the threshold was indeed found to be extremely low, of the order of one hundredth of an rf oersted. Here the threshold manifests itself, not as an extra absorption at resonance, but on the contrary, as a decline in the susceptibility. The reasons for this will be discussed in the next section.

VI. The State of the Magnetization Beyond the Instability Threshold

So far we have established only that the conditions under which strange effects are observed are also the conditions under which certain spin-wave disturbances will grow in an unstable manner. We must now establish a theory predicting the observed behavior beyond the threshold signal. At first sight this may seem a hopeless task, since the situation bears a certain resemblence to the turbulance problem in fluid dynamics. There, too, certain wavelike disturbances can grow exponentially when the velocity of suitable types of laminar flow exceeds a critical value. The theory of the ensuing turbulent state is extremely difficult, and to this day involves an element of arbitrariness. However, the case of the subsidiary absorption, and, to a lesser extent, that of the main resonance, enjoys certain simplifying features that make possible a rigorous theory of the final steady state. Still, the theory for the main resonance beyond the threshold is beset with some arithmetical difficulties. We shall, therefore, confine the discussion to the subsidiary resonance both in the case in which it is separate from, and in the case in which it coincides with, the main resonance.

So far our problem has been linear in a certain sense. The deviation δm was considered to be so small, up to

the onset of instability, that terms of second order in $\delta\vec{m}$ were neglected. The uniform precession $\vec{m}$ was assumed to be unaffected by δm and to be given by the standard small-signal theory. But in actual fact, the equation of the uniform precession contains second-order coupling terms to δm. These are negligible below the threshold. But beyond it they become large, and their effect on the uniform precession is, roughly speaking, to increase its dissipation. The problem is then truly nonlinear, but still not unsolvable provided we ask sufficiently simple questions. Before describing the mathematical steps involved in the solution we shall give an outline of the underlying physical process.

When an rf pulse not too far above the threshold signal is applied to the sample, the uniform precession will tend to build up to the value given by the conventional theory within a time of order $1/\gamma\Delta H$. As is readily verified from Section IV, the rate of buildup of the appropriate spin waves (always present due to thermal agitation) is much slower. Hence initially the precession angle is given by the conventional theory. However, gradually the relevant spin waves increase at the expense of the uniform precession. As the latter declines, so does the rate of increase of the spin waves, until finally, the uniform precession is reduced to a value just below critical. Then no further increase in the spin wave level takes place, and the final steady state is attained. An exact theory of the complete course of the transient would be very difficult to derive; however the final steady state can be evaluated by performing the following idealized experiment:

We begin by placing the sample into an extremely small signal field. The sample is always in a state of thermal agitation, which may be analyzed into a Fourier series of spin waves. To describe this thermal excitation we imagine that each spin wave is excited by a thermal driving field just sufficiently large to maintain the mean square amplitude of the spin wave at its thermal equilibrium level in the face of the dissipative term (expressed by λ_k) that tends to diminish it. The eventual origin of this thermal field is the coupling of the spins to the lattice vibrations, but its detailed form need be of no concern to us. The spin waves, excited to their thermal level in this way are coupled into the equation of the uniform precession in such a way as to enhance the dissipation to a very slightly higher value. Suppose that the signal is now increased in a series of infinitesimal steps, with a pause after each step to permit establishment of the new steady state. As it has turned out, the coupling of the uniform precession to the spin waves is such as to reduce the loss-parameter of these waves. Since the thermal driving field is not affected thereby (if the thermal reservoir has infinite capacity), their level of excitation is therefore raised. The additional losses in the uniform precession therefore experience a further very slight increase. This increase in the loss continues to be negligible until the signal field approaches the threshold to within about one thermal field. Then the loss-parameter of the critical spin waves (those that show instability for the least signal) becomes very small and hence the losses to the uniform precession very large. The precession angle, and therefore m^+ will be prevented from increasing any more. Further additions to the signal bring m^+ closer to its threshold, but then the losses to the uniform precession also increase further so that the uniform precession still cannot increase beyond the threshold. The excess signal is thus diverted entirely into the critical spin waves (or rather into spin waves whose k-values are confined to very thin conical shell of k numbers about the critical angle θ), and the uniform precession angle remains "stuck" just below its threshold. This situation represents the final steady state at any power level in excess of the threshold power. As the algebra will show, the range of the signal field over which the state changes from the usual one to the new regime is extremely small, of order of one thermal field.

Once we accept the new regime, the calculation of the new susceptibility presents no further difficulty. The uniform precession has a loss parameter given by $\Gamma=\alpha\omega$ +loss due to the spin wave excitation, and $|m^+|^2$ is "stuck" at the threshold value $|m^+|^2$ obtained by minimizing (30) appropriately. Thus we have

$$|m^+|_{\text{crit}}^2 = \frac{\omega_s^2}{(\omega-\omega_{\text{res}})^2+\Gamma^2}.$$

This is an equation for Γ as a function of signal level. If on the other hand we relate $|m^+|^2_{\text{crit}}$ to the threshold signal by:

$$|m^+|_{\text{crit}}^2 = \frac{\omega_s^2{}_{\text{crit}}}{(\omega-\omega_{\text{res}})^2+\alpha^2\omega^2}\text{[15]}$$

we find

$$\Gamma^2 = \frac{\omega_s^2}{(\omega_s)^2_{\text{crit}}}\left[\alpha^2\omega^2+(\omega-\omega_{\text{res}})^2\right]-(\omega-\omega_{\text{res}})^2.$$

The susceptibility is now, in arbitrary units

$$\chi'' = \frac{\omega_M\Gamma}{(\omega-\omega_{\text{res}})^2+\Gamma^2} = \frac{\omega_M\sqrt{(\omega-\omega_{\text{res}})^2\left(\frac{\omega_s^2}{(\omega_s)^2_{\text{crit}}}-1\right)+\alpha^2\omega^2\frac{\omega_s^2}{(\omega_s)^2_{\text{crit}}}}}{\frac{\omega_s^2}{(\omega_s)^2_{\text{crit}}}\left[(\omega-\omega_{\text{res}})^2+\alpha^2\omega^2\right]}.$$

Below the threshold χ'' has the ordinary value, given in the same units by

$$\chi_0'' = \frac{\omega_M\alpha\omega}{(\omega-\omega_{\text{res}})^2+\alpha^2\omega^2}.$$

Hence the ratio of the susceptibility in the high level to that in the small signal state is

[15] This equation must hold an infinitesimal distance below the threshold, since the contribution of the spin wave level to the losses is still negligible there.

$$\frac{\chi_P''>P_{crit}}{\chi_0''} = \frac{1}{\alpha\omega}\cdot\frac{\sqrt{(\omega-\omega_{res})^2\left(\frac{P}{P_{crit}}-1\right)+\alpha^2\omega^2\frac{P}{P_{crit}}}}{\frac{P}{P_{crit}}} \quad (37)$$

where

$$\frac{P}{P_{crit}} = \left(\frac{\omega_s}{(\omega_s)_{crit}}\right)^2$$

is the power ratio. We can now specialize (37) to our two situations. If the subsidiary absorption occurs well below the main resonance, then for P only slightly in excess of P_{crit}, the second term in the radicand is negligible and

$$\frac{\chi'' P > P_{crit}}{\chi_0''} = \frac{1}{\alpha\omega}(\omega-\omega_{res})\frac{\sqrt{\frac{P}{P_{crit}}-1}}{\frac{P}{P_{crit}}}. \quad (38)$$

This expression rises from zero (since we have neglected the second term in the radicand) at $P=P_{crit}$ to a maximum $(\omega-\omega_{res})/2\alpha\omega$ at $P=2P_{crit}$, that is 3 db above critical power, and then declines steadily to aero. Fig. 4 shows

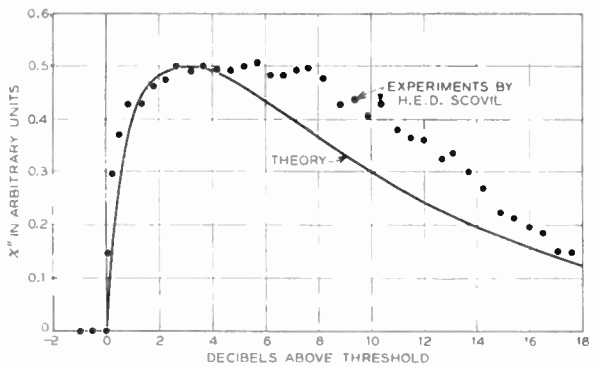

Fig. 4—Comparison of experiment and theory for the final state of the subsidiary absorption above the threshold field. The measurements were made on a manganese ferrite sphere, placed into a cavity tuned to 9300 mc per second. The power source was a pulsed magnetron. Subsidiary and main resonance were distinct in this case.

the predictions of the theory and the experimental results, measured by Dr. Scovil of Bell Telephone Laboratories, on a sphere of manganese ferrite at 10 kmc. Agreement is good except on the high power side of the peak. There Dr. Scovil observed further instabilities setting in at higher thresholds, which seem to enhance χ''. These are not yet understood. Quite possibly they are caused by the unstable growth of further spin waves that begin to feed on those on the critical cone, when the power level is high enough.[16] The agreement is also quite good with the change in $\overline{M}_z$ reported in the B.W.-D-papers for the subsidiary absorption. Since $\delta M_z \sim P\chi''$,[17] δM_z should change as

$$\sqrt{\frac{P}{P_{crit}}-1}.$$

Fig. 5 shows the agreement with the theory, in arbitrary units of δM_z.

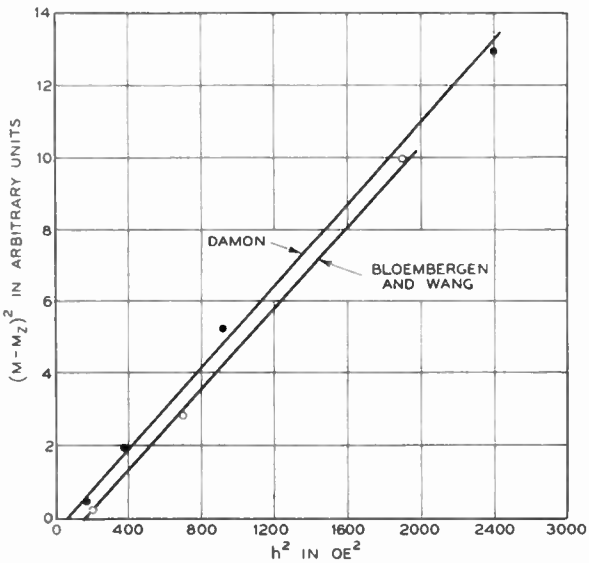

Fig. 5—$(\overline{M}_z-M)^2$ in arbitrary units, vs signal power for the Damon and the Bloembergen-Wang experiments on the subsidiary absorption in high resistivity nickel ferrite samples. Both sets of measurements agree fairly well with the predicted linear relation. However, the thresholds appear to have been different in the two samples.

The case in which the subsidiary peak coincides with the main resonance gives according to (37), with $\omega_{res}=\omega$,

$$\frac{\chi_P''>P_{crit}}{\chi_0''} = \frac{1}{\sqrt{\frac{P}{P_{crit}}}} \quad (38a)$$

so that χ'' declines steadily as $1/\sqrt{P}$ in this case. Fig. 6 shows that agreement of this formula with the authors measurement is good for manganese ferrite, less good for nonstoichiometric nickel ferrite, for which the decline in χ'' is too slow. This may be due to nonuniformities in the material which may cause different portions of the material to have different thresholds. The result would clearly be a diminished rate of decline of χ''.

We now sketch very briefly the mathematical analysis required in the proof that the uniform precession saturates at the critical precession angle. Inasmuch as all spin waves, not just one, are coupled back to the uniform precession, we have to expand the total magnetization into a complete series of spin waves, extended over the reciprocal lattice. Also, since the amplitudes of the spin

[16] They may also be connected with unstable growth of certain of the *true* modes.

[17] For the subsidiary peak, this is only approximately true, for reasons which become apparent in an analysis relating δM_z to the total dissipated power.

waves, at least collectively, become comparable with the uniform precession near the threshold, the δm-notation is really inappropriate. However for continuity with the preceding sections, we now write

$$\vec{m}_{\text{total}} = \vec{m} + \sum_k \delta m_k e^{j(\vec{k}\cdot\vec{r})}$$

and correspondingly

$$m_{\text{total}}{}^+ = m^+ + \sum \delta m_k{}^+ e^{j(\vec{k}\cdot\vec{r})}$$
$$m_{\text{total}}{}^- = m^- + \sum \delta m_k{}^- e^{-j(\vec{k}\cdot\vec{r})}$$
$$= m^- + \sum \delta m_{-k}{}^- e^{j(\vec{k}\cdot\vec{r})}.$$

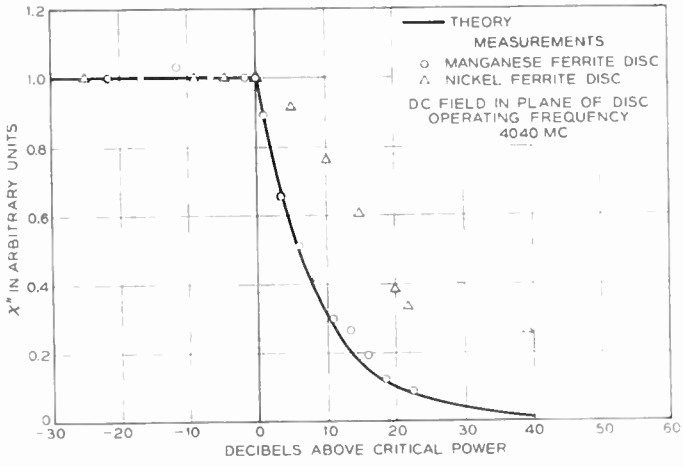

Fig. 6—Comparison of the theory with the author's measurements when the subsidiary and main resonance coincide, and the threshold signal is very low. Agreement is good for manganese ferrite, poor for nickel ferrite. This might be due to the fact that the nickel ferrite was highly nonstoichiometric ($Ni_{.75}Fe_{2.25}O_4$).

This more general formulation in no way affects the calculation of the threshold fields in both types of instability, since that calculation was linear in δm, so that coupling between δm's of different k-numbers was neglected. The only very slight modification that is needed is due to the fact that we now use traveling waves. This only requires replacement of δm^- in (10) and (21) by $\delta m_{-k}{}^-$. δm^+ is, of course, replaced by $\delta m_k{}^+$.

We shall confine ourselves to the case of the subsidiary resonance. In that case we first have to change to circularly polarized variables δn by the transformation

$$\delta m_k{}^+ = a_k \delta n_k{}^+ - b_k \delta n_{-k}{}^-$$

already discussed in Section IV. Even in the absence of coupling to m^+, the oscillators δn are no longer free oscillators, but are driven by a thermal field $h_k e^{j\omega_k t}$:

$$\delta n_k{}^+ = (j\omega_k - \lambda_k)\delta n_k{}^+ + \nu_k e^{j\omega_k t} \tag{39}$$

where $\nu_k = \gamma h_k$. The field h_k is of course only a statistically defined quantity. However we may treat it as an actual field provided we remember its statistical properties in the final results. These properties are

1) The phase of h_k is a rapidly varying random function of k. Therefore sums of the form $\sum_{k,k'} F(\vec{k}, \vec{k}')h_k h_{k'}$, will be very nearly zero, since each term has a random phase factor. Sums of the form $\sum_{kk'} F(\vec{k}, \vec{k}')h_k h_{k'}{}^*$, will reduce to $\sum_k F(\vec{k}, \vec{k})h_k h_k{}^*$, since the terms $h_k h_k{}^*$ are the only ones that are phase independent.

2) The magnitude of $h_k h_k{}^*$ can be estimated by writing down the steady state solution of (39):

$$\delta n_k{}^+ = \frac{\nu_k}{\lambda_k} e^{j\omega_k t}. \tag{40}$$

Hence

$$h_k h_k{}^* = \frac{\lambda_k{}^2 \left| \delta n_k{}^+ \right|^2}{\gamma^2}$$

and $\left|\delta n_k{}^+\right|^2$ may be interpreted as the mean square amplitude of δn_k as given by the Bose-Einstein statistics of the spin wave assembly. However, since we never actually require $h_k h_k{}^*$, we shall not give this calculation there.

Let us now include the important coupling term to m^+ in (39). Then

$$\delta n_k{}^+ = (j\omega_k - \lambda_k)\delta n_k + \rho_k m^+ \delta n_{-k}{}^- + \nu_k e^{j\omega_k t} \tag{41}$$

in the notation of Section IV. For simplicity let us restrict the argument to those spin waves for which $\omega_k = \omega/2$ holds exactly. Then (41) ,and the complex conjugate equation with $-k$ replacing k readily gives the new steady state solution that replaces (40). The new solution is

$$\delta n_k{}^+ = S_k e^{j\omega_k t} \tag{42}$$

where

$$S_k = \frac{\rho_k m_0{}^+ \nu_{-k}{}^* + \lambda_k \nu_k}{(\lambda_k{}^2 - \rho_k \rho_k{}^* \left| m_0{}^+ \right|^2)} \tag{43}$$

provided the amplitude $\left| m_0{}^+ \right|$ of the uniform precession is below the threshold $\lambda_k / \sqrt{\rho_k \rho_k{}^*}$.

It now remains to determine how this spin wave level is coupled back into the equation for the uniform precession. This is done by substituting $\vec{m}_{\text{total}}$ into the equation of motion (1), equating terms that do not vary spatially, and retaining terms of second order in the δm_k. One then finds:

$$(1 - j\alpha)\dot{m}^+ = j\omega_{\text{res}} m^+ - j\omega_s e^{j\omega t}$$
$$- j\frac{\omega_M}{2} \sum \delta m_{-k}{}^+ (\delta m_k{}^+ k^- + \delta m_{-k}{}^- k^+) \frac{k_z}{k^2} \cdot \tag{44}$$

We are looking for solutions of this equation which vary as $m_0{}^+ e^{j\omega t}$, where $m_0{}^+$ is a complex constant. Therefore we retain of the second order terms only those that also vary as $e^{j\omega t}$. In view of (42), (43) the only terms satisfying this requirement have the form $-(j/2)\rho_k{}^* S_k S_{-k} e^{j\omega t}$. We thus find, in the steady state,

$$(\omega - \omega_{\text{res}} - j\alpha\omega)m_0{}^+ = -\omega_s + \frac{j}{2} \sum_k {}^* S_k S_{-k}$$

where the sum extends over all k values satisfying $\omega_k=\omega/2$. Remembering our remarks concerning sums over terms involving h_k (and hence ν_k) twice, we find

$$(\omega-\omega_{res}-j\alpha\omega)m_0^+ = -\omega_s+\frac{j}{2}m_0^+\sum_k\frac{\rho_k\rho_k^*\lambda_k(\nu_k\nu_k^*+\nu_{-k}\nu_{-k}^*)}{(\lambda_k^2-\rho_k\rho_k+|m_0^*|^2)^2}. \quad (45)$$

This is an equation for m_0^+ below the threshold. Rearranging, and taking squares of absolute values we find

$$|m_0^+|^2=\frac{\omega_s^2}{(\omega-\omega_{res})^2+\left(\alpha\omega+\frac{1}{2}\sum\right)^2} \quad (46)$$

where $\sum$ denotes the sum in 45, and still involves $|m_0^+|^2$. In Fig. 7 the right- and left-hand sides of (46) are plotted as a function of $|m_0|^2$ for two values of ω_s^2.

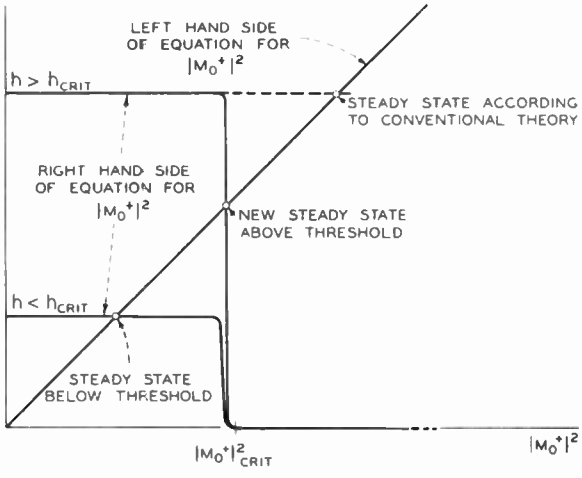

Fig. 7—Evolution of the final steady state as the signal is increased adiabatically. The uniform precession angle "sticks" at a value corresponding to the critical signal field.

The left-hand side is always a straight line of slope unity. Below the threshold the sum $\sum$ is very small, since the numerators of the various terms are small, proportional to the square of the thermal field. However, as $|m_0^+|^2$ increases, a point is reached at which $|m_0^+|^2$ approaches $\lambda_k^2/\rho_k\rho_k^*$ for *some* value, $\vec{k}_1$, of $\vec{k}$, on $\omega_k=\omega/2$. Then the sum increases sharply. When $|m_0^+|^2$ actually equals $\lambda_{k_1}^2/\rho_{k_1}\rho_{k_1}$ the sum goes to infinity. For further increases in $|m_0^+|^2$ it remains infinite, if the k values form practically a continuum, since there will then always be some $\vec{k}$ value at which one term in the sum becomes infinite. The equation

$$|m_0^+|^2=\sqrt{\frac{\lambda_{k_1}^2}{\rho_{k_1}\rho_{k_1}^*}}$$

is of course the equation for the threshold value $|m_0^+|_{crit}$. Thus the right-hand side of (46) is practically constant until $|m_0^+|^2$ approaches to within about

$$\sqrt{\frac{\lambda_k|\nu_k|^2}{\alpha\omega\rho_k\rho_k^*}}$$

of the threshold value. It then falls rapidly to zero, and thereafter remains at zero. The intersection of the left and right-hand sides (Fig. 7) gives the new value of $|m_0^+|^2$ which is practically equal to $|m_0^+|^2_{crit}$ as long as the signal exceeds the threshold, and practically equal to the conventional small signal value below the threshold. Above the threshold, (46), with the left-hand side equated to $|m_0^+|^2_{crit}$, is an equation for the effective loss

$$\alpha\omega+\frac{1}{2}\sum$$

or Γ, as this quantity was called earlier in this section. We note that in the new regime the denominator in the important term in $\sum$ is itself of order $\nu_k\nu_k^*$, so that the sum no longer depends on the magnitude of the thermal field. Hence our result is essentially temperature independent. The same remark applies to the critical S_k (43) which likewise becomes independent of the magnitude of ν_k, but still has the random phase of ν_k. Since $|m_0^+|^2$ never exceeds the critical value, it is only a narrow conical shell around the critical cone in $\vec{k}$ space that ever experiences any large excitation. However the phases of the waves within this shell are still random, so that in this sense the final state does somewhat resemble turbulence. It must be remembered however that for certain values of the dc field the critical spin waves are very long so that the true modes should be used (see Section III). These remarks are then only true in a qualitative sense. Finally, the fact that we only have considered spin waves on $\omega_k=\omega/2$ does not alter the results. More generally, it is easy to show that the denominators of the terms of $\sum$ will have an additional term $[\omega_k-(\omega/2)]^2$. $\sum$ then becomes large only for spin waves that also satisfy $\omega_k=\omega/2$.

VII. Remarks on the Final State Corresponding to the Instability Considered in Section II

The problem of the final state at the main resonance when it is distinct from the subsidiary absorption is more complicated than that of Section VI. It turns out that, if a complete spin-wave expansion is used, the equation for δm_k^+ is coupled not only to $(m^+)^2$, but also to sums of the form $\sum\delta m_k^+\delta m^-_k$ etc. The latter sums are, of course, negligible below the threshold, and therefore do not affect the calculation of the onset of instability. But, as we have just seen, above the threshold such sums can become comparable to $(m^+)^2$. For example, if in $\sum\delta m_k^+\delta m_k^-$ etc., we retain only the single term corresponding to the z-directed spin wave given by (11), we find that the growth of the spin-wave level is itself inhibited as the result of this term. In consequence, $|m^+|^2$ will not "stick" at the critical value but continue to increase at a diminished rate with increasing signal

power. Therefore χ'' will decrease to some new, but still finite value, rather than diminish to zero as was reported on the D-B.W. papers. However, it must be remembered that if $|m^+|^2$ increases beyond the threshold of a z-directed spin wave, waves propagating in other directions will become unstable, and increase the losses of $|m^+|^2$. Thus it is to be expected that χ'' will actually decline to zero, though perhaps less rapidly than in the case discussed in Section VI.

VIII. Conclusions

As we have seen, agreement of the observations available to date with the theory presented here is such as to leave little doubt about the correctness of the basic ideas. There remain a number of unresolved questions:

1) The final steady state at the main resonance when it differs from the subsidiary resonance. This problem is chiefly mathematical, and its solution, while complicated, will probably not reveal more than the precise form of the decline in χ''.
2) The precise behavior at high signal levels of the long wavelength modes evaluated by Walker. In particular it would be interesting to know if they can give rise to the further absorption peaks as observed by Scovil.
3) The stability of the highly excited spin-wave level against further spin-wave fluctuations. Any instability in this level might likewise lead to further absorption peaks.

IX. Acknowledgment

The early stage of this work, relating to the subject matter of Section II was done jointly with Dr. P. W. Anderson, to whom the author is also indebted for many discussions relating to the remainder of the paper. Thanks are also due to Drs. A. M. Clogston and L. R. Walker for their continued interest in this investigation throughout its development.

The author is especially grateful to Drs. M. T. Weiss and H. E. D. Scovil for permission to quote their unpublished data.

Microwave Resonance Relations in Anisotropic Single Crystal Ferrites*

JOSEPH O. ARTMAN†

Summary—**The ferromagnetic resonance relations in magnetically anisotropic single crystal ferrites are reexamined. Detailed analyses are presented for spherical specimens. Generalized nomograms are shown which relate the resonance frequency to static field H, anisotropy parameter K/M, and the static field orientation. The nature of the susceptibility tensor is discussed. Below magnetic saturation, multidomain structure is expected. Under these conditions, with $\vec{H}$ applied in a [110] direction, a simple multidomain arrangement is suggested by crystal geometry. Ferromagnetic resonance can be used to investigate this structure. The analysis is similar to that employed by Smit and Beljers who investigated like effects in uniaxial crystals. The domains are lamellar in form, separated by 180° walls, and lie perpendicular to $\vec{H}$. Corresponding to the two nearby easy directions of magnetization, the domains are of two varieties which alternate in sequence. Two resonance frequencies are found for a given $\vec{H}$, depending on whether the microwave magnetic field is perpendicular or parallel to $\vec{H}$. Nomograms are given relating these resonance frequencies to $\vec{H}$, K/M, and saturation magnetization M. The nature of the magnetization curve for these simple structures is also discussed. The predictions of these analyses are compared with the results of recent experiments.**

* Original manuscript received by the IRE, July 3, 1956. Supported by AF Contract 19(604)-1084.

† Gordon McKay Lab., Harvard Univ., Cambridge, Mass.

Introduction

THE THEORY of ferromagnetic resonance has been reviewed at this symposium by Bloembergen. In the most trivial case the relation between resonant angular frequency ω and applied magnetic field H is $\omega = \gamma H$, where γ is proportional to the spin g-factor. This simple expression is no longer valid when demagnetizing fields associated with the geometry of the specimen are present and must be modified further in the presence of crystalline magnetic anisotropy. These effects were considered by Kittel[1] for the case in which the magnetization $\vec{M}$ is parallel to the applied field $\vec{H}$. He obtained

$$\left(\frac{\omega}{\gamma}\right)^2 = [H + (N_y + N_y^a - N_z)M] \cdot [H + (N_x + N_x^a - N_z)M] \tag{1}$$

where z is the direction of $\vec{H}$ and $\vec{M}$; N_x, N_y, and N_z are

[1] C. Kittel, "On the theory of ferromagnetic resonance absorption," *Phys. Rev.*, vol. 73, pp. 155–161; January, 1948.

the geometrical demagnetization factors; and $N_x{}^aM$, $N_y{}^aM$ are the x and y components of the "anisotropy field." These "anisotropy fields" are directly related to K_1/M and K_2/M where K_1 and K_2 are the first and second order anisotropy constants. In any given crystal plane (1) predicts an angular variation of resonance field from which relevant crystal parameters can be determined.

A common way of doing this is to mount a spherical sample on a post normal to a (110) crystal plane. See Fig. 1. The sample is inserted in a microwave cavity

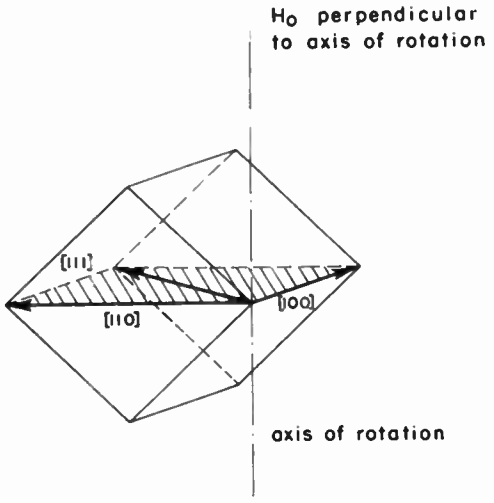

Fig. 1—Principal axes in a cubic crystal. (Artman[12])

arranged so that $\vec{H}$ and the microwave field $\vec{h}$ are perpendicular to each other and lie in the given (110) plane. At a fixed frequency ω_0, resonance field measurements in the three principal crystal directions shown in Fig. 1 are sufficient to determine ω/γ, K_1/M and K_2/M. The value of M can not be determined directly from these observations on a sphere since the geometrical demagnetizing factors cancel out. (It can be inferred from measurements of peak absorption and line breadth.) The angular variation of resonance field predicted by the Kittel formula has been verified experimentally as shown for example in Fig. 2.

The presumption that $\vec{M}$ and $\vec{H}$ are parallel can be true only in the principal crystal directions, the [100], [111], and [110] axes and their geometrical equivalents.[2] For all other orientations the direction of $\vec{M}$ approaches that of $\vec{H}$ asymptotically as $\vec{H}$ increases. The ratio of resonance field H to anisotropy parameter $|K/M|$ will be shown below to be a sensitive indication of the degree of line-up. For $H/|K/M|$ ratios of 32 or less the angular resonance curve is already visibly distorted from (1).

[2] In crystals with positive anisotropy the [100] axis is the easy anisotropy direction, and the [111] axis the hard anisotropy direction. In a negative anisotropy crystal these easy and hard directions are interchanged. In both cases the [110] axis is an "intermediate" anisotropy direction.

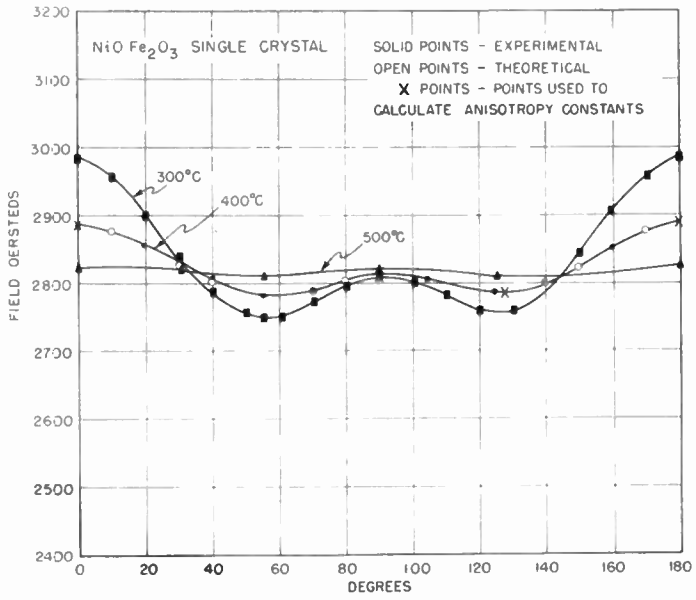

Fig. 2—H vs θ. θ equals angle in (110) plane between static field and cube edge. (D. W. Healy, Jr., Tech. Rep. 135, Cruft Lab., Harvard Univ., August 15, 1951.)

Equilibrium and Resonance Conditions in Single Domain Crystals

A more general theory of ferromagnetic resonance in magnetically anisotropic single crystal ferrites has recently been developed by Smit,[3] Zeiger,[4] and Suhl.[5] Consider a sphere oriented as in Fig. 1. $\vec{H}$ lies in the (110) plane that passes through the [100] axis and makes an angle ψ with this axis. $\vec{M}$ is inclined to the [100] axis at the angle θ. The azimuth of $\vec{M}$ with respect to the [010] axis is expressed by ϕ. See Fig. 3.[6] The

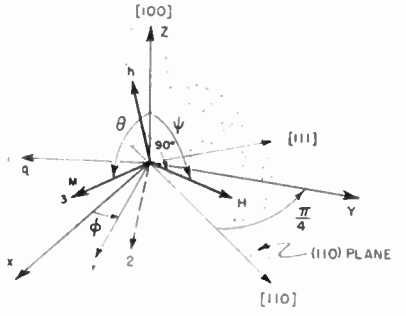

Fig. 3—Spatial configuration of $\vec{M}$ and $\vec{H}$. (Adapted from Artman.[13])

[3] J. Smit and H. G. Beljers, "Ferromagnetic resonance absorption in $BaFe_{12}O_{19}$, A highly anisotropic crystal," *Philips Res. Rep.*, vol. 10, pp. 113–130; April, 1955.

[4] H. J. Zeiger, Lincoln Lab., Lexington, Mass. (private communication).

[5] H. Suhl, "Ferromagnetic resonance in nickel ferrite between one and two kilomegacycles," *Phys. Rev.*, vol. 97, pp. 555–557; January, 1955.

[6] Strictly speaking the (110) plane and [110] direction shown in this diagram are an (01$\bar{1}$) plane and [011] direction respectively. This somewhat incorrect notation will, for convenience, be used throughout this paper, however.

total free energy per unit volume is, considering anisotropy and magnetostatic contributions only,

$$F = E_A - MH\left[\cos\theta\cos\psi + \sin\theta\sin\psi\sin\left(\frac{\pi}{4}+\phi\right)\right] + \frac{2\pi M^2}{3} \tag{2}$$

where

$$E_A = \frac{K_1}{4}\left[\sin^2(2\theta) + \sin^4\theta\sin^2(2\phi)\right] + \frac{K_2}{16}\left[\sin^2(2\phi)\sin^2(2\theta)\sin^2\theta\right]. \tag{3}$$

The equilibrium point must satisfy

$$\frac{\partial E_A}{\partial\phi} = -MH\sin\psi\sin\left(\phi-\frac{\pi}{4}\right)\sin\theta$$
$$\frac{\partial E_A}{\partial\theta} = MH\left[\sin\psi\sin\left(\frac{\pi}{4}+\phi\right)\cos\theta - \cos\psi\sin\theta\right]. \tag{4}$$

To evaluate the ferromagnetic resonant frequency and the susceptibility tensor components, departure of $\vec{M}$ from equilibrium is considered. This yields

$$\frac{\omega}{\gamma} = \frac{1}{M\sin\theta}\left[\frac{\partial^2 F}{\partial\theta^2}\frac{\partial^2 F}{\partial\phi^2} - \frac{\partial^2 F}{\partial\theta\partial\phi}\right]^{1/2}. \tag{5}$$

A "susceptibility" tensor $\overleftrightarrow{\chi}$ may be defined by relating the microwave magnetization to the applied *external* microwave field. $\overleftrightarrow{\chi}$ is not a true susceptibility but nevertheless is a most convenient way of expressing the ferrite properties.[7] With reference to the coordinate system (1, 2, 3) illustrated in Fig. 3: *1*, perpendicular to the plane formed by $\vec{M}$ and the [100] direction; *2*, normal to $\vec{M}$ and lying in the $\vec{M}$-[100] plane; *3*, parallel to $\vec{M}$;

$$\overleftrightarrow{\chi} = \begin{pmatrix} \chi_{11} & -j\kappa_{12} & 0 \\ j\kappa_{21} & \chi_{22} & 0 \\ 0 & 0 & \chi_{33} \end{pmatrix}. \tag{6}$$

[7] The *intrinsic* susceptibility tensor $\overleftrightarrow{\chi^I}$ relates the microwave magnetization to the internal microwave field. With reference to (6) the nonzero elements of $\overleftrightarrow{\chi^I}$ are:

$$\chi_{11}{}^I = \frac{\chi_{11}\left(1-\frac{\chi_{22}}{3}\right)+\frac{\kappa_{12}\kappa_{21}}{3}}{\left(1-\frac{\chi_{11}}{3}\right)\left(1-\frac{\chi_{22}}{3}\right)-\frac{\kappa_{12}\kappa_{21}}{9}} \qquad \chi_{22}{}^I = \frac{\chi_{22}\left(1-\frac{\chi_{11}}{3}\right)+\frac{\kappa_{12}\kappa_{21}}{3}}{\left(1-\frac{\chi_{11}}{3}\right)\left(1-\frac{\chi_{22}}{3}\right)-\frac{\kappa_{12}\kappa_{21}}{9}}$$

$$\kappa_{12}{}^I = \frac{\kappa_{12}\left(1-\frac{\chi_{11}}{3}\right)+\frac{\chi_{11}\kappa_{12}}{3}}{\left(1-\frac{\chi_{11}}{3}\right)\left(1-\frac{\chi_{22}}{3}\right)-\frac{\kappa_{12}\kappa_{21}}{9}} \qquad \kappa_{21}{}^I = \frac{\kappa_{21}\left(1-\frac{\chi_{22}}{3}\right)+\frac{\chi_{22}\kappa_{21}}{3}}{\left(1-\frac{\chi_{11}}{3}\right)\left(1-\frac{\chi_{22}}{3}\right)-\frac{\kappa_{12}\kappa_{21}}{9}}$$

$$\chi_{33}{}^I = \frac{\chi_{33}}{1-\frac{\chi_{33}}{3}}$$

The units are such that the demagnetizing factor for a sphere is 1/3. $\overleftrightarrow{\chi^I}$ has to be referred to the *internal* dc magnetic field to be a true susceptibility in both the dc and microwave sense.

The elements are defined as follows

$$\chi_{11} = \frac{4\pi\gamma M\left(\gamma H_z\cos\theta + \gamma H_r\sin\theta + \frac{1}{M}\frac{\partial^2 E_A}{\partial\theta^2}\right)}{D}$$

$$\chi_{22} = \frac{4\pi\gamma M\left(\frac{\gamma H_r}{\sin\theta} + \frac{\gamma}{M}\cdot\frac{1}{\sin^2\theta}\frac{\partial^2 E_A}{\partial\phi^2}\right)}{D}$$

$$j\kappa_{21} = \frac{4\pi\gamma M\left(j\omega_0 + \frac{1}{T} + \gamma Hq\cot\theta + \frac{\gamma}{M}\cdot\frac{1}{\sin\theta}\frac{\partial^2 E_A}{\partial\theta\partial\phi}\right)}{D} \tag{7}$$

$$j\kappa_{12} = \frac{4\pi\gamma M\left(j\omega_0 + \frac{1}{T} - \gamma Hq\cot\theta - \frac{\gamma}{M}\frac{1}{\sin\theta}\frac{\partial^2 E_A}{\partial\theta\partial\phi}\right)}{D}$$

$$\chi_{33} = 0$$

with

$$D = \omega^2 - \omega_0{}^2 + \frac{1}{T^2} + j\frac{2\omega_0}{T} \tag{8}$$

where ω is defined by (5) and ω_0 is the microwave angular frequency and

$$Hq = H\sin\psi\sin\left(\phi-\frac{\pi}{4}\right)$$
$$Hr = H\sin\psi\sin\left(\frac{\pi}{4}+\phi\right) \tag{9}$$
$$H_z = H\cos\psi.$$

The properties of the normal modes of oscillation of the ferrite follow from diagonalization of the tensor.

Negative Anisotropy Crystals

If second-order anisotropy can be neglected the resonance relations (5) can be displayed as a family of curves relating

$$\frac{\omega}{\gamma}\Big/\left|\frac{K_1}{M}\right| \quad \text{to} \quad H\Big/\left|\frac{K_1}{M}\right|$$

for various values of ψ. See Fig. 4. $\vec{M}$ lies in the (110) plane so ϕ equals $\pi/4$. The curves converge to

$$\frac{\omega}{\gamma}\Big/\left|\frac{K_1}{M}\right| = 4/3$$

as H approaches zero. The $\omega/\gamma - H$ relations are particularly simple in the principal crystal directions. The [111] direction corresponds to a ψ of 54°44′. θ always equals ψ in this direction and the resonance condition is simply

$$\frac{\omega}{\gamma} = H + \frac{4}{3}\left|\frac{K_1}{M}\right|.$$

The [110] direction is given by ψ equal to 90°;

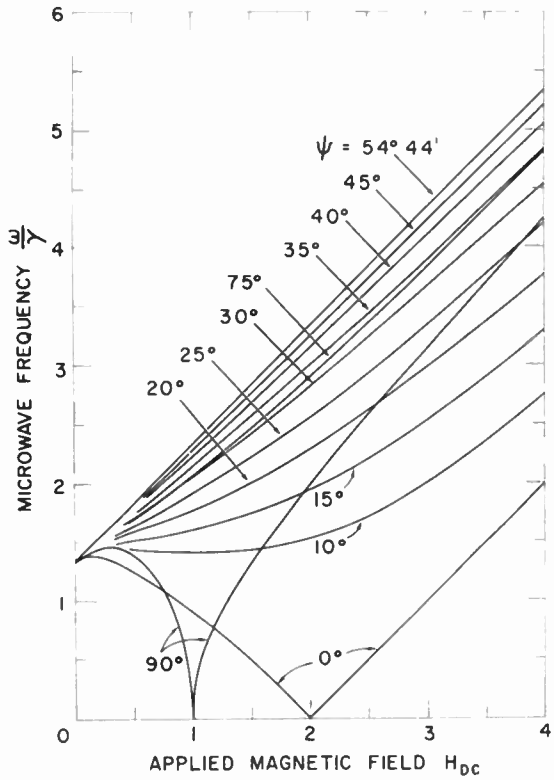

Fig. 4—Single domain resonance relations in cubic crystal for negative K_1/M. $\vec{H}$ constrained to move in (110) plane. $\vec{h_{rf}} \perp \vec{H}$. ψ-angle of $\vec{H}$ with respect to [100] axis. ω/γ and H in units of $|K_1/M|$. (Artman.[13])

$$\text{for } H \Big/ \left|\frac{K_1}{M}\right| \geqq 1,$$

$\vec{M}$ is parallel to $\vec{H}$ yielding the resonance condition

$$\frac{\omega}{\gamma} = \left[\left(H - \left|\frac{K_1}{M}\right|\right)\left(H + 2\left|\frac{K_1}{M}\right|\right)\right]^{1/2}.$$

Along the 0 degree line, the [100] axis, θ equals ψ for

$$H \Big/ \left|\frac{K}{M}\right| \geqq 2$$

for which the resonance condition reduces to

$$\frac{\omega}{\gamma} = H - 2\left|\frac{K_1}{M}\right|.$$

These formulas are just the line-up formulas which are strictly valid only in these three specific directions.

Positive Anisotropy Crystals

In a similar fashion, curves relating

$$\frac{\omega}{\gamma} \Big/ \frac{K_1}{M} \text{ to } H \Big/ \frac{K_1}{M}$$

at various ψ for positive anisotropy crystals are shown in Fig. 5. These curves converge to

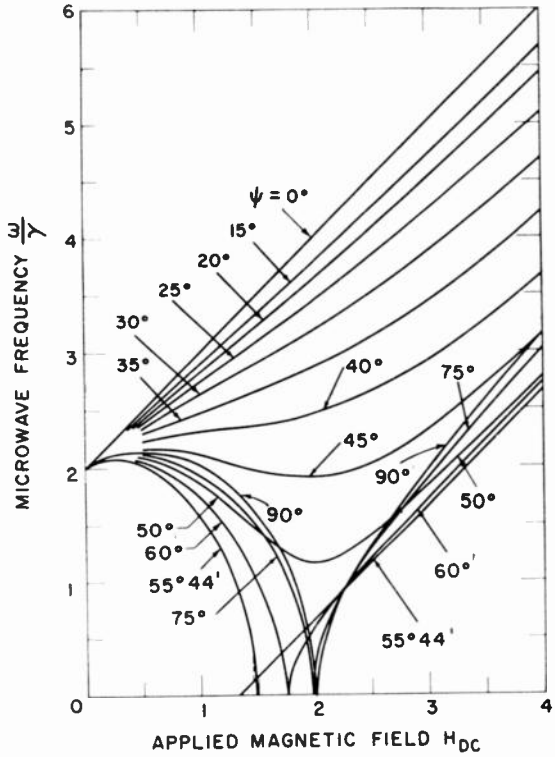

Fig. 5—Single domain resonance relations in cubic crystal for positive K_1/M. $\vec{H}$ constrained to move in (110) plane. $\vec{h_{rf}} \perp \vec{H}$. ψ-angle of $\vec{H}$ with respect to [100] axis. ω/γ and H in units of K_1/M. (Artman.[13])

$$\frac{\omega}{\gamma} \Big/ \frac{K_1}{M} = 2 \quad \text{for} \quad H = 0.$$

For $\psi = 0°$, $\vec{M}$ lies parallel to $\vec{H}$ and

$$\frac{\omega}{\gamma} = H + \frac{2K_1}{M}.$$

For $\psi = 90°$ and $H/(K_1/M)$ values greater than two, $\vec{M}$ and $\vec{H}$ are parallel and

$$\frac{\omega}{\gamma} = \left[\left(H + \frac{K_1}{M}\right)\left(H - \frac{2K_1}{M}\right)\right]^{1/2}.$$

For $\psi = 54°44'$, $\vec{M}$ is parallel to $\vec{H}$ for

$$H \Big/ \frac{K_1}{M} \geqq \frac{4}{3} \quad \text{and} \quad \frac{\omega}{\gamma} = H - \frac{4}{3}\frac{K_1}{M}.$$

As in the negative anisotropy case, these are just the Kittel line-up formulas.

Quasi-Line-Up Conditions

In both positive and negative anisotropy crystals, when sufficiently high magnetic fields are applied, $\vec{M}$ will lie close to $\vec{H}$ in the (110) plane. As the angle $\epsilon \equiv \psi - \theta$

becomes small, the equilibrium conditions (4) simplify to

$$\frac{\partial E_A}{\partial \theta} \simeq MH\epsilon. \tag{10}$$

To the first order in ϵ the value of ω/γ from (5) is

$$\frac{\omega}{\gamma} = \left[\left(H + H\epsilon\cot\theta + \frac{1}{M}\sin^2\theta\,\frac{\partial^2 E_A}{2\phi^2}\right)\cdot\left(H + \frac{1}{M}\frac{\partial^2 E_A}{\partial\theta^2}\right)\right]^{1/2}. \tag{11}$$

Upon substitution of (10) into (11), we obtain

$$\frac{\omega}{\gamma} = \left[\left(H + \frac{\cot\theta}{M}\frac{\partial E_A}{\partial\theta} + \frac{1}{M\sin^2\theta}\frac{\partial^2 E_A}{\partial\phi^2}\right)\cdot\left(H + \frac{1}{M}\frac{\partial^2 E_A}{\partial\theta^2}\right)\right]^{1/2} \tag{12}$$

which is equivalent to the Kittel-type formula derived by Bickford.[8] Thus to the first order in ϵ, the Kittel equations can still be used remembering that θ and ψ are not necessarily equivalent. Expressing ϵ in degrees, (10) becomes

$$\epsilon = \frac{57.296}{H}\sin\theta\cos\theta(3\cos^2\theta - 1)\left(\frac{K_1}{M} + \frac{K_2}{2M}\sin^2\theta\right). \tag{13}$$

These correction functions are displayed in Fig. 6 (upper right).

The use of these formulas is illustrated in Figs. 7 and 8 (opposite). In Fig. 7 resonance field data taken by Tannenwald[9] on a negative anisotropy Mn-Zn ferrite are illustrated. Agreement of the corrected formula with the experimental data is excellent. In Fig. 8 data are shown on a positive anisotropy Co ferrite.[10] Agreement between the experimental points and the computations is not as good as in the previous case. This is not too surprising since the experimental data are not internally consistent; they do not quite lie on a curve symmetrical about $\theta = 90°$.

In Figs. 9 and 10, resonance nomograms are plotted for very high fields,

$$H \Big/ \left|\frac{K_1}{M}\right| \gg 1,$$

at which $\epsilon \sim 0$ and for which (12) can be approximated by

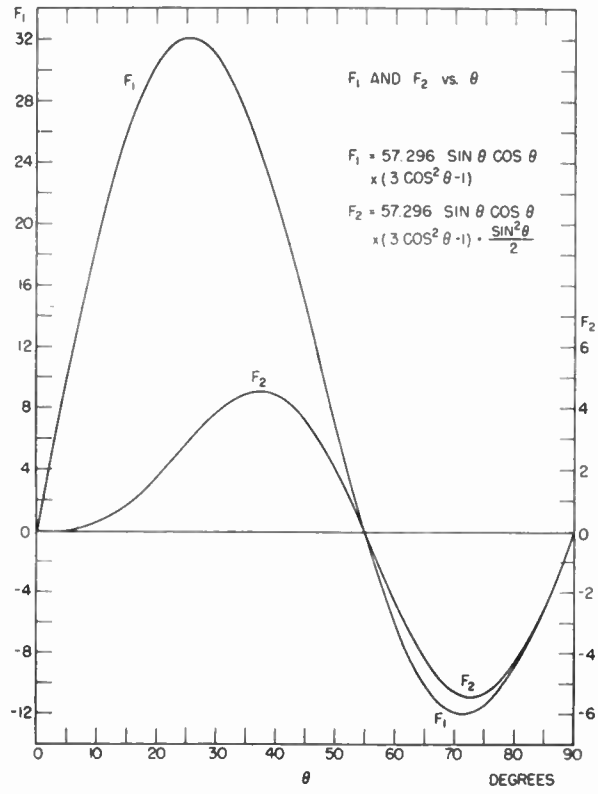

Fig. 6—F_1 and F_2 vs θ. First-order angular correction formulas for non-lineup. (Artman.[13])

$$\frac{\omega}{\gamma} = H + \frac{1}{2}\left(\frac{\cot\theta}{M}\frac{\partial E_A}{\partial\theta} + \frac{1}{M\sin^2\theta}\frac{\partial^2 E_A}{\partial\phi^2} + \frac{1}{M}\frac{\partial^2 E_A}{\partial\theta^2}\right) \tag{14}$$

which for first order anisotropy is

$$\frac{\omega}{\gamma} = H + \frac{K_1}{M}\left(2 + \frac{15}{2}\sin^4\theta - 10\sin^2\theta\right). \tag{15}$$

Figs. 9 and 10 should be compared with the previous Figs. 4 and 5. Fig. 9 is sufficient to give the theoretical curves for the Ni ferrite data presented in Fig. 3.

Under line-up conditions the tensor elements (7) simplify to

$$\chi_{11} = \frac{4\pi\gamma M\left(\gamma H + \frac{\gamma}{M}\frac{\partial^2 E_A}{\partial\theta^2}\right)}{D}$$

$$\chi_{22} = \frac{4\pi\gamma M\left(\gamma H + \frac{\gamma}{M}\cot\theta\frac{\partial E_A}{\partial\theta} + \frac{\gamma}{M\sin^2\theta}\frac{\partial^2 E_A}{\partial\phi^2}\right)}{D} \tag{16}$$

$$\chi_{12} = \chi_{21} = \kappa = \frac{4\pi\gamma M(\omega_0 - j/T)}{D}.$$

As before, D is given by

[8] L. R. Bickford, Jr., "Ferromagnetic resonance absorption in magnetite single crystals," *Phys. Rev.*, vol. 78, pp. 449–457; May, 1950.

[9] P. E. Tannenwald (private communication).

[10] P. E. Tannenwald (private communication), and "Multiple resonance in cobalt ferrite," *Phys. Rev.*, vol. 99, pp. 463–464; July, 1955.

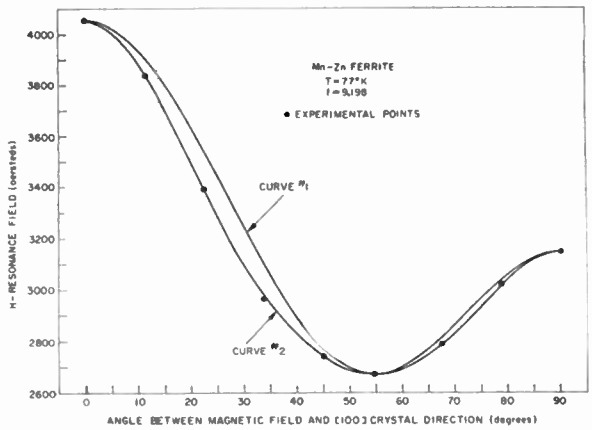

Fig. 7—Variation of resonance field with crystal orientation angle for an Mn-Zn ferrite. $T=77°K$ $f=9.198$ kmc. Computed constants: $K_1/M=-399$ oe., $K_2/M=-121$ oe., $\omega/\gamma=3256$ oe. Curve No. 1 computed under assumption $\vec{M}$ parallel to $\vec{H}$. Curve No. 2 computed allowing for angle between $\vec{M}$ and $\vec{H}$. (Experimental data from P. E. Tannenwald, private communication. Artman.[13])

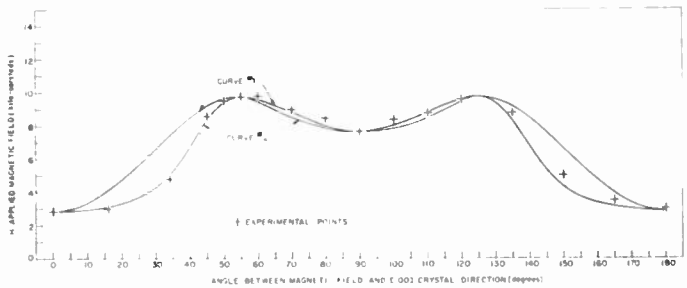

Fig. 8—Variation of resonance field with crystal orientation angle for a Co ferrite. $T=90°C$ $f=23.800$ kmc. Computed constants: $K_1/M=1.826\times10^3$ oe., $K^2/M=1.830\times10^3$ oe., $\omega/\gamma=6.502\times10^3$ oe. Curve No. 1 computed under assumption $\vec{M}$ parallel to $\vec{H}$. Curve No. 2 computed allowing for angle between $\vec{M}$ and $\vec{H}$. (Experimental data from Tannenwald, private communication. Artman.[13])

$$\omega^2 - \omega_0^2 + \frac{1}{T^2} + j\frac{2\omega_0}{T},$$

where ω now follows from (12).

Ferromagnetic Resonance in Presence of Magnetic Domain Structure

Resonances in addition to those predicted by single domain analysis have been observed experimentally in ferrites.[8,10,11] Many of these secondary resonance observations had the following common features: 1) The additional resonances did not occur when the crystal was magnetized along an easy anisotropy axis; 2) the secondary resonances were smaller in magnitude than the primary resonance and occurred at fields below the primary resonance point; 3) these secondary resonances

[11] P. E. Tannenwald, "Ferromagnetic resonance in manganese ferrite single crystals," *Phys. Rev.*, vol. 100, pp. 1713–1719; December, 1955.

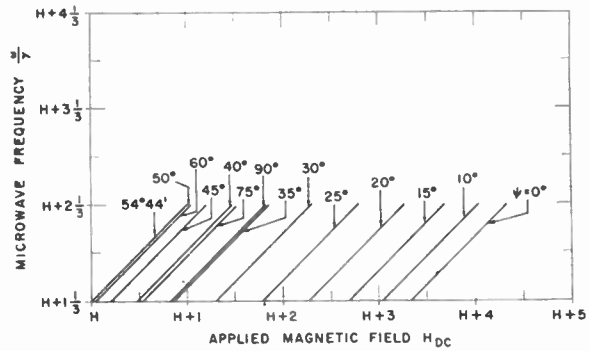

Fig. 9—Single domain resonance relations in cubic crystal at very high magnetic field. K_1/M negative. ω/γ and H in units of $|K_1/M|$. (Artman.[12])

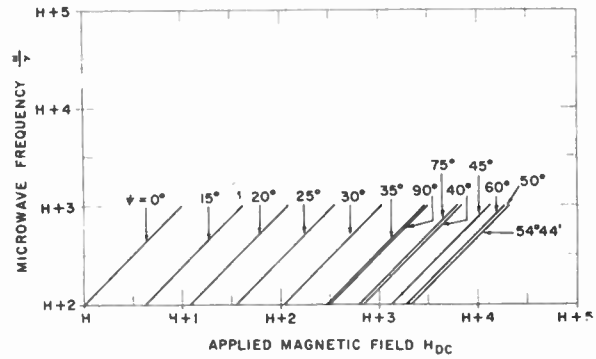

Fig. 10—Single domain resonance relations in cubic crystal at very high magnetic field. K_1/M positive. ω/γ and H in units of K_1/M. (Artman.[12])

were not seen at all at higher microwave frequencies. Such resonances have been presumed to be a consequence of the domain structure existing below magnetic saturation. Effects of this nature in magnetically uniaxial crystals have recently been demonstrated experimentally and analyzed theoretically by Smit and Beljers.[3] Nagamiya[12] has interpreted similarly the resonances observed by Bickford[8] in Fe_3O_4 at low temperatures where the magnetic anisotropy has tetragonal symmetry.

Treatment of the multiple domain structure problem in crystals with cubic symmetry is, in general, very involved. Fortunately for both negative and positive anisotropy crystals, the analysis is simplified when $\vec{H}$ lies along a [110] direction. This case has been treated by Artman[13] using the methods of Smit. Since for the [110] direction there are only two nearby easy directions of anisotropy, the crystal is assumed to consist of lamellar domains of two varieties which alternate in sequence. In each domain the magnetization tends to

[12] T. Nagamiya, "A tentative interpretation of Bickford's observation of the resonance absorption in magnetite below its transition point," *Prog. Theo. Phys.* (Japan), vol. 7, pp. 72–82; July, 1953.

[13] J. O. Artman, "Microwave resonance relations in anisotropic single crystal ferrites, *Phys. Rev.*, vol. 100, p. 1243A; November 15, 1955. Group Rep. M35–53, Lincoln Lab. (unpublished).

lie along one of the two easy directions. The domains are of equal volume, are separated by 180° walls and lie perpendicular to the dc field direction. The situation for negative anisotropy crystals is illustrated in Fig. 11.

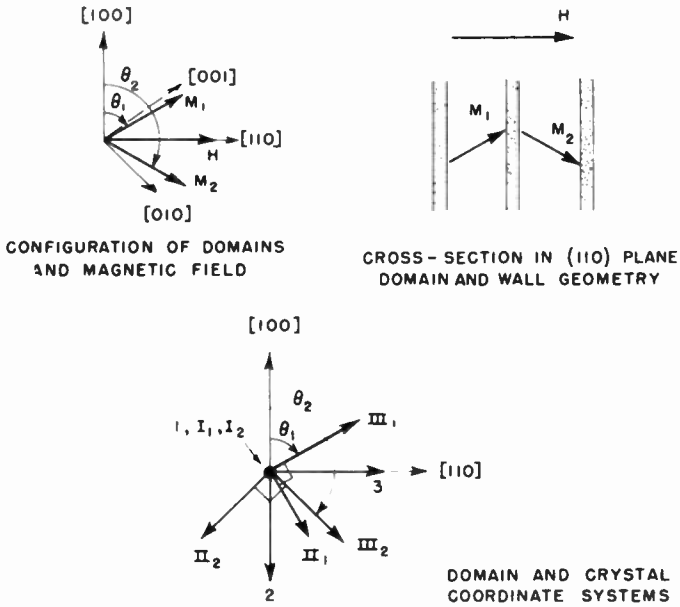

Fig. 11—Multidomain structure in negative anisotropy crystal, $\vec{H}$ in [110] direction. (Artman.[13])

The total free energy per unit volume for this multidomain structure is, for negative K_1/M:

$$F = \frac{K_1}{8}\left[\sin^2(2\theta_1) + \sin^4\theta_1 \sin^2(2\phi_1) + \sin^2(2\theta_2) + \sin^4\theta_2 \sin^2(2\phi_2)\right] - \frac{MH}{2}\left[\sin\theta_1 \sin\left(\frac{\pi}{4}+\phi_1\right) + \sin\theta_2 \sin\left(\frac{\pi}{4}+\phi_2\right)\right] + \frac{\pi M^2}{6}\left[(\cos\theta_1+\cos\theta_2)^2 + (\sin\theta_1\sin\phi_1+\sin\theta_2\sin\phi_2)^2 + (\sin\theta_1\cos\phi_1+\sin\theta_2\cos\phi_2)^2\right] + \frac{\pi M^2}{2}\left[\sin\theta_1\cos\left(\frac{\pi}{4}-\phi_1\right) - \sin\theta_2\cos\left(\frac{\pi}{4}-\phi_2\right)\right]^2 \quad (17)$$

where the angle nomenclature corresponds to that used previously. The first term represents anisotropy energy; the second, the magnetostatic energy; the third, the demagnetization energy for the average magnetization on the surface of the sample; and the fourth, the demagnetization energy of poles on the domain walls—the domain demagnetizing factor is taken as 4π.

The equilibrium conditions

$$\frac{\partial F}{\partial\theta_1} = \frac{\partial F}{\partial\theta_2} = \frac{\partial F}{\partial\phi_1} = \frac{\partial F}{\partial\phi_2} = 0$$

are, as anticipated, satisfied by $\phi_1=\phi_2=\pi/4$ and $\theta=\theta_1=\pi-\theta_2$. At a given H this resulting multidomain structure is energetically favorable with respect to the single domain originally assumed. Two resonance conditions are found

$$\left(\frac{\omega}{\gamma}\right)_\perp = \frac{1}{M\sin\theta}(AC)^{1/2} \quad (18a)$$

$$\left(\frac{\omega}{\gamma}\right)_\parallel = \frac{1}{M\sin\theta}(BD)^{1/2} \quad (18b)$$

where

$$\begin{aligned} A &= 2(F_{\theta_1\theta_1}+F_{\theta_1\theta_2}) \\ B &= 2(F_{\theta_1\theta_1}-F_{\theta_1\theta_2}) \\ C &= 2(F_{\phi_1\phi_1}+F_{\phi_1\phi_2}) \\ D &= 2(F_{\phi_1\phi_1}-F_{\phi_1\phi_2}) \end{aligned} \quad (19)$$

and $F_{\theta_1\theta_1}=\partial^2F/\partial\theta_1^2$, etc.

The $(\omega/\gamma)_\perp$ resonance is excited by microwave excitation perpendicular to $\vec{H}$, while the $(\omega/\gamma)_\parallel$ resonance is excited by radiation parallel to $\vec{H}$. The values of these resonances, unlike the usual sphere resonances, are dependent on M. In Fig. 12 families of these multidomain resonances are shown superimposed on the usual single domain $\psi=90°$ curve. M, H, and ω/γ are expressed in units of $|K_1/M|$.

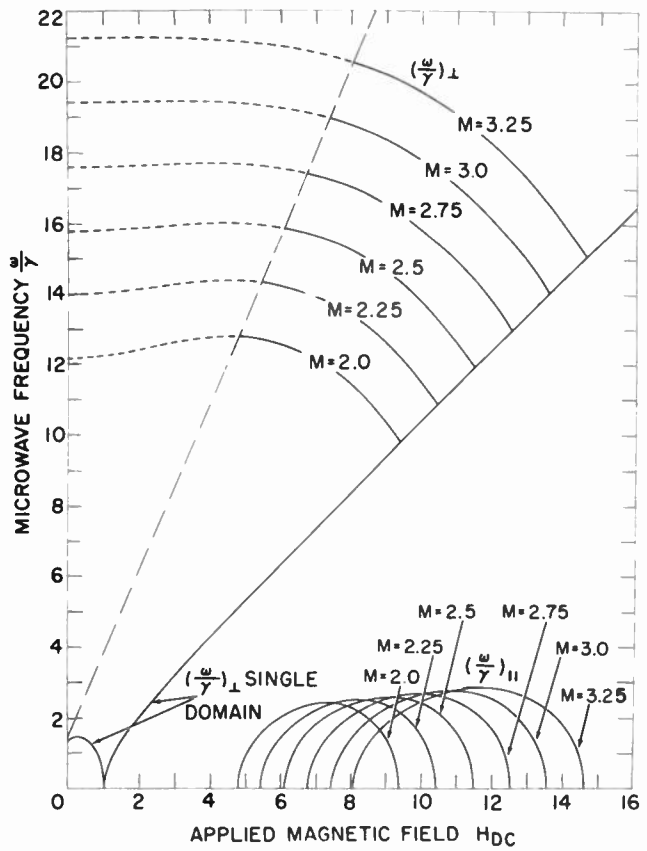

Fig. 12—Single and multidomain resonance relations in cubic crystal for negative K_1/M. $\vec{H}$ in [110] direction. ω/γ, H, and M in units of $|K_1/M|$. $(\omega/\gamma)_\parallel$ for h_{rf} in [110] direction. $(\omega/\gamma)_\perp$ for $\vec{h}_{rf}\perp$[110] direction. (Artman.[13])

The energy, equilibrium, and resonance conditions are, expressing all quantities in units of $|K_1/M|$:

$$F = -\frac{1}{4}[\sin^2(2\theta)+\sin^4\theta] - H\sin\theta + \frac{2\pi M}{3}\sin^2\theta \quad (20)$$

$$H = \left(3\sin^2\theta - 2 + \frac{4\pi M}{3}\right)\sin\theta \quad (21)$$

$$\left(\frac{\omega}{\gamma}\right)_\perp = \left\{\left[(1-\sin^2\theta)(9\sin^2\theta-2)+\frac{4\pi M}{3}(3-2\sin^2\theta)\right]\cdot\left[5\sin^2\theta-2+\frac{4\pi M}{3}\right]\right\}^{1/2} \quad (22a)$$

$$\left(\frac{\omega}{\gamma}\right)_\parallel = \left\{\left[(1-\sin^2\theta)(9\sin^2\theta-2)+\frac{4\pi M}{3}(1-\sin^2\theta)\right]\cdot|5\sin^2\theta-2|\right\}^{1/2}. \quad (22b)$$

For $(4\pi M/3) \geqq 2$ equilibria exist for all values of θ. At the point

$$H = \sqrt{\frac{2}{5}}\left(\frac{4\pi M}{3} - \frac{4}{5}\right),$$

θ equals $\sin^{-1}\sqrt{2/5}$ and $(\omega/\gamma)_\parallel$ vanishes. Since $(\omega/\gamma)_\perp$ is positive this is a free energy saddle-point. For H values less than

$$\sqrt{\frac{2}{5}}\left(\frac{4\pi M}{3} - \frac{4}{5}\right),$$

$(\omega/\gamma)_\parallel^2$ is negative. The free energy extremum hence is a local maximum and the domain structure is not stable in this region. The values of $(\omega/\gamma)_\perp$ in this unstable region are indicated by dotted lines. An analysis of the domain structure existing in this low field region has not been made. $(\omega/\gamma)_\parallel$ vanishes for all values of H greater than $(4\pi M/3)+1$. At this point, $\theta=\pi/2$, the domain structure ceases to exist and

$$\left(\frac{\omega}{\gamma}\right)_\perp = \left(\frac{\omega}{\gamma}\right) = \left[\frac{4\pi M}{3}\left(\frac{4\pi M}{3}+3\right)\right]^{1/2}.$$

It should be remembered that the existence of a local energy minimum is not really sufficient to assure the existence of the predicated domain structure. Another domain structure may exist in stable equilibrium at a lower free energy. This has not been investigated further in this case or in the analogous positive anisotropy case that is discussed later. However, at the field values for which the magnetization directions are relatively close to $\vec{H}$ our postulated structure is clearly the proper one.

A "gross susceptibility tensor" $\overleftrightarrow{\chi}$ may be defined, similar to (6), relating the internal microwave magnetization to the external field. With reference to the following axes: *1*, perpendicular to the (110) plane; *2*, directed along the $[\bar{1}00]$ axis; *3*, parallel to $\vec{H}$, the tensor elements are:

$$\begin{aligned}
\bar{\chi}_{11} &= \frac{4\pi M^2 A\sin^2\theta}{AC-z^2} \\
\bar{\chi}_{22} &= \frac{4\pi M^2 C\sin^2\theta}{AC-z^2} \\
\bar{\kappa}_{12} = \bar{\kappa}_{21} = \bar{\kappa} &= \frac{4\pi M^2 z\sin^2\theta}{AC-z^2} \\
\bar{\chi}_{33} &= \frac{4\pi M^2 D\sin^2\theta}{BD-z^2}
\end{aligned} \quad (23)$$

where A, B, C, D are defined through (19) and

$$z = (\omega_0 - j/T)\frac{M\sin\theta}{\gamma}.$$

It is clear from Fig. 12 that, at a fixed operating frequency, $(\omega/\gamma)_\perp$ resonances would be observed at fields below the usual (ω/γ) resonance. Secondary resonances will not be seen if the operating frequency is too high. The relative magnitudes of the main and secondary resonance peaks can be predicted from (21), (22) and (23). The magnetization curve predicted for this multidomain structure will be calculated. The net magnetization in the [110] direction is $M\sin\theta$. Since the fractional magnetization

$$\frac{M_{[110]}}{M} = f = \sin\theta$$

the relation between H and M follows from (21) as

$$H = (3f^2-2)f\left|\frac{K_1}{M}\right| + \frac{4\pi}{3}f \quad (24)$$

where H and $|K_1/M|$ are expressed in units of M and $1 \geqq f \geqq \sqrt{2/3}$. Analyses similar to the above could be carried out for other crystalline directions, but not as simply mathematically. No effects of this kind would be expected along an easy anisotropy axis.

Secondary resonances of the kind described here have been observed by Tannenwald[11] in a group of Mn ferrites. See Fig. 13. Secondary resonances were found at 9.150 kmc under appropriate temperature conditions but were not found at all at 23.0 kmc; this apparently was too high an operating frequency. No unusual effects were found in easy crystal directions. Tannenwald presented his [110] secondary resonance data in a Mn-Fe ferrite in the form of a resonance field vs temperature curve. This curve can be reproduced using his K_1/M results, the curves of Fig. 12, and M values which, for example, range from 591 cgs units at 40°K to 517 cgs units at 138°K. These M values are within the range deduced from magnetization data of Pauthenet[14] and x-ray observations of Vervey and Heilmann.[15] Some of

[14] R. Pauthenet, "Variation thermique de l'acmantation spontanée des ferrites de nickel, cobalt, fer et manganèse," *Compt. Rend.*, vol. 230, pp. 1842–1843; May, 1950.

[15] E. J. W. Verwey and E. J. Heilmann, "Physical properties and cation arrangement of oxides with spinel structures—I Cation arrangement in spinels," *J. Chem. Phys.*, vol. 15, pp. 174–180; April, 1947.

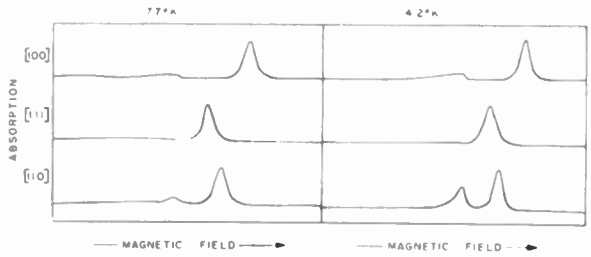

Fig. 13—Traces of absorption vs magnetic field in an Mn-Fe ferrite at 4.2°K and 77°K in the three principal crystal axes. $f=9.100$ kmc. (Tannenwald [11])

these data were criticized by Gorter[16] but the question is rather moot since the chemical and crystallographic analyses were not made on the spherical specimen actually used in these microwave experiments.

The [110] direction analysis for positive anisotropy is quite similar to that for the negative case. Two kinds of domains are postulated as before. The domain structure is illustrated in Fig. 14. The equilibrium conditions for

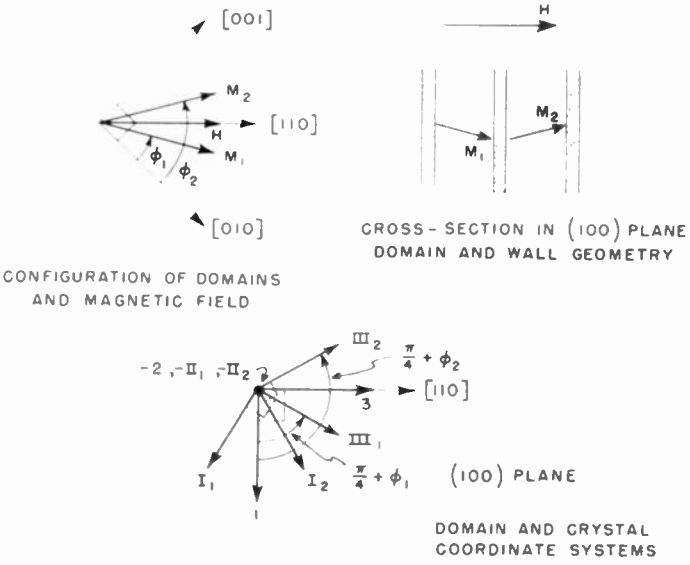

Fig. 14—Multidomain structure in positive anisotropy crystal, $\vec{H}$ in [110] direction. (Artman.[13])

the free energy (17) are satisfied by $\theta_1=\theta_2=\pi/2$ and

$$\phi = \phi_1 = \frac{\pi}{2} - \phi_2.$$

The energy, equilibrium and resonance conditions are, expressing quantities in units of K/M:

$$F = \frac{1}{4}(\sin^2 2\phi) - H\sin\left(\frac{\pi}{4}+\phi\right) + \frac{\pi M}{3}(1+\sin 2\phi) \tag{25}$$

$$H = \frac{\sin 4\phi + \dfrac{4\pi M}{3}\cos 2\phi}{2\cos\left(\dfrac{\pi}{4}+\phi\right)} \tag{26}$$

$$\left(\frac{\omega}{\gamma}\right)_\perp = \left\{\left[2 - \sin^2 2\phi + H\sin\left(\frac{\pi}{4}+\phi\right) + \frac{4\pi M}{3}\sin^2\left(\frac{\pi}{4}-\phi\right)\right]\cdot\left[2\cos 4\phi + H\sin\left(\frac{\pi}{4}+\phi\right) + 4\pi M\sin^2\left(\frac{\pi}{4}-\phi\right)\right]\right\}^{1/2} \tag{27a}$$

$$\left(\frac{\omega}{\gamma}\right)_\parallel = \left\{\left[2 - \sin^2 2\phi + H\sin\left(\frac{\pi}{4}+\phi\right) - \frac{2\pi M}{3}(1+\sin 2\phi)\right]\cdot\left[2\cos 4\phi + H\sin\left(\frac{\pi}{4}+\phi\right) - \frac{4\pi M}{3}\sin 2\phi\right]\right\}^{1/2}. \tag{27b}$$

The resonance curves (27a) and (27b) are plotted together with the usual single domain resonance curve in Fig. 15 opposite. Multiple domain effects will be seen if the operating frequency, ω/γ is not too high. The multiple domain structure collapses at $\phi=\pi/4$ for which

$$H = \frac{4\pi M}{3} + 2.$$

At this point $(\omega/\gamma)_\parallel$ becomes zero and

$$\left(\frac{\omega}{\gamma}\right)_\perp = \left(\frac{\omega}{\gamma}\right) = \left[\left(\frac{4\pi M}{3}+3\right)\frac{4\pi M}{3}\right]^{1/2}. \tag{28}$$

The gross susceptibility tensor elements are, with reference to the axes used in (23):

$$\bar{\chi}_{11} = \frac{4\pi M^2 A\sin^2\left(\dfrac{\pi}{4}+\phi\right)}{AC - z^2}$$

$$\bar{\chi}_{22} = \frac{4\pi M^2 C}{AC - z^2}$$

$$\bar{\chi}_{33} = \frac{4\pi M^2 B\sin^2\left(\dfrac{\pi}{4}-\phi\right)}{BD - z^2} \tag{29}$$

$$\bar{\kappa}_{12} = \bar{\kappa}_{21} = \bar{\kappa} = \frac{4\pi M^2 z\sin\left(\dfrac{\pi}{4}+\phi\right)}{AC - z^2}$$

[16] E. W. Gorter, "Saturation magnetization and crystal chemistry of ferrimagnetic oxides," *Philips Res. Rep.*, vol. 9, pp. 295–320; August, 1951, pp. 321–365; October 1954, pp. 403–443; December, 1954.

with z equal to

$$(\omega_0 - j/T)\frac{M \sin\theta}{\gamma}$$

and where A, B, C, and D are given by (19).

The magnetization curve for this structure is

$$H = 2f[2f^2 - 1]\frac{K_1}{M} + \frac{4\pi}{3}f \qquad (30)$$

where H and K_1/M are expressed in units of M and $1 \geqq f \geqq 1/\sqrt{2}$. The fractional magnetization f follows from

$$\frac{M_{[110]}}{M} = f = \sin\left(\frac{\pi}{4} + \phi\right).$$

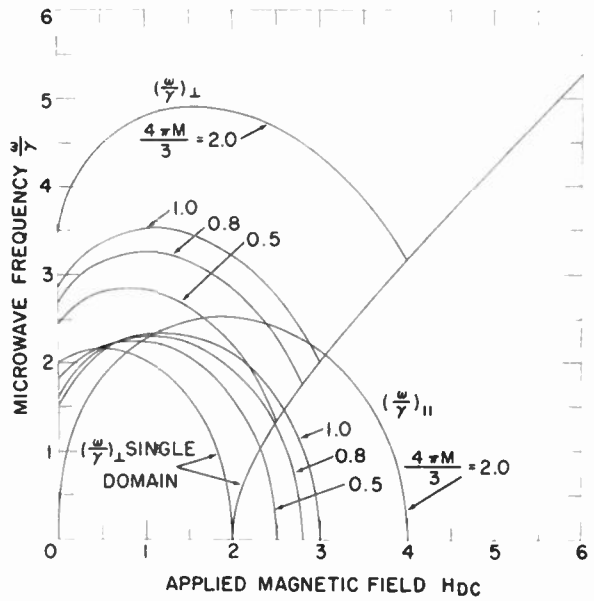

Fig. 15—Single and multidomain resonance relations in cubic crystal for positive K_1/M. $\vec{H}$ in [110] direction. ω/γ, H, and M in units of K_1/M. $(\omega/\gamma)_\parallel$ for $\vec{h_{rf}}$ in [110] direction. $(\omega/\gamma)_\perp$ for $\vec{h_{rf}} \perp$ [110] direction.

Multiple resonance observations made by Tannenwald[10] on Co ferrite at 23.8 kmc at elevated temperatures have confirmed the general features of the theory.

As expected, the secondary peaks were absent in the easy directions of magnetization. Some of the traces are shown in Fig. 16. Since second-order anisotropy is significant the curves of Fig. 15 are not quite appropriate. Nevertheless, a reasonable interpretation can still be made of the [110] direction results. The experimental conditions correspond approximately to an operating frequency

$$\frac{\omega}{\gamma} \Big/ \frac{K_1}{M} \text{ of } 3.4$$

intercepting an $(\omega/\gamma)_\perp$ curve for which

$$\frac{4\pi M}{3} \Big/ \frac{K_1}{M}$$

is 0.9. This $(\omega/\gamma)_\perp$ curve is cut on either side of its peak so that two secondary peaks occur. These blend to form a blob as shown in the figure. Further data were taken on Co ferrite at 47.3 kmc by Artman at room temperature and at 50°C. The resonances were several thousand oersteds in width, indications of multiple domain effects were observed. A detailed comparison of experiment to theory for Co ferrite is not possible because complete data on the magnetic and crystallographic properties of the samples used in the microwave experiments are not available.

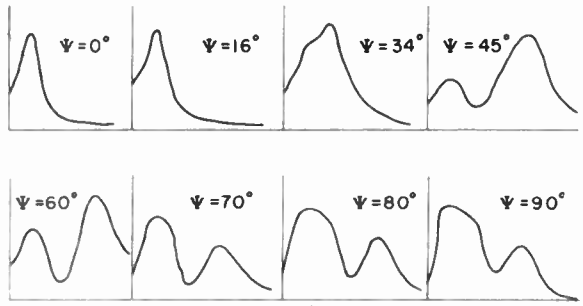

Fig. 16—Traces of absorption vs magnetic field in a Co ferrite at 90°C and 23.800 kcm. (Tannenwald.[10])

It is felt that the experimental data provide good evidence for the existence of multi domain structures which are essentially of the simple type postulated. Unfortunately a complete set of microwave, magnetic, chemical, and crystallographic measurements have never been made on any one ferrite sample. Although the $(\omega/\gamma)_\parallel$ resonance has been observed in $BaFe_{12}O_{19}$ by Smit and Beljers[3] it has not yet been seen in the cubical ferrites. Magnetization curve data which could be used as corroborative information on the domain structure are not available. Nor have any direct optical observations been made on the domain structure in cubical ferrites. Many of these investigations could be more easily done on ferrite disks, to which the sphere analysis presented here can be adapted very easily.

Acknowledgment

Much of the material presented in this paper was derived from a report prepared while the author was a staff member at Lincoln Laboratory, M.I.T. The computations were performed by Mrs. M. M. Campbell and W. D. Doyle of Lincoln Laboratory and also by the Parke Mathematical Laboratory. The author is indebted to his former colleagues, P. E. Tannenwald and S. Foner, for many valuable discussions. In closing, he would like to thank Lincoln Laboratory for making available the illustrations in the text.

Dielectric Properties of and Conductivity in Ferrites*

LEGRAND G. VAN UITERT†

Summary—**The dielectric properties of ferrites are dependent upon their methods of preparation. Low resistivity ferrites in which the individual grains are separated by air gaps or are coated with films that have high resistivities behave as inhomogeneous dielectric materials. Such low resistivity grains covered by high resistivity films are formed upon cooling slightly reduced ceramic ferrites in an oxygen containing atmosphere. Apparent low-frequency dielectric constants as high as 10^5 are found as a consequence of this. Ferrites with dc resistivities of 10^9 Ω cm or higher, in general, have dielectric losses which are low enough to meet the requirements of microwave applications. Resistivities of this order can be obtained in modified magnesium and nickel ferrites. The effects on conduction of varying composition and temperature are discussed in some detail.**

Introduction

THE FERRITES are a class of magnetic oxides which have the general formula AB_2O_4. They are structurally isomorphous with the mineral spinel ($MgAl_2O_4$) and contain eight molecules per unit cell. There are equivalent positions in this unit cell for eight metal ions surrounded tetrahedrally by four oxygen ions and sixteen metal ions surrounded octahedrally by six oxygen ions. These sites may be filled by cations having the valence combinations: 1) A^{2+}, $2B^{3+}$, 2) A^{4+}, $2B^{2+}$, 3) A^{6+}, $2B^{1+}$, and combinations wherein ($M^{+}+M^{3+}$) may be substituted for ($2M^{2+}$).

Since their introduction, by Snoek [1], as high-permeability core materials, there has been a continuing interest in their magnetic properties. As a class, the resistivities of these materials are sufficiently high that eddy current losses can be discounted in their inductor applications [2]. For this reason relatively little work has been directed at their dielectric characteristics, except in the instances where they have had a bearing on their magnetic properties. However, the current expanding interest in ferrites at microwave frequencies has served to emphasize the need for a careful examination of this field.

The ferrites are semiconductors by nature. Their resistivities can vary from 5×10^{-3} Ω-cm in the case of magnetite (Fe_3O_4) [3], a low value which is attributed to the presence of divalent iron, to well over 10^{11} Ω-cm in certain magnesium and nickel ferrites [4] at room temperature. It is possible to vary markedly the electrical properties of a given polycrystalline ferrite through the heat treatment employed in its preparation. The oxygen dissociation pressure over Fe_2O_3 increases rapidly above 1200°C. [5], which is low in the temperature range in which ferrites are normally fired. This leads to the formation of small amounts of divalent iron during firing unless sufficient ions with higher affinities for oxygen are present.

When a ferrite is sintered under slightly reducing conditions, the divalent iron formed in the body leads to high conductivity. Upon cooling such a material in an oxygen-containing atmosphere, it is possible to form films having high resistivities over its constituent grains. This occurs through the agency of oxygen migrating up pores in the material to reoxidize divalent iron ions (or any other ions that have been reduced by the high-temperature treatment) that lie near the grain surfaces. A number of investigators [6–8] have pointed out that this process, plus the contributions from air gaps between grains, can lead to the formation of an inhomogeneous dielectric structure.

In the course of this presentation, we shall consider: First, the low frequency dispersion of resistivities and dielectric constants in such materials and related phenomena; second, the general characteristics of ferrites with suitably low dielectric losses for microwave applications; and third, the cause and control of conductivity in ferrites.

Low Frequency Dispersion

Abnormally high-dielectric constants have been observed in ferrites by several investigators. In 1938, Blechstein [6] showed that certain manganese ferrites possess surprisingly high dielectric constants. Brockman, Dowling, and Steneck [9] found, in 1949, that an apparent value of approximately 10^5 in ferroxcube III—a manganese zinc ferrite—was, in part, responsible for the dimensional resonance effects observed in that material. This aroused considerable interest in the low frequency dielectric behavior of ferrites. Among others, investigations have been carried out by Koops [7] on nickel zinc ferrites, Möltgen [8] on copper zinc ferrites, and Kamiyoshi [10] on nickel ferrite and cobalt ferrite.

Fig. 1 depicts the dispersions in dielectric constants and resistivities that were obtained by Koops on a nickel zinc ferrite. These effects have been interpreted by him and by Möltgen as the result of an inhomogeneous dielectric structure discussed by Maxwell [11] and Wagner [12].

According to Koops, a good phenomenological theory of the dispersion can be based on the assumption that R_p and C_p, the parallel resistance and capacitance of the material, result from an equivalent circuit, as shown in Fig. 2, in which R_1, R_2, C_1, and C_2 are constants. AC

* Original manuscript received by the IRE, May 21, 1956. Presented at Symposium on the Microwave Properties and Applications of Ferrites, Harvard Univ., Cambridge, Mass., April 2–4, 1956.

† Bell Telephone Laboratories, Murray Hill, N. J.

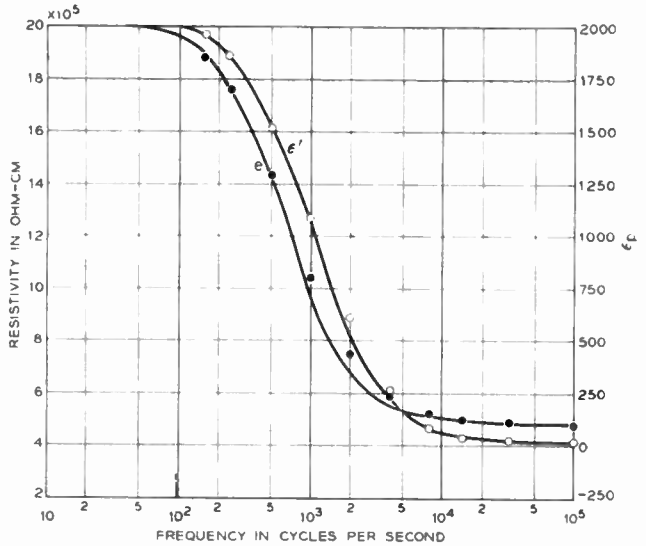

Fig. 1—Dispersions in resistivity and dielectric constant for a nickel zinc ferrite—after Koops.

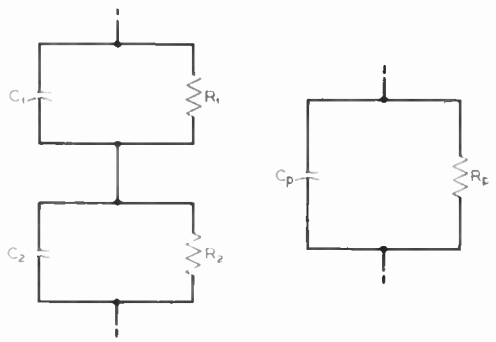

Fig. 2—If the right-hand circuit is equivalent to the left-hand one with C_1, C_2, R_1, and R_2 constants, then C_p and R_p are not constants with respect to frequency but obey dispersion formulas—after Koops.

theory predicts that R_p and C_p then obey dispersion formulas. This is equivalent to a solid state model consisting of a compact of relatively good conducting grains separated by poor conducting layers.

The dispersion equations that Koops derived from the consideration of Fig. 2 are represented by

$$\rho_p = \rho_p^{\infty} + \frac{\rho_p^{0} - \rho_p^{\infty}}{1 + T_p^{2}\omega^{2}}$$

and

$$\epsilon_p = \epsilon_p^{\infty} + \frac{\epsilon_p^{0} - \epsilon_p^{\infty}}{1 + T_\epsilon^{2}\omega^{2}}$$

where

ρ_p = the parallel resistivity
ρ_p^{∞} = the high-frequency value of ρ_p
ρ_p^{0} = the low-frequency value of ρ_p
T_p = the relaxation constant for ρ_p
ω = frequency in radians per second

and

ϵ_p = the apparent parallel dielectric constant
ϵ_p^{∞} = the high-frequency value of ϵ_p
ϵ_p^{0} = the low-frequency value of ϵ_p
T_ϵ = the relaxation constant for ϵ_p.

We may assume the following:

$x \ll 1$ where x is the ratio of the thickness of the layers to the thickness of the grains.

$\rho_1 \gg \rho_2$ where ρ_1 is the resistivity of the layers and ρ_2 is the resistivity of the grains.

$x\rho_1 > \rho_2$ by a reasonable factor, which applies for the examples of current interest. And $\epsilon_1 = \epsilon_2$ where ϵ_1 is the dielectric constant of the layers and ϵ_2 is the dielectric constant of the grains (this appears to be justifiable on the basis that most oxides have $\epsilon \simeq 10$).

It then follows

$$\text{(a)}\quad \rho_p \simeq \rho_2 + \frac{x\rho_1}{1 + c\dfrac{\rho_1\rho_2}{x}\omega^{2}}$$

and

$$\text{(b)}\quad \epsilon_p \simeq \epsilon_2 + \frac{\epsilon_2/x}{1 + c\dfrac{\rho_2^{2}}{x^{2}}\omega^{2}}$$

where $c = \epsilon_0^{2}\epsilon_2^{2} =$ a constant.

Relationship (b) indicates that the following approximations are applicable in predicting the behavior of the dielectric dispersion

1) The low frequency value of the apparent dielectric constant is approximately equal to ϵ_2/x or $10/x$.
2) The frequency at which the dispersion in dielectric constant occurs decreases as ρ_2 increases.
3) The dispersion frequency decreases as x decreases.

Relationships in Dispersion Data

The above approximations serve to correlate the data on the dielectric constant dispersions in the literature. The relationships found for a nickel zinc ferrite [7], a copper zinc ferrite [8], a manganese zinc ferrite [2], ferramics A, B, and I [13], and on the compositions $NiFe_{1.9}Mn_{.02}O_{4\pm}$ fired at 1250°C. (NM-1250) and 1350°C. (NM-1350) and $NiFe_{1.9}O_{4\pm}$ fired at 1250°C. (N1250) are shown in Fig. 3. The indicated curve numbers, the types of material, their low frequency (10^3 cps) resistivities, their high frequency resistivities, and

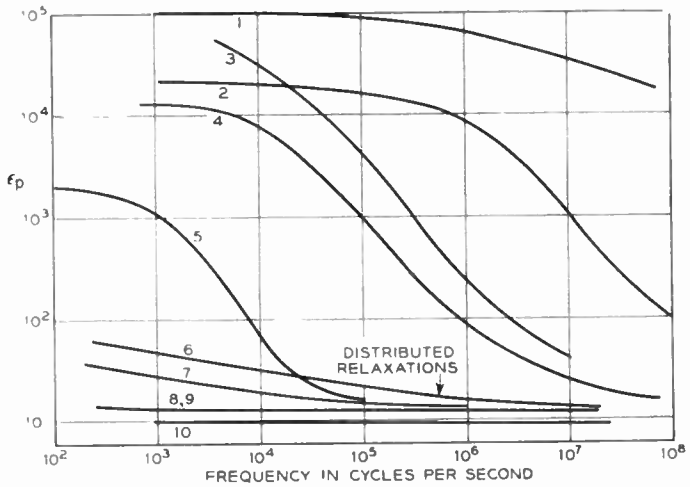

Fig. 3—Parallel dielectric constants as a function of frequency for ferrites listed in Table 1.

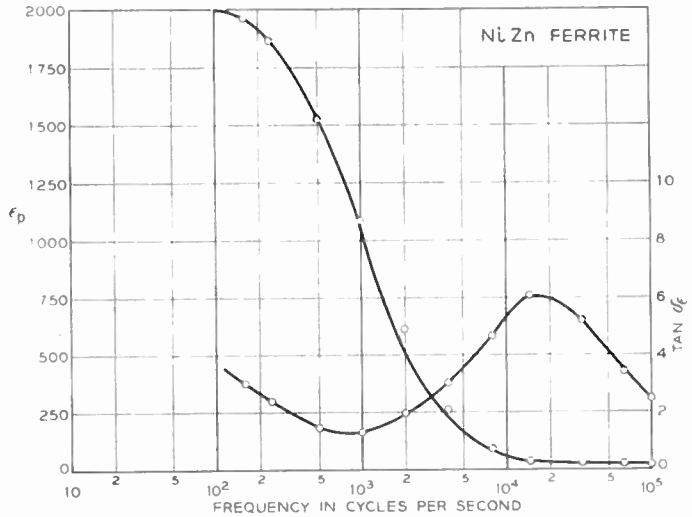

Fig. 4—Dispersions in the parallel dielectric constants and dielectric loss tangents of a nickel zinc ferrite—after Koops.

the associated frequency of measurement, at the high frequency ends of the dispersions; and references to data on the materials are given in Table I below.

TABLE I

Fig. 3 No.	Ferrite	Ref.	$\rho 10^3$ Ω cm	$\rho(x)$ Ω cm	(x)
1	Mn-Zn	2	130	10	10^8
2	Ferramic B	13	2×10^5	80	10^8
3	Cu-Zn	8	1×10^3	400	10^7
4	Ferramic I	13	5×10^5	3×10^3	10^7
5	Ni-Zn	7	2×10^6	5×10^5*	10^5
6	NM1350	14	8×10^5	1×10^6	10^7
7	N1250	14	6×10^6	4×10^5	10^7
8	NM1250	14	2×10^9	1×10^7	10^7
9	Crowloy BX113	13	6×10^8	3×10^6	10^7
10	Ferramic A	13	2×10^9	1×10^7	10^7

* Would be $\sim5\times10^4$ at 10^7 cps.

In general the points representing a 50 per cent decline of ϵ_p from $\epsilon_p 0$ occur at frequencies approximately given by

$$f(c/s) = \frac{10^{12}}{\epsilon_p{}^0 \rho_2}.$$

Materials N-1250 and NM-1350 may be considered to represent dispersions with more than one relaxation constant.

If the dispersion in ϵ_p is great enough, a noticeable peak in $\tan_{\delta\epsilon}$ $(=\epsilon''/\epsilon_p)$ occurs, as shown in Fig. 4. This peak, to a large extent, is due to the rapid increase in ϵ_p as frequency decreases through the dispersion while ϵ'', the imaginary part of the complex dielectric constant, increases much more slowly—roughly as does $1/\omega$.[1] The peak in $\tan_{\delta\epsilon}$ occurs at a frequency approximately one order of magnitude higher than that of the midpoint of the dispersion. Thus, it may be used as a reference for indicating the dependence of this midpoint upon resistivity. By comparing the temperature dependencies of dc resistivity and ω at the peak in $\tan_{\delta\epsilon}$ (see Fig. 5) Kamiyoshi [10] was able to demonstrate a direct relationship, in the absence of effects that might change the value of x. He found that the activation energies of the mechanisms responsible for the dispersion and for the dc conduction were equal. Wijn and van der Heide [15] found that low-frequency peak values that occur in the magnetic loss tangents of certain high conducting ferrites show this same dependence upon resistivity. Hence, they suggest the mechanism responsible for producing the dispersions in ϵ_p and ρ_p is also

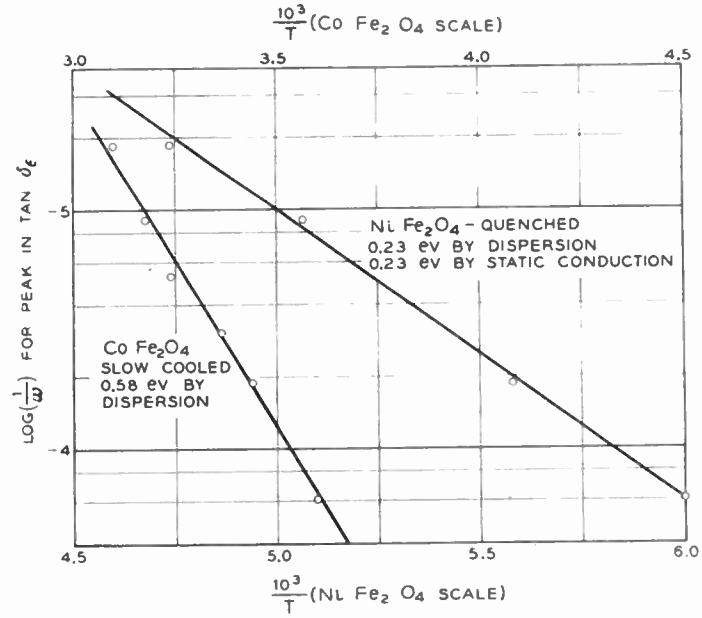

Fig. 5—The dependence of dispersion upon temperature—after Okamura and Shimoizaka.

[1] Apart from contributions that are proportional to $1/\omega$, ϵ'' itself may show a peak corresponding with the midpoint of the dispersion [10]. However, this effect is small on the scale used in Fig. 4.

responsible for certain contributions to magnetic loss.

Fig. 6 shows the relationships found by Möltgen between dc resistivity and the frequencies at which the peaks in $\tan\delta_\epsilon$ occur for a series of Cu-Zn ferrites and one Ni-Zn ferrite at room temperature. The remarkably consistent results reflect a near constant value of x with a direct dependence of ρ_1 upon ρ_2. These relationships seem reasonable when one considers that copper containing ferrites, as a class, fire well at a common temperature which in general is selected in the 1100°C. Hence, the samples were probably subjected to the same firing conditions and cooling cycle.

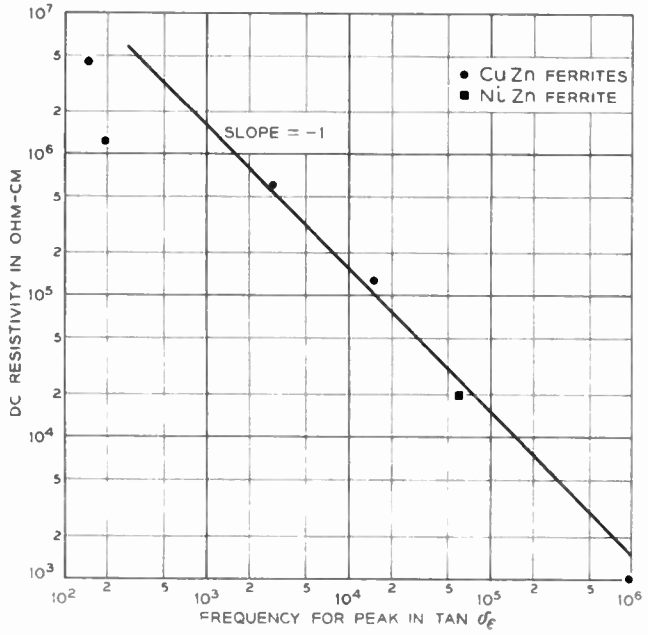

Fig. 6—The dependence of the peak in the dielectric loss tangent upon dc resistivity—based upon the data of Möltgen.

Evidence for the dependence of the thickness of the high-resistivity layers upon the conditions under which the fired parts are cooled is found in the data of Koops. The points on the two curves in Fig. 7 represent the frequencies at which the peaks in $\tan\delta_\epsilon$ occur as a function of the sample resistivities. The resistivities for the one line were measured at 10^3 cps (which is on the low-frequency side of the dispersions of ϵ_p), and the resistivities for the other line were measured at 3.5×10^7 cps (which is on the high-frequency side of the dispersions). The firing conditions, cooling conditions, and resultant values of ϵ_p measured at 10^3 cps are indicated in Fig. 7. According to the previous considerations of Koops model, one would expect x to be inversely proportional to $\epsilon_p o$, and the frequencies at which the peaks in $\tan\delta_\epsilon$ occur to be displaced in the high frequency direction by increasing values of x. The (-1) slope in Fig. 7 represents the expected dependence of this frequency upon ρ_2 for a fixed value of x. Hence, the larger negative slopes of lines through the plotted data indicate the

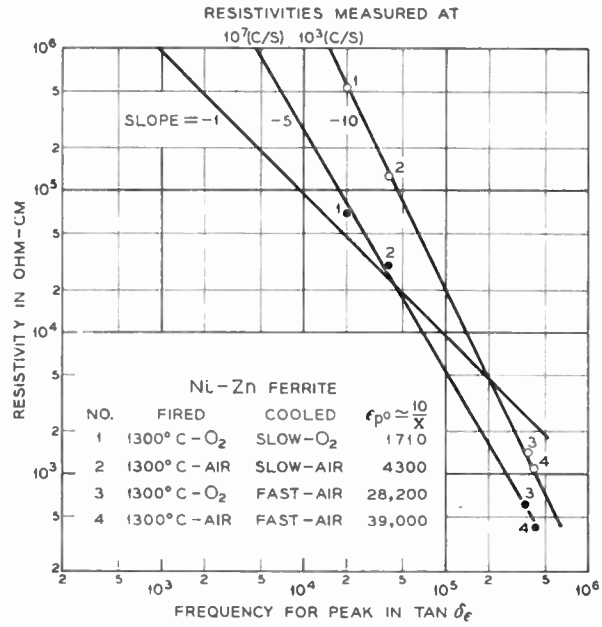

Fig. 7—The peak in the dielectric loss tangent moves to higher frequencies as wall thickness increases and as O_2 pressure during cooling and cooling time increases—based on the data of Koops.

expected displacement toward higher frequencies. These results demonstrate that both ρ_2 and x increase with the O_2 pressure over the samples during cooling and the cooling time.

Dimensional Resonance

The high apparent dielectric constants that occur at low frequencies in certain high-permeability ferrites, such as the MnZn sample and the CuZn sample in Fig. 3, can contribute to the development of resonance effects that lead to large losses in the megacycle range. The wavelength inside of the material is approximately equal to $\lambda_m = (c/f)(\mu\epsilon)^{-1/2}$. When this wavelength is less than twice the relevant dimensions of the core, standing waves are set up which cause large magnetic and dielectric losses [16]. As Brockman, Dowling, and Steneck [9] have shown, because of a large ϵ_p (*e.g.*, 10^4) together with a high μ (*e.g.*, 10^3) in the MnZn ferrite, ferroxcube III, losses from this source become important for a dimension of approximately 2 cm at 2.5 mc. Fig. 8(a) depicts the effect on the term $\epsilon_p/\epsilon_p(10^3)$, where $\epsilon_p(10^3)$ is the apparent dielectric constant at 10^3 cps, caused by reducing the relevant dimension of ferroxcube III from the critical value for dimensional resonance (lower curve) to a value sufficiently small to eliminate the effect.

Möltgen [8] was able to eliminate the effects of dimensional resonance upon ϵ_p in the 2.5 mc range in ferroxcube III by applying a magnetic field to the material at the same time as the measurements were carried out. The coil currents employed to cause the effects shown in Fig. 8(b) were sufficient to reduce the initial permeability of the material, pushing dimensional resonance to higher frequencies.

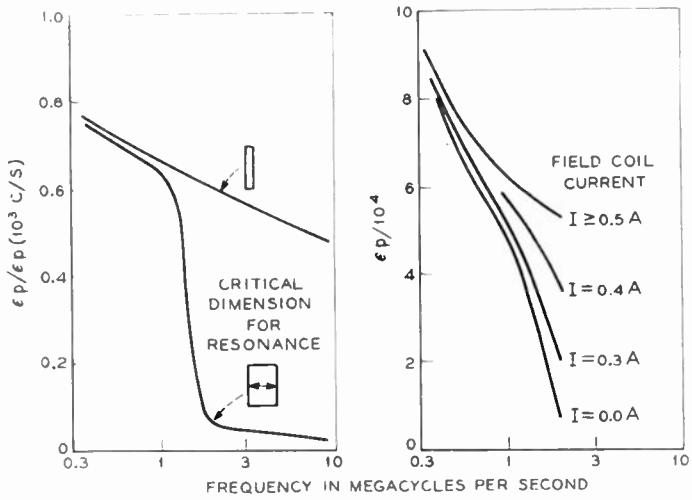

Fig. 8(a)—The effect of dimensional resonance on the apparent dielectric constant—after Brockman *et al.*
(b) The effect of a magnetic field on dimensional resonance—after Möltgen.

Characteristic Frequency Dependencies of $\tan_{\delta\epsilon}$

The courses of $\tan_{\delta\epsilon}$ as a function of frequency for several of the samples listed in Table 1 are depicted in Fig. 9.

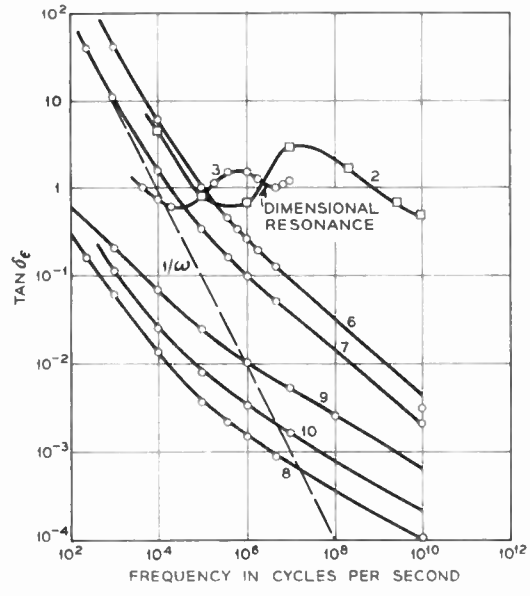

Fig. 9—The dependencies of the dielectric loss tangents upon frequency for the ferrites listed in Table 1.

The ferrites with low values of ρ_2, such as ferramic B, have high values of $\tan_{\delta\epsilon}$ extending out to the microwave region.

The curves for ferramic B and the Cu-Zn ferrite show peaks in $\tan_{\delta\epsilon}$ as a consequence of their high-dielectric constants at low frequencies. Möltgen [8] has shown that the increasing values of $\tan_{\delta\epsilon}$ at the high-frequency end of the curve for the CuZn ferrite is due to dimensional resonance. This was demonstrated by subjecting the sample to a magnetic field as in the case of ferroxcube III.

Samples that are fired to high relative densities or have high body resistivities do not show a peak in $\tan_{\delta\epsilon}$ since their low-frequency dielectric constants are not high enough (*e.g.*, ferramic A, NM-1250, NM-1350). $\tan_{\delta\epsilon}$ for these materials tends to vary as $1/\omega$ in accordance with the relationship $\tan_{\delta\epsilon} = (\rho_p \omega \epsilon_0 \epsilon_p)^{-1}$. The fact that its rate of decrease with frequency is always less than that of $1/\omega$ (as seen in Fig. 9) is attributable to the rise of conduction with frequency in these materials.

Ferrites for Microwave Applications

It is desirable to minimize both magnetic losses that can be associated with inhomogeneity and dielectric losses that are associated with conductivity in ferrites designated for microwave applications. In many instances the magnetic losses can be reduced by eliminating porosity in the material. This has the effect of minimizing the half line width for ferromagnetic resonance [17]. The dc resistivities of materials prepared to have such high relative densities correlate quite well with their microwave loss tangents. This is indicated by the curves for $\tan_{\delta\epsilon}$ in Fig. 9 which tend to converge toward their high-frequency ends. The ends near 10^{10} cps for N-1250, NM-1250, and MN-1350 in this figure were determined by Rowen and Kankowski [18].

Fig. 10 represents the relationships found between $\tan_{\delta\epsilon}$ measured at 9.4 kmc [18] and dc resistivity for a number of nickel ferrites with high relative densities. Roughly, there is a one order of magnitude decrease in $\tan_{\delta\epsilon}$ at this frequency for each two and one-half orders of magnitude increase in dc resistivity. In general it would appear that dielectric loss tangents of 5×10^{-4} or less at 9.4 kmc can be realized in materials with dc sistivities of 10^9 Ω cm or better.

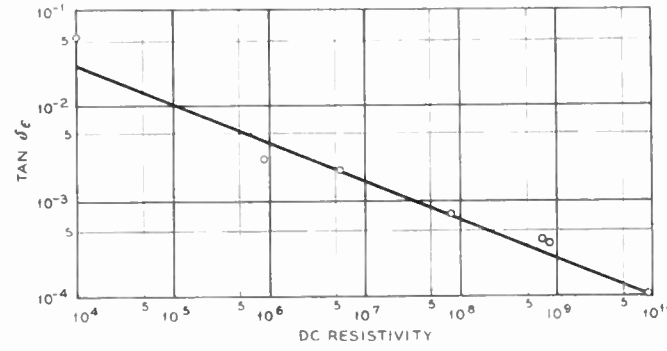

Fig. 10—The dielectric loss tangents at 9.4 kilomegacycles vs dc resistivities for a series of nickel ferrites containing various small additions of manganese. Slope = 0.40; $\epsilon \simeq 1.0$.

Measurement of Conductivity

In measuring the conductivity of ferrite materials, it is important to eliminate possible errors from contact resistance. Reliable methods that have been employed in obtaining the data reviewed herein fall into three categories:

1) The four contact method [19] where the potential drop between contacts on a sample having a known current flow through it is determined by a null point method.

2) The two contact method where metal (*e.g.* Ag, Au, Pt) is vapor deposited upon the surfaces in a vacuum [7, 8].

3) A two contact method where indium amalgam is rubbed onto freshly ground surfaces [20].

Method 1) is always free from contact-resistance difficulties and should always be employed when measuring low-resistivity materials. The contacts employed in methods 2) and 3) can be quickly checked for contact resistance or polarization by ascertaining that the resistivity of the assembly is not field dependent [8], [20], [21].

Source of Conductivity

Like other semiconducting oxides, the resistivities of ferrites are greatly affected by the presence of impurities. According to Verewey and deBoer [22] efficient electronic conduction in these compounds can be associated with the presence of ions of a given element in more than one valence state distributed randomly over crystallographically equivalent lattice points.

The classic example, Fe_3O_4, is one of the best nonmetallic conductors. Its resistivity is approximately 5×10^{-3} Ω cm at room temperature [23]. Its high conductivity is attributed to the occurrence of both Fe^{2+} and Fe^{3+} upon identical (octahedral) lattice sites in the spinel structure. In this situation electrons can move from divalent iron ions to trivalent iron ions within the octahedral positions without causing a change in the energy state of the crystal as a result of the transitions.

Verwey, Haayman, Romeijn, and Van Oosterhout [24] have shown that conduction can be enhanced in high resistivity oxides by incorporating very small amounts of foreign oxides into the structure whose metal ions take valencies other than that of the host.

Fig. 11 shows the marked effect on resistivity of adding lithium to NiO in quantities up to one atom per cent. Each lithium ion in the structure induces the formation of one Ni^{3+} ion to preserve electrical neutrality [24]. In this case, conduction occurs by the migration of holes (p-type conduction) [25]. Similar effects are observed in Fe_2O_3 by incorporating titanium into the structure giving rise to electron migration (*n*-type conduction). In general, the substitution of a cation of a high-resistivity material by a cation that tends to stay in a lower valence state leads to *p*-type conduction, and the substitution by a cation that tends to stay in a higher valence state leads to *n*-type conduction. Additions from the one category can be employed to suppress the effects of the other.

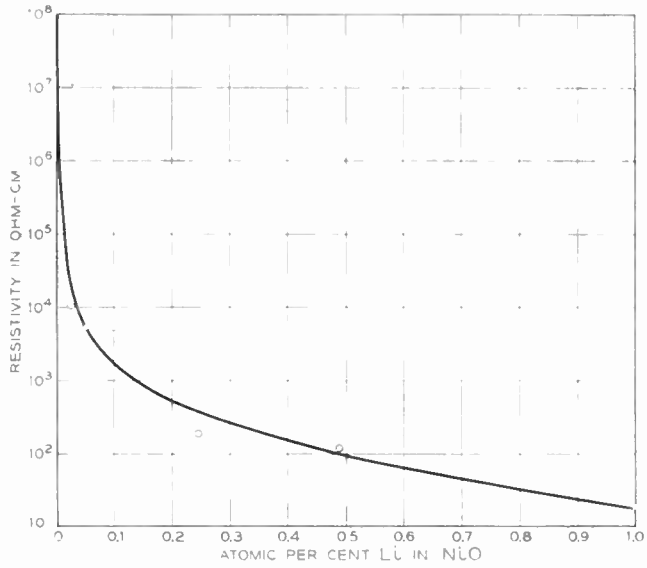

Fig. 11—The development of conduction through controlled valency —after Verwey *et al.*

Fig. 12 shows the effect on resistivity of the presence of iron in excess of the stoichiometric ratio 1(Ni+Zn):2Fe. The presence of excess iron leads to the formation of Fe^{2+} and hence high conductivity in the solid solution. While the presence of Fe^{2+} is advantageous in some instances [1], because it reduces magnetostriction, it is highly undesirable in ferrites for microwave applications [26]. As indicated by Snoek [1] the presence of Fe^{2+} can be greatly curtailed by employing less than the stoichiometric ratio of iron in the composition.

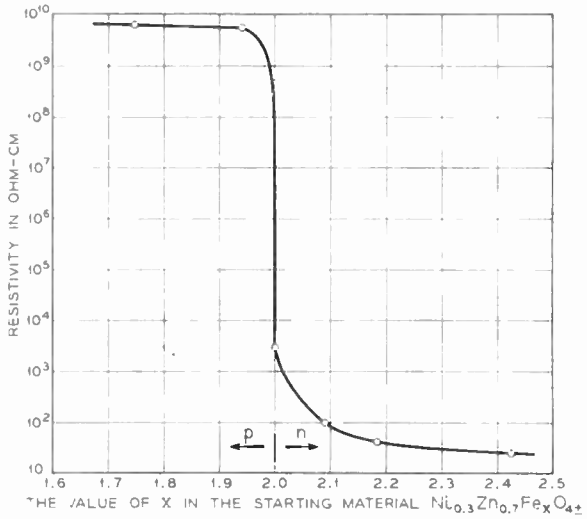

Fig. 12—The dependence of resistivity upon iron stoichiometry—materials fired at 1250°C.

Fig. 13 depicts the relationships between resistivity and composition found for high-purity nickel-zinc ferrites that are iron deficient [20]. The broken line indicates the values of resistivity that were obtained prior to grinding the surfaces of the samples and the solid line indicates the values after doing so. Chemical

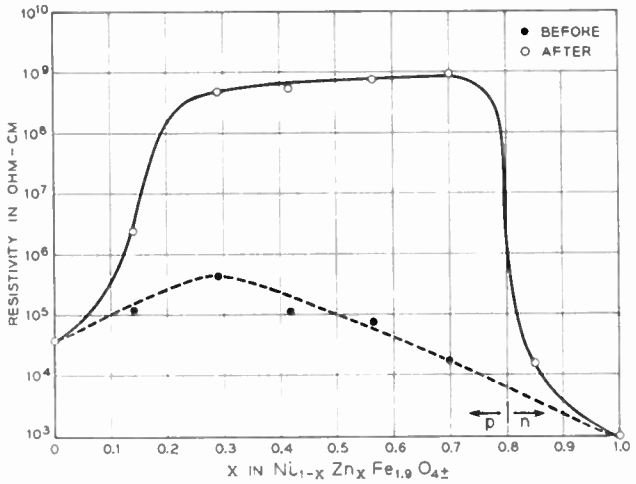

Fig. 13—The resistivities of samples fired at 1250°C. before and after surface grinding.

checks indicate zinc lost from the surface of the sample leads to the presence of Fe^{2+}, and hence to the formation of a low-resistivity surface layer. This curve indicates that the resistivity of $ZnFe_2O_4$ as well as that of $NiFe_2O_4$[1] can be increased by mixing the two. Since $ZnFe_2O_4$ is an n-type conductor and the $NiFe_2O_4$ studied in this case is a p-type conductor,[2] the high resistivity of the mixed system may, in part, be due to electron-hole compensation. Another important effect in the mixed system is the dilution of the conduction mechanisms in both sets of lattice sites. The partial substitution of nickel (which enters octahedral sites) for zinc (which has a strong affinity for tetrahedral sites) dilutes conduction that occurs through the octahedral sites. In the same manner a partial substitution of zinc for nickel in $NiFe_2O_4$ may dilute conduction effects associated with or occurring through the tetrahedral sites.

Dilution effects of this sort are evident in the series $Mg_{1.0}Al_xFe_{2-x}O_4$ fired at 1350°C. in oxygen and at 1375°C. in air (see Fig. 14). Magnesium ferrite is somewhat reduced under these conditions. As might be expected [27] the incorporation of aluminum ions, which do not lend themselves to the conduction process, limits the degree of $Fe^{2+}-Fe^{3+}$ conduction that occurs.

An efficient method of curtailing such highly effective conduction mechanisms as that for $Fe^{2+}-Fe^{3+}$ consists of replacing these by less effective ones. Verwey and deBoer [22] have shown that Co_3O_4 and Mn_3O_4, while possessing the same structure as Fe_3O_4, have resistivities that are approximately eight orders of magnitude larger than the latter. These oxides presumably differ from the familiar 2:3 spinels wherein one divalent metal ion is in combination with two trivalent ions ($M^{2+}M_2^{3+}O_4$) in that they exist as 4:2 spinels ($M^{4+}M_2^{2+}O_4$) with the M^{4+} ions occupying tetrahedral sites. Under these conditions easy conduction mechanisms do not occur, since there is an appreciable change in coulombic forces surrounding the participating ions as a result of the transfer of an electron. Since Co^{2+} and Mn^{2+} have higher affinities for oxygen than Ni^{2+}, while Co^{4+} and Mn^{4+} give up oxygen to Fe^{2+}, solid solutions of these 4:2 spinels with magnesium or nickel ferrites can serve to eliminate the most serious forms of conduction in these materials.

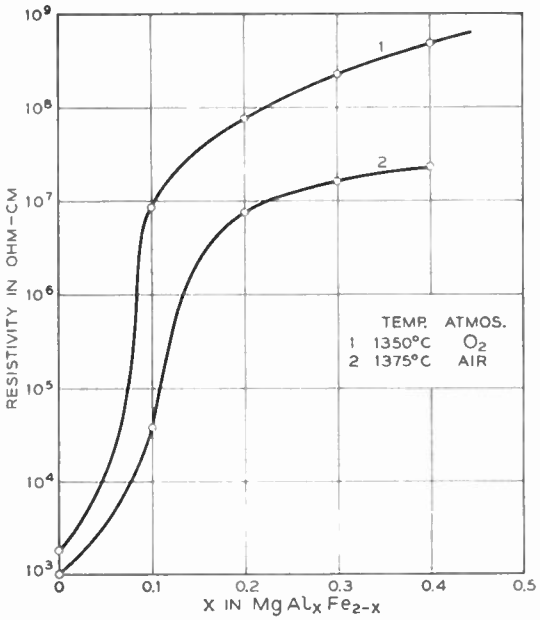

Fig. 14—Examples of the dependence of resistivity upon aluminum content in magnesium aluminum ferrites.

Fig. 15 depicts the dependencies of resistivity in nickel and magnesium ferrite upon manganese and cobalt additions when fired at 1250°C. to high relative densities [4]. One can see a large increase in resistivity, particularly in the case of magnesium ferrite where there are no canceling effects from possible p-type and n-type conduction mechanisms as in nickel ferrite. In effect, at the peak values of resistivity the Mn and Co additions are just sufficient to eliminate easier conduction mechanisms. Beyond these values, resistivity decreases with their additions.

In certain cases it is advantageous to mix copper ferrite with other ferrites to obtain more suitable characteristics [28]. One of the particular advantages of having copper present in the system is that the resulting composition can then be sintered to high densities at a much lower temperature [29]. This is of interest in preparing materials for microwave applications since magnetic losses can be minimized by achieving a high relative density (values of 98 per cent are not unreasonable). Although the substitution of copper for nickel or magnesium affects resistivity adversely, this does not appear to be serious until the copper is present in excess of 30 per cent of the total divalent ion content of MFe_2O_4. The effect of partially substituting copper for

[2] The compositions with Ni/Zn ratios $>1/4$ have positive thermoelectric voltages.

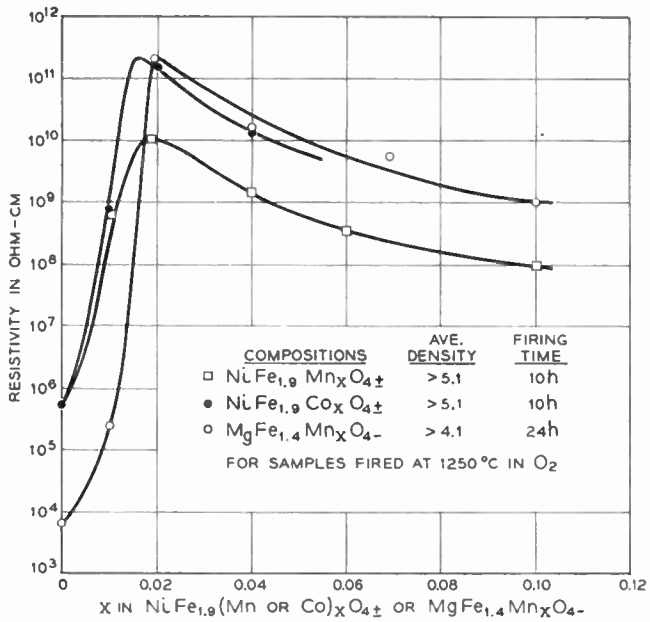

Fig. 15—The improvement of resistivity in high-density ferrites through additions of manganese or cobalt.

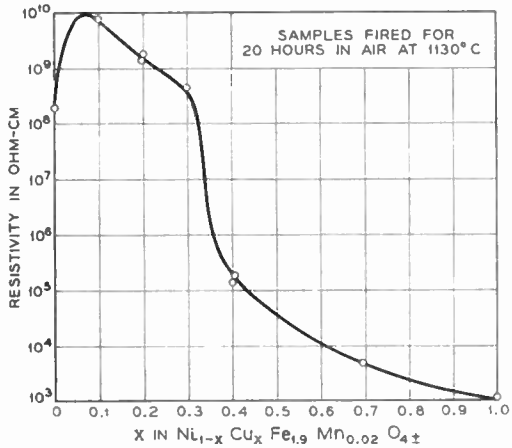

Fig. 16—The dependence of resistivity upon the copper content in nickel copper ferrites.

nickel in a high resistivity ferrite such as NM1250 is illustrated in Fig. 16.

This series of nickel copper ferrites was fired at 1130°C. for 20 hours in oxygen. The resistivity of $NiFe_{1.9}Mn_{.02}O_{4\pm}$ is low in this case because it does not sinter properly at this temperature. With the first additions of copper, however, satisfactory densities (~5.3 gms/cm³) were achieved. The curve shows a somewhat gradual decline in resistivity with copper content until one-third of the nickel has been replaced. At this point, the curve breaks rather sharply and falls in an asymptotic manner to much lower values. This break may be considered to occur at that point where, statistically, a sufficient number of copper ions, which lend themselves to conduction under these circumstances, have been introduced so that continuous conduction paths through the material begin to be realized.

Temperature Dependence of Resistivity

The equation relating resistivity ρ to activation energy (Q) is

$$\rho = Ae^{Q/kt}.$$

Where A is an essentially temperature independent constant which depends upon the nature of the material, k is the Boltzmann constant and T is the absolute temperature. Hence when the natural logarithms of resistivity are plotted vs $1/T$ the slopes of the resulting straight lines segments represent Q/k values for different conduction mechanisms. Breaks and discontinuities that are found to occur in data on ferrites represented in this way may be attributed to several sources.

Komar and Kliushin [30] have observed, as shown in Fig. 17, that changes in the activation energies for conduction which occur at high temperatures for several ferrites correlate well with the ferromagnetic Curie temperatures of the materials.

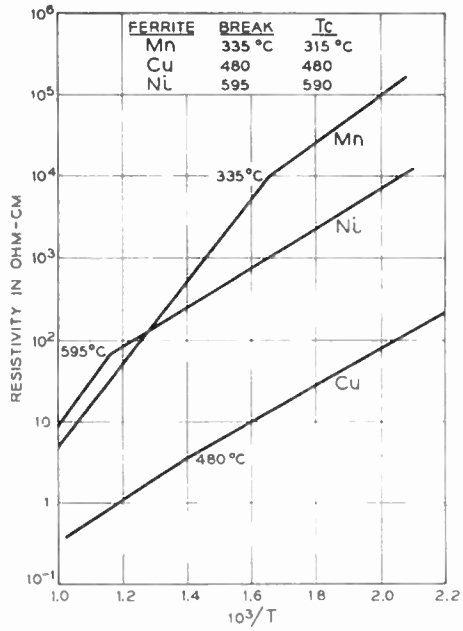

Fig. 17—Breaks occurring in the vicinities of the Curie temperatures of several ferrites—after Komar and Kliushin.

A low temperature discontinuity (see Fig. 18) that occurs in Fe_3O_4 at 120°K [31, 32] has been explained by Verwey and Haayman [23] as being due to the ordering of Fe^{2+} and Fe^{3+} ions in the octahedral lattice sites. This ordering is accompanied by a small change in crystal structure toward orthorhombic symmetry [33, 34].

Breaks in the curves representing log ρ vs $1/T$ can also occur where the dominant mechanism of conduction in the material changes [27]. In Fig. 19 the temperature dependencies of resistivity for the series of nickel ferrites containing manganese ($NiFe_{1.9}Mn_xO_{4\pm}$) shown in Fig. 15 are depicted. These measurements are all below 70°C.

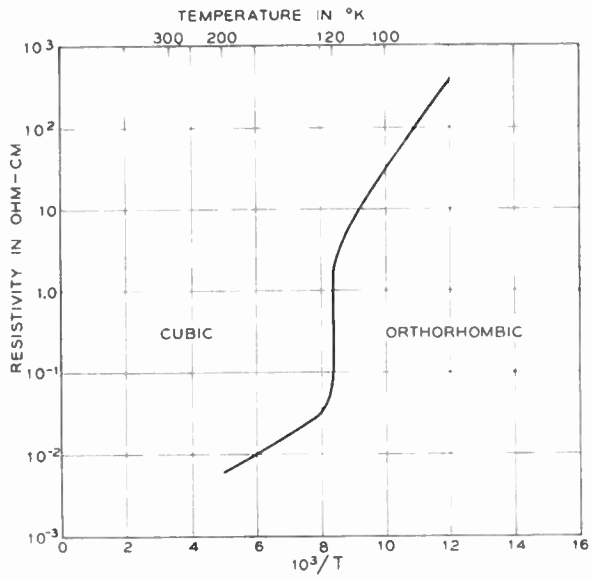

Fig. 18—Resistivity discontinuity due to $Fe^{2+}-Fe^{3+}$ ordering at the cubic-orthorhombic transition temperature of Fe_3O_4—after Verwey and Haayman.

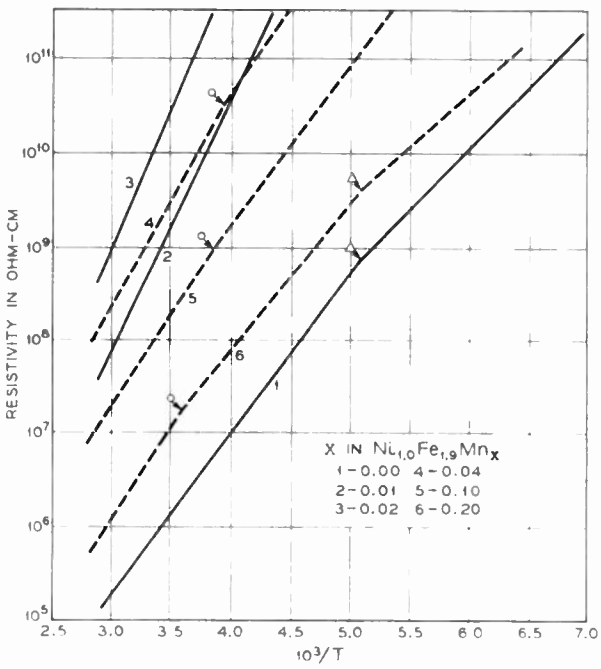

Fig. 19—The temperature dependencies of resistivities for the indicated series fired at 1250°C.

The sample numbers increase with manganese content as follows: Mn = 0.0, 0.01, 0.02, 0.04, 0.10, 0.20. The manganese free sample [1] shows one break at 195°K. The high manganese content sample [6] shows the same break as well as one at 280°K. The temperature at which this latter break occurs is dependent upon the manganese content of the sample. It drops to lower values as manganese content is decreased. As can be inferred from the slopes, in general, activation energy at room temperature increases with resistivity [27].

A final category of thermal discontinuities is that embodying hysteresis effects. Romeijn [33] has shown that a thermal hysteresis exists in the neighborhood of the transition of the low temperature (tetragonal) from of Mn_3O_4 to the cubic above 1170°C. In general, discontinuities of the type found at 120°K for Fe_3O_4 and the above mentioned thermal hysteresis effects can be related to phase transitions. Anomalous results showing a thermal low temperature hysteresis of unexplained origin, however, has been found by Morin and Geballe [35] in a single crystal of $Ni_{.8}^{2+}Fe_{.2}^{2+}Fe_2^{2+}O_4$.

Acknowledgment

The author wishes to thank C. D. Owens, J. H. Rowen, and E. F. Kankowski for making their dielectric constant data available, and also D. Edelson, J. N. Hobstetter, J. H. Scaff, and F. J. Schnettler for helpful comments on this manuscript.

Bibliography

[1] Snoek, J. L., *New Developments in Ferromagnetic Materials*. New York, Elsevier Publishing Company, 1949.
[2] Polder, D., "Ferrite Materials." *Proceedings of the Institute of Electrical Engineers*, Vol. 97, Part II (1950), p. 246.
[3] Verwey, E. J. W., and Haayman, P. W., "Electronic Conductivity and Transition Point of Magnetite (Fe_3O_4)." *Physica*, Vol. 8 (1941), p. 979.
[4] Van Uitert, L. G., "High Resistivity Nickel Ferrites—The Effect of Minor Additions of Manganese or Cobalt." *The Journal of Chemical Physics*, Vol. 24 (1956), p. 306.
[5] Hostetter, J. C., and Roberts, H. S., "Note on Dissociation of Ferric Oxide Dissolved in Glass and Its Relation to Color of Iron Bearing Glasses." *Journal of the American Ceramic Society*, Vol. 4 (1921), p. 927.
[6] Blechschmidt, E., "Dielectric Properties of Manganese Ferrites." *Physikalische Zeitschrift vereinigt mit dem Jahrbuch der Radioaktivität und Elektronik*, Vol. 39 (1938), p. 212.
[7] Koops, C. G., "On the Dispersion of Resistivity and Dielectric Constant of Some Semiconductors at Audio frequencies." *Physical Review*, Vol. 83 (1951), p. 121.
[8] Moltgen, G., "Dielektrische Untersuchungen an Ferriten." *Zeitschrift für angewandte Physik*, Vol. 4 (1952), p. 216.
[9] Brockman, F. W., Dowling, P. H., and Steneck, W. G., "Dimensional Effects Resulting from a High Dielectric Constant Found in a Ferromagnetic Ferrite." *Physical Review*, Vol. 77 (1950), p. 85.
[10] Kamiyoshi, K., "Low Frequency Dispersion in Ni and Co Ferrites." *Scientific Reports of the Research Institutes of the Tohoku University*, Vol. A3 (1951), p. 716.
[11] Maxwell, J. C., *Electricity and Magnetism*. London, Oxford University Press, Vol. 1, Section 328.
[12] Wagner, K. W., "Zur Theorie der unvollkommenen Dielektrika." *Annalen der Physik*, Vol. 40 (1913), p. 817. Also, *Archiv für Elektrotechnik*, Vol. 2 (1914), p. 371.
[13] Crowley, H. L., and General Ceramics data taken from the tables of: von Hippel, A. R., *Dielectric Materials and Their Applications*, New York, John Wiley and Sons, Inc., 1945, c.f. 36.
[14] Private communication from C. D. Owens of Bell Telephone Laboratories, Murray Hill, N. J.
[15] Wijn, H. P. J., and van der Heide, H., "A Richter Type After-Effect in Ferrites Containing Ferrous and Ferric Ions." *Review of Modern Physics*, Vol. 25 (1953), p. 98.
[16] For a concise discussion of the effects of resistivity on magnetic losses see:
Gorter, E. W., "Some Properties of Ferrites in Connection with Their Chemistry." PROCEEDINGS OF THE IRE, Vol. 43 (December, 1955), pp. 1945–1973.
[17] Kojima, Y., "The G-Factor of Ferromagnetic Spinels." *Scientific Reports of the Research Institutes of Tohoku University*, Vol. A6 (1954), p. 614.
[18] Private communication from J. H. Rowen and E. F. Kankowski of Bell Telephone Laboratories, Murray Hill, N. J. See further: Rowen, J. H., and Von Aulock, W., "Measurement of the Complex Tensor Permeability of Ferrites." *Physical Review*, Vol. 96 (1954), p. 1151.
[19] Morin, F. J., "Electrical Properties of a Fe_2O_3." *Physical Review*, Vol. 93 (1954), p. 1199.
Morin, F. J., "Electrical Properties of NiO." *Physical Review*, Vol. 93 (1954), p. 1195.

[20] Van Uitert, L. G., "DC Resistivity in the Nickel and Nickel Zinc Ferrite System." *Journal of Chemical Physics*, Vol. 23 (1955), p. 1883.
[21] Flaschen, S. S., and Van Uitert, L. G., "New Low Contact Resistance Electrode." *Journal of Applied Physics* (February, 1956).
[22] Verwey, E. J. W., and deBoer, J. H., "Cation Arrangement in a Few Oxides With Crystal Structures of the Spinel Type." *Recueil des travaux chimiques des Pays-Bas*, Vol. 55 (1936), p. 531.
[23] Verwey, E. J. W., and Haayman, P. W., "Electronic Conductivity and Transition Point of Magnetite (Fe_3O_4)." *Physica*, Vol. 8 (1941), p. 979.
[24] Verwey, E. J. W., Haayman, P. W., Romeijn, F. C., and van Oosterhout, G. W., "Controlled-Valency Semiconductors." *Philips Research Report*, Vol. 5 (1950), p. 173.
[25] Lark-Horovitz, K., "Conductivity in Semiconductors." *Electrical Engineering*, Vol. 68 (1949), p. 1047.
[26] Rowen, J. H., "Ferrites in Microwave Applications." *Bell System Technical Journal*, Vol. 68 (1949), p. 1047.
[27] Verwey, E. J. W., Haayman, P. W., and Romeijn, F. C., "Physical Properties and Cation Arrangement of Oxides With Spinel Structure." *Journal of Chemical Physics*, Vol. 15 (1947), p. 181.
[28] Albers-Schoneberg, E., "Ferrite Compounds With More Than Three Oxide Components." *Ceramic Age*, Vol. 59 (1952), p. 30.
[29] Van Uitert, L. G., "Nickel Copper Ferrites for Microwave Applications." *Journal of Applied Physics*, Vol. 27 (1956), p. 723.
[30] Komar, A. P., and Klivshin, V. V., "Temperature Dependence of the Electrical Resistivity of Ferrites." *Bulletin of the Academy of Science, USSR, Physics* Vol. 18 (1954), From Columbia University Technical Translation, p. 96.
[31] Okamura, T., "Transformation of Magnetite at a Low Temperature." *Scientific Reports of the Research Institutes of Tohoku University*, Vol. 21 (1932), p. 231.
[32] Verwey, E. J. W., "Electronic Conduction of Magnetite (Fe_3O_4) and Its Transition Point at Low Temperatures." *Nature*, London, Vol. 144 (1939), p. 327.
[33] Romeijn, F. C., "Physical and Crystallographical Properties of Some Spinels." *Philips Research Report*, Vol. 8 (1953), p. 304.
[34] Abrahms, S. C., and Calhoun, B. A., "The Low-Temperature Transition in Magnetite." *Acta Crystallographica*, Vol. 6 (1953), p. 105.
[35] Morin, F. J., and Geballe, T. H., "Electrical Conductivity and Seebeck Effect in $Ni_{0.80}Fe_{2.2004}$." *Physical Review*, Vol. 99 (1955), p. 467.
[36] Albers-Schoenberg, E., "Ferrites for Microwave Circuits and Digital Computers." *Journal of Applied Physics*, Vol. 25 (1954), p. 152.
[37] Fairweather, A., Roberts, F. F., and Welch, A. J. E., "Ferrites." *Reports on Progress in Physics*, The Physical Society, Vol. 15 (1952), p. 142.
[38] Fairweather, A., and Frost, D. J., "Dielectric Behavior of Granular Semiconducting Aggregates, With Special References to Some Magnesium Ferrites." *Proceedings of the Institute of Electrical Engineers*, Vol. 100 IIA (1953), p. 15.
[39] Okamura, T., Fujimura, T., and Date, M., "Dielectric Constant and Permeability of Various Ferrites in the Microwave Region." *Scientific Reports of the Research Institutes of Tohoku University*, Vol. 73 (1952), p. 191.
[40] Hewitt, W. H., "Microwave Resonance Absorption in Ferromagnetic Semiconductors." *Physical Review*, Vol. 73 (1948), p. 1118.
[41] Van Uitert, L. G., Schafer, J. P., and Hogan, C. L., "Low-Loss Ferrites for Application at 4000 Millicycles per Second." *Journal of Applied Physics*, Vol. 25 (1954), p. 925.
[42] Van Uitert, L. G., "Low Magnetic Saturation Ferrites for Microwave Applications." *Journal of Applied Physics*, Vol. 26 (1955), p. 1289.

Methods of Preparation and Crystal Chemistry of Ferrites*

DONALD L. FRESH†

Summary—**Conventional ceramic methods for pure oxide materials can generally be applied to the processing of ferrites. Specialized techniques such as coprecipitation and hydrostatic pressing are sometimes employed. A process involving nonaqueous milling and forming additives provides dense shapes.**

The general formula for ferrites is $MO \cdot Fe_2O_3$ (M is a divalent metallic cation). X-ray diffraction may be used to conduct unit cell and phase relation studies. Metallurgical micrographic techniques are useful in investigating grain and pore structure.

A study of the solid state reaction kinetics of an equimolar mixture of MgO and Fe_2O_3 at elevated temperatures showed that the reaction was expressed by the diffusion equation $(1-\sqrt[3]{1-.01x})^2 = K$ where x is the percentage of reaction at time t, and K is a constant.

History

FERRITES were first prepared by nature. The naturally occurring mineral magnetite, ferrous ferrite, aroused scientific curiosity among the Greeks centuries before the Christian era. Thales of Miletus (about 600 B.C.) stated that this material could attract iron. "He endowed the lodestone with a soul in the belief that nothing less than an inherent living force could account for the observed effect."[1]

Magnetite can be altered by substituting and combining other constituents with it to produce improved ferromagnetic spinels. Hilpert, one of the earliest experimenters, took out patents on magnetic core materials in 1909.[2] Forestier, in 1928, prepared ferrites by basic precipitation from chloride solutions and subsequent heat treatment.[3] Several Japanese investigators were active in ferrite preparation in the early 1930's.[4–6]

* Original manuscript received by the IRE, May 21, 1956. Presented at Symposium on the Microwave Properties and Applications of Ferrites, Harvard Univ., Cambridge, Mass.
† Bureau of Mines, College Pk., Md.

[1] C. Still, "The Soul of Lodestone," Murray Hill Books, Inc., New York, N. Y.-Toronto, Canada; 1946.
[2] S. Hilpert, German Patents 226,347 (1909), 227,787 (1909).
[3] H. Forestier, "Combinaisons du sesquioxyde de fer avec les monoxydes métalliques," *Ann. Chim. Xe serie*, vol. IX, pp. 353–401; May–June, 1928.
[4] Y. Kato, "Characteristics of metallic oxide magnets," *J. IEE (Japan)*, vol. 53, pp. 408–412; May, 1933.
[5] N. Kawai, "Studies of ferrites: formation of solid solutions," *J. Soc. Chem. Ind. (Japan)*, vol. 37 pp. 392–394; April, 1934.
[6] Y. Kato and T. Takei, U. S. Patents 1,976,230 (1934), 1,997,193 (1935).

A firm foundation for improved ferrites at high frequencies was laid by Snoek around 1940 when he established the importance of correct oxygen content and of homogeneous products.[7,8] Since this time, much work on the development of ferrite materials has been performed by many investigators. This has resulted in a very rapid growth of technical applications.

Physical and Chemical Characteristics

The usefulness of a ferrite in an electronic device is influenced by the physical and chemical properties of the material, which in turn are dependent on the method of preparation. These properties are listed in this section and then discussed with relation to processing parameters in the following sections.

The chemical composition is considered the most important of these properties. Only by virtue of the presence of certain combinations of chemical constituents can the desired electronic effects be obtained. An illustration of the dependence of Faraday rotation on composition is shown in Fig. 1. All processing variables were held constant within the accuracy of the processing method.

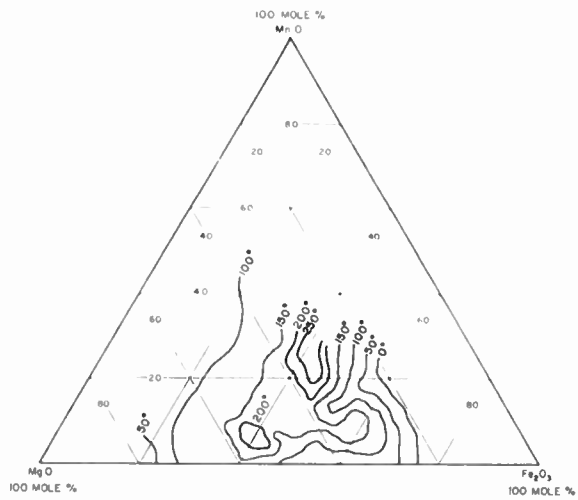

Fig. 1—Faraday rotation, degrees (sat) per inch, 9400 mc, firing temperature 1350°.

The consideration of the chemical composition, however, goes beyond the mere selection and addition of certain constituents in the reaction mixture. Of importance also are the state of valency of the cations and the amount of oxygen anion present; these are influenced by the processing parameters.

The quantity, size, and shape of air-filled pores will affect the properties of the material. These are influenced chiefly by the forming technique, firing time, and temperature.

[7] J. L. Snoek, "Magnetic and electrical properties of the binary systems $MO \cdot Fe_2O_3$," *Physica*, vol. 3, pp. 463–483; June, 1936.
[8] J. L. Snoek, "New Developments in Ferromagnetic Materials," Elsevier Publ. Co., New York, N. Y.; 1947.

The extent of internal strain within the material is of concern. This is controlled particularly by the rate of cooling during the heat treatment. It is also dependent on the homogeneity of the material and pore structure, and presence of more than one phase.

Magnetic properties are also influenced by the microscopic grain structure, such as the size, shape, and orientation of grains. The existence of more than one phase is also important. The phase relation is dependent on the original composition, the heat treating schedule, and atmosphere. Homogeneity is an important factor. The ferrite specimen should be uniform throughout from the standpoint of the above properties of 1) chemical composition, 2) porosity, 3) internal strain, 4) microscopic grain structure, and 5) phase relationships.

Reproducibility of properties is naturally of importance. The chemical composition and processing parameters must be controlled sufficiently well to permit the re-creation of properties within the narrow limits usually specified for application of microwave devices.

Finally, the ferrite specimen must have sufficient mechanical strength to allow it to be formed in a shape and/or machined to the dimensions dictated by the application. This point is quite often treated too lightly; without due care, the application may never be realized.

Methods of Preparation

Conventional Ceramic Processing

Conventional ceramic processing methods for pure oxide materials are applied with very little modification by many investigators, particularly those in industry, in preparing ferrites. When close tolerances in magnetic properties are required, as with ferrites for microwave applications, extreme care must be exercised to maintain purity and homogeneity of the material throughout the processing.

The standard procedure is shown in Fig. 2. Oxides (and often carbonates) selected chiefly on the basis of purity and particle size are mixed with a mixing medium, usually water, and milled in a steel ball mill. The mill is operated usually between four and twenty hours to obtain thorough mixing of the oxides. The grinding effect on very small particles of submicron size is minor. To minimize introduction of impurities, a rubber-lined mill with stainless balls is often employed. Although the ball mill is commonly used for the mixing step, other devices such as colloid mills and attritors may be used. Extrusion and pressing additives are occasionally introduced at this point in instances when no presintering is performed and when such additives cling to the oxides so that they are not lost when removing the milling medium.

After milling, the homogeneous oxide mixture is oven dried. To minimize preferential settling of any dense or large particles, the water is rapidly removed. Quite often the slurry is pressure-filtered prior to oven drying to expedite the removal.

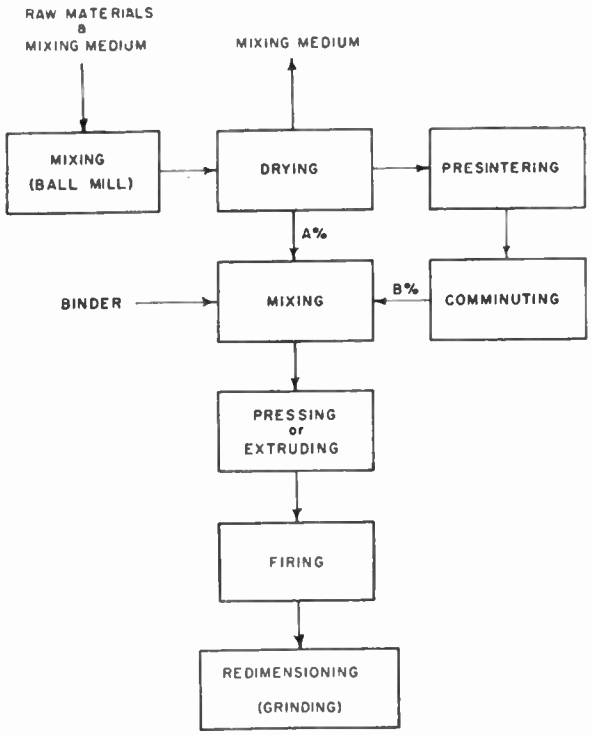

Fig. 2—Flow chart of general process used in compounding ferrites.

The dried material may then be presintered, which consists of heat-treating the oxide mixture at a temperature somewhat lower than the final firing temperature. After presintering, the oxide is comminuted to a particle size that is ceramically workable. Presintering is performed to help control shrinkage in the final shape and to influence homogeneity. All or part of the mixture may be presintered; when part is presintered, the balance is the raw oxide mixture. A definite ratio of presintered to raw oxide is often found experimentally desirable for a particular forming technique (die pressing, extrusion, etc.).

A per cent in Fig. 2 may be 100 per cent; *i.e.*, the presintering step may be completely eliminated. This is the technique that has been employed at the Bureau of Mines laboratories in preparing microwave ferrites. Comparative tests have indicated that a ferrite that is at least as dense and homogeneous as one prepared by a series of presintering and comminuting operations may be obtained by preparing the final shape directly from the raw oxide mixture. Although greater shrinkages occurred when firing shapes which were prepared by the direct method, the rupture moduli were superior to those of the presintered ferrites.

Snoek reports that properties of ferrites are influenced by the presintering and comminuting operation. He points out, however, that in certain cases the presinter method and the direct method lead to about the same results when carried out under optimum conditions.[8]

The two conventional means of forming the oxide mixture into shapes are die-pressing and extruding. With both means, organic additives are introduced (ordinarily in a water vehicle) to serve as a binder and particle lubricant. When extruding, a plasticizing agent is also needed. One organic additive occasionally serves a dual or triple role; this generally lowers the amount of organic additive needed, thereby simplifying and expediting the removal of the additive during the early stage of firing and also minimizing the voids left by the additive. Methyl cellulose is an example of a combination additive which gives fairly satisfactory results with the direct method for both pressing and extruding (considerably more methyl cellulose and water are required for extruding than for pressing).

An effective die design involves a floating die sleeve with top and bottom punches. This permits pressure to be applied from two directions and thereby reduces the packing gradient in the pressed shape. An ejection mechanism is advisable for quantity production. Proper granulation of the die charge facilitates packing. Pressures employed may vary from 1 to 10 tons per square inch or even higher depending on the nature of the charge. Vibratory and percussion pressing tends to eliminate laminations arising from air trapped among the granules. Die-pressing may be used with a variety of shapes and sizes but a serious limitation arises in that the thickness of the shape (distance between the faces bearing on the top and bottom of die) may not be large compared to the other dimensions.

Extrusion methods are preferred for the production of tubes and rods of circular, rectangular or other cross sections. They may be extruded in considerable lengths; for example, by verticle extrusion a $\frac{1}{4}$ inch diameter rod of several feet in length may be formed. The plastic mass of oxides used to charge the extruder must have the plasticizing additive blended thoroughly throughout. This is accomplished by extensive mulling of the mass. Deairing of the mass prior to extrusion by applying a vacuum is also essential. Heterogenities present in the extrusion mass will show up as imperfections in the extruded shapes. Sufficient reduction in size between the cross sectional area of the extruder barrel and the die orifice, and a proper die design to impart desirable flow characteristics to the mass are the requisites which promote knitting within the plastic mass, and the formation of dense and uniform shapes. A hydraulically actuated extruder with a five inch diameter barrel is shown in Fig. 3; this was designed at the Bureau of Mines laboratory.

For procuring the desired ferrite properties, selection of the firing schedule is preceded in importance only by selection of the composition. The firing schedule can influence chemical composition (oxygen content); phase relations; amount, size, and shape of pores; grain parameters; and strains. All of these will affect the magnetic properties.

The shapes must be heated gradually during the low temperature range of the firing cycle to slowly volatilize the organic additive. Rapid evolution of vapors will split the shapes, particularly when porosities are low. Also, at temperatures where considerable sintering and

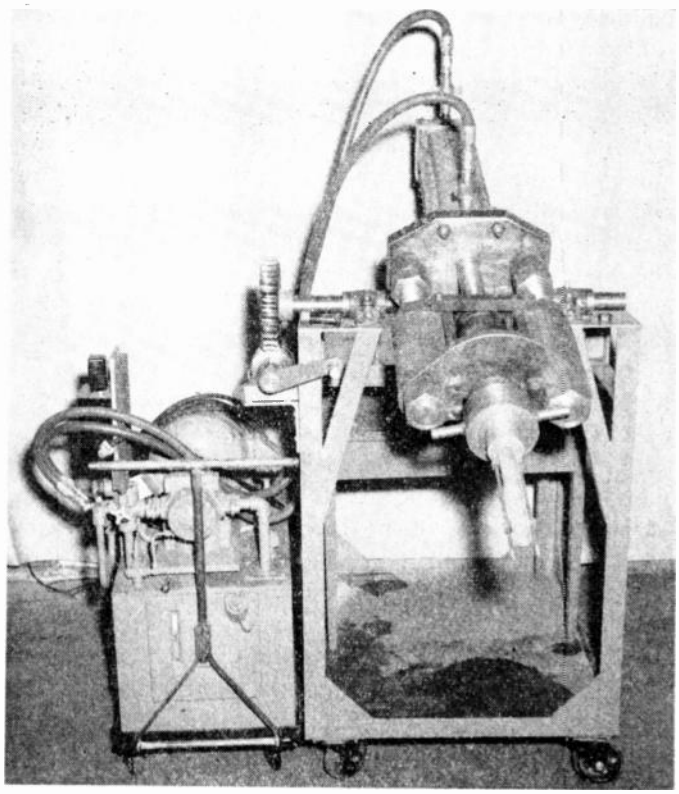

Fig. 3—Hydraulic extruder with 5-inch diameter barrel for horizontal or vertical extrusion of ferrite shapes.

shrinkage occur, the rate of heating should be slow. Fig. 4 shows typical shrinkage data which assist in selecting the schedule for a particular composition.

All ferrites, because of the presence of iron ion, are susceptible to changes in oxygen content. The equilibrium between ferric oxide and magnetite shifts very heavily to magnetite above 1370 C. in air.[9] Under reducing conditions the effect is pronounced even at lower temperatures. Since most ferrites are fired between 1100 and 1350 C., magnetite formation is not a severe problem if reducing conditions are avoided. Also, if compositions can be adjusted to contain an excess (molar) of divalent oxide, such as NiO over trivalent oxide (F_2O_3), presence of ferrous ferrite ($FeO \cdot Fe_2O_3$) is minimized further. If fired near the magnetite conversion temperature, slow cooling will tend to reoxidize any divalent iron provided the specimen is sufficiently porous.

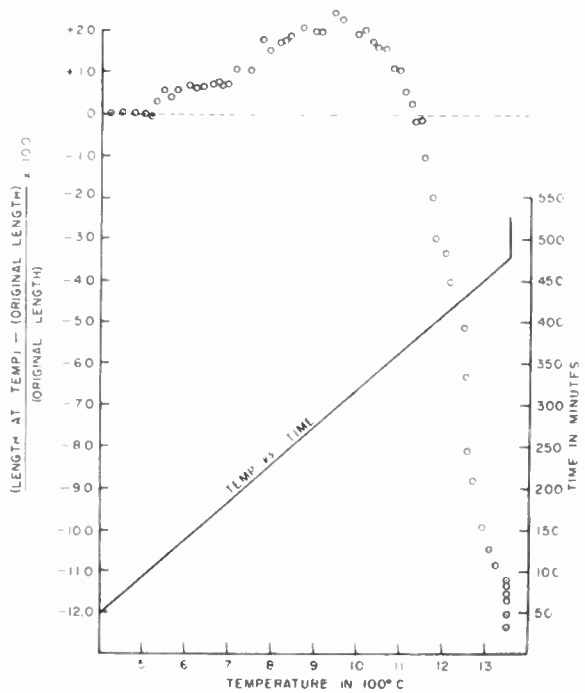

Fig. 4—Change of length of extruded shape during heating. 1.5 mol (MgO)+0.2 mol (MnO_2)+1 mol (Fe_2O_3)→ferrite.

Manganese ferrite is an extreme example of a situation where the metallic ions can exist in different states of valency and where the oxygen content can vary. If fired under ordinary conditions in air at 1300°C., an equimolar manganese ferrite composition becomes a solid solution of $MnO \cdot Fe_2O_3$, Mn_3O_4, and Fe_2O_3. With slow cooling, part of the Fe_2O_3 may separate as a discrete phase. Strong oxidizing conditions give a mixture of Mn_3O_4 and Fe_2O_3. If conditions are made more reducing in relation to those for producing $MnO \cdot Fe_2O_3$, a mixture of $MnO \cdot Fe_2O_3$ and $MnO \cdot FeO$ will result. This latter material reoxidizes on slow cooling in the same atmosphere in which it was fired provided the material is sufficiently porous. Further reduction leads first to a solid solution of MnO and FeO, then a mixture of MnO and Fe, and finally to a solid solution of Mn and Fe.[10]

The variety of products that result from a mixture of manganese oxide and iron oxide when firing parameters are altered shows the importance of the firing step. Chemical valency and oxygen content are influenced by peak temperature, heating and cooling rates, firing atmosphere, and also porosity of the shape.

In addition to the effects of firing on phase relationships as mentioned in the above example, phase relationships and solid solutions are affected also by the general rule of greater solubility at higher temperatures. The rate of cooling is therefore particularly important, and may determine whether an excess of one of the oxide components stays in solid solution or precipitates.

Quenching is a means of maintaining a high temperature equilibrium with respect to phase relations, but usually introduces appreciable internal strains in the material. Slow cooling minimizes internal strains but some internal strain in the finished piece is always encountered regardless of how slowly the material is cooled and how well it is annealed; because as room temperature is approached, the capacity to relieve strains is materially decreased. Factors that increase strain are rapid cooling, porosity, and the presence of two or more phases, where the difference in thermal

[9] O. Ralston, "Iron Oxide Reduction Equilibria," U. S. Bur. Mines Bull. 296, p. 42; 1929.

[10] E. Gorter, "Some properties of ferrites in connection with their chemistry," PROC. IRE, vol. 43, pp. 1945–1973; December, 1955.

expansion coefficients of the different phases is responsible for the strains.

The size of the crystallites or grains increases with increasing temperature. The amount of porosity tends to decrease and the pores become fewer and more spherical as higher temperatures and longer soaking periods are employed.

Although not a part of the chemical and ceramic processing, redimensioning of ferrite shapes by grinding is mentioned here since many microwave applications require special shapes. Also, when only a small number of experimental shapes are required, it is less expensive to redimension these from an available shape than to machine a new pressing or extruding die. Diamond, silicon carbide or alundum abrasive may be used in centerless grinders, surface grinders or tool-post grinders. A technique employing a tool-post grinder with a diamond wheel is used at the Bureau of Mines for obtaining small cylindrical shapes from large stock. By transmitting the thrust of the wheel toward the lathe chuck and by cutting to full depth in one pass, rods 0.015 inch diameter ×2 inches have been obtained.

Spheres for cavity measurements may be made in an abrasive-walled cylindrical chamber with a tangential air blast. Holes may be drilled with carbide or diamond tipped drills or with ultrasonic grinders.

Specialized Processing

The discussion in the above section has dealt mainly with conventional ceramic techniques as adopted for ferrite preparation. A few specialized processing methods are discussed in the following.

Certain oxides absorb and combine chemically with a sizeable quantity of water during the two mixing steps (refer to Fig. 2). Water is added to facilitate mixing in the ball-milling step and as a vehicle in the binder-introducing step. Magnesium oxide as a finely divided powder is particularly susceptible to hydration. Such hydration hinders mixing by agglomerate formation, and the water of hydration causes additional porosity in the final shape when it is removed in the early stages of kiln firing.

Experiments with nonaqueous liquids led to the development of a method at the Bureau of Mines laboratory that not only eliminated the hydration problem but it greatly aided in the forming of the oxide mixture. This method involves the use of petroleum liquids like kerosene in place of the water in the original mixing step and in the mixing step prior to forming, thereby eliminating water from the system completely. Organic wax-like additives soluble in the petroleum liquid are also introduced to facilitate pressing and extrusion. The liquid itself, however, being a very good particle lubricant and plasticizer, permits the quantity of additional additives to be lessened.

The nonaqueous processing method has resulted in more efficient mixing in the ball-milling step, the elimination of hydration, and the need for less pressing and extrusion additives. A more homogeneous and dense material is the end result. The increased density in the green shape is shown for a hydrostatic pressing experiment (discussed later) in Fig. 5.

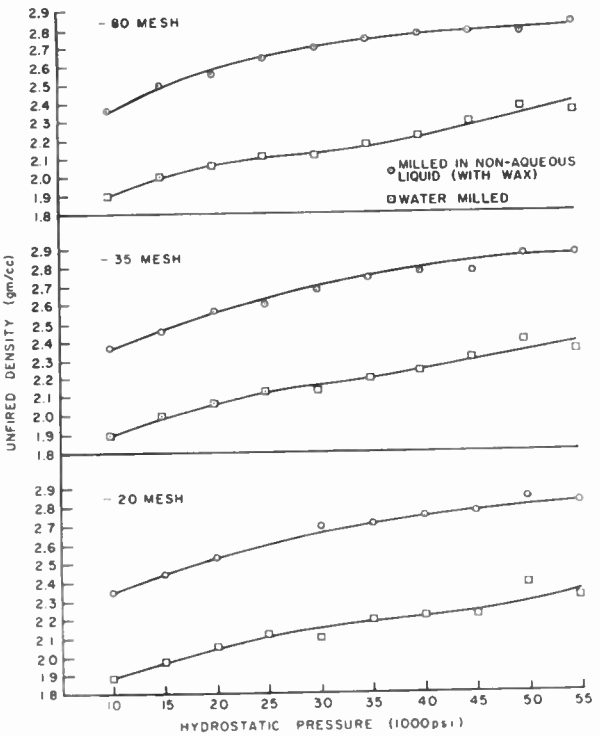

Fig. 5—Hydrostatic pressure vs unfired density experiment.

The results obtained when the nonaqueous method is used for extruded shapes prove even more gratifying. Certain magnesium ferrites and magnesium-manganese ferrites have been prepared with densities essentially equal to the theoretical density as calculated from X-ray data. In some instances densities of 99.9 per cent of theoretical density were measured. Further, this method lends to the formation of mechanically strong and dimensionally true shapes. Rods with dimensions 0.040 inch diameter ×12 inches length are formed that possess good strength and negligible camber. Dense tubes (*e.g.*, 1 inch O.D. ×½ inch I.D.) may also be prepared. When extruding tubes, an extrusion charge of stiff consistency is employed to prevent collapse or deformation during drying. Extrusion pressures as high as three tons per square inch are often required.

The nonaqueous processing method may be applied to systems other than those containing a large amount of magnesium oxide, but it is most advantageous where hydration is a problem.

Several techniques exist for obtaining more intimate contact among the reactants than is possible with conventional mixing of oxides. Basic coprecipitation from an aqueous solution of soluble salts is by no means new,[3] but it is still frequently used in the laboratory when intimate contact is desired. Particles of ferric hydroxide and magnesium hydroxide were examined by electron

microscopy in a recent coprecipitation experiment. The former had diameters of 0.01 micron; the latter were thin circular plates with diameters of 0.07 micron. Ferrite was formed under these conditions at temperatures lower than 400°C.

A technique recently reported by D. Wickham is concerned with the formation of mixed crystals (solid solutions) from ferrous oxalate dihydrate with oxalates of magnesium, manganese, cobalt, nickel, and zinc. Ferrite is formed by thermal decomposition of the mixed crystals.[11]

Hydrostatic pressing is a special shaping method that is employed when 1) the shape required is such that is cannot be formed by die-pressing or extruding, 2) extremely high packing pressures are required, or 3) directional pressing effects must be eliminated. Hydrostatic pressing is performed by placing a preformed shape (enclosed in a flexible sheath) or powder-filled flexible mold into a cylinder; the cylinder is then filled with a liquid and the system is placed under high pressure by means of a hydraulic pumping unit. Fig. 6 is a

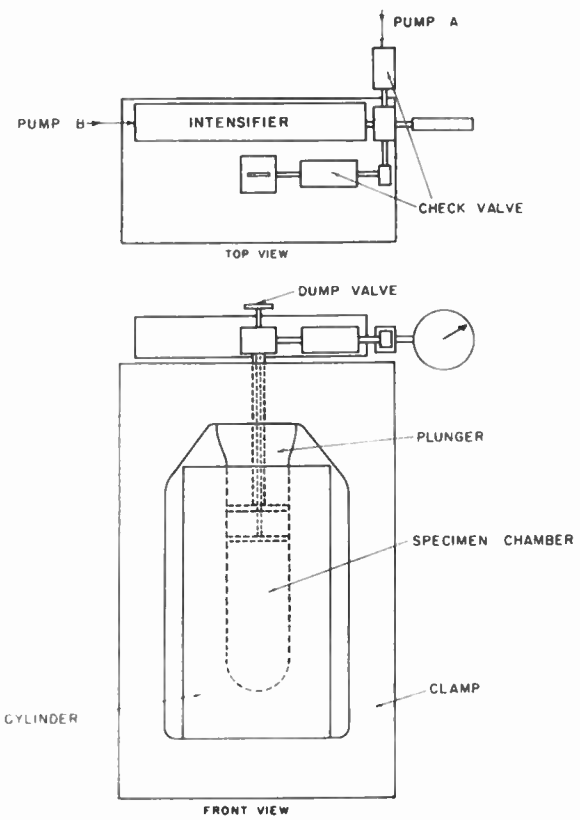

Fig. 6—Hydrostatic pressing assembly.

diagrammatic sketch of the hydrostatic pressing assembly designed and used at this laboratory. Fig. 5 indicates the effect of hydrostatic forming pressure on the density of the unfired shape.

[11] D. Wickham, "Synthesis of Ferrites and Preparation of Cobalt Ferrite Single Crystals," M. I. T. Lab. for Insulation Res., Cambridge, Mass.; October, 1954.

Controlled atmosphere firing is a specialized method that is used with ferrite compositions in which the oxygen content can vary. This is pointed out in the earlier section on the firing schedules of manganese ferrites. The compositions are fired under temperature, time and atmospheric conditions conducive to establishing the proper oxygen content. The atmosphere firing is occasionally performed as an annealing operation after the original firing is done in air.

Crystal Chemistry

The general formula of a ferrite is $MO \cdot Fe_2O_3$ where M is a divalent ion such as Mg^{++} or Ni^{++}. This material crystallizes in a face-centered-cubic form like that of the mineral spinel which is a magnesium aluminate. For this reason and because of the ferromagnetic properties, ferrites are called ferrospinels. The above formula represents the most common type of ferrospinel but other types of cubic ferromagnetic spinels exist, *e.g.*, $Mn_3O_4 \cdot (Fe_2O_3)_3$ and $Li\,Fe_5O_8$.[12,13]

A large number of different metallic ions can occur in the spinel, the primary requirement being that they are small enough so that the oxygen anions are not spread too far apart. The ionic radius of the oxygen of 1.32 A.u. is approximately twice as large as the ionic radius of the cations which fit into the lattice. With few exceptions the cation radii lie between 0.5 and 1.0 A.u. If the cations are large, as with Sr^{++} (1.35 A.u.), the spinel structure does not occur but rather a hexagonal crystal of the type $SrO \cdot 6Fe_2O_3$ is formed. Other hexagonal ferrites are $BaO \cdot 6Fe_2O_3$ and $PbO \cdot 6Fe_2O_3$.[14,15]

A unit cell of the cubic ferrite consists of eight $(MO \cdot Fe_2O_3)$'s. The 32 oxygen anions arrange in a cubic unit cell and the metallic cations fit into interstices among the anions. The geometric arrangement of the anions results in 96 interstices among the oxygens, 64 being tetrahedral (surrounded by 4 oxygen anions) and 32 octahedral (surrounded by 6 oxygen anions, each oxygen located at the 6 apexes of a regular octahedron).

The metallic cations have been found to be distributed in two ways among the oxygen anions.[16] In one case all divalent ions are placed in the tetrahedral sites and all trivalent ions in the octahedral sites. This is called the normal arrangement. In the other case, called the inverse arrangement, 8 trivalent ions are in the tetrahedral sites and the remaining 8 trivalent ions and the 8 divalent ions are in the octahedral sites. The inverse

[12] A Hoffman, "Crystal chemistry of lithium ferrites," *Naturwiss.*, vol. 26, p. 431; July, 1938.

[13] E. Verwey and M. van Bruzzen, "Structure of solid solution of Fe_2O_3 in MN_3O_4," *Zeit. für Kristallographie*, vol. 92, pp. 136–138; 1935.

[14] H. P. J. Wijn, "A new method of melting ferromagnetic semiconductors. $BaFe_{12}O_{22}$, A new kind of ferromagnetic crystal with high crystal anisotropy," *Nature*, vol. 170, pp. 707–708; October, 1952.

[15] F. G. Brockman, "A new permanent-magnet material of nonstrategic material," *Elec. Engr.* vol. 71, pp. 644–7; July, 1952.

[16] E. Verwey and E. Heilman, "Cation arrangement in spinels," *J. Chem. Phys.*, vol. 15, pp. 174–180; April, 1947.

spinel is ferromagnetic and the normal spinel is nonferromagnetic. Among the ferrites, only zinc ferrite and cadmium ferrite are normal; the others are inverse. High temperatures tend to cause intermediate arrangements between the normal and inverse structure, but at low temperature, either one is stable. Complete inverse or normal structure is obtained only if equilibrium is maintained on cooling to low temperaturse. Since it is impractical to cool that slowly, a certain combination of inverse and normal structure usually exists. The inversion parameter has been determined for some materials by X-ray diffraction.[17] Such inverse-normal studies are more conveniently conducted with neutron diffraction.[18,19] since in many cases, atomic scattering factors of the ferrite constituents are too similar to permit analysis by X-ray diffraction.

Many improved magnetic properties have been found in mixed ferrites, which are solid solutions of two or more ferrites. Mixed ferrites are not confined to cationic distributions of inverse with inverse or normal with normal crystals. Nickel-zinc ferrite is an example of an inverse-normal combination which is a very useful ferromagnetic material. Solid solutions of magnesium ferrite and magnesium aluminate, which involve a trivalent cationic substitution, are currently popular media at *S*-band microwave frequencies.[20]

Ferrite solid solutions of the system $MgO:MnO:Fe_2O_3$ have found extensive use at microwave frequencies.[21] Certain members of this system have proved valuable even when solid solution is incomplete. Compositions which contained a separate phase of MgO and which displayed very low losses at *X*-band frequencies were studied at the Bureau of Mines.

Thermodynamically speaking, solid solutions can be explained at high temperatures, but the probability of their occurrence at low temperatures is small (at zero degrees absolute, free energy considerations would render solid solutions unstable). The separation of the mixed ferrite into separate phases, however, is slow except at high temperatures; and, in practice, the cooling rates are such that insufficient time is allowed for equilibrium to be maintained. The importance of the firing schedule is indicated here. In systems where the solid solutions become unstable at temperatures where equilibrium is still maintained, rapid cooling or quenching is desirable. Gorter reports prevention of the separation of a solid solution of zinc ferrite and calcium ferrite by quenching from 1250 C.[22]

In a ferrite consisting of only two different cations, solid solutions may exist within certain limits in compositions that are nonequimolar (also called non stoichiometric); *e.g.*, $(MgO)_x \cdot (Fe_2O_3)_y$ where $x \neq y$. When $y > x$, the hexagonal Fe_2O_3 probably exists in the crystal as cubic (or gamma) Fe_2O_3. *X*-ray diffraction examination may be used to measure the extent of solid solution formation by detecting the characteristic reflections of the various phases which have not entered into solid solution or by measuring the change in unit cell dimension of the spinel. The system $(MgO)_x \cdot (Fe_2O_3)_y$ has been studied at the Bureau of Mines laboratory. Fig. 7 shows the use of the unit cell dimension method on the above system when $x > y$. According to the curve, additional MgO will not enter into solid solution when x is greater than 0.59. This was verified by the appearance of characteristic reflections of MgO in the *X*-ray pattern at this point. All specimens were heated to 1350°C. and cooled at a rate of 50°C. per hour.

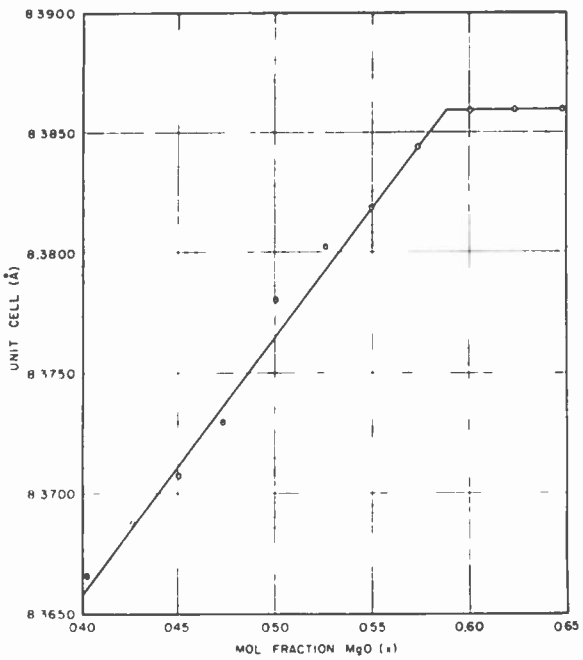

Fig. 7—Unit cell dimension (spinel) vs composition for $(MgO)_x(Fe_2O_3)_{1-x}$.

Grain structure is another aspect of crystal chemistry. The metallurgical microscope is a useful tool for studying this. Photomicrographs of polished surfaces show the size and shape of the grains, the quantity, size, and shape of the pores, and the presence of different phases. Information regarding the grain orientation may also be shown with micrographic techniques by observing the geometry of etch patterns produced on the

[17] F. J. Bertaut, "Sur quelques progres régents dans la cristallographie des spinelles, en particulier des ferrites," *de Physique et Rad.*, vol. 12, pp. 252–255; March, 1951.

[18] J. M. Hastings and L. M. Corliss, "Neutron diffraction studies of zinc ferrite and nickel ferrite," *Rev. Mod. Phys.*, vol. 25, pp. 114–121; January, 1953.

[19] L. M. Corliss, J. M. Hastings, and F. G. Brockman, "A neutron diffraction study of magnesium ferrite," *Phys. Rev.*, vol. 90, pp. 1013–1018; June, 1953.

[20] L. G. Van Uitert, J. P. Schafer, and C. L. Hogan, "Low loss ferrites for applications at 4000 mc/sec," *J. Appl. Phys.*, vol. 25, pp. 925–926; July, 1954.

[21] E. Albers-Schoenberg, "Ferrites for microwave circuits and digital computers," *J. Appl. Phys.*, vol. 25, pp. 152–154; February, 1954.

[22] E. Gorter, "Saturation magnetization and crystal chemistry of ferrimagnetic oxides," *Phillips Res. Reps.*, vol. 9, pp. 295–365, 403–443; August, October, December, 1954.

grains.[23] Caution must be exercised in interpreting micrographs since the surface is often erratically altered by polishing and etching techniques. Thermal etching is often preferrable to acid etching for this reason.

A problem encountered in ferrite processing is the inability to exactly reproduce microwave properties in successive preparations. Even when the procedure is apparently followed in detail, reproducibility is often not obtained. An explanation that can be offered is based on the complexity of structure from the standpoint of the above aspects of unit cell arrangement, phase relationship and grain structure.

In the unit cell, only 24 of 96 available interstitial sites are occupied by metallic cations. There are, therefore, many opportunities for improper positioning of the cations in the lattice with subsequent distortion of the cubic symmetry.

If a second phase exists, the concentration and location of this phase in the grain structure is a basis for the occurrance of heterogeneities, particularly since phase relationships are so sensitive to processing parameters. Other effects that may contribute to nonreproducibility are the size, shape, orientation, and imperfections of the grains. Polycrystalline ferrites are composed of grains which are not generally of the same size, shape, etc. Such differences and imperfections must be distributed uniformly throughout the structure so that the material is macroscopically homogeneous. Further, to obtain reproducibility, this homogeneity must be repeatable in successive preparation.

Solid State Reaction Kinetics

Ferrites are formed by reactions between solid components. The reaction does not usually involve a change in chemical composition but rather a transformation of crystal configurations, as indicated in the following example:

$$MgO + Fe_2O_3 \rightarrow MgO \cdot Fe_2O_3.$$

The first scientific observation of solid state reaction seems to be due to M. Faraday in 1820; this involved solid state diffusion in metals.[24] Work in the solid state reaction field was pioneered in the early 1900's by J. Hedvall,[25] G. Tammann,[26] and W. Jander.[27]

A study of the solid state reaction kinetics and the diffusion phenomena of an equimolar mixture of MgO and Fe_2O_3 at elevated temperatures was recently conducted at the Bureau of Mines Laboratory. The study was performed by observing the dependence of the extent of reaction as measured by quantitative X-ray diffraction techniques on the following variables: particle size of the reactant oxides, firing temperature, and time-at-temperature. Data for two of the reaction specimens are shown in Fig. 8.

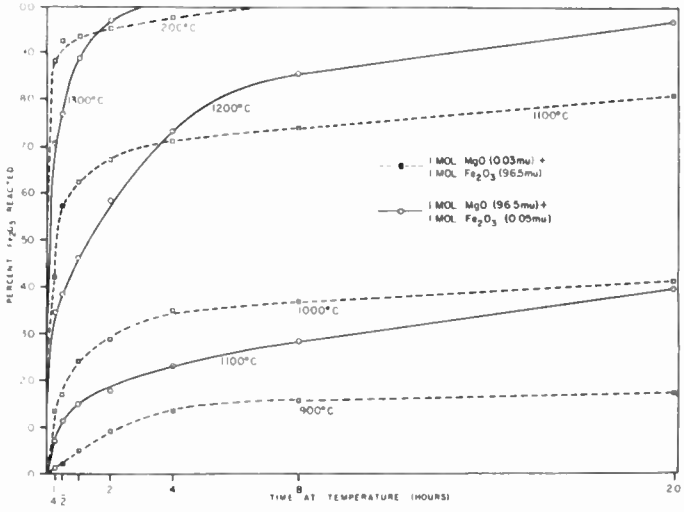

Fig. 8—Reacted ferric oxide vs time at various temperatures.

The rate determining factor was the diffusion of the reactants through the product layer as expressed by

$$\frac{dy}{dt} = \frac{k}{y} \tag{1}$$

where y is the thickness of the product layer, t is time, and k is a proportionality constant. This means that the reaction product acts as a diffusion barrier. Eq. (1) leads to the expression

$$(1 - \sqrt[3]{1 - 0.01x})^2 = Kt, \tag{2}$$

where x is the reaction percentage at time t and K is a constant.

The data were evaluated graphically and found to follow chiefly the mechanism expressed by (2). Fig. 9 is an example of the graphical interpretation. Certain specimens, particularly those involving large particles of FeO_3 and small particles of MgO (particle size ratio of approximately 1:1000) did not follow (2) as well as those involving large particles of MgO and small particles of Fe_2O_3; this relation was particularly marked at long durations of time.

By analyzing the initial reaction rates, the Fe_2O_3 component was found to migrate to a greater extent on the surface of the MgO than vice versa. Solid state diffusion rate constants and activation energies were calculated for the various reaction specimens and will be published.

[23] P. Levesque and L. Gerlach, "The metallography of ferrites," *J. Amer. Cer. Soc.*, vol. 39, pp. 119–120; March, 1956.
[24] M. Faraday and J. Stodard, "Experiments on the alloys of steel, made with a view to its improvement," *Quart. J. Sci.*, vol. 9, p. 319; July, 1820.
[25] J. Hedvall, "Platzwechselreaktionen zwischen festen phasen," *Z. anorg. Chem.*, vol. 140, p. 234; October, 1924.
[26] G. Tammann, "Chemische reaktionen in pulverförmigen gemengen zweie-kristallarten," *Z. anorg. Chem.*, vol. 149, p. 21; November, 1925.
[27] W. Jander, W., "Reaktionen im festen zustande bei höheren tempeaturen," *Z. anorg. Chem.*, vol. 163, pp. 1–30; June, 1927.

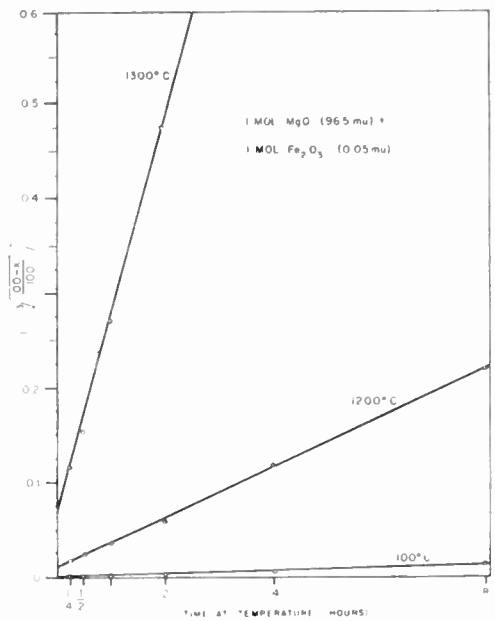

Fig. 9—Plot of $(1-\sqrt[3]{1-0.01x})^2$ vs time for solid state reaction between MgO and Fe_2O_3 (x = per cent reacted).

Results of this experiment are useful in evaluations of the processing methods and the physical and chemical behavior of materials during processing.[28]

[28] D. L. Fresh, "A Study of the Solid-State Kinetics and Diffusion Phenomena of the Reaction Between Magnesium Oxide and Ferric Oxide at Elevated Temperatures," submitted in partial fulfillment for Doctor of Philosophy degree, Catholic Univ. of America, Washington, D. C.; June, 1956.

Conclusion

Conventional ceramic methods for pure oxide materials can generally be applied to the processing of ferrites. The main operations are mixing, presintering, forming, and firing. Presintering can often be eliminated and the shape formed directly from the raw oxides. Several ferrite systems are extremely sensitive to the heat treating operation.

Certain specialized techniques have been employed in the preparation of ferrites. Hydrostatic pressing is used when high, nondirectional forming pressures are required. Coprecipitation and mixed crystal methods provide intimate contact among reactants. A process involving nonaqueous milling and extruding additives gives dense shapes.

The general formula for ferrites is $MO \cdot Fe_2O_3$ (M is a divalent metallic cation). Ferrites are normal or inverse depending on the distribution of the metallic cations in the unit cell. Improved magnetic properties have been found by forming ferrite solids solutions. X-ray diffraction may be used to detect the presence of a separate phase in ferrite materials. Metallurgical micrographic techniques are useful in studying grain and pore structure.

A study was conducted on the solid state reaction kinetics of an equimolar mixture of MgO and Fe_2O_3 at elevated temperatures. The reaction was expressed by the diffusion equation $(1-\sqrt[3]{1-0.01x})^2 = Kt$ where x is the percentage of reaction at time t, and K is a constant.

Intrinsic Tensor Permeabilities on Ferrite Rods, Spheres, and Disks*

E. G. SPENCER†, L. A. AULT†, AND R. C. LECRAW†, ASSOCIATE MEMBER, IRE

Summary—**A discussion is given of the transformation relations between the measured permeability components and the values intrinsic to the material which then do not involve the sample shape. General theoretical curves are given showing the measured permeabilities $\tilde{\mu}+\tilde{K}$ through resonance for rods and spheres deduced from the intrinsic permeability curves, $\mu+K$, which is taken to have a Landau-Lifshitz shape. Complete data are given on the four measured and intrinsic tensor permeability components through magnetic resonance for small rods, spheres, and disks of a polycrystalline magnesium-manganese ferrite. The general shape of the intrinsic curves is explained by considering the distribution of the crystallite orientation directions and the solid angles associated with these directions. The line width is of the order of magnitude to be expected by published data on other ferrite single crystals.**

* Original manuscript received by the IRE, July 3, 1956.
† Diamond Ordnance Fuze Labs., Washington, D. C.

Introduction

MEASUREMENTS of the components of the tensor permeability of polycrystalline ferrite spheres, through magnetic resonance, have been reported by the authors[1] and by Artman and Tannenwald.[2] It has been pointed out by Yager *et al.*,[3]

[1] E. G. Spencer, R. C. LeCraw, and F. Reggia, "Circularly polarized cavities for measurement of tensor permeabilities," *J. Appl. Phys.*, vol. 26, p. 354–355; March, 1955. "Measurement of microwave dielectric constants and tensor permeabilities of ferrite spheres," 1955 IRE Convention Record, Part 8 pp. 113–121.

[2] J. O. Artman and P. E. Tannenwald, "Measurement of permeability tensor ferrites," *Phys. Rev.*, vol. 91, pp. 1014–1015; August 15, 1953. "Measurement of susceptibility tensor in ferrities," *J. Appl. Phys.*, vol. 26, p. 1124: September, 1955.

[3] W. A. Yager, J. K. Galt, F. R. Merritt, and E. A. Wood, "Ferromagnetic tensor in nickle ferrite," *Phys. Rev.*, vol. 80, pp. 744–748; November 15, 1950.

and Bloembergen[4] that values derived from measurements on spheres are not intrinsic properties of the material, but depend on the sample shape. This is due to the rf demagnetizing fields changing the value of the rf magnetic field in the sample. Rowen and von Aulock[5] presented data on components of the permeability tensor of thin disks of ferrite, below magnetic resonance. They show that these measurements yield intrinsic properties since the rf demagnetizing fields are zero, the rf internal fields being equal to the externally applied rf field.

Equations have been derived[6] for obtaining the intrinsic curves from the data measured on spheres. Analogous expressions[7] have been used in obtaining intrinsic properties from measurements on rods of ferrite. These data were taken for steady magnetic fields below magnetic saturation. In extending this work measurements have been made of four components of tensor permeability through magnetic resonance on rods, spheres, and disks of a polycrystalline ferrite. For each the intrinsic components of the tensor permeability have been derived.

Experimental

The experimental techniques are described by the authors[1] with certain modifications by Artman and Tannenwald.[2] A brief résumé, but not the details, will be given here. A circularly-polarized wave is used to excite transmission-type cylindrical TE_{112} mode cavity at 9200 mc. A small ferrite sample is placed in the center of the cavity, away from the walls. The tensor permeability is given by

$$b = \begin{pmatrix} \mu & -iK & 0 \\ iK & \mu & 0 \\ 0 & 0 & 1 \end{pmatrix} h^i \qquad (1)$$

where b is the rf induction, and h^i is the rf field in the sample. For a positive and negative circularly-polarized waves, respectively, the effective permeability is a scalar, designated $\mu \pm K$. The sample is small enough so that the Bethe-Schwinger perturbation theory can be used. Using the effective scalar permeabilities for circularly-polarized waves, the Bethe-Schwinger equation becomes

$$\frac{\delta f_\pm}{f} = -\frac{4\pi m_\pm}{h_\pm{}^0}\frac{v_s}{A v_c} \qquad (2)$$

$f_\pm = f_\pm' + i f_\pm''$ is the complex frequency shift of the cavity, h^0 is the value of the applied rf magnetic field at the position of the sample before the sample is inserted in the cavity, v_s and v_c are volumes of the sample and cavity, respectively, and A is the cavity constant. The rf magnetization $m_\pm$ is given by,

$$4\pi m_\pm = (\mu \pm K - 1) h_\pm{}^i \qquad (3)$$

where $\mu \pm K = (\mu' \pm K') - i(\mu'' \pm K'')$ and $h_\pm{}^i$ are internal circularly polarized fields.

Measurements of the change in the frequency of the cavity, and the change in transmission, separately, for positive and negative circularly-polarized waves yield enough information to obtain the four tensor components.

It should be emphasized at this point that (2) is essentially exact. No approximations of rf fields in the sample have been made and there has been no statement involving sample shape.

For measurements on spheres and disks, a TE_{112} mode cavity is used. The rod is placed in a TM_{110} mode cavity[8] so that the axis of the rod is in the direction of the steady magnetic field and normal to the rf magnetic field, as shown in Fig. 1. The rod is 0.4 inch long and

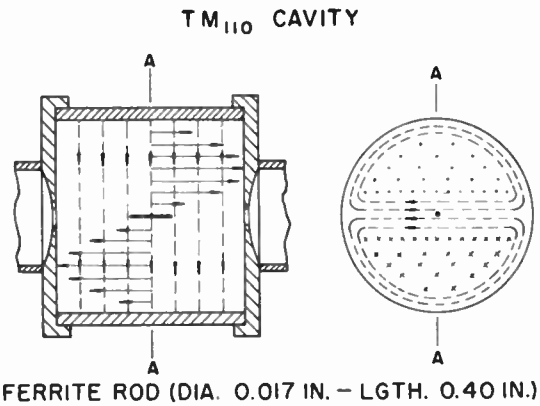

Fig. 1—Fields in a TM_{110} cylindrical transmission cavity. The ferrite rod 0.017 inch diameter and 0.4 inch long is shown in the center. The steady magnetic field is applied axially to the cavity and rod. The solid lines, dots, and crosses represent rf electric fields and the dashed lines represent rf magnetic fields.

0.017 inch in diameter, making a length-to-diameter ratio of 23. This means that the steady magnetic field is the same as the applied field, to considerably better than one per cent. The rf magnetic field is uniform and everywhere normal to the axis of the rod, so that the magnetostatic relation may be used to compute the internal rf magnetic field.

$$h_\pm{}^i = \frac{2}{\mu \pm K + 1} h_\pm{}^0. \qquad (4)$$

At the same time the rod is in a position of zero rf electric field.

[4] N. Bloembergen, "On the magnetic resonance absorption in conductors," *J. Appl. Phys.*, pp. 1383–1389; December, 1952.
[5] J. H. Rowen and W. von Aulock, "Measurement of the complex tensor permeability of ferrites," *Phys. Rev.*, vol. 96, pp. 1151–1152; November, 1954.
[6] E. G. Spencer, R. C. LeCraw, and F. Reggia, "Measurement of microwave dielectric constants and tensor permeabilities of ferrite spheres," PROC. IRE, vol. 44, pp. 790–800; June, 1956.
[7] R. C. LeCraw and E. G. Spencer, "Tensor permeabilities of ferrites below magnetic saturation," 1956 IRE CONVENTION RECORD, part 5, pp. 66–74.
[8] *Ibid.* A more complete description of properties of this mode is given.

For a homogeneous isotropic sphere placed in a uniform magnetic field, the magnetostatic equation for the internal fields is

$$h_{\pm}^{i} = \frac{3}{\mu \pm K + 2} h_{\pm}^{0}. \tag{5}$$

The applicability of this to the present case has been discussed recently by Berk and Lengyl.[9] They obtain approximate solutions of Maxwell's equations inside the sphere of tensor permeability verifying that to the first order of approximation the magnetostatic equation is applicable. The justification also has been obtained by Tompkins[10] in a more physical manner. He shows that although the sphere has different permeabilities for different directions, for any instant of time the rotating rf applied field may be considered fixed in space, for example h_x^0. Then a field distribution is obtained in the sphere, which depends only upon the permeability μ_x in the direction of this field. The boundary conditions are satisfied by the projections of h_x and b_x along normals to the sphere. μ_y and μ_z are not involved, since the solution is unique.

The spheres and disks were measured in the TE_{112} mode cavity and the rod in the TM_{110} mode cavity. The spheres could be measured in the cavity excited in either mode. However, to minimize the effects due to rf electric fields the disks are measured in the center of the TE_{112} cavity. For this mode, the disk is in a position of zero electric field. The same cavity was used in both cases, the frequency being 9200 mc for the TE_{112} mode and 9700 mc for the TM_{110} mode. The cavity constant A in (2) is 0.6416 for the TE_{112} mode and 0.6485 for the TM_{110} mode.[1,7]

The Intrinsic Permeability

In (2), the measured frequency shifts are dependent on the term $4\pi m_{\pm}/h_{\pm}^{0}$. In the past, results of experiments on spheres have been reported in which this expression was taken to be

$$\frac{4\pi m_{\pm}}{h_{\pm}^{0}} = (\tilde{\mu} \pm K - 1). \tag{6}$$

We place the tildes over $\mu \pm K$ to indicate that these are measured values. Its significance is that $(\tilde{\mu}' \pm \tilde{K}' - 1)$ is a constant times the cavity frequency shift and $(\tilde{\mu}'' \pm \tilde{K}'')$ is a constant times the change in cavity transmission.

Setting (6) equal to (3),

$$(\tilde{\mu} \pm K - 1)h_{\pm}^{0} = (\mu \pm K - 1)h_{\pm}^{i}. \tag{7}$$

It should be emphasized that $(\mu \pm K)$ is a quantity which is intrinsic to the material and does not depend at all on the shape of the sample.

Using (4) and (5), (7) becomes for the rod

$$(\tilde{\mu} \pm K - 1) = \frac{2(\mu \pm K - 1)}{(\mu \pm K + 1)}, \tag{8}$$

and for the sphere

$$(\tilde{\mu} \pm K - 1) = \frac{3(\mu \pm K - 1)}{(\mu \pm K + 2)}. \tag{9}$$

For the disk $h_{\pm}^{0} = h_{\pm}^{i}$, so, as mentioned in the introduction

$$\tilde{\mu} \pm K = \mu \pm K. \tag{10}$$

Thus, if good measurements are made on rods, spheres, or disks the derived values of $\mu \pm K$ should be the same as a function of internal steady field.

To illustrate these ideas, Fig. 2 is a plot of the real and imaginary parts of $\mu + K$, for a theoretical Landau-Lifshitz line, as a function of H_0/H_r through magnetic resonance. H_0 is the applied steady magnetic field and H_r is the value at resonance. Since the disk measurements are intrinsic, this curve is labeled "disk" in the figure. The peak of $\mu'' + K''$ which is given by $4\pi M_0/kH_r$ is normalized equal to 10 for convenience. The damping constant k in the Landau-Lifshitz equations is about 0.06, so that an approximation may be made that $1 + k^2 \approx 1$. The equations may be then written as,

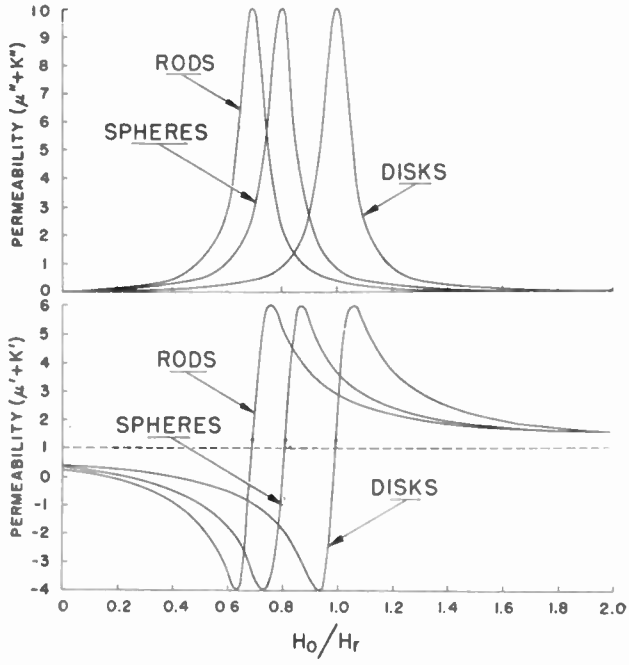

Fig. 2—Theoretical circularly-polarized wave permeabilities for rods, spheres, and disks. The disk, which is the intrinsic, permeability was computed from a Landau-Lifshitz line shape taking $4\pi M_0/kH_r = 10$ and $k = 0.6$. The rod and sphere curves were computed from the disk curve using (8) and (9).

[9] A. D. Berk and B. A. Lengyl, "Magnetic fields in small ferrite bodies with application to microwave cavities containing such bodies," PROC. IRE, vol. 43, pp. 1587–1591; November, 1955.

[10] J. E. Tompkins, "Note on the Magnetic Field in an Anisotropic Ferrite Sphere," Diamond Ordnance Fuze Labs Tech. Memo.; March 9, 1956.

$$\mu''+K''=\frac{4\pi M_0 k}{H_r}\,\frac{\left(\frac{H_0}{H_r}+1\right)^2}{\left(\frac{H_0}{H_r}-1\right)^2\left(\frac{H_0}{H_r}+1\right)^2+4k^2\frac{H_0^2}{H_r^2}} \tag{11}$$

$$\approx\frac{4\pi M_0 k}{H_r}\,\frac{1}{\left(\frac{H_0}{H_r}-1\right)^2+k^2} \tag{12}$$

$$\mu'+K'=1+\frac{4\pi M_0}{H_r}\,\frac{\left(\frac{H_0}{H_r}-1\right)\left(\frac{H_0}{H_r}+1\right)^2+2k^2\frac{H_0}{H_r}}{\left(\frac{H_0}{H_r}-1\right)^2\left(\frac{H_0}{H_r}+1\right)^2+4k^2\frac{H_0^2}{H_r^2}} \tag{13}$$

$$\approx 1+\frac{4\pi M_0}{H_r}\,\frac{\left(\frac{H_0}{H_r}-1\right)+0.5k^2}{\left(\frac{H_0}{H_r}-1\right)^2+k^2}. \tag{14}$$

The more exact form was used for plotting.

Taking values of $\mu+K$ from the disk curve, and substituting in (8) and (9) the curves for the measured values of rods and spheres are obtained and plotted. From this figure, it may be concluded that, if the tensor permeability is adequately described by the Landau-Lifshitz equations, the measurements on rods, spheres, and disks would be exactly as shown. Further, if measurements were made on rods or spheres alone, using (8) or (9) the intrinsic curve would also be obtained. It is clear that the magnitudes of the intrinsic and measured lines are the same and that the line shapes are nearly the same.

Kittel[11] has pointed out that both the rf and steady field magnetizations determine the resonance conditions. The equations defining the fields H_r at which resonance occurs for the various shaped samples then become,

$$\text{for the rod } \omega = \gamma(H_r + 2\pi M_0) \tag{15}$$

$$\text{for the sphere } \omega = \gamma H_r \tag{16}$$

$$\text{for the disk } \omega = \gamma(H_r - 4\pi M_0). \tag{17}$$

where ω is the rf angular frequency and γ is the gyromagnetic ratio.

These resonance conditions are also contained in (8) and (9). For example, by separation into reals and imaginaries, and then rationalizing, it is seen that resonance occurs for $\tilde{\mu}''$ when $\mu' = -2$ for a sphere. Remembering that the intrinsic curve is normalized for

$$(\mu'' + K'')_{\max} = \frac{4\pi M_0}{kH_r} = 10,$$

fields at which resonances occur clearly depend on the saturation magnetization and damping constants of the ferrite.

[11] C. Kittel, "On the theory of ferromagnetic resonance absorption," *Phys. Rev.*, vol. 73, pp. 155–161; January 15, 1948.

Several other comments will be made regarding Fig. 2 which will have more significance when the experimental results are considered. By comparing the real and imaginary parts of Fig. 2, it may be seen that the total excursion of the $\mu'+K'$ curve is equal to the height of the $\mu''+K''$ curve. This is the case for a Lorentzian-shaped curve and the Landau-Lifshitz curve is almost Lorentzian. For a Gaussian-shaped curve, however, the excursion in $\mu'+K'$ is 1.2 times the height of $\mu''+K''$. Since the measurements of $\mu'+K'$ and $\mu''+K''$ are independent, this comparison affords a partial check on experimental accuracy.

Some general statements on the transformations from intrinsic to measured permeabilities are as follows: If either a Landau-Lifshitz or Bloch-Bloembergen form of damping is assumed, the rf magnetization can be derived alternately in terms of internal or applied rf and dc magnetic fields. Using (3) for internal and (6) for applied rf fields, the intrinsic and measured permeabilities are obtained. The line shape of the measured permeability is found to be the same as that of the intrinsic permeability, only displaced along the applied dc field axis. This holds for rods as well as spheres. If, however, the measured line shape cannot be represented adequately by the above damping terms, line shape is not necessarily preserved upon making the above transformations. This will be shown by the results of the next section.

Experimental Results

The four measured tensor components and the derived intrinsic tensor components are shown in Figs. 3 through 8, for the rod, sphere, and disk. The samples are all from the same batch of polycrystalline Mg-Mn ferrite, General Ceramics R-1. For the rod, the measured curve has half the width of the intrinsic and the heights of the two curves are not equal. For the sphere, the measured and intrinsic absorption curves are almost mirror images while the dispersion curves are almost exact reflections through an origin. Both the rod and sphere measured curves are higher on the low field side. Upon transformation, the asymmetry changes so that the intrinsic curves have the same form of asymmetry for all three samples.

A comparison was made of the intrinsic curve in Fig. 5 and a theoretical Landau-Lifshitz curve. Normalization was made at the resonance peak and at the half-height value on the high field side. This determined $4\pi M_0$ and the damping constant k. The deviation of the theoretical values from the experimental values is shown by the dashed line.

A qualitative theory of this line asymmetry has been obtained by consideration of the polycrystalline nature of the ferrite,[12] based on the experimental data of Healy[13]

[12] R. C. LeCraw (unpublished memorandum).

[13] D. W. Healy, Jr., "Ferromagnetic Resonance in Some Ferrites as a Function of Temperature," Cruft Lab. Tech. Rep. No. 135; August 15, 1951.

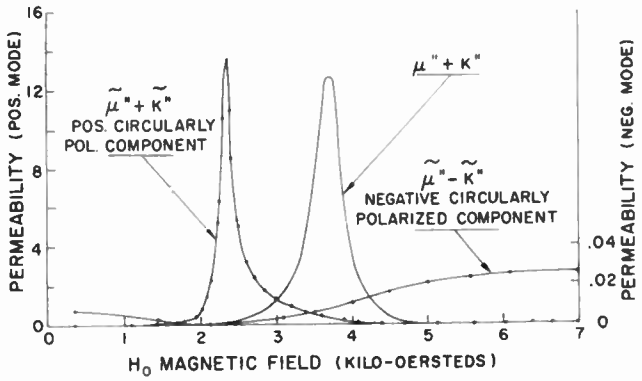

Fig. 3—Imaginary part of permeability $\tilde{\mu}''\pm\tilde{K}''$ for positive and negative circularly-polarized waves, respectively, measured on a rod. $\mu''+K''$ is the computed intrinsic curve.

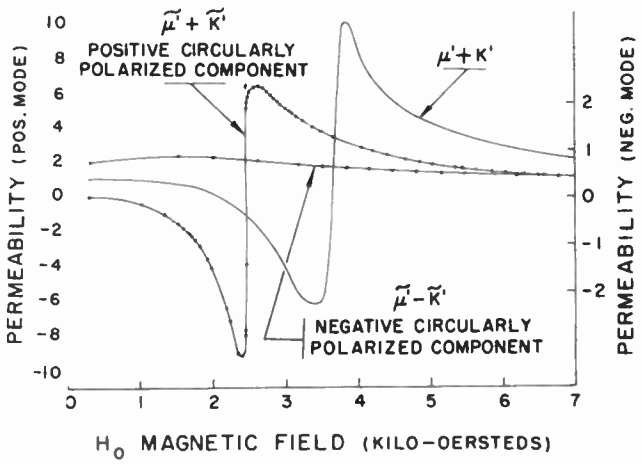

Fig. 4—Real part of permeability $\tilde{\mu}'\pm\tilde{K}'$ for positive and negative circularly-polarized waves, respectively, measured on a rod. $\mu'+K'$ is the computed intrinsic curve.

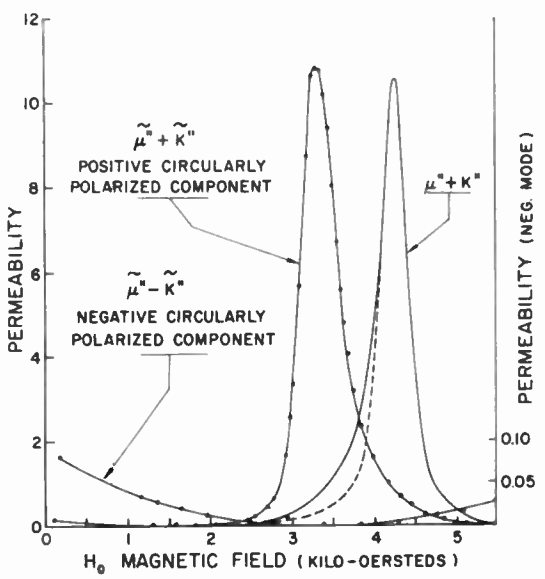

Fig. 5—Imaginary part of permeability $\tilde{\mu}''\pm\tilde{K}''$ for positive and negative circularly-polarized waves, respectively, measured on a sphere. $\mu''+K''$ is the computed intrinsic curve. The dashed curve is a theoretical Landau-Lifshitz curve normalized at the peak and at the half-height point on the high field side.

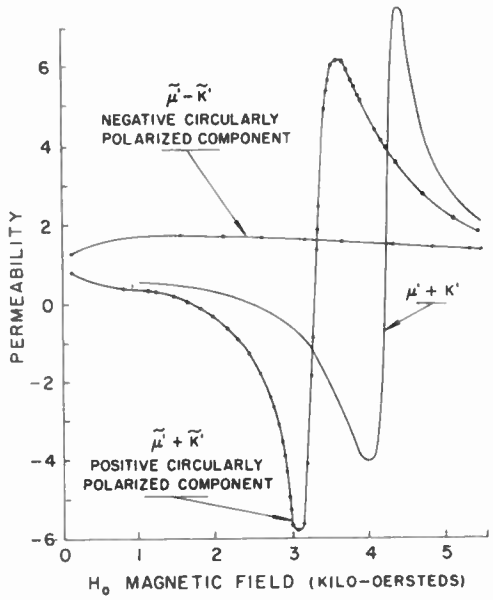

Fig. 6—Real part of permeability $\tilde{\mu}'+\tilde{K}'$ for positive and negative circularly-polarized waves, respectively, measured on a sphere. $\mu'+K'$ is the computed intrinsic curve.

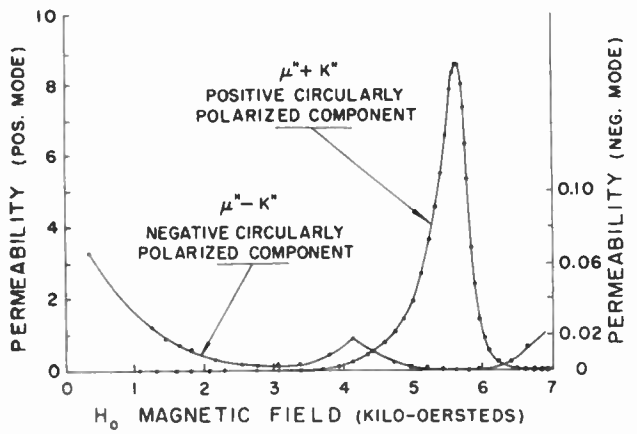

Fig. 7—Imaginary part of permeability $\mu''\pm K''$ for positive and negative circularly-polarized waves, respectively, measured on a disk. The resonance peak of the negative mode is explained in the text.

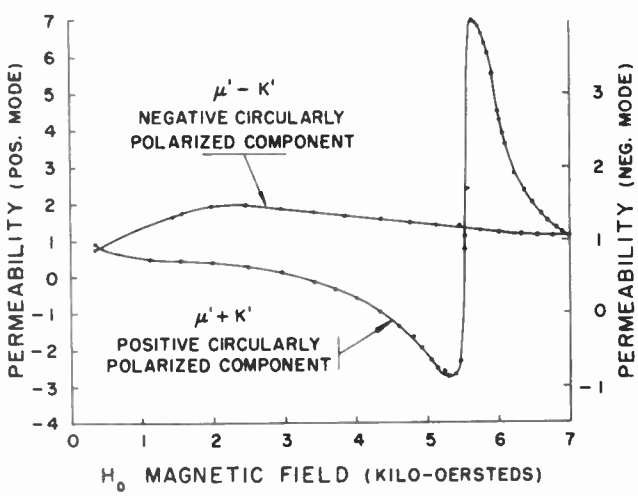

Fig. 8—Real part of permeability $\mu'\pm K'$ for positive and negative circularly-polarized waves, respectively, measured on a disk.

and Tannenwald[14] on single crystal spheres. They find that the steady field required for resonance depends on the angle θ, of this field with respect to the cube edge when rotated in the (110) plane. Tannenwald's data are shown in Fig. 9. The theory assumes that the ferrite

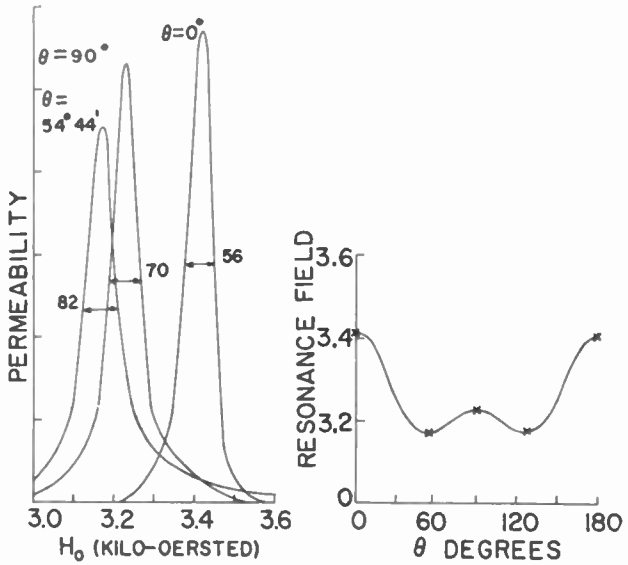

Fig. 9—Resonance absorption in the (110) plane, of a single crystal of manganese-zinc ferrite, showing variations in line width. θ is the angle in the (110) plane between the steady field and the (100) axis. This sketch was made from Fig. 5, Tannenwald.[14] The right-hand figure is a plot of the resonance field as a function of θ.

is composed of a large number of small crystallites having no preferred orientation. For each crystallite there are four easy, six medium, and three hard directions of magnetization. Consideration of the solid angels associated with each of these directions and the number of directions together with Fig. 10 leads to the conclusion that the mean value of the resonance fields is below the middle value of the two extremes. This results in asymmetry of the type shown for the polycrystalline sphere of Fig. 5. Fig. 5 is for polycrystalline magnesium-manganese ferrite. Single crystals of this ferrite were not available for direct comparison. Tannenwald's data are for a single crystal manganese-zinc ferrite and Healy's data are for a single crystal nickel ferrite. Healy's data lead to the same conclusion as above and this was confirmed by additional measurements on polycrystalline nickel ferrite. Also, the line width for the polycrystalline magnesium-manganese ferrite is 525 oersteds, which is roughly that which could be predicted for manganese-zinc polycrystalline material made from Tannenwald's crystals.

In Fig. 10 the three measured loss terms and in Fig. 11 the three intrinsic loss terms are drawn for comparison.

[14] P. E. Tannenwald, "Ferromagnetic resonance in manganese ferrite single crystal," *Phys. Rev.*, vol. 100, pp. 1713–1719; December 15, 1955.

From the displacement of the resonances, using (15), (16), and (17), the magnitude of $4\pi M_0$ is calculated to be 2000 and 2350 using the rod and disk resonance values, respectively. The peak of the $\mu''+K''$ curves is

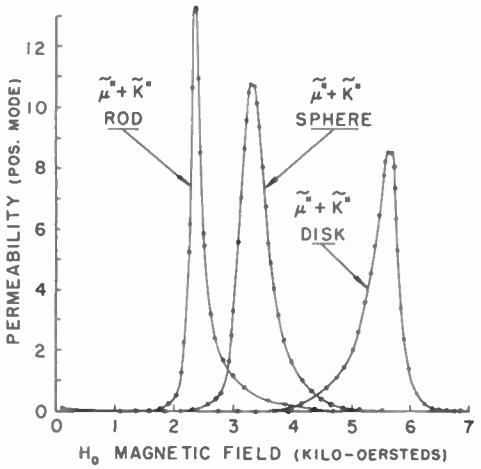

Fig. 10—The measured positive mode loss terms for the rod, sphere, and disk are shown here for comparison.

given by $4\pi M_0/kH_r$. From the intrinsic curves $4\pi M_0$ is 2450, 2290, and 2160 for the rod, sphere, and disk, respectively. The maximum of the $\tilde{\mu}''+\tilde{K}''$ loss terms varies by 33 per cent from the rod to the disk.

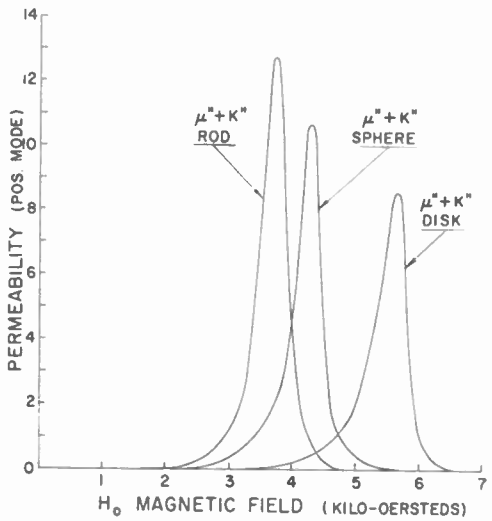

Fig. 11—The intrinsic positive mode loss terms for the rod, sphere, and disk are shown here for comparison.

We have, at present, no good explanation for the difference between the 12.5 peak value for the rod and the 10.85 peak value for the sphere. There is an explanation for the lower value for the disk. Near the edge of the disk the rf magnetic field is not perfectly circularly polarized. Also, the steady magnetic field in the

sample varies from H_0 to $H_0-4\pi M_0$ from the edge of the sample to a position in the sample several sample thicknesses from the edge. Thus, not all of the sample is is at magnetic resonance at the same time. This tends to reduce the peak value of $\mu''+K''$ from the true intrinsic value. Further weight is given these arguments by observing that in Fig. 7, an absorption resonance occurs in the negative mode. This has been observed for all disk samples. Resonance for the edge of the disk occurs near that of a sphere and shows up in the negative mode since the rf field is elliptically polarized in this region. It might be noted that for a linearly-applied wave in a circular cavity the edge effects would appear as a multiple resonance, if the diameter-to-thickness ratio is not sufficiently great. Since the line widths of the sphere and disk are equal, and the difference in heights is explained, the correlation between the disk and the sphere measurements is excellent.

Fig. 12 is included to illustrate an interesting technique in obtaining experimental data. The solid dots represent measured values of $\tilde{\mu}''+\tilde{K}''$ and $\tilde{\mu}'+\tilde{K}'$ on a sphere. The full intrinsic curves through resonance were then derived from these partial data. On many occasions utilizing this technique will save a considerable amount of experimental effort. For example, a more highly decoupled cavity may be used if only this portion of the data is to be analyzed.

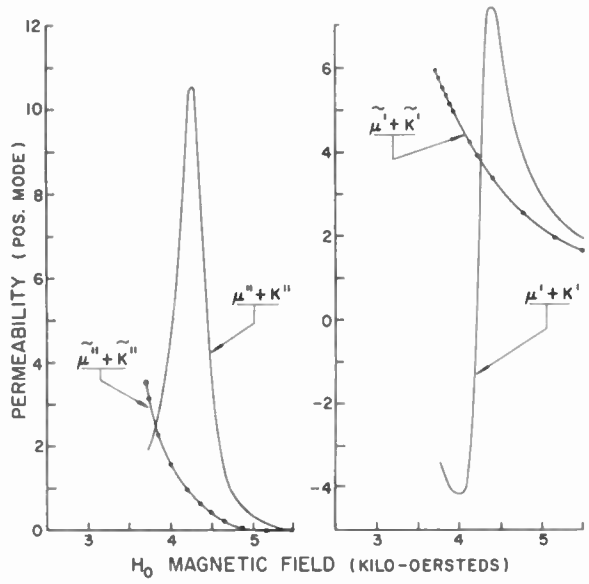

Fig. 12—The complete intrinsic resonance curves are shown derived from partial measurements on a sphere. The measurements were taken only on the side of the resonance curve.

Acknowledgment

We should like to thank J. E. Tompkins for discussions of magnetizations in the rod and the sphere, H. J. Kidd and R. J. Howell for drawing the figures, and A. J. Pannone of the National Bureau of Standards Grinding Shop for preparing the rods and disks.

Permeability Tensor Values from Waveguide Measurements*

E. B. MULLEN†, MEMBER, IRE AND E. R. CARLSON†, SENIOR MEMBER, IRE

Summary—**Measurements of the components of the microwave permeability tensor of ferrites are usually made on very small specimens, such as spheres, discs, or rods, placed in cavities. Using degenerate modes, one can relate the frequency shifts of these modes to the real parts, and the changes in Q to the imaginary parts, of the tensor components.**

The technique herein described makes use of measurements performed on a ferrite rod placed along the axis of a circular waveguide. Exciting the specimen successively with the two senses of circular polarization, one obtains phase and attenuation information for each of these modes which can then be related by a perturbation treatment back to the real and imaginary parts, respectively, of the tensor components. The variation of phase and attenuation are recorded continuously (but on successive runs) as functions of the changing applied magnetic field. The apparatus used for these purposes will be described and certain novel features pointed out.

While this method lacks the advantage of cavity techniques to separate out the dielectric contributions to the phase and attenuation shifts, it does offer a means whereby a fairly large specimen can be examined for its basic parameters in a geometrical configuration often used in applications.

Introduction

A STARTING point for all descriptions, qualitative or quantitative, of the behavior of a ferrite subjected simultaneously to a microwave field and a steady or quasi-steady magnetic field, is the permeability tensor. If the steady field is taken to be in the z-direction, this tensor is given by

$$\mu_T = \mu_0 \begin{pmatrix} \mu & -j\kappa & 0 \\ j\kappa & \mu & 0 \\ 0 & 0 & 1 \end{pmatrix}.$$

When the ferrite is of infinite extent, Maxwell's equations are fairly readily solved for plane waves. Taking the direction of propagation as parallel to that of the steady field, the natural description is in terms of circularly-polarized modes and the unequal propagation constants of these modes lead to the well-known Faraday effect. Where the direction of propagation is perpendicular to both the steady field and the microwave magnetic field, the analog to the optical Cotton-Mouton effect obtains. We shall be concerned here entirely with the first case and shall describe a method of utilizing these circularly-polarized modes which yields with fair accuracy the permeability tensor components.

* Original manuscript received by the IRE, July 3, 1956. Presented at the Symposium on Microwave Ferrites, Harvard Univ., Cambridge, Mass. April 2–4, 1956. This work was performed under Contract DA-36-039-sc-64606.

† General Electric Co., Syracuse, N.Y.

Cavity and Waveguide Methods

For practical cases of waveguide or cavity ferrite configurations, the exact behavior of the microwaves is no longer simply obtained. Complicated equations involving the propagation constant in an implicit manner are obtained, and it is only by either machine computations or simplifying approaches that quantitative information can be obtained. The former method has been used[1] to compute the field configurations and propagation constant in a rectangular waveguide with a longitudinal slab of ferrite subjected to a transverse field. Perturbation techniques were first applied[2,3] to the case of a cylindrical cavity which contained a small ferrite sphere and were particularly directed towards obtaining the tensor components in terms of the measured quantities. There are four such quantities to be determined: the real and imaginary parts of the diagonal and off-diagonal terms. The real terms are expressible in terms of the geometry of the systems and the shifts in the resonant frequencies of the two orthogonal TE_{11n} modes which are no longer degenerate. The imaginary parts are given in terms of the same geometrical parameters and the changes in the cavity Q's for the two modes. Precision measurements of this sort are not among the easiest of microwave procedures.

Berk[4] first derived an explicit form for the propagation constant of the dominant TE wave traveling down a circular waveguide in which there is axially located a thin ferrite rod. A somewhat different approach by Suhl and Walker[5] yields the same results, when account is taken of the fact that the latter authors deal with the intrinsic permeability whereas Berk works with an *effective* permeability. The distinction between the two will be enlarged upon later. In either of these approaches the expression for the propagation constant can be simply altered to give the phase and attenuation terms for either linearly or circularly polarized waves. A technique using the two senses of the latter for both phase and attenuation yields the same four quantities as did

[1] B. Lax, K. J. Button, and L. M. Roth, "Ferrite phase shifters in rectangular waveguide," *J. Appl. Phys.*, vol. 25, p. 1413; November, 1954.

[2] B. Lax and A. D. Berk, "Cavities with complex media," 1953 IRE Convention Record, part 10, pp. 65–73.

[3] J. Artman and P. Tannenwald, "Measurement of permeability tensor in ferrites," *Phys. Rev.*, vol. 91, p. 1014; August, 1953.

[4] A. D. Berk, "Cavities and waveguides with inhomogeneous and anisotropic media," thesis M.I.T., September, 1954.

[5] H. Suhl and L. R. Walker, "Guided wave propagation through gyro-magnetic media," *Bell Sys. Tech. J.*, part II, vol. 33, July, 1954.

the cavity technique. However, phase and attenuation are somewhat more readily measured in practical waveguide circuits than are cavity Q and very small frequency shifts.

Measurements

A rather elaborate automatic phase measuring device having been built previously for another purpose, it occurred to us that it might be worthwhile to utilize this apparatus to check the above theory and compare the values of the tensor components so obtained with those resulting from cavity measurements. While a number of objections could be raised against this procedure, it was thought that the results of the waveguide work would be more indicative of average material properties than those obtained by the use of extremely small spheres. Another advantage would be the presentation of data in a form directly applicable to a practical circular waveguide configuration. By the addition of the necessary microwave circuitry to give circularly polarized waves and a very sensitive bridge to give small attenuations, the apparatus was adapted for the proposed measurements.

Assuming that the transverse magnetic field does not vary by more than 10 per cent over a circular cross section concentric with the waveguide axis, a reasonable upper limit for the diameter of the ferrite rod to be used is obtained for 0.9375 inch ID waveguide. This diameter turns out to be about 0.090 inch, so rods of this diameter, and about one inch long, were used. Each rod was mounted in a polyfoam cylinder and inserted in the waveguide around which was wound a solenoid.

Fig. 1 shows the measurement circuit. Only the equipment above the line L_1 is used for the attenuation measurements. As the figure shows, the attenuation measurements are made in a bridge comprised of two (matched) barreters and two resistors. One barreter monitors the microwave power into the ferrite, and automatically corrects the bridge null point for minor power fluctuations. An amplidyne was used as a current source for the solenoid; its output was monitored to drive the X-axis input of the recorder (Moseley A-1).

When there is no ferrite in the waveguide, adjustments are made so that equal power is incident on both bolometers and, therefore, the bridge output is zero. When the ferrite is inserted, and the magnetic field applied to it varied, the relative powers incident on the bolometers change, disturbing the bridge equilibrium. For small unbalances, the bridge output voltage to the recorder is proportional to this power ratio, so that a linear db scale is obtained. The attenuation scale on the recorder is calibrated by means of the precision variable attenuator (Hewlett-Packard X382A) in series with the ferrite. By varying the gain of the recorder and adjusting the level of the power incident on the bolometers, the attenuation per chart division can be adjusted to any desired scale. For ferrite losses greater than 0.5 db, the detector output is no longer linear with the differential power to the two bolometers, but again the attenuation scale may be calibrated with the precision attenuator so that the loss measurements can still be made. The two attenuation scales, the first for losses less than about 0.7 db and the second for losses greater, are indicated in the graphs.

The stability and *resetability* of the attenuation bridge are shown in Fig. 2. The losses indicated are due to attenuations being added before shutting off the input to the recorder, preparatory to removing the ferrite-holding waveguide section. When the holder is reinserted and the recorder turned on again, it is seen that the zero level does not change by more than 0.005 db, although there is a drift in time due to thermal drift in the bolometers. It may be remarked in passing that the removable waveguide section had special noncontacting choke flanges attached to its ends, so that it could be removed simply by sliding it on guide-rails laterally in and out of the line. This feature prevented mechanical strain and, in addition, much time that would have otherwise been used to make and break conventional secure joints.

The phase measurements are somewhat more complicated to make than the attenuation measurements. Briefly, the stabilized cw signal is split in two, half serving as a reference signal, and the other half going through the ferrite and thence to a balanced modulator driven by a 10.7 mc signal. The upper sideband is filtered out, and the lower one mixed with the reference signal. The original 10.7 mc signal was obtained by mixing together the outputs of two crystal oscillators of frequency 200 kc and 10.5 mc. Part of the 10.5 mc oscillator signal is now mixed with the phase information-carrying 10.7 mc signal to obtain a phase information-carrying 200 kc signal which is fed into a 200 kc phase detector, along with a 200 kc reference signal.

The reference signal is the output of a phase shifter excited by the crystal oscillator. The phase shifter is servo-ed so as to balance the phase detector to a null. The mechanical position of the phase shifter indicates the phase shift produced by the ferrite at the X-band frequency. Figs. 3 and 4 give the results of a stability test on the phase shifter. The first is a static test of phase drift in time and the second indicates the shift in the zero position after a phase change in introduced and then removed.

Fig. 5 is a reproduction of an actual record obtained of phase shift vs applied magnetic field. Fig. 6 is, similarly, a record obtained of attenuation as a function of the magnetic field.

Results

Berk's expression for the propagation constants can be expressed, for circularly polarized waves as

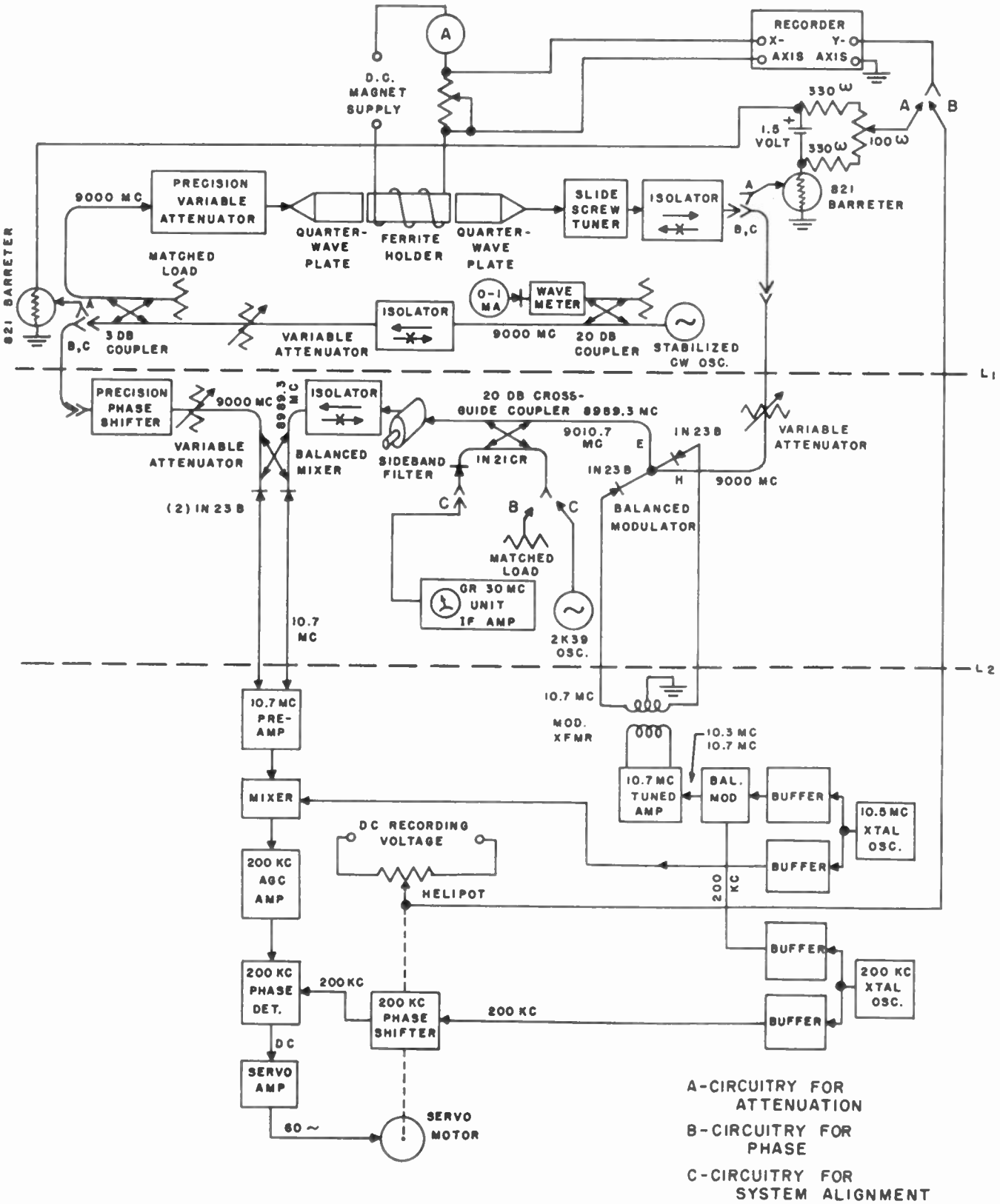

Fig. 1—Wide-range phase and attenuation recorder.

$$\beta_{\mp} = \frac{\beta_0}{2}\left\{1 - \frac{sC}{S}(\chi' \pm \kappa') + \frac{k_0^2}{\beta_0^2}\chi_e'\right\} \qquad \alpha_{\mp} = \frac{\beta_0}{2}\left\{\frac{sC}{S}(\chi'' \pm \kappa'') + \frac{k_0^2}{\beta_0^2}\chi_e''\right\}$$

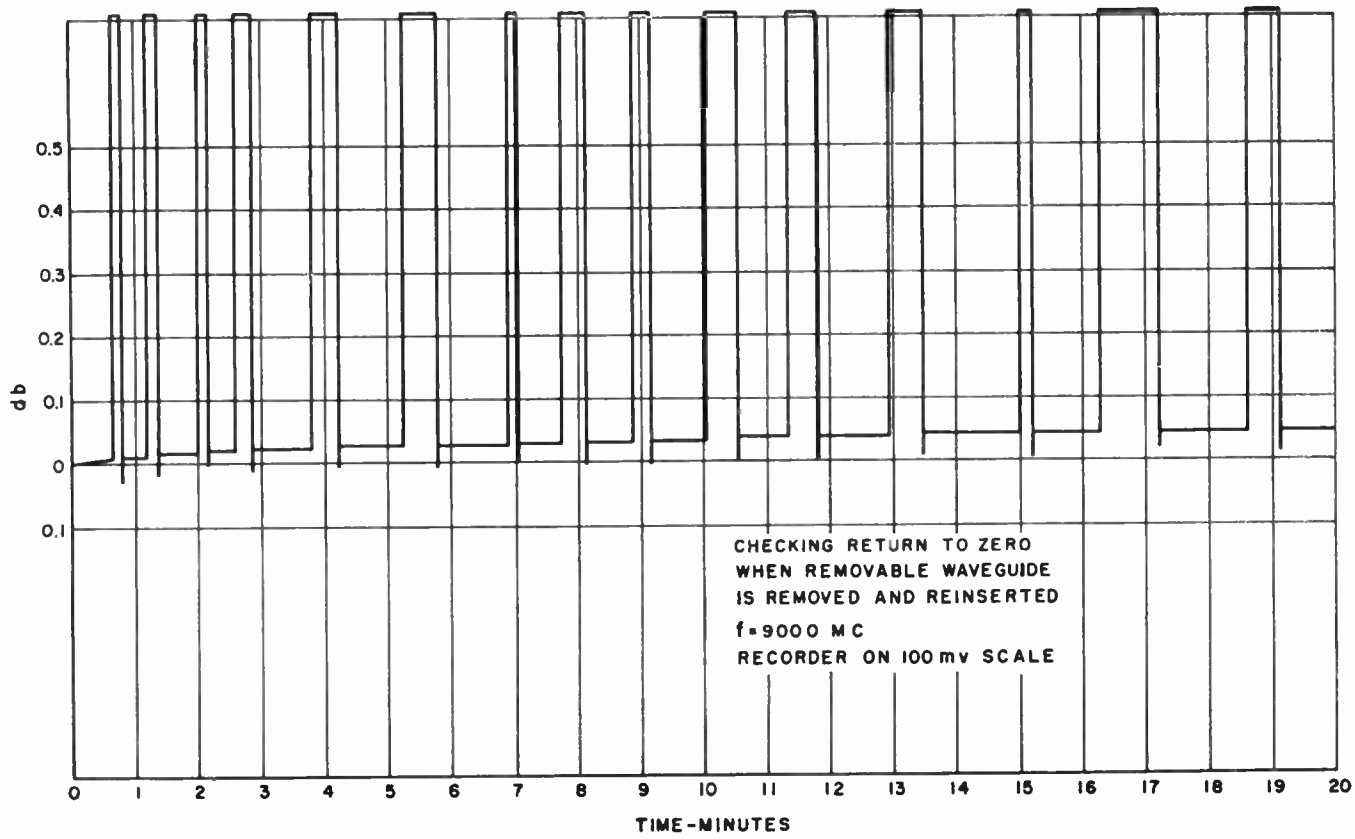

Fig. 2—Attenuation zero change.

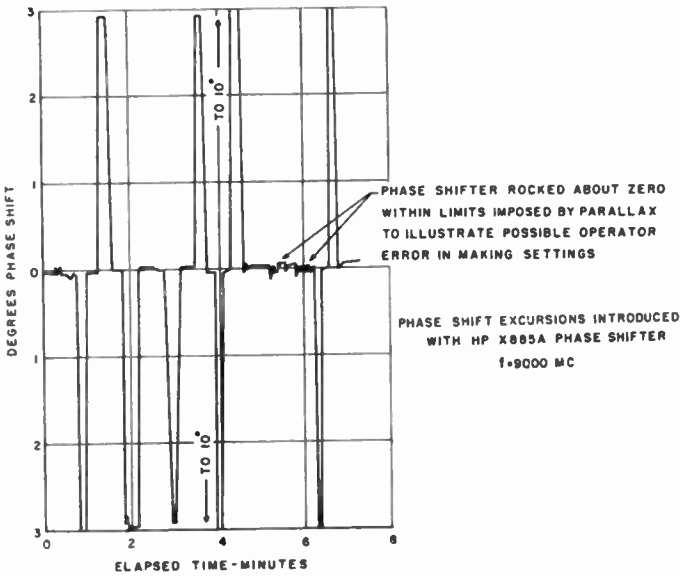

Fig. 3—Stability and resetability of bridge.

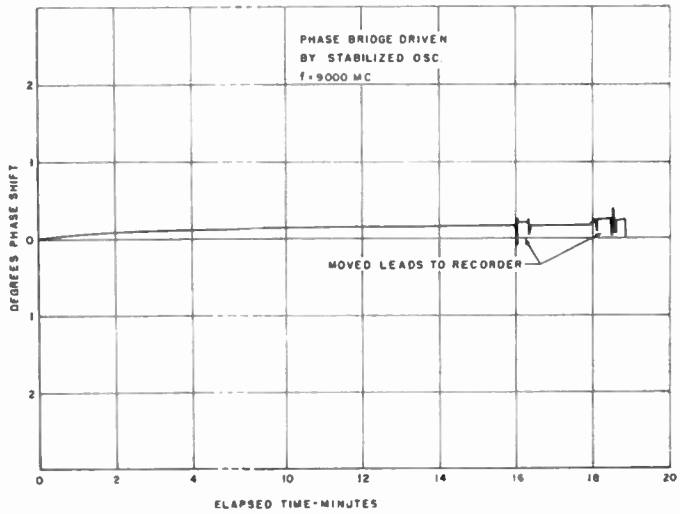

Fig. 4—Phase shift drift vs time.

where

β_0 is the phase constant for the empty waveguide

s is the cross sectional area of the ferrite rod

S is the cross sectional area of the waveguide

C is a number ($= 1.04$ for the circular guide)

$\chi' \pm \kappa'$ are the real parts of the effective susceptibilities

$\chi'' \pm \kappa''$ are the imaginary parts of the effective susceptibilities

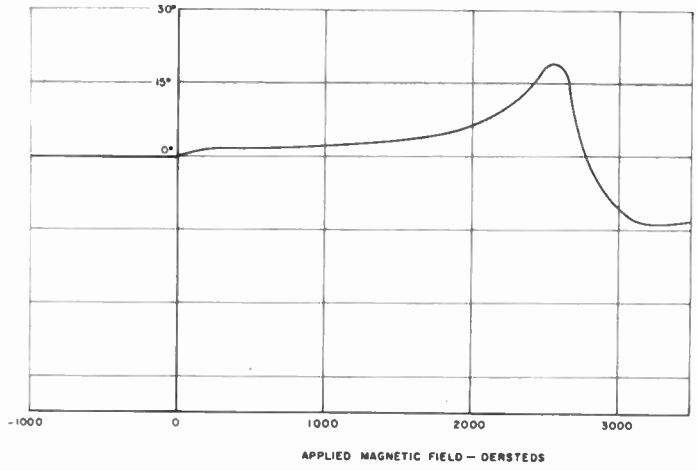

Fig. 5—Phase shift as a function of magnetic field.

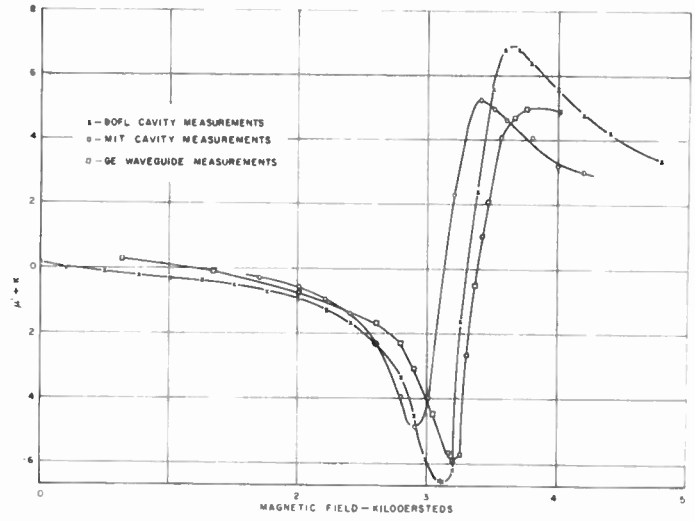

Fig. 7—The real part of the (effective) permeability tensor for ferrite 1331.

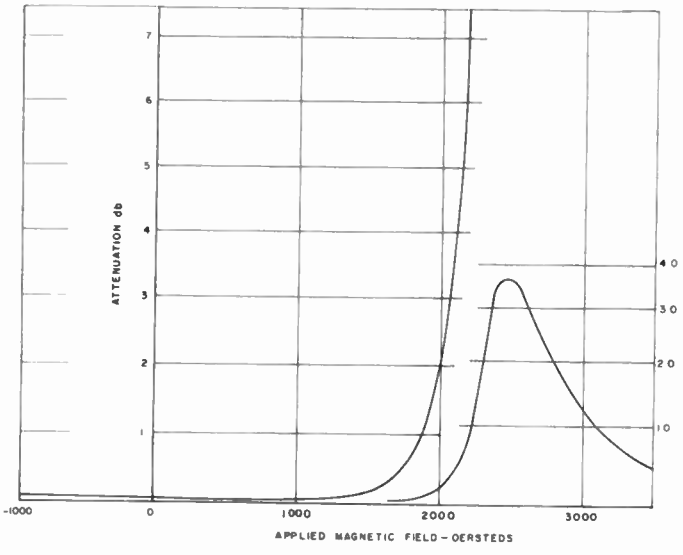

Fig. 6—Attenuation as a function of magnetic field.

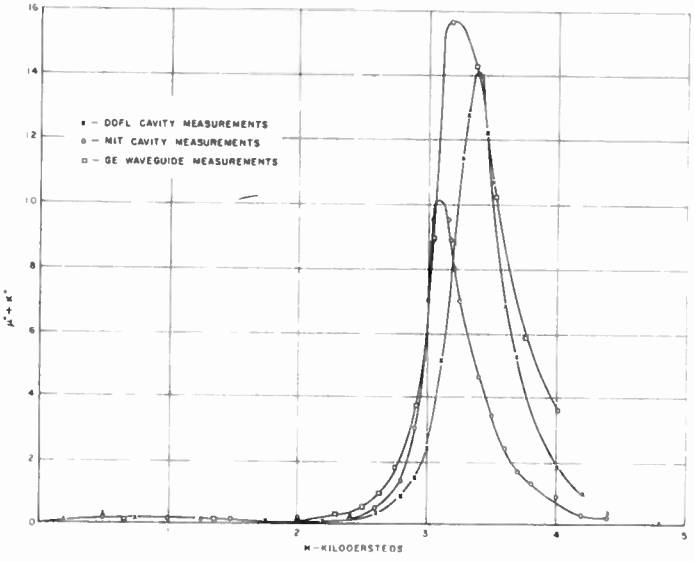

Fig. 8—The imaginary part of the (effective) permeability tensor for ferrite 1331.

k_0 is the wave number of free space

χ_e'' is the real part of the dielectric susceptibility

$\mp$ refer to the two senses of circular polarization.

We eliminate consideration of the dielectric contributions by referring all measured data to zero applied field with the ferrite present. Using the above expressions and the measurements given by Figs. 5 and 6, values of effective permeabilities were obtained. These are plotted in Figs. 7 and 8 together with comparison curves obtained by workers at *M.I.T. and the Diamond Ordnance Fuze Laboratories* using resonant cavity techniques. In order to make the comparison more readily, the *effective* permeability is used. This is the permeability obtained when the applied magnetic field is used in the mathematical expressions for the field existing in the ferrite. Strictly speaking, this is the field existing at the ferrite before the ferrite occupies the site. As Suhl and Walker[5] and lately Berk and Lengyl[6] have pointed out, the intrinsic permeability is obtained only when the actual fields existing within the ferrite are used. Both pairs of authors give the formulas relating this inner field to the applied field in terms of the geometry and the tensor permeability. In Figs. 7 and 8, the field values for the waveguide case have been increased by the amount of $4\pi M/3$ in order to facilitate comparison with the two sets of data obtained from sphere measurements, where that quantity takes account of the demagnetizing field in the sphere. (For the ratio of length/diameter of the rod, 10:1, its demagnetization is practically negligible.) The ferrite used in all three cases is General

[6] A. D. Berk and B. A. Lengyl, "Magnetic fields in small ferrite bodies with application to microwave cavities containing such bodies," PROC. IRE, vol. 43, p. 1587; November, 1955.

Ceramics 1331 (now designated as R-1). The agreement between the values deduced from the waveguide measurements and those obtained from the cavity measurements[7,8] is quite good, even in the vicinity of resonance where very large discrepancies might be expected. In view of the disparity between the two cavity sets of results, most of which is probably due to variation in material properties from ferrite to ferrite, the waveguide results can be taken as fairly reliable.

In the waveguide work, we have dealt with only one sense of the circular polarization,—the measuring apparatus was not sufficiently sensitive to give accurate data for the low field strengths at which measurements were made on the other sense of the circularly polarized wave. This is an advantage of the cavity technique.

If one allows that contributions of nonuniform applied magnetic field effects, of nonhomogeneity of the ferrite, and the anisotropy fields for the rod will be different than for the small spheres, it is not surprising that there be incomplete agreement between the tensor components derived from the two different geometries.

It has been found that, even before the reduction of the observed data to the effective permeability tensor components has been effected, valuable comparison information as to the relative properties and merits of different ferrites is immediately at hand in the curves directly obtained in a few minutes with the continuously recording apparatus described herein.

ACKNOWLEDGEMENT

The authors acknowledge the cooperation of H. C. Rothenberg for discussions regarding the physical characteristics of ferrites.

[7] J. Artman and P. Tannenwald, "Microwave susceptibility measurements in ferrites," *J. Appl. Phys.*, vol. 26, p. 1124; September, 1955.

[8] E. G. Spencer, R. C. LeCraw, and F. Reggia, "Measurement of microwave dielectric constants and tensor permeabilities of ferrite spheres," 1955 IRE CONVENTION RECORD, part 8, pp. 113–121.

Resonance Loss Properties of Ferrites in 9 KMC Region*

SAMUEL SENSIPER,† SENIOR MEMBER, IRE

Summary—**The low power level transmission loss at room temperature and at 8.2, 8.9, and 10.1 kmc of thin (nominally 0.010-inch thick) ferrite slabs placed approximately in the plane of circular polarization in rectangular waveguide (0.9×0.4 inch id) was measured as a function of applied transverse dc magnetic field. Ferramic A, B, C, D, E, G, H, H-1, I, J, N, O-1, Q, R-1, R-2, R-3, and Ferroxcube 101, 102, 103, 104, 105, 106 were measured, although graphical data are presented here only for some typical cases. The absence of resonance loss in the permanent magnet ferrite material Indox in this frequency range and for internal fields up to 5 kilo-oersteds is noted. Results of measurements on some thicker ferrite slabs and other transverse locations are also presented. The effect of temperature on the loss characteristics of Ferramic G, R-1, and Ferroxcube 104 is shown. Thin-Slab theory is used to compute the effective saturation magnetization, $4\pi M_s$, and damping parameter, α, (both defined in the text) of the measured ferrites at room temperature, and these results are presented in tabular form. For the different ferrites it is found that 2.6 kilogauss $<4\pi M_s<6.6$ kilogauss, and $0.02<\alpha<0.3$, for internal dc magnetic fields in the range from about 1 to 2 kilo-oersteds.**

I. INTRODUCTION

FERRITES have been used in recent years to produce microwave components with nonreciprocal transmission characteristics, as can be found in the literature.[1–6] However, very little data have been published comparing the properties of the various commercially available ferrites, particularly for those cases, which are of major interest here, where the material is operating at or near ferromagnetic resonance. Although it can be anticipated that improved ferrites for special applications will be developed in the future, information

* Original manuscript received by the IRE, March 23, 1956; revised manuscript received, July 18, 1956.

† Hughes Aircraft Co., Research Labs., Culver City, Calif.

[1] The references listed throughout this report are merely representative of those containing information about ferrites. They refer in turn to many others concerning the physical properties and technical applications of these materials. See also the other articles in this issue of PROCEEDINGS.

[2] E. Abrahams, "Relaxation Processes in Ferromagnetism" in "Advances in Electronics and Electron Physics," Academic Press, Inc., New York, N.Y., vol. 6, pp. 47–68, 1954.

[3] J. Smit and H. P. G. Wijn, "Physical Properties of Ferrites," in "Advances in Electronics and Electron Physics," Academic Press, Inc., New York, N.Y., vol. 6, pp. 69–136, 1954. Also, E. W. Gorter, "Some properties of ferrites in connection with their chemistry," PROC. IRE, vol. 43, pp. 1945–1973; December, 1955. Also, A. L. Aden, W. P. Ayres, and J. L. Melchor, "Ferrites, parts I, II, III," *The Sylvania Technologist*, vol. 8, pp. 76–83, pp. 108–117; July, October, 1955; vol. 9, pp. 14–21; January, 1956.

[4] J. H. Rowen, "Ferrites in microwave applications," *Bell Sys. Tech. J.*, vol. 32, pp. 1333–1369; November, 1953.

[5] A. G. Fox, S. E. Miller, and M. T. Weiss, "Behavior and applications of ferrites in the microwave region," *Bell Sys. Tech. J.*, vol. 34, pp. 5–103; January, 1955.

[6] Various authors and titles, "Conference on ferrites," *Bull. Acad. Sci. USSR* (Physical Series), vol. 18, No. 3; 1954, English translation from Columbia Technical Translation, New York, N.Y.

about presently obtainable materials is of considerable interest, not only as an aid to the microwave components designer in choosing the optimum ferrite for a particular use in the interim, but also as a guide to those developing new materials.

In Section II, in the following paper, previously used methods for measuring ferrite properties are noted. The reasons for the choice of the ferrite slab and rectangular waveguide configuration used here are given and the experimental arrangement is described. The method used for preparing the ferrite slabs is also given. In Section III, some of the experimental results are presented graphically in the form of loss per unit length vs applied transverse field for the different frequencies, and some comments are made on the relative characteristics of the various ferrites which can be deduced from the measurements. In Section IV, the effect of temperature on the loss properties of three particularly interesting ferrites is shown. In Section V, thin-slab theory is applied to compute from the measurements the effective saturation magnetizations and damping parameters (both defined in Section V), and a table is presented of these constants for essentially all the ferrite materials considered. This is followed by some discussion of these results. Section VI contains a summary of the paper, and is followed by an Appendix.

II. Choice and Description of Experimental Arrangement

Previously reported methods for measuring some of the intrinsic microwave properties of ferrite materials and the effects of surrounding boundaries are: resonant cavity measurements using a ferrite sphere, disk, or rod,[7–11] Faraday rotation measurements,[4–6,12–16] and loss and phase-shift measurements through ferrite-loaded transmission lines.[4,5,16–18] Cotton-Mouton effect measurements have also been noted.[19] The first of these methods listed can give information about the tensor permeability, $\overleftrightarrow{\mu}$, and scalar permittivity, ϵ, of ferrite materials, and a knowledge of these electromagnetic parameters would, in principle, allow one to compute the transmission characteristics of many ferrite-loaded microwave components. However, the analysis of even relatively simple arrangements is quite complex and involved[20–22] so that the relative merits of different ferrite materials in resonance loss devices may not be as directly evident from $\overleftrightarrow{\mu}$, ϵ data as would be desired. Faraday rotation measurements can yield useful data for comparing the relative properties of ferrite materials in this mode of operation, and can be used to deduce ϵ and the components of $\overleftrightarrow{\mu}$.[13] However, even aside from the fact that such $\overleftrightarrow{\mu}$, ϵ data may be of limited direct utility, very few experimenters appear to have carried Faraday rotation measurements through the region of resonance, and then only for a very limited number of materials.[4,5,12] (See also footnote 39 noted later.)

Loss and phase-shift measurements through a ferrite-loaded transmission line will, in general, give direct information solely about the particular configuration tested. Data on the relative properties of different ferrite materials deduced from such experiments can be applied to other arrangements only with extreme caution. However, if the configuration tested is quite simple, qualitative comparison among the ferrites as to resonance loss ratios, dielectric losses, bandwidths, etc., can easily be made; and if precautions are taken as to the size and shape of the ferrite pieces used, the data can be applied with some generality to other similar arrangements. Furthermore, if the configuration tested is one for which an exact solution to the boundary value problem is available, it is even possible to determine with relative ease ϵ and $\overleftrightarrow{\mu}$, or, equivalently for the latter, the effective saturation magnetization and damping constant.

The ferrite slab and rectangular waveguide arrangement used in the measurements described here is one which satisfies the requirements noted just above. The actual configuration tested is shown in Fig. 1. The in-

[7] B. Lax and A. D. Berk, "Cavities with complex media; resonance in cavities with complex media," 1953 IRE Convention Record, part 10, pp. 65–74.

[8] E. G. Spencer, R. C. LeCraw, and F. Reggia, "Measurement of microwave dielectric constants and tensor permeabilities of ferrite spheres," 1955 IRE Convention Record, part 8, pp. 113–121. See also footnote 51 noted later.

[9] J. O. Artman and P. E. Tannewald, "Measurement of susceptibility tensor in ferrites," *J. Appl. Phys.*, vol. 26, pp. 1124–1132; September, 1955.

[10] J. H. Rowen and W. von Aulock, "Measurement of the complex tensor permeability," *Phys. Rev.*, vol. 96, pp. 1151–1153; November 15, 1954.

[11] A. D. Berk and B. A. Lengyel, "Magnetic fields in small ferrite bodies with applications to microwave cavities containing such bodies," Proc. IRE, vol. 43, pp. 1587–1591; November, 1955.

[12] C. L. Hogan, "The ferromagnetic Faraday effect at microwave frequencies and its applications," *Bell Sys. Tech. J.*, vol. 31, pp. 1–31; January, 1952; also, *Rev. Mod. Phys.*, vol. 25, pp. 253–263; January, 1953.

[13] A. A. Th. M. van Trier, "Guided electromagnetic waves in anisotropic media," *App. Scien. Res.*, sec. B., vol. 3, pp. 305–371; no. 4–5; 1953; also, "Some topics in the microwave application of gyrotropic media," IRE Trans. vol. AP-4, pp. 502–507; July, 1956.

[14] H. G. Beljers, "Faraday effect in magnetic materials with traveling and standing waves," *Philips Res. Rep.*, vol. 9, pp. 131–139; April, 1954.

[15] N. G. Sakiotis and H. N. Chait, "Ferrites at microwaves," Proc. IRE, vol. 41, pp 87–93; January, 1953.

[16] Anonymous, "Interim development reports for ferrite components program." Sperry Gyroscope Co. Reps. No. 5224-1339—1, 2, 3, 4, 5; 1953, 1954.

[17] M. L. Kales, H. N. Chait, and N. G. Sakiotis, "A non-reciprocal microwave component," *J. Appl. Phys.*, vol. 24, pp. 816–817; June, 1953.

[18] N. Sakiotis and H. N. Chait, "Properties of ferrites in waveguides," IRE Trans. vol. MTT-1, pp. 11–16; November, 1953.

[19] F. K. du Pré, "On the microwave cotton-mouton effect in ferroxcube," *Philips Res. Rep.*, vol. 10, pp. 1–10; February, 1955.

[20] H. Suhl and L. R. Walker, "Topics in guided wave propagation through gyromagnetic media, parts I, II, III," *Bell Sys. Tech. J.*, vol. 33, pp. 579–659, pp. 939–986, pp. 1133–1194; May, July, September, 1954.

[21] A. D. Berk, "Cavities and waveguides with inhomogeneous and anisotropic media," Sc.D. Thesis, Dept. of Elec. Engrg., M.I.T.; September, 1954; also as M.I.T. Res. Lab. Elec. Tech. Rep. No. 284.

[22] G. Jeromson, "Perturbation Theory of Anisotropic Waveguides," Rep. No. 45, Elec. Res. Lab., Div. Elec. Engrg., Univ. of Cal., Berkeley; July, 1955.

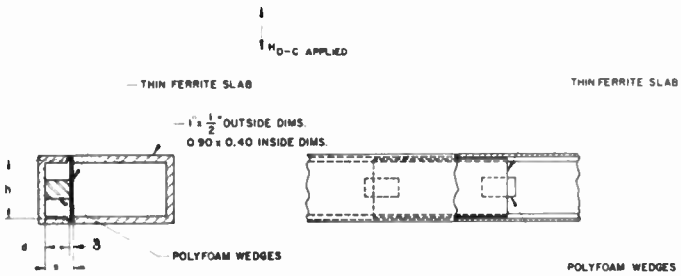

Fig. 1—Ferrite slab and rectangular waveguide (RG-52/U or WR 90) configuration used in insertion loss measurements. In all cases but one, the height of the ferrite slabs, h, was 0.425 inch and of different thickness, δ. The exception was Ferramic R-2 for which h, was 0.334 inch.

sertion loss of the waveguide containing the ferrite slab was measured as a function of applied magnetic field by replacing the empty waveguide section of equal length in the experimental setup shown in Fig. 2. All

From measurements it was determined that over the ferrite slab the space variation of the applied transverse magnetic field obtained from the electromagnet indicated in Fig. 2 was no more than ±1 per cent. The direct-reading magnetic field probe and associated indicator-amplifier referred to in Fig. 2 were calibrated with a compensated ballistic fluxmeter. A few of the calibration points were also checked with a proton resonance magnetometer. As a consequence of this calibration procedure and, also, as a result of several repeated data taking runs, it is believed that the values of the applied magnetic field used to graph the data shown in Section III have an average absolute accuracy of ±2 per cent. However, because of probable setting errors, magnetic field inhomogeneities, temperature drift, focusing effect of the ferrite slab, etc., maximum errors as large as ±5 per cent in the magnetic field values may exist in some cases.

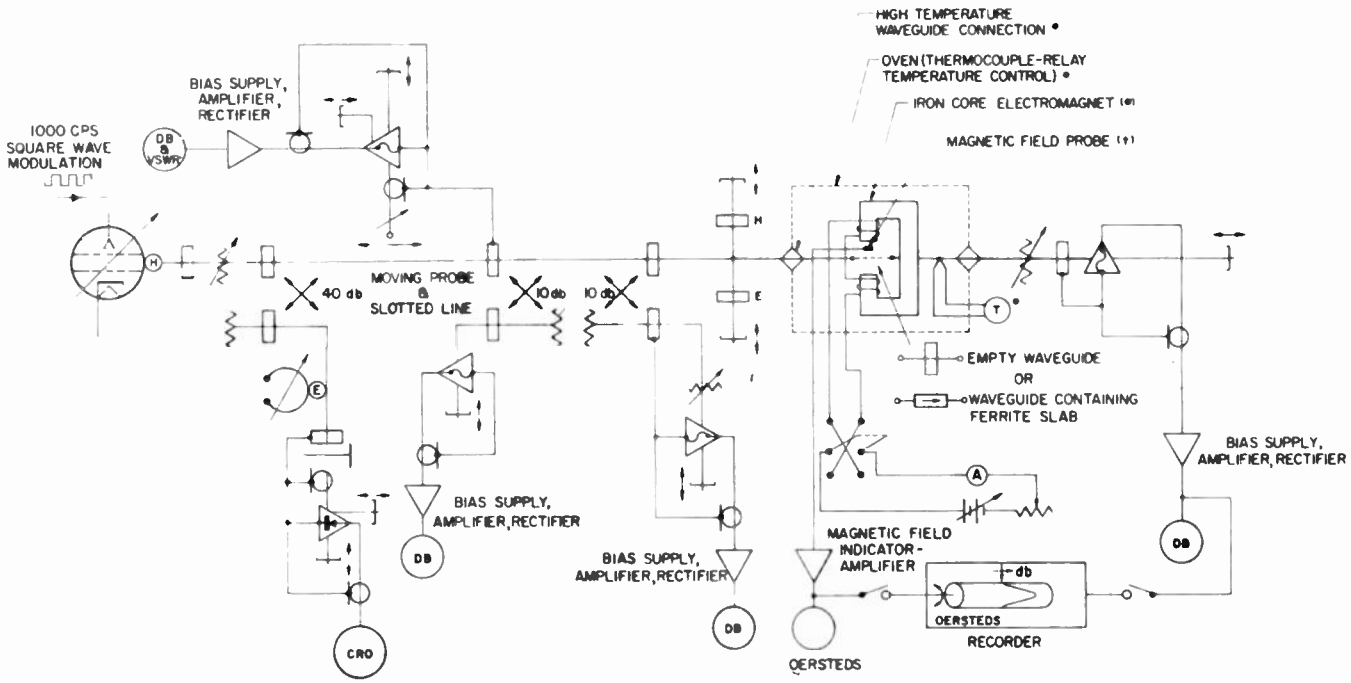

Fig. 2—Experimental arrangement for measuring the insertion loss of the ferrite slab and rectangular waveguide configuration as a function of magnetic field and frequency. The equipment modifications required for elevated temperature measurements are noted as follows:

* added, (*) altered, or (†) removed; these are discussed in Section IV.

of the microwave test equipment components were standard commercially available items. The usual precautions were taken to insure adequate padding and frequency stability, to eliminate residual reflections before insertion of the waveguide containing the ferrite slab, etc. The reflection from the ferrite-loaded waveguide section was continuously monitored as the magnetic field was varied. As a result of several calibration checks, the insertion loss data is believed to have an average accuracy of ±0.2 db in the 0 to 10 db range, and of ±2 per cent in db for losses greater than 10 db.

As can be seen in Fig. 2, provisions were made for taking the insertion loss vs magnetic field data continuously. Although this would normally have been an ideal way to obtain such information, the nonlinearities in the recording equipment available at the time made this procedure less useful than it could be, and nearly all the data were taken by a point-by-point procedure. However, the continuously scanning equipment was used for initial investigations to insure that no peculiarities would be overlooked in the point-by-point procedure.

Although some data were obtained with slabs 0.020 and 0.030 inch thick, most of the measurements were made with slabs whose thickness was nearly 0.010 inch. Because of the method of preparing the ferrite samples, this smallest dimension could not be maintained at exactly 0.010 inch without more than desirable spoilage. However, in any single sample, the variation in thickness from the average or nominal thickness was in nearly all cases less than ± 0.0005 inch. The samples were prepared from pressed or extruded ferrite rods by cutting with a diamond saw in a Di-Met machine.[23] In order to obtain the quite thin samples used here, it was found necessary to have the cutting wheel well balanced dynamically and to use a very slow feed. Final adjustment of the length and squaring the ends were readily done by hand using 320-grit aluminum oxide abrasive cloth.

Since a soluble oil lubricant was used in the cutting process, the ferrite slabs were cleaned by rinsing with trichlorethylene, decreasing in the same liquid, rinsing in methanol, and then drying in an oven at 200°C for approximately 12 hours. The slabs were then kept in tightly closed containers until tested. Recently obtained evidence is available which indicates that the chemical cleaning procedure may be superfluous as long as the ferrite material is adequately oven-dried.[24]

Some comment should be made on the reasons for the choice of 0.010 inch as the thickness of the slabs on which nearly all the measurements were performed. To avoid the so-called dimensional resonance effects,[3-5] it is to be expected that the smallest dimension of the ferrite sample in the direction of an applied space-varying rf magnetic field should be small compared to the wavelength in the ferrite medium. Thus, if δ is the thickness of the ferrite slab, $|\mu|$ the magnitude of the effective permeability, $|\epsilon|$ the magnitude of the premittivity, and λ_0 the free-space wavelength, it is required

$$\delta \ll \frac{\lambda_0}{\sqrt{|\mu||\epsilon|}}. \tag{1}$$

For a transversely magnetized infinite ferrite medium, Rowen[4] shows $|\mu| \approx 250$ as a possibly typical value in the frequency range of interest here, *i.e.*, 9 kmc. It should be emphasized that such large values of $|\mu|$ are encountered only in the region of ferromagnetic resonance, but, indeed, this is the region of major interest here. Choosing $|\epsilon| \approx 15$ as a reasonable average value for low-loss ferrites in this frequency range, we find that we require $\delta \ll 0.020$ inch, approximately. With no more specific information available at the time the series of measurements reported here was initiated, $\delta \cong 0.010$ inch was chosen as a compromise between the requirements given by (1), and the limitations of the fabrication method and the fragileness of the resulting samples. As will be seen from the results given in Section III, $\delta = 0.010$ inch is sufficiently small to avoid dimensional resonances. Further, as will be seen from Sections III and V, it is even small enough so that thin-slab theory can be used to compute with reasonable accuracy the attenuation characteristics of this arrangement for practically all the ferrite materials tested.

The thin-slab procedure would appear to have some possible advantages over other more complex methods of measuring the microwave properties of ferrites, such as the resonant cavity and Faraday rotation techniques. This is so since the ferrite samples are easily prepared, and the ferrite slab holder, which is the only special microwave component required, is simple to construct. Also, the data are easily obtained, readily interpreted, and are sufficiently accurate for most engineering purposes.

III. Experimental Results and Comments

The ratio of the transmission loss in the backward direction to that in the forward direction is a very important parameter of a ferrite-loaded resonance loss transmission system. It can be anticipated that this ratio will be at or near a maximum when the ferrite slab is located approximately where the rf magnetic field is circularly polarized.[4,5,16-18] Fig. 3, above, shows how the plane of circular polarization moves as the wavelength or frequency is varied. In spite of this variation the ferrite slabs tested here were kept in a fixed position near where the field is circularly polarized, not only

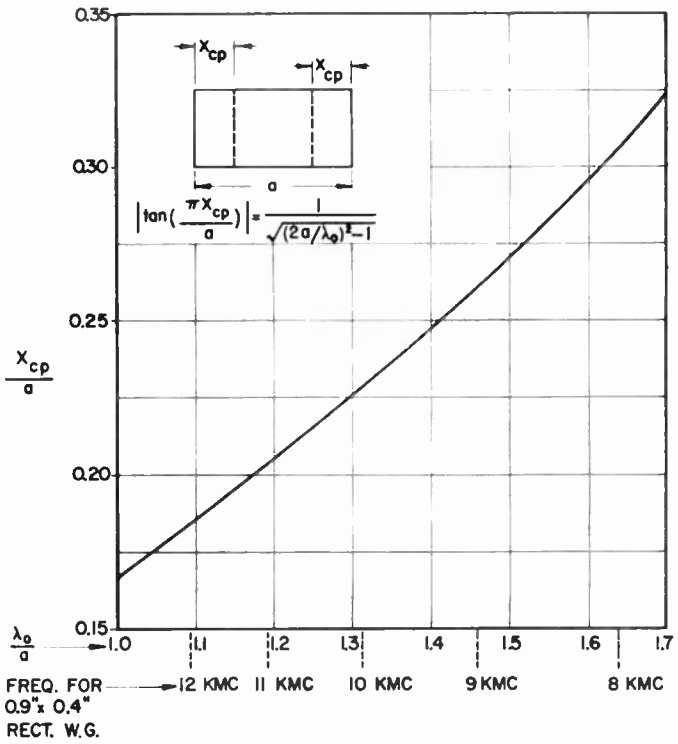

Fig. 3—Location of plane of circular polarization, x_{cp}, in rectangular waveguide as a function of the ratio λ/a, and frequency for 0.9 × 0.4 inch id (RG-52/U or WR 90) rectangular waveguide.

[23] The Di-Met machine used here is manufactured by the Felker Mfg. Co., Torrance, Calif., and is their model 80 BQ.

[24] Private communication to the author by G. S. Uebele of Hughes Aircraft Co. Research Laboratories.

because of convenience, but also because it was desired primarily to obtain only comparative information. It should be emphasized that it was not the objective of these tests to obtain a high-loss-ratio isolator. Indeed, as is now well known, the best configuration for a high-loss-ratio resonance isolator is one for which the height of the ferrite slab is less than the full narrow height of the waveguide.[5,25,26]

Data are available from measurements made on slabs of 0.010 inch nominal thickness fabricated from Ferramic A, B, C, D, E, G, H, H-1, I, J, N, O-1, Q, R-1, R-2, R-3 and from Ferroxcube 101, 102, 103, 104, 105, 106-I, 106-II; however, to conserve space, only some representative experimental results are shown here in Fig. 4 (on the next page).[27] The actual data points have been omitted for convenience. The ·, *o*, and *x* points in Fig. 4(b), 4(e), and 4(h) are calculated points about which more is said in Section V. The ordinates are given as loss in db per inch. It was found in several cases, as might be expected, that the measured db insertion loss was essentially a linear function of the length of the ferrite slab. Further, the reflection loss for these very thin slabs was, in practically all cases, less than 0.1 db at each end. As a consequence, the measured insertion loss was considered as being practically all uniform transmission loss and was, therefore, normalized in this fashion to make comparisons simpler. *f* and *b* on the curves refer to the loss characteristics in the forward and backward directions of propagation, respectively. The data were obtained by reversing the direction of the applied magnetic field, which is equivalent to reversing the direction of propagation. Hysteresis effects appeared to be quite small, and, consequently, are not shown.

Measurements were made only at one frequency, 8.9 kmc, on Ferramic C, H, H-1, I, and O-1 because of the medium-to-high dielectric losses of these materials. The reciprocal loss which occurs for both directions of polarization or propagation for applied magnetic field values greater than those required for substantial magnetic saturation, but less than those required for the onset of ferromagnetic resonance, is ascribable to dielectric loss.[4] Not shown are the results of a test made on a thin slab of the permanent magnet ferrite material Indox;[28] at 8.9 kmc and for applied fields from 0 to 5000 oersteds, no magnetic loss and a negligible dielectric loss was observed. It has been shown that for the frequency and applied fields used here the lack of magnetic loss is a result of the large internal anisotropy field which exists in such permanent magnet ferrite materials.[29,30]

Fig. 5 shows the results of measurements taken on a few slabs to determine approximately the influence of slab thickness on the loss characteristics. Even for these thicker slabs, the reflection losses were small enough to enable the results to be shown in normalized form with negligible error. In Fig. 6 are shown the data obtained with thin slabs of a few selected ferrite materials when the slabs are located against the narrow wall of the waveguide. Finally, Fig. 7 (p. 1330) shows the results obtained on a symmetrically located thin slab of Ferramic G. As before, the actual data points have been omitted for convenience in Figs. 5, 6, and 7. The · points in Fig. 6(b), 6(c), 6(d), and Fig. 7 are calculated points about which more is said in Section V.

Considerable information can be deduced from Figs. 4, 5, 6, and 7. In the following list, various points of interest are noted.

Saturation Magnetization

For the thin ferrite slab and rectangular waveguide configuration used here, the frequency for peak resonance loss is related to the applied field and the effective saturation magnetization by the following approximation:

$$f \cong 2.8\sqrt{H_{im}B_{im}} = 2.8[H_m(H_{im} + 4\pi M_s)]^{1/2}, \quad (2)$$

where the frequency f is in megacycles, the applied internal dc magnetic field at resonance, H_{im}, is in oersteds, and the magnetic induction, B_{im}, and the effective saturation magnetization, $4\pi M_s$, are in gauss. Eq. (2) is discussed in more detail in Section V. For a fixed frequency, a smaller H_{im} is required for a larger $4\pi M_s$. The magnetic field plotted in Figs. 4, 5, 6, and 7 is the applied external magnetic field, but for the thinnest slabs the demagnetization is small enough so that the applied internal magnetic field is only slightly less than the applied external magnetic field. Using (2) and the available data, one can obtain a list of the ferrites in the order of increasing effective saturation magnetization, which is approximately as follows: R-2, R-1, R-3, 101, H-1, I, 102, B, A, E, G, H, D, 106-I, 106-II, O-1, C, 103, N, Q, 105, J, and 104. The letters refer to the Ferramic materials, the numbers to the Ferroxcube materials. In Section V, where $4\pi M_s$ is computed for the various materials including the effect of loss, it is shown that the order of this list is essentially unaltered.

[25] H. N. Chait, "Non-reciprocal microwave components," 1954 IRE Convention Record, part 8, pp. 82–87.

[26] J. P. Vinding, "Microwave devices using ferrite and transverse magnetic field," 1955 IRE Convention Record, part 8, pp. 105–108. Also, A. Calvin, "High-power ferrite load isolators," IRE Trans., vol. MTT-3, pp. 38–43; October, 1955.

[27] Ferrite materials designated by Ferramic are manufactured by the General Ceramics Corp., Keasbey, N.J.; Ferroxcube materials are manufactured by the Ferroxcube Corp. of America, Saugerties, N.Y. The I and II designation used here in the case of the Ferroxcube 106 material is to distinguish between extruded rods and pressed slugs, respectively. In all other cases, the slabs of Ferroxcube materials were cut from extruded rods, and the I designation is suppressed. Complete data are shown in HAC TM-406, which interested readers can obtain by writing the author.

[28] The ferrite material Indox is manufactured by the Indiana Steel Products Co., Valparaiso, Ind.; it is apparently entirely equivalent to Ferroxdure or Magnadur made by the Ferroxcube Corp. of America, and to other similar materials now becoming available.

[29] M. T. Weiss, "The behavior of Ferroxdure at microwave frequencies," 1955 IRE Convention Record, part 8, pp. 95–99. Also, M. T. Weiss and P. W. Anderson, "Ferromagnetic resonance in ferroxdure," *Phys. Rev.*, vol. 98, pp. 925–926, May 15, 1955.

[30] J. Smit and H. G. Beljers, "Ferromagnetic resonance absorption in $BaFe_{12}O_{19}$, a highly anisotropic crystal," *Philips Res. Rep.*, vol. 10, pp. 113–130; April, 1955.

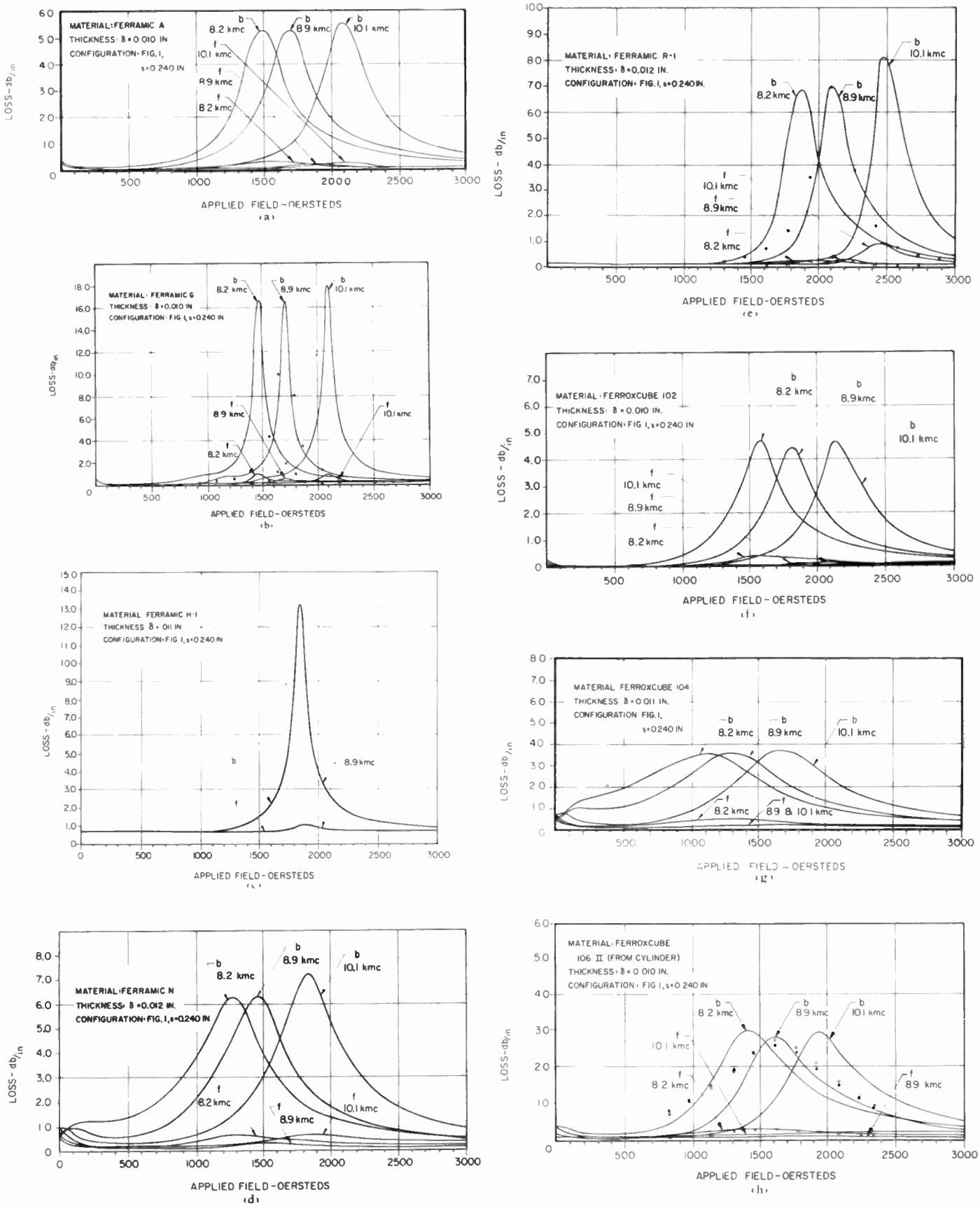

Fig. 4—Measured transmission loss at fixed frequencies as a function of applied dc magnetic field for thin ferrite slabs located approximately at the plane of circular polarization. *f* and *b* refer to loss in the forward and backward directions of propagation. In (b), (e), and (h), the · and *o* points (linear and quadratic α approximations respectively) show the calculated backward loss, while the *x* points (essentially the same for both linear and quadratic α approximations) show the calculated forward loss, all for 8.9 kmc, obtained using the derived $4\pi M_s$ and α. Section V contains further details on these calculations.

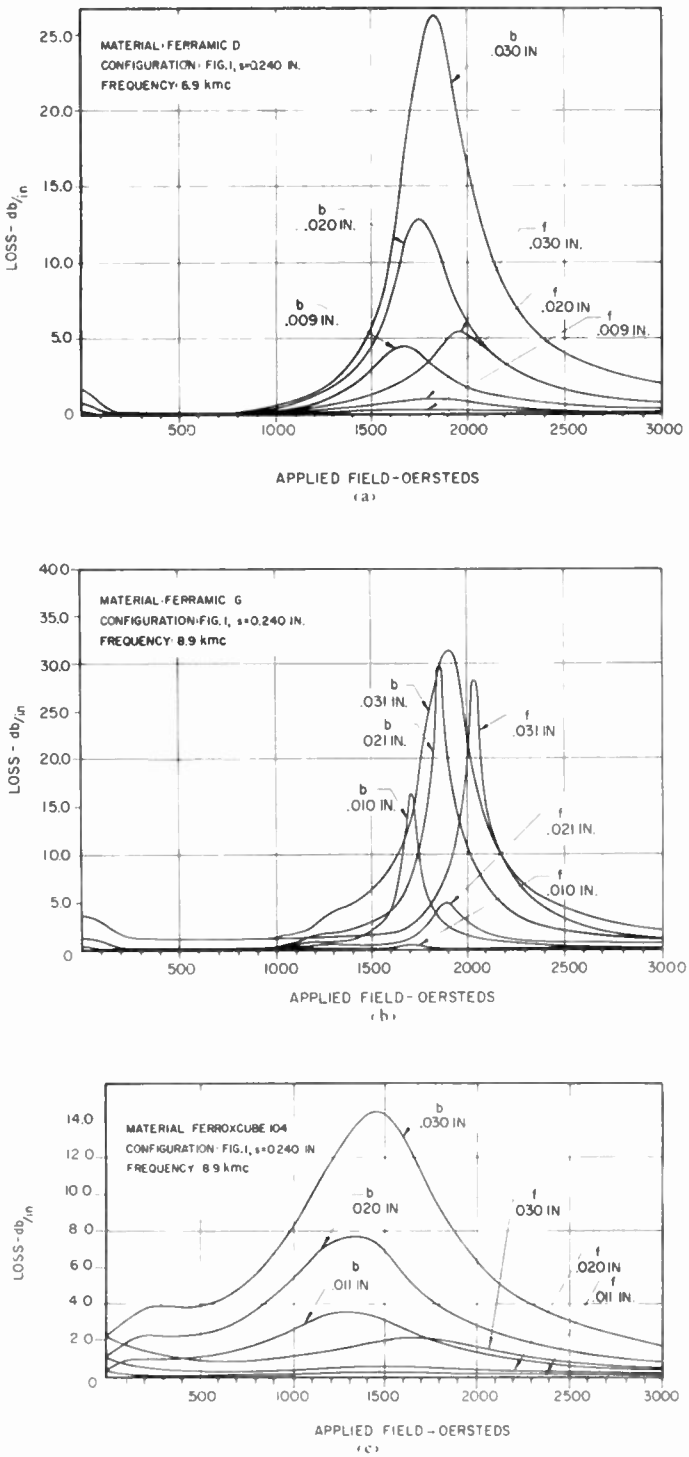

Fig. 5—Measured transmission loss at 8.9 kmc as a function of applied dc magnetic field for ferrite slabs of different thickness located approximately at the plane of circular polarization; *f* and *b* refer to loss in forward and backward directions of propagation.

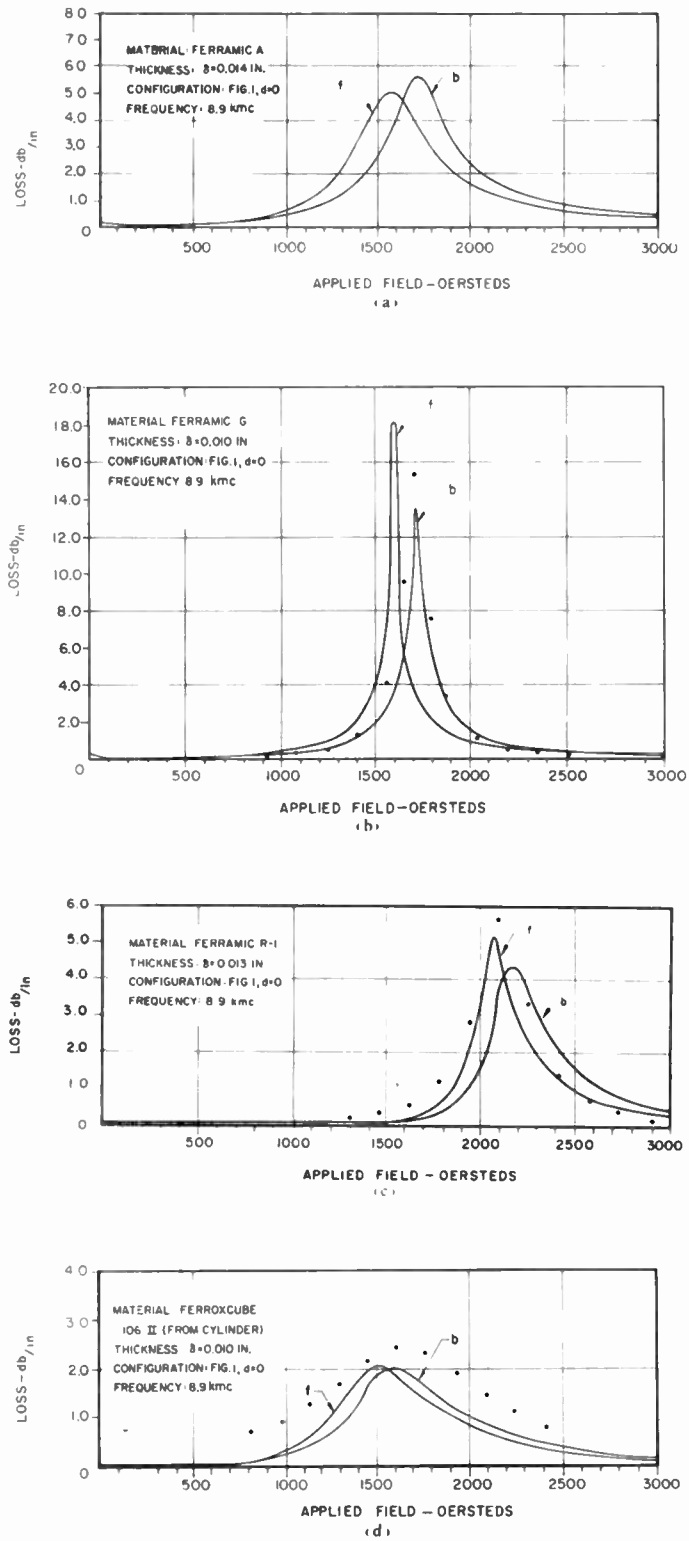

Fig. 6—Measured transmission loss at 8.9 kmc as a function of applied dc magnetic field for thin ferrite slabs located against the narrow wall of the waveguide. The convention used in Figs. 4 and 5 is maintained here; *f* and *b* refer to the loss in what would be the forward (low loss) and backward (high loss) directions of propagation, if the slabs were displaced somewhat from the sidewall. The Ferramic A and R-1 slabs were different and slightly thicker here than for Fig. 4(a) and 4(e), whereas the other slabs were the same. In Fig. 6(b), 6(c), and 6(d), the · points (linear α approximation) show the calculated loss, which would be the same in the *f* and *b* directions for a symmetrically located slab, obtained using the derived $4\pi M_s$ and α. Section V contains further details on these calculations.

Dielectric Loss

The dielectric loss in nearly all the ferrite materials tested is generally small. Exceptions are O-1 and C (very high), I (high), and H and H-1 (medium). Evidence has been given elsewhere that the rf dielectric loss is simply a result of ohmic conduction loss, and that low bulk resistivity of a ferrite material is accompanied

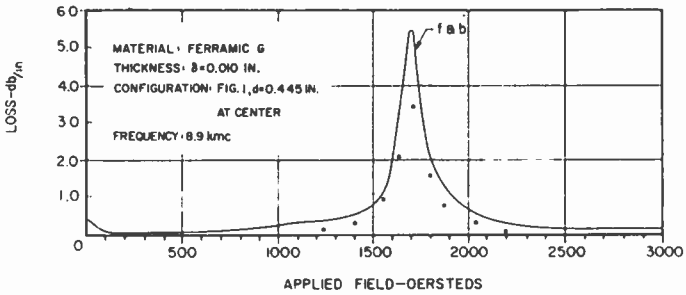

Fig. 7—Measured transmission loss at 8.9 kmc as a function of applied dc magnetic field for a symmetrically located thin slab of Ferramic *G*. The · points (linear α approximation) show the calculated loss, which would be the same in the *f* and *b* directions for a symmetrically located slab, obtained using the derived $4\pi M_s$ and α. Section V contains further details on these calculations.

by high rf dielectric loss.[4] However, as also noted, a high dc resistivity of a ferrite material is not necessarily accompanied by a low rf dielectric loss because of the granular nature of some ferrites.[4] Measurements on a few samples of O-1, C, and I led to average dc resistivity values of 8×10^4 ohm-cm, 2×10^3 ohm-cm, and 6×10^4 ohm-cm, respectively. These values agree, more or less, with those quoted in the commercial literature.[31] No dc measurements were performed on the ferrites which have a low dielectric loss, although the commercially quoted resistivities for these materials are of the order of 10^6 ohm-cm or larger. As a necessary although not sufficient criterion, it appears that a ferrite material should have a minimum dc resistivity of approximately 10^6 ohm-cm for the dielectric loss to be small. Incidentally in some applications, for example in a field-displacement isolator,[5,16] it may be desirable to use a ferrite with a medium to high dielectric loss.

Low and Medium Field Loss

By low field loss is meant that loss which is essentially the same for both polarizations or directions of propagation (*f* and *b*), and which disappears when the applied field is greater than 100 oersteds, approximately. Most of the ferrites tested possess a low field loss in the frequency range considered here. Exceptions are R-1, R-2, R-3, 101, and, possibly, H-1 and I. Perhaps C and O-1 should be included in this list of exceptions, but, more likely (this might also be the case for H-1 and I) the low field loss in these ferrites is masked by the high dielectric loss. It has been shown that as a result of the domain structure in a ferrite, low field loss will disappear in an unsaturated sample if

$$f_m > 2.8(4\pi M_s), \tag{3}$$

where f_m is the measuring frequency in megacycles, and where the anisotropy field has been assumed to be negligibly small.[3,32] If one uses the values of $4\pi M_s$ given in Section V, it is found that (3) is approximately satisfied for those ferrites with the lowest $4\pi M_s$ for which no low field loss is observed. Since the low field loss depends on the existence of domains and associated domain walls, such loss should disappear when the material is saturated, that is for applied internal fields larger than 10 to 100 oersteds, approximately. Examination of the available data shows that this is the case for nearly all the ferrite materials.

The exceptions are J, N, Q, 103, 104, 105, and possibly 106, C, and O-1. These materials have a medium field loss characteristic; by this we mean they show a substantially different loss for the different polarizations or directions of propagation (*f* and *b*) for an applied field in the range 100 to 500 oersteds, which is below the applied field required for peak ferromagnetic resonance loss. The medium field loss property is most pronounced in the case of 104, and disappears, essentially, between 8.9 and 10.1 kmc in all the cases for which tests at the different frequencies were made. It does not appear possible to ascribe the medium field loss to an effective crystalline anisotropy field, since this field would be far too small to account for such loss in this frequency range.[4,33] The presence of high internal fields resulting from magnetic poles set up on nonmagnetic grain boundaries rather than domain walls has been suggested as a possible explanation for this loss.[4] Since these high internal fields would persist when the ferrite material is magnetized to saturation, differential loss would occur because the magnetization is substantially in the same direction throughout the material. As noted in Section IV here, measurements made at various temperatures showed that the medium field loss characteristic disappears for temperatures somewhat above 100° C, at least for 104 material. It seems unlikely that the nonmagnetic grain boundaries would disappear at this temperature.

However, this temperature dependence and the fact that the medium field loss property occurs for those ferrites which have the highest effective saturation magnetization suggest another explanation for medium field loss. If relatively complete magnetic saturation did not occur for applied fields in the range from 100 to 500 oersteds in the ferrites which exhibit this characteristic, a substantial number of domains and domain walls would still exist. Consequently, the same mechanism which leads to low field loss would still be operating, but nonreciprocal losses would be observed for medium

[31] Here, more or less agreement means within a factor of three. However, in connection with C material, early data quoted by the manufacturer gave 2×10^3 ohm-cm as the resistivity, whereas more recent data give 2×10^6 ohm-cm. It would appear that the C material used here is the one to which the early data apply. In a private communication from the General Ceramics Corp. it was indicated that the resistivity of C material may vary over a wide range. It was also indicated that extremely close control of the resistivity of commercially available ferrites is quite difficult.

[32] D. Polder and J. Smit, "Resonance phenomena in ferrites," *Rev. Mod. Phys.*, vol. 25, pp. 89–90; January, 1953.

[33] From the relationship between initial permeability, saturation magnetization, and the first-order anisotropy coefficient [see (33), p. 98 of the first reference in footnote 3; also (21), p. 90 and (38), p. 106 of the same reference], it is possible to deduce the last of these from measured values of the others. The effective crystalline anisotropy field turns out to be at least an order of magnitude too small to account for medium field loss.

field strengths since a large portion of the material is magnetized in one direction. However, this nonreciprocity would be rather temperature sensitive because of the decrease in the saturation magnetization with increasing temperature. Although complete B-H data on the ferrites of interest here do not appear to be available, some published comments indicate that the Ferroxcube materials are, in fact, far from saturation for applied fields range from 100 to 500 oersteds.[19,34,35]

Whatever the reason for the medium field loss property, it should be noted that nonreciprocal loss ratios of about 10 to 1 in db can be obtained for frequencies less than 9 kmc for applied fields of the order of $\frac{1}{5}$ to $\frac{1}{3}$ of those required for peak ferromagnetic loss. This may be important for some applications, where the temperature sensitivity of this property is not significant.

Shape and Magnitude of Resonance Curve

If the low and medium field loss properties are ignored, the shapes of the resonance curves in nearly all cases are relatively simple, at least for the 0.010 inch slabs. Exceptions are C and, in particular, O-1, which have somewhat peculiar resonance loss curves, evidently because of their high dielectric losses. Except for these ferrites, the resonance curves can be reasonably well approximated by a relatively simple expression as shown in Section V. The resonance loss curves vary from the narrow, high-loss type shown by G, H-1, and I, to the quite broad, low-loss type demonstrated by J, N, Q, 104, 105, and 106. It should be noted that the internal field in the slabs was not precisely uniform because of the inhomogeneity in the applied dc magnetic field, which was as much as ± 1 per cent in some cases, and because of the inhomogeneities resulting from the departure of the slabs from a true ellipsoidal shape, *i.e.*, edge and end effects. As a consequence, it is very likely that the intrinsic peak losses are slightly higher, and the intrinsic resonance curves somewhat narrower, at least for G and H-1, shown here in Fig. 4(b) and 4(c). The resonance curves for the other ferrites are, of course, similarly affected, although in a decreasing manner as the curves broaden.

The commercially available ferrites used here are made by a sintering process and are porous.[3] In addition, as is evident on simple observation, many of them contain fissures, holes, etc. As is well known, such inhomogeneities, as well as large variations in the magnetic properties of the ferrites, are a function of the manufacturing process, *i.e.*, the handling prior to sintering, as well as the firing time, the firing temperature, and the firing atmosphere.[3] The various kinds of inhomogeneities in the material will obviously influence the shape and magnitude of the resonance loss curve. It should be emphasized that nearly all the measurements reported here were made on single, but hopefully representative, samples of the available ferrite materials. No attempt was made to determine the variation in the characteristics of all the ferrites resulting from commercial tolerances. However, tests on several samples of G, R-1, 104, and 106 indicated that for these materials, at least, variations in the resonance loss characteristics as a function of frequency and applied field are small.

Effect of Slab Thickness

It might be expected that as the slab thickness is increased the db loss/in would also increase in direct proportion, that is, in proportion to the volume. Examination of Fig. 5 shows that this is approximately true for slabs 0.010 inch and 0.020 inch thick. However, in most cases the loss is larger for the 0.030-inch slabs than would be expected from an increase in volume. A possible qualitative explanation might be that as a consequence of the high dielectric constant of ferrite materials, the fraction of the energy of the propagating wave which exists in the ferrite slab increases more rapidly than the volume increases, with a consequent more rapid increase in the loss. A peculiarity can be noted in Fig. 5(b), where the forward and backward loss are nearly the same for the case of the 0.031-inch slab of G material. Although a completely satisfactory explanation for this peculiarity is not available, one explanation for it might be in the existence of higher-order mode propagation or dimensional resonances. Another more likely explanation might be in the large distortion of the waveguide fields as a result of the high permittivity and effective permeability of the G material, so that the proper transverse location of the 0.031-inch slab of this ferrite to obtain a substantial loss ratio is considerably different than the one used for the tests here, *i.e.*, $s = 0.240$ inch.[36]

Effect of Slab Location

Intuitively, and from thin-slab theory (see Section V), it would be expected that the loss characteristics would be practically the same for both the forward and backward directions with the slab located at the waveguide wall, that is for $d = 0$. As can be seen from Fig. 6, this expectation is very nearly fulfilled, although the degree of similarity in the f and b curves is evidently

[34] du Pré, *op. cit.*, notes on page 8, that Ferroxcube IV B ferrite material is only at 85 per cent of "true" saturation even for a field as large as 2000 oersteds; "true" saturation occurs for fields in excess of 18,000 oersteds. From the exact correspondence between the listed Curie temperatures—although quoted initial permeabilities, saturation magnetizations, etc., differ somewhat, as indicated in footnote 35—the author had presumed that the correspondence between the Ferroxcube letter and number series was IV A to 102, . . . IV E to 106. In a private communication, Dr. du Pré has informed the author that this relationship is correct, although the materials are really not identical, but rather have properties which are similar.

[35] J. J. Went and E. W. Gorter, "The magnetic and electrical properties of ferroxcube materials," *Philips Tech. Rev.*, vol. 13, pp. 181–193; January, 1952.

[36] Fox et al., *op. cit.*, in their Fig. 40, show a similar peculiarity in the case of R-1 material (formerly Ferramic 1331) for the case of $s = 0.265$ inch and $\delta = 0.046$ inch (our notation), although for a slab narrower than the full height of the waveguide and for a frequency of 10.5 kmc. For the case shown there, locating the slab much closer to the side of the waveguide leads to a significant loss ratio.

a function of the ferrite material. Since the unperturbed rf magnetic field in the waveguide is linearly polarized only just at the waveguide wall, minor differences for the *f* and *b* cases would be expected even for the thinnest slabs. However, this difference may be practically negligible, so that its magnitude is a measure of how close the slabs used here approach the "ideal" thin slab. Evidently, a thickness of 0.010 inch is not too much larger than the one required for a useful "ideal" thin slab, although the maximum permissible thickness for this requirement will depend on the ferrite.

As expected from symmetry, the resonance loss curves for the forward and backward directions are the same for a ferrite slab at the center of the waveguide, as shown in Fig. 7.

Peak Loss Characteristics

Although, as already noted, no attempt was made here to maximize the loss ratio for the configuration used, a peak loss ratio of 20 to 1 in db or larger exists for several of the ferrites. Generally, peak loss ratios of this order occur only for the thinnest slabs, and for a slab location very near the plane of circular polarization of the rf magnetic field, *i.e.*, at 8.9 kmc. For other frequencies and for thicker slabs, the loss ratios are generally smaller, although this may be partly the result of a nonoptimum transverse location. Note that the applied fields for peak forward loss and peak backward loss are different; this difference is usually small for the thinnest slabs (see Fig. 4) and increases, in some cases, as the slab thickness increases (see Fig. 5). With the possible exception of the peak loss ratios shown here, other peak loss properties of full-height ferrite slabs shown here appear to be similar to those described elsewhere.[4,5,37]

IV. Effect of Temperature

The saturation magnetization of ferrite materials decreases with increasing temperature, and, in fact, essentially disappears at the Curie temperature.[3] Hence, it is clear from (2) that the applied dc field required for peak resonance loss increases as the temperature increases. Further, it can be expected that the low and medium field loss, the shape of the resonance curve, the dielectric loss, etc., are influenced by temperature. Although the effect of temperature on the magnetic properties of many special ferrites has been reported,[38] microwave resonance loss data as a function of temperature on a few of the commercially available ferrites have only been shown very recently.[39]

The procedure used here for obtaining resonance loss data at elevated temperatures was essentially the same as the one used for obtaining this information at room temperature. Only some relatively minor modifications in the experimental arrangement and equipment shown in Fig. 2 and in the procedure for determining the applied dc magnetic field were required.[40] As before the rf power level was in the 10 to 100 milliwatt range, and the measurements were performed only at 8.9 kmc. Tests were performed on G, R-1, and 104 only. Although the properties of the various ferrites are undoubtedly different,[3] these were chosen as being representative of ferrites which exhibit a range of the various resonance loss characteristics. Also, they would appear to be useful for actual application in various microwave devices. In all cases the complete resonance loss curves were recorded from room temperature up to the temperature at which resonance loss essentially disappeared. Space does not permit the presentation of all these curves, but many of the significant results are summarized in Fig. 8.

From Fig. 8 and the more complete resonance curves not shown here, the following points of interest can be noted.

Saturation Magnetization and Curie Temperature

The decreasing saturation magnetization with increasing temperature is clearly evident from the increased applied field required for peak backward resonance loss. In all cases this field and the field required for peak forward resonance loss are nearly the same, so that only the former is shown. From (2), with $4\pi M_s = 0$

[37] Fox, Miller, and Weiss *op. cit.*, indicate that their experience shows that making the slab thinner in the case where the slab extends completely from the top to the bottom of the waveguide, *i.e.*, for the full-height slab configuration identical to the one used here, does not lead to peak loss ratios in excess of about 8 or 10 to 1 in db. Considerably higher loss ratios are shown here, and the difference is believed to result from the fact that they did not investigate thin enough slabs. For example, Rowen *ibid.*, states results similar to those obtained here, and shows loss ratios for this configuration of the order of 20 or 30 to 1 in db. He indicates that these ratios are obtained only with very thin slabs.

[38] D. W. Healy, Jr., "Ferromagnetic resonance in nickel ferrite, as a function of temperature," *Phys. Rev.*, vol. 86, pp. 1009–1013; June 15, 1952.

[39] B. J. Duncan and L. Swern, "Temperature behavior of ferrimagnetic resonance in ferrites located in wave guide," *J. Appl. Phys.*, vol 27, pp. 209–215; March, 1956.

[40] Among these were 1) the substitution of a high-temperature iron core electromagnet for the one used previously, and 2) the insertion of high-temperature waveguide connections on either side of the ferrite slab and rectangular waveguide assembly to transmit microwave energy through openings in the oven walls. The high-temperature magnet was similar to the one used at room temperature except that the windings were insulated with Refrasil—a type of glass insulation manufactured by the H. I. Thompson Fiber Glass Co., Los Angeles, Calif. Since the magnetic field probe could not be used at elevated temperatures, a magnetic field vs coil current calibration taken at room temperature was used at the higher temperatures. Since the temperatures used were well below the Curie point of the core material, and since the reluctance of the air gap was large compared to that of the core, it was assumed that this calibration would be only slightly modified with temperature. It was necessary to take data only on the increasing current loop of the hysteresis curve, and to take the current up to the same maximum value on each run. Each microwave connection through the oven walls consisted of a transition from rectangular to round to round dielectric (quartz—this went through the oven wall) to round to rectangular waveguide. The effect of temperature on the insertion loss of these connections and on the waveguide run inside the oven was taken into account. The author wishes to thank G. S. Uebele of these laboratories for making the oven and the high-temperature waveguide connections available. A calibrated thermocouple in intimate contact with the waveguide in the oven was used to indicate temperature; to insure that thermal equilibrium had been reached, data were taken only when this indicated temperature and the internal wall temperature of the oven were substantially the same. Since the polyfoam wedges shown in Fig. 1 could obviously not be used at elevated temperatures, a U-shaped spring of thin molybdenum, which introduced no measurable effect, was placed on the bottom of the waveguide to force the ferrite slab against the sides of the rectangular grooves.

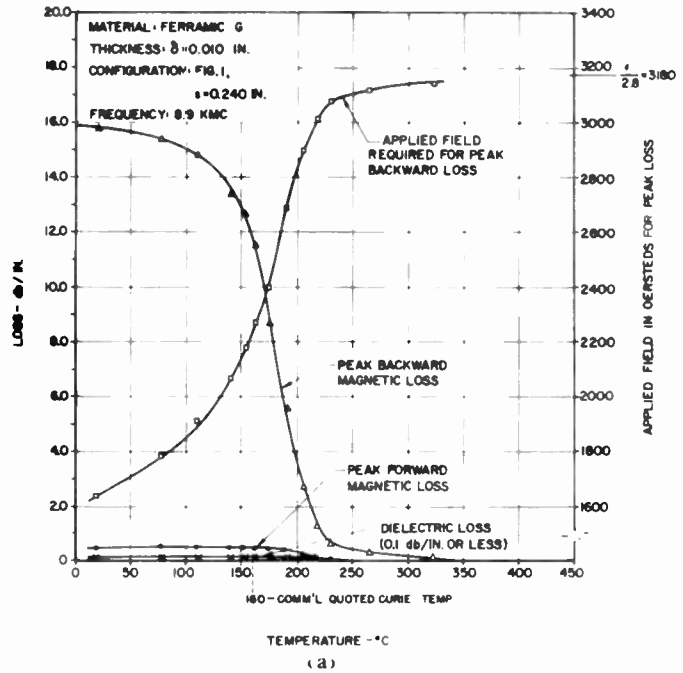

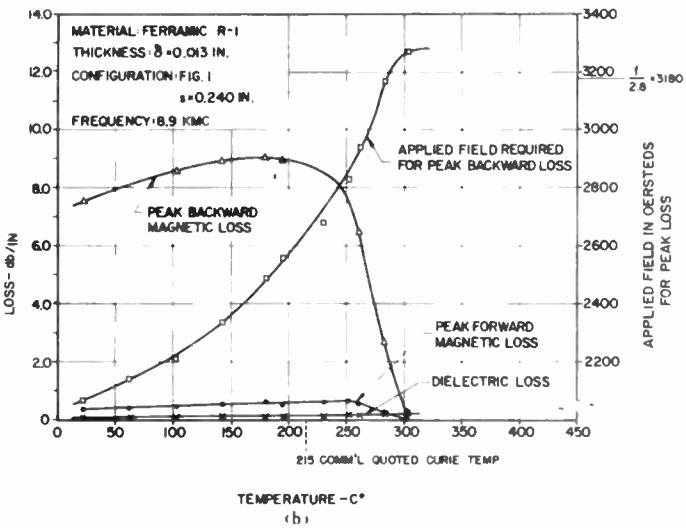

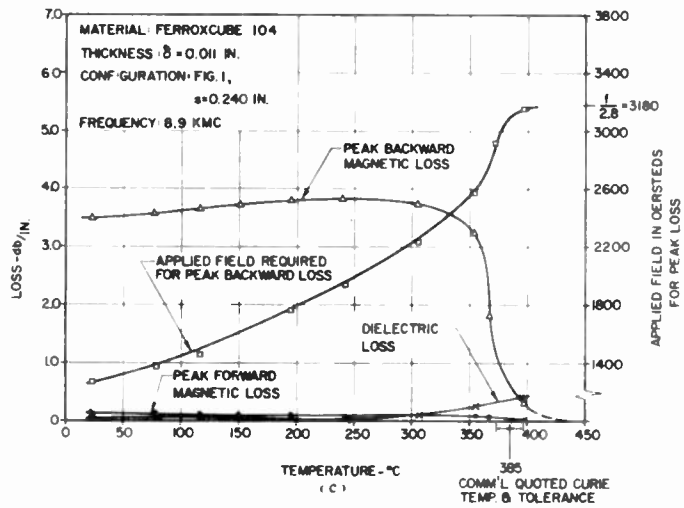

Fig. 8—Variation of applied dc magnetic field for peak forward loss, peak backward loss, and dielectric loss as a function of temperature for thin ferrite slabs. The *G* and 104 slabs were the same as for Fig. 4(b) and 4(g), whereas the R-1 slab was different and slightly thicker here than for Fig. 4(e).

at the Curie temperature T_c, $H_{im}=f_m/2.8$, and with $f_m=8.9$ kmc, $H_{im}=3180$ oersteds. The dc demagnetization effect is negligible here. Note that at the temperature at which the magnetic resonance losses essentially disappear, the required applied field for peak resonance loss is within about 5 per cent of 3180 oersteds in all cases. In view of the somewhat indirect method of determining the applied field at elevated temperatures, this agreement is quite reasonable. The precise point of disappearance of the ferromagnetic resonance loss is somewhat difficult to determine because of the tailing off of the loss curves; see, for example, Fig. 8(a) and 8(c). This property may be a result of the paramagnetic character of ferrites above T_c.[3] It will be noted from Fig. 8(a) and 8(b) that substantial resonance loss still exists for a temperature at and well above the commercially quoted Curie temperature for both G and R-1 material. The quoted Curie temperature for these materials is apparently taken to be the maximum temperature at which the low-frequency initial permeability falls below its value at about 20°C. As might be expected, the true Curie temperature, the temperature at which ferromagnetic resonance effects disappear, is somewhat higher than the Curie temperature based on this initial permeability definition.[16] On the other hand, for the 104 material, the quoted Curie temperature is quite close to the one measured here at which ferromagnetic resonance has essentially disappeared. Although only three ferrite materials have been measured, it appears that useful microwave magnetic properties may exist for some ferrites at temperatures equal to and even substantially higher than the commercially quoted Curie temperatures.

Dielectric Loss

For the ferrite materials it would be expected that the conductivity and, consequently, the dielectric loss would increase with temperature.[3] However, from Fig. 8 it is evident that the dielectric loss in G and R-1 material is practically unchanged, within experimental error, over the range of temperatures shown here. For 104 material the dielectric loss increases for temperatures above 300°C; fortunately, this occurs near where the useful microwave magnetic properties disappear, that is, near T_c.

Low and Medium Field Loss

From the complete resonance loss data not shown here, it can be determined that the low field loss for G material disappears for a temperature near 100°C, approximately. The medium field loss of 104 material disappears between 116°C and 150°C, whereas the low field loss in 104 disappears between 145°C and 248°C. R-1 material exhibits no low field loss at room temperature, and, of course, this situation is not altered at higher temperatures. From Fig. 8 and (2) the effective saturation magnetization for a given temperature can be deduced. For G and 104 it is found that (3) predicts

rather well the saturation magnetization, and consequently the temperature, at which the low field loss disappears.[3] Comments have already been made concerning the medium field loss in 104 and its temperature dependence, and these need not be repeated.

Shape and Magnitude of Resonance Curve[38]

For increasing temperatures above room temperature the resonance loss curves for both R-1 and 104 become markedly narrower as a function of applied dc field. This may also be the case for G, but was difficult to determine from this series of measurements because of the already narrow width of the resonance loss curve for G at room temperature. The comments made previously concerning the effects on the resonance curve shape and magnitude resulting from various inhomogeneities obviously apply here also.

Peak Loss Characteristics

As is evident from Fig. 8, for each of the three ferrite materials considered here the peak loss ratio is substantially unchanged, at least over the range of temperatures for which the peak backward loss remains high. A point of some interest is the increase in the peak backward loss for both R-1 and 104 between room temperature and some temperature less than T_c. Perhaps G behaves in a similar manner as tests for temperatures below room temperature might indicate. Note too that the peak backward loss of R-1 and 104 changes from essentially its peak value to practically zero with a change of 50°C. On the other hand, the change in the peak backward loss of G is much more gradual, and covers a range of 150°C or more.

V. Thin-Slab Theory

The information presented in Fig. 4 and in similar graphs not shown here has proved to be of considerable use in comparing ferrite materials qualitatively and quantitatively. Further, it turns out that numerical values of the effective saturation magnetization and damping constant of the various ferrites can be deduced through the use of so-called thin-slab theory. In this section the required formulas are developed and their use is illustrated.

The determinantal equation for a uniformly magnetized and magnetically saturated ferrite slab in a rectangular waveguide is a complicated transcendental equation.[17,20,41] It can be solved in general, even for the lossless case, only through the use of numerical methods.[41] The lossy case is even more complicated and has been solved only for a small range of parameters.[42] However, if the slab is taken to be very thin, considerable simplification results, and explicit expressions in terms of the various parameters can be obtained. A summary of the required calculative procedure and the meaning of the symbols used is given below in "Procedure for Applying the Formulas."

Derivation of Formulas

For the geometry shown in Fig. 9 the following transcendental determinantal equation applies for the "fundamental" transverse electric mode:[41]

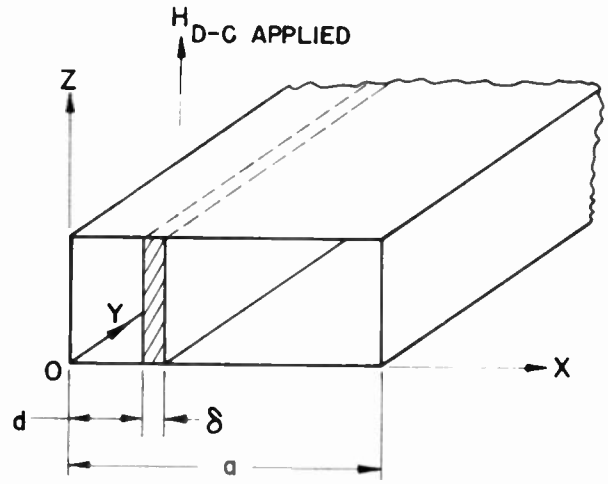

Fig. 9—Thin ferrite slab in rectangular waveguide with dc magnetic field applied along the z axis.

$$\frac{1}{2}\left(\frac{k_a^2}{\rho^2}+\frac{\beta^2}{\theta^2}-k_m^2\right)\cos k_a(a-\delta-2d)+j\frac{\beta k_a}{\rho\theta}\sin k_a(a-\delta-2d)+\frac{1}{2}\left(\frac{k_a^2}{\rho^2}-\frac{\beta^2}{\theta^2}+k_m^2\right)\cos k_a(a-\delta)+\frac{k_a k_m}{\rho}\cot(k_m\delta)\sin k_a(a-\delta)=0, \tag{4}$$

where different symbols than those used in the original reference are used here for the various transverse dimensions. In the derivation of (4), propagation like $e^{-j\beta y}$ is considered. Also,

$$\rho=\frac{1+\chi_{xx}}{(1+\chi_{xx})^2+\chi_{xy}^2}, \tag{5a}$$

$$\theta=\frac{1+\chi_{xx}}{\chi_{xy}}, \tag{5b}$$

where χ_{xx} and χ_{xy} are the components of the intrinsic magnetic susceptibility tensor

$$\overleftrightarrow{\chi}=\begin{pmatrix}\chi_{xx} & \chi_{xy} & 0\\ -\chi_{xy} & \chi_{xx} & 0\\ 0 & 0 & 0\end{pmatrix}; \tag{6}$$

that is,

$$\overleftrightarrow{\chi}=\frac{\overleftrightarrow{\mu}}{\mu_0}-\overleftrightarrow{1},$$

[41] B. Lax, K. J. Button, and L. M. Roth, "Ferrite phase shifters in rectangular wave guide," *J. Appl. Phys.*, vol. 25, pp. 1413–1421; November, 1954.

[42] K. J. Button and B. Lax, "Theory of ferrites in rectangular waveguides," IRE Trans. vol. AP-4, pp. 531–537; July, 1956.

with $\overleftrightarrow{1}$ the unit diagonal tensor. Further,

$$k_m^2 = \omega^2 \epsilon \mu_0 \left[\frac{1(+\chi_{xx})^2 + \chi_{xy}^2}{1+\chi_{xx}} \right] - \beta^2, \tag{7}$$

and

$$k_a^2 = \omega^2 \epsilon_0 \mu_0 - \beta^2, \tag{8}$$

where ϵ and ϵ_0 are the scalar permittivity of the ferrite and free space respectively, and μ_0 is the permeability of free space. Time dependence like $e^{j\omega t}$ is assumed. β is, of course, the quantity of interest.

We now make use of the expansion around $\delta = 0$, so that

$$\beta_\pm = \pm \beta_0 + \left(\frac{\partial \beta}{\partial \delta} \right)_{\delta=0, \beta=\pm\beta} \delta + \cdots, \tag{9}$$

where $\beta_0 = 2\pi/\lambda_{g0}$ is taken as an intrinsically positive quantity and is the propagation constant of the air-filled waveguide. The air-filled waveguide wavelength is λ_{g0}. Thus, for $\delta \neq 0$, propagation in the positive and negative y directions varies as $e^{-j\beta+y}$ and $e^{-j\beta-y}$, respectively; these become, in turn, $e^{-j\beta_0 y}$ and $e^{+j\beta_0 y}$ for $\delta = 0$. Upon evaluation of the derivative in (9), there results after considerable manipulation,

$$\begin{aligned} \beta_\pm &= \beta_0 \left\{ -j \frac{\pi}{\beta_0 a} \frac{\chi_{xy}}{1+\chi_{xx}} - \frac{\delta}{a} \sin \frac{2\pi d}{a} \right. \\ &= \left[1 + \frac{\omega^2 \mu_0 \epsilon_0}{\beta_0^2} \frac{\delta}{a} \chi_e \sin^2 \frac{\pi d}{a} + \frac{\chi_{xx}}{1+\chi_{xx}} \frac{\delta}{a} \sin^2 \frac{\pi d}{a} \right. \\ &\left. \left. + \left(\chi_{xx} + \frac{\chi_{xy}^2}{1+\chi_{xx}} \right) \frac{\delta}{a} \frac{\pi^2}{\beta_0^2 a^2} \cos^2 \frac{\pi d}{a} \right] \right\}.^{43} \end{aligned} \tag{10}$$

Here, χ_e has been taken to be the dielectric susceptibility; that is,

$$\chi_e = \frac{\epsilon}{\epsilon_0} - 1 = \frac{\epsilon'}{\epsilon_0} - 1 - j \frac{\epsilon''}{\epsilon_0}.$$

It will be assumed that the slab is thin enough so that the first-order term in δ is sufficient.

In principle, one might measure the phase shift and attenuation, *i.e.*, the real and imaginary parts of $\beta_\pm$ of a waveguide with a thin ferrite slab, and relate these to the real and imaginary parts of χ_{xx} and χ_{xy} through the use of (10). This might not be too difficult, particularly if measurements are made at $d = 0$ and $d = a/2$, where (10) simplifies considerably.[44] However, no phase shift measurements were made, since attenuation was of primary importance here. Consequently, it appeared more useful to assume with others that the ferrite is essentially saturated, so that the now well-known model of a ferromagnetic medium applies.[45] In this case the equation of motion of magnetization is

$$\frac{d\vec{M}}{dt} = \gamma [\vec{M} \times \vec{H}] + \frac{\gamma\alpha}{|\vec{M}|} [\vec{M} \times (\vec{M} \times \vec{H})] \tag{11a}$$

where $\vec{M}$ is the magnetization, $\vec{H}$ is the total effective magnetic field, γ is the magnetomechanical ratio which is an intrinsically *negative* number, and α, a *positive* number, is a measure of the damping. Eq. (11a) is sometimes written as

$$\frac{d\vec{M}}{dt} = \gamma [\vec{M} \times \vec{H}] - \frac{\lambda}{(\vec{M} \cdot \vec{M})} [\vec{M} \times (\vec{M} \times \vec{H})] \tag{11b}$$

where λ is a *positive* number.[2,3,12,20,46] Note that $\lambda = |\gamma| \alpha |\vec{M}|$. With the rf components of magnetic field and magnetization sufficiently small compared to the internal dc magnetic field, H_i, and saturation magnetiza-

[43] Lax, Button, and Roth, *op. cit.*, used this procedure, *i.e.*, (9), to obtain the differential phase shift for the no-loss case, here $\beta_+ + \beta_-$, but did not give the complete expression for the propagation constant. Berk *op. cit.*, also obtained the differential phase shift for thin slabs via a variational procedure. In a private communication to the author, Dr. Berk gave the complete expression for the propagation constant for this case, where a trial field which takes the magnetic field discontinuity at the surface of the ferrite slab into account was used. Berk's solution agreed exactly with (10) here. Suhl and Walker *op. cit.*, have also derived the complete expression for the propagation constant for thin slabs. Their expression appears to be equivalent to (10), although no thorough check was made.

[44] As might be expected, the possibility of using the geometry considered here for measuring the electromagnetic constants of ferrite materials, *i.e.*, the permittivity and the components of tensor permeability, has also occurred to others. For example, E. H. Turner reports on such a procedure in the Twelfth Report on Millimeter Wave Research, Contract Nonr-687(00), Bell Telephone Labs.; June, 1954. Although no data or analysis was given by Turner, it is obvious that his procedure is closely related to the one shown here.

[45] D. Polder, "On the theory of ferromagnetic resonance," *Phil. Mag.*, vol. 40, pp. 99–115; January, 1949.

[46] In both (11a) and (11b) the first term on the right-hand side describes the torque which causes the precession of the magnetization in the ferrite in a clockwise direction (it is always in this direction), when looking in the direction of the dc magnetic field. When the rf magnetic field rotates in this same direction, it is called positively polarized, and when in the opposite direction (counterclockwise) it is called negatively polarized. The second term on the right-hand side of (11a) and (11b) describes the damping torque. The significance of (11) and its various terms can be realized from the following example. Consider a small sample of ferrite in the form of a general ellipsoid with its principal axes parallel to the x, y, z axes of the coordinate system. Assume that it is magnetized to saturation by an externally applied dc field, H_a, in the z direction, and that an externally applied rf magnetic field which lies in the xy plane is driving the magnetization in precession. Then, if the external rf driving field is suddenly removed, it can be shown from the linearized form of (11a) that the total magnetization returns to its dc value along the z axis, while the components of magnetization in the xy plane vary as $e^{-t/\tau} \cos(\Omega t + \theta)$. In this,

$$\frac{1}{\tau} = |\gamma| \alpha [H_a + (2\pi - \tfrac{3}{2} N_x) M_s] \tag{a}$$

and

$$\Omega^2 = \omega_0^2 (1 + \alpha^2) - \frac{1}{\tau^2} \tag{b}$$

where

$$\omega_0^2 = \gamma^2 [H_a + (N_y - N_x) M_s][H_a + (N_z - N_x) M_s]. \tag{c}$$

N_x, N_y, N_z are the demagnetization factors in the x, y, z directions. θ is a phase angle dependent on when the rf field is removed. Eq. (c) is the Kittel relationship (see footnote 47). Here we have used the Lardau-Lifshitz form of damping rather than the Bloch-Bloembergen form. These forms as well as the problems associated with the damping term are discussed by Abrahams in footnote 2. The use of the Bloch-Bloembergen form for the thin-slab problem is shown in the Appendix.

tion, $4\pi M_s$, (11a) can be linearized and solved for the components of the tensor susceptibility. With H_i and $4\pi M_s$ directed along the positive z axis, so that p and σ below are always positive, these are:

$$\chi_{xx} = p\frac{\sigma(1+\alpha^2)+j\alpha}{\sigma^2(1+\alpha^2)-1+j2\alpha\sigma}, \tag{12}$$

and

$$\chi_{xy} = \frac{jp}{\sigma^2(1+\alpha^2)-1+j2\alpha\sigma}. \tag{13}$$

Here, the convenient normalized parameters p and σ introduced elsewhere are used,[20] although cgs magnetic units are employed here, with

$$p = \frac{4\pi|\gamma|M_s}{\omega}, \tag{14}$$

and

$$\sigma = \frac{|\gamma|H_i}{\omega}. \tag{15}$$

Substitution of (12) and (13) in (10), and separation of the real and imaginary parts of $\beta_\pm$, with $\beta_\pm = Re(\beta_\pm) + j\ \mathrm{Im}\ (\beta_\pm)$, gives

$$A - jB \equiv \frac{p}{\sigma(1+\alpha^2)(\sigma+p)-1+j\alpha(p+2\sigma)}, \tag{17}$$

$$C - jD \equiv \frac{p\sigma(1+\alpha^2)+j\alpha p}{\sigma(1+\alpha^2)(\sigma+p)-1+j\alpha(p+2\sigma)}, \tag{18}$$

$$E - jF \equiv \frac{\sigma(1+\alpha^2)}{\sigma(1+\alpha^2)+j\alpha}. \tag{19}$$

In (16), $k_0^2 = \omega^2\mu_0\epsilon_0 = (2\pi/\lambda_0)^2$ is used. For $0<d<a/2$, the rf magnetic vector in the xy plane is positively polarized for energy propagation in the positive y direction, and negatively polarized for energy propagation in the negative y direction. Thus, for $0<d<a/2$, the magnetic resonance high and low loss conditions occur for propagation in the positive and negative y directions, respectively. The total loss in the low loss, or forward, and high loss, or backward, directions, $L_t(f/b)$, can be separated into the magnetic loss part $L_{\mathrm{mag}}(f/b)$, and the dielectric loss part, L_{diel}. With the *loss* expressed in db per unit length, we find

$$L_t\left(\frac{f}{b}\right) = 20\log_{10} e^{\pm \mathrm{Im}(\beta_\mp)} = L_{\mathrm{mag}}\left(\frac{f}{b}\right) + L_{\mathrm{diel}}, \tag{20}$$

where

$$L_{\mathrm{mag}}\left(\frac{f}{b}\right) = 54.6\left\{\frac{(c_2-c_1)\alpha p[1+\sigma^2(1+\alpha^2)]+c_3\alpha p^2(p+2\sigma)(1+\alpha^2)\mp c_4\alpha p(p+2\sigma)}{[\sigma(1+\alpha^2)(\sigma+p)-1]^2+\alpha^2(p+2\sigma)^2}\right\}\frac{\delta}{a} \quad \text{for } 0 \leqq d \leqq a/2, \tag{21}$$

$$\mathrm{Re}\ (\beta_\pm) = \pm\beta_0\left\{1+\frac{\delta}{a}\frac{k_0^2}{\beta_0^2}\frac{p}{\sigma}\left(\frac{\pi}{k_0 a}\right)^2(CE-DF)\cos^2\frac{\pi d}{a} + \frac{\delta}{a}C\left(\frac{k_0^2}{\beta_0^2}\cos^2\frac{\pi d}{a}-\cos\frac{2\pi d}{a}\right) \pm\frac{\pi}{\beta_0 a}\frac{\delta}{a}A\sin\frac{2\pi d}{a} + \frac{k_0^2}{\beta_0^2}\frac{\delta}{a}\left(\frac{\epsilon'}{\epsilon_0}-1\right)\sin^2\frac{\pi d}{a}\right\}, \tag{16a}$$

and

$$\mathrm{Im}\ (\beta_\pm) = \pm\beta_0\left\{-\frac{\delta}{a}\frac{k_0^2}{\beta_0^2}\left[\frac{p}{\sigma}\left(\frac{\pi}{k_0 a}\right)^2(CF+DE)+D\right]\cos^2\frac{\pi d}{a} + \frac{\delta}{a}D\cos\frac{2\pi d}{a}\mp\frac{\pi}{\beta_0 a}\frac{\delta}{a}B\sin\frac{2\pi d}{a} - \frac{\epsilon''}{\epsilon_0}\frac{k_0^2}{\beta_0^2}\frac{\delta}{a}\sin^2\frac{\pi d}{a}\right\}. \tag{16b}$$

In (16), A, B, C, D, E, and F are real variables, functions of α, p, and σ, which are defined as follows:

and

$$L_{\mathrm{diel}} = 54.6\frac{\lambda_{g0}}{\lambda_0^2}\frac{\epsilon''}{\epsilon_0}\frac{\delta}{a}\sin^2\frac{\pi d}{a}. \tag{22}$$

In (21),

$$c_1 = \frac{1}{\lambda_{g0}}\cos\frac{2\pi d}{a}, \tag{23a}$$

$$c_2 = \frac{\lambda_{g0}}{\lambda_0^2}\cos^2\frac{\pi d}{a}, \tag{23b}$$

$$c_3 = \frac{\lambda_{g0}}{(2a)^2}\cos^2\frac{\pi d}{a}, \tag{23c}$$

$$c_4 = \frac{1}{2a}\sin\frac{2\pi d}{a}. \tag{23d}$$

p and α, or equivalently $4\pi M_s$ and α, are now determined so that the peak loss and applied field for peak loss computed from (21) agree with the measured values. The value of $4\pi M_s$ obtained from this calculation is what is meant here by effective saturation magnetization. Peak loss matching rather than "half-power points" matching is used, not only because it appears simpler and adequate, but also because the loss and the applied field can be more accurately measured at the peak loss point than elsewhere. At least this was generally true in the experimental arrangement used here. Although one might determine the point where $L_{\mathrm{mag}}(f/b)$ is a maximum by simple differentiation of (21), this leads to extremely complicated and useless algebraic equations.

Inverse interpolation in a table (or nomogram) of $L_{mag}(\frac{f}{b})$ vs σ for a useful range of values of p and α with c_1, c_2, c_3, c_4, and δ/a kept constant might be used to solve for p and α. Initial calculations for such a table led to the analysis given below, which, in view of the limitations of the ferrite model, experimental error, etc., appears quite adequate for all practical purposes.

Because α is generally small, as a function of σ the denominator in (21) is a rapidly varying quantity, whereas the numerator is a slowly varying quantity. Consequently, the maximum of $L_{mag}(\frac{f}{b})$ occurs essentially where the denominator has its minimum value. σ_m, the value of σ for the denominator to be a minimum, is given by the solution of

$$\sigma_m^2 + \sigma_m p - \frac{(1-\alpha^2)}{(1+\alpha^2)^2} = 0 \tag{24a}$$

or

$$\sigma_m = \frac{-p + \left[p^2 + 4\dfrac{1-\alpha^2}{(1+\alpha^2)^2}\right]^{1/2}}{2}. \tag{24b}$$

Note that in terms of H_i, $4\pi M_s$, and α, (24) can be written as

$$\omega = \frac{1+\alpha^2}{(1-\alpha^2)^{1/2}} |\gamma| \left[H_{im}(H_{im}+4\pi M_s)\right]^{1/2}, \tag{25}$$

where ω and H_{im} are the values at resonance. For $\alpha = 0$ this is just Kittel's formula for a thin slab.[47] Substitution of p from (24a) in (21) leads to an equation whose solution would yield the value of α. This equation is a polynomial in large powers of α whose direct solution is impractical. However, if only the lower powers of α are retained we find

$$\alpha = \frac{54.6}{L_{mag}\left(\frac{f}{b}\right)_m} \frac{(1-\sigma_m^2)}{(1+\sigma_m^2)} \times$$

$$\left[(c_2-c_1)\sigma_m + c_3\frac{(1-\sigma_m^2)}{\sigma_m} \mp c_4\right]\frac{\delta}{a}$$

$$+ \frac{54.6}{L_{mag}\left(\frac{f}{b}\right)_m} \frac{1}{(1+\sigma_m^2)^2}\left[2(c_2-c_1)\sigma_m(1-\sigma_m^2-3\sigma_m^4)\right.$$

$$\left. -\frac{3c_3}{\sigma_m}(1+\sigma_m^4-2\sigma_m^6) \pm c_4(1+5\sigma_m^4)\right]\frac{\delta}{a}\alpha^2 + \cdots. \tag{26}$$

where $L_{mag}(\frac{f}{b})_m$ is the measured peak resonance loss. In many cases, it is sufficient to use only the first term on the right-hand side of (26) to determine α.[48] Also, in view of the experimental errors, it is best to use the peak backward loss, instead of the peak forward loss, in determining α.

The formulas shown above are in terms of

$$\sigma_m = \frac{|\gamma| H_{im}}{\omega},$$

where H_{im} is the *internal* dc magnetic field at resonance, whereas only the *external* applied field is measured. Because the ferrite slab is assumed uniformly magnetized and magnetically saturated, we can write

$$\sigma = \sigma_a - \Delta p, \tag{27}$$

where

$$\sigma_a = \frac{|\gamma| H_a}{\omega}, \tag{28}$$

and

$$\Delta = \frac{N_z}{4\pi}. \tag{29}$$

H_a is the applied external dc field, and N_z is the demagnetization factor in the z direction. Since Δ and p are constant, it is obvious that σ_{am}, the value of σ_a for peak resonance loss, is a small constant value larger than σ_m. However, although Δ is known, p is initially unknown, so that the value of σ_m to insert in (26) is also unknown. It is possible to express α in terms of Δ and σ_{am}, instead of σ_m alone, along with the other known quantities; and with α determined, σ_m and p may be obtained. However, this more complicated formula for α is not required because, with Δ and α small, the formulas already presented are adequate. In some cases, a simple iterative process may be needed. This is made clear in the following where the procedure for applying the formulas is shown, and the definitions of the various symbols are summarized.

Procedure for Applying the Formulas

The steps in the computation are as follows:

1) Assume $\alpha \approx 0$.
2) Compute σ_{m_0}, the zeroth-order approximation to σ_m, from

$$\sigma_{m_0} \cong \sigma_{am} - \frac{1-\sigma_{am}^2}{\sigma_{am}}\Delta - \frac{1-\sigma_{am}^4}{\sigma_{am}^3}\Delta^2 + \cdots. \tag{30}$$

   Δ is given below.
3) With $\sigma = \sigma_{m_0}$ from (30), compute α_0, the zeroth-order approximation to α, from (26), using the measured value of $L_{mag}(\frac{f}{b})_m$. The linear approximation is adequate for many cases.

[47] C. Kittel, "On the theory of ferromagnetic resonance absorption," *Phys. Rev.*, vol. 73, pp. 155–161; January 15, 1948.

[48] Calculations show that the use of the linear approximation, rather than the complete quadratic in (26), gives a value for α which is too high by less than $50/[L_{mag}(\frac{f}{b})_m]^2$ per cent, where $L_{mag}(\frac{f}{b})_m$ is in db per inch. This applies over the frequency range of interest, *i.e.*, 8.2 to 10.1 kmc, for $d = 0$ or 0.230 inch, and $\delta = 0.010$ inch. It is of interest to note that for $d = a/2$, the error resulting from the linear approximation is in the other direction, and is only of the order of $1/[L_{mag}(\frac{f}{b})_m]^2$ per cent. In any case, for all ferrites, except possibly those with the very lowest peak resonance loss, the error in α resulting from the use of the linear approximation would seem negligible.

4) Compute p_{11}, the first-order approximation to p, from

$$p_{nn} = \frac{\sigma_{ma}(1 - 2\Delta) - \{\sigma_{ma}^2(1 - 2\Delta)^2 - 4\Delta(1 - \Delta)\sigma_{ma}p_{n,n-1}\}^{1/2}}{2\Delta(1 - \Delta)}, \qquad n \geqq 1 \tag{31a}$$

or from

$$p_{nn} = p_{n,n-1} + \frac{2\sigma_{ma}p_{n,n-1} + p_{n}^{2},_{n-1}}{\sigma_{ma}}\Delta + p_{n,n-1}\frac{2p_{n}^{2},_{n-1} + 4\sigma_{ma}^{2} + 5\sigma_{ma}p_{n,n-1}}{\sigma_{ma}^{2}}\Delta^2 + \cdots, \; n \geqq 1 \tag{31b}$$

where the partial first-order approximation to p, p_{10}, is obtained from

$$p_{n,n-1} = \frac{\dfrac{(1 - \alpha_{n-1}^2)}{(1 + \alpha_{n-1}^2)^2} - \sigma_{ma}^2}{\sigma_{ma}}, \qquad n \geqq 1. \tag{32}$$

5) Compute σ_{m_1}, the first-order approximation from

$$\sigma_{m_1} = \sigma_{am} - p_{nn}\Delta, \qquad n \geqq 1. \tag{33}$$

If σ_{m_1} is sufficiently close to σ_{m_0}, say a difference of less than one per cent, the computation can be terminated. α is taken as α_0 and $4\pi M_s$ is obtained from p_{11}.

6) If the agreement is not sufficiently close, enter step 3 above with $\sigma_m = \sigma_{m_1}$ instead of σ_{m_0} in (26) to find α_1. In step 4, use α_1 instead of α_0 in (32) to find p_{21}, and p_{21} in place of p_{10} in (31) to find p_{22}. For step 5, compute $\sigma_{m_2} = \sigma_{am} - p_{22}\Delta$ and compare with σ_{m_1}. It should now be clear how this procedure works. In general, once through is enough, although one iteration may be advisable. Because of the approximations, as well as usually limited significant figures, round-off errors, etc., continued iterations do not necessarily improve the accuracy.

A summary of the list of symbols used in the above calculations is as follows:

a, d, δ, h, s = Waveguide and ferrite slab dimensions (see Fig. 1).

λ_0 = Free space wavelength.

λ_{g0} = Air-filled waveguide wavelength.

c_1, c_2, c_3, c_4 = Parameters in loss equations dependent on a, d, λ_{g0} and λ_0; see (23).

H_{am} = Measured external applied field at peak resonance loss.

$\sigma_{am} = \dfrac{|\gamma| H_{am}}{\omega}$ = Dimensionless parameter related to frequency and applied external dc field at peak resonance loss.

$\dfrac{|\gamma|}{2\pi}$ = 1/2π of the magnitude of the magnetomechanical ratio of the electron; *taken equal to 2.8 mc/oersted.*

$\omega = 2\pi f$ = Radian frequency.

$\Delta = \dfrac{N_z}{4\pi} \cong \dfrac{\delta}{h + \delta}$ = Demagnetization constant where N_z is demagnetization factor in the z direction.[49]

$\sigma_{m_n} = \sigma_{am} - p_{nn} = \dfrac{|\gamma|}{\omega} H_{im_n}$ = nth approximation of dimensionless parameter related to frequency and applied internal field at peak resonance loss; for σ_{m0} see (30).

$n \geqq 1$

H_{im_n} = nth approximation to applied internal dc field at peak resonance loss.

α_n = nth approximation of dimensionless damping constant obtained from (26) with $\sigma_m = \sigma_{m_n}$.

$L_{\text{mag}}\left(\dfrac{f}{b}\right)_m$ = Measured peak resonance magnetic loss in db per unit length in forward (low-loss) and backward (high-loss) directions.

$p_{n,n-1} = \dfrac{4\pi|\gamma|}{\omega} M_{s_{n,n-1}}$ = Partial nth approximation of dimensionless parameter related to frequency and effective saturation magnetization given by (32).

$p_{nn} = \dfrac{4\pi|\gamma|}{\omega} M_{s_{nn}}$ = nth approximation of dimensionless parameter related to frequency and effective saturation magnetization given by (31).

$n \geqq 1$

[49] The demagnetization constant shown is an approximation based on the assumption that the slab can be considered to have an elliptical cross section in the transverse xz plane and to be infinitely long in the axial y direction (see footnote 50). If it is assumed that the slab is an ellipsoid having a finite dimension in the y direction, the change in Δ is less than about five per cent for the slab dimensions used here. Since $p\Delta$ is already quite small, the possibly more accurate value for Δ generally results in a change in σ_{m_n} of much less than one per cent. In view of the other various approximations and probable experimental errors, this difference is considered negligible.

[50] J. A. Osborn, "Demagnetizing factors of the general ellipsoid," *Phys. Rev.* vol. 67, pp. 351–357; June, 1945.

TABLE I

VALUES OF EFFECTIVE SATURATION MAGNETIZATION $4\pi M_s$, AND DAMPING CONSTANTS, α, FOR VARIOUS FERRITE MATERIALS

Material	Frequency in kmc	α	$4\pi M_s$ in kilogauss	$4\pi M_s$ in kilogauss (mean value and maximum deviation where available)
Ferramic A	8.2 8.9 10.1	0.101 0.0853 0.0623	4.50 4.49 4.45	4.48 +0.02 −0.03
Ferramic B	8.2 8.9 10.1	0.0857 0.0707 0.0502	4.70 4.60 4.57	4.62 +0.08 −0.05
Ferramic C	8.9	0.049	5.46	5.46
Ferramic D	8.2 8.9 10.1	0.116 0.0932 0.0727	4.81 4.52 4.59	4.64 +0.17 −0.05
Ferramic E	8.2 8.9 10.1	0.0658 0.0538 0.0370	4.83 4.83 4.95	4.87 +0.08 −0.03
Ferramic G	8.2 8.9 10.1	0.0330 0.0276 0.0192	4.96 4.69 4.54	4.73 +0.23 −0.19
Ferramic H	8.9	0.0334	4.57	4.57
Ferramic H-1	8.9	0.0342	3.93	3.93
Ferramic I	8.9	0.0238	3.94	3.94
Ferramic J	8.2 8.9 10.1	0.174 0.168 0.110	5.93 6.55 5.88	6.12 +0.43 −0.24
Ferramic N	8.2 8.9 10.1	0.143 0.118 0.0742	6.15 6.11 5.80	6.02 +0.13 −0.22
Ferramic Q	8.2 8.9 10.1	0.171 0.135 0.0942	6.45 6.29 6.24	6.33 +0.12 −0.09
Ferramic R-1	8.2 8.9 10.1	0.0608 0.0525 0.0361	2.91 2.93 3.01	2.95 +0.06 −0.04
Ferramic R-2	8.2 8.9 10.1	0.0482 0.0421 0.0305	2.73 2.72 2.63	2.69 +0.04 −0.06
Ferramic R-3	8.2 8.9 10.1	0.0451 0.0386 0.0281	2.93 2.95 3.03	2.97 +0.06 −0.04
Ferroxcube 101	8.2 8.9 10.1	0.0893 0.0807 0.0588	3.48 3.56 3.48	3.51 +0.05 −0.03
Ferroxcube 102	8.2 8.9 10.1	0.105 0.0898 0.0713	4.16 3.98 4.29	4.14 +0.15 −0.16
Ferroxcube 103	8.2 8.9 10.1	0.152 0.131 0.0914	5.56 5.59 5.51	5.55 +0.04 −0.04
Ferroxcube 104	8.2 8.9 10.1	0.264 0.211 0.150	6.52 6.68 6.50	6.57 +0.11 −0.07
Ferroxcube 105	8.2 8.9 10.1	0.283 0.227 0.170	5.68 5.85 5.89	5.81 +0.08 −0.13
Ferroxcube 106 I	8.2 8.9 10.1	0.288 0.256 0.183	3.50 3.69 3.91	3.70 +0.21 −0.20
*	8.9	0.229	3.92	3.92
Ferroxcube 106 II	8.2 8.9 10.1	0.198 0.177 0.134	4.60 4.56 4.97	4.71 +0.26 −0.15
*	8.9	0.167	4.63	4.63

In all cases but those marked with an asterisk, α was computed using the linear approximation; that is, only the first term on the right-hand side of (26) was used. For those cases marked with an asterisk, both terms on the right-hand side of (26) were used to compute α. In computing the characteristics of R-2 material, the experimental results were normalized to the full height of the wave guide on a simple volume basis.

Values of Effective Saturation Magnetization and Damping Constant; Discussion

The results of calculations made using the procedure described above and the experimental results presented in Fig. 4 are shown in Table I.

No calculations were performed for Ferramic O-1 because of the very high dielectric loss of this material. Incidentally, it is evident that ϵ''/ϵ_0, the imaginary part of the dielectric susceptibility might, in principle, be determined from the measured transmission loss far from resonance with the use of (22). However, even the relatively small errors in the insertion loss measurements here would result in very large errors in ϵ''/ϵ_0, so that no calculations for this quantity were made. For the calculations of $4\pi M_s$ and α it was assumed that the actual experimental configuration shown in Fig. 1 is an adequate approximation to the idealized case shown in Fig. 9; that is, the effects of the small rectangular grooves and the additional height of the ferrite slabs were assumed to be small. In view of the various experimental errors, approximations in the calculations, etc., all of the significant figures given in the values of α and $4\pi M_s$ in Table I are probably not meaningful. Note that the values of $4\pi M_s$ obtained from

TABLE II

COMPARISON OF VALUES OF SATURATION MAGNETIZATION AND PEAK VALUES OF THE SUM OF THE IMAGINARY COMPONENTS OF EFFECTIVE PERMEABILITY (SUSCEPTIBILITY) FOR FERRAMIC R-1

Entry	$4\pi M_s$ in Gauss	Source for values of $4\pi M_s$	$(\mu''+\kappa'')$ eff. max = $(\chi''+\kappa'')$ eff. max	Source for values of $(\mu''+\kappa'')$ eff. max
1	2300	Footnotes 8 & 51, but method of measurement not described	14.1 (see entry 4 below)	Graphical measurement data in footnote 8
2	2270	Footnote 9 from requirement that theoretical and experimental values of $(\chi''+\kappa'')$ eff.-max agree	9.7	Graphical measurement data in footnote 9
3[52]	2950 (average value)	Table I here via procedure outlined	Not measured directly	
4	(a) 2440	Footnote 51 from low field half-width and peak value of resonance loss curve	10.8 (a revised value from that given in footnote 8)	Graphical measurement data in footnote 52.
	(b) 2930	Footnote 51 from high field half-width and peak value of resonance loss curve		
	(c) 2800	Footnote 52 from displacement between effective and intrinsic permeability curves		

data taken at the three different frequencies have a quite small spread, in most cases. This, of course, would be expected. However, α is evidently a rather rapidly changing function of frequency. As is apparent on some examination of (21) and on comparing Fig. 4 with Table I, a small value of α corresponds to a narrow resonance line-width and a high peak loss, while a large value of α accompanies a wide resonance line-width and a small peak loss.

As a measure of how well the derived data can be used to predict the resonance loss curves of thin ferrite slabs in different positions, the values of Table I were used to compute the points shown in Fig. 4(b), 4(e), 4(h), Fig. 6(b), 6(c), 6(d), and Fig. 7. In all cases this was done for 8.9 kmc only. In spite of the departure of the slabs used here from truly thin slabs and the limitations of the model of a polycrystalline ferrite based on the parameters $4\pi M_s$ and α only, reasonable, although not excellent, agreement between the measured and calculated resonance characteristics appears evident. However, as can be seen from Fig. 4(b), 4(e), and 4(h), the calculated peak backward to forward loss ratios are somewhat less than the actual measured values. As would be expected, the use of the quadratic rather than the linear approximation to α in (26) results in a somewhat closer agreement between the measured and calculated peak backward loss for 106 II [see Fig. 4(h)]. The relatively minor influence of this approximation has already been noted,[48] and is also evident from the entries in Table I for 106 I and 106 II.

The ferrite material Ferramic R-1 has been tested in the 9-kmc region by other workers using the perturbed resonant cavity and small ferrite sphere method.[8,9] These results as well as other pertinent information are summarized in Table II (above). Note that the values of $4\pi M_s$ quoted in entries 4(b) and (c) are in excellent agreement with the value found here given in entry 3. However, these are somewhat above the values shown in entries 2 and 4(a). The value shown in entry 1 agrees very well with that of entry 2, but comparison is difficult since the procedure whereby the value in entry 1 was obtained is not known. Probable reasons for the discrepancies between the values of $4\pi M_s$ quoted in entries 2, 3, and 4 include asymmetry of the resonance loss curve, variation in the material, and influence of the sample size.

If the usually small effects of damping and demagnetization are ignored, it is easily shown from (25) with the frequency assumed constant that

$$\frac{dM_s}{M_s} = \frac{H_{am}^2 + \omega^2/\gamma^2}{H_{am}^2 - \omega^2/\gamma^2} \frac{dH_{am}}{H_{am}}; \tag{34}$$

or at 9 kmc,

$$\frac{dM_s}{M_s} \cong -\binom{1.6}{2.3} \frac{dH_{am}}{H_{am}}, \text{ for } H_{am} \binom{1500}{2000} \text{ oersteds.} \tag{35}$$

For the range of values measured here, it is evident from (35) that the fractional error in the calculated M_s is about twice the fractional error in the measured H_{am}. As already noted, the maximum errors encountered here in the magnetic field values are considered to be no more than ± 5 per cent.

[51] E. G. Spencer, R. C. LeCraw, and F. Reggia, "Measurement of microwave dielectric constants and tensor permeabilities of ferrite spheres," PROC. IRE, vol. 44, pp. 790–800; June, 1956.

[52] Incidentally, it should be noted that we have taken $|\gamma|/2\pi = 2.8$ mc/oersted here. Since all that is determined is really $p = 4\pi|\gamma| M_s/\omega$, a larger value of $|\gamma|$ would lead to a smaller value of $4\pi M_s$. Since the terms $4\pi M_s$ and $|\gamma|$ appear as a product everywhere here, and generally in using the model of a ferrite based on (11), (see footnote 20), the use of an *effective* saturation magnetization as found here with $|\gamma|/2\pi = 2.8$ mc/oersted is valid. However, comparisons of $4\pi M_s$ as obtained here with values obtained by other methods elsewhere may not be entirely justifiable.

VI. Conclusion

By the use of the thin ferrite slab and rectangular waveguide arrangement, resonance loss data at low power levels in the 9-kmc region concerning many of the commercially available ferrite materials have been obtained and presented here. Although most of the data pertain to measurements made at room temperature, for some of the ferrite materials the effects of elevated temperatures were also measured, and this information has also been summarized. Not only are the actual measured data considered to be of interest, but also the method whereby the effective saturation magnetizations and damping constants of the ferrites can be computed from the measured data through the use of thin-slab theory is thought to be useful. A table of these magnetic parameters was presented for nearly all the ferrite materials measured.

In conclusion, transmission loss measurements in the region of ferromagnetic resonance on the simply constructed thin ferrite slab and rectangular waveguide configuration are easily made and readily interpreted. The measured results can be used directly to compare the resonance loss characteristics of ferrite materials. They can also be used to compute with ease the magnetic parameters—effective saturation magnetization and damping constant—which describe a ferrite material with good accuracy in the resonance region. Finally, it appears that some readily achieved improvements and additions to equipment can be made. With these it should be possible to measure at a fixed frequency the magnetic parameters in the form of the components of the tensor susceptibility, χ_{xx} and χ_{xy}, over the entire range of magnetic field, as well as the dielectric parameter, χ_e.

Appendix

In this appendix, the Bloch-Bloembergen form of the equation of motion of magnetization is used to derive the equations for the thin slab problem. Instead of (11) we have

$$\frac{dM_{x,y}}{dt} = \gamma(\vec{M} \times \vec{H})_{x,y} - \frac{M_{x,y}}{T} . \tag{36}$$

M_x and M_y are the rf components of transverse magnetization; γ, $\vec{M}$, $\vec{H}$ are as before, and T is the transverse relaxation time or time constant. It is assumed that a dc magnetic field is applied to the ferrite in the z direction. Also, as before, we assume the rf components of magnetic field and magnetization to be sufficiently small compared to the internal dc magnetic field, H_i, and saturation magnetization, $4\pi M_s$, so that (36) can be linearized and the magnetization in the z direction can be taken to be essentially constant. The significance of (36) can be explained by considering the case of the small ferrite ellipsoid.[46] Here, when the rf driving field is suddenly removed, it can be shown from the linearized form of (36) that the components of magnetization in the xy plane vary as $e^{-t/T}\cos(\omega_0 t+\theta)$. ω_0 has been given previously[53] and θ is again a phase angle dependent on when the rf field is removed.

If (36) is used to derive the components of the intrinsic magnetic susceptibility tensor there results

$$\chi_{xx} = \frac{\sigma p}{\sigma^2 - 1 + \zeta^2 + j2\zeta}, \tag{37}$$

$$\chi_{xy} = \frac{jp(1 - j\zeta)}{\sigma^2 - 1 + \zeta^2 + j2\zeta}, \tag{38}$$

where σ and p are given by (14) and (15), and

$$\zeta = \frac{1}{\omega T} . \tag{39}$$

Substitution of (37) and (38) in (10), and separation of the real and imaginary parts of $\beta_\pm$ gives

$$\begin{aligned}\mathrm{Re}\,(\beta_\pm) = \pm\beta_0 \Bigg\{ & 1 + \frac{\delta}{a}\frac{k_0^2}{\beta_0^2}\frac{p}{\sigma}\left(\frac{\pi}{k_0 a}\right)^2 I\cos^2\frac{\pi d}{a} \\ & + \frac{\delta}{a} I\left(\frac{k_0^2}{\beta_0^2}\cos^2\frac{\pi d}{a} - \cos\frac{2\pi d}{a}\right) \\ & \pm \frac{\pi}{\beta_0 a}\frac{\delta}{a} G\sin\frac{2\pi d}{a} \\ & + \frac{k_0^2}{\beta_0^2}\frac{\delta}{a}\left(\frac{\epsilon'}{\epsilon_0} - 1\right)\sin^2\frac{\pi d}{a}\Bigg\}\end{aligned} \tag{40a}$$

and

$$\begin{aligned}\mathrm{Im}\,(\beta_\pm) = \pm\beta_0 \Bigg\{ & -\frac{\delta}{a}\frac{k_0^2}{\beta_0^2}\left[\frac{p}{\sigma}\left(\frac{\pi}{k_0 a}\right)^2 + 1\right] J\cos^2\frac{\pi d}{a} \\ & + \frac{\delta}{a} J\cos\frac{2\pi d}{a} \mp \frac{\pi}{\beta_0 a}\frac{\delta}{a} H\sin\frac{2\pi d}{a} \\ & - \frac{\epsilon''}{\epsilon_0}\frac{k_0^2}{\beta_0^2}\frac{\delta}{a}\sin^2\frac{\pi d}{a}\Bigg\} .\end{aligned} \tag{40b}$$

Eqs. (40a) and (40b) correspond to (16a) and (16b), respectively. In (40), G, H, I, and J are real variables, functions of ζ, p, and σ, which are defined as follows:

$$G - jH \equiv \frac{p(1 - j\zeta)}{\sigma p + \sigma^2 - 1 + \zeta^2 + j2\zeta}, \tag{41}$$

$$I - jJ \equiv \frac{\sigma p}{\sigma p + \sigma^2 - 1 + \zeta^2 + j2\zeta} . \tag{42}$$

As before

$$L_t\left(\frac{f}{b}\right) = L_{\mathrm{mag}}\left(\frac{f}{b}\right) + L_{\mathrm{diel}}, \tag{20}$$

where L_{diel} is, of course, the same as before and given by (22), whereas here, in place of (21), we have

[53] See (c) of footnote 46.

$$L_{\text{mag}}\left(\frac{f}{b}\right) = 54.6\left\{\frac{2(c_2 - c_1)\zeta\sigma p + 2\zeta p^2 c_3 \mp c_4 p\zeta(p\sigma + \sigma^2 + 1 + \zeta^2)}{(\sigma p + \sigma^2 - 1 + \zeta^2)^2 + 4\zeta^2}\right\}. \tag{43}$$

c_1, c_2, c_3 and c_4 are given by (23).

Since ζ is generally small the procedure outlined previously can be used to find $L_{\text{mag}}(\frac{f}{b})_m$. Here this occurs for

$$\sigma_m = \frac{-p + [p^2 - 4(\zeta^2 - 1)]^{1/2}}{2} \tag{44}$$

or, equivalently,

$$\omega = |\gamma|\left[H_{im}(H_{im} + 4\pi M_s) + \frac{1}{\gamma^2 T^2}\right]^{1/2}. \tag{45}$$

Eqs. (44) and (45) correspond to (24b) and (25), respectively. The equation which corresponds to (26) is found to be

$$\zeta = \frac{54.6}{L_{\text{mag}}\left(\frac{f}{b}\right)_m}\frac{1-\sigma_m^2}{2\sigma_m}\left[(c_2 - c_1)\sigma_m + c_3\frac{(1-\sigma_m^2)}{\sigma_m} \mp c_4\right]\frac{\delta}{a}$$
$$- \frac{54.6}{L_{\text{mag}}\left(\frac{f}{b}\right)_m}\frac{1}{2\sigma_m}\left[(c_2 - c_1)\sigma_m + 2c_3\frac{(1-\sigma_m^2)}{\sigma_m} \mp c_4\right]\frac{\delta}{a}\zeta^2 + \frac{54.6}{L_{\text{mag}}\left(\frac{f}{b}\right)_m}\frac{1}{2\sigma_m^2}c_3\frac{\delta}{a}\zeta^4. \tag{46}$$

One could now proceed with an iterative process in a manner similar to that previously described to find ζ and p, or, equivalently, T and $4\pi M_s$, from the experimental data.

Note that if only the first term on the right-hand side of (46) is retained, the approximate relationship between ζ and α is given by

$$\zeta \approx \alpha\frac{(1+\sigma_m^2)}{2\sigma_m}; \tag{47}$$

or, since to this order

$$p \approx \frac{1-\sigma_m^2}{\sigma_m}, \tag{48}$$

we can also write

$$\zeta \approx \frac{\alpha}{2}(p + 2\sigma_m). \tag{49}$$

This last is what one would expect from the apparent equivalence of the denominators of (21) and (43), and from T and τ.[54] In terms of the nonnormalized quantities, (49) yields, after some substitution and neglect of the small effect of demagnetization,

$$T \approx \frac{1.14}{\alpha(4\pi M_s + 2H_{am})\text{kilo-units}} \times 10^{-10} \text{ seconds}. \tag{50}$$

In (50), $4\pi M_s$ and H_{am} are to be expressed in kilogauss and kilo-oersteds, respectively.

No calculations have been made with the expressions derived in this Appendix. They are included for reference and possible future use.

Acknowledgment

The author wishes to acknowledge the assistance of J. Sedin and L. Wong in obtaining some of the data presented here. He also wishes to extend his appreciation to J. McLeod for making the calculations for Table I and for checking some parts of the analysis in Section V.

[54] See (a) in footnote 46.

Anisotropy of Cobalt-Substituted Mn Ferrite Single Crystals*

P. E. TANNENWALD† AND M. H. SEAVEY†

Summary—**The anisotropy of cobalt-substituted Mn Ferrite single crystals has been measured by the usual microwave techniques. Both composition and temperature have been varied, with particular emphasis being placed on achieving zero or minimum anisotropy.**

IT IS WELL KNOWN that cobalt ferrite exhibits a positive magnetocrystalline anisotropy of large magnitude. The manganese ferrites studied extensively in the past, as well as most other ferrites, have a much smaller negative anisotropy. We have substituted cobalt ions for a small fraction of the manganese ions in the ferrite spinel structure with the aim of effecting a reduction in the anisotropy.

From a practical viewpoint, low-anisotropy ferrites could be significant. In the development of polycrystalline ferrite materials for devices in which narrow resonance lines are desired, one major source of line broadening—namely, anisotropy broadening—would be diminished. Line narrowing upon cobalt addition has already been demonstrated in polycrystalline nickel ferrite.[1] However, a study of single crystals permits direct observation of the anisotropy behavior.

W. H. Bauer at Rutgers University has grown single crystals of the type $Mn_{1-x}O \cdot Co_xO \cdot Fe_2O_3$. We have examined spherical specimens[2] of compositions $x=0.04$ and $x=0.10$ by the usual microwave techniques. The results are shown in Fig. 1, which also shows the case $x=0$ (Mn ferrite). It is seen that 4 per cent cobalt substitution yields a substantial reduction in anisotropy from $K_1/M=-70$ oersteds to $K_1/M=-20$, $K_2/M=-50$. Ten per cent cobalt substitution clearly overshoots the goal since the curve has the characteristics of positive anisotropy with $K_1/M=110$. A simple interpolation would indicate that 5 per cent cobalt should give zero first-order anisotropy.

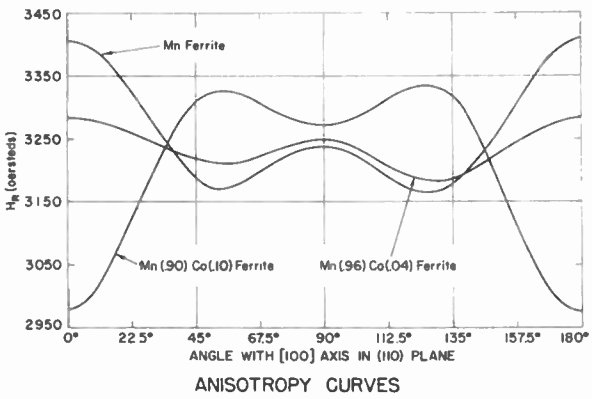

Fig. 1—Comparison of anisotropy for three different compositions. H_R is the magnetic field necessary for resonance at 9150 mc.

Instead of trying further variations in composition,[3] we investigated the anisotropy of $Mn_{.96}Co_{.04}Fe_2O_4$ at different temperatures. It might be expected that, as the temperature is lowered, the positive anisotropy contribution from the Co^{++} ions would increase faster than the negative contribution from the Mn^{++} ions. Fig. 2

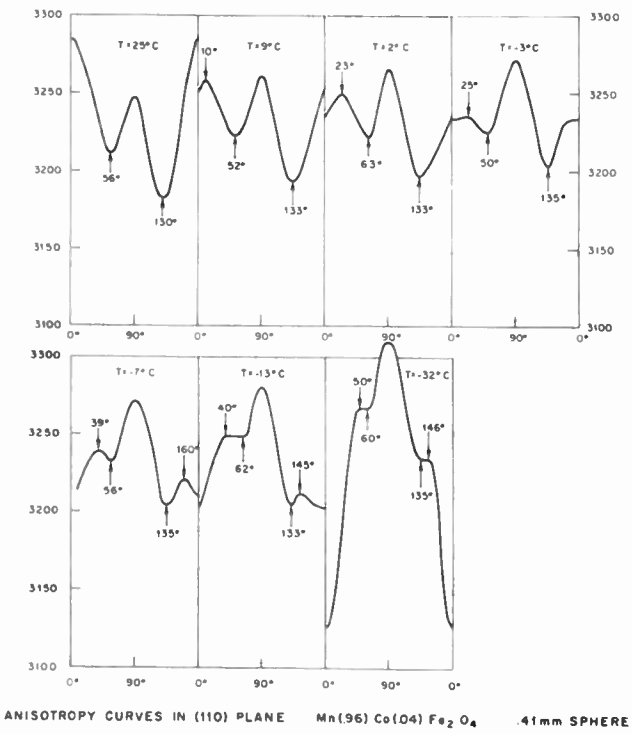

Fig. 2—Change in anisotropy curves with temperature through the region where $K_1/M=0$.

has been drawn with an enlarged vertical scale and shows that the anisotropy may be considered a minimum in the temperature region between +9°C. and −7°C. The difficulty in achieving zero anisotropy is, of course, that K_1/M and K_2/M do not go to zero at the

* Original manuscript received by the IRE, July 3, 1956. The research reported in this document was supported jointly by the Army, Navy, and Air Force under contract with the Massachusetts Institute of Technology.

† Lincoln Lab., M.I.T., Lexington, Mass.

[1] M. H. Sirvetz and J. H. Saunders, "Resonance widths in polycrystalline nickel-cobalt ferrites," *Phys. Rev.*, vol. 102; April 15, 1956.

[2] X-ray orientation by E. P. Warekois, Lincoln Laboratory.

[3] It must be remembered that the percentage compositions quoted apply to the original mixture and not to an analysis of the final crystals.

same temperature. K_1/M is zero at approximately 0°C., but here the contribution of K_2/M becomes significant.

The general way in which anisotropy curves are modified by the relative contributions of K_1 and K_2 is shown in Fig. 3. Here we have plotted the "normalized anisotropy" function

$$\frac{H_R - H_{\text{eff}}}{\frac{K_1}{2M}} = \left\{ f_x(\theta) + f_y(\theta) + \frac{K_2}{K_1}\left[g_x(\theta) + g_y(\theta) \right] \right\} \text{ vs } \theta$$

for different ratios of K_2/K_1. H_{eff} is the internal effective field at resonance and f_x, f_y, g_x, g_y are the usual angular functions which describe anisotropy in the (110) plane.

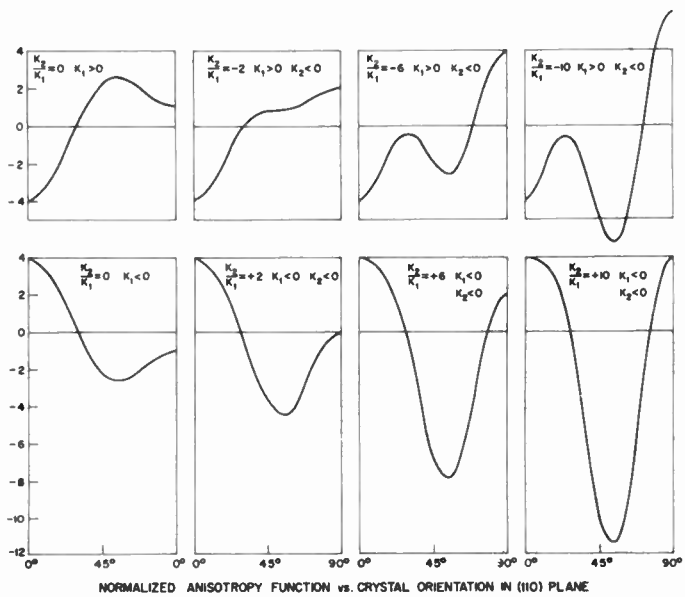

Fig. 3—Relative contributions of K_1 and K_2 to anisotropy curves. The ordinate is plotted in units of $H_R - H_{\text{eff}}/(K_1/2M)$, defined as the "normalized anisotropy function."

The cases for which K_2 is positive can be obtained by simply inverting the plots while changing the sign of K_1 also.

By comparing Fig. 3 with Figs. 2 and 4, it is seen that as the temperature is lowered, K_1/M changes sign and becomes very large and K_2/M becomes large.[4] The

[4] The curves are not symmetric, probably due to misalignment of the crystal.

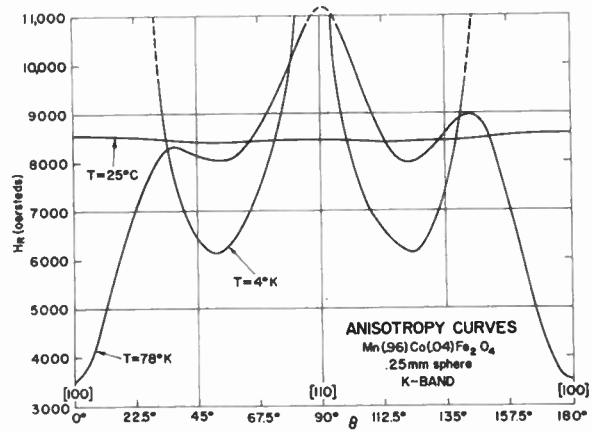

Fig. 4—Extreme anisotropic behavior at low temperatures. The peak in the [110] direction at 4°K would occur at ~14,000 oersteds as inferred from X-band data.

anisotropy constants are given in Table I as a function of temperature. The 4°K anisotropy constants are the most likely ones, but are not necessarily the only ones in view of the limited angular range of the data. $|K_2/K_1|$ is probably between 2 and 10. This behavior of $Mn_{.96}Co_{.04}Fe_2O_4$ may be contrasted with $MnFe_2O_4$, for which K_1/M stays negative and only increases to -750 oersteds at 4°K.[5]

TABLE I

T (°K)	K_1/M (oersteds)	K_2/M (oersteds)
298	−20	−50
270	+ 7	−90
266	+15	−95
260	+21	−105
241	+58	−150
78	+2330	−7100
4	>0, very large	<0, very large

The high anisotropy measurements had to be carried out both at 9150 and 24,000 mc. In crystal directions which required very low applied magnetic field for resonance the material would not be saturated at X band, while the magnetic fields required in the hard crystal directions were out of the range (>11,000 gauss) of the magnet at K band.

[5] P. E. Tannenwald, "Ferromagnetic resonance in manganese ferrite single crystals," *Phys. Rev.*, vol. 100, p. 1713; December, 1955.

The Elements of Nonreciprocal Microwave Devices*

C. LESTER HOGAN†, SENIOR MEMBER, IRE

Summary—**This paper gives an elementary but nevertheless quite complete introduction to the basic theory of nonreciprocal microwave devices. The concept of reciprocity, itself, is introduced and some of the consequences which result when one violates reciprocity are pointed out. The basic theory of microwave ferrite devices is developed from a classical theory which gives one a strong intuitive feeling for extrapolating the theory to devices not discussed in the paper.**

The analysis is extended to include basic design criterion for the three general types of microwave ferrite devices which exist today. The operation of these devices are compared and advantages and disadvantages of the various devices are pointed out for the benefit of the component engineer.

Introduction

UNTIL A few years ago, all known linear passive electrical networks obeyed the theorem of reciprocity. Today several different types of passive nonreciprocal microwave networks are in practical use, and it is to be expected that the frequency range in which they are practical will continuously expand until eventually they can be constructed to operate at any frequency which is of interest to the communications engineer. Our recent ability to build these particular nonreciprocal networks now permits the communications engineer to perform system functions which were previously impossible with passive elements. Examples of these particular functions are numerous, and many of the more practical ones will be discussed in further detail in this article. However, to give the reader an idea of the new techniques which have recently been made possible by the advent of these new circuit elements, it is worth while to point out some of the more important system functions which can now be performed by nonreciprocal microwave devices. In the first place, it is now possible to build so-called one-way transmission systems. For instance, one can now construct a microwave system which can propagate a wave in one direction with negligible attenuation, but which almost completely absorbs a wave which is simultaneously traveling in the opposite direction through the system. In addition, it is now possible to perform the operation of duplexing without power loss. In other words, the ability to violate reciprocity allows one, in principle at least, to send and receive simultaneously the same frequency from the same antenna. To be sure, this last operation would require an antenna which is much better matched to the transmission line than is the case for most systems today, but the very fact that this is at least theoretically possible without power loss gives the reader an inkling of the advance which has recently been made possible in microwave techniques by the advent of passive non reciprocal networks.

The theorem of reciprocity can be stated in many equivalent forms, and perhaps the simplest to conceive and understand is the particular form which it takes when it is expressed especially for a two terminal microwave network. Thus if we conceive of the box in Fig. 1

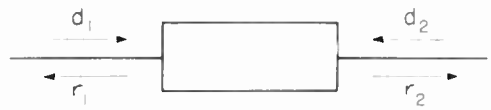

Fig. 1—Scattering matrix representation of a two terminal microwave network.

as representing such a microwave network and let d_1 represent the wave incident on the network from the left, and r_1 the wave propagating out from the network on the same side, and let d_2 and r_2 represent the same quantities on the other side, it is relatively easy to see what the theorem of reciprocity means.

It seems to be intuitively obvious that in a linear passive network, both r_1 and r_2 are made up of two components. Thus r_1 consists of a part which arises from a partial reflection of d_1 at the input terminals of the network and a part consisting of that fraction of d_2 which is transmitted through the network. Thus one can write

$$\begin{aligned} r_1 &= S_{11}d_1 + S_{12}d_2 \\ r_2 &= S_{21}d_1 + S_{22}d_2. \end{aligned} \tag{1}$$

The significance of the above coefficients becomes obvious if one lets d_1 and d_2 be separately equal to zero. Thus when d_2 is zero

$$S_{21} = \left(\frac{r_2}{d_2}\right)_{d_2=0}. \tag{2}$$

In other words, S_{21} gives the amplitude and phase of the wave emerging on the right-hand side of the network when a unit wave (with zero phase angle) is incident on the left-hand side. Thus if the network has a zero insertion loss for propagation from left to right, and if the input and output terminals are chosen to be at such a plane that the phase of r_2 is identical to that of d_1, then the quantity S_{21} would be equal to unity. The significance of all the other coefficients above should be obvious to the reader by similar arguments. Thus it is seen that if the network is perfectly matched when looking in both directions, then S_{11} and S_{22} are zero. These coefficients turn out to be very useful in the analysis and

* Original manuscript received by the IRE, June 13, 1956. This paper was presented at the Symposium on the Microwave Properties and Applications of Ferrites, Harvard Univ., Cambridge, Mass., April 2–4, 1956. The research reported in this document was supported by the U. S. Air Force, Cambridge Res. Center, under contract AF 19(604)-1084.

† Div. of Engrg. and Appl. Phys., Harvard University, Cambridge, Mass.

design of microwave networks and are referred to as the scattering matrix of the network.

Now the theorem of reciprocity demands that

$$S_{12} = S_{21}. \tag{3}$$

In other words, the network has the same transfer characteristic for one direction of propagation as it has for the other. Thus if a two-terminal matched network has a certain insertion loss or causes a certain phase shift for one direction of propagation, then it must have the same insertion loss and phase shift for the other direction of propagation.

For the reader who is more familiar with ordinary four-pole circuit analysis than he is with microwave networks, the reciprocity theorem can be equally well stated. Thus if some general network is cut at any two points and these terminals are considered as the input and output terminals of a four-pole network, then the theorem of reciprocity demands that the open circuit transfer impedance between these two sets of terminals be the same regardless of the direction in which it is measured. In other words (see Fig. 2), if a current is

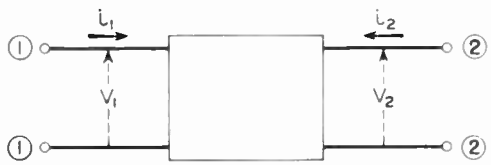

Fig. 2—Impedance matrix representation of a four-pole network.

injected into terminals ①–① and the resulting voltage is measured at terminals ②–②, then the ratio of these two quantities,

$$Z_{21} = \left(\frac{V_2}{i_1}\right)_{i_2=0}$$

is the same as the ratio,

$$Z_{12} = \left(\frac{V_1}{i_2}\right)_{i_1=0}$$

which is determined by measuring voltage which results at terminals ①–① from a current injected at ②–②.

In linear four-pole circuit analysis, it is a familiar fact that the relation between the voltages and currents at the terminals of the four-pole can be written as

$$V = Zi \tag{4}$$

where V, i, and Z are the voltage, current, and impedance matrices, respectively

$$V = \begin{bmatrix} V_1 \\ V_2 \end{bmatrix} \qquad i = \begin{bmatrix} i_1 \\ i_2 \end{bmatrix} \qquad Z = \begin{bmatrix} Z_{11} & Z_{12} \\ Z_{21} & Z_{22} \end{bmatrix}. \tag{5}$$

Thus (4) can be written in the more familiar form

$$\begin{aligned} V_1 &= Z_{11}i_1 + Z_{12}i_2 \\ V_2 &= Z_{21}i_1 + Z_{22}i_2. \end{aligned} \tag{1a}$$

The theorem of reciprocity can be simply stated for a four-pole by stating the condition

$$Z_{12} = Z_{21}. \tag{6}$$

The theorem of reciprocity has, in the past, been considered so universally valid that present-day textbooks still make the statement that if the condition stated in (6) is valid, the four-pole is passive, and if the condition does not hold for a particular network, the network must of necessity be an active network.

Actually, the theorem of reciprocity is as universally valid in mechanical, acoustical, or optical systems as it is in electrical systems, but it is known that passive systems can be built in all these fields which violate the theorem of reciprocity. These systems are so unique, though, that they have obtained special attention in the technical literature for over fifty years. Thus it has been known for some time that a mechanical system which contains a gyroscopic coupler does not obey the theorem of reciprocity,[1] and as early as the turn of the century, scientists were worried about the apparent lack of reciprocity which arose in the operation of certain electromechanical transducers.[2]

Probably one of the first passive nonreciprocal systems proposed in the literature was an optical one-way transmission system proposed by Lord Rayleigh.[3] Lord Rayleigh's "one-way" system made use of the Faraday rotation of the plane of polarization and consisted of two polarizing Nicol prisms (oriented so that their planes of acceptance made an angle of 45° with each other), with the material causing the Faraday rotation placed between them. Thus, light which was passed by the first crystal and whose plane of polarization was rotated 45° would be passed by the second crystal also. But, in the reverse direction, the rotation would be in such a sense that light which was admitted to the system by the second crystal would not be passed by the first. This device is shown in Fig. 3.

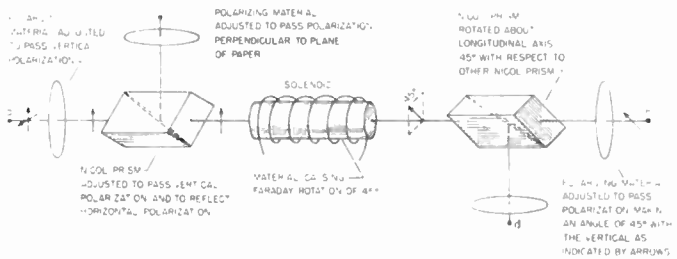

Fig. 3—Lord Rayleigh's optical one-way transmission system.

[1] A Bloch, "A new approach to the dynamics of systems with gyroscopic coupling terms," *Phil. Mag.*, Series 7, vol. 35, p. 315; 1944.

[2] H. Poincare, "Étude du récepteur téléphonique," *L'Éclairage Electrique*, vol. 50., p. 221; 1907.

For an excellent analysis of this subject, see Ph. LeCorbeiller, "Origine des termes gyroscopiques," *Annales des Postes, Télégraphes et Telephones*, vol. 18, pp. 1–22; 1929.

[3] Lord Rayleigh, "On the magnetic rotation of light and the second law of thermodynamics," *Nature*, vol. 64, p. 577; 1901.

In 1946, McMillan[4] published an interesting paper in which he showed that an antireciprocal four-pole electrical network could be obtained by properly coupling electromechanical transducers. This probably constituted the first practical proposal for realizing a passive electrical system which violated the reciprocity theorem. The main results of McMillan's paper can be demonstrated from the following rather simple analysis.

A linear electromechanical transducer can be treated as a four terminal network with voltages and currents applied at one end, and forces and velocities at the other end. In a steady state condition these quantities can be related to each other by

$$\begin{aligned} V &= ai + bv \\ F &= ci + dv \end{aligned} \tag{7}$$

where

V = voltage, F = force, v = velocity, and i = current.

For electrostatic transducers, such as a crystal or condenser transducer, $b=c$ in the above equations. For electromagnetic transducers it can be easily shown[5] that $b=-c$ in the above equations. Hence, it is obvious that electrostatic transducers obey reciprocity, and electromagnetic transducers violate reciprocity, provided that the correlation is made between electrical and mechanical quantities

$$\text{Force} \sim \text{Voltage}$$

$$\text{velocity} \sim \text{current}.$$

It should be pointed out, however, that this is not the only correlation that can be made. It is equally possible to make the correlation

$$\text{Force} \sim \text{current}$$

$$\text{velocity} \sim \text{Voltage}.$$

With this analogy, it is more enlightening to put (7) in the following form

$$\begin{aligned} V &= \frac{ad-bc}{d} i + \frac{b}{d} F \\ v &= \frac{-c}{d} i + \frac{1}{d} F. \end{aligned} \tag{8}$$

It is seen that with this analogy one is led to the opposite conclusion, namely, that the electromagnetic transducer is reciprocal and the electrostatic transducer is antireciprocal. Be that as it may, in any one system containing both kinds of transducers, one must use a consistent analogy, and as McMillan showed, it is possible to build an electrical network which is antireciprocal by mechanically coupling an electromagnetic and an electrostatic transducer. If these are coupled as shown in Fig. 4, then the equation relating the voltages and currents at the input and output of this combination can be written as

$$V = Zi$$

where

$$Z = \begin{vmatrix} \dfrac{a_1a_2 + a_1d_1 - b_1c_1}{a_2 + d_1} & \dfrac{b_1b_2}{a_2 + d_1} \\ \dfrac{c_1c_2}{a_2 + d_1} & \dfrac{d_1d_2 + a_2d_2 - b_2c_2}{a_2 + d_1} \end{vmatrix}. \tag{9}$$

If transducer 1) is electrostatic, $b_1 = c_1$, and if transducer 2) is electromagnetic, $b_2 = -c_2$, and the matrix expressed in (9) becomes

$$Z = \begin{vmatrix} \dfrac{a_1a_2 + a_1d_1 - b_1^2}{a_2 + d_1} & \dfrac{b_1b_2}{a_2 + d_1} \\ \dfrac{-b_1b_2}{a_2 + d_1} & \dfrac{d_1d_2 + a_2d_2 + b_2^2}{a_2 + d_1} \end{vmatrix}. \tag{10}$$

Thus the network in Fig. 3 is seen to be antireciprocal.

McMillan also showed that a one-way transmission system could be built by using any such antireciprocal network. For instance, if the network shown in Fig. 4 is connected to an impedance as shown in Fig. 5, and

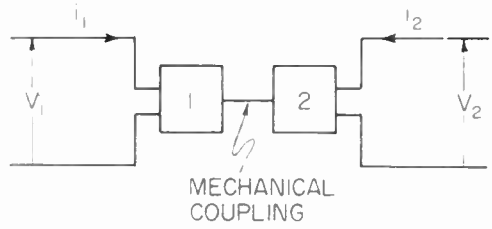

Fig. 4—Gyrator constructed from coupled electromagnetic and electrostatic transducers.

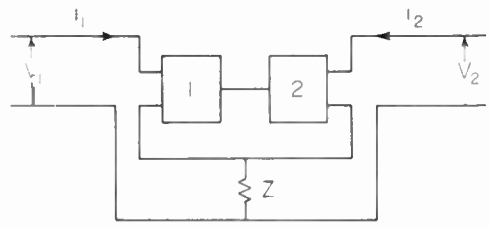

Fig. 5—Network which transmits signals in one direction only.

if we denote the matrix given in (10) by the usual notation, *i.e.*,

$$Z_{11} = \frac{a_1a_2 + a_1d_1 - b_1^2}{a_2 + d_1} \tag{11}$$

$$Z_{12} = \frac{b_1b_2}{a_2 + d_1} \tag{12}$$

$$Z_{21} = -Z_{12} \tag{13}$$

[4] E. M. McMillan, "Violation of the reciprocity theorem in linear passive electromechanical systems," *J. Acoust. Soc. Amer.*, vol. 18, pp. 344; 1946.

[5] W. P. Mason, "Electromechanical Transducers and Wave Filters," D. Van Nostrand Co., Inc., New York, N. Y.
Also, E. V. Hunt, "Electroacoustics," Harvard University Press, Cambridge, Mass.; 1951.

$$Z_{22} = \frac{d_1 d_2 + a_2 d_2 + b_2^2}{a_2 + d_1} \tag{14}$$

then the equations of the network in Fig. 5 are

$$\begin{aligned} V_1 &= (Z_{11} + Z)i_1 + (Z_{12} + Z)i_2 \\ V_2 &= (Z - Z_{12})i_1 + (Z_{22} + Z)i_2. \end{aligned} \tag{15}$$

If the impedance Z is taken equal to Z_{12}, then (15) becomes

$$\begin{aligned} V_1 &= (Z_{11} + Z_{12})i_1 + 2Z_{12}i_2 \\ V_2 &= (Z_{22} + Z_{12})i_2. \end{aligned} \tag{16}$$

Thus currents or voltages applied to the first set of terminals produce no effect at the second set, while signals are transmitted in the opposite direction. This system violates reciprocity in an extreme way, even though it is made up of linear passive elements.

There are several other methods of realizing one-way transmission systems from any antireciprocal device such as the coupled transducers. One of these, which is of interest because of its close analogy to some microwave devices, is shown in Fig. 6, where:

$$Z = \frac{Z_{11}Z_{22} + Z_{12}^2}{Z_{12}}. \tag{17}$$

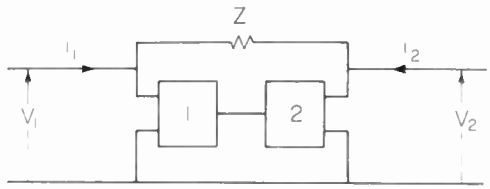

Fig. 6—One-way transmission network with properties similar to network shown in Fig. 5.

The first comprehensive treatment of antireciprocal four-poles was given in 1948 by Tellegen,[6] and he coined the word gyrator to describe such networks. Tellegen restricted his analysis to a so-called ideal gyrator in which the impedance matrix had the following form

$$Z_{11} = Z_{22} = 0 \tag{17a}$$

$$Z_{12} = -Z_{21} = -R. \tag{17b}$$

Now it is easily shown that for such a gyrator to be nondissipative, the transfer impedances must be real as Tellegen has shown them; however, it is not necessary that the diagonal terms of the impedance matrix be zero (*i.e.*, Z_{11} and Z_{22}). In addition, the restriction imposed by (17a) is also not necessary in order to realize two of the most important properties of the gyrator (*i.e.*, construction of one-way transmission systems and phase inversion of signal polarity for one direction of transmission). As a result of the restriction placed on the so-called ideal gyrator by (17a), Tellegen's gyrator has the additional interesting property of impedance inversion. Thus, if Tellegen's gyrator is terminated by an impedance Z_L, the input impedance of the gyrator is

$$Z_{in} = \frac{V_1}{i_1} = \frac{R^2}{Z_L}. \tag{18}$$

This property of impedance inversion is not, however, a distinguishing property of an antireciprocal network; for if we make the same requirement that in a nondissipative reciprocal four-pole, $Z_{11} = Z_{22} = 0$, we find that the input impedance of the terminated network is

$$Z_{in} = \frac{V_1}{i_1} = \frac{X_{12}^2}{Z_L}. \tag{19}$$

Such a reciprocal impedance inverting network can be easily realized and has been used by Doherty[7] in his high efficiency amplifier.

Much has been written about the conditions under which it might be possible to build an antireciprocal element such as the gyrator. Onsager[8] has recently shown that in order for a *completely* electrical passive system to violate reciprocity, a nonchanging magnetic field must be present. Only two types of practical gyrators have been built to date. Needless to say, they both satisfy the requirement of having a dc biasing magnetic field acting on them. One gyrator, proposed by Goldstein and Lampert,[9] arises from the behavior of electric charges moving in a magnetic field, and the other, proposed by the author, arises from the behavior of magnetic dipoles in a magnetic field. The basic operation of both types can be understood from a rather simple physical or mathematical analysis, but since the most useful devices today result from the use of magnetic materials (ferrites) in the presence of a dc magnetic field, it is this type which will be discussed in detail

Basic Theory of Operation of Microwave Ferrite Devices

Modern physical analysis shows that the ferromagnetic property of matter arises from the spin property of the electron. Since the effective quantum number of concern in the ferromagnetic case is extremely large, most of the important aspects of ferromagnetism can be understood from a rather simple classical theory. In this classical theory, the magnetic moment of the electron arises from its spinning motion and hence the electron can be regarded as a spinning magnetic top. Thus every electron has an invariable angular momentum due to spin which is given by

$$|\vec{J}| = 1/2 \frac{h}{2\pi}.$$

[6] B. D. H. Tellegen, "The gyrator, a new electric network element," *Philips Res. Reps.* vol. 3, p. 81; 1948.

[7] W. H. Doherty, "A new high efficiency power amplifier for modulated waves," Proc. IRE, vol. 24, pp. 1163–1182; September, 1936.

[8] H. B. G. Casimir, "On Onsager's principle of microscopic reversibility," *Rev. Mod. Phys.*, vol. 17, pp. 343; 1945.

[9] L. Goldstein and M. A. Lampert, "New linear passive nonreciprocal microwave circuit component," Proc. IRE, vol. 41, p. 295; February, 1953.

$\vec{J}$ = Angular momentum of electron $\frac{(\text{gm cm}^2)}{\text{sec}}$.

h = Planck's constant (erg-sec).

The magnetic moment which arises due to this rotation is

$$\vec{\mu_\beta} = g\frac{e}{2mc}\vec{J} = \gamma\vec{J}.$$

μ_β = magnetic moment of electron (emu).
γ = gyromagnetic ratio of electron.
e = charge on electron (esu).
m = mass of electron (gm).
g = Landé g factor for electrons of concern (approximately 2 for ferromagnetic electrons in ferrites).

If an electron is placed in a magnetic field which is not parallel to its magnetic moment as indicated in Fig. 7,

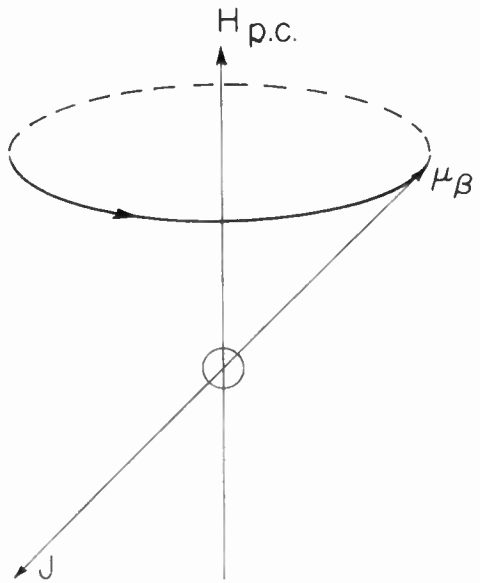

Fig. 7—Classical representation of electron precessing about an applied magnetic field (Larmour precession).

the torque exerted on the electron by the magnetic field causes the electron to precess about the field with an angular velocity given by

$$\omega_0 = \gamma H_{\text{dc}}. \tag{20}$$

This precessional motion is highly damped in ferromagnetic solids so that the magnetic moment vector gradually spirals in until it comes into alignment with the magnetic field. If it were not for this damping, it would be impossible to magnetize a ferromagnetic material, since the electrons would just precess indefinitely around the applied field without ever coming into alignment with the field. In most ferromagnetic materials, the effective damping of this precessional motion is large enough so that it requires only about one one-hundredth of a microsecond for the precessional motion to become effectively damped out, and hence this represents a theoretical lower limit to the time required to magnetize a ferromagnetic body.

Now if one makes a simple analysis of an electron placed in a dc magnetic field acting along the Z axis and an alternating magnetic field acting in the XY plane, a rather unusual property of ferromagnetic materials which arises from the gyroscopic property of the electron can be readily understood. To do this the linearly polarized alternating magnetic field is decomposed into two counter-rotating circularly polarized components in the XY plane, and the circular component which is rotating in the direction which the electron precesses about the dc field is called a positive circular component, (h_+), and the component rotating in the opposite direction is labeled the negative circular component. Now it is well known that the torque exerted on the electron by the positive circular component is given by

$$\vec{\tau_+} = (\vec{\mu_\beta} \times \vec{h_+}) \tag{21}$$

and hence the torque is a vector which is perpendicular to the plane of μ_β and h_+. In Fig. 8 these vectors are

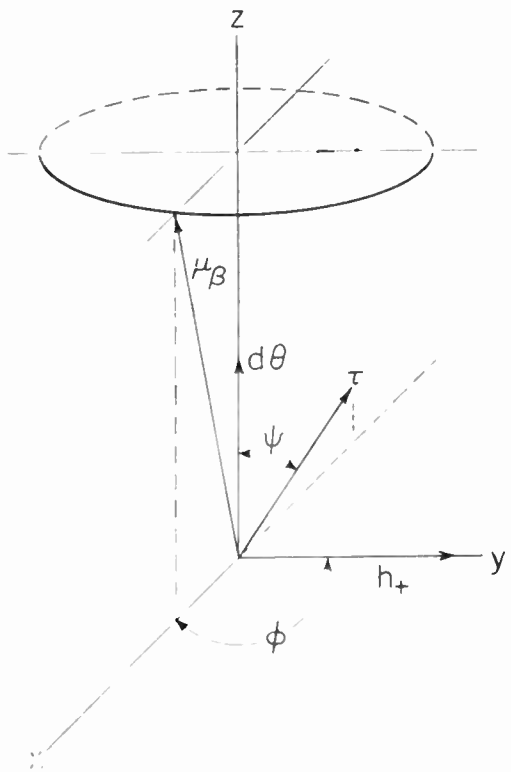

Fig. 8—Classical representation of electron motion when subjected to a dc magnetic field along z axis and a positive circularly polarized magnetic field in xy plane.

shown at a given instant under certain assumed conditions concerning their orientation. The magnetic moment vector is shown at the particular instant to be lying in the XZ plane, and the rotating magnetic field vector is shown lying along the positive Y axis. Under these conditions, the torque vector given by (21) would also be in the XZ plane, perpendicular to the plane

formed by μ_β and h_+. An exact analysis of this problem shows that these relative orientations are correct provided the frequency of the alternating field corresponds to the natural precessional frequency of the electron about the dc field H_Z as given by (20). Now during an infinitesimal rotation of all these vectors about the Z axis, work is done on the electron by the positive circular component of the alternating field. This work is given by

$$dW = \vec{\tau} \cdot \vec{d\Theta} = |\vec{\tau}| \, |\vec{d\Theta}| \cos \psi, \tag{22}$$

and in one complete cycle the total work done is

$$W = \int_0^{2\pi} \vec{\tau} \cdot \vec{d\Theta} = 2\pi\tau \cos \psi. \tag{23}$$

Hence there is a net transfer of energy from the positive circularly polarized alternating field to the electron. This causes the electron's magnetic moment vector to *fan out* so that it makes a larger and larger angle with the direction of dc field acting along the Z axis. Thus a positive circular component in the XY plane can act to maintain the precessional motion of the electron at some constant amplitude, even though this motion is heavily damped. The energy fed into the electron by the rotating magnetic field just makes up for the energy dissipated by the damping.

If the same analysis is made for the negative circular component of the alternating field (*i.e.*, the component which is rotating in the opposite direction to the precessional motion), it is seen that there is no net transfer of energy from the rotating field to the electron since the torque reverses twice each cycle. Hence the magnetic moment vector of the electron would not be expected to respond to a negative circular component in the X-Y plane.

In other words, if a block of ferromagnetic material is saturated by a large dc magnetic field acting in the Z direction, and if oppositely rotating circularly polarized magnetic fields acting in the XY plane are applied to it, the material will present a different effective permeability to the two oppositely rotating circularly polarized fields.

An exact analysis of this problem is relatively simple and was first carried out by Polder[10] and extended to include damping by the author.[11] In the general case when the frequency of the alternating field does not necessarily coincide with the natural resonant frequency given in (20), the magnetic moment vector does not lag the magnetic field vector by exactly 90 degrees as shown in Fig. 7 (the angle ϕ) but might lag by anywhere from zero to one hundred and eighty degrees as they both rotate about the Z axis. Hence, the effective permeability which relates the circularly polarized flux in the medium with the circularly polarized field must be complex to indicate the component of flux in phase (or 180° out of phase) with the field and the component which is exactly 90° out of phase with the field. Thus the relation between the circularly polarized flux (in the XY plane) and the circularly polarized magnetic field in the XY plane is

$$\vec{b}_\pm = \mu_\pm \vec{h}_\pm \tag{24}$$

where the plus or minus sign refer to the direction of rotation as previously defined. Under the conditions shown in Fig. 7, μ_+ is imaginary since the component of flux in phase with the rotating magnetic field is zero. However, in general, both μ_+ and μ_- are complex with their real parts indicating the reactive component of the flux and their imaginary parts indicating the lossy or resistive component of the alternating flux.

If now we consider a block of ferromagnetic material subjected to the above dc and circularly polarized fields, it is enlightening to plot the behavior of μ_+ and μ_- at a given frequency as a function of the strength of the dc field acting along the Z axis. This is done in Figs. 9 and 10 opposite. The curves are calculated for a frequency of 9000 mc, and the constants chosen for the medium are typical of many ferrites.

The above discussion has attempted to explain in a rather qualitative way the basic features of the phenomenon of ferromagnetic resonance which one must understand in order to understand the operation of microwave ferrite devices. These relations can be derived in a more quantitative way following the theory developed in the paper by Bloembergen.[12]

As shown in Bloembergen's paper, the equation of motion of magnetization of a saturated ferromagnetic medium can be written as

$$\frac{\vec{dM}}{dt} = \gamma(\vec{M} \times \vec{H}) - \lambda\left[\frac{(\vec{H} \cdot \vec{M})\vec{M}}{M^2} - \vec{H}\right]. \tag{25}$$

To obtain quantitative relations for the phenomenon of ferromagnetic resonance, it is necessary to solve the above equation under the conditions that both a dc and an alternating magnetic field are applied to the medium. It turns out that the proper method of solving this problem is not at first completely obvious. The reason for this is, that in practice, the actual macroscopic magnetic field within a ferromagnetic material is seldom equal to the applied magnetic field. This results because: 1) the sample has a finite size and hence there is a divergence of magnetization on the surface of the sample, which sets up magnetic fields in addition to those applied, or 2) the sample is large compared to the wavelength of the alternating field and in some cases there results a volume divergence of the magnetization, which also sets up magnetic fields in addition to those which

[10] D. Polder, "On the theory of ferromagnetic research," *Phil. Mag.*, vol. 40, pp. 99–115; 1949.

[11] C. L. Hogan, "The microwave gyrator," *Bell Sys. Tech. J.*, vol. 31, pp. 1–31; 1952.
Also, C. L. Hogan, *Rev. Mod. Phys.*, vol. 25, p. 253; 1953.

[12] N. Bloembergen, p. 1259, this issue.

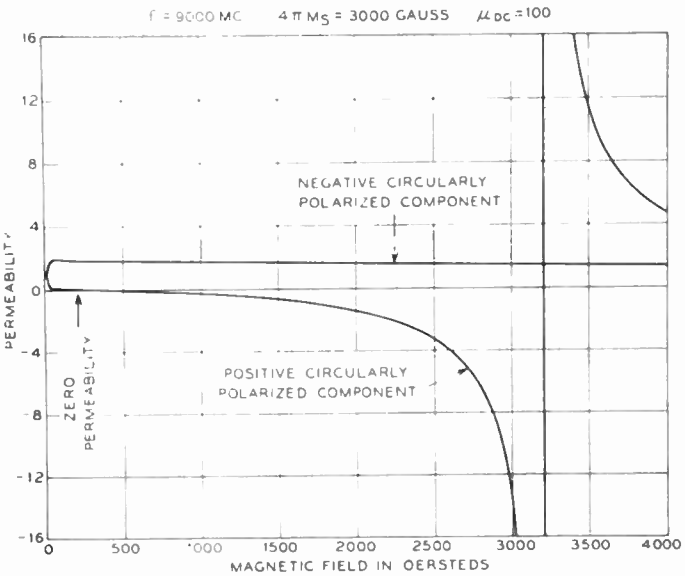

Fig. 9—Real part of the effective permeability of a ferromagnetic medium which is magnetized parallel to the direction of propagation of an infinite plane wave. The curves are computed for a medium whose saturation moment $4\pi M_s = 3000$ gauss and for a wave whose frequency is 9000 $\mu dc = 100$.

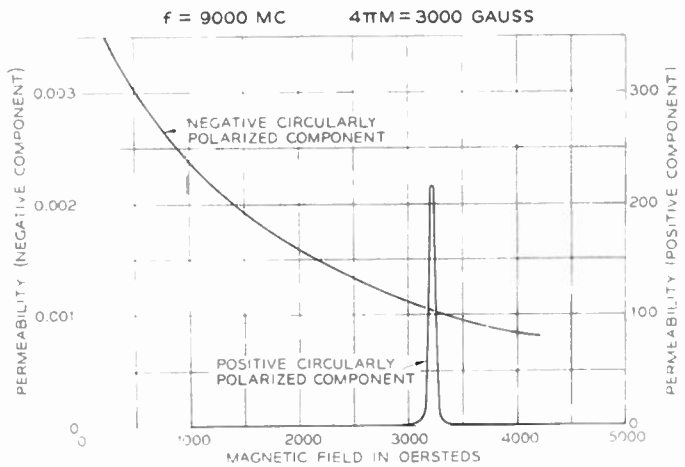

Fig. 10—Imaginary part of the effective permeability of a ferromagnetic medium which is magnetized parallel to the direction of propagation of an infinite plane wave. The constants chosen to compute the curves were the same as those in Fig. 1. In addition the relaxation frequency, λ, was arbitrarily taken as 1.9×10^7 for the curves.

arise from electric currents (applied fields). Kittel[13] first showed how to solve the problem provided the sample was small compared to the wavelength of the ac magnetic field, and Polder[14] then solved the problem more generally so that it could be applied to the case which Kittel treated, or to the more general case listed in 2) above. In a paramagnetic material these problems do not arise, because the magnetic fields set up by the poles, which exist where the magnetization has a divergence, are negligible compared to the applied fields.

[13] C. Kittel, "On the theory of ferromagnetic resonance absorption," *Phys. Rev.*, vol. 73, p. 155; 1948.
[14] Polder, *loc. cit.*

These ideas will become clearer after we have solved the problem and applied the solution to certain specific cases.

We shall follow the general method of Polder in obtaining the solution. What we are attempting to find is a relation between the alternating field and the alternating flux, so that we can have some expression which we can call the permeability of the medium. Now, as generally used in conjunction with Maxwell's equations, the permeability gives the relation between the flux density and the total macroscopic field. As such, it is not a property of the size and shape of the sample but is an intrinsic property of the material. Once we know the intrinsic permeability of the material, we can, in principle at least, find the flux density which results from any particular applied field to any particularly shaped sample by simply solving the appropriate boundary value problem, which will automatically take into account the additional magnetic fields set up by a divergence in the magnetization, if it exists.

Thus, in order to find the intrinsic permeability of the medium, we can neglect any surface divergence by assuming that the sample is infinite in size,[15] and we can avoid any volume divergence by making the wavelength of the alternating magnetic field infinite. Thus, let

$$H_z = \text{dc magnetic field in } Z \text{ direction}$$

$$\chi_0 = \text{static susceptibility} \left(\frac{M_z}{H_z}\right) \tag{26}$$

$$H_0 = H_z\left[1 + \frac{\lambda^2}{\gamma^2 M^2}\right]^{1/2} \approx H_z.$$

Now if the alternating components of the magnetic field are small compared to the dc field applied along the Z axis, and if the alternating field has a harmonic time dependence, $\exp[j\omega t]$, then it can be shown from (25) that the correct relation between the alternating magnetic field and the alternating flux density is given by

$$\vec{b} = |\mu_{ij}|\vec{h} \tag{27}$$

(lower case letters denote alternating quantities; upper case, dc) where the permeability is a tensor of the following form

$$|\mu_{ij}| = \begin{vmatrix} \mu & -j\kappa & 0 \\ +j\kappa & \mu & 0 \\ 0 & 0 & 1 \end{vmatrix} \tag{28}$$

[15] The mathematically-inclined reader will recognize that if we approach infinite size as a limiting process the demagnetizing fields do not disappear and hence we can in practice never build a sample in which the surface can really be neglected. If no volume divergence exists a more correct statement might be to simply state that we are concerned with internal fields.

and

$$\mu = \mu' - j\mu'' \tag{29}$$

$$\kappa = \kappa' - j\kappa'' \tag{30}$$

$$\mu' = 1 + \frac{[\gamma^2 H_0^2 - \omega^2]4\pi M_z \gamma^2 H_0 \chi_0^2 + 8\pi\omega^2\lambda^2\chi_0}{\chi_0^2[\gamma^2 H_0^2 - \omega^2]^2 + 4\omega^2\lambda^2}. \tag{31}$$

$$\kappa' = \frac{4\pi M_z \gamma\omega\chi_0^2[\gamma^2 H_0^2 - \omega^2]}{\chi_0^2[\gamma^2 H_0^2 - \omega^2]^2 + 4\omega^2\lambda^2} \tag{32}$$

$$\mu'' = \frac{4\pi\lambda\omega\chi_0^2[\gamma^2 H_0^2 + \omega^2]}{\chi_0^2[\gamma^2 H_0^2 - \omega^2]^2 + 4\omega^2\lambda^2} \tag{33}$$

$$\kappa'' = \frac{8\pi\omega^2\gamma\lambda H_z\chi_0^2}{\chi_0^2[\gamma^2 H_0^2 - \omega^2]^2 + 4\omega^2\lambda^2}. \tag{34}$$

The constant λ in the above expressions can be easily related to the ferromagnetic resonance line width which is a more easily determined quantity by the relation

$$\lambda = \frac{\gamma M \Delta H}{2H_r} \tag{35}$$

where

ΔH = resonance line width in oersteds (*i.e.*, distance between half-power points of resonance line shown in Fig. 10).

H_r = magnetic field required for resonance.

As was pointed out previously, these expressions are valid only for the internal fields within the ferrite and then only if the alternating fields are uniform throughout all space. If we are dealing with a finite sized sample it is often more convenient to deal with the so-called external magnetic fields since they are more readily measured. For mathematical reasons it is necessary to confine our interest to ellipsoids. All other shapes have nonuniform magnetization, and hence the macroscopic field varies from point to point within the sample, and there is thus no macroscopic field which can be defined for the sample as a whole. In ellipsoids, which are small compared to the wavelength, the relation between the external field and internal field can be very simply written as

$$\begin{aligned} h_x &= h_x^e - N_x m_x \\ h_y &= h_y^e - N_y m_y \\ H_z &= H_z^e - N_z M_z \end{aligned} \tag{36}$$

where h_x^e, h_y^e, and H_z^e are the externally applied magnetic fields, and N_x, N_y, and N_z are the so-called demagnetization factors.

Now from (27) and (28) we may write

$$\begin{aligned} b_x &= h_x + 4\pi m_x = \mu h_x - j\kappa h_y \\ b_y &= h_y + 4\pi m_y = j\kappa h_x + \mu h_y \\ b_z &= h_z + 4\pi m_z = h_z. \end{aligned} \tag{37}$$

If the expressions for the internal magnetic fields given in (36) are inserted into the above expressions and then these expressions are solved for the alternating components of magnetization, we have

$$m_x = (\mu - 1)\frac{\left\{4\pi + (\mu-1)N_y - \frac{\kappa^2}{\mu-1}N_y\right\}h_x^e}{[4\pi + (\mu-1)N_x][4\pi + (\mu-1)N_y] - \kappa^2 N_x N_y} - \frac{j\kappa 4\pi h_y^e}{[4\pi + (\mu-1)N_x][4\pi + (\mu-1)N_y] - \kappa^2 N_x N_y} \tag{38}$$

$$m_y = \frac{j\kappa 4\pi h_x^e}{[4\pi + (\mu-1)N_x][4\pi + (\mu-1)N_y] - \kappa^2 N_x N_y} - \frac{(\mu-1)\left\{4\pi + (\mu-1)N_x - \frac{\kappa^2}{\mu-1}N_x\right\}h_y^e}{[4\pi + (\mu-1)N_x][4\pi + (\mu-1)N_y] - \kappa^2 N_x N_y}. \tag{39}$$

In order to find the susceptibility tensor in terms of the external fields, it is necessary to insert the values for μ and κ, given in (29) to (34), into the above expressions. The algebraic manipulation required is quite formidable, and so we shall find the expressions for the case in which the damping parameter, λ, is zero. It turns out that the expressions obtained are quantitatively valid everywhere, except in the vicinity of the ferromagnetic resonance absorption line. Under these conditions, the equations for μ and κ are

$$\mu = \mu' = 1 + \frac{4\pi M\gamma^2 H_z}{\gamma^2 H_z^2 - \omega^2}, \qquad \mu'' = 0 \tag{40}$$

$$\kappa = \kappa' = \frac{4\pi M\gamma\omega}{\gamma^2 H_z^2 - \omega^2}, \qquad \kappa'' = 0. \tag{41}$$

Using these, (38) and (39) become

$$m_x = \frac{\gamma^2 M[H_z^e + (N_y - N_z)M]h_x^e}{\gamma^2 H_{\text{eff}}^2 - \omega^2} - \frac{jM\gamma\omega h_y^e}{\gamma^2 H_{\text{eff}}^2 - \omega^2} \tag{42}$$

$$m_y = \frac{jM\gamma\omega h_x^e}{\gamma^2 H_{\text{eff}}^2 - \omega^2} + \frac{\gamma^2 M[H_z^e + (N_x - N_z)M]h_y^e}{\gamma^2 H_{\text{eff}}^2 - \omega^2} \tag{43}$$

where

$$H_{\text{eff}}^2 = [H_z^e + (N_x - N_z)M][H_z^e + (N_y - N_z)M]. \tag{44}$$

This equation was first derived by Kittel and will be referred to as Kittel's equation in the future.

The most important result of this calculation is the fact that the resonant frequency now depends upon the shape of the sample. Thus, in the infinite medium where no divergence of the magnetization exists, the ferromagnetic resonance frequency occurs for

$$\omega_0 = \gamma H_z. \tag{45}$$

For an ellipsoidal specimen which is small compared to the wavelength of the radiation being used, the resonant frequency occurs at

$$\omega_0 = \gamma H_{\text{eff}}. \tag{46}$$

This effect is sometimes confusing to the novice in this field since it is obvious that if a magnetized piece of ferrite is subjected to an applied alternating magnetic field, the frequency of the internal field must be equal

to the frequency of the applied field. This paradox can be removed in the following way.

Consider a cylinder of ferrite whose axis lies along the Z axis as shown in Fig. 11. Assume $N_z=0$. It is exposed to an external rf magnetic field which lies in the xy plane. Now, it is known from the previous discussion that if the magnetization is expressed in terms of the internal fields, a resonance exists at the frequency given by (45). If, however, the magnetization is expressed in terms of the external fields, the resonance occurs at a frequency [given by (46)]

$$\omega = \gamma(H_z + 2\pi M_s). \tag{47}$$

The question logically arises: How is this possible? The frequency of the internal and external fields must be identical.

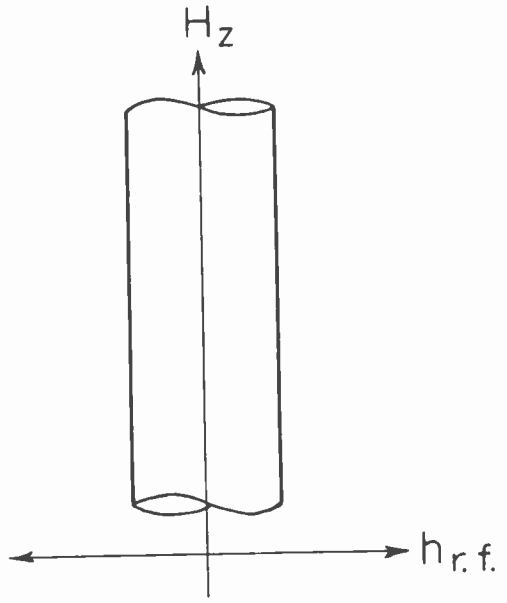

Fig. 11—Infinite cylinder subjected to a axial dc magnetic field and an rf magnetic field perpendicular to axis.

This question can be answered from purely physical reasoning. It is known that the internal fields are given by (36), and if we imagine the rf field in Fig. 11 to start with a zero frequency and to gradually have the frequency increased until it passes through both frequencies given in (45) and (47), the following sequence of events takes place. When the frequency is far below the resonant frequencies, the response of the magnetization vector is small. In other words, m_x and m_y are small, and according to (36), there is little difference between the magnitudes of the internal and external fields. However, as the frequency corresponding to (45) is approached, the magnetization responds more readily to the applied field, and according to (36), the magnitude of the internal field approaches zero. [In the absence of damping, the internal field is exactly zero at the frequency given in (45).] Since the magnitude of the internal field becomes vanishingly small at this frequency, the magnetization vector is not fanned out into a violent precessional motion as would at first be expected. In fact, it fans out just enough to reduce the internal field to just the right magnitude to just make up for losses of energy. As the frequency is increased beyond this point the phase of the alternating magnetization reverses with respect to the applied fields and hence when dealing with magnitudes we can replace the minus signs in (36) by plus signs. Thus the magnitude of the internal field increases and reaches its maximum amplitude at the frequency given in (47).

These results can be easily shown mathematically. However, to do it simply we shall neglect damping. This allows the magnetization to go to infinity and hence reduces the internal field to exactly zero at the frequency given in (45), and allows the magnitude of the internal field to become infinite at the frequency given in (47). In any actual case, it is not quite zero (but almost) at the one point and is not quite infinite at the other.

From (36) and (37), it is possible to write

$$\begin{aligned} h_x^e &= (1 + N_x\chi_{xx})h_x - jN_x\chi_{xy}h_y \\ h_y^e &= (1 + N_y\chi_{xx})h_y + jN_y\chi_{xy}h_x \end{aligned} \tag{48}$$

where the χ's are the diagonal and off-diagonal components of the susceptibility tensor.

At the *infinite medium resonance* of (45), the susceptibilities in the above equation are infinite. Hence, if the external fields are finite, the internal fields are zero.

If (41) is inverted we get

$$h_x = \frac{(1 + N_y\chi_{xx})h_x^e + iN_x\chi_{xy}h_y^e}{(1 + N_x\chi_{xx})(1 + N_y\chi_{xx}) - N_xN_y\chi_{xy}^2} \tag{49}$$

with a similar equation for h_y. The denominator of this expression has a zero at the frequency given in (47), and hence the internal fields become *infinite* at this frequency, and thus the magnetization vector is driven into a large amplitude of precessional motion. The reader should be warned that this analysis is valid only if the diameter of the cylinder is small enough so that transverse propagation in the cylinder can be neglected; and in addition it refers only to that component at the magnetic field for which a resonance occurs (*i.e.*, h_+).

Another problem of some interest deals with the behavior of an infinite saturated ferromagnetic medium when the wavelength of the radiation is finite. This problem was first solved by Polder, who showed that the resonant frequency of the medium depended upon the polarization and direction of propagation of the wave. Actually, the reason for this is quite simple. The magnetic dipoles in the medium are caused to precess around the dc magnetic field by the rf field of the wave. Since the phase of this precessional motion is determined by the strength of the dc field and the relative phase of the rf magnetic field, it follows that the magnetic dipoles will be 180° out of phase with those one-half wavelength away. Thus, at one instant of time the magnetic dipoles in the sample are not all pointing in the same direction. This may or may not cause a divergence (volume divergence) in the magnetization of the medi-

um. If a divergence does result, then additional internal fields not normally present in the wave motion arise, and these cause the resonant frequency to shift in the same way that the demagnetizing fields which arise from a surface divergence shift the resonant frequency.

This can be understood better by looking in detail at a few particular problems of wave propagation in an infinite medium. Thus, if an infinite plane wave is propagated through an infinite medium saturated in the Z direction, it can be easily shown by solving Maxwell's equation in conjunction with (27) that the propagation constant of the wave is given by

$$\Gamma_{\pm} = j\omega(\mu_0\epsilon)^{1/2}\left[\frac{\mu^2 - \mu - \kappa^2)\sin^2\theta + 2\mu \pm (\mu^2 - \mu - \kappa^2)^2\sin^4\theta + 4\kappa^2\cos^2\theta^{1/2}}{2[(\mu - 1)\sin^2\theta + 1]}\right]^{1/2} \tag{50}$$

where the angle between the Z axis and the direction of propagation of the wave is θ, and polarization of the wave is determined by the choice of signs above. Now, when the wave is propagated along the Z axis (around which the magnetic dipoles are precessing), there is no divergence of the magnetization. (If the reader will take a few seconds to sketch the orientation of the dipoles as functions of X, Y, and Z, this statement will be obvious.) Hence we should expect the resonant frequency to be given by (45). To check this prediction, we need only set θ equal to zero in (50). When this is done, it is found that the propagation constants are given by

$$\Gamma_{\pm} = j\omega[\epsilon\mu_0(\mu \pm \kappa)]^{1/2}. \tag{51}$$

This expression has a resonance at the value of ω, given by (45), for a circularly polarized wave that is rotating in the direction which the electrons precess about the dc field. If, however, the wave is propagated along the Y axis ($\theta = 90°$) and is polarized so that the rf magnetic field vector lies along the X axis, the propagation constant as found from (50) is

$$\Gamma = j\omega\left[\epsilon\mu_0\frac{\mu^2 - \kappa^2}{\mu}\right]^{1/2}. \tag{52}$$

If one substitutes into this expression the values of μ and κ given in (40) and (41), the propagation constant given in (52) becomes

$$\Gamma = j\omega\left[\epsilon\mu_0\frac{\gamma^2B_z^2 - \omega^2}{\gamma^2H_zB_z - \omega^2}\right]. \tag{53}$$

The resonance occurs at the same frequency as it would if the sample were a thin disc rather than an infinite medium, and for approximately the same reason. In the case of a thin disc, an rf magnetic field is set up in the Y direction, due to the surface divergence of M on the faces of the disc as the dipoles precess about the Z axis. In the case of the infinite medium above, an rf magnetic field is set up in the Y direction, due to a volume divergence in the magnetization which results from the fact that the spins are not all parallel. In both cases, the rf magnetic field set up in the Y direction is

$$h_y = -4\pi m_y. \tag{54}$$

In both cases this additional magnetic field is in the direction in which the wave is being propagated. In other words, it is a longitudinal component. In a sense, then, the infinite plane wave is no longer a purely transverse wave in the ferromagnetic medium. However, it is transverse in terms of the B vector, since the net flux density in the longitudinal direction is always zero. Thus, there is no electric field vector directly associated with this longitudinal magnetic field vector.

A problem of more concern to the engineer than Polder's infinite medium or Kittel's finite medium which is smaller than a wavelength, is the problem of a finite medium in which at least one dimension is large compared to the wavelength of the radiation. This problem cannot be solved exactly, except for particularly shaped samples; but in most cases approximate relations can be deduced from the above arguments, which are often quite valid for quantitative applications. A few examples will make this method clear.

Assume that an infinite cylindrical rod is exposed to an external alternating magnetic field with a finite wavelength, as shown in Fig. 12. The axis of the cylindrical specimen lies along the Z axis, and the wave is being propagated along the Z axis.

Fig. 12—Infinite plane wave being propagated along axis of an infinitely long magnetized ferrite cylinder.

The exact solution to this problem involves the solution of Maxwell's equations, both inside and outside the medium, matching boundary conditions. However, if the diameter of the rod is small compared to the wavelength (roughly $5d < \lambda$), the resonant frequency can be found approximately, using the above reasoning. The only divergence in the magnetization occurs on the cylindrical surface (assuming infinite length). This results from the precessional motion of the magnetization vector about the Z axis. Hence if the appropriate rf demagnetizing factors for this shape can be deduced, the resonant frequency can be obtained from Kittel's equation. In order to find the correct rf demagnetizing factors, it is necessary to find the magnetic field in the X and Y directions which results from the divergence of magnetization on the cylindrical surface. The pole

distribution on the surface is a helical distribution of north and south poles as shown in Fig. 13. Obviously, if the wavelength is very large compared to the diameter of the rod, then the magnetic fields in the X and Y direction are the same as they would be for an infinite wavelength, and hence Kittel's equation should hold exactly where

$$N_x = N_y = 2\pi, \qquad N_z = 0.$$

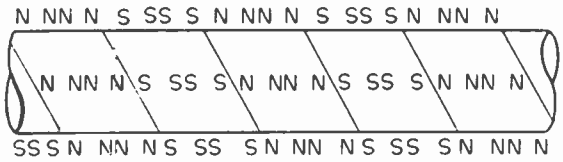

Fig. 13—Resulting pole distribution on surface of cylinder shown in Fig. 12.

If in the other extreme, the diamenter of the rod is very large compared to the wavelength (roughly $d = 5\lambda$), no demagnetizing factor can be defined, due to the fact that right under the surface the effective demagnetizing field is just $h_x = -2\pi M_x$. However, in the bulk of the material the north poles on the surface cancel the south poles (due to their proximity when $d \gg \lambda$) and the effective demagnetizing field is zero. This effect tends to broaden the absorption line, since dipoles at different radii see different effective fields. However, in the limit as $d \to \infty$ one can neglect the small amount of material near the surface, and the correct effective demagnetizing factors are $N_x = N_y = N_z = 0$, and the resonant frequency of a large cylinder is then the same as for an infinite medium regardless of the fact that it has cylindrical symmetry. Where $d \approx \lambda$, there must be a smooth transition from the resonant frequency.

$$\omega = \gamma(H_z + 2\pi M) \tag{55}$$

to

$$\omega = \gamma H_z. \tag{56}$$

The trend from a resonant frequency given by (55) to that given by (56) has actually been observed experimentally as the diameter is increased. However, before the frequency given in (56) is reached the diameter is so large that transverse propagation in the cylinder becomes important and the problem is much more complicated than the above analysis would indicate.

If now the cylinder is finite in length in the Z direction, the same problem arises that no demagnetizing factor can be defined for the entire length of the cylinder. If we assume the cylinder is uniformly magnetized (not a bad approximation if the dc field in the Z direction is very large, *i.e.*, $H_z > 2\pi M_s$), then again, there is a field in the Z direction just inside the butt ends of the cylinder equal to $H_z(\text{demag}) = 2\pi M_z$. However, again if the cylinder is long, the demagnetizing field in the Z direction near the center is zero. Obviously then, a finite cylinder cannot be uniformly magnetized in weak fields, and hence the absorption line is broadened especially if the resonant field for the major portion of the sample is less than $2\pi M_s$. If the ends of the cylinder are tapered in order to approximate an ellipsoid, the broadening of the absorption line due to the finite length can be greatly reduced. In order to obtain sharp absorption lines using the above geometry, it is obvious that either extremely small diameter tapered cylinders should be used or very thin discs with large diameter.

Another configuration of engineering interest is that shown in Fig. 14. In this configuration a wave polarized with its magnetic field vector along the X axis is propagated along the Y axis past a thin slab of material which is uniformly magnetized in the Z direction. In this problem, a true volume divergence of the magnetization exists such that there is a magnetic pole distribution which varies harmonically along the Y axis. If the wavelength is very long compared to the thickness of the slab, this volume divergence can be neglected, since it will lead to a small density of magnetic poles within the material. Thus a close approximation would allow one to set the effective demagnetizing factors equal to the following

$$N_z = N_y = 0, \qquad N_x = 4\pi.$$

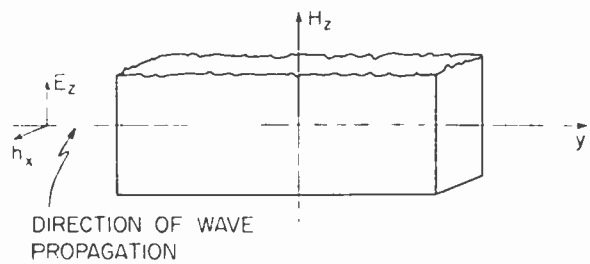

Fig. 14—Infinite plane wave being propagated past a slab of magnetized ferrite.

If, however, the thickness of the slab becomes appreciable compared to the wavelength, the effective demagnetizing factors will change to the extreme values, $N_z = N_x = 0$, $N_y = 4\pi$ (as the wavelength becomes very small compared to the thickness of the slab). In any case, the effective demagnetizing fields in the X and Y direction are not uniform throughout the volume of the sample, and hence there is a broadening of the absorption line in this geometry.

In any actual problem the resonant frequency is not easily obtained, due to the effects of volume and surface divergence of the magnetization. However, close inspection of the problem often leads to the establishment of effective rf demagnetizing factors from which the resonant frequency can be calculated.

Thus even though the problem of wave propagation in magnetized ferrites is extremely complicated the major point of the above analysis is that the permeability which an infinite saturated ferromagnetic material exhibits to superposed alternating magnetic fields is a tensor quantity. Likewise, if the magnetization of a

finite ellipsoid is expressed in terms of the externally applied magnetic fields, the permeability or susceptibility which results is also a tensor quantity. If the ellipsoid has cylindrical symmetry ($N_x = N_y$), the tensors are practically identical, except for the value of the resonant frequency. Thus for both the case of an infinite medium and an ellipsoid with cylindrical symmetry, the diagonal component of the tensor can be written as

$$\mu' = 1 + \frac{(4\pi - N_t)\gamma M \omega_0}{\omega_0^2 - \omega^2} \tag{57}$$

and the off-diagonal component becomes

$$\kappa' = \frac{(4\pi - N_t) M \gamma \omega}{\omega_0^2 - \omega^2} \tag{58}$$

where ω_0 is the appropriate resonant frequency for the particular sample, and N_t is the transverse demagnetizing factor which is set equal to zero if one is dealing with internal fields rather than external fields. It should be pointed out, though, that if the finite sized ellipsoid does not have cylindrical symmetry, then the diagonal components of the tensor are all different when the magnetization is expressed in terms of the externally applied fields.

If now we restrict ourselves to circularly polarized alternating magnetic fields, it turns out that the tensor describing an infinite medium or a cylindrically symmetrical ellipsoid can be reduced to a scalar quantity. This has an important engineering advantage, because it is easy to think intuitively in terms of scalar permeabilities but difficult, without more practice than most of us have, to think intuitively in terms of tensor permeabilities. There is really no great restriction imposed by requiring that we limit our discussion to circularly polarized fields, because the most general polarization can be decomposed into counter-rotating circularly polarized fields with arbitrary amplitudes. The only restriction which we shall find annoying is the fact that the ellipsoid must have cylindrical symmetry in order to simply reduce its tensor permeability to a scalar quantity for circularly polarized external fields.

Thus for any material which is described by

$$\begin{aligned} b_x &= \mu h_x - j\kappa j_y, \\ b_y &= j\kappa h_x + \mu h_y, \end{aligned} \tag{59}$$

whether the magnetic fields are internal or external fields, it is possible to write

$$\vec{b}_{cp} = (\mu \pm \kappa)\vec{h}_{cp} \tag{60}$$

for the circularly polarized magnetic fields. The choice of signs is determined by the direction of rotation of the fields.

From (57) and (58) we may write (neglecting the damping of precessional motion)

$$\mu' \pm \kappa' = 1 + \frac{(4\pi - N_t)\gamma M}{\omega_0 \pm \omega}. \tag{61}$$

Since the Kramers Kronig relation must hold for these quantities, we can write the imaginary (or lossy) part of the above effective scalar permeability from (29) to (34) above (neglecting the difference between H_z and H_0).

$$\mu'' \pm \kappa'' = \frac{4\pi\lambda\omega[\omega_0 \pm \omega]^2}{[\omega_0^2 - \omega^2]^2 + \dfrac{4\omega^2\lambda_0^2\omega_0^2}{\gamma^2 M_z^2}}. \tag{62}$$

Everywhere except in the vicinity of the absorption line, (62) reduces to

$$\mu'' \pm \kappa'' \frac{4\pi\lambda\omega}{(\omega_0 \mp \omega)^2}. \tag{63}$$

The permeabilities given in (61) and (63) are plotted in Figs. 9 and 10.

Thus it is apparent that if an infinite plane wave is propagated in the Z direction through the medium described by (27), it will split into two counter-rotating circularly polarized components which will travel with different velocities, since the medium presents a different permeability to these two components.

Since the two circularly polarized components travel at different velocities there is a continuous rotation of the plane of polarization of the net wave. It is to be expected that the rotation of the plane of polarization will be proportional to the difference between the square roots of the two permeabilities shown in Fig. 9. Fig. 15

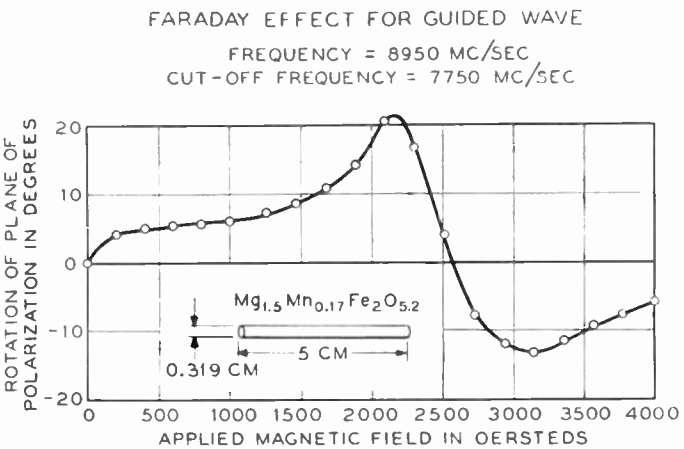

Fig. 15—Measured Faraday rotation of TE_{11} mode for a cylinder of ferrite in a circular x-band waveguide.

shows the rotation of the plane of polarization actually measured in a round waveguide carrying the dominant mode. It is seen that this is qualitatively identical to what one would predict from Fig. 9. In Fig. 16 is shown the measured attenuation of circularly polarized TE_{11} modes in a circular waveguide when they were propagated through a guide containing a small cylinder of ferrite, supported along the axis of the guide. It is seen that these data support the prediction of Fig. 10, that the medium should be practically lossless for both

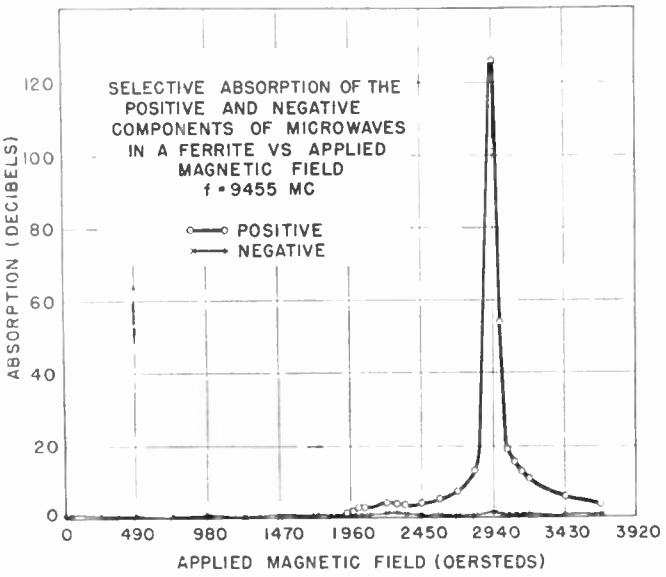

Fig. 16—Measured absorption of a positive and negative circularly polarized TE_{11} mode in a circular waveguide with a thin cylinder of ferrite located along the axis of the waveguide. The cylinder was 0.123 inch diameter and 0.815 inch long. The magnetic field was applied along the axis of the waveguide.

circular components, except in the region of the absorption line, where it should become very lossy for the positive circularly polarized component only.

Fig. 15 constitutes data taken on a magnesium manganese ferrite, and Fig. 16, a nickel zinc ferrite. Fig. 17 shows the experimental apparatus in which the rotation of the plane of polarization is measured.

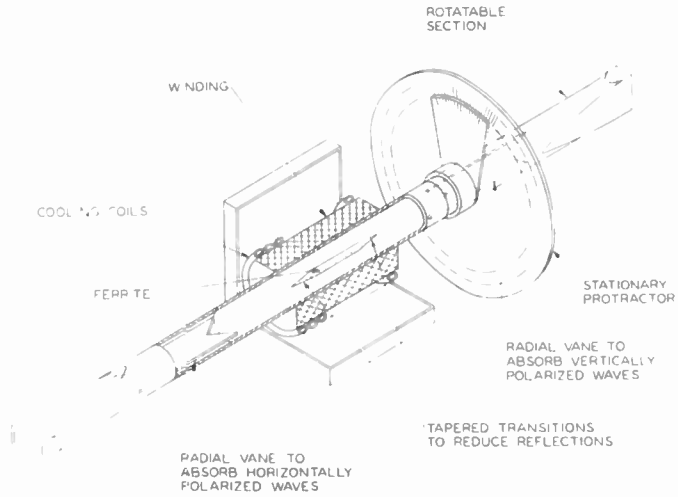

Fig. 17—Typical experimental set-up for measuring Faraday rotation.

For most practical applications the Faraday rotation is used in relatively weak applied magnetic fields. An inspection of Figs. 15 and 16 indicates why this is so. The rotation in weak fields is relatively large and the loss is relatively small. In this region, it is easy to derive a very fundamental equation for rotation per unit path length. Thus, the rotation per unit path length is obviously given by

$$\frac{\theta}{l} = \frac{\omega}{2}\left[\frac{1}{v_-} - \frac{1}{v_+}\right], \tag{64}$$

where

$v_\pm$ = velocity of positive and negative circularly polarized components.

Eq. (64) can be written in terms of the phase constant of the wave,

$$\frac{\theta}{l} = \frac{1}{2}[\beta_- - \beta_+]. \tag{65}$$

The phase constants can be evaluated from (51). If losses are neglected, (65) becomes

$$\frac{\theta}{l} = \frac{\omega}{2}\sqrt{\mu_0\epsilon}\left[\left(1 + \frac{4\pi M\gamma}{\gamma H_z + \omega}\right)^{1/2} - \left(1 + \frac{4\pi M\gamma}{\gamma H_z - \omega}\right)^{1/2}\right]. \tag{66}$$

In weak fields, $\gamma H_z \ll \omega$, and if the saturation moment is low enough or the frequency high enough so that

$$\frac{4\pi M\gamma}{\omega} \ll 1 \tag{67}$$

then (66) can be put into the extremely simple form

$$\frac{\theta}{l} = \frac{1}{2}\sqrt{\mu_0\epsilon}[4\pi M_s\gamma] \text{radians/meter}. \tag{68}$$

For assumed values

$$\epsilon = 10\epsilon_0, \qquad 4\pi M_s = 3000 \text{ gauss},$$
$$\gamma = 17.6 \times 10^6 \text{ radians/sec/oersted},$$

(12) predicts rotations of 160 degrees/cm.

This rotation of the plane of polarization is known as the Faraday effect. It has long been known that the Faraday rotation of the plane of polarization in optics is antireciprocal. Its antireciprocal property distinguishes the Faraday effect from optical rotations caused by birefringent crystals, or by the Cotton-Mouton effect, which are reciprocal. That is, if a plane polarized light wave is incident upon a birefringent crystal in such a manner that the plane of polarization is rotated through an angle θ in passing through the crystal then this rotation will be cancelled if the wave is reflected back through the crystal to its source. In the Faraday rotation, however, the angle of rotation is doubled if the wave is reflected back along its path. Hence, if the length of path through the *active* material is adjusted so as to give a 90° original rotation, the beam on being reflected will have its plane of polarization rotated a total of 180° in passing in both directions through the material. This accounts for the one way transmission system which Lord Rayleigh discussed and which is shown in Fig. 3.

The antireciprocal property of the Faraday effect affords a means of realizing a microwave circuit element

which is analogous to Tellegen's gyrator. Such a gyrator is illustrated in Fig. 18 along with diagrams which help explain its action. Beneath the gyrator are construction lines which indicate the plane of polarization of a wave as it travels through the gyrator in either direction. On each diagram is a dotted sine wave for reference only which indicates the constant plane of polarization of an unrotated wave. It is noticed that for propagation from left to right in Fig. 18, the screw rotation introduced by the twisted rectangular guide adds to the 90° rotation given to the wave by the ferrite element making a total rotation of 180°. For a wave traveling in the reverse direction these two rotations cancel each other, producing a net zero rotation through the complete element. The unique property of the Faraday rotation becomes immediately apparent from this diagram. In the case of the rotation induced by the twisted rectangular guide, the wave rotates in one direction in going from left to right through the twisted section, and rotates in the opposite direction when it traverses the section from right to left. For the case of the rotation induced by the ferrite element, the direction of rotation is indicated by the arrow in the upper figure for either direction of propagation. The important characteristic of the element is the time phase relation between two points such as A and B in the upper diagram. It is seen with the help of the diagrams illustrating the rotating waves that the field variations are in phase at points A and B for propagation from left to right and they are 180° out of phase for propagation from right to left. In other words the transmission line is an integral number of wavelengths long between A and B for propagation from left to right and is an odd integral number of half-wavelengths long for propagation from right to left.

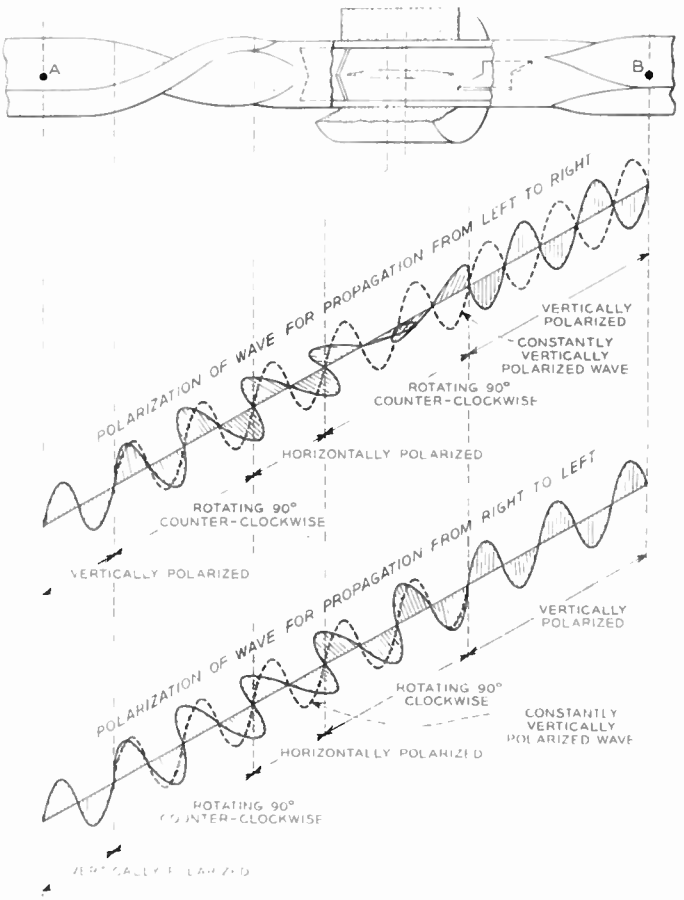

Fig. 18—Microwave gyrator with diagrams which explain its action.

If the rectangular wave guides on each side of the ferrite are rotated about their common axis so as to make an angle of 45° with each other, then a one-way transmission system can be created which is similar to Lord Rayleigh's one-way transmission system of optics. This one-way transmission system can be used, for example, to isolate the generator or detector from the wave guide in microwave systems. In this application it has the great advantage over the attenuators which are presently used for this purpose in that it can be made practically lossless for the direction of propagation which is desired but the reflected wave will be completely absorbed and hence more complete isolation can be effected.

This device which makes use of the 45° rotation has been called a circulator since it is essentially a more complex and more useful circuit element than its simple one-way transmission property would at first indicate. The word was coined by A. G. Fox. The circulator actually has four output branches corresponding to the two different polarizations at each end of the device. The polarizations of the four output branches are indicated schematically in Fig. 19(a). It is noticed that power sent into the polarization circulator with polarization a is turned into polarization b, also b is turned into c, c is turned into d, and d is turned into minus a. This property is indicated very clearly by the circuit symbol suggested in Fig. 19(a) the phase inversion between arms d and a being indicated by the minus sign between the d and a arms.

Another one-way transmission system can be created by combining the gyrator with two magic tees. This combination is indicated in Fig. 19(b). Since this device has all of the fundamental properties of the polarization circulator with the exception of the phase inversion between arms d and a it is suggested that it be called a circulator and the circuit symbol suggested which indicates its properties is also given in Fig. 19. The circulator can also be constructed by using other forms of the hybrid junction than the normal magic tees.

Kales[16] and his associates at the Naval Research Laboratories have shown that gyrators can be built in rectangular waveguides and by extending their reasoning to other guided wave systems, a very powerful approach is available for designing gyrators for many different types of guided wave systems. As an introduction to Kales' work on the partially loaded rectangu-

[16] M. L. Kales, H. N. Chait, and N. G. Sakiotis, "A non-reciprocal microwave component," *J. Appl. Phys.*, vol. 24, p. 816; 1953.

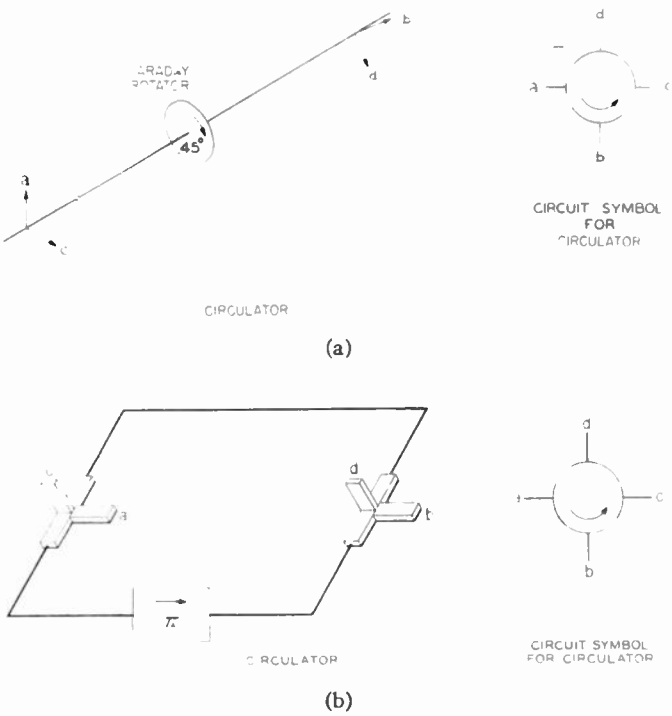

Fig. 19—(a) One type of Faraday rotation circulator, and (b) general circulator employing a gyrator and hybrid junctions.

lar waveguide, it is enlightening to examine the problem of the completely filled rectangular guide. This problem was first solved by Van Trier[17] by a rather general and very powerful mathematical method. For our purpose, we shall arrive at the solution by a less powerful but more direct route. In the first place we shall be interested in only the lowest or dominant mode that exists in a completely filled guide. The system of axes is illustrated in Fig. 20.

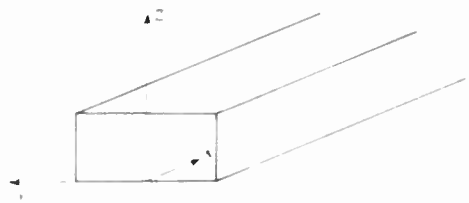

Fig. 20—System of axes for analysis of rectangular waveguide loaded with magnetized ferrite.

To find a solution to the problem of the completely filled guide, we begin with Maxwell's equations (mks).

$$\vec{\nabla} X \vec{E} = -\frac{\partial \vec{B}}{\partial t}, \qquad \vec{\nabla} X \vec{H} = \frac{\partial \vec{D}}{\partial t}. \tag{69}$$

[17] A. A. Th. M. Van Trier, "Guided electromagnetic waves in anisotropic media," *Appl. Sci. Research*, vol. B3, pp. 305–371; 1953.

To these we must add the relations

$$\vec{D} = \epsilon \vec{E} \tag{70}$$

and

$$b_x = \mu_0(\mu h_x - j\kappa h_y)$$
$$b_y = \mu_0(j\kappa h_x + \mu h_y) \tag{71}$$
$$b_z = \mu_0 h_z.$$

If now we assume that the fields in the guide are all proportional to $\exp[-ay-bz-\Gamma x]$, we can derive from Maxwell's equations the explicit form of the wave equation which applies in this case. For a TE mode we require that $E_x=0$. If this condition is placed on the set of equations, we are led to the result that $B=0$. The resulting equation for the magnetic field vectors then becomes

$$\left[\omega^2\epsilon\mu_0\mu + a^2 + \Gamma^2 + j\frac{\kappa}{\mu}a\Gamma\right]h_x + \left[-j\frac{\kappa}{\mu}(\omega^2\epsilon\mu_0\mu + \Gamma^2)\right]h_y = 0, \tag{72}$$

$$\left[j\frac{\kappa}{\mu}(\omega^2\epsilon\mu_0\mu + a^2)\right]h_x + \left[\omega^2\epsilon\mu_0\mu + a^2 + \Gamma^2 - j\frac{\kappa}{\mu}a\Gamma\right]h_y = 0.$$

In order for this set of equations to have a solution, the determinant must vanish. If the determinant is set to zero and then factored, two equations result, the solutions of which would allow wave propagation under the conditions which we have imposed. It can be shown that one equation leads to the trivial case that

$$\omega^2\epsilon\mu_0\mu = 0. \tag{73}$$

The other equation leads to the result

$$\omega^2\epsilon\mu_0\left(\frac{\mu^2-\kappa^2}{\mu}\right) + a^2 + \Gamma^2 = 0 \tag{74}$$

which is the identical result for a dielectric loaded waveguide, except that the relative permeability of the medium is given by the expression in the parentheses above. In order to satisfy the boundary conditions on the edges of the guide (E_z must vanish), it is obvious that

$$a = j\frac{n\pi}{y_0}. \tag{75}$$

From here the solution of the problem is similar to that for guides loaded with isotropic material. The field components are

$$E_x = E_y = 0$$
$$E_z = E_0 \cos\frac{\pi y}{y_0} \exp\left[-j\beta x\right], \tag{76}$$

$$B_x = \frac{-j\pi}{\omega y_0} E_0 \sin\frac{\pi y}{y_0} \exp\left[-j\beta x\right]$$
$$B_y = \frac{-}{\omega} E_0 \cos\frac{\pi y}{y_0} \exp\left[-j\beta x\right] \tag{77}$$
$$B_z = 0$$

$$h_y = \frac{-E_0 \exp\left[-j\beta x\right]}{\omega\mu_0\left(\frac{\mu^2-\kappa^2}{\mu}\right)}\left[\beta\cos\frac{\pi y}{y_0} + \frac{\pi\kappa}{\mu y_0}\sin\frac{\pi y}{y_0}\right]$$
$$h_x = \frac{-jE_0 \exp\left[-j\beta x\right]}{\omega\mu_0\frac{\mu^2-\kappa^2}{\mu}}\left[\frac{\pi}{y_0}\sin\frac{\pi y}{y_0} + \frac{\beta\kappa}{\mu}\cos\frac{\pi y}{v_0}\right]. \tag{78}$$

Now the surface current density in the wall of the guide, necessary to terminate the tangential component of the magnetic field, is

$$\vec{K} = \vec{n} \times \vec{h} \tag{79}$$

where $\vec{n}$ is a unit vector normal to the surface.

For the top and bottom walls of the guide, it is possible to find an expression for the longitudinal (x component) and transverse (y component) current flowing in the guide walls from (78) and (79). From this one obtains

$$|K_y| \sim \frac{\pi}{y_0}\sin\frac{\pi y}{y_0} + \frac{\beta\kappa}{\mu}\cos\frac{\pi y}{y_0}, \tag{80}$$

provided the guide is above cutoff.

If a longitudinal slot is cut in the broad wall of the guide, it must be cut in a position where $|K_y|$ is zero in order to be a nonradiating slot. If we set (80) equal to zero and solve we find the value of y which gives the position of a nonradiating slot. This is

$$y = \frac{y_0}{\pi}\tan^{-1}\left(-\frac{\beta\kappa y_0}{\pi\mu}\right). \tag{81}$$

If the off-diagonal component of the tensor permeability κ is zero, the position of the nonradiating slot occurs at $y=0$ or the center line of the guide as usual. However, as the ratio of κ/μ increases, the position of the nonradiating slot moves over to one side of the guide. The direction which it moves depends upon the sign of β, or in other words, on the direction of propagation. Thus a slot can be cut in a ferrite filled guide that is radiating for one direction of propagation but not for the other.

The problem of the partially filled guide rectangular waveguide has been solved in part by many authors since Kales first showed that it could be made anti-reciprocal. The most complete solution is that due to B. Lax, K. J. Button, and L. M. Roth at Lincoln Laboratory. We shall not present their solution here but instead we shall present an intuitive explanation of the problem which can be extrapolated more rapidly to other configurations.

Fig. 21 shows a diagram of the field patterns associated with the dominant mode in rectangular guide.

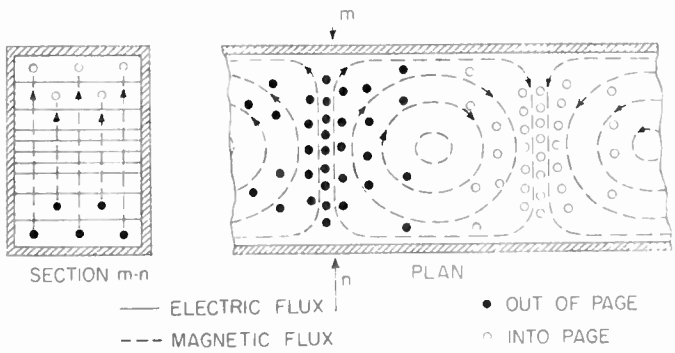

Fig. 21—Magnetic and electric field lines in a rectangular waveguide propagating the dominant mode.

The magnetic field associated with this pattern is usually decomposed into longitudinal and transverse fields, such that we can write

$$H_y = C\sqrt{\left(\frac{\omega}{\omega_c}\right)^2 - 1}\cos\frac{y\pi}{y_0}\sin(\beta x - \omega t),$$
$$H_x = C\sin\frac{\pi y}{y_0}\cos(\beta x - \omega t). \tag{82}$$

The field can be equally well decomposed into counter rotating circularly polarized vectors in the xy plane. Thus from (82) it is easy to show that the magnitudes of the circularly polarized fields that are equivalent to the fields given in (82) are

$$|H_{+cp}| = \frac{C}{2}\left|\left[\sqrt{\left(\frac{\omega}{\omega_c}\right)^2 - 1}\cos\frac{\pi y}{y_0} + \sin\frac{\pi y}{y_0}\right]\right|,$$
$$|H_{-cp}| = \frac{C}{2}\left|\left[\sqrt{\left(\frac{\omega}{\omega_c}\right)^2 - 1}\cos\frac{\pi y}{y_0} - \sin\frac{\pi y}{v_0}\right]\right|. \tag{83}$$

If these are plotted as a function of position in the guide, the results are as indicated in Fig. 22.

At points A and B in the rectangular guide, the magnetic field is purely circularly polarized but in opposite senses. If the direction of propagation is reversed, the pattern shown in Fig. 21 remains unchanged but the sense of rotation assigned to the two curves reverses. Thus an observer standing at point A would see a pure positive circularly polarized field for one direction of propagation and a pure negatively polarized field for the other direction of propagation. The position of point A or B can be easily calculated from (83), which yields the relation

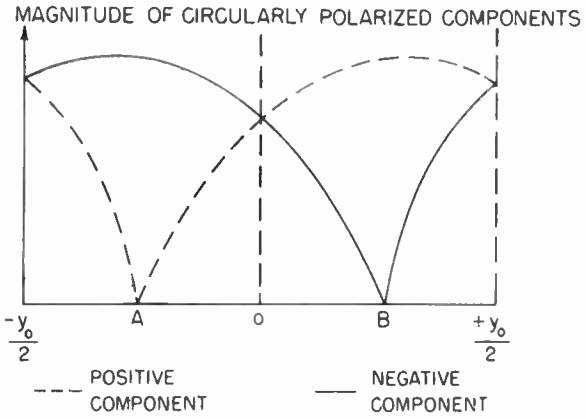

Fig. 22—Magnetic field components in a rectangular waveguide propagating the dominant mode.

$$\tan \frac{\pi y_A}{y_0} = \sqrt{\left(\frac{\omega}{\omega_c}\right)^2 - 1} \tag{84}$$

so that point A exists at the center of the guide when the frequency is just equal to the cutoff frequency and moves toward the side wall as the frequency is increased. As an example, a guide operating at 10,000 mc, whose cutoff frequency is 8000 mc, has the points of pure circular polarization at

$$y_A = 0.41\left(\frac{y_0}{2}\right). \tag{85}$$

If now a slab of ferrite were placed at point A and biased in the z direction, it would be expected that the slab would present the permeabilities given in Fig. 9, for the two different directions of propagation. Such a device is illustrated in Fig. 23.

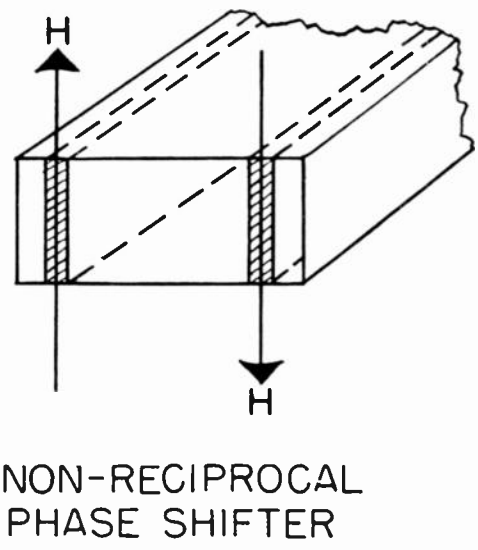

Fig. 23—Rectangular waveguide loaded with magnetized slabs of ferrite in a manner so as to make it nonreciprocal.

Actually it is not quite so simple, because the curves of Fig. 9 apply either for internal fields or for external fields if the ferrite has cylindrical symmetry about the z axis. Obviously, the slab given in Fig. 23 does not have cylindrical symmetry about the z axis. Hence, if it were placed in a region where the external fields were circularly polarized, the internal fields would be elliptically polarized and the sample would show resonance absorption for both directions of propagation. A closer approximation can be found by finding what conditions must be placed on the external fields so that the internal fields will be circularly polarized. This relation is very easily derived from (48). If the following requirement is placed on the internal fields (*i.e.*, they can be circularly polarized)

$$h_x = \pm j h_y \tag{86}$$

we are led to the following relation between the components of the external field

$$h_x^e = \pm j \frac{[1 + N_x X_{xx} \mp N_x X_{xy}]}{[1 + N_y X_{xx} \mp N_y X_{xy}]} h_y^e \tag{87}$$

where

$$X_{xx} = \frac{\mu - 1}{4\pi} = \frac{M\gamma\omega_0}{\omega_0^2 - \omega^2},$$

$$X_{xy} = \frac{K}{4\pi} = \frac{M\gamma\omega}{\omega_0^2 - \omega^2}.$$

If now the slabs shown in Fig. 22 are extremely thin, it was shown in the above discussion that the demagnetizing factors can be set approximately equal to

$$N_x = 0 \qquad N_y = 4\pi \qquad N_z = 0$$

regardless how long the slabs may be. (See Fig. 14.)

For this geometry, (87) reduces to:

$$h_x^e = \pm \frac{j h_y^e}{\mu \mp \kappa}. \tag{88}$$

Thus it is impossible to put the slab into the guide, in a manner such that it sees a pure positively rotating internal field for one direction of propagation and a negatively rotating internal field for the other direction unless the off diagonal component of the permeability tensor is zero. If the element is being used as a differential attenuator rather than a differential phase shifter, it is important that the ferrite see a pure negative circularly polarized wave for one direction of propagation so that there will be no absorption. For the other direction of propagation the internal field will be elliptically polarized, but that makes little difference. Thus, if the effective permeability for the negative circular component $(\mu - \kappa)$ is approximately two, then the relation between the external fields, so that the internal fields will be circularly polarized, is

$$h_x^e = \frac{j h_y^e}{2}, \tag{89}$$

which means the ferrite must be closer to the center than the point A in Fig. 22, if it is to have zero loss for

the one direction of propagation. It is difficult, using this approach, to say anything about the point of maximum differential phase shift for a long thin slab. However, it is interesting to note that if in place of a long thin slab, extremely thin cylinders were placed in the guide with their axes parallel to the Z axis, then the position of maximum differential phase shift and maximum differential attenuation would occur when the cylinders were placed at point A or B in Fig. 22. The above analysis is valid only if the fields in the waveguide are undisturbed by the dielectric loading caused by inserting the ferrite. Experimental data indicates that if the slab goes all the way from top to bottom of the guide as indicated in Fig. 23 then the slabs must be thinner than 0.010 inch in order for this assumption to hold at X band. If, however, pieces of ferrite are placed against the upper and lower walls the pieces can be considerably thicker and the above analysis can be applied

Comparison of Various Microwave Devices

Differential Phase Shifter

The above theory makes it evident that several different types of nonreciprocal microwave devices can now be built in rectangular, round or square waveguide and it is often a perplexing problem for the component engineer to decide which particular geometry he should pick to realize a particular system function. Often the criterion which decides this for the engineer is a consideration which is not even included in the above theory, such as picking a particular geometry so that the ferrite can be kept in intimate contact with the waveguide walls, making it possible to dissipate the energy which it absorbs from the microwave fields rapidly enough so that it does not heat up above the Curie temperature. However, in spite of the complexity of the problem many general statements can be made about the various devices so that some guide can be given to the design engineer.

Thus a differential phase shifter operates best when the ferrite is biased with a weak magnetic field which is just sufficient to magnetize it. The strength of the field required is relatively independent of the frequency of operation of the device but since waveguide components get successively smaller as one goes to higher frequencies, the problem of providing the magnetic field for a differential phase shifter becomes increasingly easier as one operates at higher frequencies. For this reason alone, differential phase shifters look increasingly more attractive as one operates at frequencies above K band.

In addition, since (68) indicates that the differential phase shift (or Faraday rotation) per unit length is sensibly the same for two waveguides whose cross-sections contain the same amount of ferrite regardless of whether the guide is operating at 10,000 mc or 100,000 mc it turns out that the approximate length required to obtain a certain amount of differential phase shift is sensibly independent of the frequency of operation. The same equation indicates that a differential phase shifter can in principle be made as broad band as the waveguide itself.

As an example one can predict that if it is possible to build a 45° Faraday rotator which is 3 inches long with an applied field of 300 oersteds at a frequency of 24,000 mc then a 45° Faraday rotator to operate at 100,000 mc will be about 3 inches long and will require a magnetic field of approximately 300 oersteds.

The main advantages of a differential phase shifter can be summarized by stating that a very small biasing magnetic field relative to other microwave ferrite devices is required for its operation, and the ferrite need not necessarily absorb any microwave energy itself and hence the heating can be kept to a minimum. This turns out to be an important consideration for high average powers.

One disadvantage of the differential phase shifter is that it requires a great deal of other external circuitry (such as hybrid junctions) in addition to the phase shifter in order to build a simple isolator. (Of course if one is attempting to build a circulator then this extra circuitry is essential.) In addition as one goes to frequencies below 1000 mc the properties of a phase shifter deteriorate rapidly as shown in the paper by Lax.[18] Thus it is probably impossible to build a circulator to operate at 1000 mc with an insertion loss less than 1 db, and impossible to reduce the insertion loss below 2 db at 500 mc with any kind of ferromagnetic material which is known today regardless of whether it has ideal properties or not with respect to all its other characteristics.

This low frequency limitation, in itself, is really not too severe and if it were possible to build ferrites today whose other properties were ideal, differential phase shifters operating at 1000 mc and perhaps 500 mc would be available today. To realize this ultimate low frequency limit, we must develop materials which more nearly approach the ideal material assumed in the above discussion. The problems are well understood and research is now underway to develop materials which will make these devices operable. It is outside the realm of this paper to discuss these problems in detail. However it is felt that this paper would be incomplete without indicating the nature of the problem.

It has been shown by Polder and Smit[19] that demagnetized ferrites would be expected to have a large magnetic loss tangent between the frequencies of

$$\gamma H_a \leqq \omega \leqq \gamma(H_a + 4\pi M_s) \tag{90}$$

where

$$H_a = \text{effective anistropy field} = \frac{2K_1}{M} .$$

[18] B. Lax, p. 1368, this issue.

[19] D. Polder, and J. Smit, "Resonance phenomena in ferrties," *Rev. Mod. Phys.*, vol. 25, p. 89; 1953.

(See Van Vleck.[20]) Thus it is to be expected that all demagnetized ferrites will have a large magnetic loss in this frequency region. However, when the ferrite is magnetized, this loss is not spread out over such a large band of frequencies but exists in a relatively narrow region (line width) around a frequency given by Kittel's equation.

If we assume a ferrite for which

$$\frac{2K_1}{M} = 400 \text{ oersteds} \tag{91a}$$

$$4\pi M_s = 2000 \text{ gauss} \tag{91b}$$

$$\nu_z = 0; \quad N_x = N_y = 2\pi \text{ (long cylinder)} \tag{91c}$$

and if we assume the wavelength of the radiation being considered is always much larger than the diameter of the ferrite (so that Kittel's equation can be applied), then one of the low frequency problems becomes immediately evident.

Eq. 90 indicates that this ferrite cylinder will be very lossy between 1120 mc and 6720 mc when it is demagnetized. When the ferrite is just magnetized (say in an applied field of 200 oersteds), the ferromagnetic resonance occurs at 3360 mc. If measurements are being taken at 4000 mc, a cylinder of the above ferrite will be at ferromagnetic resonance in an applied field of 430 oersteds. Thus, if the attenuation of a 4000 mc wave is measured as a function of the applied longitudinal field as the wave is propagated through a round waveguide containing the above cylinder two components are evident in the loss. First there is the initial loss which occurs in the demagnetized ferrite which approaches zero as the ferrite is magnetized, and then the ferromagnetic resonance of the magnetized cylinder which reaches a maximum in an applied field of 430 oersteds. This is indicated in Fig. 24.

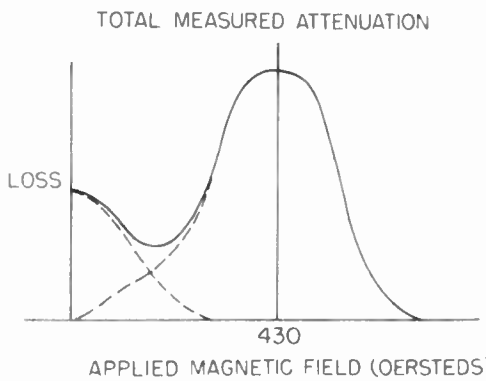

Fig. 24—Measured attenuation as a function of applied magnetic field for a cylinder of ferrite being used as a Faraday rotator at 4000 mc. (See text.)

Now if the saturation moment of the cylinder is reduced so that

$$(H_a + 4\pi M_s) < \omega, \tag{92}$$

then the initial loss in the demagnetized state will not occur for the frequency being used and the ferromagnetic resonance of the magnetized cylinder will not occur until higher magnetic fields are applied. Hence, the total loss in weak applied fields can be greatly reduced. Fig. 25 shows the measured loss and rotation of the plane of polarization for several samples of magnesium ferrite to which aluminum has been added to reduce the saturation moment of the material.[21] The data were

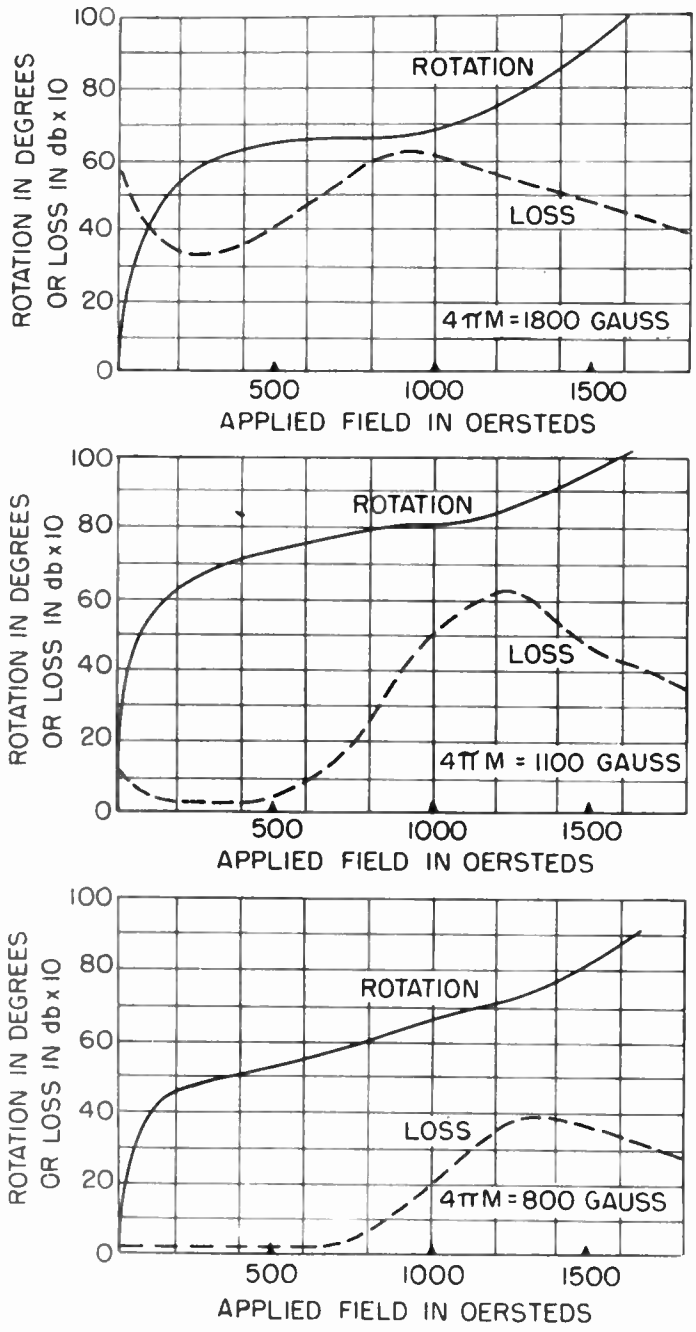

Fig. 25—Measured rotation and attenuation of cylinders of ferrite with various saturation moments when used as Faraday rotators at 4000 mc.

[20] J. H. Van Vleck, p. 1248, this issue.

[21] L. G. Van Uitert, J. P. Shafer, and C. L. Hogan, "Low loss ferrites for applications at 4000 mc/sec.," *J. Appl. Phys.*, vol. 25, p. 925; 1954.

taken at 4000 mc. It should be pointed out in this connection that the initial low-field loss does not completely disappear until the microscopic saturation moment of the individual ferrite grains has been reduced below that given in (92). Often the microscopic saturation moment is 10 per cent or 20 per cent larger than the macroscopic moment since the ferrites are usually not fired to maximum density. It can be easily shown, however, that the macroscopic moment is the quantity required in Kittel's equation, unless the ferrite is grossly nonhomogeneous.

Thus it is evident that if the major loss in a differential phase shifter is a magnetic loss it can be greatly reduced by reducing the saturation moment of the ferrite. (This is the major reason why some ferrites show an increase in the factor of merit when the temperature of the ferrite is increased.) However, as shown in (68), the rotation of the plane of polarization or the phase shift per unit length in a rectangular guide are proportional to the saturation moment of the ferrite, thus if the saturation moment is reduced too far, the physical size of the ferrite needed to obtain the desired result will become prohibitive. Thus a long cylinder of ferrite whose saturation moment is only 720 gauss will be at ferromagnetic resonance by the time it is magnetized, when it is subjected to a 1000 mc alternating field. Thus it appears that long cylinders are practical for a phase shifter only down to frequencies of the order of 1000 mc, unless one operates on the high field side of the resonance line. If on the other hand one uses a thin disc of ferrite rather than a cylinder, and magnetizes the disc perpendicular to the plane of the disc, then one can extend the low frequency limit of a particular ferrite. For instance, if the ferrite whose properties are described in (91a) and (91b) is cut into a thin disc instead of a cylinder, the demagnetizing factors for this geometry become

$$N_x = N_y = 0; \qquad N_z = 4\pi \tag{93}$$

and hence from Kittel's equation it is seen that the applied magnetic field necessary for resonance is

$$H_a = \frac{f(mc)}{2.8} + 4\pi M_s. \tag{94}$$

Thus if this ferrite is again used at 4000 mc ferromagnetic resonance will not occur in the disc until an applied field of

$$H_a = 1430 + 2000 = 3430 \text{ oersteds} \tag{95}$$

is reached.

On the other hand, the disc will almost completely saturate in an applied field of 2000 oersteds, and hence the low field loss will disappear long before the peak in the ferromagnetic resonance occurs. Thus, in place of Fig. 23, the loss vs applied field for the disc will be as indicated in Fig. 26.

It is seen by comparing Fig. 23 with Fig. 26 that the identical piece of ferrite might be usable at 4000 mc when cut into a thin disc but not when cut into a long cylinder, and hence part of the low frequency problem can be considered a geometry problem as well as a materials problem.

In addition, a polycrystalline ferrite has a ferromagnetic resonance absorption line width at least of the order of magnitude of the effective crystalline anisotropy field. Thus a polycrystalline nickel ferrite would have a resonance absorption line width of approximately 500 oersteds. Obviously, these wide lines hurt more and more as one attempts to operate at lower frequencies, and hence for extremely low microwave frequencies (below 1000 mc), it becomes increasingly important to obtain polycrystalline ferrites with low crystalline anisotropy, or in lieu of this, to obtain good single crystals.

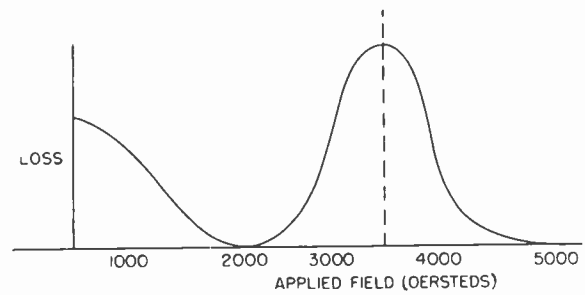

Fig. 26—Measured attenuation as a function of applied field of same ferrite as shown in Fig. 24. Here the ferrite is cut as a disc and located coaxially in a round waveguide or as thin slabs in a rectangular waveguide as shown in Fig. 27.

Resonance Absorption Devices

It is obvious that if a ferrite is placed in a waveguide and biased with a dc magnetic to its resonant frequency as given by Kittel's equation it will be extremely lossy provided the internal rf magnetic field vector in the ferrite has a positive circularly polarized component. It is on the basis of this phenomenon that microwave isolators can be built. Perhaps the simplest is that described above where a rectangular waveguide is loaded as shown in Fig. 23 and the magnetic field is adjusted to bring the ferrite to resonance. Usually in practice the slabs do not go all the way across the guide as shown in Fig. 23 but consist of small pieces placed in contact with the upper and lower walls of the guide.

This device has the advantages of constituting one of the simplest microwave ferrite devices from a circuit point of view and also having the best low frequency limit as shown by Lax.[22] As shown in that paper the back to front loss ratio in this device can be as high 10 db to 1 db for such a device operating at 200 mc. Certainly until ferrite materials are developed which overcome the problems discussed in the above section on differential phase shifters, resonance absorption devices are the only practical devices which can be built for operation at 1000 mc or lower today.

[22] Lax, *loc. cit.*

In reference to Figs. 24 and 26 it is evident that one should choose a geometry for the ferrite which maximizes the difference between the field required to magnetize and the field required for resonance as one goes to very low frequency operation (below 2000 mc). The simplest geometry which affords this result is with thin flat slabs in contact with the upper and lower walls of the guide as indicated in Fig. 27. This geometry also improves the thermal contact of the ferrite with the waveguide walls and thus allows the ferrite to dissipate the heat absorbed from the microwave energy more readily.

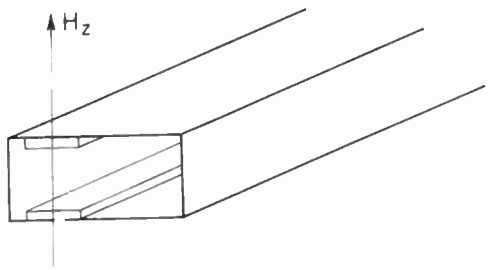

Fig. 27—Optimum geometry for loading a rectangular waveguide at very low microwave frequencies.

One of the main disadvantages of a resonance absorption isolator is that the ferrite, itself, must absorb all of the backward wave and in microwave systems which operate at large average power levels into loads with a high vswr this disadvantage can become disastrous if one does not resort to forced cooling. Another disadvantage of a resonance absorption isolator is that the magnetic field required for resonance becomes prohibitively high as one goes to very high frequency microwave systems even it one chooses optimum geometries. Thus if a resonance absorption isolator to operate at 56,000 mc is built with the geometry of Fig. 23 (optimum geometry for minimizing the dc magnetic field) an applied magnetic field of approximately 18,500 oersteds will be required if the ferrite has a saturation moment of 3000 gauss. It is doubtful if any permanent magnet today can produce this field over the volume required and at the same time have the high stability which is necessary.

Two considerations enter into determining the band width of a resonance absorption isolator. The first is related to the geometry of the guide itself. Thus to maximize the reverse loss and minimize the forward loss the ferrite should be placed in a position such that it sees a pure positive circular polarization for one direction of propagation and a negative circular polarization for the other direction of propagation. As we saw from (87) above this is in general impossible for a rectangular waveguide and even if one selects the optimum position, it is easily shown from (82) and (87) that this optimum position is in itself a function of frequency. Recently this problem has been partially overcome by dielectrically loading the waveguide. Even if the position of pure circular polarization does not change with frequency the resonance absorption isolator must have a bandwidth determined by the width of the resonance absorption line in Fig. 10 unless the ferrite is placed in a grossly inhomogeneous magnetic field.

By a combination of dielectric loading and inhomogeneous field, Melchor, Ayers, and Vartanian[23] at the Electronic Defense Laboratory have produced the broadest band resonance absorption isolator known to the author. The characteristics of this device are shown in Fig. 28. It seems apparent that slightly more development of this particular device would give front to back ratios in excess of 75 db to 1 db over a band from 8000 mc to 14,000 mc.

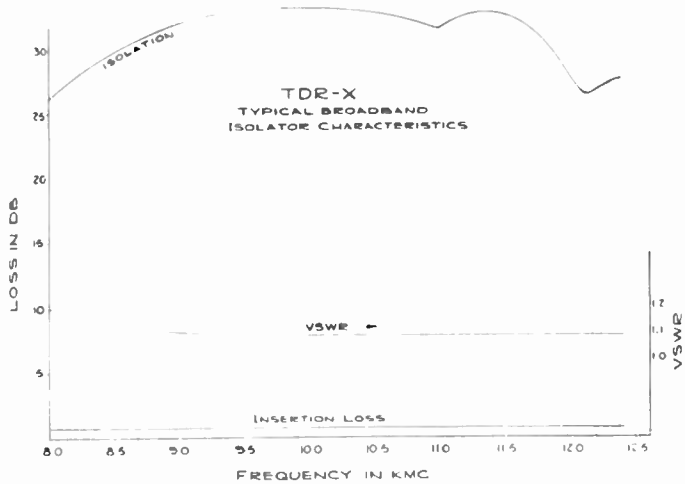

Fig. 28—Measured characteristics of dielectrically loaded ferrite isolator developed at the Electronic Defense Laboratory.

Field Displacement Devices

Field displacement devices are probably the most difficult to understand from an intuitive point of view since they cannot be completely understood either from an infinite plane wave analysis, or from perturbation theory of the loaded waveguide. However much can be said about the design of a field displacement isolator from the theory which has been developed above.

Thus if an infinite plane wave is incident upon a semi-infinite slab of ferrite magnetized in the direction of propagation of the wave as indicated in Fig. 29, some rather interesting aspects of the wave motion can be deduced from the above theory.

Thus as was shown in (51), the propagation constant for the two counter-rotating circularly polarized components of the wave can be written as

$$\Gamma_{\pm} = j\omega[\epsilon\mu_0\mu_{\pm}]^{1/2} \tag{96}$$

where

$$\mu_{\pm} = \mu \pm \kappa.$$

The real and imaginary parts of $\mu \pm \kappa$ are plotted in Figs. 9 and 10 for a particular set of values of the

[23] Private communication.

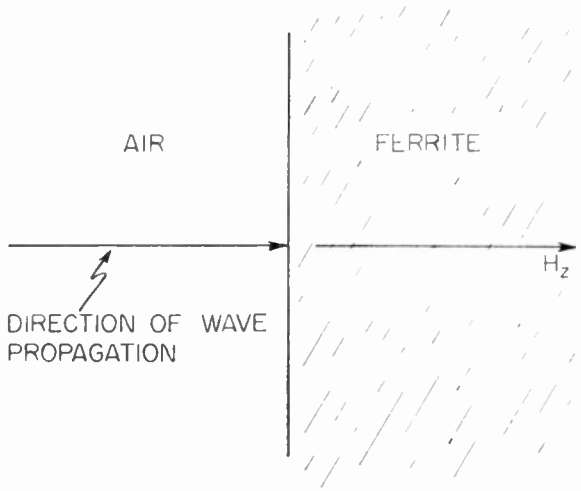

Fig. 29—Infinite plane wave incident upon a ferrite-air interface. Ferrite is magnetized in the direction of propagation of the wave.

parameters. Now if (96) is solved for the attenuation and phase constant under the assumption that the only loss is due to the imaginary part of the effective permeability shown in Fig. 10, one gets

$$\begin{aligned} \alpha_{\pm} &= \omega\sqrt{\epsilon\mu_0\mu_r^{\pm}} \\ \beta_{\pm} &= \omega\sqrt{\epsilon\mu_0\mu_l^{\pm}} \end{aligned} \tag{97}$$

where

$$\mu_r^{\pm} = \frac{[(\mu_{\pm}')^2 + (\mu_{\pm}'')^2]^{1/2} - \mu_{\pm}'}{2}$$

$$\mu_l^{\pm} = \frac{[(\mu_{\pm}')^2 + (\mu_{\pm}'')^2]^{1/2} + \mu_{\pm}'}{2}.$$

If we refer to Fig. 9 we should expect some rather startling behavior for the positive circular component if the magnetic field is raised to the point where the effective permeability (*i.e.*, μ_+') is zero or negative. In fact if we neglect the losses associated with the *tail end* of the absorption line at first we see that the semi-infinite ferrite medium behaves like a waveguide beyond cutoff for the positive circular component. That is, neglecting all losses, when the magnetic field is adjusted to the zero permeability value for the positive component both α_+ and β_+ are zero. When the magnetic field is adjusted so that the effective permeability, μ_+', is negative we find that

$$\begin{aligned} \beta_+ &= 0 \\ \alpha_+ &= \omega\sqrt{\epsilon\mu_0|\mu_+'|}. \end{aligned} \tag{98}$$

Thus we have an attenuation constant but no phase constant. This is obviously a reactive attenuation such as one encounters in a lossless waveguide beyond cutoff. In other words the wave is reflected from the air-ferrite interface. Thus we can define a skin depth which is the distance into the ferrite which the wave will penetrate before it is reduced to $1/e$ of its initial amplitude. On the basis of this

$$\delta_+ = \frac{1}{\omega\sqrt{\epsilon\mu_0|\mu_+'|}}. \tag{99}$$

As the effective permeability for the positive circular polarization takes on larger and larger negative values (increasing the applied magnetic field) the depth of penetration becomes smaller and smaller. The effective depth of penetration assuming no loss can be easily computed from the above equation. Thus, for instance, if one assumes an operating frequency of 9000 mc, a relative dielectric constant of 10, and in addition assumes that the biasing magnetic field is adjusted so that the effective permeability of the medium for the positive circular component is minus 1, then (99) indicates that the effective depth of penetration of the wave into the medium is

$$\delta_+ = 1.7 \text{ mm.} = 0.067 \text{ inch.}$$

A similar effect occurs if the ferrite is placed in the waveguide at a position where it sees a positive circular polarization for one direction of propagation and a negative circular polarization for the other direction. For the direction of propagation in which the magnetic field vector is positively polarized the rf fields tend to be expelled from the ferrite loaded region and penetrate the ferrite to a depth indicated by (99). If the ferrite dimensions are large compared to the effective skin depth thus calculated, then appreciable field displacement effects should take place in the waveguide. More exact criteria can be established by the reader by the use of (97) and the theory developed above.

It will be recognized by the reader that the criteria given above are greatly oversimplified. Some field displacement takes place whenever β_+ is different from β_- in (97) and the effect is maximized by maximizing the difference. In practice, however, it is found the effect is not large unless the effective permeability for the positive circular polarization is zero or negative.

It is apparent that in order to build a good field displacement device it is necessary to bias the ferrite into the region where it has zero or negative permeability for the positive circular component but on the other hand the magnetic field must be low enough so that losses due to the resonance absorption line are negligible. These requirements of course put frequency limitations in which a practical field displacement device can be built. At too high a frequency (above K band) the magnetic field required to reach the zero permeability region is becoming prohibitively high. At too low a frequency (below L band) the ferrite will have considerable loss when the real part of the permeability is zero and like the cutoff in a very lossy guide, the field displacement effect deteriorates rapidly.

The behavior of a field displacement device is clearly illustrated in some calculations made by Lax and Button[24] and two of the modes which they calculated are shown in Fig. 30. The propagation constants for

[24] B. Lax and K. J. Button, "Theory of new ferrite modes in rectangular waveguide," *J. Appl. Phys.*, vol. 26, p. 1185; 1955.

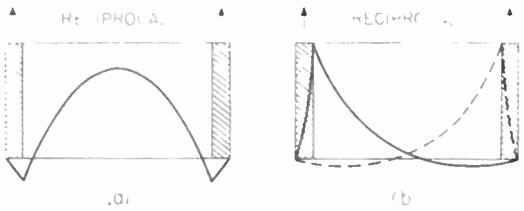

Fig. 30—Modes in a ferrite loaded rectangular waveguide. Magnetic field directions shown by arrows.

these modes are shown in Fig. 31. It is noticed that for very thin slabs of ferrite only mode A exists which is not radically different from the empty wave guide mode. However when the slabs are thick enough a strong field displacement toward one side of the waveguide takes place for one direction of propagation and toward the other side of the guide for the opposite direction of propagation. It is thus obvious that if a resistance card is placed on the surface of one of the slabs in Fig. 30(b) it will cause a very large attenuation for one direction of propagation and a very small attenuation for the other direction of propagation.

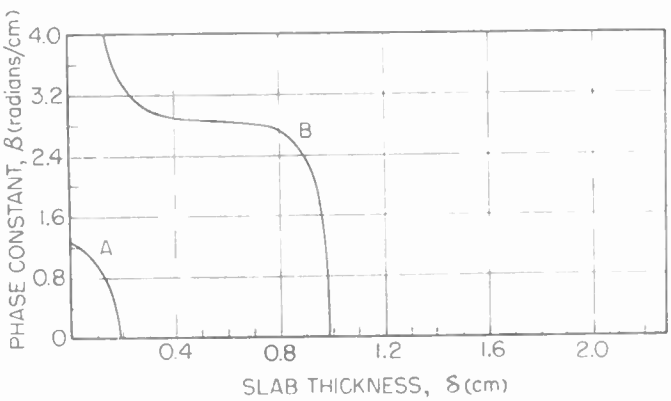

Fig. 31—Propagation constants for modes shown in Fig. 30 as a function of slab thickness. (In both cases the magnetic field is such that the ferrite has an intrinsic negative permeability for positive circular polarization.)

Commercial Ferrite Devices

In conclusion it is felt that this article would not be complete without indicating to the reader the types of commercial devices which have already come into wide use today. The list is not complete but is meant only to show the reader the extent of present day development.

Figs. 32 and 33 show an assembled and exploded view of a Faraday rotator isolator developed at Hughes Research and Development Laboratories. It has an isolation greater than 18 db and an insertion loss less than 0.5 db over a 10 per cent band centered around X band. It will handle a peak power of 300 kw and an average power of 300 watts with forced air cooling. The ferrite is magnetized by means of bar magnets on the outside wall of the waveguide. One of these magnets is shown in Fig. 33.

Fig. 34 shows an X-band circulator developed at Airtron, Inc. It is capable of handling a peak power of

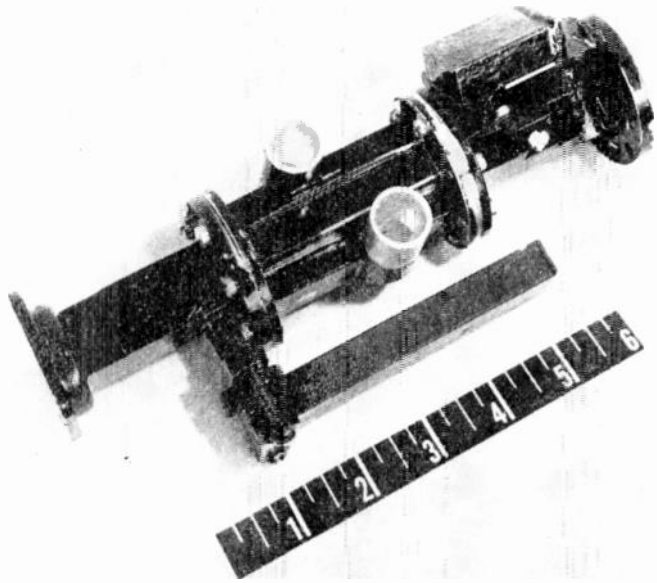

Fig. 32—Assembled view of high power isolator developed at Hughes Research Laboratories.

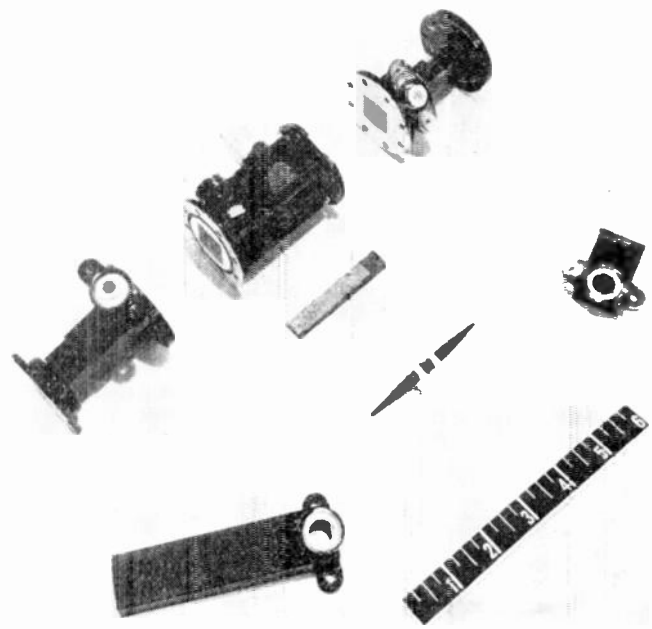

Fig. 33—Exploded view of isolator shown in Fig. 32.

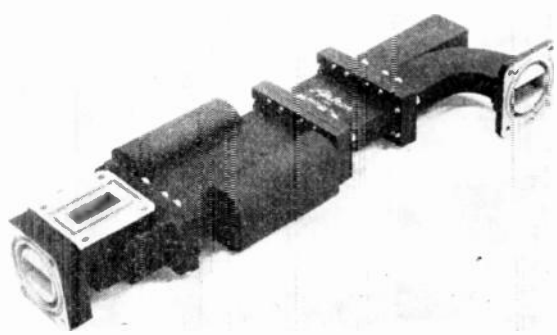

Fig. 34—Typical ferrite circulator using one folded hybrid and one Riblet hybrid.

500 kw and an average power of 500 watts without cooling. This circulator gives an insertion loss of 0.5 db and the cross coupling is down by 20 db.

Fig. 35 shows a typical rectangular waveguide resonance absorption isolator also developed at Airtron. This particular device gives an isolation greater than 10 db and an insertion loss less than 0.5 db while handling 2.5 megawatts of power at S band. It will work into a 2 to 1 load mismatch.

This list is not complete and there are available on the market today dozens of different types of microwave ferrite devices made by at least a dozen different concerns.

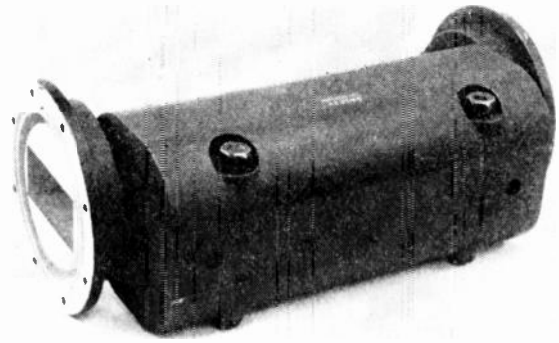

Fig. 35—High power S-band isolator developed by Airtron, Inc.

Frequency and Loss Characteristics of Microwave Ferrite Devices*

BENJAMIN LAX†

Summary—**The four major microwave ferrite devices, *i.e.*, the Faraday rotator, the resonance isolator, the nonreciprocal phase shifter, and the field displacement devices are discussed in terms of their loss properties over a range of frequencies. By means of perturbation theory the figure of merit of these devices is derived in the idealized limits for various ferrite geometries. These limiting values are analyzed in terms of the experimental results of the resonance loss for polycrystalline and single crystal measurements and compared with existing data on practical devices. The analysis indicates a possible low-frequency limit of Faraday and nonreciprocal phase shift circulators at about 1000 mc. The low-frequency limit of the resonance isolator is estimated at about 200 mc with a reverse-to-forward ratio of about 10. The problem of broad banding is also discussed in terms of the perturbation results.**

Introduction

EVER SINCE the development of practical microwave ferrite devices the principal problem that has faced the engineers and physicists working in this field is that of extending the usefulness of these devices over a wider frequency range. In particular, many of the designers of radar and communications systems have been asking for such devices in the ultra-high frequency region, that is, 1000 mc or below. The problem of extending the ferrite devices into the millimeter region has not been quite as serious or as urgent. The question that has to be answered is: *What are the factors which determine the limitations of these devices at either low or high frequencies?* The problem is now reasonably well crystallized and understood. However, although the diagnosis exists, the cure has not been obtained. As a matter of fact, we are able to go beyond the qualitative stage and even assign numbers which measure the limitations of the application of ferrites at these edges of the microwave spectrum.

An additional problem confronting the designers of ferrite devices is that of broad banding some of these devices in terms of the ferrite elements themselves. Finally, a problem that has been drawing a great deal of attention is that of using these devices at high power levels. I shall touch upon all of these considerations in the discussion of each of the four principal devices to be considered in this lecture, namely, the Faraday rotator, the resonance isolator, the nonreciprocal phase shifter, and the field displacement devices.

At low frequencies the factors which determine the limitations of a ferrite device are size and loss. As we go to lower frequencies the size and weight of the device normally become greater until it may become impractical economically and physically. Furthermore, it becomes increasingly more difficult to avoid dielectric and magnetic losses. The dielectric losses can be minimized by the proper preparation of the ferrite itself. The magnetic losses in the ferrite in the unsaturated state at very low frequencies may be due to domain wall motion. These can be reduced to about 100 mc or less in suitable ferrite materials. Another type of loss in the unsaturated state is due to the creation of dipole charges at the domain walls such that resonance losses can occur up to frequencies as high as $\omega = 4\pi\gamma M$ in the

* Original manuscript received by the IRE, May 21, 1956. Presented at Symposium on the Microwave Properties and Applications of Ferrites, Harvard Univ., Cambridge, Mass., April 2–4, 1956. The research reported in this document was supported jointly by the Army, Navy, and Air Force under contract with Massachusetts Institute of Technology.

† Lincoln Laboratory, M.I.T., Lexington, Mass.

most unfavorably oriented domains. This effect may be reduced through the proper choice of ferrite geometry. For example, a disc may be magnetized perpendicular to the broad face in order to maximize the difference between the field required for resonance and the field required for the magnetic saturation of the sample. Thus, the overlap region of the resonance and low-field loss may be reduced and result in a lower minimum loss. However, this geometry may frequently be inconvenient. Furthermore, this technique is not adequate at lower frequencies if the resonance line half-width is relatively large (see Fig. 1). In that case, the zero-field loss

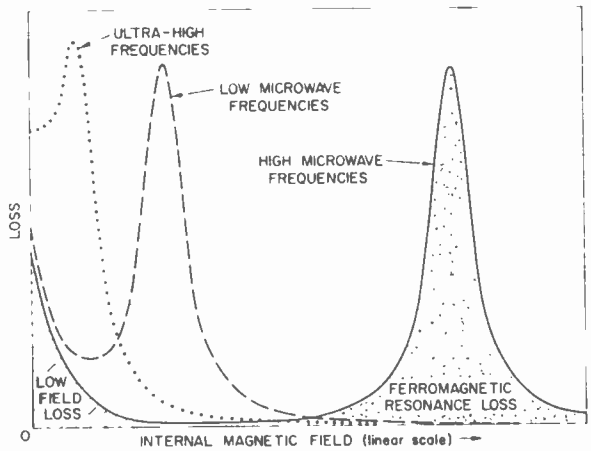

Fig. 1—Schematic representation of absorption as a function of magnetic field for a typical ferrite. Resonance line-width is assumed independent of frequency. Low-field loss (which is exaggerated for high microwave frequencies) increases with $4\pi M_s$ and with decreasing frequency.

may be reduced further through the use of special ferrites such as the aluminates and others in which the saturation moment has been substantially reduced. This, of course, may have the disadvantage of a low Curie temperature. In that case it may be necessary to consider the use of magnetic fields large enough to bias the ferrite for operation above ferromagnetic resonance. This would eliminate the zero-field losses since the sample should be magnetically saturated. However, above resonance, the differential properties of the ferrites are substantially smaller. We can compensate for this since high magnetization ferrites can be used above resonance. Nevertheless, the over-all effect in either of the last two possibilities is the net reduction of Faraday rotation or differential phase shift per unit length such that longer ferrites are required. An additional factor, magnetic anisotropy, enters into the zero-field loss and also the resonance loss. Thus, even if the zero-field loss is eliminated through the use of low-saturation material, the anisotropy field still remains and the lowest operating frequency which can be reached is given by $\omega = \gamma H_{anis}$. The use of Ni-Zn ferrites with proportionately larger amounts of zinc will help to reduce the anisotropy but again the Curie temperature becomes too low for most devices. Possibly a more satisfactory solution is in the addition of cobalt to the ferrite mixture. Cobalt ferrite has a positive anisotropy whereas manganese or nickel ferrite has negative anisotropy. It should, therefore, be possible to make low-anisotropy materials in this way without reducing the Curie temperature.

In principle, the dielectric and low-field magnetic losses may be eliminated. The ferromagnetic resonance-loss must still be considered. It will be shown later that whatever operating conditions we choose, the optimum operation of these devices will require that the loss associated with resonance must be minimized in at least one direction of transmission. This condition can be achieved only through the use of ferrite materials which have narrow resonance line widths. Thus, in preparing the ferrite material for microwave devices, this is one of the most important considerations. As a matter of fact the evaluation of the devices which we shall discuss will be made in terms of idealized materials in which one can represent the resonance loss rather simply by a relaxation time of a phenomenological type. Then in terms of this relaxation time, the frequency and the magnetic field, we shall arrive at figures of merit for some of these devices.

A great body of experimental information has been obtained in recent years on the behavior and design of ferrite components and, to a lesser extent, some theoretical work has been done to explain the behavior of these devices. In some cases quite satisfactory explanations have been given concerning some of the phenomena encountered. In particular the articles of Hogan,[1] Rowen,[2] and Fox, Miller, and Weiss[3] and others have provided excellent expositions of some of these. Nevertheless, in some cases, no mathematical formulation of a qualitative or semiquantitative nature has been offered. It is the purpose of this paper to review the situation and to try to bring up to date the experimental evidence and to use in some instances, idealized models of the infinite medium or through the use of perturbation theory, to arrive at an analytical result for the figures of merit of these devices in some of the limiting situations. Although the perturbation theory may not provide quantitative results in some practical cases, it can be an extremely useful tool in gaining a better understanding of the fundamental principles of design and operation of ferrite media in waveguides and cavities. It can also be useful in developing and explaining new design principles and existing ones which many of the workers have devised on either an intuitive or empirical basis.

[1] C. L. Hogan, "The ferromagnetic Faraday effect at microwave frequencies and its applications," *Bell Syst. Tech. J.*, vol. 31, pp. 1–31; January, 1952.
C. L. Hogan, "The ferromagnetic Faraday effect at microwave frequencies and its applications," *Rev. Mod. Phys.*, vol. 25, pp. 253–263; January, 1953.
[2] J. H. Rowen, "Ferrites in microwave application," *Bell Syst. Tech. J.*, vol. 32, pp. 1333–1369; November, 1953.
[3] A. G. Fox, S. E. Miller, and M. T. Weiss, "Behaviour and applications of ferrites in the microwave region," *Bell. Syst. Tech. J.*, vol. 34, pp. 5–103; January, 1955.

Faraday Rotator

Infinite Medium

The phenomenon which best illustrates the basic principles of the interaction of ferrites with electromagnetic waves is the Faraday rotation in an infinite medium. The usual method of considering this phenomenon is to treat the two contra-rotating circularly polarized waves in terms of their effective scalar permeabilities

$$\mu_\pm = \mu \mp \kappa = \mu_0\left(1 + \frac{\omega_M}{\omega_0 \mp \omega + j/T}\right) \tag{1}$$

where $\omega_M = 4\pi\gamma M$, $\omega_0 = \gamma H$ and T is a phenomenological relaxation time.

The quantity that distinguishes the positive and negative permeabilities is the off-diagonal component of the permeability tensor

$$\kappa = \mu_0 \frac{\omega_M \omega}{\omega_0^2 - \omega^2} \approx -\mu_0 \frac{\omega_M}{\omega} \text{ for } \omega \gg \omega_0 \text{ (below resonance)} \tag{2}$$

$$\kappa \approx \mu_0 \frac{\omega_M \omega}{\omega_0^2} \text{ for } \omega \ll \omega_0 \quad \text{(above resonance)} \tag{3}$$

which is responsible for the existence of the Faraday rotation. Thus, we see that as we increase the frequency in (2) the absolute value of κ decreases. Eq. (2) indicates that the Faraday rotation per unit length should decrease as we approach the millimeter region. However, κ does not necessarily increase [as indicated by (2)] as we approach the lower end of the microwave spectrum. It has already been pointed out that the low-field loss limits us to $\omega_M < \omega$. Therefore, ω_M must be reduced eventually and then the Faraday rotation which is proportional to the ratio of ω_M and ω should become approximately independent of frequency at the lower end of the spectrum. If we consider the other possibility of $\omega_0 > \omega$ for operation above resonance (3) suggests that κ decreases with decreasing frequency. Now it is possible to select $\omega_M > \omega_0$ so that in the practical regions of a few hundred megacycles the large value of the magnetization may compensate to yield a Faraday rotation comparable to the low-magnetization case.

Using the expression of (1) it is a simple matter to evaluate the complex propagation constant for an infinite medium from

$$\Gamma_\pm = j\omega\sqrt{\epsilon\mu_\pm} \tag{4}$$

by expanding the radical in terms of T^{-1} since $\omega_0 \pm \omega \gg 1/T$ for a good Faraday rotator. The losses in this application should be nearly equal for the positive and negative circularly polarized waves. This can be achieved in the high- and low-frequency regions where $\omega \gg \omega_0$ or $\omega \ll \omega_0$ respectively. For the low-frequency case (4) can be expanded to give the components of $\Gamma = \alpha + j\beta$ as follows:[4]

$$\alpha_\pm \approx \frac{\omega\omega_M\sqrt{\epsilon\mu_0}}{2\omega_0^2 T\sqrt{1 + \omega_M/\omega_0}}$$

$$\beta_\pm = \omega\sqrt{\epsilon\mu_0}\left[\sqrt{1 + \omega_M/\omega_0} \pm \frac{\omega_M\omega}{2\omega_0^2\sqrt{1 + \omega_M/\omega_0}}\right]. \tag{5}$$

The rotation per unit length is given by

$$\theta = (\beta_+ - \beta_-)/2 = \omega\sqrt{\epsilon\mu_0}\omega_M\omega/2\omega_0^2\sqrt{1 + \omega_M/\omega_0}.$$

The figure of merit for the Faraday rotator is defined as the ratio of the rotation to the attenuation θ/α. The result becomes

$$F = \omega T. \tag{6}$$

Using the equations above one can obtain the same result for the high-frequency case when $\omega \gg \omega_0$ and $\omega \gg \omega_M$. The above result has been derived for circularly polarized plane waves in an infinite medium.

Perturbation Theory

In practice, the Faraday rotator is a cylindrical ferrite rod in a circular or a square waveguide. To solve such a problem for the complex propagation constant has been found to be rather difficult. However, if we consider the limiting case of a thin ferrite sliver the solution can be obtained by means of first order perturbation theory. The result for the propagation constant Γ of the perturbed system is given by the following expression:

$$\Gamma + \Gamma_0^* = \frac{i\omega\int_{\Delta S}[(\overleftrightarrow{\Delta\mu}\cdot\vec{H})\cdot\vec{H}_0^* + (\overleftrightarrow{\Delta\epsilon}\cdot\vec{E})\cdot\vec{E}_0^*]dS}{\int_S \vec{k}\cdot(\vec{E}\times\vec{H}_0^* + \vec{E}_0^*\times\vec{H})dS} \tag{7}$$

where Γ_0 is the propagation constant of the unperturbed system (which in this case is assumed to be lossless), ω is the angular frequency of the rf field, and the differences in the tensors between the perturbed and unperturbed situations are denoted by $\overleftrightarrow{\Delta\mu}$ and $\overleftrightarrow{\Delta\epsilon}$ for the permeability and permittivity respectively. This difference may be an actual or a mathematical one. $\vec{E}$ and $\vec{H}$ are the electric and magnetic field configurations everywhere across the section of the guide including the ferrite. Thus, if one knew the true analytical relations for the field components, the above formula would give the exact results for the propagation constant. Since this is seldom possible, it is necessary to use the known relations for the unperturbed fields $\vec{E}_0$ and $\vec{H}_0$ everywhere. Of course, there is a large discontinuity of both

[4] B. Lax, "A figure of merit for microwave ferrites at low and high frequencies," *J. Appl. Phys.*, vol. 26, p. 919; July, 1955.

the permeability and the dielectric constant at the ferrite boundary and the field components inside the ferrite are modified considerably. It is a simple matter to use Kittel's relations to calculate the internal fields in terms of the external field components if the demagnetizing and depolarizing factors are obtained from the geometry of the ferrite sliver. The expressions for the numerator of (7) can then be rewritten using the following relations:

$$\overleftrightarrow{\Delta\mu}\cdot\vec{H} = \mu_0\overleftrightarrow{\chi}\cdot\vec{H} = \mu_0\overleftrightarrow{\chi}_{eff}\cdot\vec{H}_0 \tag{8}$$

where $\overleftrightarrow{\chi}$ is the magnetic susceptibility tensor for the infinite medium as given in (1) and $\overleftrightarrow{\chi}_{eff}$ is that of the ferrite rod taking into account the demagnetizing factors as follows:

$$\chi_{xx}^{eff} = \frac{\omega_M\left[\omega_0 + \frac{j}{T} + (N_y - N_z)\omega_M\right]}{\left(\omega_r + \frac{j}{T}\right)^2 - \omega^2}$$

$$\chi_{yy}^{eff} = \frac{\omega_M\left[\omega_0 + \frac{j}{T} + (N_z - N_z)\omega_M\right]}{\left(\omega_r + \frac{j}{T}\right)^2 - \omega^2}$$

$$\chi_{xy}^{eff} = -\chi_{yx}^{eff} = -j\frac{\omega_M\omega}{\left(\omega_r + \frac{j}{T}\right)^2 - \omega^2} \tag{9}$$

where N_x, N_y and N_z are the demagnetizing factors of an equivalent ellipsoid [the sum of which are unity in the representation of (9)] and z is the direction of the applied dc field. The representation of the loss in (9) by the relaxation time T is essentially a Landau-Lifshitz parameter rather than the Bloch-Bloembergen parameter which is inappropriate. The resonance frequency ω_r is that derived by Kittel, *i.e.*,

$$\omega_r = \sqrt{[\omega_0 + (N_x - N_z)\omega_M][\omega_0 + (N_y - N_z)\omega_M]}. \tag{10}$$

By the same procedure which has been used for the magnetic field components it can be shown that the electric field for a ferrite which has a scalar dielectric constant is given by the following

$$E_j = \frac{1}{1 + N_j\chi_e}E_{0j}, \qquad \chi_e = (\epsilon - \epsilon_0)/\epsilon_0$$

or

$$\chi_e^{eff} = \chi_e/(1 + N_j\chi_e) \tag{11}$$

where E_j is the component of the internal electric field for $j = x$, y or z and E_{0j} and N_j are the external field and depolarizing factors for the corresponding directions. The phase constant and attenuation constant are derivable from (7) to (11) and are given by:

$$\beta_\pm = \beta_0 + A\frac{S'}{S}\left[\chi_\pm'^{eff}\beta_0 - \frac{\beta_0^2}{\beta_0}\chi_e^{eff}\right]$$

$$\alpha_\pm = A\frac{S'}{S}\chi_\pm''^{eff}\beta_0 \tag{12}$$

where β_0 is the propagation constant of the unperturbed waveguide filled with a lossless dielectric, $\beta_0^2 = \omega^2\epsilon_0\mu_0$, S' and S are the cross-sectional areas of the ferrite and the waveguide respectively, A is a constant which is 2.1 for a circular waveguide[5] and unity for a square waveguide.[6] Finally, the effective magnetic and electric susceptibilities are those derived from (9) and (11). For a long circular cylinder these become

$$\chi'^{eff} \mp \kappa'^{eff} = -\frac{\omega_M(\omega_r \mp \omega)}{(\omega_r \mp \omega)^2 + \frac{1}{T^2}}$$

$$\chi_\pm''^{eff} = -\frac{\omega_M/T}{(\omega_r \mp \omega)^2 + \frac{1}{T^2}} \tag{13}$$

where

$$\omega_r = \omega_0 + \frac{\omega_M}{2}$$

and

$$\chi_e^{eff} = \frac{2\left(\frac{\epsilon}{\epsilon_0} - 1\right)}{\frac{\epsilon}{\epsilon_0} + 1}. \tag{14}$$

The result of (12) is similar to that given by Suhl and Walker.[5] From (12) one can derive the value for the Faraday rotation and the figure of merit F. For a good Faraday rotator $\alpha_+ \approx \alpha_- = \alpha$ and consequently

$$F = \frac{\beta_+ - \beta_-}{2\alpha} = \frac{\kappa'^{eff}}{\chi_\pm''^{eff}} \approx \omega T \tag{15}$$

since at low and high frequencies the susceptibilities are given by:

$$\chi_\pm''^{eff} = \frac{\omega_M/T}{(\omega_r \mp \omega)^2 + \frac{1}{T^2}} \approx \frac{\omega_M/T}{\omega_r^2} \text{ or } \frac{\omega_M/T}{\omega^2}$$

and

$$\kappa'^{eff} \approx \omega_M\omega/(\omega_r^2 - \omega^2) \approx \omega_M\omega/\omega_r^2 \text{ or } \sim\omega_M/\omega \tag{16}$$

where $\omega_r \gg \omega$ or $\omega \gg \omega_r$ respectively. Thus, we see that at least in the limiting case of a thin rod at high and low

[5] H. Suhl and L. R. Walker, "Topics in guided-wave propagation through gyromagnetic media," *Bell Syst. Tech. J.*, vol. 33, pt. III, "Perturbation theory and miscellaneous results," *Bell Syst. Tech. J.*, pp. 1133–1194; September, 1954.

[6] A. D. Berk, "Ferrites at Microwave Frequencies," Quart. Prog. Rep. Res. Lab. of Elec., Mass. Inst. Tech., pp. 53–55; January, 1954.

frequencies the geometry of either the ferrite sample or that of the waveguide has not altered the situation from that of the infinite medium. For intermediate frequencies where the difference between ω and ω_r for the ferrite rod or ω and ω_0 for the infinite medium is not so great $\alpha_+ \neq \alpha_-$. In this case one should define the figure of merit somewhat differently, namely let:

$$F = \frac{2\theta}{\alpha_+ + \alpha_-} = \frac{\beta_+ - \beta_-}{\alpha_+ + \alpha_-} = \frac{\kappa_{eff}'}{\chi_{eff}''}. \tag{17}$$

Here in essence one defines the ratio in terms of the total loss for both circularly polarized components. The result becomes

$$F \approx \frac{\omega T}{2}\left|\frac{\omega}{\omega_r} - \frac{\omega_r}{\omega}\right| \tag{18}$$

depending on whether one operates above or below resonance. Thus, we see that if ω/ω_r is of the order of 2 or $\frac{1}{2}$ the figure of merit is of the same order as before. If the ratio is 3 or more ($\frac{1}{3}$ or less) the derivation leading to (15) is valid.

Figure of Merit

We have shown that $F=\omega T$ is a reasonable criterion for an ideal device using the Faraday rotation at microwave frequencies. Such a device might be a circulator in which the total rotation $\Theta=\theta l$ in a length of ferrite l is 45°. Hence, the total attenuation is given by:

$$\alpha l = \frac{\Theta}{\omega T} \approx \frac{0.8}{\omega T}. \tag{19}$$

If the circulator has an insertion loss of 0.5 db then $\alpha l = 0.06$. This would yield a value of $\omega T \approx 13$. To find the lowest frequency for which this value of the figure of merit can be achieved it is necessary to find a ferrite with the maximum available value of T. The best experimental value quoted at the present has been for a single crystal which for practical purposes has a resonance line width $\Delta H \approx 50$ oersteds. Such a resonance line taken by Tannenwald[7] is shown in Fig. 2 and is a reasonable fit for a Lorentzian line using the phenomenological relaxation time T. Using the relation $T = 1/\gamma\pi\Delta H$, where γ is the gyromagnetic ratio, we obtain the maximum figure of merit $F_m \approx 14\nu$ (ν in kmc). For $F=13$ for a 0.5 db device this corresponds to a low frequency limit of about 1000 mc. This represents at the present time the low-frequency limit for a Faraday rotation device whether we work with magnetic fields above or below resonance. Since single crystals of sufficiently large size and high resistivity are not available, the low-frequency limit, based upon 0.5 db insertion loss, has to be revised upwards. If we consider that properly prepared sintered ferrites can be made having

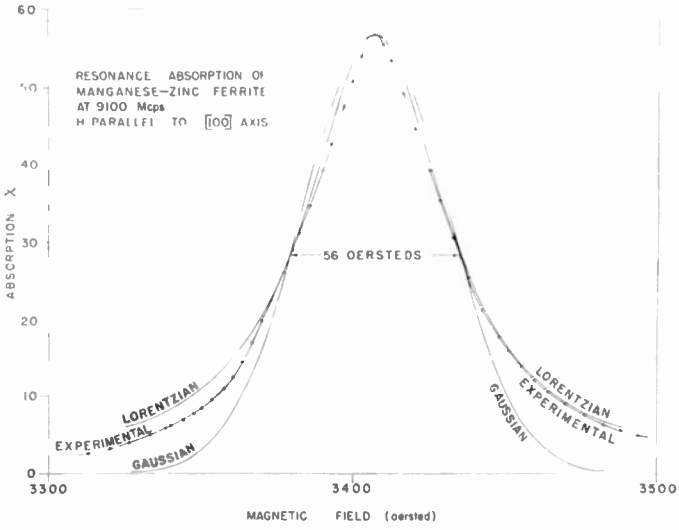

Fig. 2—Comparison of experimental line shape with theoretical Lorentzian line represented by relaxation time T (after P. E. Tannenwald).

halfwidths of $\Delta H \approx 100$ oersteds then it should be possible to build Faraday circulators at about 2000 mc.

Let us now look into the higher frequency situation. Obviously it is not difficult to meet the necessary requirement of 0.5 db insertion loss since the figure of merit increases with frequency. However, it will be instructive to compare the theoretical limits of the values of F with the experimental values reported and attempt to account for whatever differences appear. Some of the values of F obtained from the literature are given in Table I.

TABLE I
FIGURE OF MERIT FOR FARADAY ROTATOR

Source	F	Ferrite	Freq (mc)	Diam
Sakiotis and Chait[8]	~32	Ferramic A-34	9,375	0.25 inch
Rowen[2]	11	Ni-Zn	9,000	—
Hogan[1]	~55	Mg	9,000	0.32 inch
Fox, Miller, and Weiss[3]	~110	Ni-Zn	11,200	0.15 inch

The best value is that of Fox, Miller, and Weiss and corresponds to a value of $\Delta H \approx 50$ oersteds. This effective line width for a polycrystalline material is remarkably narrow and is comparable to that reported for single crystals. This situation could be deceptive for the following reason. The value of ΔH for Ferramic 1331 (or R-1) at about 9000 mc is between 400 and 500 oersteds. It is conceivable that the corresponding values of F of about 12 and 15 could be exceeded in practice. This is the case since the observed losses below resonance where the device operates may be lower than that predicted by a Lorentzian line corresponding to the

[7] P. E. Tannenwald, "Ferromagnetic resonance in manganese ferrite single crystals," *Phys. Rev.*, vol. 100, pp. 1713–1719; December, 1955.

[8] N. G. Sakiotis and H. N. Chait, "Ferrites at microwaves," PROC. IRE, vol. 41, pp. 87–93; January, 1953.

T value obtained from the half width. In Fig. 3 the comparison of theory and experiment is shown on the curve of the lossy part of the susceptibility for Ferramic R-1 for the positive circularly polarized wave as obtained by Artman and Tannenwald.[9] This situation is, however, not true for the single crystal where the line shape is nearly Lorentzian. Hence, one may conclude that $F=120$ for $\Delta H=50$ begins to approach a realistic upper limit of performance for the Faraday rotator.

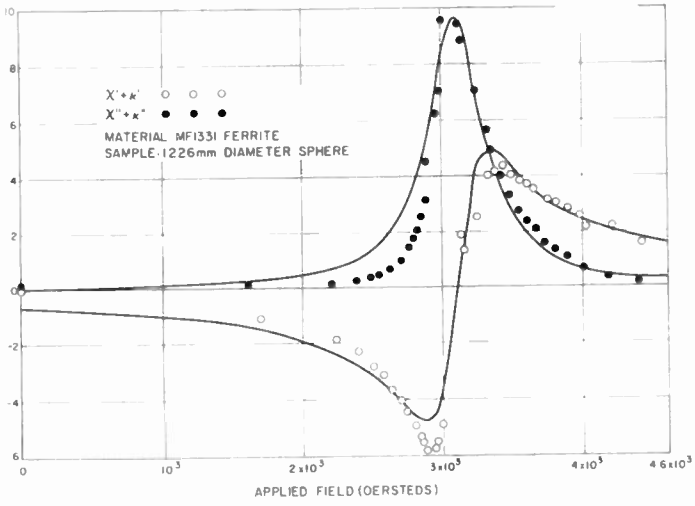

Fig. 3—Real and imaginary parts of the component of the microwave susceptibility for the positive circularly polarized wave. The solid lines are theoretical and the points are experimental (after Artman and Tannenwald).

Dielectric Modes

One of the questions that arises is the effect of the dielectric modes on the operation of the Faraday device and its possible effect on the figure of merit. It has been shown by a number of workers that as one increases the diameter of the ferrite rod in a circular waveguide the angle of rotation increases rapidly beyond a certain value. Such a curve of rotation as a function of diameter is shown in Fig. 4. The effect is well understood qualitatively and is attributed to the existence of a dielectric mode for the negative circularly polarized wave and the rejection of the electromagnetic field from the ferrite for the positive circularly polarized component. The existence or absence of the electromagnetic field concentration in the ferrite was experimentally demonstrated recently by Melchor, Ayres, and Vartanian.[10] The equation for the modes of a partially filled circular guide has been set up;[5,11,12] the solution for the mode

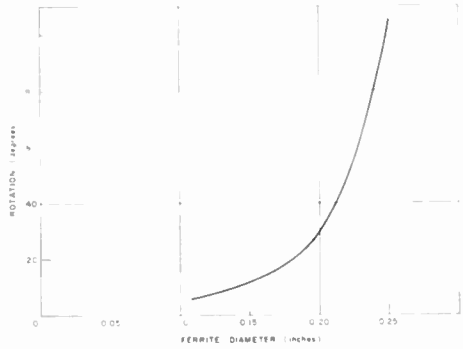

Fig. 4—Typical curve of Faraday rotation as a function of the diameter of the ferrite rod for frequency ≈9000 mc and applied field ≈400 oe. The sharp increase in rotation at larger diameters is attributable to the onset of the dielectric mode.

configurations as a function of the diameter of the ferrite rod has not been given.

Again, perturbation theory can be very helpful in explaining, at least qualitatively, the nature of the phenomenon that occurs as the diameter of the rod is increased. The thought behind the particular use of the perturbation theory is inspired by the suggestion of Fox and Weiss[13] that as the diameter of the ferrite rod is increased the TE_{11} mode is converted partially into the TM_{11} mode. This is probably correct but not complete. Not only is there mode conversion or coupling of the TM_{11} mode but also of the TE_{12}, TM_{12}, and all the other modes whose rotational symmetry is the same as the TE_{11} mode and whose field components are given by the form

$$J_1\left(\frac{rr_j}{a}\right)e^{i\theta} \quad \text{or} \quad J_1'\left(\frac{rr_j'}{a}\right)e^{i\theta}$$

where r_j and r_j' are the roots of $J_1=0$ and $J_1'=0$. Using the original perturbation expression of (7) and assuming that the actual field is a linear combination of all the modes including the unperturbed mode, then we can show that the coupling coefficient and the new value of the phase constant, neglecting losses, are given by:

$$C_j=\frac{W_{1j}}{(\beta_1-\beta_j)W_j}$$

$$\beta=\beta_1+\frac{W_{11}}{W_1}+\frac{W_{j1}W_{1j}}{(\beta_1-\beta_j)W_1W_j} \tag{20}$$

where C_j is the coupling coefficient, β_1 the phase constant for the unperturbed mode, β_j of the other modes, β the perturbed value, and the matrix elements W represent the following integrals:

$$W_{j1}=\omega\mu_0\int_{S'}(\overleftrightarrow{\chi_m}\cdot\vec{H}_j)\cdot\vec{H}_1^*dS+\omega\epsilon_0\int_{S'}(\overleftrightarrow{\chi_e}\cdot\vec{E}_j)\cdot\vec{E}_1^*dS$$

$$W_j=\int_S\vec{k}\cdot[\vec{E}_j\times\vec{H}_j^*+\vec{E}_j^*\times\vec{H}_j]dS \tag{21}$$

[9] J. O. Artman and P. E. Tannenwald, "Measurement of susceptibility tensor in ferrites," *J. Appl. Phys.*, vol. 26, pp. 1124–1132; September, 1955.
[10] J. L. Melchor, W. P. Ayres, and P. H. Vartanian, "Energy concentration effects in ferrite loaded wave guides," *J. Appl. Phys.*, vol. 27, pp. 72–77; January, 1956.
[11] M. L. Kales, "Modes in wave guides containing ferrites," *J. Appl. Phys.*, vol. 24, pp. 604–608; May, 1953.
[12] A. A. T. M. Van Trier, "Guided electromagnetic waves in anisotropic media," Martinus Nijoff, *'S-Gravenhage* (The Netherlands), pp. 32–40; 1953.
[13] A. G. Fox and M. T. Weiss, "Discussion, mode conversion problem," *Rev. Mod. Phys.*, vol. 25, pp. 262–263; January, 1953.

where $\overleftrightarrow{\chi_m}$ and $\overleftrightarrow{\chi_e}$ are the magnetic and dielectric tensor susceptibilities of the ferrite and W_{1j} is analogous to the expression above with the subscripts interchanged in the integrals. The analytical expression for the field components are appropriately normalized. If we evaluate these integrals for the circular case we obtain for the coupling coefficient the following

$$C_j = \frac{r_1' r_j' [\beta_1\beta_j(\chi \pm \kappa) + \beta_0^2\chi_e]_{eff} S}{2(\beta_1 - \beta_j)\beta_j(r_j'^2 - 1)J_1^2(r_j')S} \quad \text{(TE modes)}$$

$$C_j = \frac{\omega\mu_0 r_1' [\beta_1(\chi \pm \kappa) + \beta_j\chi_e]_{eff} S'}{2(\beta_1 - \beta_j)\beta_j r_j J_1'^2(r_j)S} \quad \text{(TM modes)} \quad (22)$$

where $r_1' = 1.84$ is the root for the TE_{11} mode, $\beta_0 = \omega^2\epsilon_0\mu_0$, J_1 is the first Bessel function, r_j' and r_j the appropriate roots for the higher TE and TM modes respectively, and the subscript *eff* implies that the susceptibilities take into account the proper demagnetizing and depolarizing factors.

The important thing to observe in the above relation for the coupling coefficients is that the coupling of the higher order modes is accomplished both by the magnetic and dielectric properties of the ferrite rod. The dielectric coupling for the TM_{11} mode appears to be slightly larger than the magnetic. However, it becomes less for the other modes with the magnetic coupling dominating eventually. It is the reversal in sign of the susceptibilities for the positive circularly polarized component as compared to the negative, which is responsible for the absence and concentration respectively of the electromagnetic field in the ferrite. In a crude way we might imagine that along a given direction the electric field has the configuration shown in Fig. 5(a) for

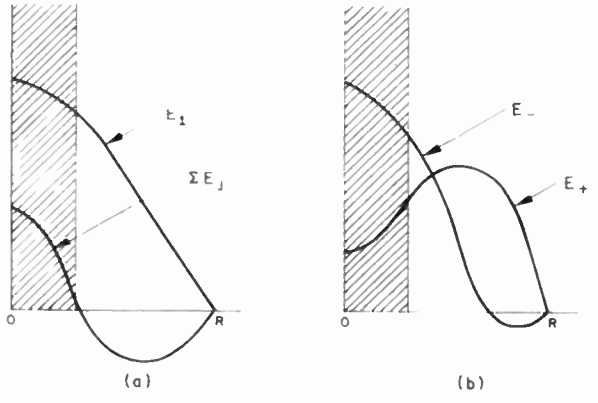

Fig. 5—Approximate configuration of the rf electric field intensities in cylindrical waveguide as a function of the radial dimension. (a) The unperturbed mode, E_1, represents the field in the waveguide with a dielectric equivalent to ferrite (shown shaded). ΣE_j is the composite of higher modes coupled by the rf permeability of the ferrite.

the unperturbed mode E_1 and ΣE_j for the others. Perturbation theory which can be formulated for the magnetic effect alone (since we might assume that the unperturbed system included an equivalent dielectric rod) would suggest that for the negative circularly polarized wave the modes for the two configurations shown would give rise to the sum of their amplitudes and for the positive polarized wave the two configurations would subtract. The result of such a combination is shown schematically in Fig. 5(b). Qualitatively this type of argument accounts for the origin of the dielectric mode.

The question now arises as to whether the existence of these dielectric modes degrade or improve the figure of merit. According to Fox, Miller, and Weiss[3] the figure of merit is more or less independent of ferrite diameter for small diameters. For large ferrite diameters, the figure of merit should decrease because for both the positive and negative modes of rotation there is an admixture of the opposite sense of circularly polarized field away from the center of the ferrite rod. The theoretical problem is difficult to analyze exactly although Suhl and Walker have treated it approximately. Their analysis indicates that the figure of merit is relatively insensitive to the size of the ferrite. However, Fox, Miller, and Weiss[3] show a graph (see Fig. 6) of the figure

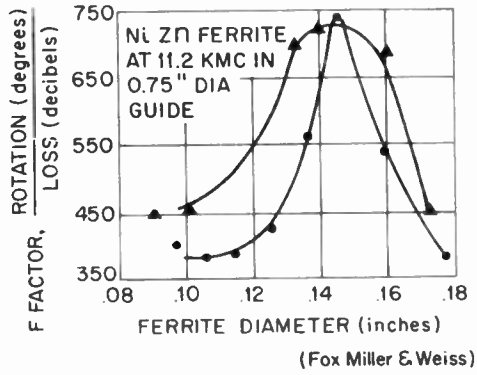

Fig. 6—Figure of merit for a Faraday rotator as a function of ferrite diameter for two different low-loss ferrites. $F_{max} \approx 740$ degrees/db ≈ 110 radians.

of merit as a function of ferrite diameter which was obtained by J. P. Shafer for two different low-loss ferrites. These curves show a maximum in the figure of merit for 0.15 inch diameter at 11.2 kmc which is still below the theoretical limit. The curves demonstrate that an increase in diameter produces a reduction of the figure of merit as one approaches the dimensions which result in the dielectric modes. Another interesting feature discussed by Fox, Miller, and Weiss is that the characteristic shape of this curve is partially accounted for by the presence of dielectric loss in the ferrite. Suhl and Walker have calculated a theoretical curve of loss and rotation as a function of diameter taking this into account. These curves are shown in Fig. 7. This shows a maximum loss corresponding nearly to the diameter at which the dielectric mode sets in. When the energy is concentrated in the ferrite for the negative wave, the dielectric loss is at a maximum. Hence, this result is not surprising. As the diameter is increased, of course,

both the positive and negative circular modes become more nearly equally distributed in the ferrite and consequently the loss is reduced.

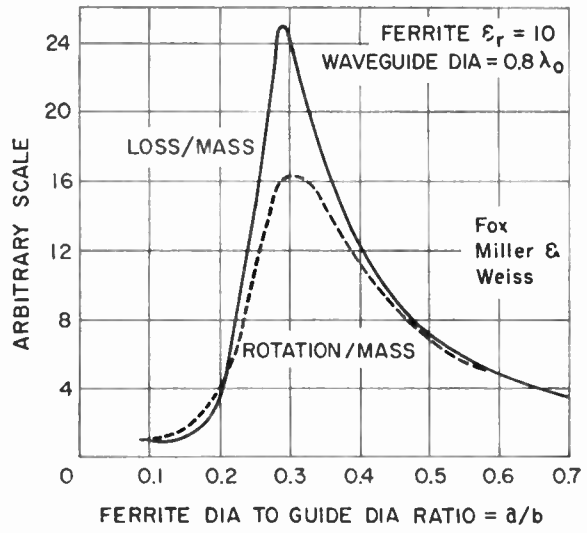

Fig. 7—Theoretical curves (calculated by Suhl and Walker) of the loss and rotation as a function of ferrite diameter taking dielectric loss into account (after Fox, Miller, and Weiss).

Broad Banding

One of the problems that concerns engineers is that of broad banding the Faraday rotator. Three suggestions have been given in the literature. One of the most effective schemes is that suggested by Kales.[14] The diagram of Fig. 8 shows the usual characteristics of the Faraday

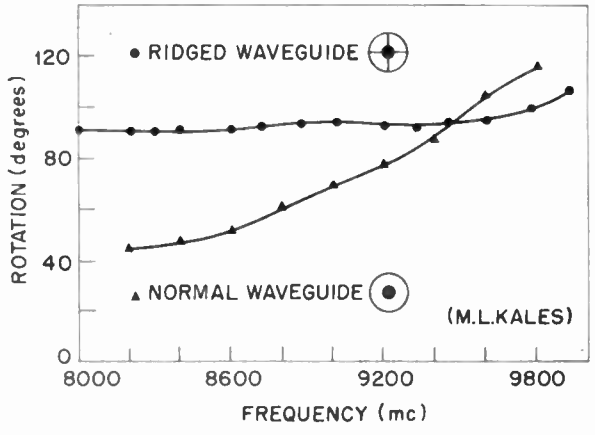

Fig. 8—Faraday rotation as a function of frequency for normal waveguide and for waveguide containing two orthogonal pairs of ridges. The flat response is apparently due to the compensation of the frequency variation of the ridged waveguide modes and the permeability of the ferrite.

rotation which increases as a function of frequency. This can again be seen qualitatively from the results of the perturbation theory which is given by:

$$\theta = A\frac{S'}{S}\kappa_{\text{eff}}\beta_e = \frac{r_0^2}{R^2}\frac{\omega_M\omega}{\omega^2-\omega_r^2}\sqrt{\omega^2\epsilon\mu_0-\frac{(1.84)^2}{R^2}}$$

$$\sim\frac{r_0^2}{R^2}\omega_M\sqrt{\epsilon\mu_0-\frac{(1.84)^2}{\omega^2R^2}} \qquad (23)$$

where r_0 and R are the radii of the ferrite and the waveguide respectively.

Hence, as the frequency is increased the angle θ increases asymptotically for the normal waveguide to $\theta_{\max}=\omega_M r_0^2\sqrt{\epsilon\mu_0}/R^2$. In the ridge waveguide apparently the frequency variation in the permeability is compensated by that of the modes to give a flat response. A second scheme for broad banding has been given by Rowen in which he surrounds the ferrite with a dielectric. Again if we look at the equations of the perturbation theory we can see why such a scheme should be helpful. If the dielectric constant is raised this reduces the cutoff frequency of the mode and hence $\beta_e\approx\omega\sqrt{\epsilon\mu_0}$ and $\theta\rightarrow\theta_{\max}$ which is the asymptotic limit. Of course, the presence of the dielectric cylinder helps in a number of other ways also. It was demonstrated by Rowen that it increases the Faraday rotation, as we can again see from the results of the perturbation theory. The reason for this for a small diameter rod is that the dielectric reduces the depolarizing effects and increases the electromagnetic field in the ferrite. For larger ferrites the presence of the dielectric reduces the possibility of field concentrations in the ferrite. This in essence reduces the perturbation of the ferrite in the waveguide since if the dielectric constant of the surrounding medium is the same then only the magnetic perturbation exists. Under these circumstances the perturbation theory is valid for larger diameters. Finally the perturbation results show that if the outer diameter of the waveguide R is reduced the rotation is again enhanced. This too was demonstrated experimentally by Rowen.

A third method of broad banding the Faraday rotator shown in Fig. 9(a) has been suggested by M. B. Loss.[15] He uses two ferrite rods in the waveguide which are magnetized in opposite senses. He suggests that broad banding can be achieved by compensating the frequency changes of Faraday rotation in the two rods, either by choosing two ferrites of different magnetization or by using rods having different diameters. Of course, H_{1a} and H_{2a}, the applied fields, can also differ. By this scheme Loss has broad banded devices over a 12 per cent frequency band using Ferramic A-106 and Ferramic R-1 rods.

The principle of broad banding can be examined very conveniently by the use of perturbation theory

$$\theta=\theta_1-\theta_2\sim S_1\kappa_1-S_2\kappa_2=\frac{S_1\omega_{M1}\omega}{\omega_{r1}^2-\omega^2}-\frac{S_2\omega_{M2}\omega}{\omega_{r2}^2-\omega^2} \qquad (24)$$

where S_1 and S_2 are the areas of the ferrite rods, ω_1

[14] M. L. Kales, "Propagation of fields through ferrite-loaded guides," *Proc. of Symposium on Modern Advances in Microwave Techniques*, Polytechnic Inst. of Brooklyn, pp. 215–228; July, 1955.

[15] M. B. Loss, "Broadband characteristics of ferrites," 1955 IRE Convention Record, part 8, pp. 109–112.

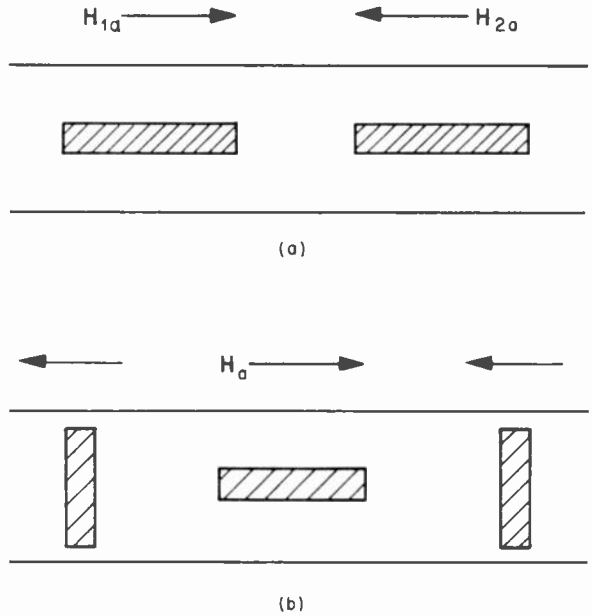

Fig. 9—Two possible methods of broad banding the Faraday rotator. (a) (suggested by M. B. Loss) Different applied fields or different ferrite dimensions or magnetization may be used. (b) The magnetization of the rod and two disks can be chosen such that the former will operate above resonance and the latter below resonance.

and ω_2 are the resonant frequencies given by (10) and ω_{M1} and ω_{M2} are the magnetization parameters. Perhaps one can set up the criterion here that at the design frequency the slope of the change should be zero, *i.e.*, $d\theta/d\omega = 0$ and that $d^2\theta/d\omega^2 \neq 0$ insuring either a maximum or a minimum. Such a situation should provide for optimum broad banding. The above equations are very suggestive of the method in which this type of scheme may be used to the best advantage. If one of the ferrites were biased above resonance and the other below then again the changes of the Faraday rotation in the two rods would compensate. Furthermore, the rotation for each rod would add rather than subtract which would provide a device having a better figure of merit than the one that uses opposing fields. The disadvantage of the necessity for higher applied fields would not be serious at the lower frequencies and here larger dimensions facilitate the application of opposing fields. A convenient arrangement to achieve the desired result is shown in Fig. 9(b) where a rod and two disks are used. The former would operate above resonance since $\omega_1 = \omega_0 + \omega_{M1}/2$ and the latter below resonance, since $\omega_2 = \omega_0 - \omega_{M2}$. The magnetization of each ferrite could be selected to give best operation for a given frequency. For example, at 10,000 mc, a field of 3000 oersteds is required for resonance in the infinite medium. If the disk were made of material having a magnetization of 2000 Gauss, an applied field of 3000 oersteds would provide an internal field of 1000 oersteds which is well below resonance. Then the rod should be made of a material having a magnetization of 3000 to 4000 Gauss so that the internal field is about 5000 oersteds which is well above resonance.

Resonance Isolator

Cylindrical Waveguide

Perhaps one of the most useful and simplest devices is the resonance isolator. This can be built in two forms, one using a circular guide and the other rectangular. The latter has been more practical since it is much simpler to construct as one can see from Fig. 10. The

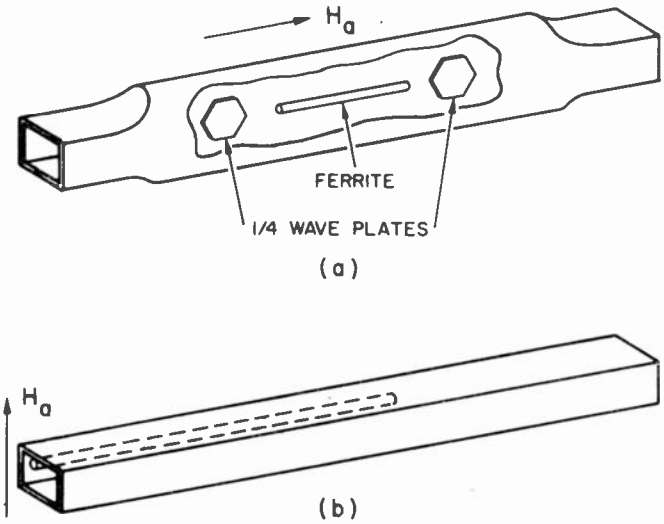

Fig. 10—Resonance isolator in (a) cylindrical waveguide and (b) rectangular waveguide. The cylindrical version requires quarter-wave plates to provide circularly polarized modes.

circular one may consist of two transitions from rectangular to circular waveguide with two quarterwave plates one on either side of the cylindrical ferrite rod. The field is then circularly polarized in the positive sense in one direction and the negative sense in the opposite direction. The applied field H_a is that required for resonance, so that the absorption is large for the positively rotating wave and is small in the opposite direction. The purpose of presenting the circular guide device is to demonstrate in a simple case the analytical results for the limit of the figure of merit which, for such a device, is the ratio of the reverse-to-forward loss. From perturbation theory we can show that for a thin ferrite rod

$$\alpha_{\pm} = C(\chi''_{eff} \pm \kappa''_{eff})$$

where $\alpha_{\pm}$ are the attenuation constants for the two circularly polarized waves, C is a constant proportional to the ratio of the area of ferrite cross section to that of the waveguide, and χ''_{eff} and κ''_{eff} are the imaginary (or lossy) components of the susceptibilities for the rod. These are given by the following for a thin circular rod:

$$\chi''_{eff} \pm \kappa''_{eff} = \frac{\omega_M/T}{(\omega_r \mp \omega)^2 + \dfrac{1}{T^2}} \tag{25}$$

where $\omega_r = \omega_0 + \omega_M/2$. It can be shown that the ratio in

decibels of the reverse loss to the forward loss on resonance is given by the following expression:

$$R = \frac{\alpha_+}{\alpha_-} \approx (2\omega T)^2 \tag{26}$$

since $\omega = \omega_r$ and $\omega \gg 1/T$. Consequently this expression represents the ideal limit of performance of a resonance isolator for a given ferrite. One may ask whether the above figure of merit for the resonance isolator can be improved by the use of larger rods and take advantage of the dielectric modes in the rod. The answer is that this effect actually works against attaining the desired objective of improving the reverse-to-forward ratio. For the negative wave the energy transmitted is concentrated in the ferrite rod. Hence, although the loss is not large for this case it is, nevertheless, increased since the loss is the product of $\mu'' h^2$ over the volume and h, the rf field amplitude in the ferrite has been enhanced by the dielectric effect. For the positive circular wave, the opposite effect takes place. As the rod diameter is increased the radius may exceed the skin depth which on resonance is given by the following:

$$\delta = \frac{\lambda}{2\pi}\sqrt{\frac{2}{\epsilon \chi''_+}}. \tag{27}$$

For Ferramic R-1 at 10,000 mc the value of $\delta \approx 1$ mm, since $\epsilon \approx 13$, and $\chi''_+ = \omega_M T \approx 8$. The consequence is that the field penetrates a smaller volume for the positive wave and the field is excluded from a good portion of the ferrite. The net result of these two effects is to degrade the performance of the isolator, *i.e.*, reduce the value of R from the theoretical limit.

Rectangular Waveguide

The resonance isolator in the rectangular waveguide is a very simple structure, which requires no transitions or quarter wave plates but simply a ferrite rod or slab with a transverse magnetic field as shown in Fig. 10(b). The ferrite may be a long slab which is either horizontally or vertically oriented across the guide or it may be a cylindrical rod. These arrangements are shown in Fig. 11. As we shall see the position of the slab for optimum performance will depend on the geometry of the ferrite cross section and for a thin slab or rod will ***not necessarily occur at the position of circular polarization*** for the empty guide. Also contrary to some of the statements found in the literature the position will not necessarily correspond to the point of circular polarization of the internal rf field in the ferrite. Such a position may not even exist for some of the geometries used. We can analyze this situation as follows. The components of the internal field h_{ix} and h_{iy} are given as follows:

$$\begin{aligned} h_{ix} &= h_{ox} - N_x M_x = h_{ox} - N_x(\chi h_{ix} - j\kappa h_{iy}) \\ h_{iy} &= h_{oy} - N_y M_y = h_{oy} - N_y(j\kappa h_{ix} + \chi h_{iy}). \end{aligned} \tag{28}$$

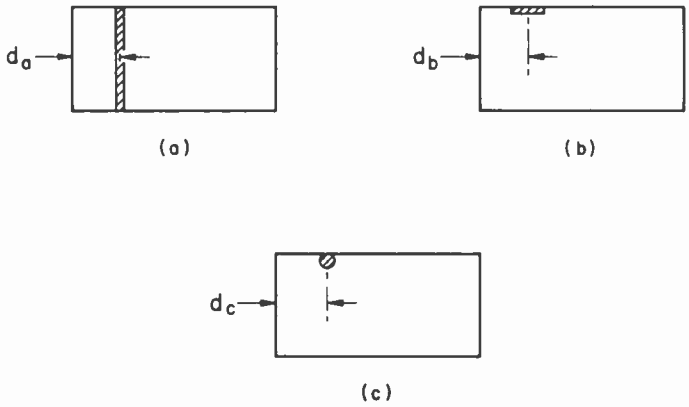

Fig. 11—The resonance isolator in rectangular guide showing three possible ferrite shapes which may be used. The optimum position for the ferrite depends upon the shape and frequency.

Solving these equations for h_{ix} and h_{iy} we obtain:

$$\begin{aligned} h_{ix} &= \frac{(1 + N_y\chi)h_{ox} + jN_x\kappa h_{oy}}{1 + (N_x + N_y)\chi + N_xN_y(\chi^2 - \kappa^2)} \\ h_{iy} &= \frac{(1 + N_x\chi)h_{oy} - j\kappa N_y h_{ox}}{1 + (N_x + N_y)\chi + N_xN_y(\chi^2 - \kappa^2)}. \end{aligned} \tag{29}$$

If we express the external field components for the empty guide for the TE_{01} mode as follows we have:

$$\begin{aligned} h_{ox} &= (-j\beta \sin kx) \exp[-j\beta y] \\ h_{oy} &= (-k \cos kx) \exp[-j\beta y] \end{aligned} \tag{30}$$

where $k = \pi/L$ and $\beta^2 = \omega^2\epsilon_0\mu_0 - k^2$. If we use these in (29) and obtain the ratio of h_{ix} and h_{iy} we get

$$\frac{h_{ix}}{h_{iy}} = \frac{j(1 + N_y\chi)\beta \sin kx + jN_x\kappa k \cos kx}{(1 + N_x\chi)k \cos kx + N_y\kappa\beta \sin kx}. \tag{31}$$

For circular polarization of the internal field components it is required that $h_{ix}/h_{iy} = \pm j$. From this we can solve for the position for which this is true. We can of course obtain the solution for any value of N_y. However, the perturbation theory was developed for infinitely long sections of waveguide and, hence, $N_y \to 0$. The value of the position is then given by:

$$\tan kx = \pm \frac{k}{\beta}[1 + N_x(\chi \mp \kappa)] \tag{32}$$

where x is the ferrite position which must be real. But if $N_x \neq 0$ no real solution exists for x, since χ and κ are complex quantities. Therefore, for the thin vertical slab for which $N_x \approx 1$ and for the circular rod, $N_x = \frac{1}{2}$, the internal field is not circularly polarized. For the thin slab which is oriented with its broad surface perpendicular to the magnetic field $N_x \approx 0$ and x can, therefore, be real. In this case the point of circular polarization is the same as that in the empty guide.

Let us now consider the problem of positioning the ferrite in the waveguide for the maximum reverse-to-forward ratio. To do this we again use perturbation

theory. We can show that the loss in the ferrite for the two directions of propagation is given by:

$$\begin{aligned}\alpha_{\pm} &= C(\chi_{xx}''h_{ox}^2+\chi_{yy}''h_{oy}^2\pm 2\chi_{xy}''h_{ox}h_{oy})\\ &= C(\chi_{xx}''\beta^2\sin^2 kx+\chi_{yy}''k^2\cos^2 kx\\ &\quad \pm \chi_{xy}''\beta k\sin 2kx)\end{aligned} \tag{33}$$

where C is a constant depending on the cross section of the ferrite waveguide and the result for the ratio R becomes

$$R=\frac{\alpha_+}{\alpha_-}=\frac{\chi_{xx}''\beta^2+\chi_{yy}''k^2-(\chi_{xx}''\beta^2-\chi_{yy}''k^2)\cos 2kx+2\chi_{xy}''\beta k\sin 2kx}{\chi_{xx}''\beta^2+\chi_{yy}''k^2-(\chi_{xx}''\beta^2-\chi_{yy}''k^2)\cos 2kx-2\chi_{xy}''\beta k\sin 2kx}. \tag{34}$$

To maximize the value of R as a function of position we set $dR/dx=0$. The result gives an equation for the position of the ferrite which is given by:

$$\cos 2kx=\frac{\chi_{xx}''\beta^2-\chi_{yy}''k^2}{\chi_{xx}''\beta^2+\chi_{yy}''k^2}. \tag{35}$$

When this is substituted into (34) the result for R_{max} becomes

$$R_{max}=\frac{\sqrt{\chi_{xx}''\chi_{yy}''}+\chi_{xy}''}{\sqrt{\chi_{xx}''\chi_{yy}''}-\chi_{xy}''}. \tag{36}$$

We can evaluate this expression on resonance when $\omega=\omega_r$ for the lossy part of the effective susceptibilities, where we obtain

$$\chi_{xx}''=\frac{\omega_M T\left\{2\omega_r[\omega_0+(N_y-N_z)\omega_M]+\frac{1}{T^2}\right\}}{4\omega_r^2+\frac{1}{T^2}}$$

$$\chi_{yy}''=\frac{\omega_M T\left\{2\omega_r[\omega_0+(N_x-N_z)\omega_M]+\frac{1}{T^2}\right\}}{4\omega_r^2+\frac{1}{T^2}}$$

$$\chi_{xy}''=2\omega_M T\omega_r^2\Big/\left(4\omega_r^2+\frac{1}{T^2}\right)$$

$$\begin{aligned}&\sqrt{\chi_{xx}''\chi_{yy}''}\\ &\approx \omega_M T\frac{\left\{2\omega_r^2+\frac{1}{2\omega_r}[2\omega_0+(1-3N_z)\omega_M]/T^2\right\}}{4\omega_r^2+\frac{1}{T^2}}.\end{aligned} \tag{37}$$

If the above expressions are substituted in (36) for R_{max} we obtain

$$R_{max}\approx(2\omega T)^2\frac{\omega_r}{\omega_0+(1-3N_z)\omega_M/2} \tag{38}$$

since $1/T^2$ is assumed to be a small quantity. The above expression closely resembles the one obtained for the resonance isolator in a circular waveguide. To a good approximation the results for the three geometries of ferrites that are shown in Fig. 11 are given by

$$R\approx(2\omega T)^2. \tag{39}$$

The optimum ferrite location for each geometry shown in Fig. 11 has been computed from (35) for the TE_{01} mode at 9280 mc using the values of $4\pi M$ and T of Ferramic R-1. The results are $d_a=0.30L$, $d_b=0.25L$, and $d_c=0.27L$ where L is the internal width of standard X-band waveguide. It can be seen by inspection of (35) that the position for the maximum ratio will be frequency dependent.

Fig. 12 shows the relative loss in the two directions

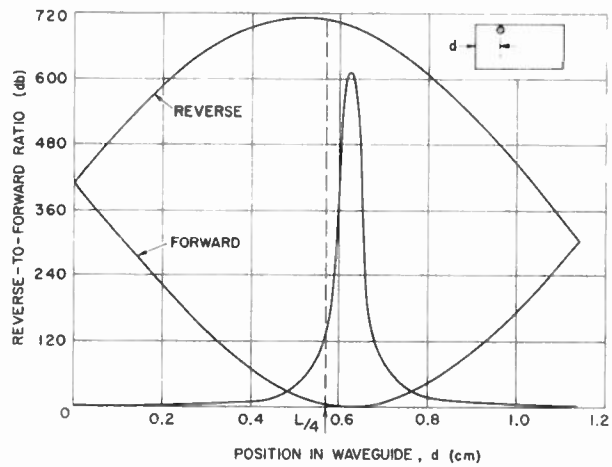

Fig. 12—Theoretical curves of loss in the reverse and forward directions (arbitrary scale) and the reverse-to-forward ratio as a function of ferrite position for a resonance isolator using a round ferrite rod. The computations were made from (34) for Ferramic R1 at 9280 mc in standard X-band guide. The dashed line marks the quarter-point.

and the reverse-to-forward ratio as a function of ferrite position for a round rod. It can be seen that the position for R_{max} is very close to the value for the minimum of the forward loss. This is the criterion that Fox, Miller, and Weiss have established from experimental results and is the one used by Heller[16] for treating the resonance isolator by perturbation methods.

An experimental curve very similar to that shown in Fig. 12 has been obtained at 9000 mc by Momo and Heller for a thin cylindrical rod and is shown in Fig. 13.

[16] G. S. Heller, "Theory of the Resonance Isolator," Lincoln Lab. Quart. Prog. Rep. on Solid State Research, pp. 56–57; November, 1955.

Although the absolute values of the ordinates do not agree the shape of the curves are remarkably similar and the position for maximum reverse-to-forward ratio corresponds quite well to that predicted for this geometry. The discrepancy in line width is probably due to the broadening effect of the large diameter rod which was used.

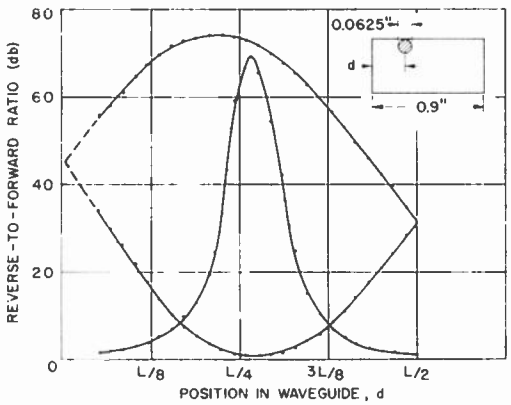

Fig. 13—Experimental curves (taken by L. R. Momo and G. S. Heller) of the relative loss in the reverse and forward directions (arbitrary scale) and the reverse-to-forward ratio as a function of ferrite position for a resonance isolator using a round ferrite rod. The data were taken for Ferramic R1 at 9000 mc.

We have shown that to a good approximation the maximum value of the reverse-to-forward loss is given by $R \doteq (2\omega T)^2$ for the resonance isolator. If we evaluate this quantity at 9280 mc for Ferramic R-1 for which $\Delta H \approx 500$ oersteds we find from the relation

$$\omega T = \frac{2H_r}{\Delta H} = \frac{6600}{500} = 13.3$$

$$R = (2\omega T)^2 \approx 700 \qquad (40)$$

where $H_r \approx 3300$ oersteds is the value of the field for resonance. At this frequency no one has yet achieved such a high ratio. Until recently some of the best values given in the literature have been of the order of 20:1 to 30:1 considerably below the theoretical limit. The vertical slab with full height across the guide gave a ratio of about 10:1 and with a reduction in height this was improved to about 20 or 25 to 1.[3] The use of thin circular rods and thin flat slabs against the top or bottom of the guide have produced ratios of about 70:1.[14] At the recent meeting of the IRE, Weiss reported ratios as high as 150:1 obtained through the use of dielectric material placed adjacent to or surrounding the ferrite. At the same meeting of the IRE in Philadelphia, Blasburg reported ratios of 300:1 using flat slabs of ferrite against the top or bottom wall of the guide with an applied magnetic field which had a gradient in the horizontal direction. Each of these schemes has approached the theoretical limit closer with Blasburg's reported result nearly $\frac{1}{2}$ of the maximum. But perhaps the best performance yet is that achieved by Heller who used a modified version of the dielectric scheme of Weiss to obtain a resonance isolator at 1300 mc with reverse-to-forward ratio of 15:1. At this frequency $\omega T \approx 2.5$ for Ferramic R-1 making $R_{max} \approx 25$ using (40). Thus, he has approached the ideal situation in this case.

The explanation of the phenomenon is perhaps suggested by the theoretical analysis used in obtaining the limiting figure. The theory is based upon the idea that the ferrite does not perturb the field configuration in the guide. This means that the energy in the ferrite is small compared to that in the empty guide. It also assumes that the field in the ferrite is uniform. Let us now examine the three configurations in the light of these facts and see which geometry is the most favorable in approximating the ideal situation. The vertical slab has been shown theoretically to exhibit strong dielectric effects. The exact solution which is applicable for the forward propagation where the loss is not great has shown that even for a ferrite which is 1 mm thick, the magnetic field perturbations within the ferrite are far from uniform. Since the field is also peaked at the ferrite it can be shown that the electromagnetic energy in the ferrite for this thickness is comparable to that in the empty waveguide. Finally, we have shown that since the field inside the ferrite cannot be circularly polarized for this configuration it would be difficult to match it to the electromagnetic system of the empty guide. Fox, Miller, and Weiss have reported results for a slab of this size and have shown that reducing the vertical height improved the performance. This is understandable since the dielectric effect was reduced. Use of even smaller vertical slabs by Weiss produced better results. Thin circular rods and flat slabs which minimize the dielectric effects also gave good results for this reason.

The notable success of Weiss, Blasburg, and Heller with flat slabs suggests that this geometry is optimum. There may be several reasons for this. First, we have shown that the field in the ferrite can be circularly polarized in this arrangement. The polarization in the ferrite corresponds to that in the empty guide. This is a great help in matching the impedance of the ferrite to that of the guide. The dielectric surrounding the ferrite does this approximately for the reverse direction permitting more energy to go into the ferrite. For the forward direction the lossless dielectric prevents a large concentration of energy in the ferrite and thus reduces the forward loss. Finally, the slab can be made thinner than a skin depth so that the rf magnetic field in the reverse direction is fully effective. Blasburg's dc magnetic field gradient helps to reduce the forward loss since he applies the resonance value only at the position of negative circular polarization; at other points in the waveguide where the undesired positive circular polarization component exists the dc magnetic field is not the resonance value.

These recent techniques which have improved the performance of the resonance isolator approaching the theoretical limit with ordinary commercial ferrites, should make it possible to build isolators which can operate at a lower frequency than any other type of

ferrite device. If practical polycrystalline ferrites can be prepared with a resonance half-width of about 100 oe then it should be possible to build resonance isolators at 200 mc with a ratio of $R \approx 10$.

Nonreciprocal Phase Shifters

Figure of Merit

Although the Faraday rotator was first used for constructing nonreciprocal devices such as the circulator, the nonreciprocal phase shifter in rectangular guide introduced by Kales, Chait, and Sakiotis[17] promises to be more practical. For a vertical slab which occupies the full height of the waveguide the exact theoretical treatment has been carried out in great detail for nonlossy ferrite material.[18] The lossy case has also been considered but in most cases detailed treatment is very laborious.[19] For geometrical shapes of ferrite other than the slab the theory is extremely difficult in general. However, the perturbation treatment which we have used throughout this paper permits us to compare the various geometries and analyze their performance in terms of a figure of merit. Before we do this it would be helpful to examine the polarization of the field inside the ferrite when losses can be neglected as in the phase shifter. We showed (32) that if the internal field is to be circularly polarized then the position of the ferrite for an infinite guide is given by:

$$\tan kx = \pm \frac{k}{\beta} \left[1 + N_z(\chi \mp \kappa)\right]. \tag{41}$$

For the three geometries of Fig. 11 ($N_z = 1, 0, \frac{1}{2}$ respectively) we obtain the following results:

$$\begin{aligned} x_a &= \frac{L}{\pi} \tan^{-1}\left[1 + \frac{\omega_M}{\omega_0 \mp \omega}\right] \\ x_b &= L/4 \\ x_c &= \frac{L}{\pi} \tan^{-1}\left[1 + \frac{1}{2}\,\frac{\omega_M}{\omega_0 \mp \omega}\right] \end{aligned} \tag{42}$$

at the midband frequency where $k = \beta$.

Thus, we see that for the vertical slab and the circular rod the position for circular polarization for the forward and reverse propagation do not coincide. However, for the flat horizontal slab the position is one-quarter of the guide width from the wall for both directions of propagation. It can be shown from perturbation theory that the complex propagation constant for the nonreciprocal phase shifter is given by the following expression

$$\Gamma = j\beta_e + j\frac{S'}{S\beta_e}\left[\beta_e^2\chi_{xx}\sin^2 kx + k^2\chi_{yy}\cos^2 kx \pm \chi_{xy}\beta_e k \sin 2kx + \omega^2\epsilon_0\mu_0\chi_e\right] \tag{43}$$

where S' and S are the cross section of the ferrite and guide respectively, χ_e is the effective electric susceptibility, χ_{xx}, χ_{yy} and χ_{xy} are the effective magnetic susceptibilities of (9), and β_e is the phase constant of the empty waveguide. From this one finds that the differential phase shift is given by

$$\beta_+ - \beta_- = 2\chi_{xy}' k \frac{S'}{S} \sin 2kx. \tag{44}$$

This states that for a ferrite of any shape the position of maximum differential phase shift for thin slabs or rods is at L/4 in rectangular guide where L is the guide width. Consequently for the vertical slab and the circular rod the position for maximum differential phase shift does not correspond to the position for circular polarization inside the ferrite.

The quarter position is not necessarily the position for the maximum value of the ratio of the differential phase shift to the total loss in a device such as a circulator. This again we shall call the figure of merit F and shall define as

$$F = \frac{\beta_+ - \beta_-}{\frac{1}{2}(\alpha_+ + \alpha_-)}. \tag{45}$$

The factor of $\frac{1}{2}$ for the attenuation constant arises from the fact that the ferrite loaded waveguide in a circulator carries only one-half the energy in either direction of transmission. Using the results of (43) and (44) we obtain

$$F = \frac{4\chi_{xy}'\beta k \sin 2kx}{\beta^2\chi_{xx}'' + k^2\chi_{yy}'' + (k^2\chi_{yy}'' - \beta^2\chi_{xx}'')\cos 2kx}. \tag{46}$$

When the above is maximized for the figure of merit as a function of position, *i.e.*, $dF/dx = 0$, we obtain

$$\cos 2kx = \frac{\beta^2\chi_{xx}'' - k^2\chi_{yy}''}{\beta^2\chi_{xx}'' + k^2\chi_{yy}''}. \tag{47}$$

This is exactly the same result that we derived for the resonance isolator. This means that the position is frequency dependent. At midband frequency for the flat horizontal slab the position is again at the quarter point. Hence, since this again corresponds to circular polarization within the ferrite, it appears that this geometry should provide the most effective phase shifter in a practical device. This should permit a closer approach to the theoretical figure of merit if an appropriate matching dielectric is used. The exact theory has shown[18] that the vertical slab with its dielectric effect which concentrates the energy in the ferrite may provide the largest differential phase shift for a given cross sectional area of ferrite. From (46) and (47) we find that the value of F_{max} becomes

[17] M. L. Kales, H. N. Chait, and N. G. Sakiotis, "A nonreciprocal microwave component," *J. Appl. Phys.*, vol. 24, pp. 816–817; June, 1953.

[18] B. Lax, K. J. Button, and L. M. Roth, "Ferrite phase shifters in rectangular waveguide," *J. Appl. Phys.*, vol. 25, pp. 1413–1421; November, 1954.

[19] K. J. Button (unpublished).

$$F_{max} = \frac{2\chi_{xy}'}{\sqrt{\chi_{xx}''\chi_{yy}''}}. \quad (48)$$

For operation below resonance where $\omega \gg \omega_r$ we can show that for all the geometries

$$F_{max} \approx 2\omega T. \quad (49)$$

Above resonance at low frequencies where $\omega_r \gg \omega$ the figure of merit differs for the three ferrite configurations as follows

$$F_a \approx 0.9\omega T\left[1 + \frac{2\omega_0 + \omega_M}{5\sqrt{\omega_0(\omega_0 + \omega_M)}}\right]$$

$$F_b \approx 2\omega T$$

$$F_c \approx 0.9\omega T\left[1 + \frac{4\omega_0 - \omega_M}{5\sqrt{4\omega_0^2 - 2\omega_0\omega_M}}\right]. \quad (50)$$

For typical values of ω_0 and ω_M the horizontal slab has a slightly higher figure of merit above resonance, namely, $2\omega T$. This then can be used as the upper limit for the nonreciprocal phase shifter. It turns out that this value is equivalent to its analog for the Faraday rotator since for a circulator in rectangular guide the total differential phase shift required is 180°. The allowable attenuation (equivalent to 0.5 db insertion loss in the Faraday rotator) in this case is 2 db for a round trip, since only one-half of the energy passes through the ferrite. Therefore,

$$F = \frac{\beta_+ - \beta_-}{\frac{\alpha_+ + \alpha_-}{2}} = \frac{\pi}{\frac{0.24}{2}} = 2\omega T$$

or

$$\omega T = 13. \quad (51)$$

This is exactly the value obtained before for the circulator using the Faraday rotator. Hence, the low-frequency limit of the phase shifter under the most favorable circumstances, *i.e.*, single crystal with $\Delta H \approx 50$ oersteds, is about 1000 mc. With a polycrystalline ferrite the limit is approximately 2000 mc.

Broad Banding

A number of schemes for broad banding the nonreciprocal phase shifter have been proposed in the past. Perhaps the best scheme is the analog of the compensation method used by Murray Loss for broad banding the Faraday rotator. This method has been used by Weisbaum and Boyet[20] with success. The method involves the use of two ferrites on either side of the center of the waveguide as shown in Fig. 14(a). By varying any of the parameters such as the applied fields H_{1a}, H_{2a}, the magnetizations M_1, M_2, the positions d_1 and d_2 or the ferrite thickness δ_1 and δ_2 or any combinations of these

[20] S. Weisbaum and H. Boyet, "A double slab ferrite field displacement isolator at 11 kmc," PROC. IRE, vol. 44, pp. 554–555; April, 1956.

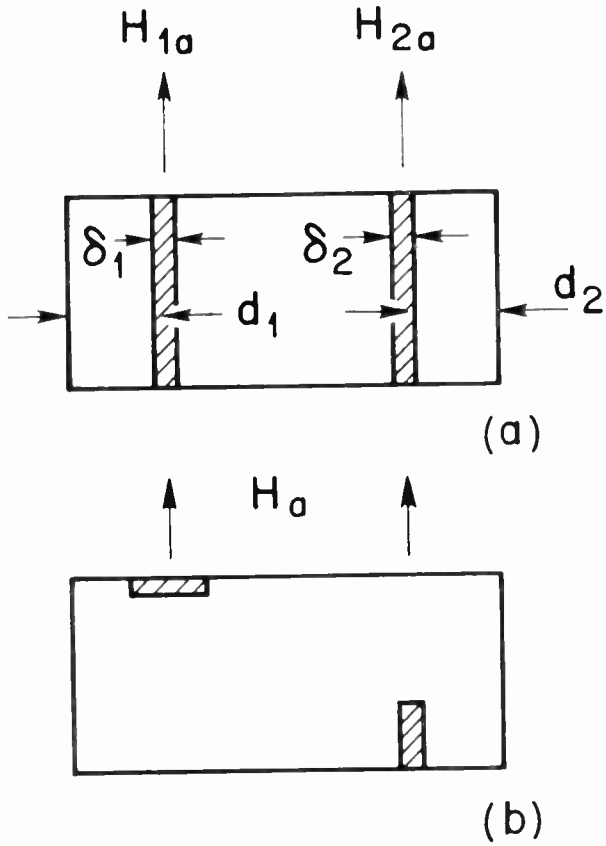

Fig. 14—Schemes for broad banding the nonreciprocal phase shifter. Compensation of phase shift variations due to frequency changes depend in (a) on different values of applied field, magnetization, thickness or position and in (b) on operation of one ferrite element above resonance and another below resonance.

it is possible in principle to obtain broad-band characteristics since the change in differential phase shift for the two ferrites compensate one another. This can again be readily seen from the perturbation results of (44) when applied to the two ferrite phase shifters

$$\Delta\beta = \Delta\beta_1 - \Delta\beta_2 = C\left[S_1\frac{\omega_{M1}\omega}{\omega^2 - \omega_{r1}^2} - S_2\frac{\omega_{M2}\omega}{\omega^2 - \omega_{r2}^2}\right] \quad (52)$$

assuming the positions of the two ferrites have been selected for optimum operation. This equation except for the constant C is identical to (24) for the Faraday rotator, emphasizing the analogy. Again, to obtain best performance, $\Delta\beta/d\omega = 0$ and

$$\frac{d^2\Delta\beta}{dx^2} \neq 0.$$

Using the same reasoning as before it may be possible to construct a better broad-banded shifter by operating one ferrite above resonance and the other below. This can be accomplished in either of two ways shown in Fig. 14(b) and Fig. 14(c). In either case the magnetization of each ferrite and the applied field can be chosen suitably. The advantage as before is that frequency compensation is obtained in a device in which the differential phase shifts add resulting in a better figure of merit. It is necessary, however, to use higher fields.

Another consideration that also arises in these compensated devices is that the change in the reciprocal parts of the phase shift should be broad banded. For instance, in the case of a circulator, the absolute phase shift is balanced in one direction by a dielectric in an adjacent branch. When both ferrites are operated below resonance the reciprocal part of the phase shifts add and hence changes in both ferrites with frequency will add. However, if one ferrite is operated above and the other below resonance, the reciprocal portions of the phase shift oppose and so will the changes with frequency. This can be seen readily from the expressions for the reciprocal phase shift obtained from (43) as follows:

$$\beta = C\left\{\beta_e\left[\frac{S_1\omega_{M1}(\omega_{01} - N_z\omega_{M1})}{\omega^2 - \omega_{r1}^2} + \frac{S_2\omega_{M2}(\omega_{02} - N_z\omega_{M2})}{\omega^2 - \omega_{r2}^2}\right] + \frac{k^2}{\beta_e}\left[\frac{S_1\omega_{M1}(\omega_{01} + \omega_{M1} - 2N_z\omega_{M1})}{\omega^2 - \omega_{r1}^2} + \frac{S_2\omega_{M2}(\omega_{02}\omega_{M2} - 2N_z\omega_{M2})}{\omega^2 - \omega_{r2}^2}\right] + \frac{2\omega^2\epsilon_0\mu_0}{\beta_e}\chi_e(S_1 + S_2)\right\}. \quad (53)$$

The frequency dependence of the phase shift due to the dielectric component of the ferrite can be balanced by the lossless dielectric in the adjacent arm.

Field Displacement Devices

Field Displacement Isolators

The two principal devices which use the field displacement properties of ferrite loaded waveguides are the field displacement isolator and the field displacement circulator. The former may be constructed in circular or rectangular waveguide. Melchor, Ayres, and Vartanian[10] constructed the circular type by placing an aquadag resistance strip inside a split ferrite rod 0.250 inch diameter as shown in Fig. 15. The loss for the negative polarized wave was large due to the electric field concentration in the ferrite and the loss for the positive polarized wave was small since the electric field was concentrated outside the ferrite. As in the case of the resonance isolator the corresponding structure for the rectangular waveguide field displacement isolator is simpler. The basic phenomenon in the two is very similar. If we use an analysis similar to that given for the circular guide we can again demonstrate the field displacement phenomenon from the results of the perturbation theory.

For practical reasons we shall only consider the TE_{on} modes. The presence of a slab in a rectangular waveguide will couple the higher modes to give a new field configuration which will differ for the two directions of propagation. Using the results of (20) and (21) we can calculate the coupling coefficients for these modes as follows:

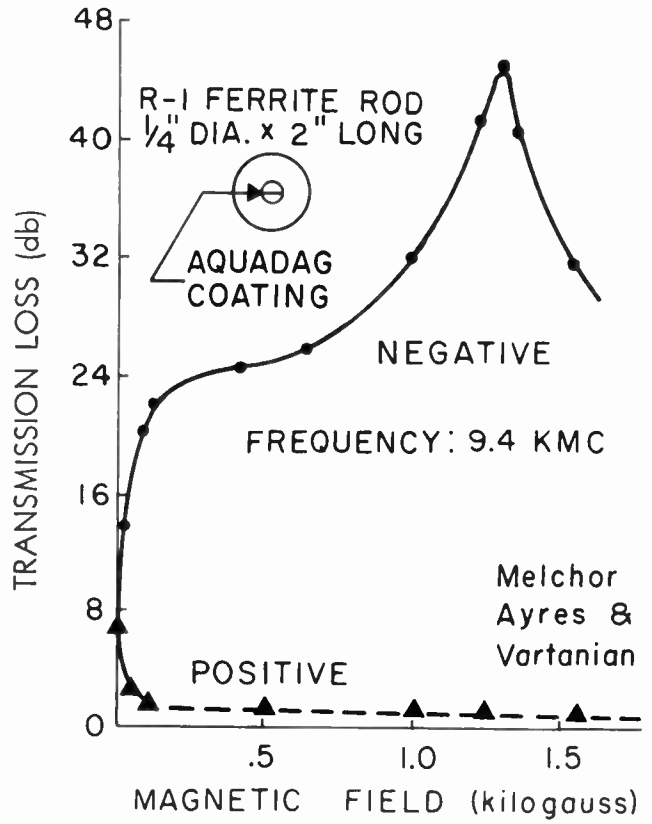

Fig. 15—Transmission loss in the reverse (negative polarization) and forward (positive polarization) direction of propagation for the cylindrical waveguide field displacement isolator. Reverse loss is provided by an aquadag coating inside a split ferrite rod.

$$C_n = \left[\chi_{xx}\beta_n\beta_1\int \sin k_n x \sin k_1 x dx + \chi_{yy}k_n k_1\int \cos k_n x \cos k_1 x dx \pm \kappa\left(k_n\beta_1\int \cos k_n x \sin k_1 x dx + \beta_n k_1\int \sin k_n x \cos k_1 x dx\right) + \frac{\omega^2}{C^2}\chi_e\int \sin k_n x \sin k_1 x dx\right]\frac{1}{(\beta_1 - \beta_n)\beta_n}. \quad (54)$$

If the slab is near the wall the expression for a slab which is not too large may be approximated by

$$C_n \approx \frac{k_n k_1}{(\beta_1 - \beta_n)\beta_n}\left[\chi_{xx}\beta_n\beta_1\frac{\delta^3}{3} + \chi_{yy}\delta \pm \kappa(\beta_1 + \beta_n)\frac{\delta^2}{2} + \frac{\omega^2}{C^2}\chi_e\frac{\delta^3}{3}\right]. \quad (55)$$

Again the dielectric coupling of the higher modes is comparable to that of the magnetic coupling when the slab is of reasonable thickness. Since this is the case in an actual device we could consider the perturbation for the problem when the waveguide is solved for a thick dielectric slab against the wall. The functions in the

integrals would still be sinusoidal functions with more rapid variation within the dielectric than in the empty portion of the waveguide. Hence, in (54) the terms involving κ, the off-diagonal component of the tensor, can be made larger than the terms involving χ_{xx} and χ_{yy} by choosing the appropriate thickness and position of the slab. Under these circumstances a reversal of sign for the reverse direction of propagation can couple the higher modes in the manner shown in Fig. 16. For one direction of propagation we can concentrate the electromagnetic field in the ferrite and in the other, in the empty part of the waveguide.

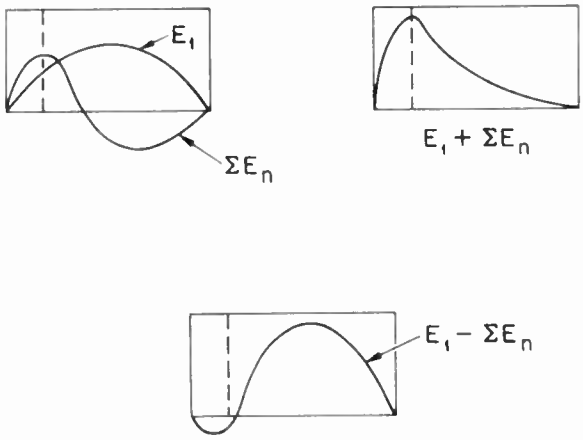

Fig. 16—Electric field intensities in rectangular waveguide with a ferrite slab against the side wall. The unperturbed mode, E_1, represents the field in the waveguide with a dielectric equivalent to ferrite (shown by dashed line). ΣE_n is the composite of higher modes coupled by the rf permeability of the ferrite

The field displacement isolator developed by Weisbaum and Seidel[21] uses the modified form of these configurations shown in Fig. 17. Here the ferrite slab is

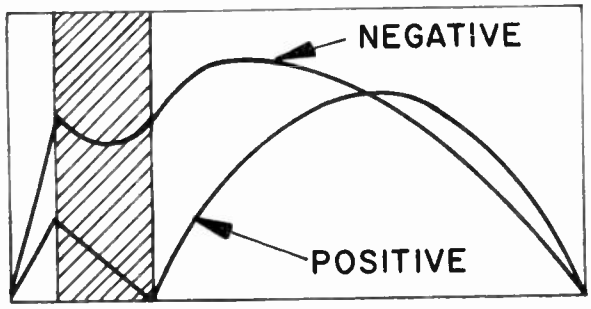

Fig. 17—Electric field configurations for a resistance-sheet field displacement isolator. A resistance sheet is placed against the face of the ferrite where, for the forward direction, the electric field intensity is zero.

displaced from the side wall and a resistance strip is placed on one side of the ferrite. This field configuration can be derived exactly theoretically when the losses in the ferrite and the resistance strip are neglected. As shown by Weisbaum and Seidel, the field at the resistance strip can be made zero for one direction of propagation resulting in little loss in this direction. For the other direction the energy is absorbed by the strip.

It is now necessary to define the figure of merit. Evidently for such an absorption device one should consider the ratio of the reverse-to-forward loss. In the forward direction the loss is primarily due to the ferrite. This small loss can be evaluated by perturbation theory because the exact field configurations can be utilized for this particular geometry. The loss calculation is carried out with integrals involving the imaginary components of the magnetic and dielectric susceptibilities and the analytical expressions for the rf fields. In the reverse direction one can again estimate the loss by perturbation theory if one integrates the field over the cross sectional area of the resistance sheet, knowing its conductivity or resistivity. These results will not be as simple as those for the idealized limits of the other three devices, but may be useful in estimating the possible limit of performance of this device.

Field Displacement Circulators

The four-port and three-port circulators,[3] shown in Fig. 18, also use the field displacement properties of

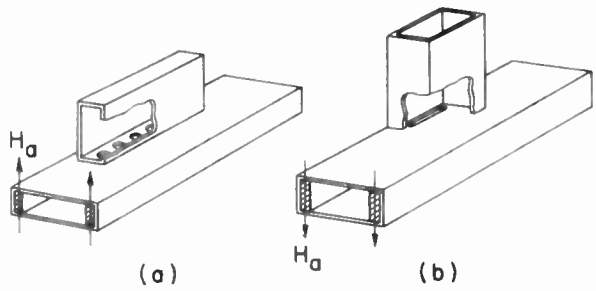

Fig. 18—The four-port and three-port field displacement circulators. These require the rf magnetic field to be displaced toward one side of the guide for forward propagation and toward the other side for reverse propagation (after Fox, Miller, and Weiss).

ferrite loaded rectangular guide. However, the circulators depend upon the property that the rf magnetic field is displaced to one side of the guide for the forward direction of propagation and to the other side for reverse propagation. The rf magnetic field configuration for forward propagation is shown in Fig. 19. These are theoretical results obtained for the lossless case.[22] The component which is of interest is the h_y or longitudinal rf field which couples energy into the holes or slot at the top of the guide near one ferrite. For one direction of propagation the amplitude near the face of the left-hand slab is large and with the proper circuitry nearly all the energy is coupled to the upper guide. For the other direction of propagation the peak intensities of the h_y field will appear on the right so that the field is small near the slot and very little energy is coupled to the upper guide.

[21] S. Weisbaum and H. Seidel, "The field displacement isolator" (to be published).

[22] K. J. Button and B. Lax, "Theory of Ferrites in Rectangular Waveguides," M. I. T. Lincoln Lab. Tech. Rep. No. 89; August, 1955.

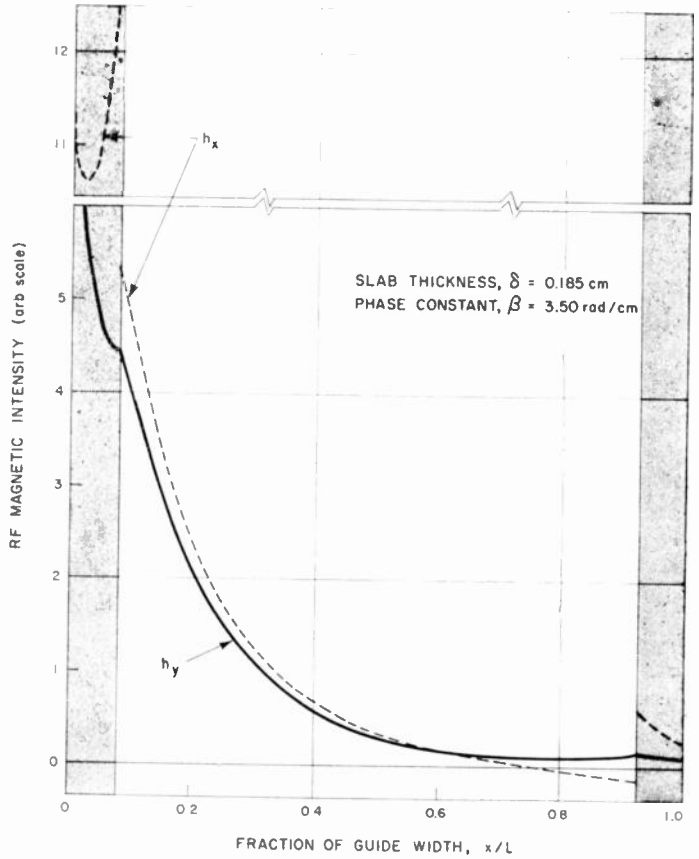

Fig. 19—The rf magnetic field components of the dielectric (field displacement) mode for one direction of propagation. The peak intensities will appear on the right for the opposite direction of propagation.

It is difficult to define a figure of merit for this device. However, what is desired is a low insertion loss and a large differential coupling of the longitudinal rf magnetic field near the ferrite slabs. Fundamentally this type of structure has a fair amount of loss associated with it since the electromagnetic field is concentrated in the ferrites. This means that the losses due to the magnetic and dielectric absorption are high. Assuming that one obtains low-loss ferrites, then one can again evaluate the insertion loss by the perturbation theory since one can solve for the field configuration from the nonlossy case. When the loss is larger the problem is more difficult. K. J. Button has obtained the exact solution for the case of a ferrite dielectric mode for such a lossy situation taking into account only the magnetic loss. He has shown that the loss decreases with magnetic field as one approaches resonance. This is shown in Fig. 20. The reason for this decrease in loss is accounted for by the fact that as one increases the dc magnetic field the permeability for the medium becomes more negative and the penetration into the ferrite decreases resulting in less concentration of electromagnetic energy in the ferrite. Consequently the loss is reduced. One of the difficulties with this scheme of using a dc magnetic field near resonance is that the longitudinal rf field minimum increases, reducing the effectiveness of the device. The most effective operational point of the device according to E. H. Turner[23] is where $\mu \approx \kappa$. This is also the criterion for the optimum operation of the resonance isolator leading to an electric field null. For the field displacement circulator essentially the same principle applies. One can write the dispersion relation for the electromagnetic wave in the ferrite medium as follows:

$$k_m^2 + \beta^2 = \omega^2 \epsilon \mu_{eff} \tag{56}$$

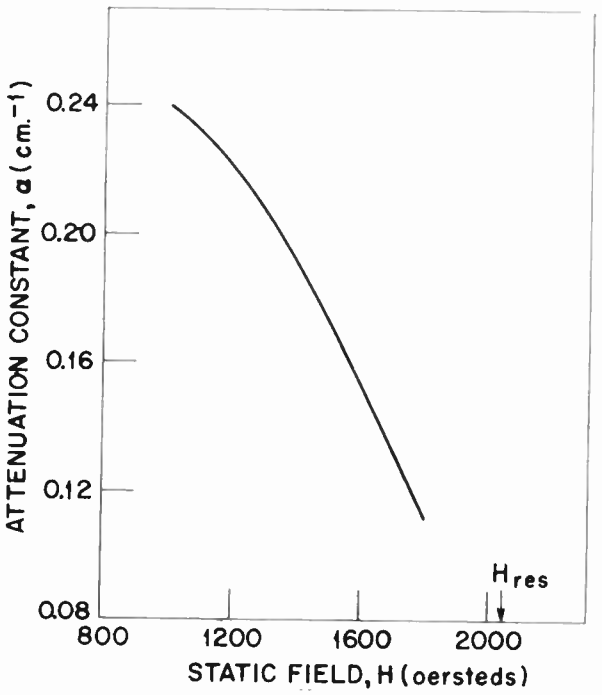

Fig. 20—Attenuation constant vs internal dc field for the rectangular waveguide dielectric mode. This computation was carried out at 9000 mc for a single ferrite slab, 1 millimeter thick, against the side wall of the guide.

where k_m is the transverse wave number and $\mu_{eff} = (\mu^2 - \kappa^2)/\mu$ is the effective permeability which is plotted in Fig. 21. Evidently when $\mu = \kappa$, $\mu_{eff} = 0$ and for propagation we obtain real values of β resulting in imaginary values of k_m or hyperbolic dependence of the field components. This signifies an exponential or decaying penetration of the electromagnetic wave into the ferrite medium in the transverse plane. Such exponential field patterns are characteristic of the field displacement devices and are only obtained when the magnetic field is below resonance since μ_{eff} must be $\leqq 0$.

When $\mu_{eff} = 0$, it can be shown that the field configuration for a single slab against the wall is that given by Fig. 22(a).

[23] E. H. Turner, "Field displacement isolators at 55 kmc," URSI-Michigan Symposium on Electromagnetic Wave Theory, Ann Arbor, Michigan; June, 1955.

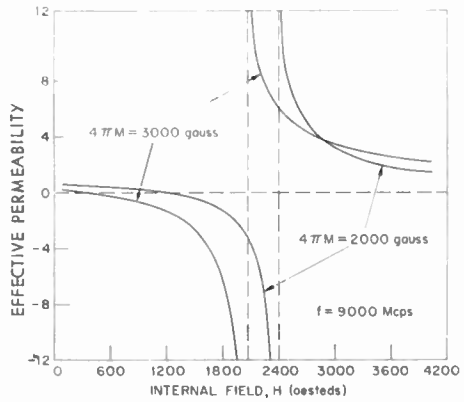

Fig. 21—Effective permeability of ferrite for transverse propagation vs internal dc magnetic field for two different values of saturation magnetization.

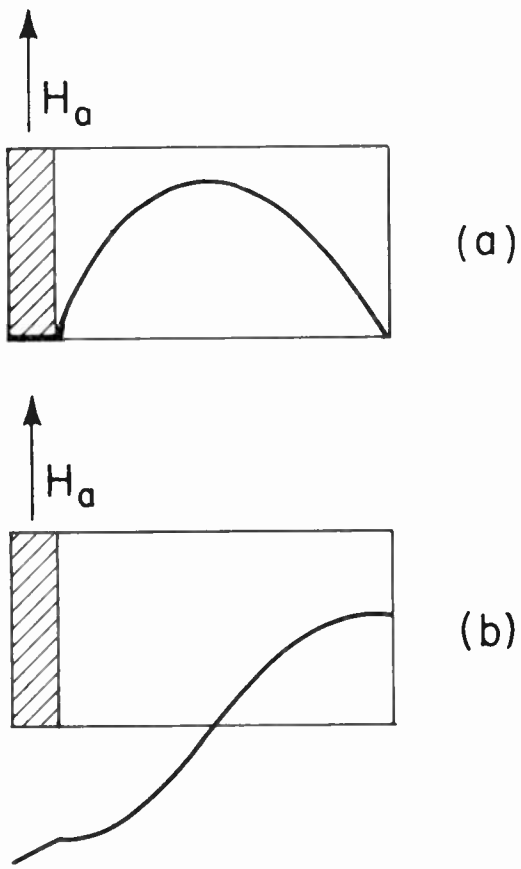

Fig. 22—RF field configurations for $\mu_{eff}=0$ for transverse magnetization: (a) electric field, (b) longitudinal component of magnetic field.

Therefore

$$\beta^2 = \omega^2\epsilon_0\mu_0 - \left(\frac{\pi}{L-\delta}\right)^2. \tag{57}$$

Since all parameters of (57) are determined, this implies that the mode is reciprocal. Consequently, one cannot build a nonreciprocal field displacement device with the slab against the wall. It is, therefore, not surprising that Weisbaum and Seidel found that the slab displaced from the wall provided an optimum design.

Another interesting fact is revealed by the longitudinal component of the rf magnetic field shown in Fig. 22(b). This indicates that the magnetic field is rather large in the ferrite and, therefore, must be taken into account in calculating the forward loss in an isolator.

Discussion

We have neglected the discussion of the influence of dielectric losses on each of the ferrite devices because, in principle, the proper ferrites should contribute little or no such losses. However, some results have been reported in the literature which indicate the existence of dielectric loss. These losses can bring about a reduction in the figure of merit of the devices that we have treated. In particular, the absorption isolators would fare badly because the dielectric loss would increase the forward loss in greater proportion than the reverse loss. This would reduce the reverse-to-forward ratio considerably. For the other devices, it would simply result in an increased insertion loss.

In discussing the four principal ferrite devices the theoretical treatment tacitly assumed that the ferrite medium was operating at low power levels. The values of line width used it to obtain the figure of merit are those measured at low levels. At high powers the situation may change. It was shown by Bloembergen and Damon[24] and also by Bloembergen and Wang[25] that at high power levels the rf magnetic field may reach a critical value which produces broadening of the lines and increases the loss. The explanation of this phenomenon has been discussed by H. Suhl.[26] The consequences of this phenomenon have also been observed by Sakiotis, Chait, and Kales[27] in waveguides. They have carried out measurements in both circular and rectangular guides with ferrite bodies sufficiently large to produce the dielectric modes in the guide. The resultant enhancement of the rf field in the ferrite produced losses which increased with power level as shown in Fig. 23. This is another manifestation of the instability of the spin system which can absorb additional energy beyond a critical value of the rf field. The obvious consequence

[24] N. Bloembergen and R. W. Damon, "Relaxation effects in ferromagnetic resonance," *Phys. Rev.*, vol. 85, p. 699; February, 1952.
R. W. Damon, "Relaxation effects in the ferromagnetic resonance," *Rev. Mod. Phys.*, vol. 25, pp. 239–245; January, 1953.

[25] N. Bloembergen, and S. Wang, "Relaxation effects in para- and ferromagnetic resonance," *Phys. Rev.*, vol. 93, pp. 72–83; January, 1954.

[26] H. Suhl, "Subsidiary absorption peaks in ferromagnetic resonance at high signal levels," *Phys. Rev.*, vol. 101, pp. 1437–1438; February, 1956.
P. W. Anderson and H. Suhl, "Instability in the motion of ferromagnets at high microwave power levels," *Phys. Rev.*, vol. 100, pp. 1788–1789; December, 1955.

[27] N. Sakiotis, H. N. Chait, and M. L. Kales, "Nonlinearity of propagation in ferrite media," Proc. IRE, vol. 43, p. 1011; August, 1955.

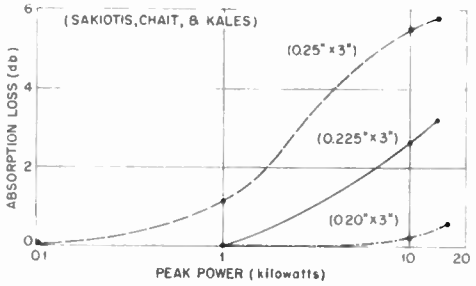

Fig. 23—Absorption loss of a negative circularly polarized wave in a rod of magnesium-manganese ferrite vs rf peak power for three different ferrite diameters. The applied dc field is 450 oersteds.

of the increased loss and reduction of the figure of merit of the devices at high power will raise the lower frequency limit of the application of these devices. To counteract this we must reduce the dimension of the ferrite to avoid the onset of the dielectric modes. We should also use the configurations of the ferrite bodies which are unfavorable for exciting the growth of spin waves at high power level.

Acknowledgment

I would like to express my appreciation to K. J. Button for a great deal of assistance in the preparation of this paper and for many helpful discussions and suggestions on the technical aspects of this material. The author also acknowledges the fruitful discussions and suggestions of Dr. Gerald S. Heller. I am grateful to Drs. S. Weisbaum and H. Seidel for sending me a copy of their article on the field displacement isolator prior to publication.

Ferrites as Microwave Circuit Elements*

GERALD S. HELLER†

Summary—**This paper is intended to be tutorial in nature and its purpose is the description of the effects of magnetically saturated ferrites in microwave structures from the more general approach of microwave circuit theory. This is done via the scattering matrix rather than the impedance matrix. Since most of the important properties of such circuits depend on the fact that the circuit behaves differently when the direction of propagation is reversed, the scattering matrix seems to be a more natural mode of description than the impedance matrix from which these effects are not immediately evident.**

The properties of the scattering of microwave junctions containing magnetically saturated media are discussed. It is shown that except for nonreciprocity, the scattering matrix of such junctions satisfy the same requirements as that of junctions containing ordinary scalar media. The general scattering matrix of a lossless two port device is given. The circulator is discussed and a particular microwave circuit, of which several proposed circulators are a special case, is treated. Conditions on the elements of this circulator, in order that it be a perfect circulator, are derived. Finally deviations from the ideal circulator conditions are considered.

Introduction

THE SOLUTION of boundary value problems in which ferrite media are involved is a formidable task. Even the simpler cases of infinitely long waveguides, completely filled with magnetically saturated ideal ferrite media, yield solutions which are amenable to computation in only very special cases.[1–4] Infinitely long waveguides whose cross sections are not completely filled with ferrite are still more complicated and only one such solution has yielded numerical values of propagation constant and field configurations for some of the modes.[5] The perturbation theory,[6–8] is available for the approximate solution of such problems if a small enough fraction of the cross section is filled. The use of variational principles also shows some promise.[9,10]

Numerical solutions for waveguides containing pieces of ferrite of finite length are at present unavailable. In

* Original manuscript received by the IRE, July 3, 1956. The research reported in this document was supported jointly by the Army, Navy, and Air Force, under contract with the Massachusetts Institute of Technology, Cambridge, Mass.

† Lincoln Lab., M.I.T., Lexington, Mass.

[1] M. L. Kales, "Modes in waveguides containing ferrites," *J. Appl. Phys.*, vol. 24, p. 604; May, 1953.

[2] H. Suhl and L. R. Walker, "Topics in guided wave propagation through gyromagnetic media," *Bell Sys. Tech. J.*, vol. 33, p. 579; May, 1954.

[3] H Gamo, "Faraday rotation of waves in a circular waveguide," *J. Phys. Soc. (Japan)*, vol. 8, p. 176; March, 1953.

[4] A. A. Th. M. Van Trier, "Guided electromagnetic waves in anisotropic media," *Appl. Sci. Res.*, sec. B, vol. 3, p. 142; 1953.

[5] B. Lax, K. J. Button, and L. M. Roth, "Ferrite phase shifters in rectangular waveguide," *J. Appl. Phys.*, vol. 25, p. 1413; November, 1954.

[6] A. D. Berk and B. Lax, "Cavities with complex media and resonances in cavities with complex media," 1953 IRE Convention Record, part 10, pp. 65–74.

[7] H. Suhl and L. R. Walker, "Topics in guided wave propagation through gyromagnetic media," Part III, "Perturbation theory and miscellaneous results," *Bell. Sys. Tech. J.*, vol. 32, pp. 1133–1194; September, 1954.

[8] G. S. Heller and B. Lax, "Use of perturbation theory for cavities and waveguides containing ferrites," URSI/Symposium on Electromagnetic Theory, Univ. of Michigan, Ann Arbor, Mich.; June 21–25, 1955.

[9] A. D. Berk, Sc. D. Thesis, M. I. T.; September, 1954.

[10] W. Hauser, Lincoln Lab. Quart. Prog. Rep. (Solid-State Group) 1954–1955.

practice the cross section of the ferrite is either very small or the ends are tapered so that the reflection from the ends of the ferrite are negligible. In this case the infinitely long waveguide solutions can give useful information concerning the propagation properties of finite ferrite filled waveguides. The effect of such tapers is at this time empirical. For unbounded media, there is theoretical numerical data showing the effect of finite length on the Faraday rotation of a plane wave due to a finite slab of infinite lateral extent.[11] Even the simple analytical solution of Van Trier,[4] for the transversely magnetized completely filled rectangular waveguide, cannot be used to give numerical results for the reflection from a finite piece of ferrite without laborious mathematical computation.

Most ferrite devices may be considered as a junction of several ordinary transmission lines (coaxial lines or waveguides) which at reference planes far enough from the junction containing the ferrite, support the usual modes of transmission whose field configurations are known. The behavior of such junctions may be described by the various transmitted and reflected amplitudes of the waves in the various leads of the junction (scattering matrix of the junction) when either all or some of the leads are excited rather than the detailed description of the electromagnetic fields in the junctions. Although knowledge of this detailed description is necessary for the exact calculation of the elements of the scattering matrix certain general relations concerning these elements may be inferred from energy considerations and from the physical structure (symmetry) of the junction. Although the junction may also be described in terms of an impedance matrix the scattering matrix seems to be a more *natural* mode of description.

It will be our purpose here to introduce the concept of the scattering matrix to those who are not familiar with it and to discuss some of the properties of the scattering matrix of junctions containing ferrite media. Finally, some applications to devices such as circulators will be discussed.

Scattering Matrix of Junctions Containing Asymmetrical Tensor Media

The scattering matrix of junctions containing isotropic media have been described by Montgomery, Dicke, and Purcell.[12] A more complete account and the extension to media, described by symmetrical tensors, has been given by Kerns[13] and an extension to junctions containing ferrite media was made by Fowler.[14]

[11] M. A. Gintzberg, "On the propagation of electromagnetic waves in gyromagnetic layers," Doklady, A. N. USSR, vol. 95, p. 753; 1954.

[12] C. G. Montgomery, R. H. Dicke, and E. M. Purcell, "Principles of Microwave Circuits," McGraw-Hill Book Co., Inc., New York, N. Y., chs. 5 and 12; 1948.

[13] D. M. Kerns, "Analysis of symmetrical waveguide junctions," *J. Res. NBS*, vol. 46, p. 4; April, 1951.

[14] H. Fowler, paper presented at Symposium on Microwave Properties and Applications of Ferrites, Harvard Univ., Cambridge, Mass; April, 1956. Also, private communication, February, 1955.

Consider a junction of several empty waveguides whose walls are of perfect conductors (Fig. 1). Each guide can be considered as propagating only one mode to which corresponds a single propagation constant. If the frequency or size of the guide is such that a single physical guide can support more than one mode then a separate junction lead or port is assigned to each mode. Thus the number of ports may be a function of frequency. The orthogonality of the modes in any one lead insures that there is no coupling between them.

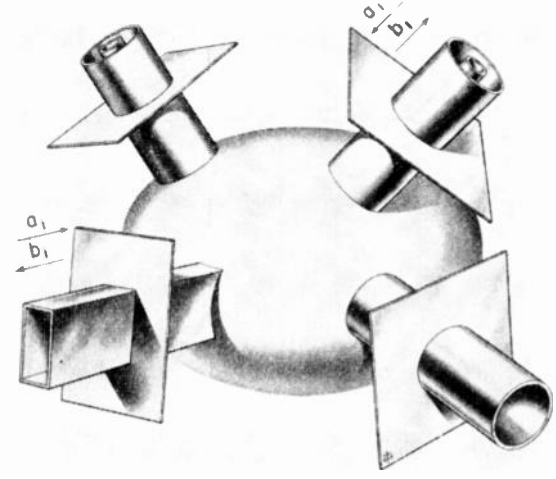

Fig. 1—General microwave junction showing reference planes. The first and ith incident and reflected waves are labeled at their respective reference planes.

Reference planes for each of the leads are chosen far enough away from the junction so that all cutoff modes excited by the junction are of negligible amplitude. The electromagnetic fields in the various leads may be normalized so that the elements of the scattering matrix are independent of the different characteristic impedances of each of the lead guides.[15] Then if a_i represents the incident wave at the reference plane of the ith lead, then the reflected amplitude b_j at the reference plane of the jth lead is given by

$$b_j = S_{j1}a_1 + S_{j2}a_2 + \cdots + S_{jn}a_n.$$

There is one such relation for each port and in matrix notation they may be written

$$\begin{bmatrix} b_1 \\ b_2 \\ \cdot \\ \cdot \\ b_n \end{bmatrix} = \begin{bmatrix} S_{11} & S_{12} \cdots S_{1n} \\ S_{21} & S_{22} \cdots S_{2n} \\ \cdot & \\ \cdot & \\ S_{n1} & S_{n2} \cdots S_{nn} \end{bmatrix} \begin{bmatrix} a_1 \\ a_2 \\ \cdot \\ \cdot \\ a_n \end{bmatrix}$$

The square array of quantities S_{ij} is the scattering matrix of the junction. Note that S_{jj} represents the reflection coefficient in the jth lead so that if that lead

[15] A. E. Pannenburg, "Scattering Matrices of Symmetrical Networks," Philips Res. Rep., vol. 7, pp. 131–57, 169–88, and 270–302; 1952.

is matched $S_{jj}=0$. The incident and reflected mean square power in the ith lead are given by $\frac{1}{2}a_ia_i^*$ and $\frac{1}{2}b_ib_i^*$ respectively where a_i^* is the complex conjugate of a_i. S_{ij} represents the wave traveling out of the ith lead due to an incident wave of unit amplitude on the jth lead.

Nonreciprocity of the Scattering Matrix

It is instructive to observe the way in which nonsymmetry of the tensor describing the media inside the junction induces a nonsymmetric scattering matrix. Let us assume that within the junction there is a volume V_1 which contains a material whose dielectric constant and permeability are given by the tensors $\epsilon_{ij}=\overleftrightarrow{\epsilon}$ and $\mu_{ij}=\overleftrightarrow{\mu}$. Then inside V_1, Maxwell's equations are, for harmonically time dependent fields,

$$\nabla \times \boldsymbol{E} = -j\omega\overleftrightarrow{\mu}\cdot \boldsymbol{H},$$

$$\nabla \times \boldsymbol{H} = +j\omega\overleftrightarrow{\epsilon}\cdot \boldsymbol{E},$$

while outside V_1 the tensors μ and ϵ reduce to ordinary scalars. Let $\boldsymbol{E}^{(1)}$, $\boldsymbol{H}^{(1)}$ represent the electromagnetic field in the junction when there is an incident wave only on the mth lead. Similarly $\boldsymbol{E}^{(2)}$, $\boldsymbol{H}^{(2)}$ represents the electromagnetic field in the junction when only the nth lead is excited (Fig. 2). Then

$$\nabla\cdot(\boldsymbol{E}^{(1)}\times\boldsymbol{H}^{(2)} - \boldsymbol{E}^{(2)}\times\boldsymbol{H}^{(1)}) = j\omega[(\boldsymbol{H}_1\cdot\overleftrightarrow{\mu}\boldsymbol{H}_2 - \boldsymbol{H}_2\cdot\overleftrightarrow{\mu}\boldsymbol{H}_1) + (\boldsymbol{E}_2\cdot\overleftrightarrow{\epsilon}\boldsymbol{E}_1 - \boldsymbol{E}_1\cdot\overleftrightarrow{\epsilon}\boldsymbol{E}_2)]. \quad (1)$$

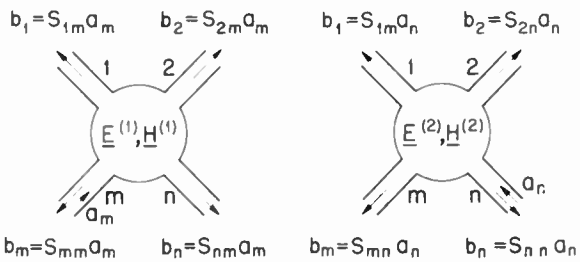

Fig. 2—Definition of the fields ($\boldsymbol{E}^{(1)}$, $\boldsymbol{H}^{(2)}$), and ($\boldsymbol{E}_2$, $\boldsymbol{H}_2$) used in the derivation of the nonreciprocity relation for the scattering matrix of a junction containing a magnetically saturated ferrite.

If (1) is integrated over the volume bounded by the junction and the reference planes in the various leads, and the divergence theorem applied to the left hand side, we have

$$\sum_i \int (\boldsymbol{E}_i^{(1)}\times\boldsymbol{H}_i^{(2)} - \boldsymbol{E}_i^{(2)}\times\boldsymbol{H}_i^{(1)})\cdot\boldsymbol{n}_i ds^i = j\omega\int[(\boldsymbol{H}_1\cdot\overleftrightarrow{\mu}\boldsymbol{H}_2 - \boldsymbol{H}_2\overleftrightarrow{\mu}\boldsymbol{H}_1) + (\boldsymbol{E}_2\cdot\overleftrightarrow{\epsilon}\boldsymbol{E}_1 - \boldsymbol{E}_1\overleftrightarrow{\epsilon}\boldsymbol{E}_2)]dV \quad (2)$$

where $\boldsymbol{n}_i$ and ds^i represent the outward normal to the ith reference plane and the element of area in that plane respectively. The integration over the surface of the junction has vanished everywhere except at the reference planes because of the boundary condition that the electric field be normal to the perfectly conducting surface of the junction. In terms of the scattering matrix (2) becomes:

$$S_{mn} - S_{nm} = \frac{j\omega}{2a_na_m}\left[\overleftrightarrow{(\mu - \tilde{\mu})}\cdot\int_{V_1}\boldsymbol{H}^{(1)}\boldsymbol{H}^{(2)}dV + \overleftrightarrow{(\epsilon - \tilde{\epsilon})}\cdot\int_{V_1}\boldsymbol{E}^{(1)}\boldsymbol{E}^{(2)}dV\right] \quad (3)$$

where $\tilde{\overleftrightarrow{\mu}}$ and $\tilde{\overleftrightarrow{\epsilon}}$ are defined by $\tilde{\mu}_{ij}=\mu_{ji}$ and $\tilde{\epsilon}_{ij}=\epsilon_{ji}$. Eq. (3) as pointed out by Fowler,[14] shows the nonsymmetry of the scattering matrix in terms of the nonsymmetry of the permeability and dielectric-constant tensors. For a magnetically saturated ferrite medium the relation between $\boldsymbol{B}$ and $\boldsymbol{H}$ may be written (See Appendix)

$$B = \mu_0[j\kappa\boldsymbol{k}\times\boldsymbol{H} - \chi\boldsymbol{k}\times\boldsymbol{k}\times\boldsymbol{H} + \boldsymbol{H}] \quad (4)$$

where $\boldsymbol{k}$ is a unit vector in the direction of the applied magnetic field and χ and κ are the usual diagonal and off-diagonal components of the permeability tensor. Eq. (3) now becomes

$$S_{mn} - S_{nm} = \omega\mu_0\kappa\int_{V_1}\boldsymbol{k}\cdot(\boldsymbol{H}^{(1)}\times\boldsymbol{H}^{(2)})dV_1. \quad (5)$$

where the incident amplitudes have been set equal to unity. Note that if the direction of $\boldsymbol{k}$ is reversed (*i.e.*, the applied magnetic field) then the sign of $S_{mn}-S_{nm}$ is reversed. Note that the scattering matrix is nonsymmetrical only if the integral in (5) is nonvanishing so that only certain special field configurations will lead to nonsymmetrical matrices. This is discussed further by Fowler.[14]

Conservation of Energy

We shall now see what conditions are imposed on the scattering matrix by requiring that energy be conserved. The difference between the total power incident, P_{in}, and total power reflected, P_r, from the junction is given by

$$P_{in} - P_{out} = 1/2\sum_i a_ia_i^* - b_ib_i^* \geqq 0. \quad (6)$$

This difference must be equal to the power dissipated in the junction. This power dissipation may be due to either dielectric or magnetic loss within the junction, and must always be positive except for the lossless case when it is zero.

If (6) is rewritten in terms of the scattering matrix, we have

$$\sum_i\left[a_ia_i^* - \sum_{jk}S_{ij}S_{ik}a_ja_k^*\right] \geqq 0$$

or, in terms of matrix notation

$$\tilde{a}^*[I - \tilde{S}^*S]a \geqq 0 \tag{7}$$

where a is the (column) matrix of the input amplitudes, the symbol $\tilde{S}$ means the transposition (interchange of rows and columns) of S and I is the unit matrix. The condition (7) occurs frequently in the theory of quadratic forms, and the conditions on the matrix $I-\tilde{S}^*S$ such that (7) be satisfied is that all the determinants that can be formed from $I-\tilde{S}^*S$ by striking out rows and columns containing elements from the principal diagonal be positive, *i.e.*, all the principal minors are positive.[16]

This criterion is independent of whether the junction is reciprocal or not and can be used to test a scattering matrix as to its reliability.

If there is no loss in the junction, then condition (7) becomes

$$\tilde{S}^*S = I. \tag{8}$$

A matrix which satisfies (8) is called a *unitary* matrix. Therefore, a lossless nonreciprocal device of the type considered has a unitary scattering matrix.

Scattering Matrix for a Nonreciprocal Lossless Two Port Junction

A two-port junction has the general scattering matrix,

$$\begin{pmatrix} S_{11} & S_{12} \\ S_{21} & S_{22} \end{pmatrix},$$

where in general $S_{21} \neq S_{12}$. If we substitute this matrix into (8), we have the following relations.

$$\begin{aligned} S_{11}S_{11}^* + S_{21}S_{21}^* &= |S_{11}|^2 + |S_{21}|^2 = 1 \\ S_{12}S_{12}^* + S_{22}S_{22}^* &= |S_{12}|^2 + |S_{22}|^2 = 1 \\ S_{11}^*S_{12} + S_{21}^*S_{22} &= 0 \\ S_{11}S_{12}^* + S_{21}S_{22}^* &= 0. \end{aligned} \tag{9}$$

Only three of the above equations are independent since the last is merely the complex conjugate of the third. Since the elements of the scattering matrix are complex, (9) gives 4 relations among the eight independent matrix elements. This must yield four independent parameters for the scattering matrix. The physical meaning of (9) is apparent from Fig. 3. The first two equations are expressions of conservation of energy when there is an incident wave only on either port 1 or port 2 respectively. The third or fourth takes care of the *interference* between waves when both ports are simultaneously excited. From the above relations it is easy to see that it is impossible to make a lossless one-way transmission line. If there is no transmission of energy from port 1 to port 2 then $S_{21}=0$. Then according to the first of (9) we must have $|S_{11}|^2=1$, *i.e.*, perfect reflection. The third then yields $S_{12}=0$ or no transmission from port 2 to port 1.

[16] H. J. Carlin, "Principles of Gyrator Networks," Proc. Symposium Modern Advances in Microwave Techniques, Polytech. Inst. of Bklyn., Bklyn, N. Y.; November 8–10, 1954.

Utilizing the relations between the matrix elements given by (9), the scattering matrix for a general nonreciprocal two-port may be written

$$\begin{pmatrix} ae^{j\alpha} & \sqrt{1-a^2}e^{j(\alpha-\phi)} \\ -\sqrt{1-a^2}e^{j(\delta+\phi)} & ae^{j\delta} \end{pmatrix} \tag{10}$$

where a, α, ϕ, and δ are real quantities. By shifting reference planes (Appendix) the above matrix may be written in terms of two real parameters a and θ.

$$\begin{pmatrix} a & \sqrt{1-a^2}e^{j\theta} \\ -\sqrt{1-a^2}e^{-j\theta} & a \end{pmatrix}. \tag{11}$$

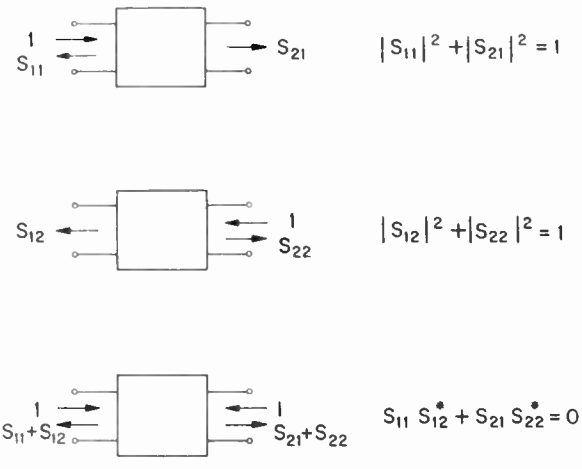

Fig. 3—Physical significance of the unitary condition for a lossless two-port junction.

The above matrix is of course a special case in which particular reference planes are chosen. All two-port lossless junctions containing saturated ideal ferrite media must be of the form shown above. It is interesting to note that the scattering matrices derived for several specific two-port devices are all of the form given above. For example, Steinman[17] has considered the scattering matrix of a lossless nonideal gyrator containing a 90° ferrite rotator in which the effect of deviations from the ideal 90° rotation are considered.

In passing it may be mentioned that a nonreciprocal lossless n-port device can in general be described by n^2 independent real parameters while the reciprocal network requires only $n(n+1)/2$ parameters.

Application to Circulator

A circulator[18] is a network which may be represented by the circuit shown in Fig. 4(a). Each of the numbered arms are microwave transmission lines. In an ideal circulator, power may flow only from port 1 to port 2, port 2 to port 3, etc. Although there is no restriction on the number of ports, most of the circulators proposed have been four-port circulators. All of these may

[17] B. Steinman, "Analysis of Some Microwave Ferrite Devices," Rep. R-367/54, M. R. I., Polytech. Inst. of Bklyn.; February, 1954.

[18] C. L. Hogan, "The microwave gyrator," *Bell Sys. Tech. J.*, vol. 31, pp. 1–31; January, 1952.

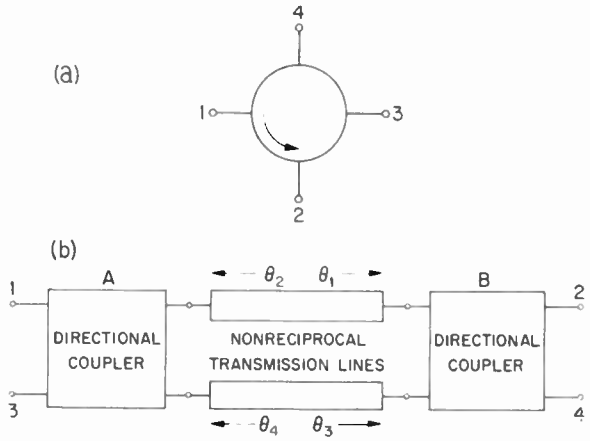

Fig. 4—(a) Symbol for a circulator. (b) Representation of a four-port circulator in terms of two directional couplers A and B, and two lossless nonreciprocal transmission lines.

be represented by a combination of directional couplers and nonreciprocal transmission lines.[19] Fig. 5 shows several types of circulators and Fig. 4(b) their common schematic representation in terms of the two directional couplers A and B and the nonreciprocal transmission lines.

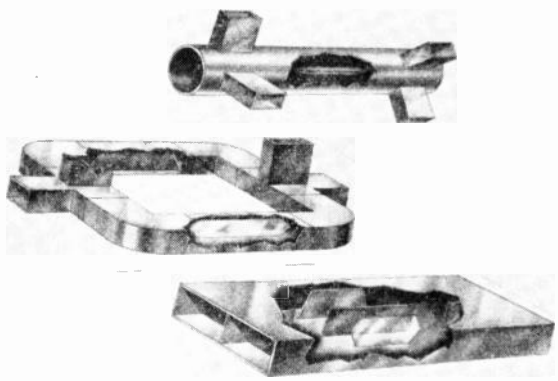

Fig. 5—Several four-port circulators.

We can now discuss the conditions on the directional couplers and the nonreciprocal transmission lines in order that the diagram of Fig. 4(b) be a circulator. In order to do this we shall have to obtain the scattering matrices of circulators and directional couplers.

The general 4-port has a scattering matrix

$$\begin{pmatrix} S_{11} & S_{12} & S_{13} & S_{14} \\ S_{21} & S_{22} & S_{23} & S_{24} \\ S_{31} & S_{32} & S_{33} & S_{34} \\ S_{41} & S_{42} & S_{43} & S_{44} \end{pmatrix}$$

If the four-port is matched at all terminals then $S_{21}=S_{22}=S_{33}=S_{44}=0$. If transmission is not allowed from port 2→1 then $S_{12}=0$, similarly (Fig. 3) $S_{41}=S_{34}=S_{23}=0$. Further, since ports 1 and 3 and 2 and 4 are decoupled, $S_{13}=S_{31}=S_{42}=0$. By suitable choice of reference planes,

$$S_{21} = S_{14} = S_{43} = S_{32} = 1.$$

The scattering matrix then becomes

$$S = \begin{pmatrix} 0 & 0 & 0 & 1 \\ 1 & 0 & 0 & 0 \\ 0 & 1 & 0 & 0 \\ 0 & 0 & 1 & 0 \end{pmatrix}.$$

It is more convenient for our purpose to renumber the ports replacing 1 2 3 4 by 1 4 2 3 respectively, giving as the scattering matrix

$$S = \begin{pmatrix} 0 & 0 & 1 & 0 \\ 0 & 0 & 0 & 1 \\ 0 & 1 & 0 & 0 \\ 1 & 0 & 0 & 0 \end{pmatrix}.$$

If the reference planes had been chosen arbitrarily, then each of the nonzero elements in the above matrix would contain an arbitrary phase factor.

The scattering matrix of a directional coupler depends on symmetry of the coupler. We consider first a coupler consisting of two guides side by side with the coupling in the common side wall as shown in Fig. 6(a). If the coupler is matched, $S_{11}=S_{22}=S_{33}=S_{44}=0$. From symmetry $S_{14}=S_{23}$, $S_{24}=S_{13}$ and $S_{12}=S_{34}$. Since this is a reciprocal device, the scattering matrix is symmetrical.

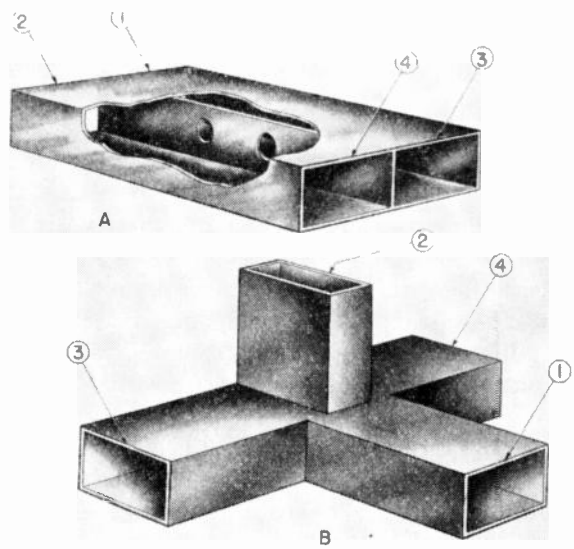

Fig. 6—(a) Side wall directional coupler. (b) Magic T.

We now have three independent elements S_{12}, S_{13}, and S_{14}. Applying the condition that the scattering matrix is unitary, we find that either S_{12}, S_{13}, or S_{14} vanishes, and the remaining two are orthogonal in the complex plane. By choosing the reference planes judiciously we

[19] R. H. Fox, A Non-Reciprocal Four-Pole Ring Circuit," M.I.T. Lincoln Lab. Tech. Rep., T-68; November, 1954.

can show that the scattering matrix may be written

$$\begin{pmatrix} 0 & 0 & \sqrt{1-f^2} & if \\ 0 & 0 & if & \sqrt{1-f^2} \\ \sqrt{1-f^2} & if & 0 & 0 \\ if & \sqrt{1-f^2} & 0 & 0 \end{pmatrix}$$

where $0 \leqq f \leqq 1$, and f is real. It is sometimes convenient to replace f by $\sin\theta$, where $0 \leqq \theta \leqq (\pi/2)$.

In the case of a rectangular waveguide hybrid magic T (Fig. 6(b)), the symmetry is such that we must have $S_{23} = -S_{24}$. This leads to a scattering matrix of the type

$$S = \frac{1}{\sqrt{2}} \begin{pmatrix} 0 & 0 & 1 & 1 \\ 0 & 0 & -1 & 1 \\ 1 & -1 & 0 & 0 \\ 1 & 1 & 0 & 0 \end{pmatrix}$$

The scattering matrices for lossless nonreciprocal transmission lines are given in Fig. 7.

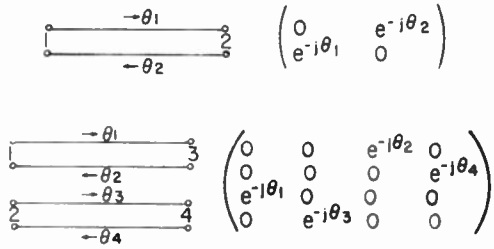

Fig. 7—Scattering matrices for a single and two decoupled lossless nonreciprocal transmission lines.

The scattering matrix for a cascade or chain of networks is not easily obtained from the scattering matrix of the individual networks. For simple cases this may be done by inspection, but for more complicated cases use is made of the transfer matrix,[16] T, which relates the incident and scattered waves on one side of the network to those on the other side. The T matrix is defined by

$$g = Th$$

where (see Fig. 8)

$$g = \begin{pmatrix} a_1 \\ b_1 \\ a_2 \\ b_2 \\ \cdot \\ \cdot \\ \cdot \\ a_n \\ b_n \end{pmatrix} \quad \text{and} \quad h = \begin{pmatrix} a_3 \\ b_3 \\ a_4 \\ b_4 \\ \cdot \\ \cdot \\ \cdot \\ a_m \\ b_m \end{pmatrix}.$$

Although the elements of the T matrix can be simply written in terms of the elements of the scattering matrix for a two-port network, there is unfortunately no general rule for the relation between the two. The importance of T matrix is that the T matrices of several networks in cascade is the product of the individual T matrices.

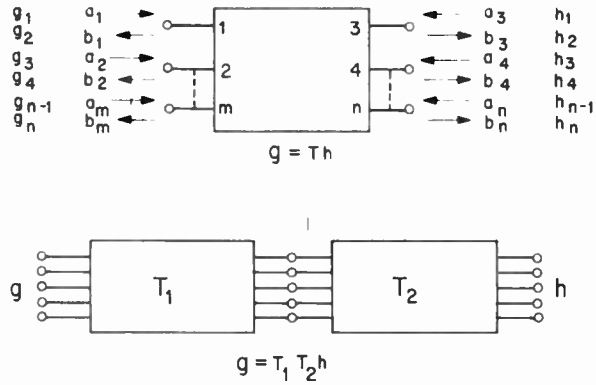

Fig. 8—Definition of the elements of the T matrix in terms of the elements of the scattering matrix.

The T matrices for several four-port elements are given in Fig. 9.

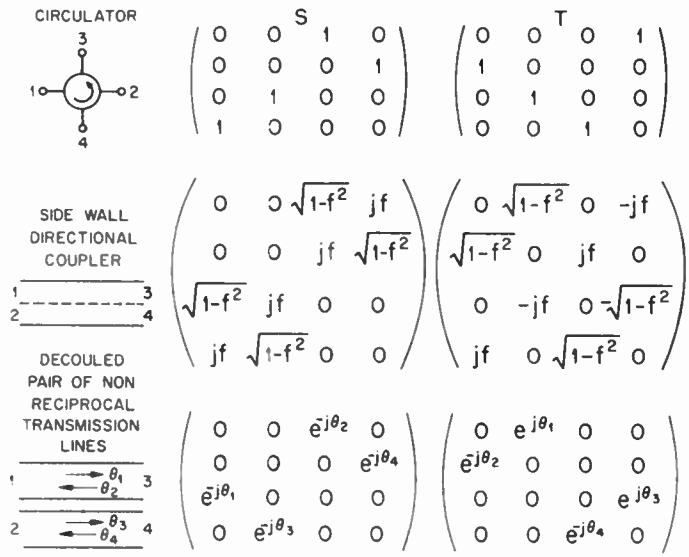

Fig. 9—Scattering and transfer matrices for a circulator and several microwave elements used in the circulator.

Circular Conditions

The condition that the arrangement of Fig. 4(b) be an ideal circulator can now be found by setting the product of the individual T matrices of the various elements equal to the T matrix of a circulator. This yields the following conditions.[19]

It is necessary that both couplers be 3 db couplers and that the total differential phase shift $(\theta_1-\theta_2)-(\theta_3-\theta_4)$, be an odd multiple of 180°. If both couplers are alike then it is possible to have all of the nonreciprocal differential phase shift in only one of the transmission lines. If the couplers are different, for example: one a side wall hybrid and the other a magic T, then one must have a 90° phase shift in each of the transmission lines. For the case of a Faraday rotation-type circulator, the two nonreciprocal transmission lines represent the two circular polarized modes in the circular wave guide. The

above necessary conditions then require the Faraday rotation of the ferrite element be an odd multiple of 45°.

The above conditions are summarized in Fig. 10. Of course, some of these conditions may be arrived at by simpler considerations. We have used this more general approach as an illustration of a method which can be used for more complicated considerations such as the effect of deviations from ideal elements on the performance of circulators.

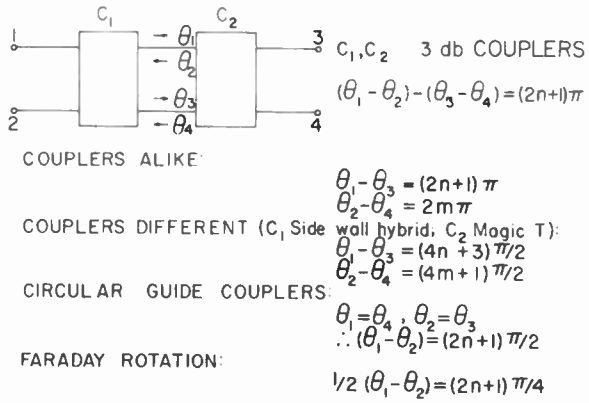

Fig. 10—Summary of the conditions that the microwave circuit of Fig. 4(b) be an ideal circulator.

Effects of Deviations from Ideal Circulator Elements

The scattering matrix analysis may be used to investigate the effect of deviations from ideal circulator elements on the operation of a circulator. Deviations from the ideal have the effect of removing zero elements from the scattering matrix. Nonzero elements along the diagonal mean that the circulator is no longer matched. The other nonzero elements correspond either to *reverse coupling*, that is, coupling between adjacent ports in the reverse direction or a *cross coupling*, *i.e.*, coupling between the usual completely decoupled ports. The scattering matrix of a circulator with nonideal phase shift and imperfect coupling reveals that only reverse coupling occurs. Cross coupling can be due to reflection from the ferrite or from imperfect directivity of the couplers. R. H. Fox[20] has considered the effects of nonideal coupling and phase shift on the bandwidth of the circulator. We repeat some of his results here to show the order of magnitudes of some of these effects.

Consider the case of a circulator utilizing a ferrite in only one of the transmission lines. If the phase shift of the ferrite is imperfect, reverse coupling occurs between the ports shown in Fig. 11. Reverse coupling between two ports is equivalent to insertion loss between those ports. If the differential phase shift of the ferrite is $\theta_1-\theta_2=\pi\pm\epsilon$, then the insertion loss is given by

[20] R. H. Fox, "Bandwidth of Microwave Ferrite Devices," M. I. T. Lincoln Lab. Tech. Rep., T-65; November, 1954.

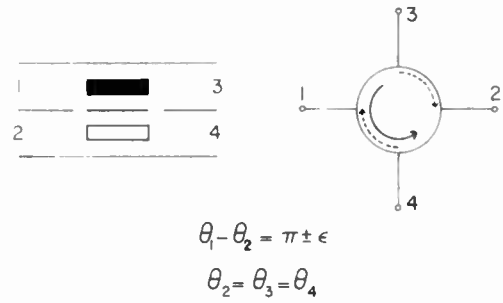

$L_{23}=L_{14}=20\log_{10}\sec\epsilon/2$

Fig. 11—Insertion loss and cross-coupling for a side wall hybrid circulator due to imperfect ferrite phase shift.

$$L = 20\log_{10}\sec\frac{\epsilon}{2}\ \text{db}.$$

This equation is plotted in Fig. 12. Note that even for $\epsilon=30°$ the insertion loss is only 0.30 db.

If both couplers have coupling which differs slightly from 3 db, then reverse coupling occurs at all ports.

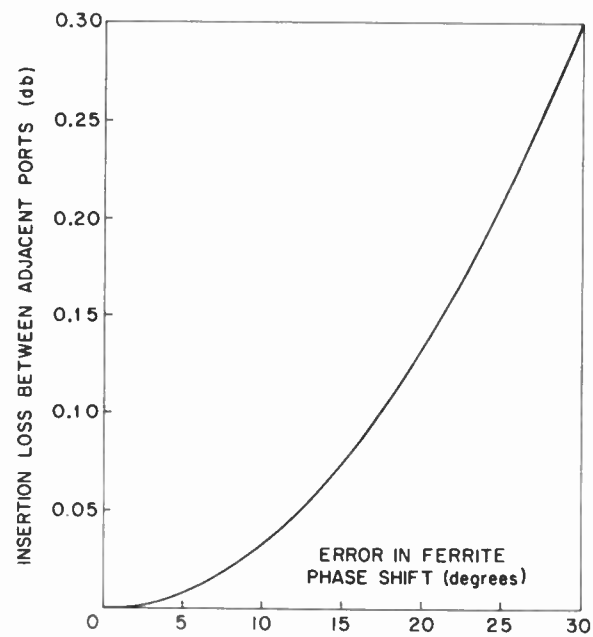

Fig 12—Insertion loss vs error in ferrite phase shift for the circulator of Fig. 11.

Referring to Fig. 4(b), if ΔC_A and ΔC_B are the deviations in db from perfect or 3 db coupling, then the insertion loss is given by

$$L = 0.058(\Delta C_A \pm \Delta C_B)^2\ \text{db}$$

where the plus sign is for insertion loss for transmission from ports 1→4 and 2→3, the minus sign for insertion loss for transmission from ports 3→1 and 4→2.

The effects of imperfect directivity have not yet been investigated but their computation via the S and T matrices is straightforward though laborious.

Generalized Circulator

An extension of the circulators described thus far, which can be treated by the methods described, is the generalized circulator shown in Fig. 13. This device consists of alternate directional couplers and transmission lines. This device may be more broadbanded or serve to reduce the effect of ferrite reflections. It may also be useful at the lower frequencies where it may be more convenient to split the ferrite elements into several sections because of the long length required due to either the lower magnetization of the ferrite required or to operation above resonance, where the phase shift is smaller.

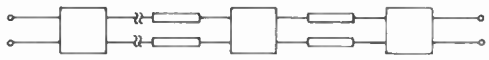

Fig. 13—Generalized circulator composed of alternate directional couplers and pairs of nonreciprocal transmission lines.

Conclusion

We have attempted to review some of the microwave circuit properties of microwave junctions and their extension to junctions containing ferrites. We have seen that the scattering matrix of junctions containing saturated ferrite media satisfies the same requirements as that of junctions containing scalar media, with the exception that the scattering matrix may be nonreciprocal for the former. We have illustrated the use of the scattering matrix treatment by applying it to the four-port circulator.

Unfortunately, time did not permit the discussion of several other interesting aspects of the general problem. In particular, the use of group theoretical methods for computation of the elements of the scattering matrices from the symmetry of the junction was not covered. For reciprocal networks these methods were originally used by Dicke[12] and extended by Auld.[21] The extension to nonreciprocal networks has been started by Fowler.[1]

A mathematical study of the form of scattering matrix which can represent a circulator has been made by Treuhaft.[22] The interesting problem of the synthesis of nonreciprocal networks has been considered by Carlin.[23]

Much of the material presented, especially the treatment of the four-port circulator, was taken from Lincoln Laboratory Reports and other unpublished works of R. H. Fox, formerly of this laboratory.

[21] B. A. Auld, "Use of group theoretical methods for the investigation of symmetrical waveguide junctions," Microwave Lab. Rep. 157, Stanford Univ., Stanford, Calif.; March, 1952.

[22] M. A. Treuhaft, "Network Properties of Circulators, Based on the Scattering Concept," Rep. R-453-55, P. I. B.-383, M. R. I., Polytech. Inst. of Bklyn.; December, 1955.

[23] H. J. Carlin, "Synthesis of Non-Reciprocal Networks," presented at Symposium on Modern Network Synthesis, Polytech. Inst. of Bklyn.; April 13–15, 1955.

Appendix

Relation Between B and H for Magnetically Saturated Ferrite Media

The relation between $\boldsymbol{B}$ and $\boldsymbol{H}$ written in vector form (4) can be derived in a straightforward manner from the equation of motion of the magnetization. If M_T is the magnetization and H_T the magnetic field intensity then

$$\frac{d\boldsymbol{M}_T}{dt} = \gamma \boldsymbol{M}_T \times \boldsymbol{H}_T \tag{12}$$

where γ is 2.8 mcps/oersted. Let $\boldsymbol{M}_T = \boldsymbol{M}_0 + \boldsymbol{M}$ and $\boldsymbol{H}_T = \boldsymbol{H}_0 + \boldsymbol{H}$, where $\boldsymbol{M}_0$ and $\boldsymbol{H}_0$ are the static and $\boldsymbol{M}$ and $\boldsymbol{H}$ are the rf parts of the magnetization and magnetic field intensities. If $\boldsymbol{M}$ and $\boldsymbol{H}$ are small compared to the static values then (12) may be written,

$$\frac{d\boldsymbol{M}}{dt} = \gamma \boldsymbol{M}_0 k \times \boldsymbol{H} + H\gamma_0 \boldsymbol{M} \times k, \tag{13}$$

where $M_0 = |\boldsymbol{M}_0|$, $H_0 = |\boldsymbol{H}_0|$, and k is a unit vector in the direction of $\boldsymbol{H}_0$. By differentiating (13) and eliminating the term $\boldsymbol{M}_0 \times d\boldsymbol{H}/dt$ by the original equation we find

$$\frac{d^2\boldsymbol{M}}{dt^2} + \gamma^2 H_0^2 \boldsymbol{M} = \gamma M_0 k \times \frac{d\boldsymbol{H}}{dt} - \gamma^2 M_0 H_0 k \times k \times \boldsymbol{H}. \tag{14}$$

The above equation bears formal resemblance to the forced oscillation of a simple harmonic oscillator with resonant frequency γH_0. For harmonic time variations of the form $e^{j\omega t}$, (14) is easily solved for $\boldsymbol{M}$ giving,

$$\boldsymbol{M} = j\kappa k \times \boldsymbol{H} - \chi k \times k \times \boldsymbol{H}$$

where κ and χ are the usual components of the permeability tensor given by,

$$\kappa = \frac{\omega_0 \gamma M_0}{\omega_0^2 - \omega^2}; \qquad \chi = \frac{\omega \gamma M_0}{\omega_0^2 - \omega^2}$$

where $\omega_0 = \gamma H_0$.

Eq. (4) follows directly from $B = \mu_0(H + M)$. For the special case in which the magnetic field H_0 is in the z direction, (4) reduces to the ordinary tensor equation as written by Polder.

Shift of Reference Planes

The effect of the shifting of reference planes on the scattering matrix is discussed by Montgomery, Dicke, and Purcell.[12] This is independent of whether or not the microwave junction is reciprocal.

Consider a junction whose scattering matrix has elements S_{mn}. If the n reference plane is shifted away from the junction by θ_n electrical degrees, then the new scattering matrix elements S_{mn}' referred to the new reference planes is given by

$$S_{mn}' = S_{mn} e^{-j(\theta m + \theta n)}.$$

Network Properties of Circulators Based on the Scattering Concept*

MILTON A. TREUHAFT, SENIOR MEMBER, IRE

Summary—**By treating the scattering matrix as an operator, it is possible to relate the properties of cirulators to the cyclic substitutions of group theory and the oriented 1-circuits of topology. The body of knowledge made available by these two branches of mathematics is shown to yield precise definitions of circulator performance. Useful results in treating the symmetries, interconnections and cascade combinations of circulators are found by further application of group theory and topology.**

Practical application of the symmetry analysis is made to the design of circulators. It is shown that a necessary condition for circulator performance is that the structure under consideration possess no symmetry other than those specified in the circulator group. Thus, structures proposed for circulator development which do not meet this necessary requirement may be eliminated immediately with consequent savings in development time and expense.

Introduction

IN RECENT literature there appeared many devices known as circulators.[1–3] In some, a piece of ferrite material is used to obtain a nonreciprocal effect. Recent low frequency circulators use the Hall effect on semiconductors. Although these devices are all classified as circulators, there is little outward physical resemblance. Certainly the Faraday rotation ferrite circulator bears little resemblance to the type which uses two Magic-*T*'s with a ferrite strip gyrator between. However, performance of these devices is sufficiently similar to justify classing both as circulators.

It is the purpose of the present paper to examine this common property of circulator performance and to precisely define this property, making use of the concise terminologies of two mathematical disciplines, namely, topology and the theory of finite groups. Those properties of circulators will be studied which may be deduced from these definitions. It is rather surprising to find how much may be said about the performance of circulators, their physical appearance, and their combinatorial properties, merely from a knowledge of the basic definition of circulator performance.

The Problem of the Definition of Circulator Performance

If one were to put into words the rather intuitive and informal notion of circulator performance, which has been so useful to the present time, one might say that "A device which may be nonreciprocal, in which energy may be transferred from port to port, suffering, at most, a change of phase, may be called a circulator." The energy need not return from a port by the same path that it came to the port. This situation gives rise to the need for nonreciprocity. The change of phase, mentioned above, may be eliminated for purposes of simplicity, by affixing suitable line lengths to the ports. These lines may be reciprocal or nonreciprocal. This simplification will be assumed throughout this paper.

An attempt at a more formal definition of circulator performance was made by R. Fox.[4] Fox gives the scattering matrix below as that of a 4-port circulator having a given system of port numbering. (Fox actually gives a

$$S^{v} = \begin{bmatrix} 0 & 0 & 1 & 0 \\ 0 & 0 & 0 & 1 \\ 0 & 1 & 0 & 0 \\ 1 & 0 & 0 & 0 \end{bmatrix} \tag{1}$$

matrix having four general phase shifts. These have been reduced to zero in the above matrix for the aforementioned purpose of simplicity.) Other systems of port numbering will give different matrices and this complicates the task of recognizing the presence of circulator performance from the scattering matrix. For a 4-port circulator, this is not serious since there are only 6 distinct scattering matrices which may represent circulator performance. However, if one goes to the next higher circulator with an even number of ports, the 6-port, there are 120 distinct scattering matrices that may be obtained by various port numbering systems! The difficulties with definition solely by scattering matrices are, therefore, rather obvious.

Definition by Means of Cyclic Substitution

In the theory of finite groups,[5] an operation, called cyclic substitution, is defined. This operation is usually illustrated as being performed on a sequence of letters or numbers. For example, the operation of cyclic substitution $(abcd)$ means that a be replaced by b, b by c, c by d, and d by a. If this operation is performed on the sequence $bdac$, the result is

$$(abcd) \rightarrow bdac = cabd. \tag{2}$$

* Original manuscript received by the IRE, July 31, 1956. Reprinted from IRE Trans., vol. CT-3, pp. 127–135; June, 1956.

† Microwave Res. Inst., Polytechnic Inst. of Brooklyn, N.Y.

[1] C. L. Hogan, "The ferromagnetic Faraday effect at microwave frequencies and its applications," *Bell Sys. Tech. J.*, vol. 31, pp. 1–31; January, 1952.

[2] J. H. Rowen, "Ferrites in microwave application," *Bell Sys. Tech. J.*, vol. 32, pp. 1333–1369; November, 1953.

[3] A. G. Fox, S. E. Miller, and M. T. Weiss, "Behavior and applications of ferrites in the microwave region," *Bell Sys. Tech. J.*, vol. 34, pp. 5–103; January, 1955.

[4] R. H. Fox, "A Non-Reciprocal Four-Pole Ring Circuit," M.I.T. Lincoln Lab. Tech. Rep., no. 68.

[5] G. A. Miller, H. F. Blichfeldt, and L. E. Dickson, "Theory and Application of Finite Groups," Stechert; 1938.

In the scattering relationship between incident and reflected voltages, the scattering matrix may be considered as indicating an operation performed on the incident voltages, the result of which yields the reflected voltages. Thus, in the matrix relation

$$E^r = S^v E^i \tag{3}$$

the result of applying the operation S^v to E^i yields E^r. If the operator S^v corresponds to a cyclic substitution, then it can be seen that the device having such a scattering matrix corresponds to the intuitive notion of the circulator property. Consequently, a circulator may be defined as: "A device, whose scattering matrix operates on the incident voltages so as to produce the same result as the operation of a cyclic substitution on these incident voltages, is called a circulator."

For example, the equation

$$\begin{pmatrix} E_1^r \\ E_2^r \\ E_3^r \\ E_4^r \end{pmatrix} = \begin{pmatrix} 0 & 0 & 1 & 0 \\ 0 & 0 & 0 & 1 \\ 0 & 1 & 0 & 0 \\ 1 & 0 & 0 & 0 \end{pmatrix} \begin{pmatrix} E_1^i \\ E_2^i \\ E_3^i \\ E_4^i \end{pmatrix} \tag{4}$$

corresponds to

$$[E_1^r\ E_2^r\ E_3^r\ E_4^r] = (1\ 3\ 2\ 4) \rightarrow [E_1^i\ E_2^i\ E_3^i\ E_4^i] \tag{5}$$

where (1 3 2 4)→means that E_1^i is replaced by E_3^i, E_3^i is replaced by E_2^i, etc. [The incident and reflected voltages have been written as row matrices in (5)].

It is interesting to note that when the number of ports is reduced to two, the cyclic substitution is reduced to what is known in group theory as a "transposition." The corresponding equation is

$$[E_1^r\ E_2^r] = (1\ 2) \rightarrow [E_1^i\ E_2^i] = [E_2^i\ E_1^i] \tag{6}$$

and the matrix equation is

$$\begin{pmatrix} E_1^r \\ E_2^r \end{pmatrix} = \begin{pmatrix} 0 & 1 \\ 1 & 0 \end{pmatrix} \begin{pmatrix} E_1^i \\ E_2^i \end{pmatrix}. \tag{7}$$

The S^v matrix in (7) is that of an ideal transformer with a 1 to 1 ratio. The interesting thing about it is that under the definition given above, it may be classified as a circulator and yet it is a completely reciprocal system.

If this is carried even further and the number of ports is reduced to one, then the scattering equation reduces to

$$E_1^r = E_1^i. \tag{8}$$

This is the equation of a 1-port which looks into an open circuit. This also would have to be called a circulator under the cyclic substitution definition, although it is a rather degenerate form of circulator.

It should also be pointed out that a collection of dissociated 1-ports, having the scattering relationship given by (8), has the scattering matrix I, the identity matrix.

Symmetry and Group Properties of Circulators

In the preceding section, a concept of group theory was used in formulating an exact definition of a circulator. In this section, those properties of circulators which follow directly from this definition will be examined. Primarily, it will be shown how the various symmetries that a circulator may possess are derived from its definition.

Symmetries of microwave structures have been studied by Dicke.[6] According to Dicke, the network whose scattering matrix is S^v will possess a symmetry if

$$FS^v = S^v F \tag{9}$$

where F is a "symmetry operator." The problem of finding all the symmetries of S^v reduces to finding all the symmetry operators which commute with S^v. Fortunately, this can be done.

Since the S^v matrices of circulators are, by definition, equivalent to cyclic substitutions, a theorem which has been proved for cyclic substitutions will apply. This theorem states,[7] "The only substitutions on n letters which are commutative with a cyclic substitution are the powers of this cyclic substitution." Since, the F operators of Dicke are essentially substitutions, these F operators may be found by taking the powers of S^v as indicated by the theorem. Accordingly, taking a 4-port circulator as an example

$$F_1 = (S^v)^1 = \begin{pmatrix} 0 & 0 & 0 & 1 \\ 0 & 0 & 1 & 0 \\ 1 & 0 & 0 & 0 \\ 0 & 1 & 0 & 0 \end{pmatrix} \tag{10}$$

$$F_2 = (S^v)^2 = \begin{pmatrix} 0 & 1 & 0 & 0 \\ 1 & 0 & 0 & 0 \\ 0 & 0 & 0 & 1 \\ 0 & 0 & 1 & 0 \end{pmatrix} \tag{11}$$

$$F_3 = (S^v)^3 = \begin{pmatrix} 0 & 0 & 1 & 0 \\ 0 & 0 & 0 & 1 \\ 0 & 1 & 0 & 0 \\ 1 & 0 & 0 & 0 \end{pmatrix} \tag{12}$$

$$F_4 = (S^v)^4 = \begin{pmatrix} 1 & 0 & 0 & 0 \\ 0 & 1 & 0 & 0 \\ 0 & 0 & 1 & 0 \\ 0 & 0 & 0 & 1 \end{pmatrix}. \tag{13}$$

Since $(S^v)^4$ is equal to I, the identity matrix, the powers of S^v are said to form a cyclic group with S^v as the "generator" of the group.

The F operators listed above would comprise a mathematically complete list of the symmetries of the

[6] C. Montgomery, R. H. Dicke, and E. M. Purcell, "Principles of Microwave Circuits," McGraw-Hill Book Co., Inc., New York, N.Y., Chap. 12; 1948.

[7] Miller, Blichfeldt, and Dickson, *op. cit.*, p. 19.

4-port circulator, except for the fact that negative F operators, which are permissible, also satisfy (9). Therefore, the complete and mathematically exhaustive list of symmetries of the 4-port circulator is contained in the following group whose order is 8.

$$F_1, F_2, F_3, I, -F_1, -F_2, -F_3, -I. \tag{14}$$

If a structure possesses a symmetry not contained in this group, then it cannot be a circulator.

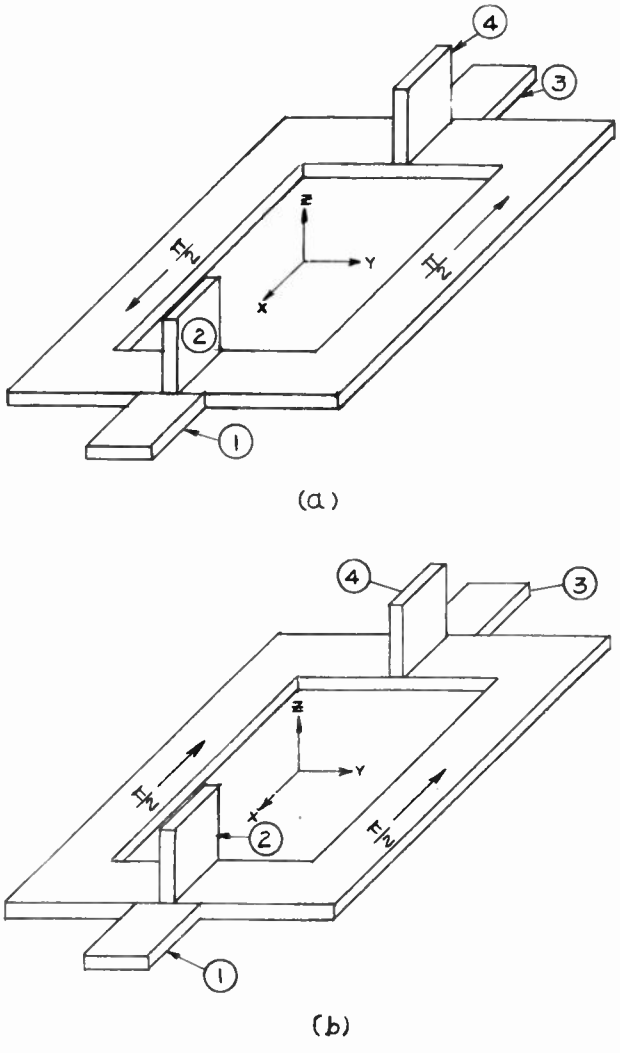

Fig. 1—Structures having nonpermissible symmetries.

In Fig. 1, two examples of 4-port structures are given which, from experience with similar structures, look like they might possibly be circulators. [The symbol $(\pi/2)\rightarrow$indicates a 90° nonreciprocal phase shift.] However, it will be seen that the structure of Fig. 1(a) is symmetrical about the z axis. Therefore, by rotating the structure 180° about the z axis port 1 replaces port 3 and port 2 replaces port 4 with no change in polarity of the ports. The symmetry operator which describes this operation is given by F_z below in (15). In Fig. 1(b), the structure is symmetrical about the xz plane. In a reflection through the xz plane, port 1 and port 3 remain unchanged whereas port 2 and port 4 have their polarities reversed. The reflection operator which specifies this operation is given by F_{xz} in (16) below.

$$F_z = \begin{bmatrix} 0 & 0 & 1 & 0 \\ 0 & 0 & 0 & 1 \\ 1 & 0 & 0 & 0 \\ 0 & 1 & 0 & 0 \end{bmatrix} \tag{15}$$

and

$$F_{xz} = \begin{bmatrix} 1 & 0 & 0 & 0 \\ 0 & -1 & 0 & 0 \\ 0 & 0 & 1 & 0 \\ 0 & 0 & 0 & -1 \end{bmatrix}. \tag{16}$$

Neither one of these F operators may be found in the group of the circulator given in (10) to (14). Hence, without going through any further analysis, it is known that these structures cannot be circulators.

Topological Definition of Circulators

A commonly used symbol for a circulator is shown in Fig. 2(a). The symbol illustrates in a rather graphical way that energy which enters port 1 emerges at port 2, etc. The purpose of the symbol is merely to provide a notation which can be recognized as designating a circulator. It serves this purpose very well, but there its utility ends. In this section, an attempt will be made to formalize this symbolic representation, by means of the precise language of topology, into an alternative definition of the circulator.

If Fig. 2(b) be observed, there will be seen two points with a directed path between them. In topological language, this is an oriented 1-cell having the 0-cell a as the initial point and the 0-cell b as the terminal point.[8] If it is agreed that the 0-cells represent ports and the oriented 1-cell the path and direction of energy flow, then *a circulator may be defined as any structure which may be represented by an "oriented 1-circuit."* (The word "circuit" is used in a different sense than the ordinary electric circuit.) Its topological definition is mathematically precise and it is given in Veblen.[9] However, an informal definition of an oriented 1-circuit would not be amiss here and it is accordingly given below.

Topologically, the notion of an n circuit involves its behavior at its intersections. If two and only two n cells intersect with one $(n-1)$ cell, the system is called a circuit. Under this definition, the figure of Fig. 2(d) is also a circuit in the topological sense, although it is not what is generally thought of as a circuit in electric net-

[8] O. Veblen, "Analysis Situs," American Mathematical Society; 1931.
[9] *Ibid.*, p. 24.

work theory. Fig. 2(d) is a 2-circuit since two and only two of its 2-cells (the faces), intersect with each 1-cell. It serves to illustrate the difference between the precise topological meaning of the term "circuit" as compared with its ordinary usage. A 1-circuit is then a system of 1-cells and 0-cells such that two 1-cells intersect with each 0-cell. An oriented 1-circuit simply means that if arrows are used to indicate the orientation of the 1-cells, all the arrows will be pointed in the same direction.

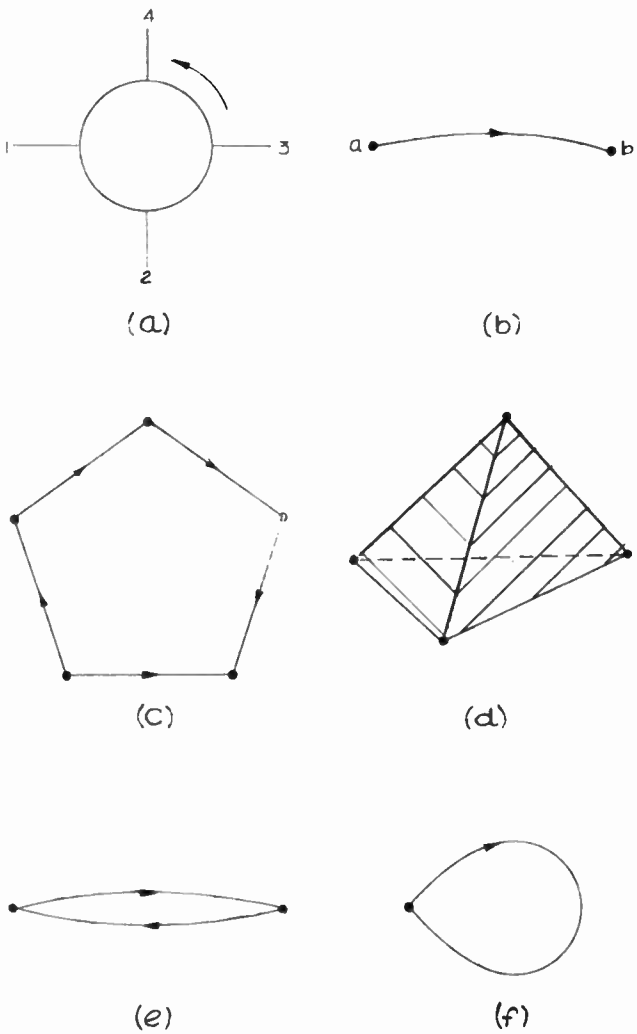

Fig. 2—The topological n circuit.

If incident voltages are thought of as entering the ports or 0-cells of an oriented 1-circuit and emerging at the succeeding ports as reflected voltages, then it will be seen that the topological definition of the circulator is in every way equivalent to the cyclic substitution definition. The oriented 1-circuit is more or less a precise graphical representation of a cyclic substitution. It is interesting to note here, as in the case of cyclic substitutions, what occurs as the number of ports is brought down to two and then to one. Again the ideal transformer and the open circuit are classified as circulators and Fig. 2(e) and Fig. 2(f) are respectively their graphical representations.

Topological Combination and Interconnection of Circulators

In order to study the result of interconnecting the ports of circulators, it is necessary to set up a formal rule which accurately describes the physical situation. In Fig. 3(a), two ports b and b' are shown which are to be connected. After connection, the energy flowing along the directed path ab emerges at b and flows along the directed path $b'c'$. Similarly, the energy flowing along the path $a'b'$ will continue along path bc. This situation can be described formally by means of a topological concept[10] called the product of two oriented 1-cells. An illustration of this product is shown in Fig. 3(b). The oriented 1-cell g_1, g_2 is the product of the two oriented 1-cells g_1 and g_2 since, according to the definition of the product, it contains all the points of g_1 and g_2 and has the same initial point as g_1 and the same terminal point as g_2.

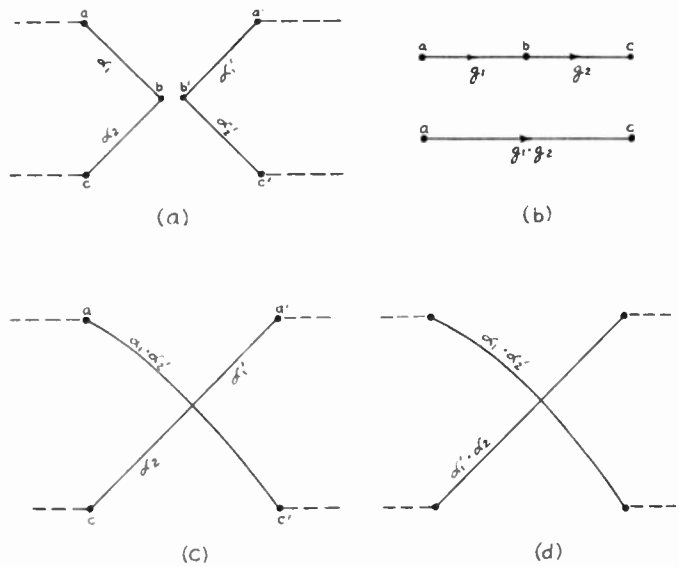

Fig. 3—Interconnection by means of multiplication.

Now the operation of interconnection shown in Fig. 3(a) may be described by a formal rule, as follows.

Rule for Interconnection—Superimpose the two 0-cells which represent the two ports to be interconnected. Form the product of an oriented 1-cell whose terminal point is one of the 0-cells that have been superimposed and another oriented 1-cell whose initial point is the other 0-cell that has been superimposed. Replace the two oriented 1-cells by the product. Then replace the two remaining oriented 1-cells, at the junction, with their product.

[10] *Ibid.*, p. 139.

To illustrate this rule the interconnection of b and b' in Fig. 3(a) will be shown. Fig. 3(c) represents the first step where b and b' have been superimposed and the oriented 1-cells α_1 and α_2' have been replaced by $\alpha_1 \cdot \alpha_2'$. The next step is to replace α_1' and α_2 by $\alpha_1' \cdot \alpha_2$ as shown in Fig. 3(d).

The interconnection technique is now in form to be applied to actual circulators. Fig. 4 shows several interesting cases. In the first column are shown the original circulators that are to be interconnected. There follows, in the succeeding columns, the steps necessary to make the interconnections. In Fig. 4(a), the connection of a 3-port and a 4-port circulator is shown. The result is a 5-port circulator. Fig. 4(b) illustrates how to handle the singular case where the initial and terminal points of g_3 coincide. If the rule for interconnection is followed carefully, then the result is a 3-port circulator. Fig. 4(c) shows what happens when two circulators are interconnected at two ports. (This is equivalent to cascading these circulators.) The result is two through connections. This result may also be shown to be true by matrix methods, but certainly not as simply. By topological methods, the result is practically obvious. Fig. 4(d) illustrates how the singular case may be encountered in the course of interconnection although neither of the original circulators was singular.

Another result, which is also practically obvious by topological means, is the fact that any higher order circulator can be constructed by interconnecting 4-port circulators. Fig. 4(b) shows how a 3-port circulator may be realized from a 4-port. The interconnection of this 3-port with successive 4-ports will give circulators of odd order 5, 7, 9, etc., and the interconnection of 4-ports will give even order circulators 6, 8, 10, etc. This is a rather important consideration if one is interested in constructing higher order circulators since much is known about the construction of 4-port circulators whereas, with the exception of Carlin,[11] there has been very little work on higher order circulators.

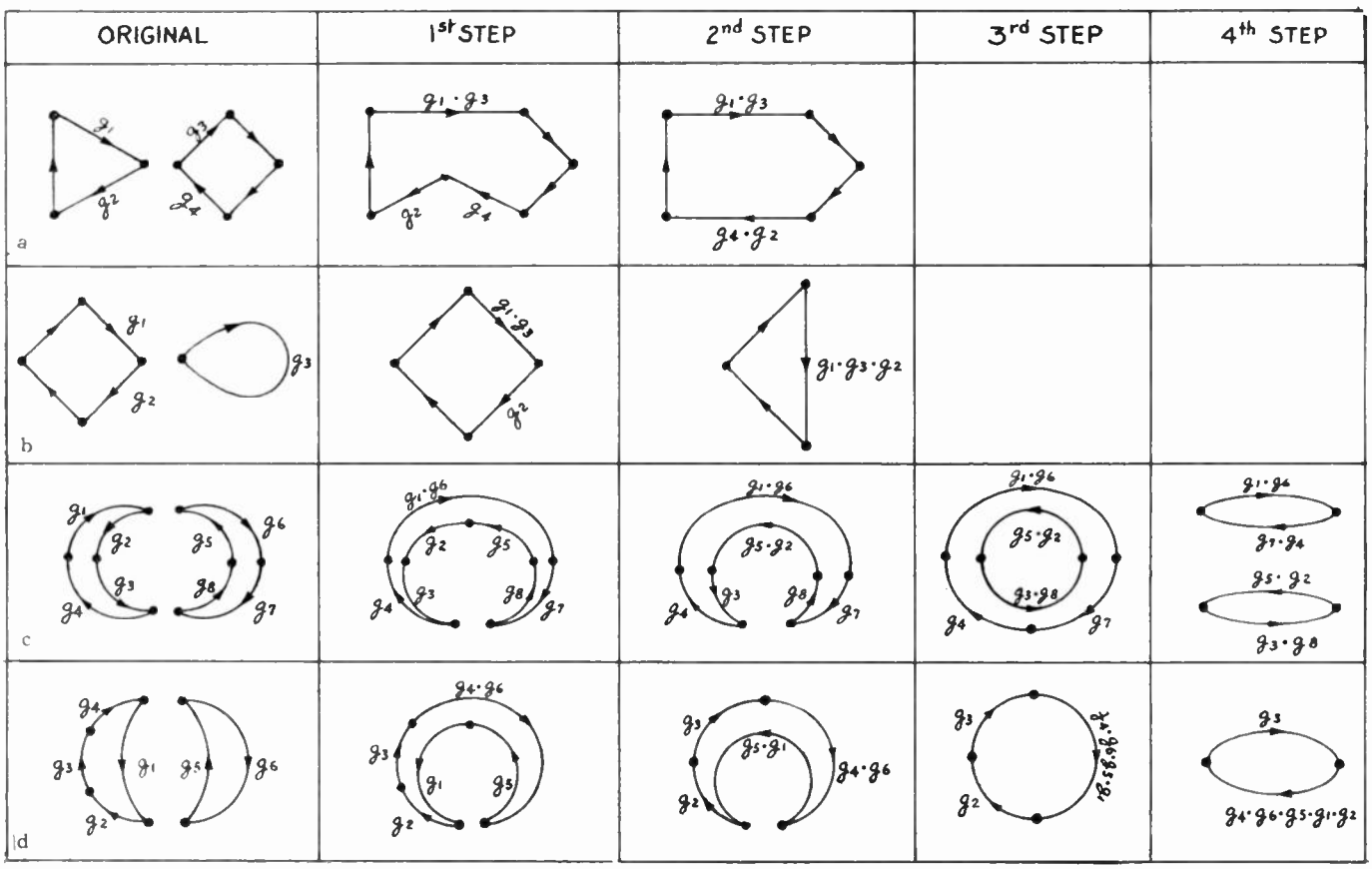

Fig. 4—Some examples of the interconnection technique.

Cascading of Circulators

In the previous section some general rules were defined for the interconnection of circulators. There was no real restriction on the type of interconnection considered. In this section, a special, but important, type interconnection will be investigated, namely, the cascade connection. The very nature of the cascade connection assumes that there are an equal number of input ports and output ports so that, immediately, the study is limited to

[11] H. J. Carlin, "Principles of gyrator networks," *Proceedings of Symposium on Microwave Techniques*, Polytechnic Inst. of Brooklyn, N.Y., p. 197; November, 1954.

circulators having an even number of ports. Also, there is another restriction that follows quite naturally from practice with 4-port circulators where two decoupled ports are paired as input ports and the other two decoupled ports are paired as output ports. This restriction is that no input port be directly coupled to any other input port and no output port be directly coupled to another output port. Several circulators satisfying these requirements are shown in Fig. 5. It may be verified that each of the networks of Fig. 5 is an oriented 1-circuit and that no pair of input or output ports are directly coupled by an oriented 1-cell.

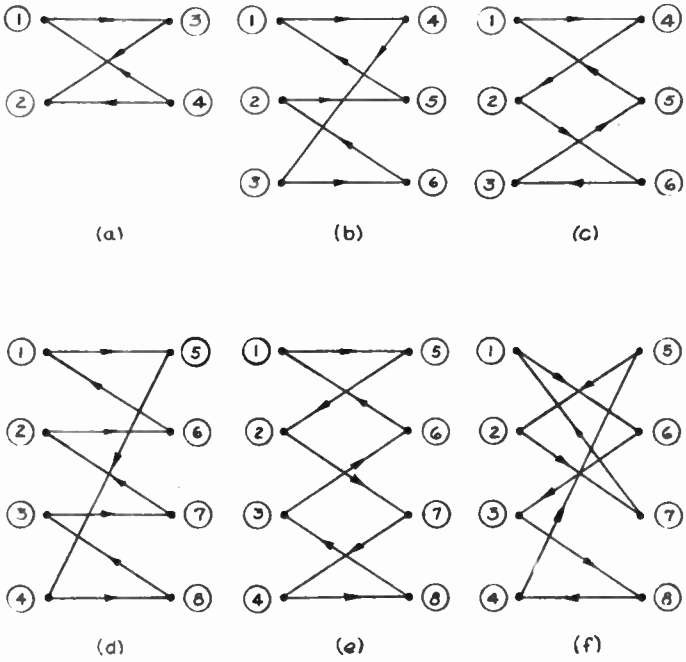

Fig. 5—Some even-port circulators with decoupled input and decoupled output ports.

As may be seen from Fig. 5, that although several restrictions have been placed on the type of circulator to be considered, there are, within these restrictions, a multitude of circulators for each given number of ports. As a matter of fact, for an n-port circulator having decoupled input and output ports, there are exactly

$$\left(\frac{n}{2}\right)!\left(\frac{n}{2}-1\right)!$$

circulators possible. If these circulators are cascaded with themselves or in various combinations, the number of resultant networks becomes completely unwieldly. Therefore, in order to bring the study of cascaded circulators within reasonable limits where some simple, useful results are possible, a further restriction is that the circulators considered be of the form shown in Fig. 5(a), (b), and (d). If the scattering matrices for these circulators be written, they will be seen to be of the following forms, respectively,

$$S_4^v = \left[\begin{array}{cc|cc} 0 & 0 & 0 & 1 \\ 0 & 0 & 1 & 0 \\ \hline 1 & 0 & 0 & 0 \\ 0 & 1 & 0 & 0 \end{array}\right] \tag{17}$$

$$S_6^v = \left[\begin{array}{ccc|ccc} 0 & 0 & 0 & 0 & 1 & 0 \\ 0 & 0 & 0 & 0 & 0 & 1 \\ 0 & 0 & 0 & 1 & 0 & 0 \\ \hline 1 & 0 & 0 & 0 & 0 & 0 \\ 0 & 1 & 0 & 0 & 0 & 0 \\ 0 & 0 & 1 & 0 & 0 & 0 \end{array}\right] \tag{18}$$

$$S_8^v = \left[\begin{array}{cccc|cccc} 0 & 0 & 0 & 0 & 0 & 1 & 0 & 0 \\ 0 & 0 & 0 & 0 & 0 & 0 & 1 & 0 \\ 0 & 0 & 0 & 0 & 0 & 0 & 0 & 1 \\ 0 & 0 & 0 & 0 & 1 & 0 & 0 & 0 \\ \hline 1 & 0 & 0 & 0 & 0 & 0 & 0 & 0 \\ 0 & 1 & 0 & 0 & 0 & 0 & 0 & 0 \\ 0 & 0 & 1 & 0 & 0 & 0 & 0 & 0 \\ 0 & 0 & 0 & 1 & 0 & 0 & 0 & 0 \end{array}\right]. \tag{19}$$

These matrices are seen to be of the "block" form

$$S_n^v = \begin{pmatrix} 0 & S_{12} \\ S_{21} & 0 \end{pmatrix} \tag{20}$$

where

$$S_{21} = I_{n/2}\left(\text{the identity for an } \frac{n}{2} \times \frac{n}{2} \text{ matrix}\right) \tag{21}$$

and S_{12} is of the form

$$S_{12} = \left[\begin{array}{c|c} 0 & \\ 0 & \\ \vdots & I_{[(n/2)-1]} \\ 0 & \\ \hline 1 \cdots 0 & 0 \quad 0 \end{array}\right] \tag{22}$$

where, as in (21), $I_{[(n/2)-1]}$ is the identity matrix for an

$$\left(\frac{n}{2}-1\right) \times \left(\frac{n}{2}-1\right)$$

matrix. It is the circulator having this type of a scattering matrix which will be considered in the present study of cascaded circulators. This form of circulator matrix will be called, for purposes of references, the "reduced form."

Fortunately, for the reduced form of circulator matrices, there is a very simple rule whereby the scattering matrix of the cascaded combination can be computed from the individual scattering matrices. If the circulators X and Y be cascaded so that the output ports of X are connected to the input ports of Y and if the scattering matrices of X and Y are in block form as below

$$S_X{}^v = \begin{pmatrix} 0 & X_{12} \\ X_{21} & 0 \end{pmatrix} \tag{23}$$

and

$$S_Y{}^v = \begin{pmatrix} 0 & Y_{12} \\ Y_{21} & 0 \end{pmatrix} \tag{24}$$

then the scattering matrix of the cascaded combination is given by

$$S_{XY}{}^v = \begin{pmatrix} 0 & X_{12}\ Y_{12} \\ Y_{21}\ X_{21} & 0 \end{pmatrix}. \tag{25}$$

This rule depends only on the fact that X and Y are block matrices. If, in addition, the matrices of the circulator X and Y are in reduced form, then

$$X_{21} = Y_{21} = I_{n/2} \tag{26}$$

and

$$S_{XY}{}^v = \begin{pmatrix} 0 & X_{12}\ Y_{12} \\ I_{n/2} & 0 \end{pmatrix}. \tag{27}$$

Now that the type of circulator, whose cascading properties are to be studied, has been defined and a rule stated for the computation of the cascade scattering matrix, the preliminaries are over and the objectives and plan of cascade study may be stated. Essentially the objectives of the cascade study are as follows.

1) To determine whether the cascading of n-port circulators, when n is even, always yields an n-port circulator.

2) If the above is not true, to determine a rule by which one might tell in advance which cascade combinations will yield circulators and which will not for each value of n.

3) To allow one to predict what the form of the resulting network will be in the event that it is not an n-port circulator.

These objectives can be achieved and the plan of the work is as follows.

1) The properties of any circulator, X, will be shown to be completely derivable from the properties of X_{12}.

2) The powers of X_{12}, which result from cascading, will be shown to form a cyclic group of order $n/2$.

3) It will then be shown that when the cyclic group of the powers of X_{12} breaks up into subgroups, the member of these subgroups cannot be n-port circulators.

4) It will also be shown that the members of the subgroups, mentioned above, also represent circulators, but of orders lower than n. The relation of this multiplicity of lower order circulators to the properties of the subgroup will be given.

The proof of statement 1) directly above is straightforward but lengthy. Therefore, it has been relegated to the Appendix. The results may profitably be summed up here, though. Essentially, it is shown in the Appendix that if the matrix X_{12} represents a certain substitution, for example

$$(1\ 2\ 3\ 4) \tag{28}$$

then the substitution which represents the whole scattering matrix is

$$(1\ 6\ 2\ 7\ 3\ 8\ 4\ 5). \tag{29}$$

It is seen that each number x of the substitution (28) has been preceded by the number

$$\left(x + \frac{n}{2}\right),$$

where n is the order of the circulator. If the substitution which represents X_{12} is made up of a numer of disjoint cycles, then the substitution which represents the whole matrix is also made up of the same number of disjoint cycles, each cycle being double in length. For example, if X_{12} is represented by

$$(1\ 3)\ (2\ 4) \tag{30}$$

then the whole matrix is represented by

$$(1\ 7\ 3\ 5)\ (2\ 8\ 4\ 6). \tag{31}$$

Also, conversely, the substitutions for X_{12} may be derived from those of the whole matrix by simply omitting alternate numbers. Hence, if the whole scattering matrix is the matrix of a circulator, then it is by definition a simple (nondisjoint) cyclic substitution and X_{12} will also be a nondisjoint cyclic substitution.

It is known from a standard theorem in group theory that: "The powers of a cyclic substitution of k letters form a cyclic group of order k." Therefore, it immediately follows that the powers of X_{12} form a cyclic group order $n/2$. This means, for example, that if an 8-port circulator be cascaded four times, then

$$X_{12}{}^4 = I \tag{32}$$

and the block matrix of the network is

$$S^v = \begin{pmatrix} 0 & I_{n/2} \\ I_{n/2} & 0 \end{pmatrix}. \tag{33}$$

This is the matrix of four dissociated through connections.

A study of the cyclic group of the powers of X_{12} will now reveal the properties of cascaded circulators. The question as to whether cascading of circulators always yields a circulator can be definitely answered in the negative. It will now be shown that any member of the subgroups of the cyclic group, formed by the powers of X_{12}, cannot be a circulator. For, if a member of a sub-

group contained a cyclic substitution, it would have to contain all the powers of that cyclic substitution since every group contains all the powers of every element. But all the powers of cyclic substitution form a group of order $n/2$. Since the order of a subgroup is less than $n/2$, the subgroup cannot contain a cyclic substitution of order $n/2$ and hence no member of the subgroup can have an S^v which represents an n-port circulator.

Each of the members remaining in the group, after the subgroups are removed, may act as a "generator" of a cyclic group whose order is the same as the original group, namely, $n/2$. Since powers of these residual members generate groups of order $n/2$, they can contain no cyclic substitutions of order less than $n/2$. Therefore, the residual members must be cyclic substitutions of order $n/2$ and the corresponding S^v matrices must represent n-port circulators.

For example, every group contains the subgroup I, the identity. Eq. (33) above shows the identity to be a collection of separate through connections or ideal transformers. Each of these in itself may be classified as a circulator. However, the collection of a multiplicity of circulators is certainly not an n-port circulator.

Fortunately, with cyclic groups the subgroups can be simply determined in advance. For a cyclic group of order $n/2$, the powers of any member whose exponent is an integral divisor of $n/2$ form a subgroup. For example, if $n/2 = 6$, the group may be symbolized as

$$a,\ a^2,\ a^3,\ a^4,\ a^5,\ I. \tag{34}$$

The subgroups are

$$a^2,\ a^4,\ I \tag{35}$$

$$a^3,\ I \tag{36}$$

$$I. \tag{37}$$

Therefore, in cascading 12-port circulators, only the cascade combination of 5 circulators yields a circulator, since a^5 is not a member of any subgroup. When $n/2$ is 5, a prime number, the only subgroup is I and all cascade combinations of 10-port circulators, which are not a multiple of 5, yield circulators.

An interesting corollary of the above work is the fact that given any circulator, another circulator always exists such that the cascade combination gives the collection of through connections which corresponds to the identity of the cyclic group of X_{12}. This is true since every group must contain the inverse of every element and the inverse of a cyclic substitution is a cyclic substitution.

Since the networks in the subgroups do not represent n-port circulators, the question arises as to what they do represent. From group theory, it is known that the powers of a cyclic substitution of order $n/2$ may lead to other $n/2$ order substitutions or to the product of disjoint cycles. As an illustration, consider

$$(1\ 2\ 3\ 4)^2 = (1\ 3)\ (2\ 4). \tag{38}$$

Apparently, the subgroups must be composed of disjoint cycles and the number of substitutions in the largest cycle must be equal to the order of the subgroup. This means that the subgroups represent lower order circulators having no interconnections with each other and the order of the highest circulator present is twice the order of the subgroup.

Conclusion

Consideration of the scattering matrix as an operator has led to the definition of circulator performance as a cyclic substitution which relates the incident voltages to the reflected voltages. By means of the full group of "symmetry operators" of this cyclic substitution, it is possible to specify which symmetries circulators may have and to exclude all others. This is useful since the outward physical structure of a network may be examined for symmetries which might preclude its use as a circulator.

Definition of the circulator as an oriented 1-circuit, the topological analog of a cyclic substitution, has allowed the statement of a formal rule for the interconnection of circulators. By means of this rule, the orderly determination of the results of interconnections, in rather complicated situations, is made possible.

By specifying that the port numbering system of a circulator be arranged to give a certain form of scattering matrix, the multiplicity of possible cascade combinations of circulators is reduced to a simple and, it is hoped, useful situation. The cascade combinations of n-port circulators is shown to produce other n-port circulators provided that a certain block matrix, which is part of the scattering matrix, is not a member of any subgroup of the cyclic group formed by the cascading operation.

Appendix

Theorem

When the scattering matrix of an n-port circulator (n even) is put into "reduced form,"

$$S^v = \begin{pmatrix} 0 & X_{12} \\ I_{n/2} & 0 \end{pmatrix}, \tag{39}$$

then the cyclic substitution which represents X_{12} is related to the cyclic substitution for S^v in the following fashion. If the cyclic substitution, of order n, for S^v be written as

$$\left\{1(k_1)\left(k_1 - \frac{n}{2}\right)(k_2)\left(k_2 - \frac{n}{2}\right)\cdots (k_{x-1})\left(k_{x-1} - \frac{n}{2}\right)(k_x)\right\} \tag{40}$$

where the integers designated by the k's lie in the interval $(n/2) < k \leqq n$. Then the cyclic substitution for X_{12} is found by simply taking the alternate members of (40). The substitution, of order $n/2$, for X_{12} is then

$$\left\{1\left(k_1-\frac{n}{2}\right)\left(k_2-\frac{n}{2}\right)\cdots\left(k_{x-1}-\frac{n}{2}\right)\right\}. \tag{41}$$

[Or, it may also be stated that S^v may be found from X_{12} by inserting the appropriate k's in alternate positions as in (40) and (41).]

Proof

The block scattering matrix relationship for an n-port circulator, (n even), is

$$\begin{pmatrix} E_1{}^r \\ E_2{}^r \end{pmatrix} = \begin{pmatrix} E_1{}^{i'} \\ E_2{}^{i'} \end{pmatrix} = \begin{pmatrix} 0 & X_{12} \\ I_{n/2} & 0 \end{pmatrix} \begin{pmatrix} E_1{}^i \\ E_2{}^i \end{pmatrix}, \tag{42}$$

where each E element is itself a column matrix or order $n/2$ and the primed incident voltages indicate the result of substitution on the original incident voltages. Then

$$\begin{pmatrix} E_1{}^{i'} \\ E_2{}^{i'} \end{pmatrix} = \begin{pmatrix} X_{12} & E_2{}^i \\ E_1{}^i & \end{pmatrix}. \tag{43}$$

This means that every element of the column matrix $E_1{}^i$ is transformed into an element of $E_2{}^{i'}$ and every element of $E_2{}^i$ goes into an element of $E_1{}^{i'}$. If the column matrices $E_1{}^i$ and $E_2{}^i$ be written for an n-port circulator

$$E_1{}^i = \begin{Bmatrix} e_1{}^i \\ e_2{}^i \\ \cdot \\ \cdot \\ \cdot \\ e_{n/2}{}^i \end{Bmatrix} \tag{44}$$

and

$$E_2{}^i = \begin{Bmatrix} e_{n/2+1}{}^i \\ e_{n/2+2}{}^i \\ \cdot \\ \cdot \\ \cdot \\ e_n{}^i \end{Bmatrix}. \tag{45}$$

Similarly for $E_1{}^{i'}$ and $E_2{}^{i'}$.

The substitution operation represented by the block matrix

$$\begin{pmatrix} 0 & X_{12} \\ I_{n/2} & 0 \end{pmatrix} \tag{46}$$

will now be derived. The first element of column matrix $E_1{}^i$, due to (43), will be replaced by a member of the column matrix $E_2{}^i$. Let this member of $E_2{}^i$ be called $e_{k_1}{}^i$. From (45) it is seen that $(n/2)<k_1\leqq n$. If k_1 is taken to indicate the substitution of $e_{k_1}{}^i$, then the substitution operation thus far may be written as $\{1(k_1)\cdots\}$. The next letter in this substitution is found by noting what replaces k_1. Again referring to (43) this is equivalent to asking what does $e_{k_1}{}^{i'}$ equal. Due to the fact that $E_2{}^{i'}$ has been carried into $E_1{}^i$ by the identity $I_{n/2}$, then $e_{k_1}{}^{i'}$ must equal $e_{k_1}{}^{i-(n/2)}$. The substitution may now be written as

$$\left\{1\,(k_1)\left(k_1-\frac{n}{2}\right)\cdots\right\}.$$

By continuing this process, (40) is obtained.

There yet remains to show that the substitution for X_{12} is given by (41). It is important in considering X_{12} to realize that the rows of X_{12} have the identical numbers that the rows of S^v have. However, the relation between the columns of X_{12} and S^v is given by

$$k \text{ column of } S^v = \left(k-\frac{n}{2}\right) \text{column of } X_{12}. \tag{47}$$

Therefore, whereas the substitution for S^v started as $1(k_1)\cdots$, the corresponding substitution for X_{12} is

$$\left\{1\left(k_1-\frac{n}{2}\right)\cdots\right\}.$$

Since the $|k_1-(n/2)|$ row in X_{12} is identical with the $|k_1-(n/2)|$ row in S^v, the next step in the substitution is to go to what was formerly the k_2 column of S^v and which is now the $|k_2-(n/2)|$ column of X_{12}. Therefore, the substitution for X_{12} proceeds as given in (41) and the theorem is proven.

Note that if X_{12} is composed of disjoint cycles, then S^v is also composed of the same number of disjoint cycles except that each cycle of S^v will have twice as many numbers as those of X_{12}.

Acknowledgment

The author wishes to acknowledge the sponsorship of the Evans Signal Corps Laboratory of the Department of the Army in sponsoring the research required for the work in this report. The encouragement and advice of Dr. Herbert J. Carlin of the Microwave Research Institute is also hereby acknowledged.

Topics in Guided-Wave Propagation in Magnetized Ferrites*

MORRIS L. KALES†, MEMBER, IRE

Summary—Contributions of various authors to the linear theory of propagation in magnetized ferrites are briefly reviewed. Modes of propagation are discussed for the cases where a static magnetic field is applied to a ferrite in directions parallel and perpendicular respectively to the direction of propagation of the microwave field. Various properties of propagation are described for waveguides of rectangular or circular cross section which are either partially or completely filled with ferrites.

Emphasis is placed on those characteristics of propagation in ferrite media which are in contrast with those obtained in conventional media. Unusual types of mode "cutoffs" are described, as well as various nonreciprocal propagation properties resulting from the particular type of anisotropy which is present in a magnetized ferrite.

The review closes with a brief discussion of some results obtained by perturbation methods.

Introduction

IN ACCORDANCE with the linear theory of propagation, if a ferrite is magnetized in the direction of the z-axis by the application of a static magnetic field H_0, the relation between the rf components of $\vec{B}$ and $\vec{H}$ is given by the equations[1,2]

$$B_x = \mu H_x - j\kappa H_y$$

$$B_y = j\kappa H_x + \mu H_y$$

$$B_z = \mu_z H_z.$$

For a given unbounded ferrite medium, and at a given frequency, the components of the permeability tensor

$$\bar{\bar{\mu}} \equiv \begin{pmatrix} \mu & -j\kappa & 0 \\ j\kappa & \mu & 0 \\ 0 & 0 & \mu_z \end{pmatrix}$$

will depend on H_0.

Recent investigations have shown that propagation in a ferrite medium may be nonlinear at power levels normally encountered in practical applications.[3] The discussion that follows, however, is confined to the case where the propagation is linear.

Although the subject of this discussion is guided-wave propagation, it will be instructive to consider first the case of uniform plane waves in an unbounded ferrite medium. Polder has shown that for any direction of propagation there are two such waves.[1] In general these waves are elliptically polarized, and have unequal propagation constants. Two cases are of particular interest: they are the ones for which the directions of propagation are either parallel or perpendicular to the static magnetic field. In the first case, the waves are circularly polarized with opposite senses of rotation. Each of these waves is identical in structure with a circularly polarized plane wave in an isotropic, homogeneous medium having an appropriate permeability. For the wave rotating in the positive sense with respect to the magnetizing field the permeability is $\mu_+ = \mu - \kappa$. For the other wave the permeability is $\mu_- = \mu + \kappa$. These "effective" values of permeability depend only on the sense of rotation with respect to the magnetizing field and not on the sense of propagation. When two circularly polarizing plane waves of equal amplitudes and opposite senses of rotation propagate simultaneously in the direction of the magnetizing field, their sum is linearly polarized at every point in space, but the plane of polarization rotates as the wave advances. This is the well-known Faraday rotation. As a consequence of the fact that the propagation constants for each of the circularly polarized waves depend only on the sense of the magnetizing field, and not on the sense of the propagation direction, the rotation is nonreciprocal.

When the direction of propagation is at right angles to the magnetizing field, one of the two possible plane waves has a component of $\vec{H}$ in the direction of the z-axis only. For this wave only the μ_z component of the tensor permeability enters into consideration and, as a result, the wave is identical in form with a uniform plane wave in an isotropic, homogeneous medium of permeability μ_z. The second plane wave has no component of $\vec{H}$ in the direction of the z-axis. This wave has the $\vec{E}$-vector in the direction of the z-axis, and insofar as $\vec{E}$ and $\vec{B}$ are concerned, it is identical with a plane wave in an isotropic medium with permeability $\mu\{1-(\kappa/\mu)^2\}$. With respect to the vector $\vec{H}$, however, there is an important difference. In this case the $\vec{H}$-vector has a component in the direction of propagation and is elliptically polarized.

Ferrite-Loaded Waveguide Longitudinally Magnetized

We turn now to the consideration of propagation in a waveguide. Most of the studies of propagation in a ferrite-loaded waveguide have treated the case where the

* Original manuscript received by the IRE, May 21, 1956. Presented at Symposium on the Microwave Properties and Applications of Ferrites, Harvard Univ., Cambridge, Mass., April 2–4, 1956.

† Microwave Antennas and Components Branch, Electronics Div., Naval Res. Lab., Washington 25, D. C.

[1] D. Polder, "On the theory of ferromagnetic resonance," *Phil. Mag.*, vol. 40, pp. 99–115; 1949.

[2] C. L. Hogan, "The microwave gyrator," *Bell. Sys. Tech. J.*, vol. 31, pp. 1–31; January, 1952.

[3] N. G. Sakiotis, H. N. Chait, and M. L. Kales, "Nonlinearity of propagation in ferrite media," PROC. IRE, vol. 43, p. 1011; August, 1955.

magnetizing field is either parallel or transverse to the longitudinal axis of the waveguide.[4-9] We shall consider first the case where the magnetizing field is parallel to the longitudinal axis which is taken as the z-axis. It is assumed that the ferrite is uniformly magnetized, and that its cross section is uniform with respect to z. As in the case of an isotropic medium, all the field components of any mode can be expressed in terms of the longitudinal components E_z and H_z. These components satisfy a pair of equations of the form

$$\Delta^2 E_z + aE_z + b\,H_z = 0.$$
$$\nabla^2 H_z + cH_z + dE_z = 0.$$

The coefficients in these equations are functions of the propagation constant of the mode, and other physical constants of the medium. Formal solutions for the modes which depend on the solution of a transcendental equation for the propagation constant can be obtained in the case of a round guide filled or partially filled with ferrite in an axially symmetric fashion. A complete study of the modes is very difficult, but certain general properties can be readily obtained. For example, it can easily be shown that no TE, TM, or TEM modes are possible. The modes fall into two groups; those having an $e^{jn\theta}$ and those having an $e^{-jn\theta}$ θ-dependence. The transverse field vectors of these modes are circularly polarized in opposite senses on the axis of the guide. (If $|n|>1$ this statement must be interpreted in a limiting sense, inasmuch as the transverse field components vanish on the axis in this case.) For a given direction of propagation, the propagation constant of a mode with an $e^{jn\theta}$ dependence differs from one with an $e^{-jn\theta}$ dependence. In other words, as in the case of the unbounded medium, modes which are circularly polarized in opposite senses have unequal propagation constants. This leads to a rotation of the plane of polarization when an incident linearly polarized mode passes through a ferrite waveguide section. This situation differs from the unbounded medium case, inasmuch as the counter-rotating circularly polarized modes not only have unequal propagation constants, but have different field configurations as well. It has been pointed out by some writers that two such modes do not combine to give a linearly polarized transverse field pattern which simply rotates as the wave progresses in the direction of propagation. While this is true within the ferrite medium itself, in the usual application one is not concerned with the field configuration within the ferrite medium, but rather with the relation between input and output waves on passing through a ferrite section of waveguide which joins two empty sections. From symmetry considerations, it is clear that an incident circularly polarized mode will emerge circularly polarized, in the same sense. However, the phase change on passing through the ferrite section will be different for two incident circularly polarized modes of opposite sense. Thus if a linearly polarized mode is incident on the ferrite section, the relative phase of its two circularly polarized components will be altered on passing through the section. If the insertion losses are equal for the two components they will recombine to form a linearly polarized mode, rotated with respect to the incident mode. If the amplitudes of the transmitted components are unequal, the resultant will be elliptically polarized, but the major axis of the ellipse will make the same angle with the direction of polarization of the incident wave as would be the case if the amplitudes were equal.

For the case of the completely filled circular waveguide, calculated values of the propagation constant for several special cases are given in a paper by Gamo.[5] Suhl and Walker[6] have made an extensive study of the behavior of the modes as a function of various physical constants of the medium. The results which they have obtained, as well as the analysis, are rather involved and we shall not attempt to summarize them here. Instead we shall single out for discussion just one of the interesting results which they present, which serves to illustrate some of the novel features of propagation in the ferrite medium. This has to do with the cutoffs of the modes. The analysis of Suhl and Walker shows that there are three different types of cutoffs. One of these types has been obtained by others, and is similar to the cutoff which occurs if the circular waveguide is filled with a homogeneous, isotropic medium. In such a waveguide, when the propagation constant β becomes zero, the field can be represented as a superposition of plane waves propagating at right angles to the longitudinal axis of the guide. It was pointed out earlier that in the unbounded ferrite medium two plane waves propagating at right angles to the direction of the magnetizing field were possible. With respect to the vectors $\vec{E}$ and $\vec{B}$ these waves are identical with plane waves in an isotropic medium. Since the boundary conditions in the filled guide involve only the tangential components of $\vec{E}$, it is clear that a cutoff condition can be obtained in the ferrite waveguide by a superposition of plane waves propagating at right angles to the axis. In calculating the cutoff one has only to use the effective value of μ, which is μ_z if the $\vec{H}$-vector of the plane waves is parallel to the axis, and $\mu(1-(\kappa/\mu)^2)$ if the $\vec{H}$-vector is perpendicular to the axis of the waveguide. Fig. 1 is a plot of the normalized propagation constant vs the normalized wave-

[4] M. L. Kales, "Modes in waveguides containing ferrites," *J. Appl. Phys.*, vol. 24, pp. 604–608; May, 1953.
[5] H. Gamo, "The Faraday rotation of waves in a circular waveguide," *J. Phys. Soc. Japan*, vol. 8, pp. 176–182; March–April, 1953.
[6] H. Suhl and L. R. Walker, "Topics in guided-wave propagation through gyromagnetic media, Part I—The completely filled cylindrical guide," *Bell Sys. Tech. J.*, vol. 33, pp. 579–659; May, 1954.
[7] H. Suhl and L. R. Walker, "Topics in guided-wave propagation through gyromagnetic media, Part II—Transverse magnetization and the non-reciprocal helix," *Bell. Sys Tech. J.*, vol. 33, pp. 939–986; July, 1954.
[8] H. Suhl and L. R. Walker, "Topics in guided-wave propagation through gyromagnetic media, Part III—Perturbation theory and miscellaneous results," *Bell Sys. Tech. J.*, vol. 33, pp. 1133–1194; September, 1954.
[9] A. A. Th. M. VanTrier, "Guided electromagnetic waves in anisotropic media," *Appl. Sci. Res.*, sec. B, vol. 3, pp. 305–371; 1953.

guide radius for a value of $\kappa/\mu=\frac{1}{2}$. (Modes are referred to as quasi-TE or quasi-TM if the limit of zero magnetizing field they reduce to TE or TM modes.) Note that the cutoff occurs at the same value of the radius for both the positive and negative circularly polarized modes. The dashed line is the asymptotic value of the propagation constant for the positive circularly polarized modes, as the waveguide radius becomes infinite. This value is that which would be obtained in the unbounded magnetized ferrite medium.

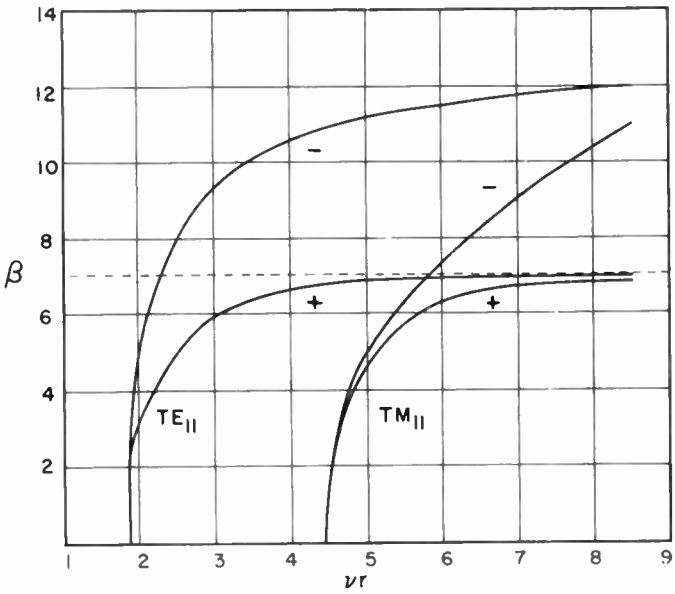

Fig. 1—Normalized propagation constant vs normalized radius. (Reproduced, with minor change in notation, from Gamo.[5])

The second type of cutoff, for which β is zero, is one for which the longitudinal components E_z and H_z both vanish. An examination of the equations which express the transverse components of the field in terms of the longitudinal components reveals that a nonzero solution is possible only if $\kappa/\mu=\pm 1$. It then turns out that $\vec{E}$ and $\vec{B}$ are both zero, and we are left only with a circularly polarized $\vec{H}$-vector rotating in planes perpendicular to the axis of the guide. For an $e^{jn\theta}$ θ-dependence it can be shown that $\vec{H}=\nabla r^n e^{jn\theta}$, where r and θ are the polar-coordinates of a point in the transverse plane. The striking feature of this solution is the existence of a time-varying $\vec{H}$-field, without an accompanying $\vec{E}$-field. Such a situation cannot exist in an isotropic medium, but is here possible because the appropriate effective μ, which is $\mu\pm\kappa$ when the $\vec{H}$-vector is circularly polarized in a transverse plane, vanishes. The occurrence of this type of cutoff can be seen in Fig. 2, where a normalized value of the propagation constant is plotted vs a parameter p for several values of a normalized radius. The parameter p is proportional to the magnetization of the ferrite. When $p=-1$, $\mu+\kappa=0$, which is a condition for cutoff. Note that the cutoff does not occur if the guide radius

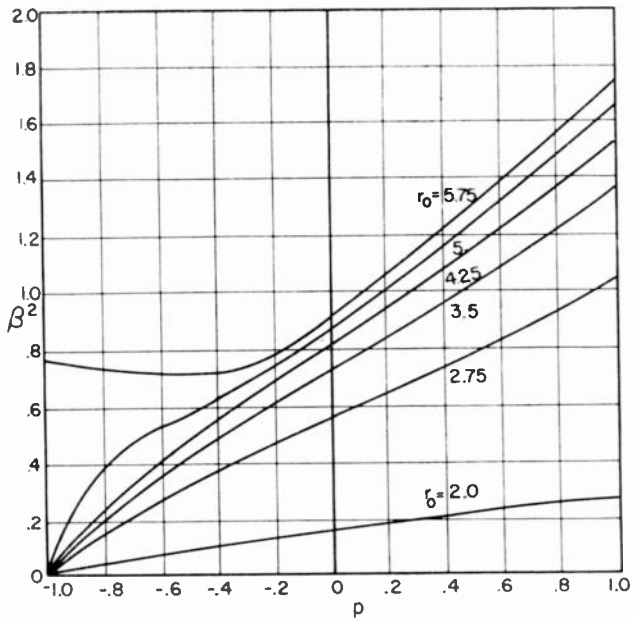

Fig. 2—Square of normalized propagation constant vs parameter p. (Reproduced from Suhl and Walker.[6])

is sufficiently large. The curves shown are for just one sense of polarization. Curves for the other sense may be obtained by reflection in the vertical axis.

The third type of cutoff is perhaps the most unusual in that, when it occurs, β is not zero. This cutoff occurs when the main diagonal component μ of the tensor permeability becomes zero. It is not clear from the analysis whether this mode still exists as a nonpropagating mode or simply ceases to exist when μ becomes negative. It appears to the writer that the method of analysis is such, that only those values of β^2 which are real can be obtained. The question then arises whether or not β can become complex, even though the medium is assumed to be lossless. (Continuity considerations would appear to rule out the possibility of an imaginary value of β.) Such a result would be in contrast with the homogeneous, isotropic case where for a lossless medium the propagation constant is always real or imaginary. (According to Adler this is true even for an inhomogeneous, isotropic medium.)[10]

We turn now to a recent publication by Chambers which deals with the case of a waveguide of *arbitrary* cross section completely filled with ferrite and magnetized in the longitudinal direction.[11] The author treats the case where the main diagonal components of the tensor μ and μ_z are equal. The longitudinal field components and the square of the propagation constant are represented as series in powers of κ/μ. When $\kappa/\mu=0$, these quantities reduce to the corresponding values appropriate to a particular mode which exists for the waveguide filled with the unmagnetized and therefore iso-

[10] R. B. Adler, "Properties of Guided Waves on Inhomogeneous Cylindrical Structures," Res. Lab. Elec. Tech. Rep. No. 102; 1949.
[11] L. L. G. Chambers, "Propagation in a ferrite-filled waveguide," *Quart. J. Mech. and Appl. Math.*, vol. VIII, Part 4; December, 1955.

tropic, ferrite medium. The determination of the coefficients requires the solution of an infinite set of pairs of wave equations. However, the solution of each pair depends only on the solutions of the preceding equations. Thus, in principle, it is possible to obtain any given number of coefficients. This writer is of the opinion that in its present form the development is not generally valid, although it may be possible to modify it so that it is. For example, the results which Chambers obtains indicate that when the ferrite is weakly magnetized the change in the propagation constant is of the second order in κ/μ, whereas it has been found by other methods to be of the first order in the case of the circularly polarized TE_{11} mode. Furthermore, it would appear from Chambers' results that a linearly polarized mode could be obtained as a limiting form of a single mode in the weakly magnetized ferrite. On the other hand, it is known that if the unmagnetized ferrite medium supports a linearly polarized mode in a circular waveguide, as soon as a longitudinal magnetizing field is applied, the mode splits into *two* counter-rotating circularly polarized modes. These two modes have unequal propagation constants, and therefore cannot combine to form a single mode which would reduce to the linearly polarized mode in the limit of zero magnetizing field.

Ferrite-Loaded Waveguide Transversely Magnetized

The next problem which we shall consider is the one where the magnetizing field is transverse to the longitudinal axis of the guide. The problem which has received the most extensive theoretical treatment is the case of the rectangular waveguide with the magnetizing field perpendicular to the broad faces of the guide. If the z-axis is again taken in the direction of the magnetizing field it can be shown that modes which are independent of z can have only an $\vec{E}$ component in the z-direction, and that $\vec{H}$ is transverse to the z-direction. For the completely filled guide these modes can be found in the same way that they are frequently obtained in the isotropic case: that is, by a superposition of two uniform plane waves traveling in directions which are parallel to the broad faces and make a suitable angle $\pm\theta$ with the longitudinal axis. It will be recalled that, in the unbounded ferrite medium, uniform plane waves exist which propagate in any direction perpendicular to the magnetizing field, have their $\vec{E}$-vector in the direction of the magnetizing field, and insofar as $\vec{E}$ and $\vec{B}$ are concerned are identical in form with uniform plane waves in an isotropic, homogeneous medium of permeability $\mu\left[1-\left(\frac{K}{2}\right)^2\right]$. Since in the completely filled guide the boundary conditions involve only the tangential components of $\vec{E}$, it is obvious that for these z-independent modes the solutions are the same as in the empty waveguide insofar as $\vec{E}$ and $\vec{B}$ are concerned. It should be emphasized at this point that these remarks do not apply in the case where the ferrite only partially fills the cross section of the guide. In such a case the boundary conditions involve the tangential components of $\vec{H}$ at an interface between the ferrite and the air.

If we solve for the components of $\vec{H}$ in terms of those of $\vec{B}$ we find that

$$H_x = (\mu B_x + j\kappa B_y)(\mu^2 - \kappa^2)^{-1}$$
$$H_y = (-j\kappa B_x + \mu B_y)(\mu^2 - \kappa^2)^{-1}.$$

Thus we see that if the components of $\vec{B}$ are the same as they would be in an isotropic, homogeneous guide, the components of $\vec{H}$ must differ.

As a consequence of the distortion of the $\vec{H}$-field in the ferrite medium, if a normal waveguide mode is incident on a ferrite-filled section of waveguide an infinite number of modes must be excited in order to satisfy the boundary condition. This differs from the case of the isotropic medium where only modes of the same type are needed to satisfy the boundary conditions.

From the point of view of practical applications, the case where the ferrite only partially fills the cross section of the guide has received the greatest amount of study. The simplest case to analyze is that in which the ferrite consists of one or more slabs of rectangular cross section which fill the guide in height, and for which the modes are independent of z. In this case formal solutions which depend on the solution of a transcendental equation for the propagation constants can be obtained. An examination of the equation which determines the propagation constants reveals that when a single slab is asymmetrically located in the waveguide, the propagation constants of the modes depend upon the direction of propagation. The same thing is true for an asymmetrical distribution of several slabs. (Throughout this discussion a distribution will be considered asymmetrical even in the case where there is geometrical symmetry, if the geometrically similar portions are oppositely magnetized.) From the fact that the propagation constants are dependent on the direction of propagation, it may be concluded that the relation between the transmitted wave and the wave which is incident on such a section is dependent on the direction of propagation. In other words the ferrite section is "nonreciprocal." From a rigorous mathematical point of view this argument is not conclusive since, for either direction of propagation, an infinite number of modes are excited at the transitions between the empty and ferrite sections of guide. Intuitively, however, one might except nonreciprocal behavior, and this is borne out by experimental results.[12-14] The nonreciprocal character of the propaga-

[12] M. L. Kales, H. N. Chait, and N. G. Sakiotis, "A nonreciprocal microwave component," *J. Appl. Phys.*, vol. 24, pp. 816–817; June, 1953.

[13] N. G. Sakiotis and H. N. Chait, "Properties of ferrites in waveguides," Trans. IRE, vol. MTT-1, pp. 11–16; November, 1953.

[14] H. N. Chait, "Non-reciprocal microwave components," 1954 IRE Convention Record, Part 8, pp. 82–87.

tion can also be accounted for by a physical argument which is useful in analyzing other cases. When the ferrite is magnetized, the spin axes of the electrons in the ferrite have a natural sense and frequency of precession about the direction of magnetization. If the rf magnetic vector is circularly polarized, in a plane perpendicular to the magnetizing field, its interaction with the electron spins will depend on whether the sense of rotation is the same or opposite to the sense of precession of the spin axes. If the rf magnetic vector is elliptically polarized, it can be resolved into unequal circularly polarized components of opposite sense. The effect of the medium on propagation will depend on which sense of circular polarization is greater. Now let us consider the rf magnetic vector of the dominant mode in empty waveguide. This vector is elliptically polarized in planes parallel to the broad faces of the guide. In passing from one side of the guide to the other the sense of rotation of the vector reverses. If the direction of propagation is reversed, the senses of polarization on the two sides are interchanged. Thus, when the dominant mode is incident on the ferrite section for one direction of propagation one sense of circular polarization is greater, but when the direction of propagation is reversed the other sense of polarization is greater at the place where the ferrite is located. Here again the argument is not conclusive since it is the resultant field in the ferrite medium which is the determining factor. Again intuition suggests that if the polarization of the incident field is different for the two directions of propagation, the same will be true of the resultant field.

If the ferrite is symmetrically distributed, it follows from symmetry considerations that the relationship between incident and transmitted fields is independent of the direction of propagation. One of the interesting features of the ferrite medium is that the field distribution is asymmetrical even though the medium has physical symmetry. We have already seen that this is true of the $\vec{H}$-field in the case of the filled waveguide. When the waveguide is only partially filled, both the $\vec{E}$-field and $\vec{H}$-field may be asymmetrical. This fact has an important bearing on the design of ferrite devices. For example, if a scanning antenna is designed by cutting slots in the narrow wall of a ferrite-loaded guide, the field configuration at the slots depends on the direction of propagation. Thus the identity of the transmitting and receiving pattern that exists in the case of conventional antennas is destroyed. This violation of reciprocity is not surprising when it is considered that the slots on one side of the guide destroy the symmetry which otherwise leads to reciprocal propagation characteristics. Although the nonreciprocal field distribution is a disadvantage in the case of antennas, there are other applications which take advantage of this fact. One of these is the so-called field displacement isolator where the displacement of the field from one side of the guide to the other, when the propagation direction is reversed, is used to produce a much greater dissipation of energy for one direction of propagation than the other.[15]

Lax and his co-workers have made a study of the propagation constants and the mode configurations for a number of reciprocal and nonreciprocal cases.[16,17] We shall here review some of the results which appear to be of particular interest. The first deals with the case where slabs of equal thickness are placed adjacent to each of the narrow walls of the guide and magnetized in the same direction. The electric field distributions and a plot of the phase constant vs slab thickness for two propagating modes are shown in Figs. 3 and 4. The first

Fig. 3—Electric field patterns for ferrite modes in rectangular waveguide. (Reproduced from Lax and Button.[16,17])

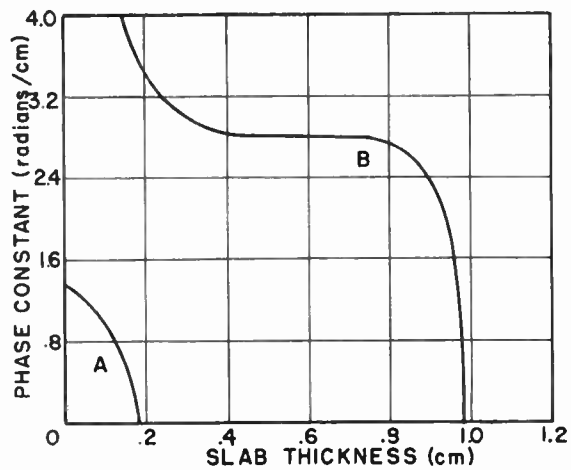

Fig. 4—Phase constant vs slab thickness. (Reproduced from Lax and Button.[16,17])

mode designated by "A" has an electric field distribution similar to that of the dominant mode of the empty guide, and in the limit of zero slab thickness this mode reduces to the dominant TE_{10} mode. On the other hand when the slab thickness exceeds a certain critical value this mode is cut off. At first glance, it seems rather surprising that the mode should be cut off when the slab thickness increases. One, perhaps, thinks of the case of pure dielectric slabs where, as the slab thickness increases, the electrical width of the waveguide increases

[15] A. G. Fox, S. E. Miller, and M. T. Weiss, "The behavior and applications of ferrites in the microwave region," *Bell Sys. Tech. J.*, vol. 34, pp. 6–103; January, 1955.

[16] B. Lax and K. J. Button, "Theory of new ferrite modes in rectangular wave guide," *J. Appl. Phys.*, vol. 26, pp. 1184–1185; September, 1955.

[17] B. Lax and K. J. Button, "New ferrite mode configurations and their applications," *J. Appl. Phys.*, vol. 26, pp. 1186–1187; September, 1955.

and therefore there is no tendency for a mode to be cut off. However, it will be recalled that for plane waves traveling at right angles to the direction of static magnetization, the effective permeability is given by $\mu_{eff}=\mu(1-(\kappa/\mu)^2)$. We see that μ_{eff} can be made arbitrarily small, and even negative, by making κ/μ close to unity. We can think of the electrical thickness of the slab as being given by $\omega\sqrt{\epsilon\mu_{eff}}\,t$, where t is the actual thickness. Thus, even though the dielectric constant of the ferrite is rather large, the electrical thickness of the slab can be made smaller than that of air, by making μ_{eff} small. If this is true, making the slabs thicker would narrow the electrical width of the guide, and tend to suppress the dominant mode.

The second mode which is designated by "B" does not make its appearance until the slab thickness reaches a certain minimum value, and it is cut off as soon as the thickness exceeds a critical value. This mode has been compared by Lax and Button with a so-called "ferrite dielectric" mode, shown in Fig. 5. The "ferrite dielectric"

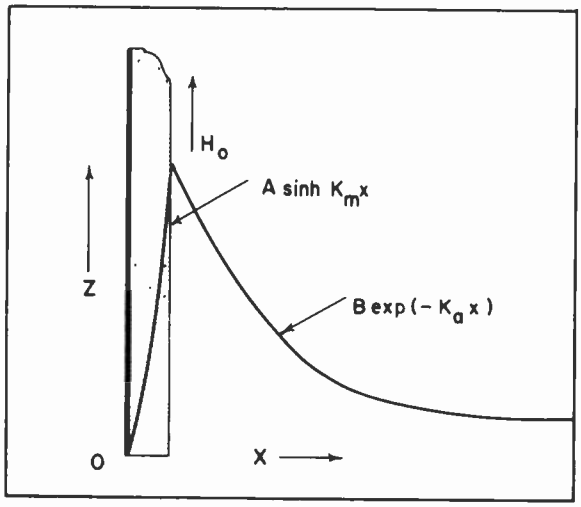

Fig. 5—Electric field distribution of the "ferrite dielectric" mode. (Reproduced from Lax and Button.[16,17])

mode is a bound wave which propagates in the semi-infinite space consisting of the space on one side of an infinite perfectly conducting plane, with an infinite magnetized slab adjacent to it. It is possible for a wave to be guided by this slab for one direction of propagation, but not the other. For this wave the electric field reaches a peak value at the interface between the ferrite and air, and is then attenuated exponentially with distance from the conducting plane. In the waveguide, the second slab and waveguide wall are in a region where the field of the mode guided by the first slab is weak. Presumably, therefore, the effect of the second wall and slab is to perturb the "ferrite dielectric" mode somewhat. If the direction of propagation is reversed, the second slab guides the mode, and thus the peak field intensity shifts from one side of the guide to the other.

If a single slab is placed in the waveguide, Lax and Button have shown that a situation may exist which has aroused wide interest. This is the fact that if the thickness and magnetizing field are properly chosen, a propagating mode will exist for one direction of propagation, but there will be no propagating modes for the other. From energy considerations it is known that if two ports of a junction are coupled by a lossless transmission path in such a way that energy can be transmitted from one to the other, then transmission in the reverse direction is possible. Ferrite circuits do exist which permit energy to be transferred from one port to a second, but not from the second to the first. In these cases, energy transmitted from the second port is transferred to a load, and the transmission path must be regarded as a lossy path for that direction of transmission. It might at first seem that the conditions described by Lax and Button, where a propagating mode is possible in one direction, but none is possible in the opposite, violate these energy principles. However, it should be kept in mind that in discussing a single mode, the waveguide must be considered to extend to infinity in both directions, and have no available ports. It is helpful, perhaps, to think of the waveguide as being in the form of a closed circle of infinite radius. It is then not difficult to think of energy circulating around this path in one sense, but not in the other, and no energy principles are violated. On the other hand if the ferrite section is finite, and leads at both ends into an empty section of waveguide, then an infinite number of modes must be excited at the transition planes. Now, even in the case of a conventional waveguide at a frequency for which all modes are cut off, it is possible to transmit energy through a finite length. This requires only that two properly phased modes of the same kind, and attenuated in reverse direction, be present. It therefore does not seem unreasonable to expect that propagation through the finite ferrite section is possible for either direction of propagation, when modes belonging to both directions are present simultaneously.

The modes which have been discussed thus far are those which have no z-dependence, and for which the magnetizing field is parallel to the z-axis. The more general problem of finding modes of the completely filled rectangular waveguide which are z-dependent has been solved by Mikaelyan.[18] The method used by Mikaelyan is a modified form of one which has been used in the case of conventional waveguides. A parallel plate ferrite medium is first considered with planes perpendicular to the z-axis. A pair of plane waves of the type discussed in the first section of this paper are combined to give a mode for which the components of $\vec{E}$, which are normal to the z-axis, have a sin $n\pi z/z_0$ dependence on z, where z_0 is the distance between the parallel plates, and n is an integer. It is found that for each integer n there are two such modes propagating in an arbitrary direction parallel to the plates. If a third perfectly conducting

[18] A. L. Mikaelyan, "Electromagnetic waves in a rectangular wave-guide filled with a magnetized ferrite," *Doklady, A. N., USSR*, vol. 98, pp. 941–944; 1954.

plane perpendicular to the first two is introduced, it is found that when one of these parallel plate modes is incident on the third plane, two are reflected. Therefore when the waveguide is completed by adding a fourth plane parallel to the third, two incident and two reflected waves are needed to satisfy the boundary conditions at both walls. These boundary conditions then lead to a transcendental equation for the determination of the propagation constants, and the modes are completely determined when the propagation constants are found.

Perturbation Theory

The final theoretical topic to be discussed is that of perturbation theory. A number of writers have made contributions in this area, but probably the most comprehensive treatment is that of Suhl and Walker.[8] Two types of problems have been treated. One of these is where the magnetization of the ferrite is of arbitrary magnitude, but because the appropriate dimensions of the ferrite are small the perturbation of the homogeneous, isotropic mode is small. The other is the case where the ferrite dimensions are unrestricted, but the magnetizing field is weak. This represents a perturbation of a mode corresponding to an isotropic, but not necessarily homogeneously filled waveguide. The perturbation theory has been applied principally to cavity techniques for determining the intrinsic physical constants of the medium. From the point of view of propagation studies, it is usually the case that when the perturbation is sufficiently small to permit accurate quantitative calculation, the desired effect is too small to be of practical value. Nevertheless, the perturbation theory is often useful in providing a qualitative guide to the behavior of various ferrite devices. Thus, for example, if the dominant linearly polarized mode in a circular waveguide is incident on a longitudinally magnetized ferrite section, the propagation constants of the positive and negative circularly polarized components in the ferrite section are given by formulas of the form

$$\beta_+ = \beta_0 + A\kappa + 0(\kappa^2)$$
$$\beta_- = \beta_0 - A\kappa + 0(\kappa^2).$$

Here β_0 is the propagation constant in the unmagnetized ferrite medium and A is a constant. If the ferrite is in the form of a cylinder which is long compared to its diameter, κ will vary linearly with the applied magnetizing field. If the effect of multiple reflections can be neglected, the angle of rotation of the transmitted wave is determined by $(\beta_+ - \beta_-)/2 = A\kappa + 0(\kappa^2)$ and the phase is determined by $(\beta_+ + \beta_-)/2 = \beta_0 + 0(\kappa^2)$. Thus we see that a ferrite section can be devised which, when second and higher order terms are neglected, produces a rotation of the incident wave which varies linearly with the magnetizing field, but for which the phase of the transmitted wave is independent of the magnetization. Such a device is useful when it is desired to produce an amplitude modulation without any accompanying phase modulation.

Conclusion

At the present time the exact theory of propagation in ferrite-loaded waveguides is inadequate and too involved for the treatment of practical problems. Nevertheless, much has been learned by using the theory as a qualitative guide in conjunction with experimental methods. We shall close with a discussion of a configuration which has been investigated experimentally, but for which a rigorous theory is not available. If, in the case of the transverse magnetizing field, the rectangular waveguide which can propagate only the dominant mode is replaced by a circular waveguide, an added degree of freedom is obtained. (Actually, for this added degree of freedom, it is only necessary that the waveguide be capable of supporting two orthogonally polarized modes.) We shall assume that the axis of the ferrite cylinder coincides with the axis of the waveguide. By analogy with the unbounded ferrite medium theory for the case of propagation perpendicular to the direction of magnetization, we find that what we can call an effective propagation constant depends on whether the $\vec{E}$-vector of an incident linearly polarized mode is parallel or perpendicular to the direction of the magnetizing field. Experimentally, it has been determined in these two cases, that after passing through the ferrite section, an incident linearly polarized mode emerges linearly polarized. If the $\vec{E}$-vector of the incident mode makes some other angle θ with the direction of the magnetizing field, the incident mode can be resolved into a parallel and perpendicular mode. After emerging from the ferrite section, the relative phase of these two component modes will depend on the length of the section, and the two modes can be recombined to form a single elliptically polarized mode. For proper lengths a half-wave or quarter-wave plate can be produced.

If the axis of the ferrite cylinder is displaced from the axis of the guide, it is possible to obtain either reciprocal or nonreciprocal propagation characteristics. In particular, as Turner has shown, a nonreciprocal phase shifter can be obtained.[19] Another possibility is a ferrite section which acts as a half-wave plate for one direction of propagation, and a quarter-wave plate for the other.[20]

The discussion in this paper has been limited principally to topics which have been treated theoretically. Although some of the experimental results have been touched upon, a great deal more has been presented in a number of published articles during the past few years. The knowledge gained from these theoretical and experimental studies of propagation in ferrite media has already led to the development of a number of important ferrite devices of both the reciprocal and nonreciprocal variety, and probably in time we shall see many more such developments.

[19] E. H. Turner, "A new nonreciprocal waveguide medium using ferrites," Proc. IRE, vol. 41, p. 937; July, 1953.
[20] N. G. Sakiotis, "Ferrite quarter-wave and half-wave plates at X-band," 1954 IRE Convention Record, Part 8, p. 88.

Anomalous Propagation in Ferrite-Loaded Waveguide*

HAROLD SEIDEL†, MEMBER, IRE

Summary—**Gyromagnetic loading of waveguide structures curiously modifies the conventional modal description of propagation. Among the anomalies produced is that in which propagation is found to occur in vanishingly small waveguide cross sections at a given frequency. Another is the appearance of spurious resonances in an ostensibly single mode waveguide. A physical basis of such phenomena is described employing the birefringent character of the gyromagnetic medium, and corroborating experimental evidence is offered.**

ANOMALOUS RESULTS are quite often experimentally observed in ferrite-loaded microwave devices. One finds, for instance, that the reverse loss of a field displacement isolator in rectangular guide is not a linear function of length of the loss film. Another illustration is the appearance of spurious spikes of transmission loss that occur as a function of swept fields or frequency. In each of these two cases calculations indicate that but a single TE mode is propagating in the guide. The argument is employed that it is only TE modes which propagates since the narrowness of the guide height precludes the formation of other types of modes. The nature of these phenomena is therefore not directly evident.

The key to the situation is in the fact that modes of non-TE variety may propagate irrespective of the guide height, and as it will be shown, irrespective of guide width as well. This statement may be understood only by appreciating the character of propagation in birefringent media. That the magnetized ferrite medium is birefringent is not surprising in view of the medium anisotropy in the direction of the magnetic field.

Let us consider the propagation of plane waves in a gyromagnetic medium. If the plane wave is represented by a dependence of the form $\epsilon^{-ik\cdot R}$, we may expect the scalar wave equation to be a function of k_z and k_t, where these are the components along the magnetic field and along some transverse axis, respectively. The equation is not homogeneous in these quantities, as it would be in isotropic media, and we find two values of k_t^2 corresponding to one of the k_z^2. As shown in Fig. 1, a specification of k_z gives rise to two possible values of the vector k. Since the transverse axis is arbitrary the two solutions k_1 and k_2 form cones having semivertical angles θ_1 and θ_2 with the z axis, respectively.

Let us fix one degree of freedom by requiring that the projections along one transverse axis, say the y axis, are equal in magnitude (Fig. 2). Thus, the two values of k_x are unequal. Although all projections are shown real we may not exclude complex projections. In particular, let us seek that situation in which k_y is real and both

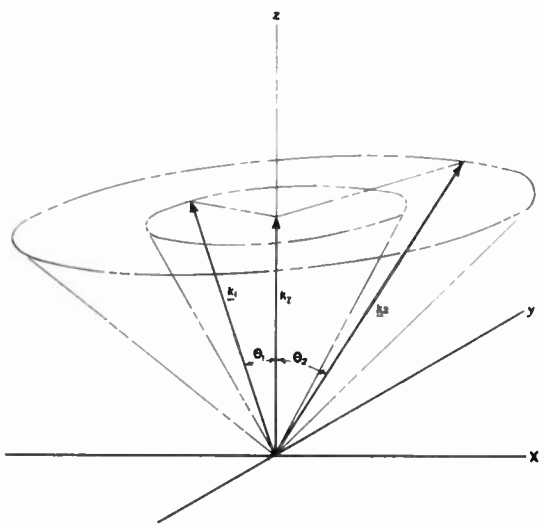

Fig. 1—Splitting of propagation vector by magnetic field.

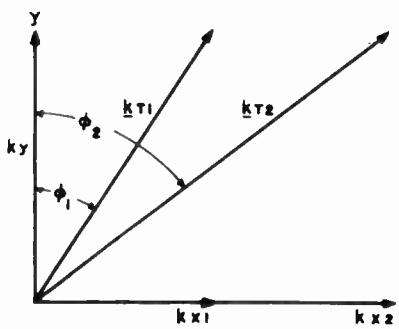

Fig. 2—Transverse projection of propagation vectors uniquely defining k_y.

values of k_x are imaginary. Under these circumstances

$$k_{1,2}^2 = k_z^2 + k_y^2 - |k_{x1,2}|^2. \tag{1}$$

The quantity k_z may be made arbitrarily large if $|k_x|$ increases in proportion.

We may understand now the nature of propagation in an arbitrarily small size waveguide. Demonstrated in Fig. 3 is the relation sought of the various components of the propagation vectors. Cutoff occurs transversely instead of longitudinally. There is no contradiction since there are two types of transverse decay to provide the null requirements at each wall. Multiple half wave variations occur in the guide height and the modes are ordered by the number of such variations. Considering the unique longitudinal wave numbers k_y, the birefringent rays are appropriately welded into true modes of propagation.

It may be shown, incidentally, that the pairing of wave number values only takes place along the x axis

* Original manuscript received by the IRE, July 3, 1956.
† Bell Telephone Labs., Inc., Murray Hill, N.J.

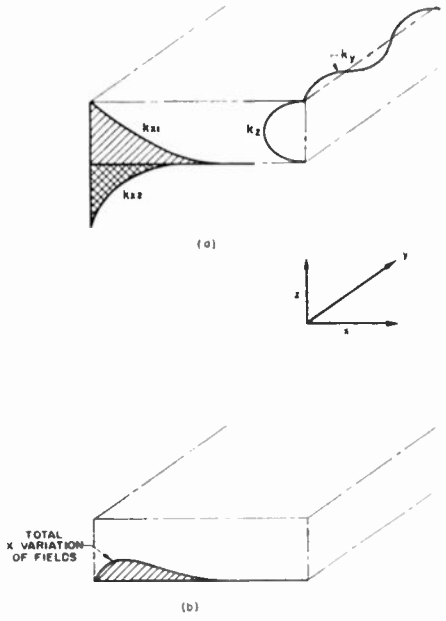

Fig. 3—Mode of propagation in small size waveguide.

for the geometry shown. The distribution shown in Fig. 3 is made unique by the satisfaction of the vector boundary condition which defines exactly the direction cosines of k_1 and k_2.

Analysis indicates that propagation occurs for this type of mode for

$$\mu^2 < \kappa^2, \qquad \mu > 0, \tag{2}$$

where μ and κ are components of the permeability tensor. It is of interest at this point to remark that particular feature of ferrites which causes $\mu^2 = \kappa^2$ to denote that condition for which the waveguide generally initiates some peculiar mode of behavior. It is at precisely this condition that the permeability tensor becomes singular since its determinant vanishes. The consequence of this singularity is generally given in the formation of branch points in the complex propagation constant plane with a consequent result.

The type of action taking place in the small rectangular guide may be extended by treating the concentration of energy at one face of the guide as a surface wave. We then have the open slab type guide shown in Fig. 4 in which k_z is assumed large. The ground plane may be wrapped into a cylinder with either the z or the y axis going into the circumference, as shown in Fig. 5(a) and 5(b). Fig. 5(a) indicates a circumferentially applied magnetic field whereas Fig. 5(b) requires a more simply achieved axial field. If either guide is of small circumference the wave periodicity around the guide contour requires large wave numbers, which is consistent with the assumed nature of the mode. The center void of material at the guide center may be filled or left as is without undue consequence.

Propagation is therefore likewise initiated at the condition $\mu^2 = \kappa^2$ in a small circular guide. This unusual characteristic of the undersized circular guide first came to

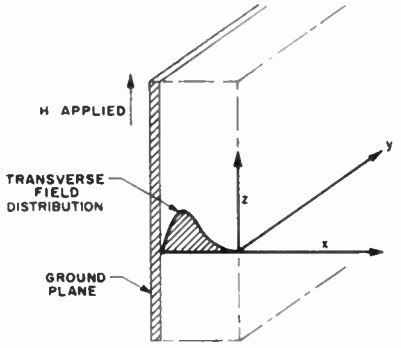

Fig. 4—Ferrite slab surface wave mode.

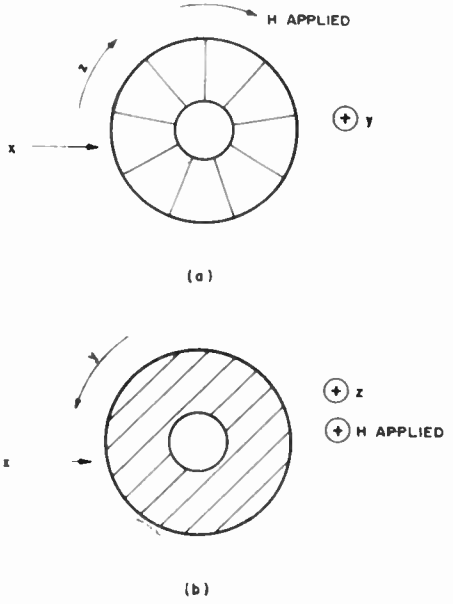

Fig. 5—Wrapping of ferrite slabs into cylinders.

light in Part I of Suhl and Walker's analytic treatment of ferrite propagation.[1] The mode in question was referred to by them as "unclassical" and its physical character was not investigated in detail. Thompson[2] subsequently reexamined this mode of behavior and felt that propgatation was attributable to the negative effective permeability of the preferred circular polarization spin sense. Actually, one determines analytically that both senses of polarization appear over the range $\mu^2 < k^2$. While it may be shown to be true that only one sense of polarization propagates over the positive μ portion of the range, both senses propagate when μ is negative.

The analysis may be sketched briefly as follows. Maxwell's equations lead to

$$[\text{curl}^2 - \omega^2\epsilon_0\mu_0 T\cdot\,]H = 0 = [k^2 I - kk - \omega^2\epsilon_0\mu_0 T]\cdot H, \tag{3}$$

[1] H. Suhl and L. R. Walker, "Topics in guided wave propagation through gyromagnetic media," *Bell Sys. Tech. J.*, vol. 33, p. 3; May, 1954. See Fig. 9(g), p. 915 and Table I, p. 642.

[2] G. B. H. Thompson, "Unusual waveguide characteristics associated with the apparent negative permeability obtainable in ferrites," *Nature*, vol. 175, p. 1135; June 25, 1955.

where the right-hand side is the expansion for plane waves of vector wave number k, and I is the idemfactor. If we represent the dyadic operator on the right by a matrix, we must require that its determinant vanish. In terms of the colatitude angle θ between k and z axis, we obtain the following

$$\cos^4\theta[(\mu^2-\kappa^2)h + k_z^2(\mu^2-\kappa^2-\mu h)] + \cos^2\theta[(h-\mu)k_z^4 - k_z^2(\mu^2-\kappa^2+\mu h)] + k_z^4\mu = 0, \tag{4}$$

where we have used the transformations

$$\omega^2\epsilon_0\mu_0\mu \longrightarrow \mu,$$
$$\omega^2\epsilon_0\mu_0\kappa \longrightarrow \kappa,$$
$$\omega^2\epsilon_0\mu_0 \longrightarrow h.$$

Birefringence is confirmed through the existence of two solutions of $\cos^2\theta$. In the limit of small guide sizes, in general, k_z becomes infinitely large and the two solutions become

$$\cos^2\theta_1 = \frac{\mu}{\mu - h},$$
$$\cos^2\theta_2 = \frac{(\mu-h)}{\mu-\kappa^2-\mu h}k_z^2. \tag{5}$$

If ϕ is the angle made between the transverse component of the vector k and the y axis, using the solutions of (5), one finds that $\cos\phi_{1,2}$ is imaginary if k_y is to be real for the rectangular guide case. Satisfying boundary conditions at the "active" guide wall produces the propagation condition

$$\cos^2\phi_1 = \frac{\mu^2}{\mu^2-\kappa^2}, \qquad \mu > 0. \tag{6}$$

Propagation thus occurs for $\mu^2<\kappa^2$. It may be shown[3] that yet another class of modes occurs for $\mu<0$, which is still in the range of $\mu^2<\kappa^2$. These modes employ the birefringent character of the modum but differ in some basic respects from those being presently considered.

Solution for circular guide are formed by an integration of the plane wave solutions about the cone of propagation vectors suitably weighted by a periodic phase factor. The modes are ordered by the number n of peripheral variations, and n takes on both negative and positive values corresponding to clockwise and counterclockwise polarization respectively.

Let $\rho = k_z\mu^{-1/2}R$, where μ is the original Polder tensor diagonal component, and where R is the guide radius. The character of propagation is then obtained in the following two equivalent equations for $\mu>0$.

$$\frac{\mu}{\kappa}I_n'(\rho) - \frac{n}{\rho}I_n(\rho) = 0, \tag{7a}$$

[3] A parallel publication has been submitted by the author to the *Bell Sys. Tech. J.* covering all analytic details of statements made for both the undersized rectangular and circular waveguides.

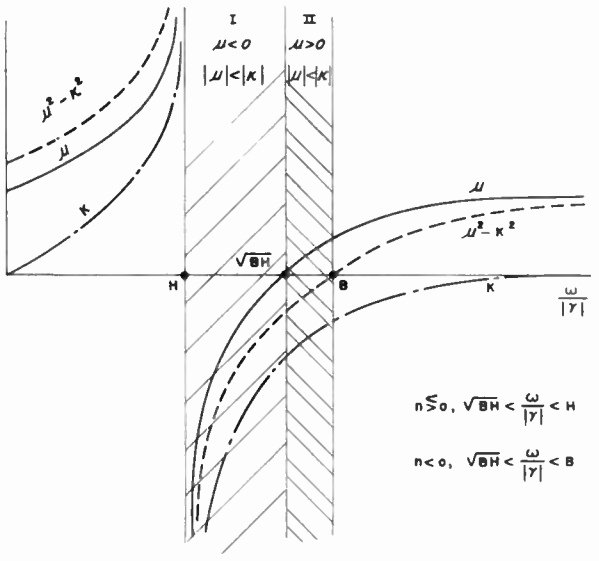

Fig. 6—Regions of propagation of undersized circular guide.

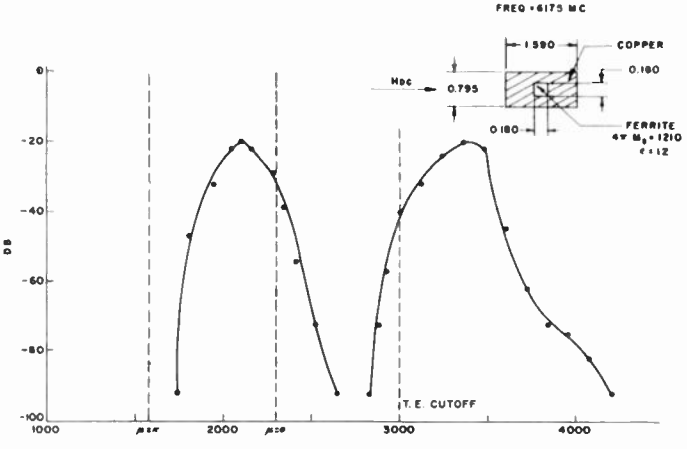

Fig. 7—Applied magnetic field oersteds.

$$\left|\frac{\kappa}{\mu}\right| - 1 = \frac{\rho}{|n|}\frac{I_{|n|+1}(\rho)}{I_{|n|}(\rho)}, \tag{7b}$$

where $I_n(\rho)$ is the modified Bessel function of the first kind. We find from (7a) that reversing the sign of the spin sense, namely n, reverses the sign of μ/k (magnetic field reversal). Eq. (7b), related by recursion formulas, is placed in such form to reflect these sign reversal properties. The double sign relates to the relative direction of the applied field and the sense of polarization. Since the right-hand side of (7b) is positive and monotonic, a single solution exists for $|\mu| < |k|$ for the appropriate direction of magnetic field.

It may be shown that solutions of (7a) indicate propagation in the region of $\mu<0$ for both signs of n and for a fixed direction of applied magnetic field. Singular values of ρ occur for slightly positive values of μ suggesting a resonance occurring at $\mu=0+$. The small circular guide propagating regions are shown in Fig. 6.

Experiment gives startling verifications of the small guide properties deduced from theory. Fig. 7 shows

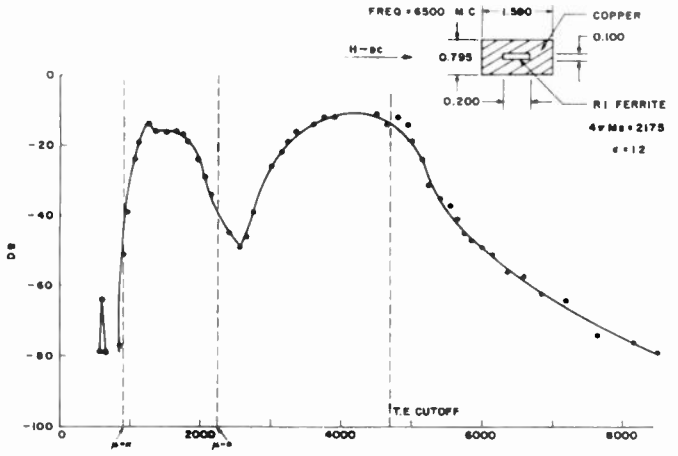

Fig. 8—Applied magnetic field oersteds.

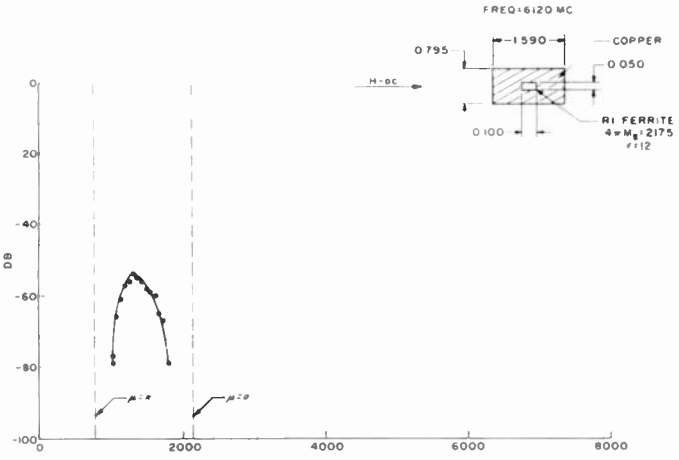

Fig. 9—Applied magnetic field oersteds.

data of a small square guide approximately 0.180 inch on a side and filled with a ferrite of 1210 gauss saturation magnetization and operating at a frequency of 6175 mc. Two regions of energy transmission are shown. Assuming an appropriate average demagnetization factor, the first region essentially spans the range of $\mu = \kappa$ to $\mu = 0$, as a function of magnetic field. The second region is initiated after $\mu = 0$ and persists for some range of magnetic field.

The first region fits the theory described here well considering the approximations involved in taking an average demagnetizing factor. We may interpret the second region by recognizing the massive effective permeability on the high field side of ferromagnetic resonance, with its consequent effect of producing TE transmission in a small guide size. There is no propagation of either form at the condition of susceptibility resonance because of the large loss.

Fig. 8 shows the effect of modifying the aspect ratio of the ferrite-loaded section to obtain a smaller demagnetization and similar data to that of Fig. 7 is obtained. The guide cross section here is 0.1×0.2 inches and the material is now of 2175 gauss saturation.

Fig. 9 shows the effect of reducing the size of the last cross section but maintaining the same aspect ratio. The second region of transmission has disappeared since the effective permeability required for propagation in the TE mode is so large as to be operating well within the region of large resonance loss.

An entirely different type of effect is that observed of spikes of loss appearing in conventional slab type configurations. The following mechanism is suggested:

Birefringent modes are weakly excited in slab type geometries and may resonate for critical slab lengths and positions in the guide. Spikes of extreme loss are caused by a combination of birefringent resonance and destructive interference between the enhanced birefringent mode and the conventional TE mode. The spike is generally deeper and narrower for smaller slab lengths because of the more intense resonance in the smaller, and therefore less lossy, volume. Fig. 10 shows two typical spikes in widely differing geometries and for radically different ferrite materials. The spikes are observed in tracing through the BH loop, and we find that the difference of the interrelationships between B and H around the loop causes the spike to change in appearance.

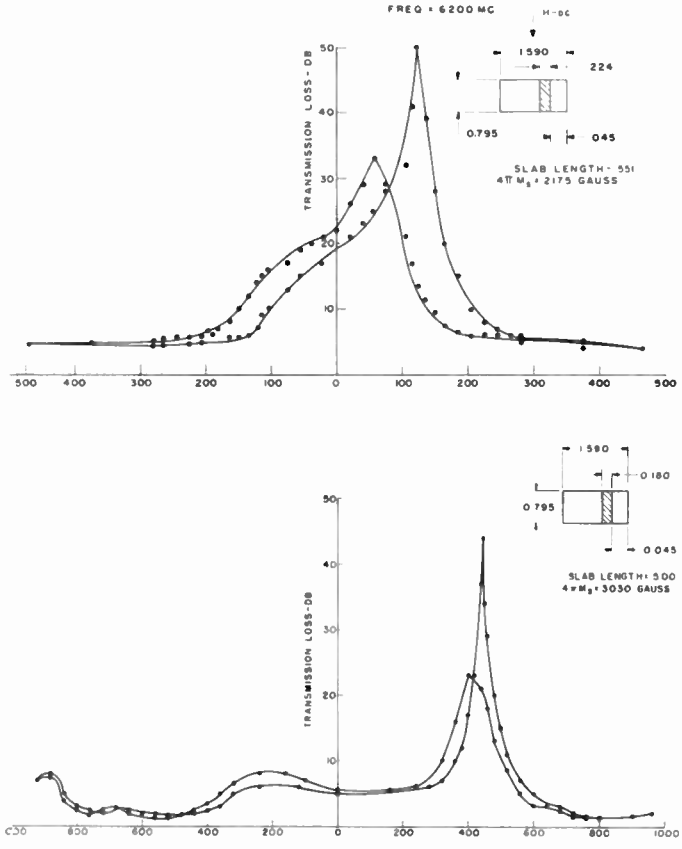

Fig. 10—Magnetic field oersteds.

The nature of such spikes incidentally suggests the need for frequency swept characteristics where ferrite structures are being studied.

Birefringent modes seem to be of importance in tentatively explaining a novel resonance condition observed by S. Weisbaum of the Bell Telephone Laboratories.

Weisbaum observed a geometry independent resonance to exist well above the conventionally described gyromagnetic resonance. Birefringent modal analysis seems to predict its appearance with some accuracy. One may assert simply that the ferrite slab takes on an effective demagnetization appropriate to these modes and leads to results considerably different from that of ordinary slab resonance. It is not surprising therefore to find gyromagnetic resonance recurring at a higher field. These results will be reported on shortly.

Conclusion

The physical character of certain anomalous propagation characteristics has been shown in ferrite-loaded structures. It would seem important for the designer to recognize their effects in addition to conventional design considerations.

Acknowledgment

I should like to thank W. A. Dean for his help in obtaining the experimental data for this paper.

Birefringence of Ferrites in Circular Waveguide*

N. KARAYIANIS† AND J. C. CACHERIS†, SENIOR MEMBER, IRE

Summary—**The objective of this study was to measure the birefringence of different ferrite configurations in circular waveguide. Large differential phase shifts relatively independent of frequency have been obtained with low external magnetic fields. A half-wave plate requiring an external magnetic field of 210 oersteds has been designed with a conversion loss of 3 db or less over the frequency range 9.0 to 9.7 kmc.**

Introduction

THE IMPORTANCE of ferrite devices in microwave electronics has definitely been established. Faraday rotation and the birefringent properties of ferrites have been utilized to develop reciprocal and nonreciprocal devices which, previous to ferrites, were impossible or impractical to design. Examples of dielectric and ferromagnetic birefringence are shown in Fig. 1. A thin dielectric plate placed diametrically across a circular waveguide produces the greatest phase delay when its principal plane lies parallel to the electric field of a dominant mode and least when it is perpendicular. The device introduces a phase difference between the two components of a wave and is called a differential phase shift section. Differential phase shifts can also be achieved by means of a ferrite in a circular waveguide with a static magnetic field transverse to the direction of propagation.[1-3]

The purpose of the experiments to be described in this paper was to investigate the birefringence of circularly symmetrical ferrite geometries in circular waveguide and to design a magnetic half-wave plate which has the following characteristics: Maximum magnetic field 225 oersteds; length 2 inches or less; conversion loss of 3 db or less, and frequency range from 9.0 to 10.0 kmc.

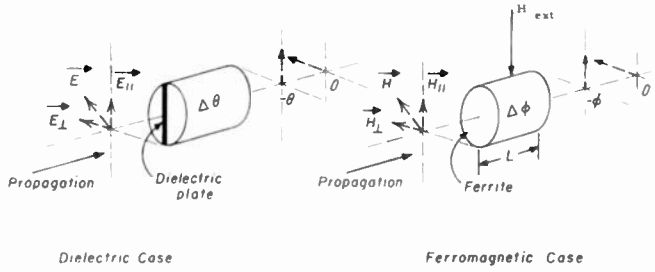

Fig. 1—Birefringence in circular waveguide.

Theory

In order to define conversion loss as a figure of merit for a half-wave plate, the following must be considered: A half-wave plate changes the sense of polarization of a circularly polarized wave. If the half-wave plate is imperfect, *i.e.*, if it differs from 180° differential phase shift by $\Delta\theta$, an elliptically polarized wave will be transmitted. Ellipticity in the transmitted wave will also be produced if the linearly polarized components of the incident circularly polarized wave are unequally attenuated. The resultant elliptically polarized wave may be resolved into two oppositely rotating circularly polarized waves. Conversion loss is defined as the ratio, in decibels, of the power of the incident circularly polarized wave to the power of the transmitted component circularly polarized in the correct sense. It may easily be shown that the formula for computing conversion loss of a lossy, imperfect half-wave plate is

$$-\log_{10} 1/4\left|\gamma_1^2 + \gamma_2^2 + 2\gamma_1\gamma_2 \cos(\Delta\theta)\right|$$

* Original manuscript received by the IRE, July 3, 1956.
† Diamond Ordnance Fuze Labs., Washington 25, D. C.
[1] J. C. Cacheris, "Microwave Single-Sideband Modulator Using Ferrites with Transverse Magnetic Fields," Natl. Bur. Stand. Rep. No. 17-77; September 29, 1952.
[2] M. T. Weiss and A. G. Fox, "Magnetic double refraction at microwave frequencies," *Phys. Rev.*, vol. 88, pp. 146-147; October, 1952.
[3] N. G. Sakiotis, "Ferrite quarter-wave and half-wave plates at x-band," 1954 IRE Convention Record, part 8, p. 88

where γ_1^2 is the ratio of transmitted to incident power of the ordinary wave, γ_2^2 is the same ratio for the extraordinary wave, and $\Delta\theta$ is the phase error of the half-wave plate.

From the above equation, if $\Delta\theta$ is as large as 90°, the conversion loss of the half-wave plate is only 3 db, providing the ordinary and extraordinary waves have 0 db insertion loss ($\gamma_2^1 = \gamma_2^2 = 1$). Similarly the conversion loss is 3 db if $\Delta\theta = 0$ and $\gamma_1^2 = \gamma_2^2 = 0.5$ (3 db), or if $\Delta\theta = 0$ and $\gamma_1^2 = 1$, $\gamma_2^2 = 0.172$ (7.6 db).

The behavior of a *saturated* ferrite magnetized in an arbitrary direction with respect to the direction of propagation has been analyzed by Polder.[4] He has shown that an infinitely large ferrite which is homogeneously magnetized in the z direction becomes birefrigent when electromagnetic plane waves are propagated in the y direction. For two linearly polarized plane waves with microwave magnetic field vectors, $\vec{H}$, respectively parallel and perpendicular to the applied dc magnetic field, the effective microwave permeabilities are

$$\mu_\parallel = \mu_0$$

and

$$\mu_\perp = \frac{\mu^2 - K^2}{\mu}$$

where μ and K are components of Polder's permeability tensor

$$\begin{Vmatrix} \mu & -jK & 0 \\ jK & \mu & 0 \\ 0 & 0 & \mu_\parallel \end{Vmatrix}.$$

At saturation, the effective permeability, $\mu_\parallel$, is independent of the dc magnetic field, while $\mu_\perp$ is a function of the field. For an *unsaturated* medium, both permeabilities are functions of the applied magnetic field.[5] The variation of the two permeabilities with the magnetic field inside the ferrite is shown in Fig. 2. In the low field region, the parallel permeability reaches its maximum value and then remains constant, whereas the perpendicular permeability continues to vary with the internal magnetic field. In this region, $\mu_\parallel$ is greater than $\mu_\perp$ and the phase velocity for the parallel wave is less than that for the perpendicular wave. Consequently, as in optics, the parallel wave will be called the ordinary wave and the perpendicular wave the extraordinary wave. The differential phase shift per unit length of the ordinary wave with respect to the extraordinary wave is given by[6]

[4] H. Polder, "On the theory of ferromagnetic resonance," *Phil. Mag.*, vol. 40, pp. 99–114; January, 1949.
[5] J. C. Cacheris, G. Jones, and R. Van Wolfe, "Topics in the Microwave Applications of Ferrites," Diamond Ordnance Fuze Lab. Tech. Rep. TR-188; July 28, 1955.
[6] J. C. Cacheris, "Microwave single-sideband modulator using ferrites," PROC. IRE, vol. 42, pp. 1242–1247; August, 1954.

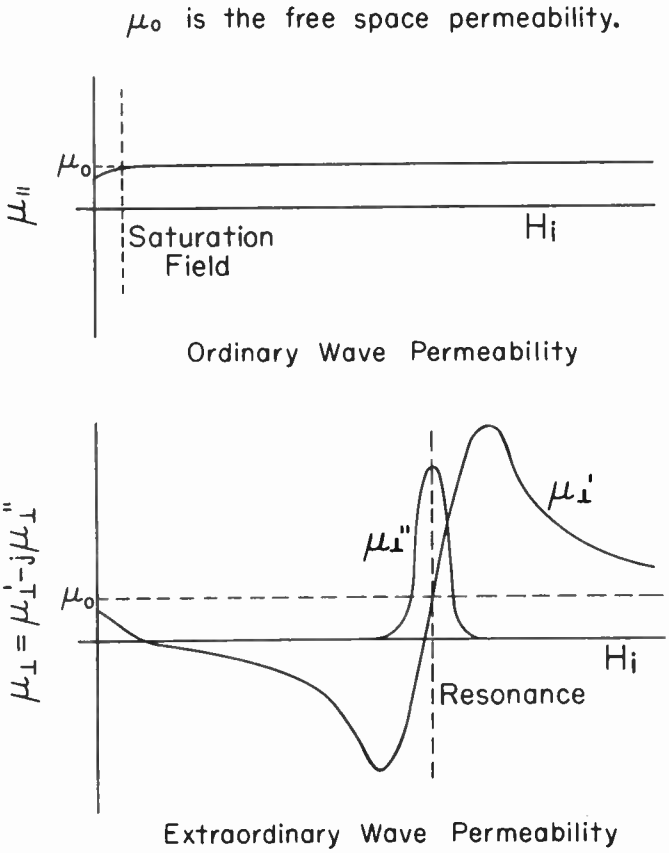

Fig. 2—Qualitative variation of the permeabilities for ordinary and extraordinary plane waves in an infinite ferrite medium as functions of the internal static magnetic field.

$$\frac{\Delta\phi}{l} = \frac{\sqrt{\epsilon}}{2c} \frac{(\gamma^2 B^2 - \gamma^2 HB)}{\omega}$$

where

c is the velocity of light,
ϵ is the dielectric constant of the ferrite,
γ is the magnetomechanical ratio of the spinning electron, (magnetic moment/angular momentum),
B is the internal static flux density,
H is the internal static magnetic field, and
ω is the microwave angular frequency.

In the analysis of the behavior of ferrites in circular waveguide, it will be assumed that the pure TE_{11} mode exists as in empty waveguide. Although the microwave fields in waveguide are curved, the ordinary and extraordinary waves may be defined by referring to the plane of polarization of the TE_{11} mode. The ordinary wave has its $\vec{E}$ vector perpendicular to the external magnetic field. Similarly, the microwave $\vec{E}$ vector of the extraordinary wave is parallel to the external magnetic field. These definitions of ordinary and extraordinary waves agree with those for the infinite medium when very small ferrite pencils are inserted along the axis of circular waveguide.

Relatively small phase shifts are obtained with thin ferrite rods in circular waveguide because only a small part of the microwave energy propagates through the ferrite medium. If the diameter of the rod is increased without decreasing the waveguide diameter, the phase shift will increase, but higher order modes will be excited in the waveguide.[7] Greater differential phase shift can be obtained by filling a reduced circular waveguide section with ferrite (Fig. 3) so that all the microwave energy propagates in the ferrite. The diameter of the reduced section should be chosen so that higher modes cannot exist. The microwave $\vec{H}$ field in circular waveguide is curved and is, in general, parallel or perpendicular to the static magnetic field at only a few points. Nevertheless, the microwave behavior of ferrites can be qualitatively explained by the application of plane wave theory at particular points in the ferrite, and averaging these effects over the waveguide cross section.

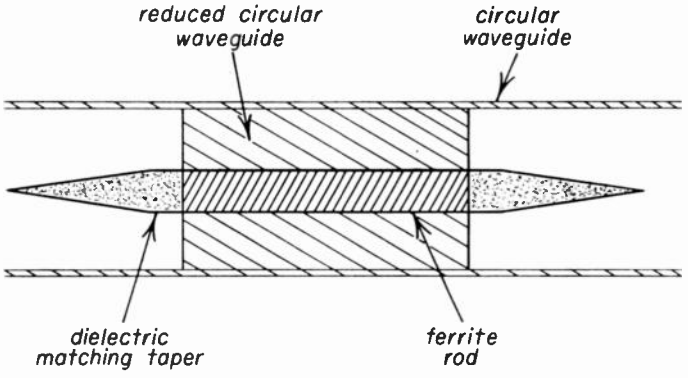

Fig. 3—Ferrite-filled circular waveguide section with dielectric matching tapers.

The analysis of ferrite tubes in circular waveguide is further complicated by the nonuniformity of the static magnetic field inside the ferrite. Polder's permeability tensor, which is derived for a uniform magnetic field, cannot strictly be applied to ferrite tubes. Nevertheless, in this paper, Polder's tensor will be applied to the ferrite tube as though the static magnetic field at any particular point is the same field that would exist in an infinite medium.

The static magnetic field configuration is shown in Fig. 4(a) for a ferrite tube where the dc permeability, μ_{DC}, is greater than that of free space. For a thin walled tube, the static magnetic field at B is μ_{DC} times the field at A. As the wall thickness increases, the ratio of the magnetic field at B to that at A approaches one. The microwave magnetic field, configuration for a thin ferrite tube, assuming that the TE_{11} mode exists as in

[7] N. Karayianis, "The Phase Shift and Insertion Loss of Microwaves in Ferrite Rods Subjected to Transverse D.C. Magnetic Fields," (unpublished Master Thesis, George Washington Univ.).

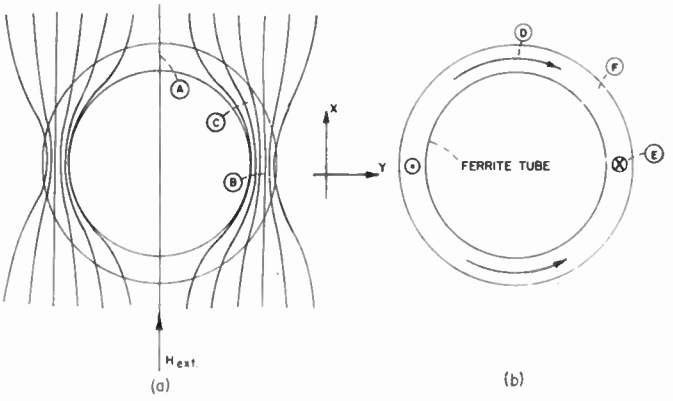

Fig. 4—(a) Static applied magnetic field pattern in a ferrite tube. (b) Microwave $\vec{H}$ field configuration in a ferrite tube assuming the TE_{11} mode.

empty waveguide, is shown in Fig. 4(b). The relative orientation of microwave $\vec{H}$ field to static magnetic field as shown in Fig. 4 is the extraordinary wave orientation. The microwave magnetic field at point E is perpendicular to a strong static field, and the permeability at this point is $\mu_\perp$. At D the microwave magnetic field is perpendicular to a weak static field, and the permeability is also $\mu_\perp$. Since the static field is different at A and B, the microwave permeabilities at these points will differ (Fig. 2). The $\vec{H}$ field orientation of the ordinary wave to the static magnetic field may be seen by rotating Fig. 4(a) 90°. For such an orientation the permeability at point B is $\mu_\parallel$, and at point A it is $\mu_\perp$.

Experimental Procedure

A schematic of the microwave apparatus used for the measurements is shown in Fig. 5. Separate measure-

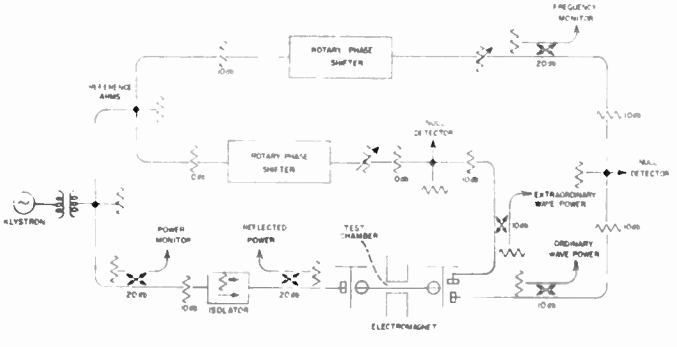

Fig. 5—Schematic of the microwave measuring equipment.

ments were made with ordinary and extraordinary waves in the ferrite test chamber. However, the power of both waves was measured in order to determine the ellipticity introduced by the ferrite. Sets of phase shift and insertion loss measurements were made as functions of the applied magnetic field for the three ferrite geometries described in the Theory section. The phase shifts are relative to the phase when the magnetic field is zero. Magnesium-manganese ferrites were used.

Results and Discussion

Ferrite-Filled Reduced Circular Waveguide

The microwave phase shift and insertion loss of the two waves as functions of the external magnetic field for a ferrite-filled reduced circular waveguide are shown in Fig. 6. As the magnetic field is increased from zero,

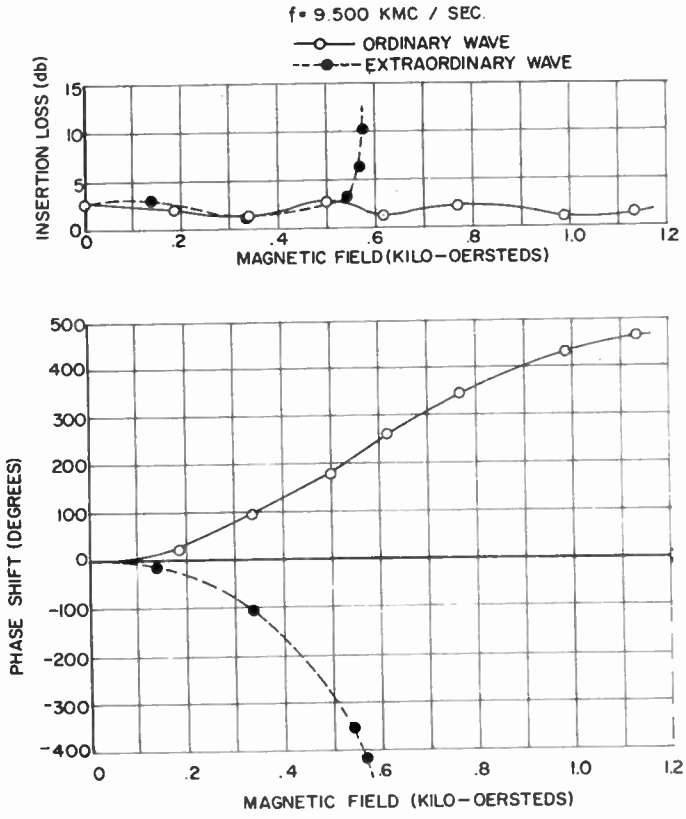

Fig. 6—Insertion loss and phase shift variations with external magnetic field of the ordinary and extraordinary waves propagating through a ferrite-filled reduced guide (L = 1.940 inch; d = 0.248 inch).

the phase velocity of the ordinary wave decreases; consequently, the phase shift is positive. Similarly, the phase velocity of the extraordinary wave increases, and the phase shift is negative. The insertion loss of the extraordinary wave becomes large at a field of 0.55 kilo-oersted. The permeability is small and the waveguide approaches cutoff so that most of the loss is due to reflection. A diameter study was made at a frequency of 9.375 kmc for completely filled reduced waveguide. The phase shift data as functions of waveguide diameter for various values of the external magnetic field are shown in Fig. 7. It was found that the phase shift is sensitive to reflections from the ferrite. The dashed curves are drawn to average out these effects. For a fixed magnetic field, cutoff is approached as the waveguide diameter is decreased and the phase shift increases in magnitude. Further, for a fixed change in the external magnetic field, the smaller the diameter of the waveguide, the greater the change in phase shift. The phase shift of

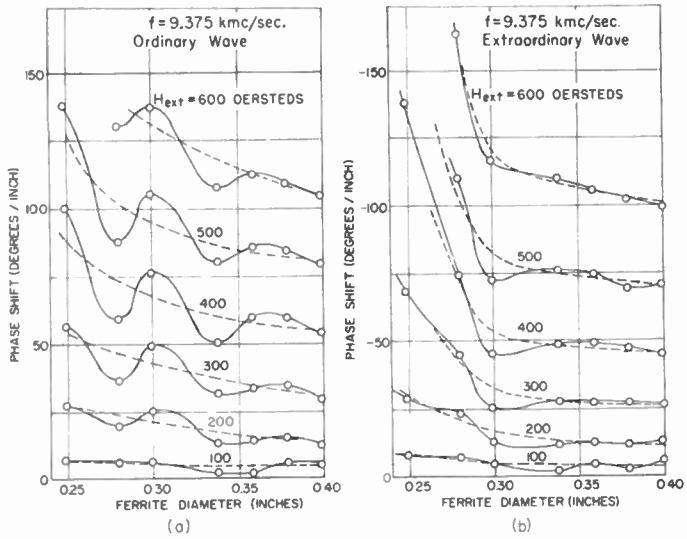

Fig. 7—Phase shift per unit length of the ordinary and extraordinary waves as a function of ferrite diameter for varous values of the external magnetic field.

the two waves in ferrite-filled reduced waveguide (0.338-inch diameter) as a function of frequency, with the magnetic field as a parameter, is shown in Fig. 8.

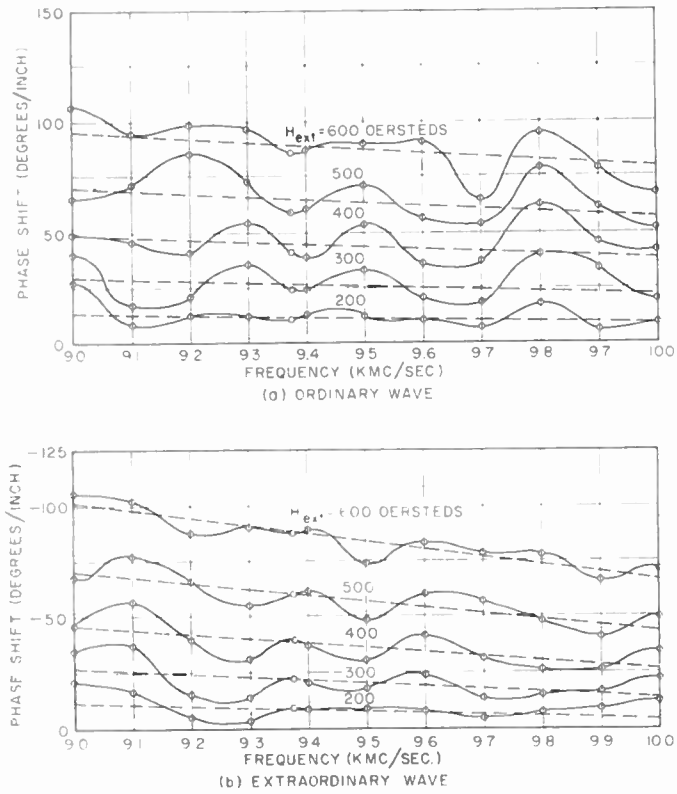

Fig. 8—Phase shift per unit length of the ordinary and extraordinary waves, produced by a rod of ferrite in reduced guide, as a function of frequency for various values of the external magnetic field (d = 0.338 inch).

For a 180° differential phase shift, with a 2-inch length of ferrite, the field required is 400 oersteds at 9.0 kmc, and 500 oersteds at 10.0 kmc. To decrease the field required for the same differential phase shift, the wave-

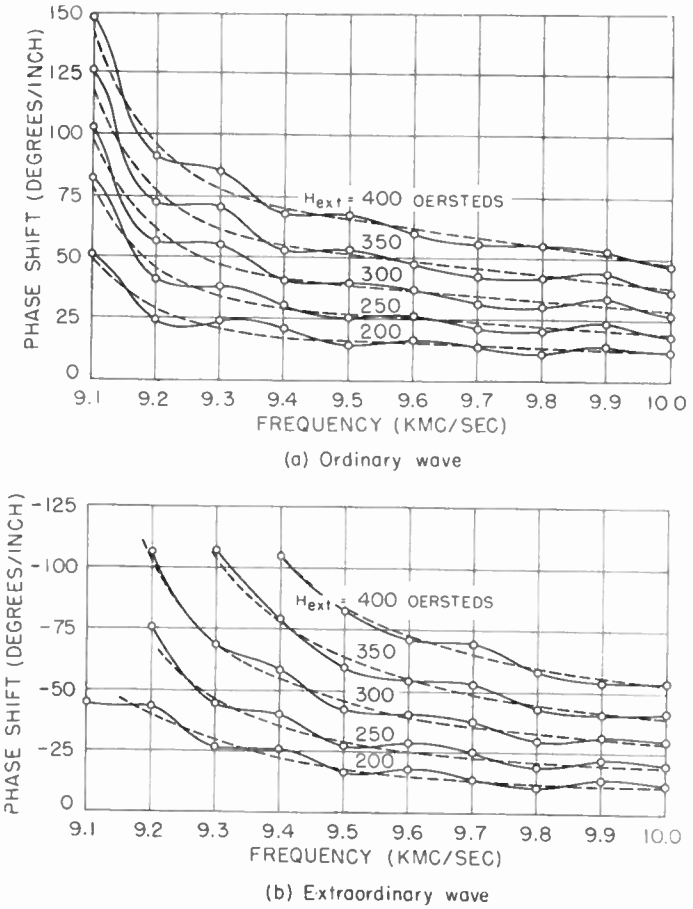

Fig. 9—Phase shift per unit length of the ordinary and extraordinary waves, produced by a rod of ferrite in reduced guide, as a function of frequency for various values of the external magnetic field (d = 0.248 inch).

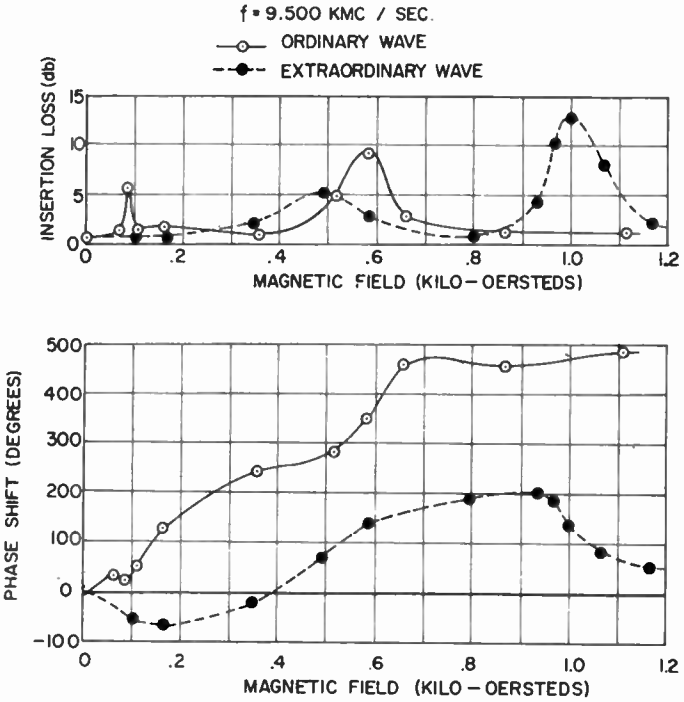

Fig. 10—Insertion loss and phase shift variations with external magnetic field of the ordinary and extraordinary waves propagating through a tube of ferrite (L = 4.000 inches; od = 0.935 inch; id = 0.760 inch).

guide diameter must be reduced. Fig. 9 is similar to Fig. 8 except that the diameter of the waveguide has been reduced to 0.248 inch. In this case, with a 2-inch length of ferrite, a 180° differential phase shift can be obtained with a magnetic field of 200 oersteds at 9.1 kmc, and 400 oersteds at 10.0 kmc. These measurements indicate that for 180° differential phase shift with fields below 225 oersteds, a waveguide near cutoff must be used. Consequently, the reflections will be large, and the differential phase shift will be very sensitive to frequency changes. It is evident that fulfilling the characteristics for the half-wave plate, as given in the Introduction, will not be possible using reduced waveguide filled with this type of ferrite.

Ferrite Tubes in Circular Waveguide

In Fig. 10, the phase shift and insertion loss of the two waves are shown as functions of the external magnetic field for a tube of ferrite whose outer diameter is equal to the inner diameter of the circular waveguide. In the very low field region, the phase shift of the ordinary wave is positive, and the phase shift of the extraordinary wave is negative as qualitatively predicted by the theory. As the static magnetic field is increased, the ferrite tube becomes saturated at points B, C, and A respectively [Fig. 4(a)]. For moderate static fields, the point B is saturated while C is near saturation and A is unsaturated. Since the permeability for the extraordinary wave at B is near zero (Fig. 2), the ferrite at this point is near cutoff. In a large region around C, the microwave field is parallel to the static field. The permeability averaged over the ferrite cross section is $\mu_{\parallel}$, since the ferrite is near cutoff at B, and the phase shift is positive. For large static fields, point A is near saturation, and the ferrite at this point is near cutoff. The effective permeability averaged over the cross section is $\mu_{\parallel}$, but less than that for moderate fields; consequently, the phase shift is decreased but remains positive.

The phase shift and differential phase shift of the two waves for a ferrite tube are shown in Fig. 11 as functions of wall thickness with the external magnetic field as parameter. The outside diameter of the tubes remains constant and equal to the inner diameter of the waveguide. For a given external magnetic field, the differential phase shift increases with wall thickness. For a 180° differential phase shift at the field of 200 oersteds, a length of 3 inches with a wall thickness of 0.095 inch is required. For the same wall thickness and differential phase shift with a 2-inch section, a field of over 300 oersteds is required. Tubes with wall thickness greater than 0.095 inch have larger differential phase shifts but are difficult to match over the required frequency range.

The phase shift and differential phase shift as functions of frequency are shown in Fig. 12 for a ferrite tube [Fig. 12(d)]. The curves of Fig. 12(a) and (b) were drawn to average out the effect of reflections from the

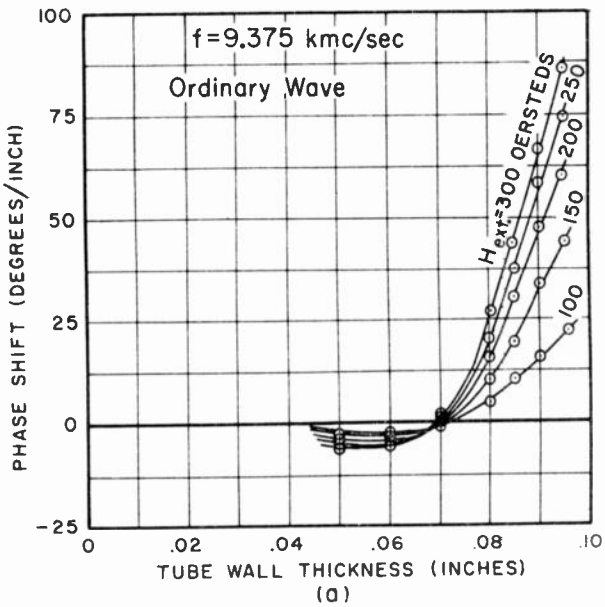

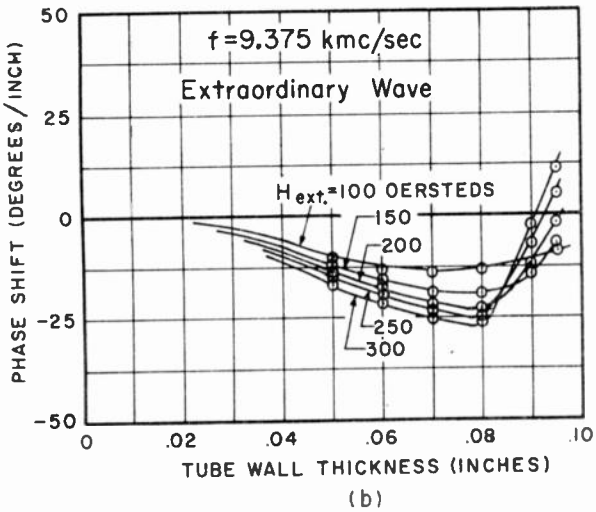

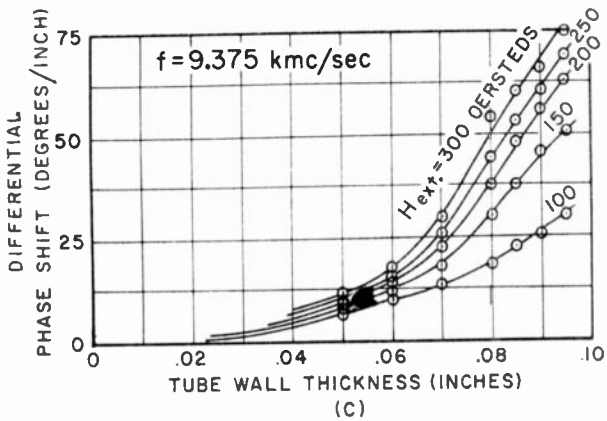

Fig. 11—Phase shift per unit length of the (a) ordinary and (b) extraordinary waves and (c) the differential phase shift as functions of the ferrite tube wall thickness for various values of the external magnetic field

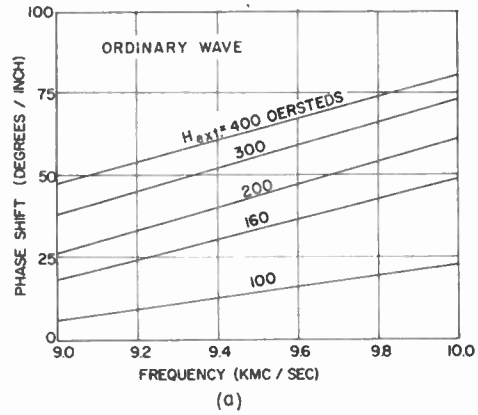

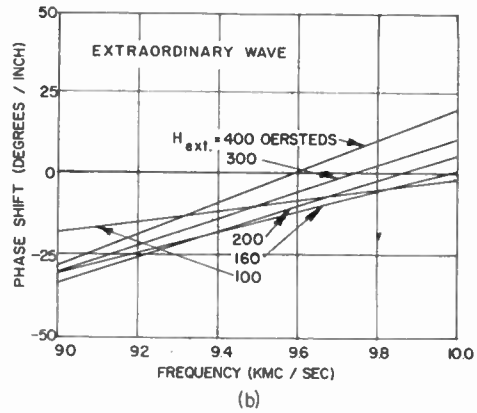

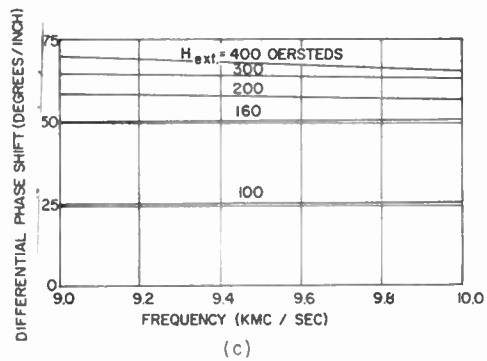

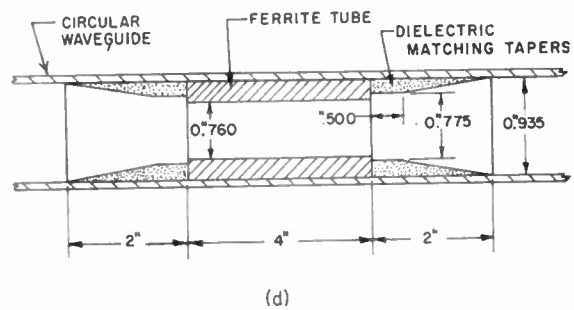

Fig. 12—Phase shift per unit length of the (a) ordinary and (b) extraordinary wave and (c) the differential phase shift as functions of frequency for various values of the external magnetic field. (d) Dimensions of the ferrite tube and dielectric matching tapers.

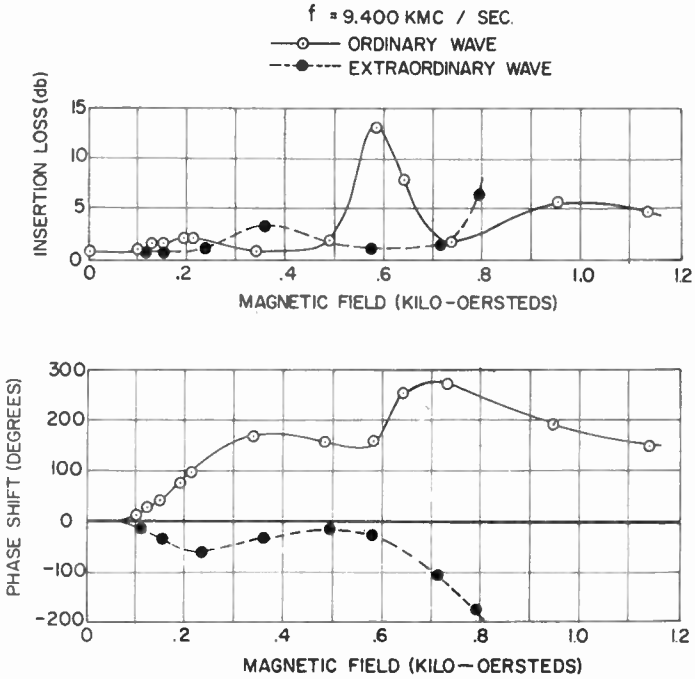

Fig. 13—Insertion loss and phase shift variations with external magnetic field of the ordinary and extraordinary waves propagating through a tube of ferrite in reduced guide (L = 2.000 inches; od = 0.698 inch; id = 0.500 inch).

ferrite. The differential phase shift of this ferrite tube is essentially independent of frequency.

To obtain 180° differential phase shift in a ferrite tube 2 inches long, tubes with relatively thick walls must be used. However, the presence of higher modes would make matching over the frequency band difficult if not impossible. The conversion loss would then be greater than 3 db.

Ferrite Tubes in Reduced Circular Waveguide

The information gained from the measurements on rods and tubes of ferrite was valuable in designing a ferrite section which produces large differential phase shifts at low fields. In comparing the phase shifts of the extraordinary waves for a typical rod and tube of ferrite (Figs. 6 and 10), it was concluded that the cutoff effects of reduced guide would increase the negative phase shift produced by a tube of ferrite. Further, if the reduced guide were not too close to cutoff at zero applied field, the phase shifts produced would not be too frequency sensitive. The phase shift and insertion loss of the ordinary and extraordinary waves for a ferrite tube in reduced circular waveguide (0.700-inch diameter) are shown in Fig. 13 as functions of the external magnetic field. At 9.4 kmc the 180° differential phase shift is obtained with an external magnetic field of 230 oersteds. The phase shift and differential phase shift of the two waves are shown in Fig. 14 as functions of frequency for the same tube used in Fig. 13. The average external magnetic field required to produce the desired phase shift is 216 oersteds for the frequency range 9.0 to 9.7 kmc. Large mismatches at the higher frequencies prevented accurate measurements of phase shift. The computed conversion loss for this tube is plotted as a function of frequency in Fig. 15. This half-wave plate has the desired characteristics, except that the frequency

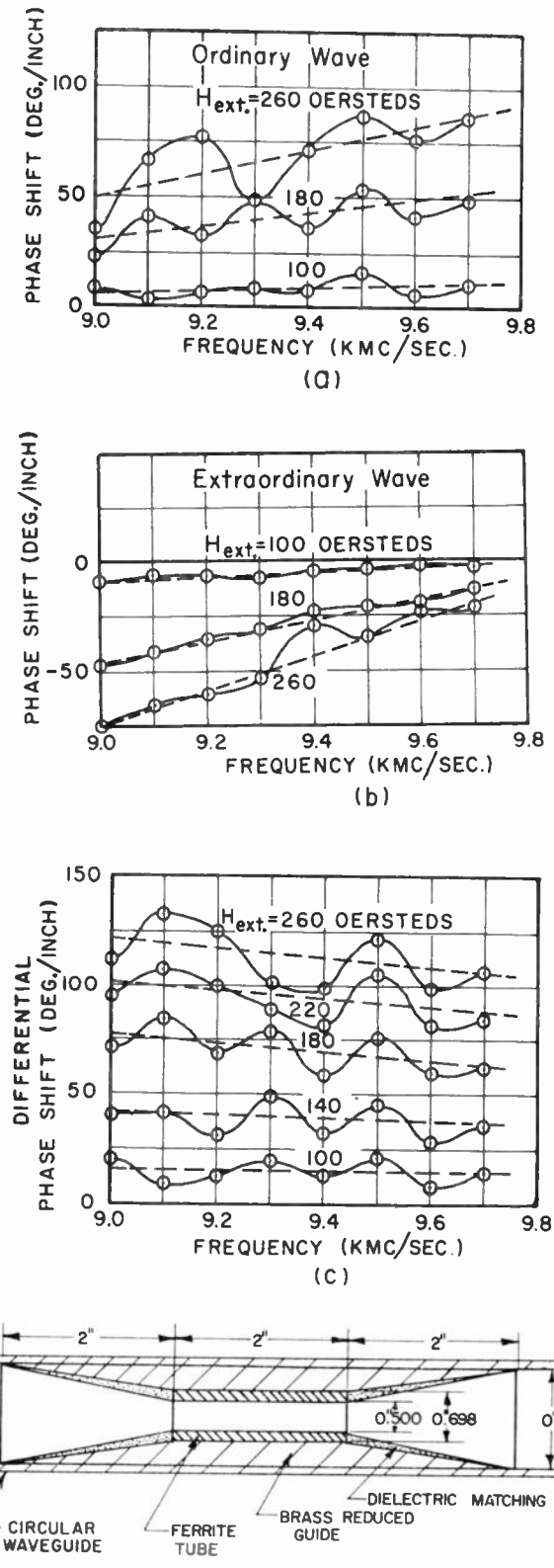

Fig. 14—Phase shift per unit length of the (a) ordinary and (b) extraordinary waves and (c) the differential phase shift as functions of frequency for various values of the external magnetic field for a tube of ferrite in reduced guide.

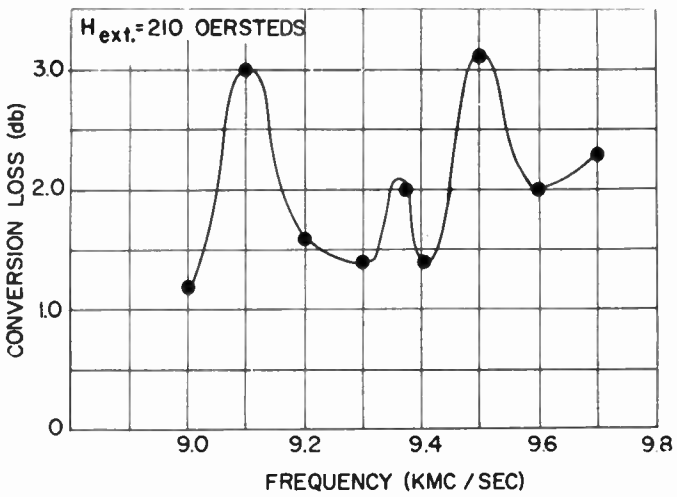

Fig. 15—Conversion loss of the ferrite half-wave plate as a function of frequency.

range is 9.0 to 9.7 kmc. Additional work is being done to extend the range to 10 kmc.

Conclusion

It has been shown that large differential phase shifts relatively independent of frequency can be obtained with low external magnetic fields. These characteristics were achieved with ferrite tubes in reduced circular waveguide. In particular, a half-wave plate requiring an external magnetic field of 210 oersteds has been designed with a conversion loss of 3.1 db or less in the frequency range 9.0 to 9.7 kmc. The conversion loss may possibly be reduced by better matching techniques.

Acknowledgment

The authors wish to thank C. A. Morrison and H. A. Dropkin for their constructive criticism of the material contained in this paper.

A New Ferrite Isolator*

BENGT N. ENANDER†, ASSOCIATE MEMBER, IRE

Summary—**A new ferrite isolator is described, which uses a helical transmission line. The main advantage of the new isolator, as compared to other isolators, is that no externally applied magnetic field is required. This has been achieved by using closed rings of soft ferrites with a square-loop magnetization curve. Although designed primarily for use in traveling-wave tubes, the new isolator should also find other applications. By suitable modifications, it can be used as an isolator, switch, or modulator with helical as well as hallow waveguide and coaxial lines.**

The best ratio of backward-loss to forward-loss in decibels obtained with the new isolator is 25:1 at 6500 mc, with a ratio better than 15:1 over a 25 per cent frequency band. Ratios of 100:1 were measured when a small external magnetic field was applied. Switching times of less than a microsecond are feasible.

Introduction

A MICROWAVE isolator is a transmission line with nonreciprocal attenuation. Isolators have important applications in microwave systems. One application is for reducing frequency pulling of an oscillator due to reflections from the load. Another application exists in high-gain traveling-wave tube amplifiers. The maximum gain in present tubes is limited, because reflections from the output end will make the tube oscillate above a certain critical gain. By means of an isolator this limitation can be overcome without affecting the tube performance in any way. When ferrite materials suitable for lower frequencies have been developed, isolators might also be used in uhf color television to reduce *ghost effects* caused by reflected signals on the line between the tv receiver and the antenna.

A ferrite isolator has three necessary components: a transmission line, a ferrite sample, and a dc magnetic field applied to the ferrite. However, a ferrite isolator having these three components can be built according to at least three rather different principles: Faraday rotation, field displacement, and resonance absorption. The most commonly used of these isolator principles is the resonance isolator. It uses the phenomenon of ferromagnetic resonance between a circularly polarized rf magnetic field and the precessing electron spins in the ferrite. A disadvantage of present resonance isolators is the large external magnetic field that has to be applied to the ferrite. This field becomes a particularly severe problem in an isolator for traveling-wave tubes; a large magnetic field near the tube will easily upset the focusing of the electron beam in the tube. Cook, *et al.*,[1] proposed to use ferrite rings linked by a number of turns of wire carrying the magnetizing dc current. To avoid this extra current, they further presented a very elegant solution by using the same field for focusing the beam and magnetizing the isolator. The practical use of this isolator, however, seems rather limited, as it requires a ferrite helix which is very difficult to produce.

* Original manuscript received by the IRE, July 3, 1956.
† RCA Laboratories, Princeton, N. J.

[1] J. S. Cook, R. Kompfner, and H. Suhl, "Nonreciprocal loss in traveling-wave tubes using ferrite attenuators," PROC. IRE, vol. 42, pp. 1188–1189; June, 1954.

This paper describes a different solution to the problem of an isolator for a helical transmission line: it consists of ferrite rings which once magnetized, remain magnetized. No external magnetic field is required. Turns of current-carrying wire are not required either. The isolator is especially suitable for use in traveling-wave tubes.

Description of the Isolator

Fig. 1 shows a schematic drawing of the new isolator. Pictures of an isolator design are shown in Figs. 2 and 6. The two essential components of the isolator are a helical transmission line and a ferrite cylinder. The ferrite should have a magnetization curve of the type shown in Fig. 3 with the remanent magnetization, M_r almost equal to the saturation magnetization, M_s. Ferrites of this type have been developed for use in memory cores and are, therefore, readily available. The ferrite cylinder is permanently magnetized in circumferential direction. This is done by passing a current through the cylinder as shown in Fig. 1(b). The current magnetizes the cylinder circumferentially and will saturate the ferrite if it is large enough (corresponding to point *a* on the magnetization curve). Since the ferrite is in the form of a closed ring it stays almost saturated when the current is removed (point *b* in Fig. 3).

The isolator uses the phenomenon of ferromagnetic resonance absorption. A short and simplified description of the theory of resonance isolators will be given here. For a better and more detailed account the reader is referred to an article by Fox *et al.*[2] A resonance isolator consists of a transmission line which operates in a mode that provides a circularly polarized rf field in some region, and a ferrite sample which is situated in this region and magnetized perpendicular to the plane of circular polarization. When an electromagnetic wave propagates along one direction of the transmission line, the sense of rotation of the polarized rf magnetic field is such that it is in synchronism with the precessional motion of certain electron spins in the ferrite. As there are damping effects associated with the precession, rf energy will be absorbed in the ferrite. The magnitude of the applied dc magnetic field determines the natural frequency of precession and is chosen so that it is equal to the signal frequency of the rf signal. In this case the precessional motion is excited strongly, the dissipation of rf energy in the ferrite becomes large, and the electromagnetic wave is attenuated. This is called ferromagnetic resonance absorption. If the wave propagates in the reverse direction, the rf magnetic field is circularly polarized in the opposite sense and does not interact with the precessing electron spins. The wave remains, therefore, essentially unattenuated in this direction.

In the isolator shown in Fig. 1, the type of helix used is such that the rf magnetic field outside the helix is

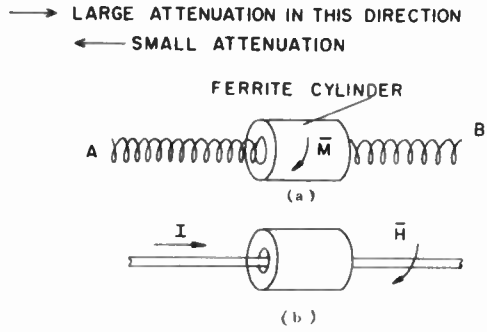

Fig. 1—(a) Nonreciprocal attenuator. (b) Magnetization of ferrite cylinder.

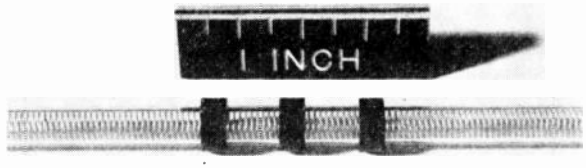

Fig. 2—An isolator consisting of three ferrite rings around a helical line.

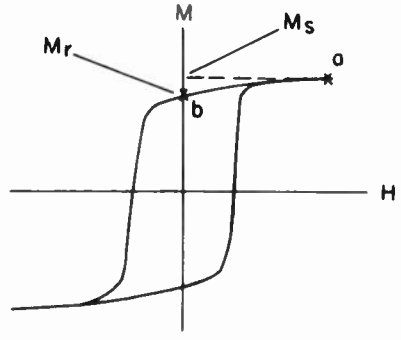

Fig. 3—Magnetization curve for ferrite used in the nonreciprocal attenuator.

essentially circularly polarized in a plane through the axis. As the direction of magnetization in the ferrite is perpendicular to this plane the conditions for nonreciprocal attenuation are fulfilled for a signal frequency which corresponds to the ferromagnetic resonance frequency of the magnetized ferrite. The directions of propagation that give large and small loss are indicated in Fig. 1 for the direction of magnetization indicated by M in the figure. If the magnetization is reversed, the directions of large and small loss will be interchanged. For simplicity the direction of propagation with large attenuation will be called the backward direction, the low-loss direction the forward direction.

The frequency f, at which ferromagnetic resonance absorption occurs in the ferrite cylinder, can be derived approximately from Kittel's[3] equation:

[2] A. G. Fox, S. E. Miller, and M. T. Weiss, "Behavior and applications of ferrites in the microwave region," *Bell Sys. Tech. J.*, vol. 34, pp. 5–103; January, 1955.

[3] C. Kittel, "On the theory of ferromagnetic resonance absorption," *Phys. Rev.*, vol. 73, p. 115; 1948.

$$f = \frac{|\gamma|}{2\pi}\sqrt{(H_a + (N_x - N_z)M_s)(H_a + (N_y - N_z)M_s)} \quad (1)$$

where

γ = the gyromagnetic ratio ($|\gamma|/2\pi = 2.8$ mc/oersted)

H_a = the externally applied field in the z-direction

N_x, N_y, N_z = demagnetization factors in x, y, and z-directions

$4\pi M_s$ = saturation magnetization of the ferrite,

with the additional relation

$$N_x + N_y + N_z = 4\pi. \quad (2)$$

Kittel's equation holds exactly for a ferrite ellipsoid which is magnetically saturated in the z-direction by the applied field. However, it can be used with good approximation for other shapes of the ferrite sample. To be able to apply it to our ferrite ring, we assume the ring to have a thickness and an axial length which are small compared to the circumference of the ring (this is not the case for the ring shown in Fig. 1). The x, y, and z-directions we take as the r, z, and ϕ-directions in a cylindrical coordinate system.

Then

$$N_\phi = 0$$

$$N_r + N_z = 4\pi$$

and from (2)

$$f = \frac{|\gamma|}{2\pi}\sqrt{(H_a + N_z M_s)(H_a + N_y M_s)}. \quad (3)$$

If

$$N_z = N_y = 2\pi$$

then

$$f = \frac{|\gamma|}{2\pi}(H_a + 2\pi M_s) \quad (4)$$

which is the maximum resonance frequency that can be obtained from (1), when H_a is kept constant and N_x, N_y and N_z are varied. For the ring in Fig. 1, which is saturated (although the externally applied field is zero) we therefore would expect to obtain a resonance frequency

$$f = \frac{|\gamma|}{2\pi}\cdot 2\pi M_s \quad (5)$$

or somewhat lower. Suhl and Walker[4] have derived resonance conditions for a ferrite loaded helix in a more rigorous way. Their results indicate that the resonance frequency for a ferrite ring with infinite length and infinite outer diameter is given by (5) for zero applied field.[5]

[4] H. Suhl and L. R. Walker, "Topics in guided wave propagation through gyromagnetic media," *Bell Sys. Tech. J.*, vol. 33, pp. 939–986; 1954.

[5] *Ibid.* This result is obtained by using the formula in Fig. 3, p. 105.

Thus, the isolator of Fig. 1 should have a resonance frequency which is essentially determined by the saturation magnetization of the ferrite. By using materials with various saturation magnetization it should be possible to make isolators for a wide range of frequencies.

To show, that the H-component of the electromagnetic field outside the helix can be made essentially circularly polarized, we use expressions derived by Pierce[6] for the helically conducting sheet:

$$\frac{|H_\phi|}{|H_r|} = \frac{\beta_0^2}{\beta\gamma}\cdot\frac{K_1(\gamma r)}{K_0(\gamma r)}\cdot\cot\psi \quad (6)$$

$$\frac{|H_z|}{|H_r|} = \frac{\gamma}{\beta}\frac{K_0(\gamma r)}{K_1(\gamma r)}.$$

H_ϕ, H_r and H_z are the components of the magnetic field in the circumferential, radial and axial directions; r is the radial coordinate. For an explanation of the other symbols the reader is referred to Pierce. For tightly wound helices, in which the phase velocity is small compared to the velocity of light,

$$\gamma \approx \beta \gg \beta_0.$$

Then

$$|H\phi| \ll |H_r|$$

and

$$\frac{|H_z|}{|H_r|} \approx \frac{K_0(\gamma r)}{K_1(\gamma r)}.$$

Using the first two terms of the asymptotic series for the modified Bessel functions K_0 and K_1 we obtain for large γr

$$\frac{|H_z|}{|H_r|} \sim \frac{1 - \dfrac{.125}{\gamma r}}{1 + \dfrac{.375}{\gamma r}}. \quad (7)$$

Eq. (7) shows, that for large values of γr, $|H_z| = |H_r|$ and the H-field is essentially circularly polarized in a plane through the axis of the helix. The circular polarization is better far away from the helix than near it. Actually the field distribution around the helix is disturbed due to the presence of the ferrite ring. The results should still hold qualitatively, however.

Fig. 4 shows the rf magnetic field distribution outside a helix. It is easily seen that the magnetic vector at a point P outside the helix rotates counter clockwise for a wave traveling from left to right, but clockwise for a wave traveling from right to left.

Measurements

In order to determine how the properties of the isolator depend upon its physical dimensions and upon

[6] J. R. Pierce, "Traveling-Wave Tubes," D. Van Nostrand and Co., New York, N. Y.; 1950.

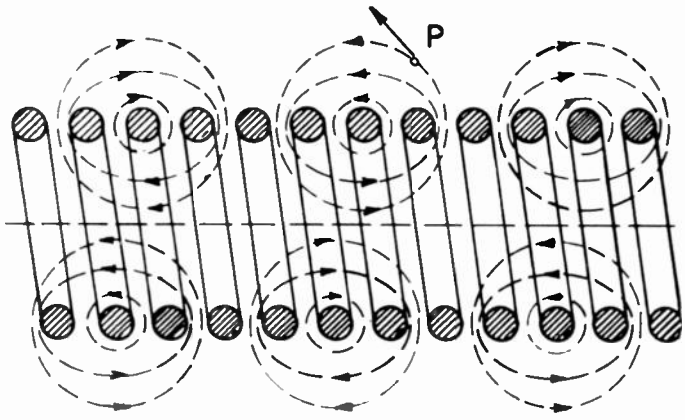

Fig. 4—Magnetic field distribution around a helix.

its material properties, measurements were made using various ferrite materials with different helices. For practical applications we want to know how the ratio of backward-loss to forward-loss can be optimized, how the isolator can be made to work over a large band of frequencies and how to make isolators for various frequency bands by using different ferrites. Considering the application to traveling-wave tubes, we have to investigate how the isolator works in an axial magnetic field of the strength used in traveling-wave tubes to focus the electrom beam.

Measuring Equipment and Technique

The isolation quality of a nonreciprocal attenuator is measured by the ratio of backward loss in db to forward loss in db. The equipment shown in Fig. 5 has been used to measure the two losses on the new isolator at 5000–10,000 mc. The essential components in the setup are a signal generator, a variable precision attenuator, the isolator under test fed by suitable waveguide coupling sections, and a detector circuit. The transitions from the waveguide sections to the isolator helix are shown in detail in Fig. 6. To ascertain that the transitions were matched, a slotted line was inserted to check the standing-wave ratio.

The increase in loss of the helix circuit, when the ferrite rings were inserted, was measured by decreasing the attenuation of the calibrated attenuator keeping the detector output constant. To obtain the loss caused by the ferrite rings for the reverse direction of propagations, the magnetization direction of the ferrite rings was reversed and the loss measured. It should be stressed that the loss which is measured, and which will be discussed subsequently, is the absorption loss of the ferrite rings only and does not include the constant loss of the helix and the glass tube surrounding the helix.

For convenience, data for the ferrites used in the measurements have been compiled in Table I while dimensions of helices and ferrite rings are contained in Table II, both opposite.

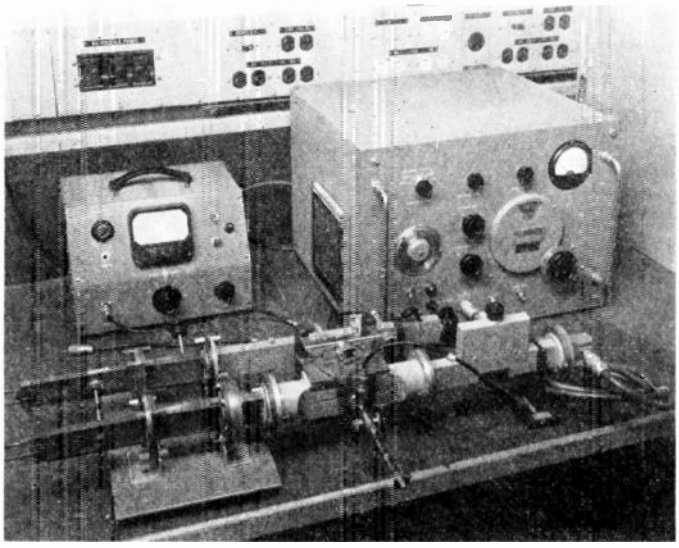

Fig. 5—Attenuation measurement apparatus around 6000 mc. The transitions from waveguide to helix, and the ferrite isolator are at the left.

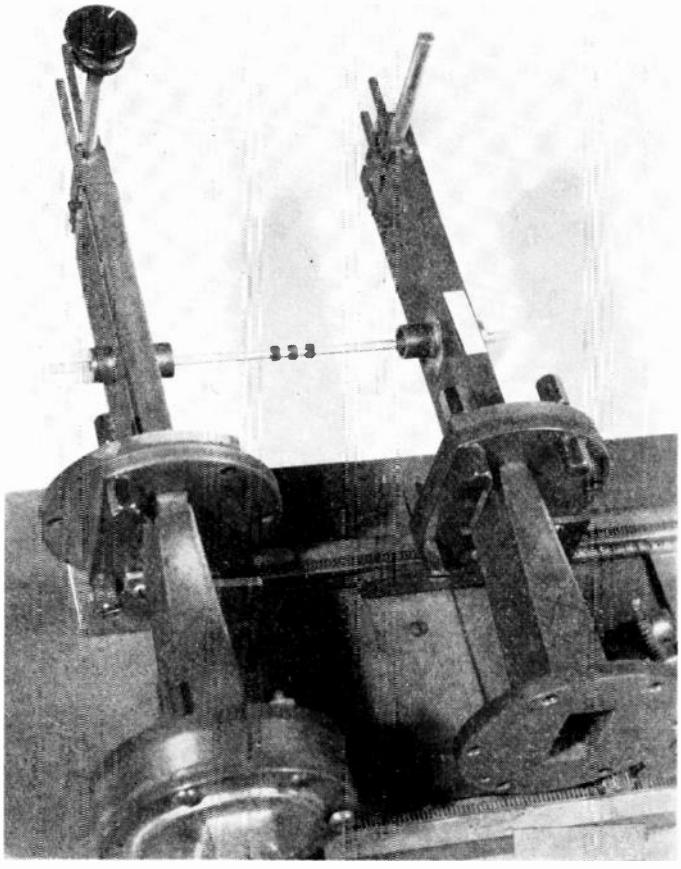

Fig. 6—Enlarged view of waveguide to helix transitions.

Results

The losses in backward and forward directions for the isolator which produced the best isolation characteristics, are shown in Fig. 7 as a function of frequency. A maximum isolation of 25:1 (backward-loss to forward-

TABLE I

COMPOSITIONS AND MAGNETIC CHARACTERISTICS OF SOME FERRITES

No.	Composition	B_m gauss	H_c oersted	B_r/B_m	f_0 mc	R_1	R_2	T_c °C
1	45 Fe, 50 Mn, 5 Zn (a)	3100	0.55	0.94	8500	20	36	250
2	45 Fe, 50 Mn, 5 Zn (b)	2490	2.8	0.55	7500	4	10	250
3	45 Fe, 50 Mn, 5 Zn (c)[e]	2850	0.25	0.90	8000	15	70	250
4	40 Fe, 30 Mn, 30 Mg (a)	1770	1.2	0.94	6000	17	23	310
5	40 Fe, 30 Mn, 30 Mg (b)	1980	2.2	0.85	5000	13	24	310
6	35 Fe, 32.5 Mn, 32.5 Mg	1780	1.5	0.96	4500	10	50	265
7	35 Fe, 65 Mn	1960	0.62	0.78	6000	10	48	240
8	45 Fe, 55 Mn	2320	0.56	0.86	7000	8	36	280
9	48 Fe, 52 Mn	2620	0.79	0.80	8000	6	13	—
10	49 Fe, 41 Mn, 10 Zn	2670	0.52	0.88	7500	17	25	235
11	45 Fe, 5 Mn, 47 Mg, 3 Zn	1680	3.5	0.91	5000	14	20	310
12	39 Fe, 21 Mn, 18 Mg, 22 Zn	1660	0.14	0.94	4500	—	—	100
13	80 Fe, 15 Li, 5 Zn	2340	2.8	0.86	6500	7	8	500
14	60 Fe, 10 Li, 30 Zn	1850	1.4	0.68	—	10	14	215

Composition: Figures in second column give the mole percentage of the oxides Fe_2O_3, MnO, MgO, ZnO, Li_2O.
B_m, H_c and B_r/B_m: See Fig. 14.
f_0: Resonance frequency for isolator with dimensions according to Table II.
R_1: Maximum ratio of backward loss to forward loss for isolator with dimensions given in Table II(f) with no external magnetic field.
R_2: The same ratio for field of about 10 oersteds, applied by a few turns of current-carrying wire linking the ferrite.
T_c: Curie temperature.

TABLE II

DIMENSIONS OF HELICES AND FERRITE RINGS

	D_1 inches	D_2 inches	D_3 inches	D_4 inches	*TPI*	l inches	*N*	Remarks
(a)	0.070	0.080	0.127	0.205	96	0.105	5	Quartz glass tube between helix and ferrite rings.
(b)	0.070	0.080	0.151	0.205	44	0.105	3	
(c)	0.096	0.110	0.210	0.500	30	0.59	5	
(d)	0.096	0.110	0.151	0.205	30	0.105	4	
(e)	0.100	0.110	0.120	0.200	40	0.056 −0.115	1	Quartz rod inside helix. Ferrite rings separated from helix by teflon sheet.
(f)	0.070	0.080	0.120	0.200	44	0.056 −0.105	1	

The symbols used in the table are explained in Fig. 14.
TPI: Number of turns per inch of the helix.
N: Number of ferrite rings.

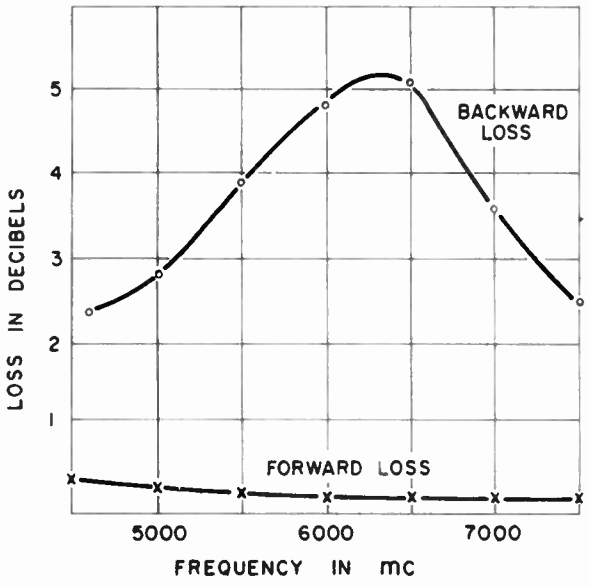

Fig. 7—Loss as a function of frequency for helix surrounded by ferrite rings. Ferrite No. 1. Dimensions of circuit given in Table II(a).

loss in decibels) was measured at 6500 mc, and the isolation was better than 15:1 over the frequency range from 5500 to 7000 mc. The forward-loss curve shows an effect obtained for all isolator circuits: the forward loss increases with decreasing frequency. This is probably due to the fact that the magnetic rf field in the region of the ferrite cylinder deviates more from circular polarization at lower frequencies.

For switching and modulation purposes it is important to measure how the loss of the isolator is influenced by a circumferential magnetic field. Also, such measurements give information on the absorption mechanism. Some isolators were therefore provided with a small coil as shown in Fig. 8 and the loss measured for various currents through the coil. Fig. 9 shows the results obtained for the Mn-Zn ferrite used in the previous measurement, which has a square-loop magnetization curve. Fig. 10 shows the data measured for a ferrite which does not have a square magnetization loop. The curves show hysteresis behavior and they should be interpreted similarly to ordinary magnetization hysteresis loops.

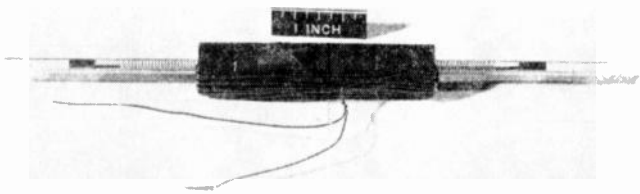

Fig. 8—Ferrite isolator with coil to vary the magnetic field.

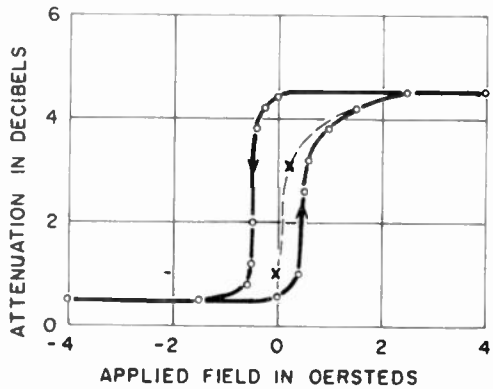

Fig. 9—Hysteresis loop showing loss as a function of applied field for helix surrounded by ferrite rings. The measurement was made at 6500 mc using ferrite No. 1. Dimensions of circuit given in Table II(b).

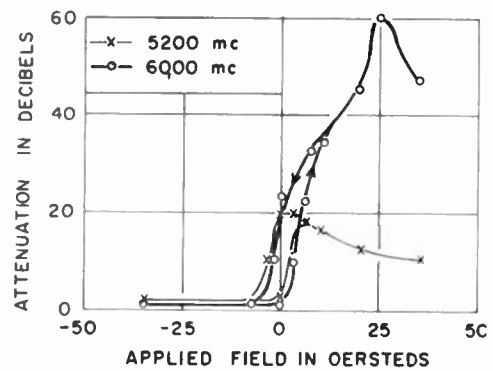

Fig. 10—Hysteresis loop showing loss as a function of frequency for helix surrounded by ferrite rings. The measurement was made using ferrite No. 15. Dimensions of circuit given in Table II(c) and Fig. 6.

The curve in Fig. 9 was measured at the resonance frequency of the attenuator. If the magnetic field was increased to much higher values than those shown in the figure the upper horizontal part of the curve started to go down towards zero loss. This is because the resonant condition will not be fulfilled any more for the particular frequency if the applied field becomes large compared to the effective internal field caused by shape anisotropy. The dashed branch of the curve is obtained when one starts with an unmagnetized ring. The curve in Fig. 9 shows that for this particular isolator very little is gained in isolation by applying externally a small circumferential field. The curve also illustrates how the loss of the circuit can be switched from a high to a low value and *vice versa* by sending a current pulse, corresponding to a circumferential field of about 1 oersted, through the coil.

The curves in Fig. 10 show how a small applied field has a much greater influence on the loss, when a ferrite with a low ratio of remanent magnetization to saturation magnetization is used. The circuit of Fig. 8 was used for this measurement. In Fig. 11 the loss of this

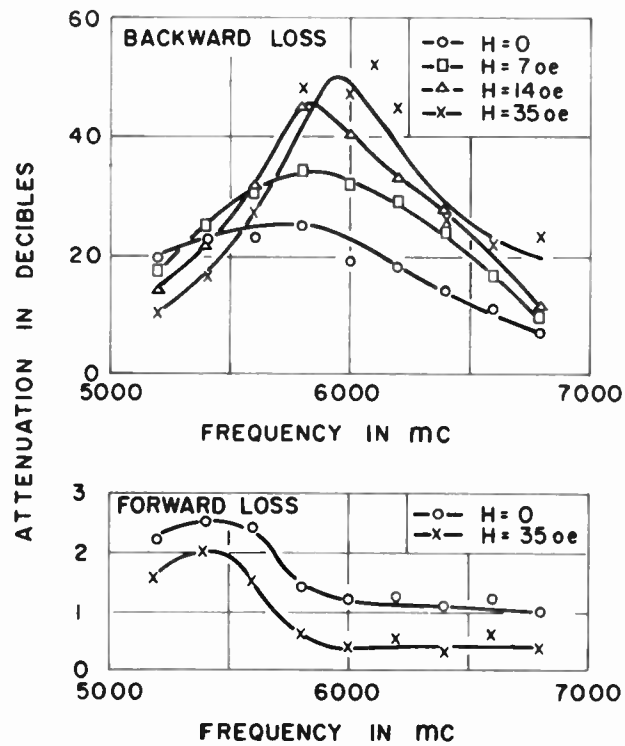

Fig. 11—The backward and forward losses of helix surrounded by ferrite rings, measured for various applied circumferential magnetic fields as a function of frequency. Ferrite No. 15. Dimensions of circuit given in Table II (c) and Fig. 6.

circuit is given as a function of frequency. The ratio of backward-loss to forward-loss is in this case greatly improved when a small field is applied. An isolation of 100:1 is obtained when a field of 35 oersteds is used. This is a surprisingly high value considering that no particular efforts were made to optimize the isolation. The peak of the backward-loss curve moves towards higher frequencies, when the applied field is increased. This is in accordance with (4); however, the peaks are not well enough defined to allow a quantitative comparison with (4).

The first measurements on the isolator indicated that the measured resonance frequencies were appreciably higher than would be expected theoretically from (5). As it is important both for practical and theoretical reasons to know what factors determine the resonance frequency in the ferrite, extensive measurements were made using 13 different ferrites. For each material the

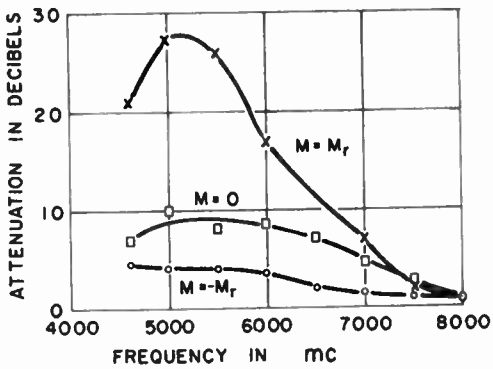

Fig. 12—Loss as a function of frequency for three different states of the magnetization of ferrite rings. Ferrite No. 5 used. M_r is the remanent magnetization [See Fig. 4 (c)]. Dimensions of circuit given in Table II (e).

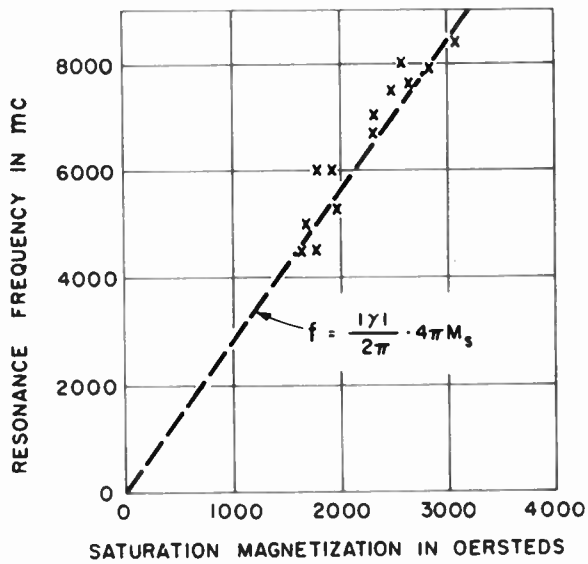

Fig. 13—Resonance frequency measured at zero applied field as a function of the saturation magnetization of the ferrite for helix surrounded by ferrite rings. Thirteen different ferrites were used. The dimensions of the circuit are given in Table II (e).

absorption of a ring of the material inserted on the helix was measured as a function of frequency. The measurements were made for three different states of magnetization of the rings: unmagnetized, permanently magnetized in one circumferential direction, and permanently magnetized in the other circumferential direction. As an example, the results of one of these measurements are shown in Fig. 12. The maximum of the backward-loss curve is taken as the resonance frequency f_0 of the magnetized ferrite material. Measured values of the resonance frequency, f_0, and the saturation magnetization, $4\pi M_s$, for the different ferrites are given in Table I and plotted in Fig. 13.

Table I also gives two isolation ratios: R_1, which is the maximum ratio obtained on the measurements exemplified by Fig. 12, and R_2, which was obtained when the rings were magnetized by a circumferential field of about 2 oersteds. The saturation magnetization, $4\pi M_s$, has been approximated by the maximum flux density, B_m (see Fig. 14), measured by a 60 cycle hysteresis-loop tracer. To obtain true values of saturation magnetization, much higher magnetizing fields should be applied, than the 1–10 oersteds used in these measurements of B_m.

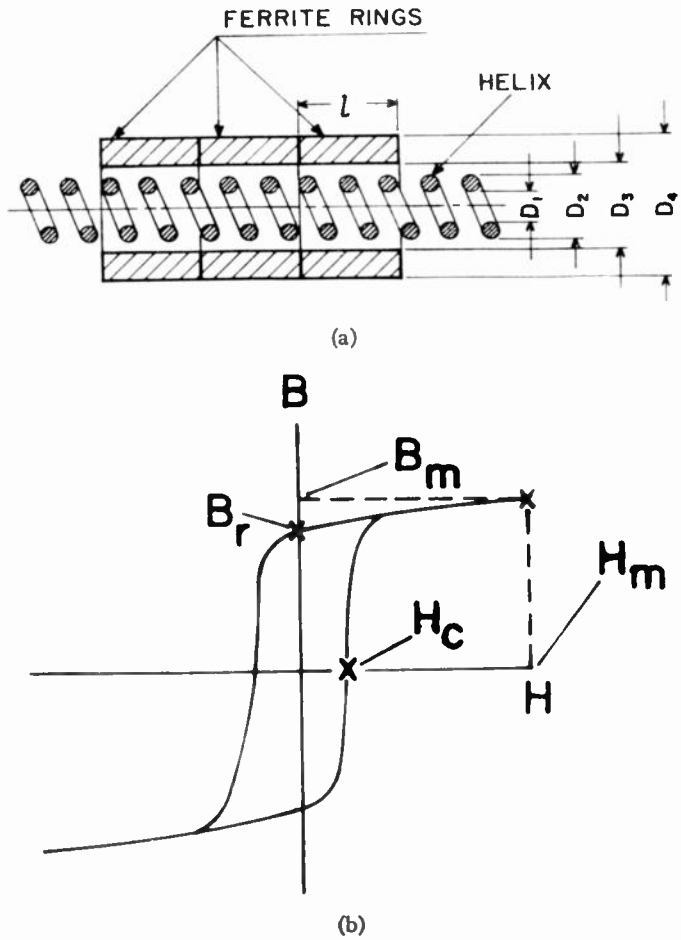

Fig. 14—Explanation of symbols used in Tables I and II. (a) Dimensions of circuit. (b) Magnetization curve.

As has been shown above, the resonance frequency of a saturated ferrite should depend only upon the saturation magnetization, $4\pi M_s$:

$$f = \frac{|\gamma|}{2\pi} \cdot 2\pi M_s. \tag{5}$$

To compare this relationship with the results obtained from the experiments, the resonant frequencies for the different materials were plotted as a function of the respective saturation magnetizations in Fig. 13. It is evident that the resonance frequencies are mainly determined by the saturation magnetization of the ferrite, as expected. The relation, however, is not the one of (5) but rather

$$f = \frac{|\gamma|}{2\pi} \cdot 4\pi M_s. \tag{8}$$

The spread of the points in Fig. 13 may be explained by the fact that the values of f and $4\pi M_s$ are not determined with better accuracy than approximately 10 per cent.

Thus, the measured resonance frequencies are twice as high as those predicted from (5). The discrepancy must be due to internal fields in the ferrite, other than the demagnetizing fields, which depend upon the shape of the ferrite sample and which are not taken into account in (5). These internal fields must be proportional to the saturation magnetization of the ferrite because of the correlation between resonance frequency and the saturation magnetization. According to present theories, there are two such internal field effects that can cause ferromagnetic resonance at these relatively high frequencies, when the applied field is small. One of these was first described by Snoek[7] and is caused by the crystalline anisotropy. The other one is ascribed to demagnetization fields due to domain walls.

If the crystalline anisotropy of the ferrites used in Fig. 9 had been large, the measured resonance frequencies would have been considerably influenced by the anisotropy fields. In that case, however, the resonance frequencies would not have been proportional to the saturation magnetization as the anisotropy fields are not directly correlated to the saturated magnetization. We therefore conclude from Fig. 13, that the anisotropy fields for the ferrites used are relatively small and that they do not account for the discrepancy between measured and calculated frequencies.

Smit and Polder[8] have described how demagnetization effects due to the presence of domain walls in a ferrite influence the ferromagnetic resonance conditions. Their results show that ferromagnetic resonance absorption in an unmagnetized ferrite sample occurs up to the frequency:

$$f = \frac{|\gamma|}{2\pi} \cdot 4\pi M_s. \qquad (9)$$

This result has been confirmed experimentally by Beljers *et al.*[9] As (9) is identical with the experimentally found relation (8) between frequency and saturation magnetization, the results in Fig. 13 might be explained on the basis of the influence of domain walls. There are two objections to this, however. The loss curve, from which the resonance frequencies in Fig. 13 are derived, is obtained for samples that are almost magnetically saturated in the remanent state. There should, therefore, be only few domain walls present and the influence of them should be small. Furthermore, the theory does not predict a resonance peak at the frequency given by (9), but a broad band of resonances extending up to this frequency. In spite of these objections, the author does not feel that domain wall effects can be ruled out as a possible cause of the high resonance frequencies.

[7] J. L. Snoek, "Dispersion and absorption in magnetic ferrites," *Physics*, vol. 14, pp. 207–217; 1948.
[8] D. Polder and J. Smit, "Resonance phenomena in ferrites," *Rev. Mod. Phys.*, vol. 25, pp. 89–90; 1953.
[9] H. G. Beljers, W. J. Van der Lindt, and J. J. Went, "A new point of view on magnetic losses in anisotropic bars of ferrite at ultra high frequencies," *J. Appl. Phys.*, vol. 22, p. 1506; 1951.

Influence of Helix Geometry and Axial Magnetic Field

The maximum backward loss obtained for a particular isolator depends, of course, upon the dimensions of the helix and the ferrite rings as well as upon the properties of the ferrite. In Fig. 15 the maximum backward loss of a number of isolators, made of the same ferrite material, is plotted as a function of a parameter which characterizes the isolator dimensions and the signal frequency. For a given helix, this parameter is an approximate expression for the ratio of the magnitude of rf H-field at the helix to the magnitude of this field at the inner surface of the ferrite cylinder. Instead of trying to explain why the backward loss should depend upon this parameter only, for a given ferrite material, we let the results in Fig. 15 justify the choice of parameters. It should be observed that the thickness of the rings, x_1 was not taken into account in Fig. 15 although the rings used in the measurements had different thicknesses. This shows that the rf field from the helix decreases rapidly in radial direction and therefore, only a very small part of the loss occurs in the outer regions of the rings, as long as the rings are relatively thick. The rings used for the measurements had a relative thickness x_1/x_0 between 0.7 and 1.5.

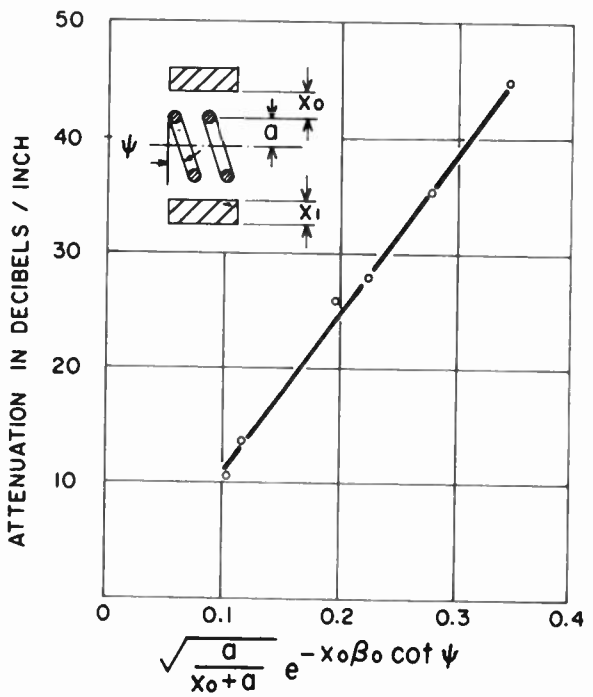

Fig. 15—Maximum loss as a function of dimensions of ferrite rings and helix. B_0 is the free-space phase constant ($=2\pi/\lambda_0$). Measurements made for ferrite No. 1.

It would have been interesting to show the forward loss vs the parameter used in Fig. 15 because this would

have given a correlation between the parameter and the isolation ratio. It was not possible, however, to obtain a good correlation between the parameter and the forward loss. Isolators using the Mn-Zn ferrite for which the measurements were made can be designed from Fig. 15. Experience shows that Fig. 15 also gives a good estimate of the relative backward loss for isolators using other ferrites.

If the isolator is used in a traveling-wave tube, it is subjected to the axial magnetic field used to focus the electron beam. This field tends to change the magnetization in the rings from a circumferential to an axial direction and, therefore, deteriorates the nonreciprocal characteristics. Fig. 16 shows how a homogeneous axial

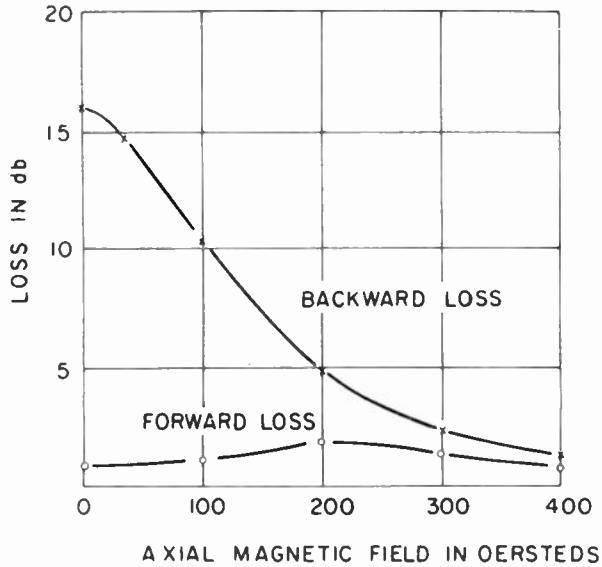

Fig. 16—Effect of an axial magnetic field on backward and forward losses at 6500 mc. Ferrite No. 1 used. Dimensions of circuit given in Table II (d).

field decreases the backward loss and increases the forward loss of an isolator consisting of several ferrite rings located close together. As the focusing field in a traveling-wave tube is of the order 500 gauss, this isolator is much too sensitive to the axial field. By separating the ferrite rings and by using thinner rings the effects of the axial field can be made much smaller. If the rings are shielded magnetically by high-permeability metal rings, in a way shown in Fig. 17 case *D*, the effects of an axial field of 500 oersteds becomes negligible. The isolation ratio for the shielded isolator was not as good as for the same isolator without shielding, a disadvantage that might be overcome by proper dimensioning. By using a soft ferrite with a somewhat higher coercive force, this effect of an axial field upon the internal field can be greatly reduced.

As mentioned earlier, the ferrite rings of the isolators are magnetized in advance by sending a current through the rings [Fig. 1(a)]. For the isolators used in the above measurements the magnitude of the magnetizing current was well above the magnitude needed to saturate the rings, so that nothing could be gained in isolation ratio

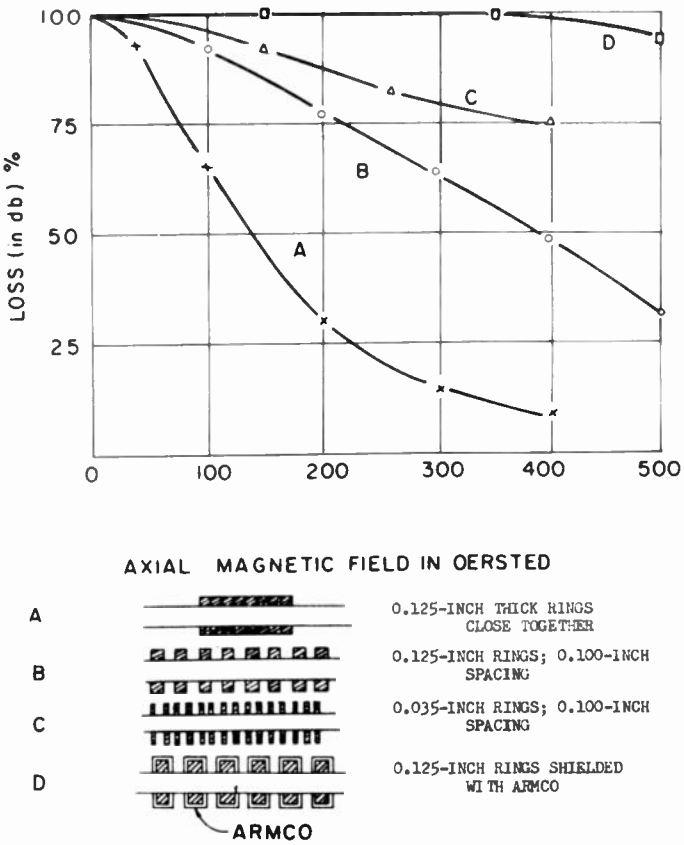

Fig. 17—Effect of an axial field on the backward loss for some different arrangements. The arrangements of ferrite No. 1 rings in the cases *A*, *B*, and *C* are as above.

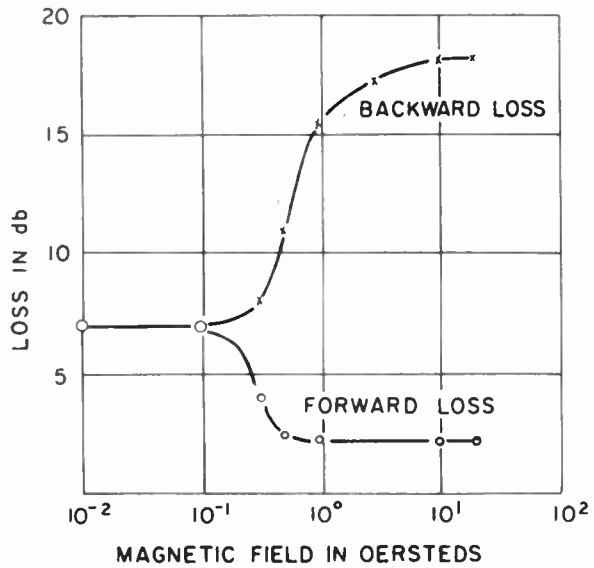

Fig. 18—Backward and forward losses as a function of the circumferential field for helix surrounded by ferrite rings. The measurement was done at 6500 mc using ferrite No. 1.

by using a higher current. Fig. 18 shows how the isolation depends upon the magnetizing field. The field used in this figure is the one produced by the premagnetizing current at the inner surface of the ferrite ring.

Conclusion

The main advantage of the new isolator is that it does not require any externally applied magnetic field. The best ratio of backward-loss to forward-loss obtained for the isolator (25:1) is not quite as good as the ratio for the best isolators. The loss ratio can probably be improved by choosing more suitable dimensions and ferrite materials. For most practical applications, however, the loss ratio obtained should be good enough. The bandwidth of the isolator, on the other hand, is appreciably larger than that of other isolators. No work has been done to determine the maximum power for which the isolator can be used. As the ferrite rings are easily accessible for cooling, the isolator should compare favorably with other isolators in this respect.

The isolator should be very suitable for use in traveling-wave tubes. It still remains to be shown that the design of an isolator with good isolation characteristics in the magnetic focusing field of a traveling-wave tube is possible without upsetting the focusing of the beam. To get enough backward attenuation, the ferrite rings have to be rather close to the helix and must, therefore, probably be inside the vacuum envelope of the tube. The ferrite can be magnetized after tube processing by passing a current pulse through the helix.

Because of its simplicity, the isolator might also find use in waveguide and coaxial-line systems. It can be used in its original form with the ends coupled to waveguides or coaxial lines, or waveguide and coaxial versions of the isolator can be designed as shown in Fig. 19. The waveguide isolator is the same in principle as the ordinary waveguide resonance isolator,[2] but the design of Fig. 19 does not require any applied magnetic field if a ferrite with a square-loop magnetization curve is used.

In its original form as well as in the waveguide or coaxial version, the isolator can be used as a switch or modulator, if the ferrite rings are provided with a small coil. The loss of the isolator can then be controlled by sending current pulses through the coil. Switching times of the order of 1 μsec can be obtained. The advantage of the present circuit for switching and modulating purposes is that the ferrite forms a closed magnetic circuit and that the magnetization, therefore, can be controlled by very small applied fields.

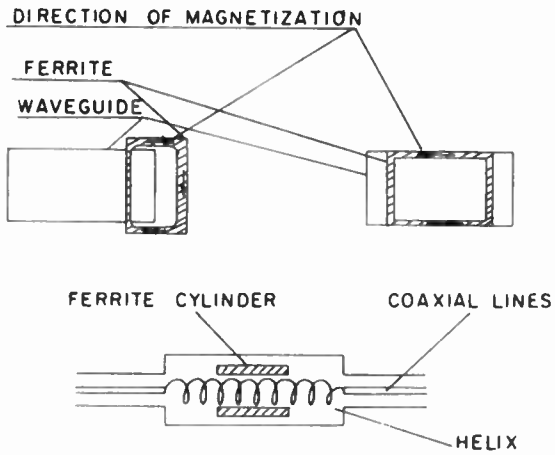

Fig. 19—Nonreciprocal waveguide attenuator. Coaxial line attenuator.

The isolators which have been measured have worked in the frequency range 4000–8000 mc. It should be possible to make isolators up to 10,000 mc by using ferrites with higher saturation magnetization. Above 10,000 mc ferrites with high magnetic anisotropy can be used.[10] The present lower frequency limit is about 3000 mc because there are no square-loop ferrites available with a saturation magnetization below 1000 gauss. However, if square-loop ferrites with very low magnetic anisotropy are developed a similar ring-type isolator operating at frequencies of around 1000 mc should be obtainable.

Acknowledgment

The author wishes to thank R. W. Peter for his invaluable help, and his continued interest in this work, R. S. Weisz for suggesting and making a wide variety of excellent ferrites, and P. K. Baltzer for many helpful discussions.

[10] M. T. Weiss, "The behavior of ferroxdure at microwave frequencies," 1955 IRE Convention Record, part 8, pp. 95–99.

Magnetic Tuning of Resonant Cavities and Wide-band Frequency Modulation of Klystrons*

G. R. JONES†, ASSOCIATE MEMBER, IRE, J. C. CACHERIS†, SENIOR MEMBER, IRE, AND C. A. MORRISON†

Summary—**General expressions are obtained for the perturbation of transmission cavities at microwave frequencies by the magnetic properties of ferrites. Experimental results are given for a number of ferrite slabs and magnetic field orientations. The frequency shift of the cavities is given for the range of magnetic field strength from 0 to 1,000 oersteds and slab thicknesses of 0.010 to 0.100 inch. The microwave permeability of a ferrite in the direction of the applied magnetic field is also determined. Two magnetically-tuned x-band klystrons are described for applications requiring very wide-band frequency modulation with low amplitude modulation. Linear frequency deviations as large as 240 mc are obtained with only 13 per cent change in amplitude. This deviation can be extended by proper magnet design.**

Introduction

WHEN FERRITES are placed in a microwave cavity, the resonant frequency of the cavity is a function of the magnetic field applied to the ferrite. This effect has been used in the study of the microwave behavior of ferrites[1,2] to determine experimentally the components of the permeability tensor. It can also be utilized to vary the resonant frequency of an *x*-band klystron having an external cavity.[3] Klystrons can be frequency modulated by conventional methods; however, the accompanying amplitude modulation restricts the frequency variation to a very narrow band. With magnetically-tuned klystrons, it is possible to obtain very wideband frequency modulation with low amplitude modulation.

The purpose of the work described in this paper was to determine the limitations of the applicability of the perturbation theory when applied to moderately large ferrite samples in a rectangular transmission cavity and to relate the theoretical and the experimental results to the behavior of magnetically-tuned klystrons.

Theory for the Transmission Cavity

Polder[4] has shown that the alternating flux density $\bar{b}$ in a ferromagnetic material saturated in the *z*-direction is related to the internal alternating magnetic field $\bar{h}$ by a tensor permeability of the form

$$\overleftrightarrow{\mu} = \begin{pmatrix} \mu & -jK & 0 \\ jK & \mu & 0 \\ 0 & 0 & \mu_0 \end{pmatrix} \tag{1}$$

where μ_0 is the permeability of free space. For an unmagnetized ferrite, however, Rado, *et al.*[5], have observed a resonance absorption in the microwave region and initial permeabilities less than that of free space. Consequently, as a ferrite is magnetized, the permeability in the direction of the applied field, $\mu_\parallel$, increases to μ_0. It will be assumed that the above tensor also represents the unsaturated ferrite with $\mu_\parallel$, a function of the magnetic field replacing μ_0.

If the time dependence of the microwave field components is of the form $e^{j\omega t}$, then in a ferrite region, Maxwell's equations are

$$\nabla \times \bar{h} = j\omega\epsilon\bar{e}$$

$$\nabla \times \bar{e} = -j\omega\overleftrightarrow{\mu}\cdot\bar{h}$$

where $\bar{e}$ is the alternating electric field, ω is the angular frequency of the microwave field, and ϵ is the scalar permittivity of the ferrite.

These equations can be used to derive the wave equation for the alternating magnetic field.

$$\nabla \times \nabla \times \bar{h} = \omega^2\epsilon\overleftrightarrow{\mu}\cdot\bar{h}.$$

By manipulating the above equation, either two coupled second-order differential equations or the following can be derived

$$\left[\left(\frac{\mu}{\mu_\parallel}\frac{\partial^2}{\partial x^2} + \frac{\mu}{\mu_\parallel}\frac{\partial^2}{\partial y^2} + \frac{\partial^2}{\partial z^2} + \omega^2\mu\epsilon\right) \cdot \left(\frac{\partial^2}{\partial x^2} + \frac{\partial^2}{\partial y^2} + \frac{\partial^2}{\partial z^2} + \omega^2\mu_e\epsilon\right) + \frac{K^2}{\mu}\omega^2\epsilon\frac{\partial^2}{\partial z^2}\right] h_i = 0$$

where μ, K, and $\mu_\parallel$ are components of the permeability tensor with $\mu_e = (\mu^2 - K^2)/\mu$ and $h_i = h_x, h_y, h_z$. In general, the above wave equation is very difficult to solve. Solutions have been found for only a few special cases. Hence, most of the analysis given in this paper will be based on the perturbation theory of Bethe-Schwinger.[6] Consequently, correlation between theoretical and experimental results can be expected only if the ferrite

* Original manuscript received by the IRE, July 3, 1956.
† Diamond Ordnance Fuze Labs., Washington 25, D. C.

[1] J. O. Artman and P. E. Tannenwald, "Measurement of permeability tensor in ferrites," *Phys. Rev.*, vol. 91, pp. 1014–1015; August 15, 1953.

[2] E. G. Spencer, R. C. LeCraw, and F. Reggia, "Measurement of microwave dielectric constants and tensor permeabilities of ferrite spheres," 1955 IRE Convention Record, part 8, pp. 113–121.

[3] J. C. Cacheris, G. Jones, and L. Diehl, "Magnetic tuning of klystron cavities," Proc. IRE, vol. 43, p. 1017; August, 1955.

[4] D. Polder, "On the theory of ferromagnetic resonance," *Phil. Mag.*, vol. 40, pp. 99–115; January, 1949.

[5] G. T. Rado, R. W. Wright, and W. H. Emerson, "Ferromagnetism at very high frequencies III. Two mechanisms of dispersion in a ferrite," *Phys. Rev.*, vol. 80, pp. 273–280; October 15, 1950.

[6] H. A. Bethe and J. Schwinger, NDRC Rep. D1-117, Cornell University, Ithaca, N.Y., March, 1943.

volume is small compared to the volume of the cavity.

The frequency shift δf, due to the perturbation is given by

$$\frac{\delta f}{f} = -\frac{\int_{V_s} (\bar{e}_1 \cdot \bar{d}_2 - \bar{e}_2 \cdot \bar{d}_1 + \bar{h}_1' \cdot \bar{b}_2' - \bar{h}_2' \cdot \bar{b}_1') dv}{\int_{V_c} (\epsilon_0 \bar{e}_1^2 + \mu_0 \bar{h}_1'^2) dv} \tag{2}$$

where f is the complex frequency. The subscripts 1 and 2 denote the unperturbed and the perturbed states of the cavity respectively. The electric field is $\bar{e}$. The magnetic field $\bar{h}$ is related to $\bar{h}'$ by $\bar{h} = j\bar{h}'$. The volume of the ferrite sample is V_s and the volume of the cavity is V_c.

In this paper, the TE_{101} mode will be assumed for the empty cavity. The microwave field components are

$$\begin{aligned} e_x &= 0 \\ e_y &= A \sin \frac{\pi}{a} x \sin \frac{\pi}{c} z \\ e_z &= 0 \\ h_x &= \frac{-jAa\sqrt{\epsilon_0/\mu_0}}{\sqrt{a^2 + c^2}} \sin \frac{\pi}{a} x \cos \frac{\pi}{c} z \\ h_y &= 0 \\ h_z &= \frac{jAc\sqrt{\epsilon_0/\mu_0}}{\sqrt{a^2 + c^2}} \cos \frac{\pi}{a} x \sin \frac{\pi}{c} z. \end{aligned} \tag{3}$$

where a, b, and c are the x, y, and z dimensions of the cavity respectively. These are also assumed to be the field components of the empty region of the ferrite-loaded cavity and are the quantities having the subscript 1 in (2).

At the ferrite surface, the normal components of $\bar{b}$ and $\bar{d}$ and the tangential components of $\bar{h}$ and $\bar{e}$ are continuous. In Fig. 1, at $x = T$ and $a - T$ the boundary

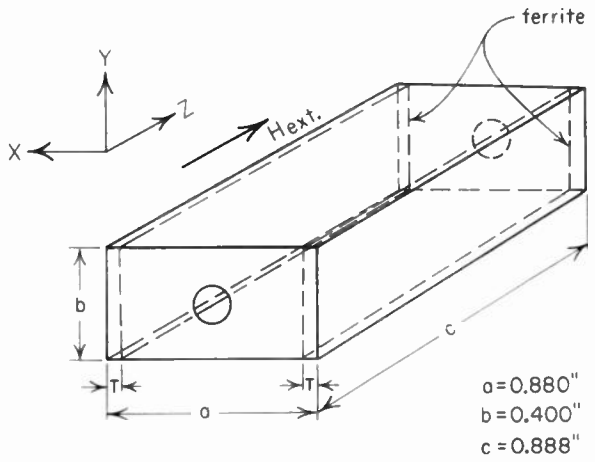

Fig. 1—Transmission cavity.

conditions are $b_{1x} = b_{2x}$, $h_{1z} = h_{2z}$, $h_{1y} = h_{2y}$, and $e_{1y} = e_{2y}$, where the subscript 2 refers to the ferrite region. From the permeability tensor

$$b_{2x} = \mu h_{2x} - jK h_{2y},$$
$$b_{2y} = \mu h_{2y} + jK h_{2x} \quad \text{and} \quad b_{2z} = \mu_\parallel h_{2z}.$$

Since $h_{1y} = 0$,

$$h_{2x} = \frac{b_{1x}}{\mu} = \frac{\mu_0}{\mu} h_{1x} \quad \text{and} \quad b_{2y} = \frac{jK}{\mu} b_{1x}.$$

Notice that b_{2y} does not vanish at $y = 0$ and $y = b$ unless the ferrites are very thin ($b_{1x} \sim 0$) or the magnetic field is zero ($K = 0$). By substituting these quantities and the field components given by (3) into (2) and integrating, the following equation is obtained

$$\begin{aligned} \frac{\delta f}{f} = {} & \frac{T}{a}\left(1 + \frac{\mu_\parallel}{\mu_0}\right)\left\{1 + \frac{\sin \dfrac{2\pi T}{a}}{\dfrac{2\pi T}{a}}\right\}\left(\frac{c^2}{a^2 - c^2}\right) \\ & + \frac{T}{a}\left(\frac{\mu_0}{\mu} - 1\right)\left\{1 - \frac{\sin \dfrac{2\pi T}{a}}{\dfrac{2\pi T}{a}}\right\}\left(\frac{a^2}{a^2 + c^2}\right) \\ & + \frac{T}{a}\left(1 - \frac{\epsilon}{\epsilon_0}\right)\left\{1 - \frac{\sin \dfrac{2\pi T}{a}}{\dfrac{2\pi T}{a}}\right\}. \end{aligned} \tag{4}$$

The real part of $\delta f/f$ is related to the change in the resonant frequency of the cavity, while the imaginary part is related to the change in Q. Only the real part is considered in this paper. For very thin samples, (4) reduces to

$$\frac{\delta f}{f} = \frac{-2T}{a}\left(\frac{\mu_\parallel}{\mu_0} - 1\right)\left(\frac{c^2}{a^2 + c^2}\right). \tag{5}$$

This equation predicts a linear dependence of frequency on sample thickness (T). From frequency shift measurements and (5), the permeability tensor component $\mu_\parallel$ has been determined as a function of the magnetic field for a magnesium-manganese ferrite.[7] If $\mu_\parallel$ as a function of the magnetic field is known, then the frequency shift can be predicted.

With the magnetic field applied to the ferrite of Fig. 1 in the y direction instead of the z direction as in the previous discussions, the permeability tensor becomes

$$\overleftrightarrow{\mu} = \begin{pmatrix} \mu & 0 & -jK \\ 0 & \mu_\parallel & 0 \\ jK & 0 & \mu \end{pmatrix}.$$

The microwave fields inside the ferrite, obtained as before from the boundary conditions and permeability tensor, are

[7] J. C. Cacheris, G. Jones, and R. Van Wolfe, "Topics in the Microwave Applications of Ferrites," Diamond Ordnance Fuze Labs. Tech. Rept. TR-188; July 28, 1955.

$$h_{2x} = \frac{\mu_0}{\mu} h_{1x} + \frac{jK}{\mu} h_{1z}, \quad h_{2z} = h_{1z}$$

$$b_{2x} = b_{1x}, \quad b_{2y} = 0, \quad b_{2z} = \left(\frac{\mu^2 - K^2}{\mu}\right) h_{1z} + \frac{jK}{\mu} b_{1x}$$

$$e_{2y} = e_{1y}, \quad d_{2y} = \epsilon e_{1y}.$$

The expression

$$\left(\frac{\mu^2 - K^2}{\mu}\right)$$

is the effective microwave permeability, μ_e, when none of the field components vary in the direction of the applied magnetic field. Another point to be noted is that b_{2z} does not vanish at the ends of the cavity ($z=0$, c) unless the term $(jK/\mu)b_{1x}$ is zero. This term vanishes when the samples are very thin ($b_{1x}\sim 0$) or when the magnetic field is zero ($K=0$). If the above field quantities are substituted in (2) and the integration is performed, then the frequency shift is

$$\frac{\delta f}{f} = \frac{T}{a}\left(1 - \frac{\mu_e}{\mu_0}\right)\left\{1 + \frac{\sin\frac{2\pi}{a}T}{\frac{2\pi}{a}T}\right\}\left(\frac{c^2}{a^2 + c^2}\right)$$

$$+ \frac{T}{a}\left(\frac{\mu_0}{\mu} - 1\right)\left\{1 - \frac{\sin\frac{2\pi}{a}T}{\frac{2\pi}{a}T}\right\}\left(\frac{a^2}{a^2 + c^2}\right) \quad (6)$$

$$+ \frac{T}{a}\left(1 - \frac{\epsilon}{\epsilon_0}\right)\left\{1 - \frac{\sin\frac{2\pi}{a}T}{\frac{2\pi}{a}T}\right\}.$$

For very thin samples, (6) becomes

$$\frac{\delta f}{f} = -\frac{2c^2T}{a(a^2 + c^2)}\left(\frac{\mu_e}{\mu_0} - 1\right). \quad (7)$$

As before, the frequency shift is a linear function of T, and the equation can be used to determine μ_e.

With the magnetic field applied in the x direction (Fig. 1), the demagnetizing factors are such that the field inside the ferrite is small as compared to the external field. Consequently, a large magnet would be required in order to obtain an appreciable internal field. Further, misalignment of the slab may cause the internal field to have large components in directions other than the x direction. For these reasons, this configuration was not investigated.

For a ferrite slab in the $x-z$ plane, and the magnetic field applied in the x direction, the permeability tensor is

$$\overleftrightarrow{\mu} = \begin{pmatrix} \mu_\parallel & 0 & 0 \\ 0 & \mu & -jK \\ 0 & jK & \mu \end{pmatrix}. \quad (8)$$

Applying the usual boundary conditions with $b_{2y} = \mu h_{2y} - jKh_{2z}$ and $b_{2z} = \mu h_{2z} + jKh_{2y}$ from the permeability tensor shows the microwave fields inside the ferrite to be

$$h_{2x} = h_{1x}, \qquad h_{2z} = h_{1z}, \qquad h_{2y} = \frac{jK}{\mu} h_{1z}$$

$$b_{2x} = \mu_\parallel h_{1x}, \quad b_{2y} = 0, \qquad b_{2z} = \mu_e h_{1z}.$$

If these quantities are substituted in (2) and the integration is performed, the frequency shift is

$$\frac{\delta f}{f} = -\frac{T}{2b}\left[\frac{\left(\frac{\mu_\parallel}{\mu_0} - 1\right)a^2}{(a^2 + c^2)} + \frac{\left(\frac{\mu_e}{\mu_0} - 1\right)c^2}{(a^2 + c^2)} + \left(1 - \frac{\epsilon_0}{\epsilon}\right)\right]. \quad (9)$$

This equation predicts the frequency shift to be a linear function of T. No higher order terms are obtained for this geometry.

In the derivation of (4) and (6), it is possible, for the thicker ferrites, to obtain from the boundary conditions at the ferrite-air interface components of $\bar{b}$ inside the ferrite which are normal to the walls of the metal cavity. These components of b_{2y} and b_{2z} which do not vanish at the metal surfaces ($y=0$ and $z=0$, respectively) drop out of the scalar product in (2). This boundary violation may be a further limitation of the applicability of perturbation theory to the experimental results.

When the applied magnetic field is zero, the wave equation can be solved exactly for the fundamental TE mode. With the ferrite slabs as shown in Fig. 1, only one half of the cavity is considered since the electric field is symmetrical about the center ($x=a/2$, Fig. 1). The electric field can then be written

$$e_y = A\cos\beta_1\xi \sin\frac{\pi}{c}z, \quad 0 < \xi < \frac{a}{2} - T, \quad \xi = x - \frac{a}{2}$$

$$\beta_1^2 + \left(\frac{\pi}{c}\right)^2 = \omega^2\epsilon_1\mu_0$$

$$e_y = B\sin\beta_1\left(\xi - \frac{a}{2}\right)\sin\frac{\pi}{c}z, \quad \frac{a}{2} - T < \xi < \frac{a}{2}$$

$$\beta_2^2 + \left(\frac{\pi}{c}\right)^2 = \omega^2\epsilon_2\mu$$

where

ϵ_1 = permittivity of the region between the ferrite slabs (polyfoam);

ϵ_2 = permittivity of ferrite slabs, and

μ = permeability of the ferrite when the dc internal magnetic field is zero.

By matching e_y and h_z at the slab surface

$$\left(\xi = \frac{a}{2} - T\right)$$

the equation

$$\frac{\mu_0}{\beta_1}\cot\beta_1\left(\frac{a}{2}-T\right)=\frac{\mu}{\beta_2}\tan\beta_2 T$$

is obtained. This equation can be written in terms of ω by using the relations

$$\beta_1=\left[\omega^2\epsilon_1\mu_0-\left(\frac{\pi}{c}\right)^2\right]^{1/2}$$

and

$$\beta_2=\left[\omega^2\epsilon_2\mu-\left(\frac{\pi}{c}\right)^2\right]^{1/2}.$$

Then

$$\cot\left\{\left(\frac{a}{2}-T\right)\left[\omega^2\epsilon_1\mu_0-\left(\frac{\pi}{c}\right)^2\right]^{1/2}\right\}=\frac{\mu}{\mu_0}\left[\frac{\omega^2\epsilon_1\mu_0-\left(\frac{\pi}{c}\right)^2}{\omega^2\epsilon_2\mu-\left(\frac{\pi}{c}\right)^2}\right]^{1/2}\cdot\tan\left\{T\left[\omega^2\epsilon_2\mu-\left(\frac{\pi}{c}\right)^2\right]^{1/2}\right\}. \quad (10)$$

The permittivity of the polyfoam is determined by the resonant frequency of the cavity when filled with polyfoam. That is,

$$\epsilon_1\mu_0\omega_0^2=\left(\frac{\pi}{a}\right)^2+\left(\frac{\pi}{c}\right)^2$$

or

$$\frac{\epsilon_1}{\epsilon_0}=\left(\frac{v_c}{\omega_0}\right)^2\left[\left(\frac{\pi}{a}\right)^2+\left(\frac{\pi}{c}\right)^2\right],$$

where $\omega_0=2\pi\times 9.214$ kmc and v_c is the velocity of light.

Eq. (10) was used to determine the resonant frequency of the cavity for $0<T<0.100$ inch, $\mu/\mu_0=0.780$, and $\epsilon/\epsilon_0=13.6$.[8] The results are shown in Fig. 5 and Fig. 8 (exact curves). The difference between the exact curve and the experimental curve may be due to the choice of ϵ and μ. The experimental values of frequency can be used in (10) to determine quite accurately the permeability and dielectric constants for thick samples of ferrite.

Experimental Procedure

In studying the properties of ferrite-loaded cavities, most of the analyses and measurements were made for transmission cavities instead of klystron cavities. This avoided the following difficulties in making the measurements: The coupling effects between the cavity in the klystron and the external cavity; the necessity for tuning the ferrite-loaded klystron through a continuous range of frequencies, and the effects of changes in the ferrite properties due to heating by the klystron.

A block diagram of the microwave apparatus is shown in Fig. 2. The test cavity which was mounted

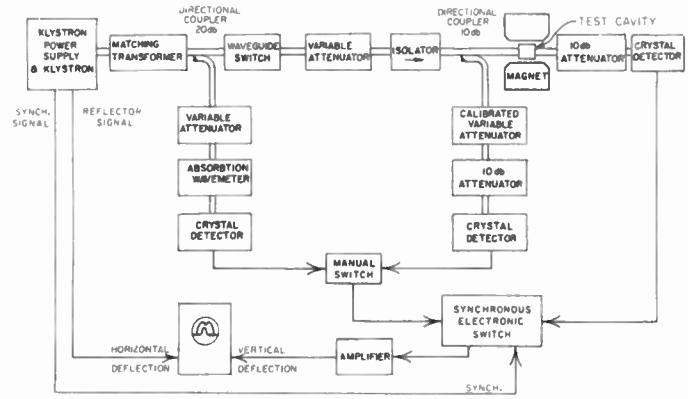

Fig. 2—Block diagram of the system for the transmission cavity measurements.

between the pole pieces of a laboratory magnet, received energy from a frequency-modulated klystron. The power incident upon and transmitted through the cavity was measured. Incident and transmitted signals were simultaneously viewed on an oscilloscope by means of an electronic switch. Frequencies were measured with an absorption type wavemeter. The applied external magnetic field was measured with a rotating coil gaussmeter. The internal field was computed using a B-H[9] curve and by approximating the slab by an appropriate ellipsoid. Sets of frequency measurements were made as a function of the magnetic field with the ferrite geometry and position as parameters. The accuracy of the frequency measurements was ± 1 mc.

The insertion of ferrite slabs into the transmission cavity had a large effect on the Q of the cavity. However, this change in Q of the transmission cavity was not important for the magnetically-tuned klystron because the Q of the klystron-loaded cavity was comparatively low and was not appreciably affected by introduction of the ferrite.

The experimental setup for the klystron-loaded cavity was relatively simple. Energy from the klystron was fed through a pad and wavemeter to a crystal detector connected to a wattmeter. For some of the measurements, the magnetic field was supplied by a large laboratory magnet and was measured with a rotating coil gaussmeter. Other measurements were made with the field supplied by a coil wound on a toroidal core, mounted on the tube cavity as shown in Fig. 3.

[8] R. C. LeCraw and E. G. Spencer, "Tensor permeabilities of ferrites below magnetic saturation," 1956 IRE Convention Record, Part 5, pp. 66–74.

[9] The B-H curves were obtained from measurements made by R. E. Mundy and I. L. Cooter of the National Bureau of Standards, Washington, D. C.

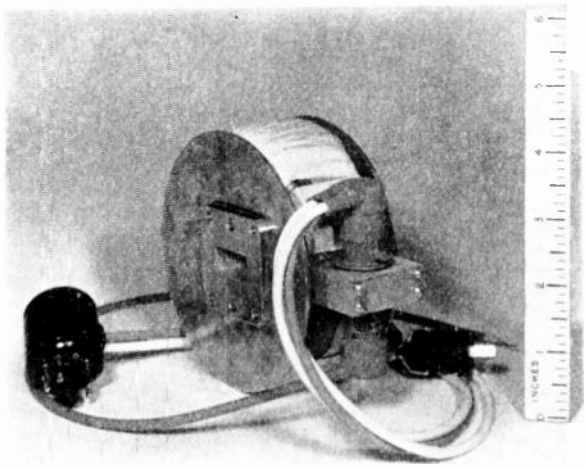

Fig. 3—Magnetically-tuned klystron.

Results and Discussions

The frequency dependence of the cavity upon the internal magnetic field in the z direction for magnesium-manganese ferrites of various thicknesses is shown in Fig. 4. For very thin samples (0.020 inch or less), as the

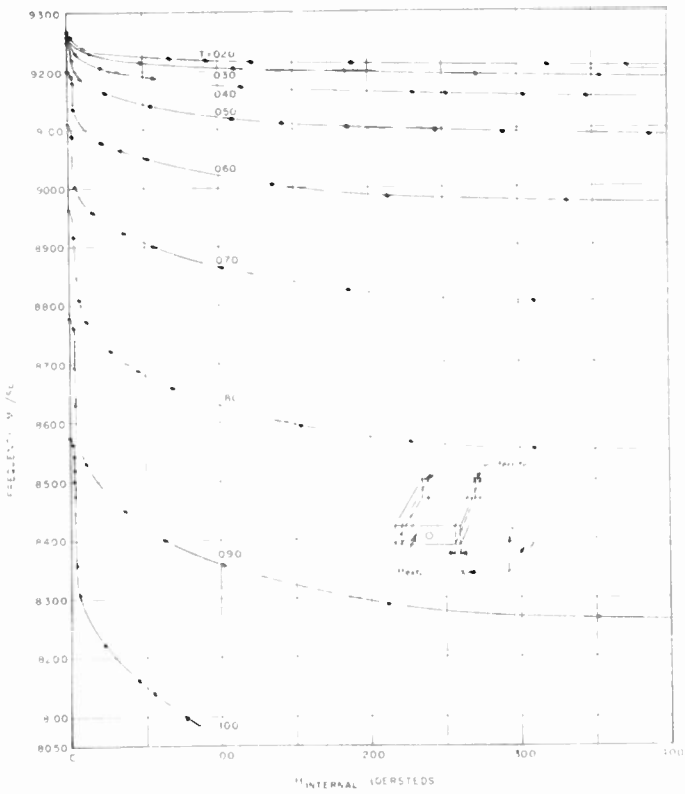

Fig. 4—Cavity frequency as a function of internal magnetic field applied parallel to the z axis.

magnetization approaches saturation, $\mu_\parallel$ approaches μ_0, and the frequency becomes asymptotic to the frequency of the empty cavity (9214 mc), as predicted in (5). For slightly thicker samples, with magnetic fields of about 300 oersteds, the frequency shift approaches that of the cavity with only the dielectric effect of the ferrite. This is in agreement with (4), as the first two terms are negligible for this range of magnetic fields. Measurements made with higher fields for the thicker samples show that the frequency increases with field, *i.e.*, $\delta f/f$ decreases, as can be predicted by the second term of (4).

Fig. 5, which can be obtained from data presented in Fig. 4, shows the variation of cavity frequency with ferrite thickness for several values of internal field. The frequency as a function of slab thickness was calculated from (4) with $\epsilon/\epsilon_0 = 13.6$ and $\mu_\parallel/\mu_0 = 0.780$. The theoretical curve fits the experimental data as well as can be expected, since the maximum frequency shift is only a very small percentage of the empty cavity frequency.

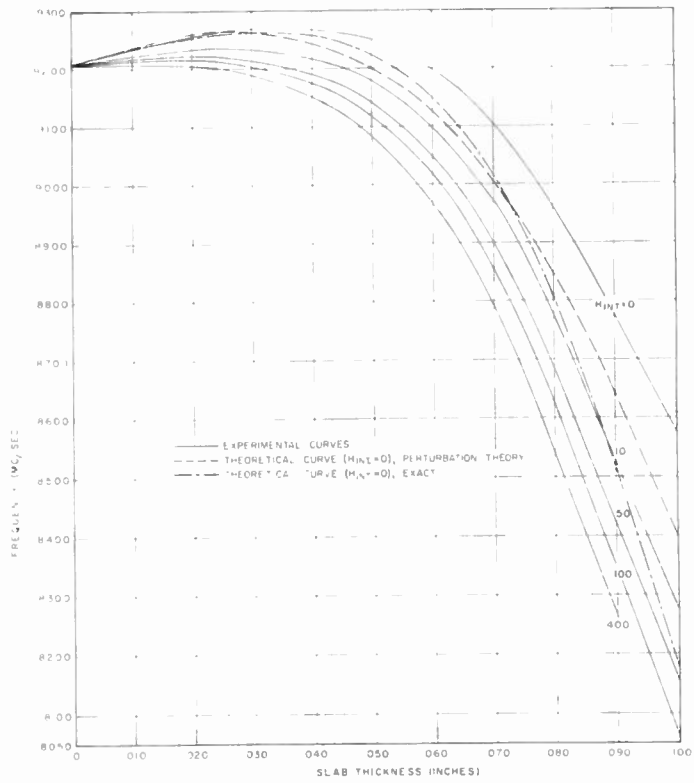

Fig. 5—Cavity frequency as a function of ferrite thickness with the magnetic field applied parallel to the z axis.

Eq. (5) was used with frequency shift measurements to compute $\mu_\parallel$ for slabs 0.005 inch thick whose height was less than b (Fig. 1). The variation of the microwave permeability, $\mu_\parallel$, is shown in Fig. 6 as a function of the internal magnetic field. At this frequency (9241 mc), the relative permeability of the ferrite at zero field is 0.78. The permeability $\mu_\parallel$, which is an intrinsic property of the material, changes only in the interval 0 to 350 oersteds. It is over this range that the cavity's resonant frequency is dependent upon the magnetic field.

The frequency of the cavity as a function of the in-

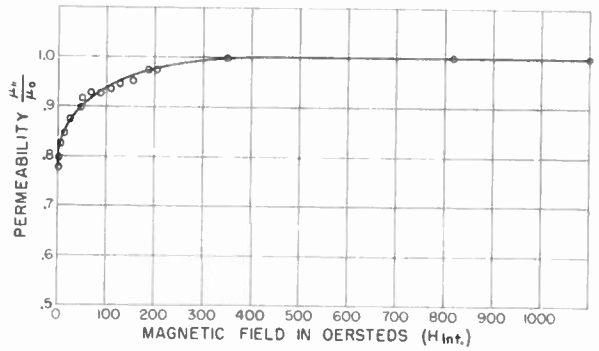

Fig. 6—Measured microwave permeability in the direction of dc magnetization.

ternal magnetic field in the y direction is shown in Fig. 7, with ferrite thickness as a parameter. In Fig. 8, data obtained from these curves shows the cavity frequency as a function of slab thickness for a range of values of internal magnetic field.

For very thin samples (0.020 inch or less), the frequency shift is positive and increases with increasing magnetic field as predicted by (7). For thicker samples, the frequency decreases, due mainly to the large dielectric constant of the ferrite. Eq. (6) shows that this term should subtract from the terms involving the permeability. The theoretical curve in Fig. 5 also applies to this configuration for zero magnetic field.

Fig. 9 shows the frequency of the cavity as a function of the internal magnetic field in the x direction for various slab thicknesses with the ferrite completely covering the x, z plane at $y=0$. Fig. 10 was plotted from Fig. 9 for comparison with the results of perturbation theory. For thin samples (0.030 inch or less), the frequency is a linear function of the thickness; this is in agreement with (9). For thicker samples, the frequency decreases very rapidly with increase in thickness. No terms of higher order than linear in T were obtained from perturbation theory for this case, since the assumed microwave fields did not vary in the y direction.

Some outstanding features of the geometries investigated that are useful for the design of magnetically tuned klystrons can be summarized by means of Figs. 5, 8, and 10. With the ferrite slabs at the side walls and with z magnetization, large negative frequency shifts can be obtained by small changes in the magnetic field. However, the nonlinearity may not be desirable for practical applications. With y magnetization and the ferrite slabs placed as before, very large positive frequency shifts having excellent linearity can be obtained. With the ferrite slab on the bottom of the cavity ($y=0$) and with x magnetization, small frequency shifts are obtained with good linearity.

An x band klystron with an external cavity was magnetically tuned by a field applied in the z direction to two ferrite slabs (0.870 inch $\times$ 0.100 inch $\times$ 0.300 inch) in the cavity. Fig. 11 shows the frequency deviation and power change as functions of the magnetic field supplied by a laboratory magnet. As the field is increased, the mode of oscillation (ordinarily only 80 mc wide) shifts so that very wide deviations are pos-

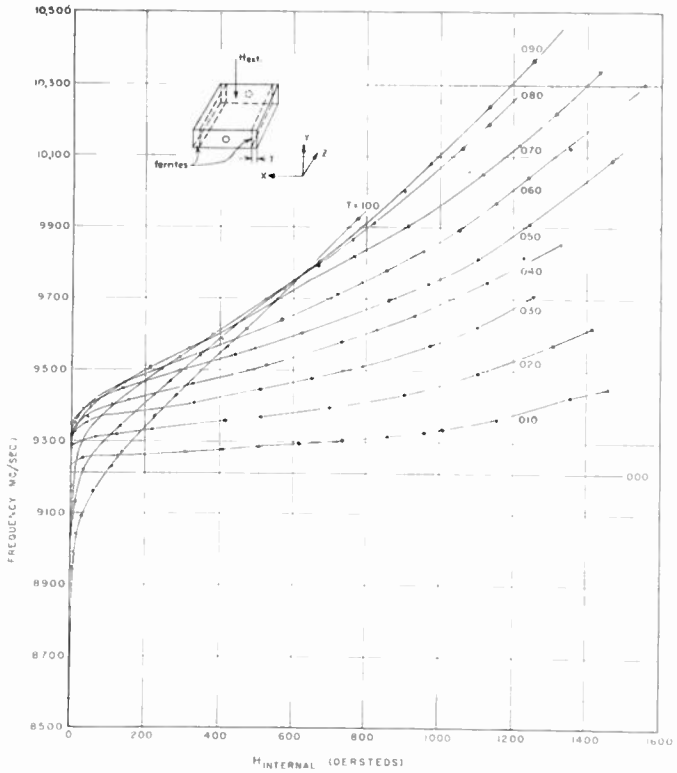

Fig. 7—Cavity frequency as a function of internal magnetic field applied parallel to the y axis.

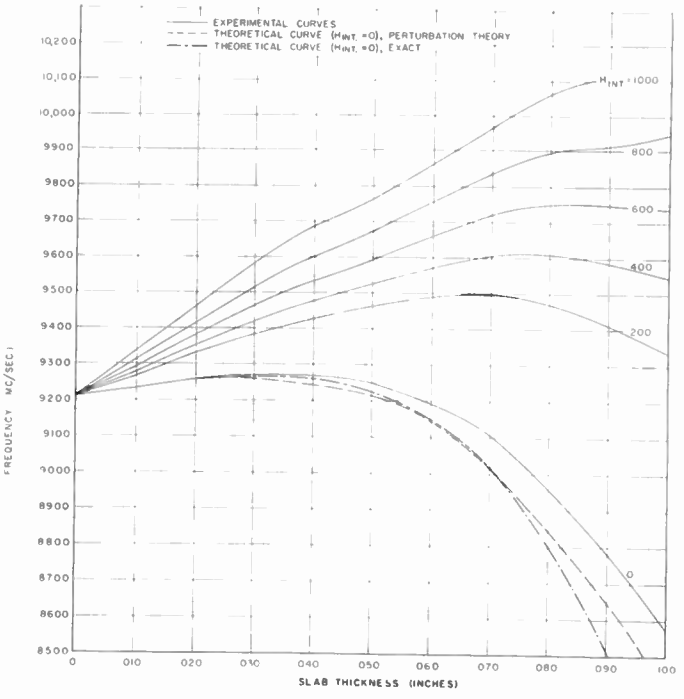

Fig. 8— Cavity frequency as a function of ferrite thickness with the magnetic field applied parallel to the y axis.

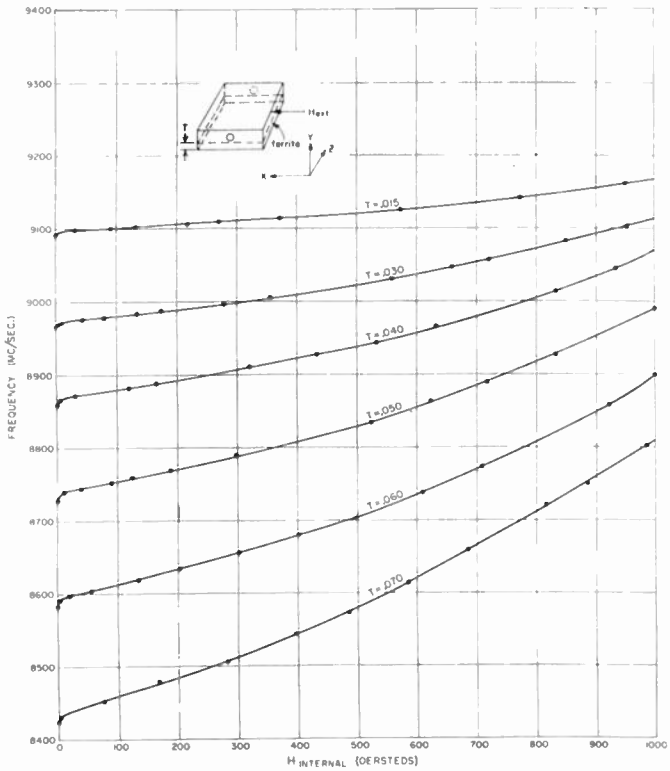

Fig. 9—Cavity frequency as a function of internal magnetic field applied parallel to the x axis.

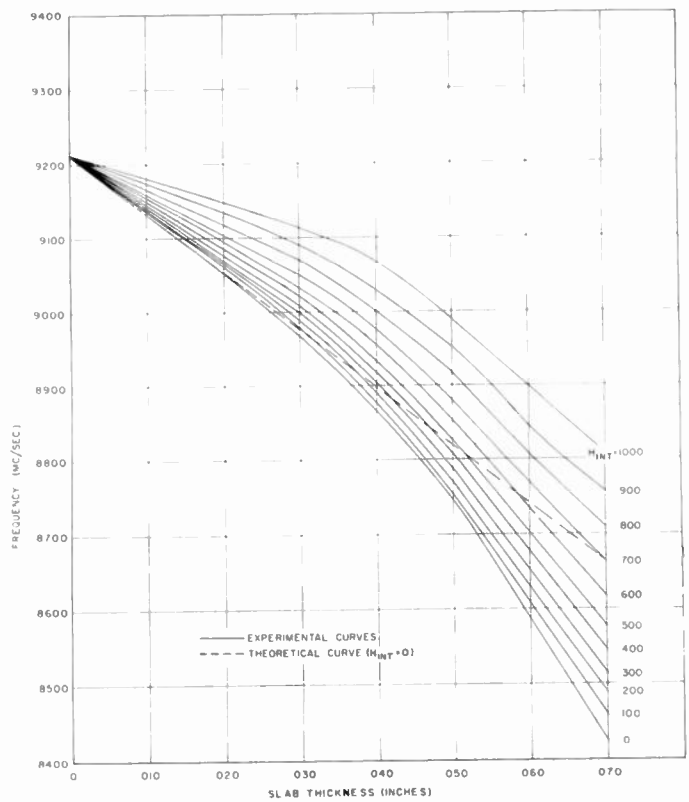

Fig. 10—Cavity frequency as a function of ferrite thickness with the magnetic field applied parallel to the x axis.

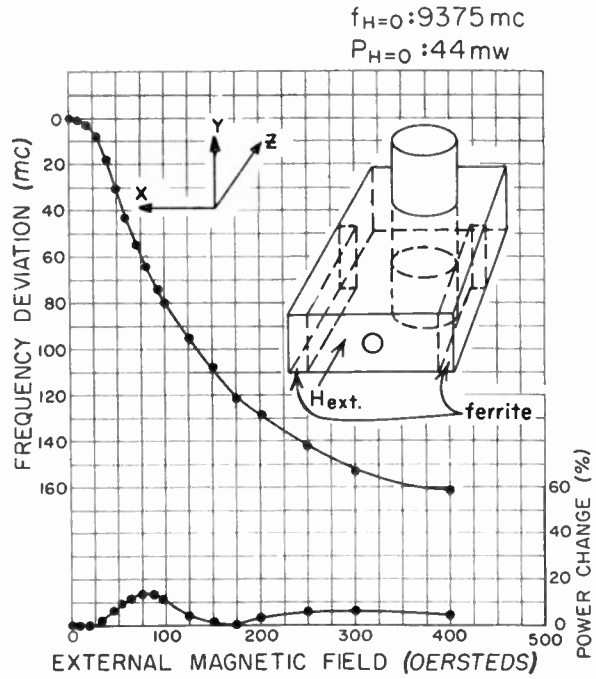

Fig. 11—Frequency deviation and power change of the klystron as functions of a magnetic field applied along the z axis.

sible. With the repeller voltage adjusted for minimum amplitude modulation, the maximum frequency deviation for less than 15 per cent power change is 160 mc, compared to 20 mc obtained by varying the repeller voltage. These results are in agreement with the data in Fig. 5 and with additional transmission cavity measurements not given here. The frequency deviation increases with increasing magnetic field up to 400 oersteds, but decreases for fields above 400 oersteds.

The frequency deviation and power change of the klystron assembly shown in Fig. 3 are given in Fig. 12 (slab dimensions: 0.833 inch $\times$ 0.100 inch $\times$ 0.384 inch) as functions of the current in the coil. As predicted by the curves in Fig. 8, a large frequency deviation (240 mc) is obtained that is linear with magnetic field. In this linear region, the power change is less than 13 per cent. The linearity, which was limited by saturation of the magnet, can be extended by a redesigned magnet.

For frequency modulation applications the klystron cavity can be made of bakelite and the inside plated with a thin layer of silver. This reduces the alternating magnetic field loss due to eddy currents induced in the cavity walls. It is also possible to wind the coil on a dielectric of low heat conductivity surrounding the ferrite. The dielectric will prevent the heat generated in the coil from reaching the ferrite slab. This assembly can then be placed in an ordinary cavity in a position where the wires do not interfere appreciably with the microwave fields in the ferrite. The bias field for linear operation can be supplied by an external magnet, and modulation can be achieved by applying a signal to the coil inside the cavity.

On the basis of the qualitative agreement between measurement with the transmission cavity and ferrite-loaded klystron cavity with z and y magnetization, small frequency shifts with very good linearity are to be expected for the klystron with the ferrite slab in the position shown in Fig. 9. These properties of magnetically-tuned klystrons are useful for wideband frequency modulation applications requiring low amplitude modulation.

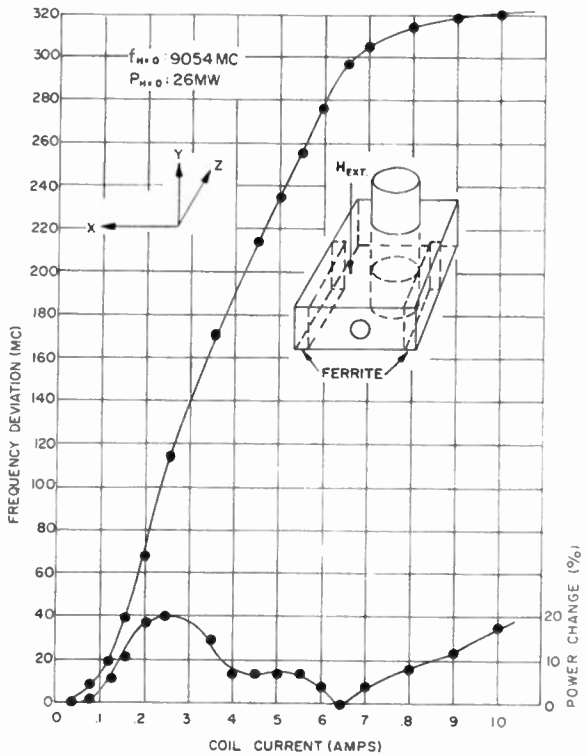

Fig. 12—Frequency deviation and power change of the klystron as functions of current in the coil producing a magnetic field along the y axis.

Conclusion

This paper gives experimental and theoretical values of the frequency shifts of a transmission cavity for several different ferrite slab locations and magnetic field directions over a wide range of slab thicknesses and magnetic field strengths.

Experimental measurements of frequency shift in ferrite-loaded klystrons are in excellent agreement with transmission cavity measurements. Hence, statements concerning the transmission cavity can be applied to the klystron cavity. Since ferrites are essentially lossless in the low field region, measurements of Q were not made with the transmission cavity. Further, these measurements cannot be simply related to the klystron-loaded cavity.

The results indicate that with ferrites located at the sides of the cavity and the magnetic field applied parallel to the long dimension of the slabs, large negative frequency shifts can be obtained for small changes in magnetic field. The nonlinearity of the ferrite material chosen may not be desirable for practical applications. To obtain large frequency shifts the ferrites used should have microwave permeabilities at zero magnetization that differ greatly from μ_0. For good linearity, ferrites should be chosen such that $\mu_\parallel$ is linear with the external magnetic field. For the above ferrite slabs and the magnetic field applied perpendicular to the broad face of the cavity, very large frequency shifts can be obtained. The linearity is excellent, especially with proper bias fields. With the ferrite on the bottom of the cavity and the magnetic field applied perpendicular to the side walls of the cavity, small frequency shifts are obtained having good linearity. The linearity in the low field region is dependent on the dimensions of the sample and can be improved by changing a or c as can be shown in (9). Two magnetically-tuned x band klystrons were designed; the frequency deviation of the first was 160 mc and nonlinear with magnetic field, while the frequency deviation of the second was linear over a range of 240 mc. The linearity of the second was limited by saturation of the material in the core of the magnet. The range of linearity can be extended by redesigning the magnet.

It is expected that further work to obtain optimum parameters will yield greater frequency shifts while minimizing the amplitude effects and reducing the required magnetic fields.

Acknowledgment

The authors wish to thank C. W. Carnahan, Varian Associates, for suggesting the use of ferrites to magnetically tune klystrons, and Miss Isabelle Arsham for the computation of the theoretical results presented in Figs. 5 and 8.

Ferrite Directional Couplers*

A. D. BERK† AND E. STRUMWASSER†, MEMBER, IRE

Summary—**A novel directional X-band coupler based on the nonreciprocal scattering properties of a ferrite cylinder is described. Experimental data for coupling and directivity are given as a function of various parameters. Approximate theoretical expressions for coupling and directivity are derived and discussed.**

Introduction

A THEORETICAL STUDY of the scattering produced by a ferrite cylindrical post in a rectangular waveguide has revealed the possibility of a novel directional coupler at microwave frequencies. Whereas conventional directional couplers are invariably based on the coupling properties of one or more holes in the common wall of two waveguides, the performance of the ferrite directional coupler depends entirely on the nonreciprocal property of the ferrite material. In the following pages, after a qualitative description of the physical principle[1] is given, approximate theoretical expressions for the coupling and directivity will be offered. Experimental results showing the effect of changing various parameters as well as data describing the performance of experimental couplers will then be presented and discussed. Finally in the Appendix the derivation of the formulas used in the text will be given together with a discussion of some of the theoretical aspects of the problem.

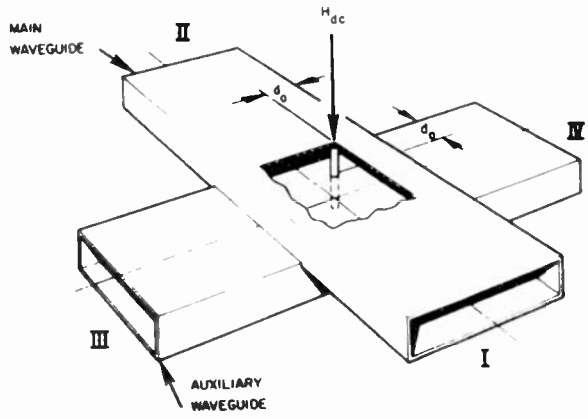

Fig. 1—Crossguide ferrite directional coupler.

Qualitative Description

Fig. 1 illustrates the basic arrangement. A thin ferrite cylindrical post extends through both the main and the auxiliary waveguides. It is located at a point where the rf magnetic field in both waveguides is circularly polarized. An adjustable dc magnetic field is applied parallel to the axis of the post and the electric field. The crossguide coupler shown in Fig. 1 is one possible configuration, the collinear coupler with two waveguides joined at their broad faces as shown in Fig. 7 is another. It is clear that the angle between the axes of the two waveguides is completely arbitrary.

To understand the directional nature of the coupler we must examine the behavior of the ferrite post in some detail. The ferrite cylinder transfers power from the main waveguide to the auxiliary waveguide by two mechanisms: dielectric coupling and magnetic coupling.

Dielectric Coupling

The incident wave in the main waveguide, assumed to be of the fundamental mode, produces a dielectric polarization current which is parallel to the axis of the post. This polarization current is not confined in the upper half of the ferrite cylinder but penetrates into the lower half. The latter behaves, therefore, as a dielectric rod antenna radiating into the auxiliary waveguide. Since such an antenna radiates equally in both directions of the auxiliary waveguide the power transfer from the main waveguide to the auxiliary waveguide is *nondirectional.*

Magnetic Coupling

The electron spins in the upper half of the ferrite post are made to precess about the orienting field, H_{dc}, by the circularly polarized rf magnetic field of the incident wave. With the direction of H_{dc} as shown in Fig. 1, the amplitude of precession will remain small and fairly independent of the magnitude of H_{dc} if the wave in the main guide travels from terminal II to terminal I, whereas it can assume large values depending on the strength of the dc magnetic field if power in the main guide flows from terminal I to terminal II. Because of spin to spin coupling, this precessional motion is transferred to the spins of the lower half of the post. Thus, the ferrite cylinder acts like a stack of magnetic dipoles rotating about its axis at the frequency of the rf field. It is physically clear, and it will be shown mathematically in the Appendix, that for a fixed sense of rotation of these dipoles there is a corresponding fixed direction in which power in the auxiliary waveguide can propagate. In Fig. 1, for example, this direction is from terminal IV to terminal III. Thus, the transfer of energy due to the magnetic properties of the post is *directional.*

As the intensity of the dc magnetic field approaches the value required for ferromagnetic resonance the

* Original manuscript received by the IRE, July 6, 1956.
† Hughes Aircraft Co., Culver City, Calif.
[1] See also, R. W. Damon, "Magnetically controlled microwave directional coupler," *J. Appl. Phys.*, vol. 26, p. 1281; October, 1955. Dr. Damon's letter appeared while the research reported in the present paper was in progress.

magnetic coupling becomes predominant and the overall coupling becomes directional.

Theoretical Results

The following approximate analytical expressions for the coupling and the directivity are valid when the diameter of the post is small as compared to the wavelength and the effect of the dielectric coupling can be neglected. The derivation of these expressions together with formulas which include the effect of the dielectric coupling is given in the Appendix.

Coupling

According to the standard definition this is the ratio in decibels of the input power at terminal I to the power received at terminal III when all the remaining terminals are matched (see Fig. 1). We have

$$\text{Coupling} = -20\log\left(\frac{Q_m\pi D^2}{a^2}\sin^2\frac{\pi d_0}{a}\,\frac{\chi-\kappa}{\chi-\kappa+2}\right), \qquad (1)$$

where D is the diameter of the post, a the width of the waveguide, d_0 the distance from the points of circular polarization to the nearest wall of the waveguide. The symbols χ and κ are defined by the *intrinsic* susceptibility tensor,

$$\overleftrightarrow{\chi}_m = \begin{pmatrix} \chi & -j\kappa & \\ j\kappa & \chi & 0 \\ 0 & 0 & 0 \end{pmatrix}.$$

Q_m is an empirical factor measuring the extent to which magnetic polarization currents in the upper half of the ferrite post penetrate into the lower half.

Directivity

This is defined as 10 log (P_a/P_c), where P_a is the power measured at terminal III due to input at terminal I with terminals II and IV matched and P_c is the power measured at terminal III due to the same power input at terminal II with terminals I and IV matched. It is shown in the Appendix that

$$\text{Directivity} = 20\log\frac{(\chi-\kappa)(\chi+\kappa+2)}{(\chi+\kappa)(\chi-\kappa+2)} \qquad (2)$$

Experimental Results

The preceding theoretical expressions predict that the coupling and the directivity should go through a single resonance as the strength of the dc magnetic field varies and that this resonance should occur when the dc magnetic field is

$$H_{dc} = \frac{\omega}{\gamma} - 2\pi M_s,$$

where ω is the angular frequency, γ the gyromagnetic ratio and $4\pi M_s$ is the saturation magnetization of the ferrite material. It was found that the diameters of the ferrite samples used in the experiments were too large for the theoretical expressions to be valid. Reasonable agreement between theory and experiment was obtained only with a Ferramic R-1 post of 0.030 inch diameter. The results are shown in Fig. 2. The theoretical curve was plotted from (1) by assuming a saturation magnetization of 2400 oersteds, a gyromagnetic ratio of 2.89 and by adjusting the line width and the absolute value of the coupling to fit approximately the experimental curve. Note that in spite of the general agreement between the two curves in the neighborhood of resonance, a difference in character is definitely apparent. Therefore, even a 0.030 inch diameter is not small enough for the theoretical expression to be applicable. There is no room for comparison between theory and experiment for a 0.030 inch diameter post made of Ferroxcube 106 material as the experimental coupling curve exhibits two resonant dips instead of the one predicted by theory. Further efforts to compare theory and experiment were postponed because of the difficulty of obtaining thin enough cylinders and also because the size of ferrite posts required for practical values of coupling is well beyond the limit of applicability of the approximate theory developed in the Appendix.

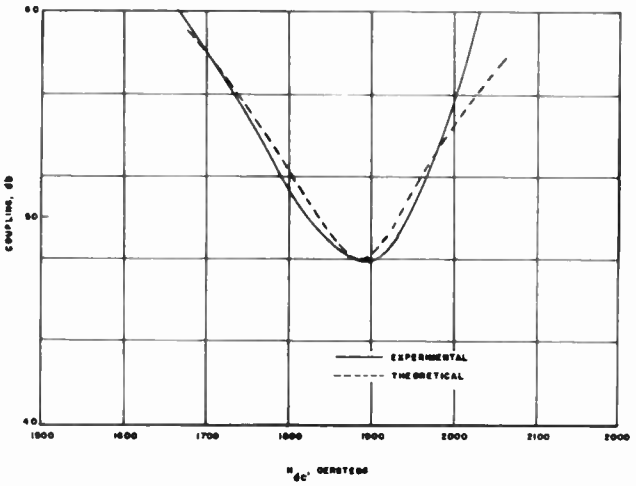

Fig. 2—Comparison of theoretical and experimental coupling curves for a 0.030-inch diameter General Ceramics R-1 ferrite.

The information presented in the following series of curves should not be considered as final engineering design data, but rather the result of various exploratory experiments performed to determine the practical feasibility of the ferrite directional coupler. The ferrite materials used were General Ceramics R-1 and Ferroxcube 106. Waveguides with a 0.200 inch b dimension were used in order to shorten the gap between the pole faces of the electromagnet and thereby reduce its size and power input requirements.

Figs. 3 and 4 show typical behavior of coupling for three frequencies as a function of the dc magnetic field. The measurements were made for both 0.062 inch di-

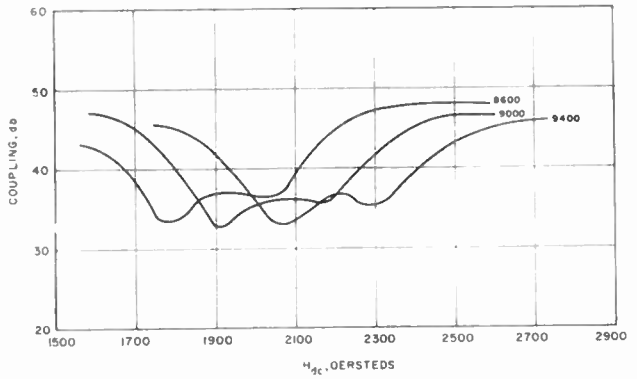

Fig. 3—Coupling vs H_{dc} for a 0.061-inch diameter General Ceramics R-1 ferrite.

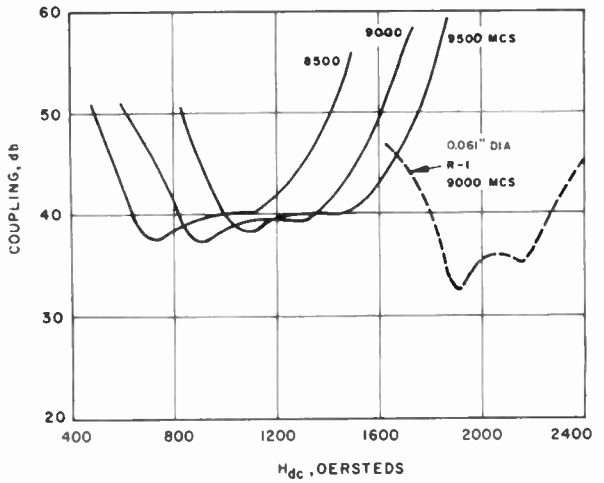

Fig. 4—Coupling vs H_{dc} for a 0.062-inch diameter Ferroxcube 106 ferrite.

ameter R-1 and 0.061 inch diameter 106 ferrite posts. Each set of curves exhibits a double resonance, both dips occurring in the general neighborhood of the ferromagnetic resonance. From the practical point of view the resonance dip occurring at the higher value of the dc magnetic field (from hereon referred to as the "second dip") is of prime importance because it is wider with respect to H_{dc} and consequently more broadband with respect to frequency.

From Fig. 4 it may also be noted that the 106 ferrite has an inherently broader resonance than R-1. Furthermore, because of its higher saturation magnetization Ferroxcube 106 requires a much lower dc biasing field to produce resonance, which results in a marked advantage in the size and weight of the magnet. From the set of the three coupling curves one may deduce the frequency response of the coupler when operated at a fixed dc magnetic field. For the R-1 ferrite post, when operated at an H_{dc} value of 2000 oersteds, the expected variation according to Fig. 3 would be confined to ± 1 db between the frequency limits of 8600 to 9400 mc. The frequency curve of Fig. 5 shows a coupling variation of the same order of magnitude. The optimum magnetic field for broadband operation of the

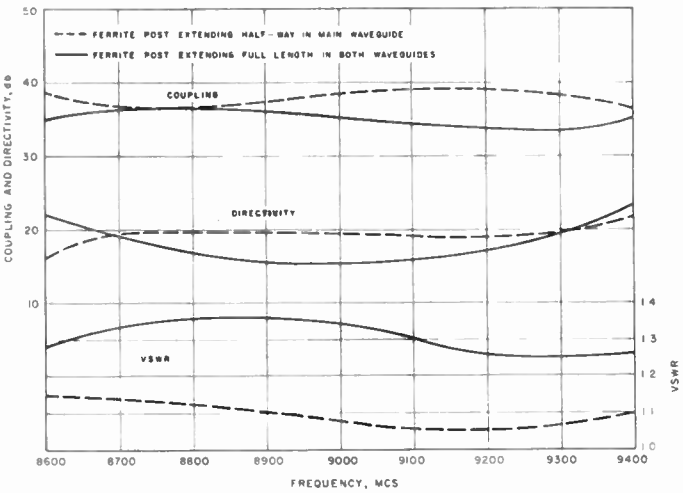

Fig. 5—Coupling, directivity, and vswr vs frequency. $H_{dc}=2000$ oersteds. General Ceramics R-1, 0.061-inch diameter post.

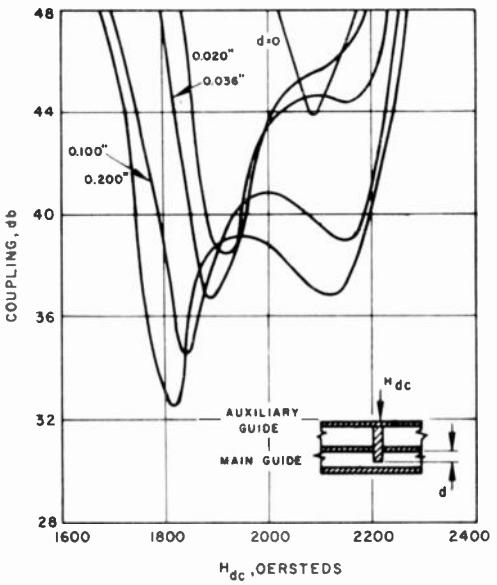

Fig. 6—Coupling as a function of height of insertion of ferrite post in main waveguide. General Ceramics R-1, 0.061-inch diameter.

single 106 ferrite post is approximately 1200 oersteds and the frequency curve plotted in Fig. 12 shows a coupling value of 41.5 db ± 1 db from 8200 to 9800 mc, while the directivity remained above 20 db throughout. The directivity and vswr for the single R-1 ferrite post coupler were measured and the results are also given in Fig. 5. In order to reduce the reflections in the main waveguide the extension of the ferrite post into the main waveguide was reduced to one-half the b dimension. The results are compared to the full insertion case in Fig. 5 and show an appreciable reduction in vswr and only a 3 db drop in coupling. A more complete picture of the coupling behavior as a function of height of insertion in the main guide is given in Fig. 6.

Within certain limits one may increase the coupling values by increasing the diameter of the ferrite or by using an array of ferrite posts in a collinear coupler as

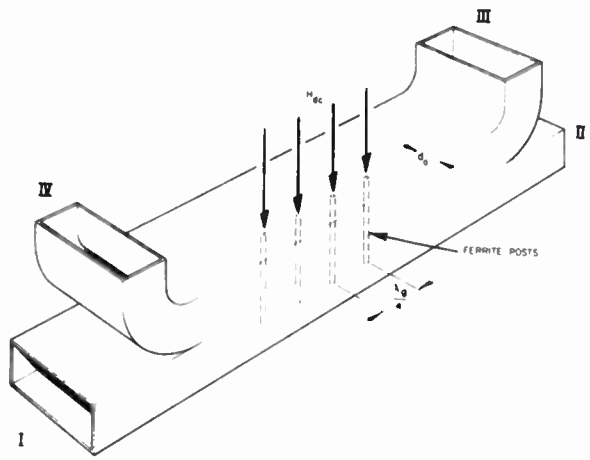

Fig. 7—Collinear ferrite array directional coupler.

shown in Fig. 7. Curves of coupling as a function of magnetic field for various diameters of R-1 and 106 ferrites are shown in Figs. 8 and 9. These figures also indicate that one should be able to optimize the ferrite diameter to yield the flattest coupling response curve and consequently the most broadband coupler.

One advantage of using an array of ferrite posts is the fact that reflections in the main waveguide may be cancelled by spacing an even number of ferrite posts a quarter wavelength apart. The directivity of the array coupler is primarily dependent on the reflections in the main waveguide from every second ferrite, since the reflected energy will couple to the auxiliary waveguide by virtue of the same phenomenon that produces the direct coupling. Thus, for an array of two ferrites the directivity in db would be the sum of the reflection in db in the main waveguide and the coupling value for a single ferrite. This effect was experimentally verified. By reducing the ferrite length extending into the main waveguide an improvement in the directivity was obtained over a restricted bandwidth at the expense of somewhat reduced coupling.

Couplers employing an array of four R-1 and one, two, and four 106 ferrites were built and the results are plotted in Figs. 10, 11, and 12 opposite. The insertion loss of the main waveguide was measured for most of the experimental couplers and a typical loss curve is plotted in Fig. 13. Note that the value of H_{dc} at which maximum insertion loss occurs is outside the region of broadband operation. The insertion loss therefore remains less than 0.5 db for the single R-1 full length ferrite coupler.

One of the interesting features of this device, which cannot be realized with the conventional type coupler, is the electronic control of coupling possible over a restricted frequency band. Fig. 14 shows coupling from 8900 to 9100 mc for four magnetic field values.

If both the direction of the magnetic field and the direction of propagation in the main waveguide are reversed, coupling and directivity should not be altered. Therefore, bidirectional coupling may be achieved by

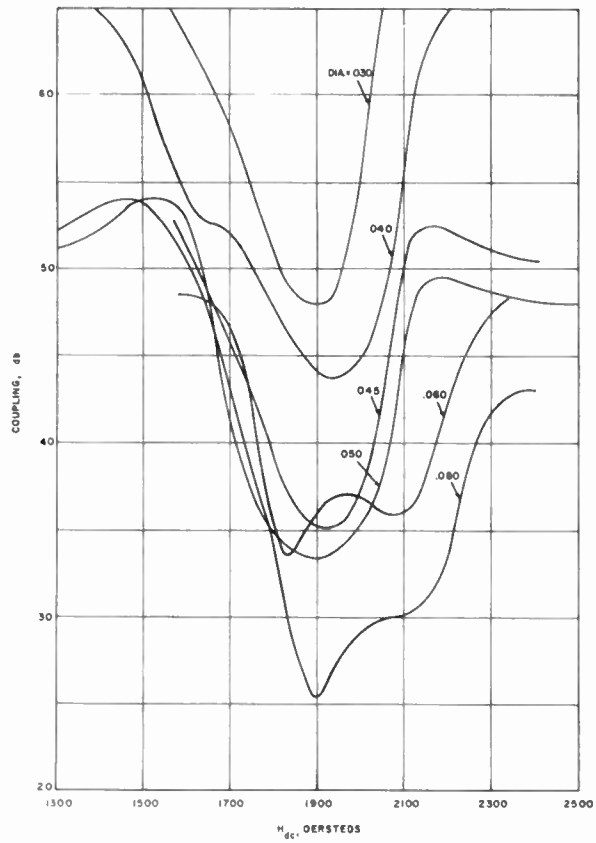

Fig. 8—Coupling vs H_{dc} as a function of diameter. General Ceramics R-1. Frequency, 9000 mc.

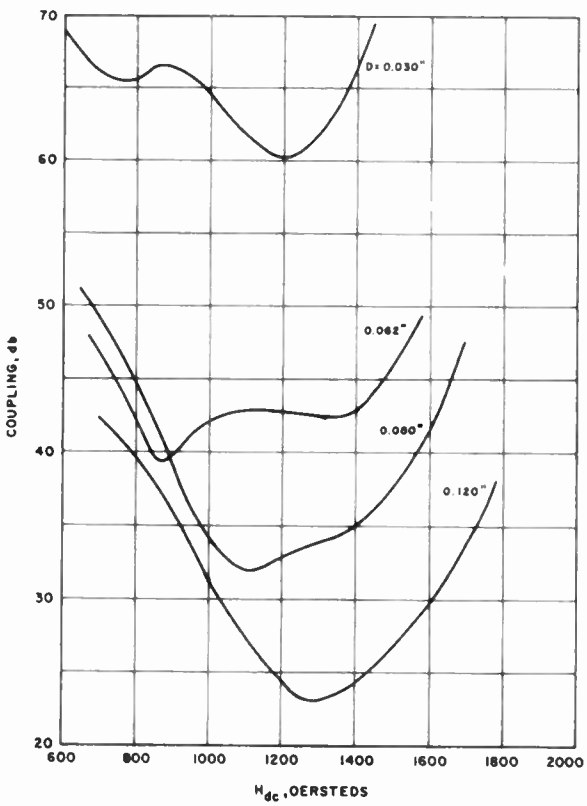

Fig. 9—Coupling vs H_{dc} as a function of diameter. Ferroxcube 106. Frequency, 9000 mc.

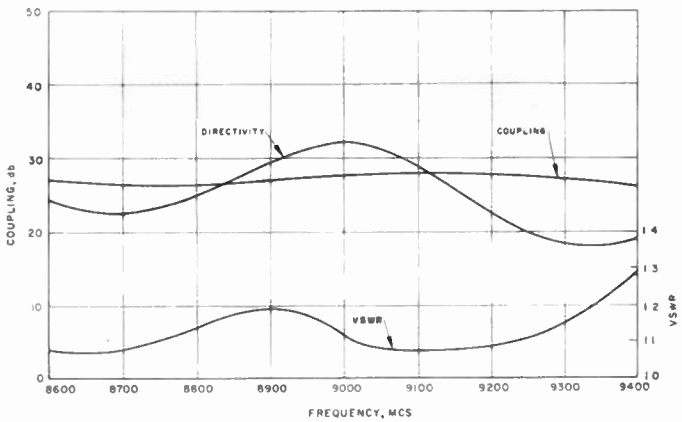

Fig. 10—Coupling, directivity, and vswr vs frequency for an array of four 0.060-inch diameter R-1 ferrite posts.

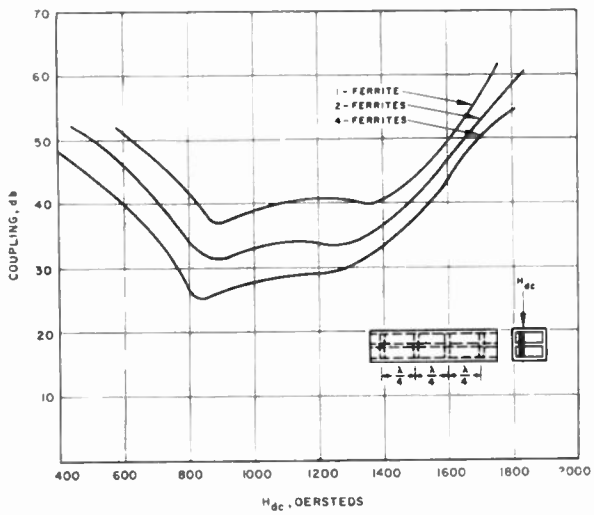

Fig. 11—Coupling vs H_{dc} for one, two, and four 0.060-inch diameter Ferroxcube 106 ferrite posts. Frequency, 9000 mc.

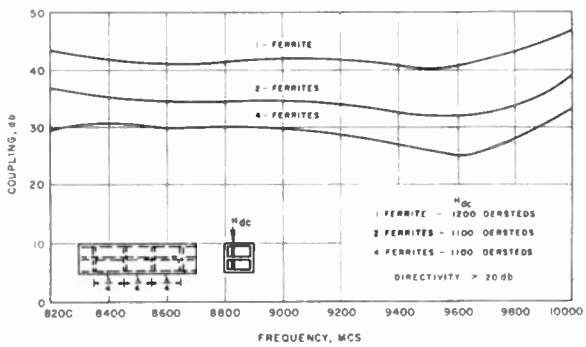

Fig. 12—Coupling vs frequency for one, two, and four 0.060-inch diameter Ferroxcube 106 ferrite posts.

providing a means for the reversal of the magnetic field. This was experimentally verified with the single R-1 ferrite post in the crossguide coupler. Bidirectional coupling is also realizable with a unidirectional magnetic field by locating two ferrite posts (see Fig. 15).

Standard microwave techniques were used for the measurement of coupling, directivity, insertion loss and

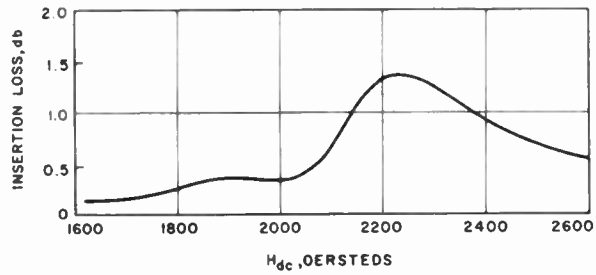

Fig. 13—Insertion loss vs H_{dc} for a single 0.61-inch diameter R-1 ferrite post.

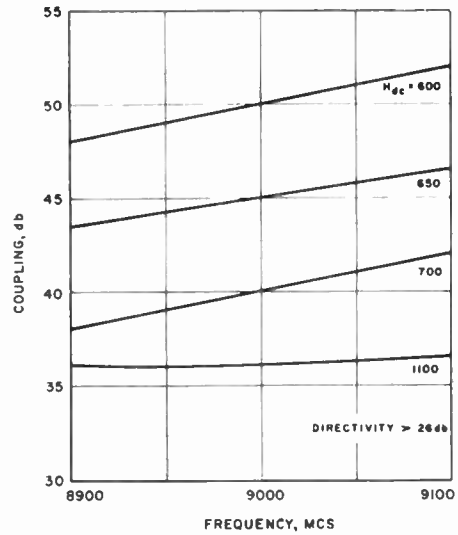

Fig. 14—Performance of electronically controlled coupler.

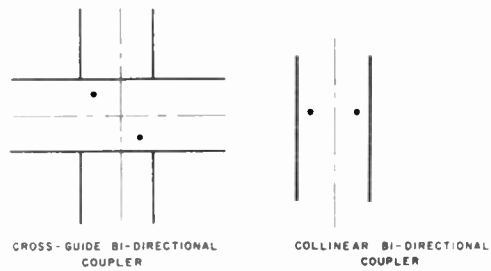

Fig. 15—Bidirectional couplers.

vswr. All but that of vswr are straight attenuation measurements. For coupling values up to 50 db a Hewlett-Packard 415B Standing Wave Indicator was used. Above 50 db and for the measurement of directivity a Vectron spectrum analyzer with 70 db sensitivity and two Hewlett-Packard No. 382A Precision Attenuators were used. In order to minimize load reflections, (vswr of 1.10 will introduce sufficient reflections to cause an intrinsically perfect coupler to have an effective directivity of 26.5 db) special precautions were taken to insure a vswr of less than 1.02 for all loads over the whole operating band. The accuracy of the coupling measurement involving the Hewlett-Packard 415B Standing Wave Indicator are ± 0.5 db, while the measurements employing the spectrum analyzer are accu-

rate to ±1.0 db. Directivity values requiring attenuation measurements above 70 db were not measured to any degree of accuracy and were recorded as minimum values. The insertion loss data are correct to within ±0.1 db and the vswr to within ±2 per cent.

Larger errors than those intrinsic to the measuring equipment were due to the fact that the dc magnetic fields could not be repeated with an accuracy better than ±5 per cent. The electromagnet was calibrated with a Dyna-Lab gaussmeter.

Conclusion

It should again be emphasized that the experimental data presented in this paper are not to be considered optimum design information for the ferrite directional coupler. The experimental results however did establish the practical feasibility of this device. Potential advantages over the conventional coupler include the possibilities of bidirectional coupling, electronic control of coupling, and extremely broad bandwidth. Further investigation is planned along the following lines: 1) optimizing the ferrite diameter to obtain the widest possible bandwidth, 2) extending the ferrite post only partially into the main waveguide, 3) the use of an array of ferrite posts with either a tapered magnetic field or appropriately spaced values of saturation magnetization for each element, such that for a given frequency only one ferrite in the array produces the primary coupling action.

Appendix

We shall treat first the problem of the scattering of the fundamental mode in a rectangular waveguide by a thin cylinder of ferrite as shown in Fig. 16. The cylinder will be assumed arbitrarily located, *i.e.*, not necessarily at a point of circular polarization.

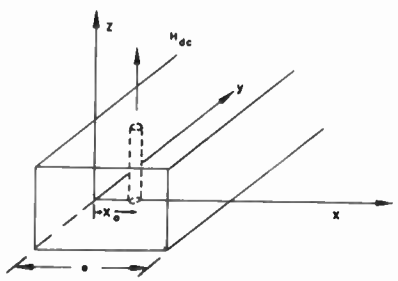

Fig. 16—A cylindrical ferrite post in a waveguide.

The general method of attack is well known and can be found in Morse and Feshbach.[2] Details will therefore be omitted. The electric field vector $\vec{E}$ at any point (x_0, y_0) within the waveguide satisfies

$$\nabla^2\vec{E} + k_0^2\vec{E} = j\omega\mu_0\vec{J}_e + \operatorname{curl}\vec{J}_m, \tag{3}$$

where $\vec{J}_e = j\omega\epsilon_0\chi_e\vec{E}$ is the electric current density, $\vec{J}_m = j\omega\mu_0\chi_m\vec{H}$ the magnetic current density and $k_0^2 = \omega^2\mu_0\epsilon_0$. Eq. (3) can be integrated with the help of the Green's dyadic G defined as follows:

$$\nabla^2\overleftrightarrow{G}(x_0, y_0; x, y) + k_0^2\overleftrightarrow{G}(x_0, y_0; x, y) = \overleftrightarrow{I}\delta(x - x_0)\delta(y - y_0), \tag{4}$$

$\overleftrightarrow{G}_{\text{tangential}} = 0$, $\operatorname{div}\overleftrightarrow{G} = 0$, at the walls of the waveguide. $\overleftrightarrow{I}$ is the idemfactor and δ is Dirac's delta function. Eqs. (3) and (4) can be combined in the manner indicated. The result, which takes into account the discontinuity of $\vec{J}_m$ at the surface of the ferrite post, is

$$\vec{E} = a_z \sin\frac{\pi x}{a}\exp(-j\gamma_1 y) + j\omega\mu_0\int\overleftrightarrow{G}(x_0, y_0; x, y)\cdot\vec{J}_e(x_0, y_0)\,dx_0\,dy_0 + \int\vec{J}_m(x_0, y_0)\cdot\operatorname{curl}\overleftrightarrow{G}(x_0, y_0; x, y)\,dx_0 dy_0, \tag{5}$$

where a_z is the unit vector in the z-direction and γ_1 the propagation constant of the fundamental mode. For the particular geometry at hand it suffices to write

$$\overleftrightarrow{G}(x_0, y_0; x, y) = \sum_n \overleftrightarrow{G}_n,$$

$$\overleftrightarrow{G}_n = a_z a_z (j/a\gamma_1)\sin\frac{n\pi x_0}{a}\sin\frac{n\pi x}{a}\exp(j\gamma_n|y - y_0|), \tag{6}$$

where

$$\gamma_n^2 = k_0^2 - (n\pi/a)^2.$$

The first term in (3) represents the incident wave assumed to propagate in the y direction. The integrals are over the cross section of the post and represent the field scattered by the electric and magnetic polarization currents in the ferrite post. The electric and magnetic polarization currents are not known since they depend on the unknown electric and magnetic fields within the ferrite. Reasonable approximations to the latter can be made however if the diameter of the post is sufficiently small as compared to the wavelength. The electric field can then be assumed equal to the field of the incident wave evaluated at the post. The computation of the internal magnetic field is a little more involved. We shall write down the result and refer the reader to the literature.[3]

$$\begin{aligned} H_x &= 2U^{-1}[(2 + \chi)B + j\kappa P], \\ H_y &= 2U^{-1}[(2 + \chi)P - j\kappa B], \\ U &= (2 + \chi)^2 - \kappa^2, \quad B = (\gamma_1/\omega\mu_0)\sin(\pi x_0/a), \\ P &= (\pi/j\omega\mu_0 a)\cos(\pi x_0/a). \end{aligned} \tag{7}$$

[2] P. M. Morse and H. Feshbach, "Methods of Theoretical Physics," McGraw-Hill Book Co., New York, N. Y., Chapter 13; 1953. See also, D. Saxon's notes on lectures by J. Schwinger, "Discontinuities in Waveguides," Section II, where the problem of the dielectric post in a rectangular waveguide is treated.

[3] See for example, A.D. Berk and B. A. Lengyel, "Magnetic fields in ferrite bodies," Proc. IRE, vol. 43, pp. 1587–1591, eq. (13); November, 1955.

Before substituting these expressions in (5) we observe that for large distances from the post ($|y-y_0| \gg$ wavelength of the fundamental mode) all G_n's vanish except G_1. Taking this fact into account and observing that for sufficiently small diameters of the post the integrals can be replaced by products of the integrands and the cross sectional area of the ferrite cylinder, $(\pi D^2/4)$, we obtain for the voltage reflection coefficient R,

$$\begin{aligned} R &= R_e + R_m, \\ R_e &= -j\frac{k_0^2\chi_e\pi D^2}{4a\gamma_1}\sin^2\frac{\pi x_0}{a}, \\ R_m &= j\frac{\pi D^2}{2a\gamma_1}\left[\gamma_1^2\sin^2\frac{\pi x_0}{a} - \left(\frac{\pi}{a}\right)^2\cos^2\frac{\pi x_0}{a}\right] \\ &\quad \cdot\frac{\chi(2+\chi)-\kappa^2}{(2+\chi)^2-\kappa^2}, \end{aligned} \tag{8}$$

and for the voltage transmission coefficient T,

$$T = 1 + S, \tag{9}$$

where

$$S = R_e + S_m, \tag{10}$$

with R_e already defined and

$$S_m = -j\frac{\pi D^2}{2a\gamma_1}\cdot\frac{[\chi(2+\chi)-\kappa^2]\left[\gamma_1^2\sin^2\frac{\pi x_0}{a} + \left(\frac{\pi}{a}\right)^2\cos^2\frac{\pi x_0}{a}\right] - 2\kappa\gamma_1\frac{\pi}{a}\sin\frac{2\pi x_0}{a}}{(2+\chi)^2-\kappa^2}. \tag{11}$$

The preceding expressions are valid regardless of the value of x_0 (the distance of the ferrite post from the waveguide wall). Note that the scattering produced by the dielectric property of the post is the same in the forward and backward directions. The magnetic property of the post, on the other hand, scatters the incident field unequally in the forward and in the backward directions. It is precisely this property that permits the realization of the ferrite directional coupler. Indeed all we have to do to obtain directional coupling is to extend the ferrite post shown in Fig. 16 beyond the wall of the guide into an auxiliary waveguide. The equivalent circuit of the impedance presented to the incident wave consists of a series inductance L and a shunt capacitor C where

$$\begin{aligned} C &= \frac{\epsilon_0\chi_e\pi D^2}{a}\sin^2\frac{\pi x_0}{a}, \\ L &= \frac{\mu_0\pi D^2}{a}\left[\sin^2\frac{\pi x_0}{a} - (\lambda_g/2a)^2\cos^2\frac{\pi x_0}{a}\right]\frac{\chi(2+\chi)-\kappa^2}{(2+\chi)^2-\kappa^2}. \end{aligned}$$

Note that the inductance L can be positive, zero, or negative depending on the location of the ferrite post x_0, on the guide wavelength λ_g, and on the values of χ and κ. The two latter parameters are governed by the strength of the dc magnetic field.

In the special case when the post is situated at the point of circular polarization of the rf magnetic field, we have $x_0 = d_0$,

$$\tan(\pi d_0/a) = (\pi/a\gamma_1), \tag{12}$$

and therefore $R_m = 0$, $L = 0$ and

$$S_m = -j\frac{\pi D^2}{a\gamma_1}\left(\frac{\pi}{a}\right)^2\cos^2\frac{\pi d_0}{a}\cdot\frac{\chi-\kappa}{\chi-\kappa+2}. \tag{13}$$

To obtain an expression for the forward coupling of the directional coupler we multiply R_e and S_m by empirical factors Q_e and Q_m, respectively, and substitute in the expression:

$$\text{Coupling} = -20\log|Q_eR_e + Q_mS_m|. \tag{14}$$

These empirical factors are a measure of the extent to which the electric and magnetic polarization currents penetrate into the portion of the post extending into the auxiliary waveguide. Similarly for the directivity we obtain,

$$\text{Directivity} = 20\log\frac{Q_eR_e + Q_mS_m}{Q_eR_e + Q_mS_m^+}, \tag{15}$$

where S_m^+ equals S_m except with the sign of κ reversed.

This reversal of sign corresponds to reversing the direction of propagation of the incident wave in the main waveguide. The factor $(\chi-\kappa)/(\chi-\kappa+2)$ appearing in S_m varies with H_{dc} and resonates at the expected value[4] $H_{dc} = (\omega/\gamma) - 2\pi M_s$ as it can be shown by substituting Polder's expression for χ and κ:

$$\chi = 4\pi M_s\gamma^2H_{dc}/\Delta, \quad \kappa = 4\pi M_s\gamma\omega/\Delta, \quad \Delta = \gamma^2H_{dc}^2 - \omega^2.$$

Experiments indicated that R_eQ_e can be neglected in comparison to both Q_mS_m and $Q_mS_m^+$, except when H_{dc} is far removed from ferromagnetic resonance. Hence the expressions for coupling and directivity reduce to

$$\begin{aligned} \text{Coupling} &= -20\log(Q_mS_m), \\ \text{Directivity} &= 20\log(S_m/S_m^+). \end{aligned} \tag{16}$$

Eqs. (1) and (2) of the text were obtained from the two preceding expressions by assuming that the post is situated at a point of circular polarization of the rf magnetic field.

ACKNOWLEDGMENT

The authors are indebted to B. Mills for making most of the measurements.

[4] C. Kittel, "On the theory of ferromagnetic resonance absorption," *Phys. Rev.*, vol. 73, pp. 155–161; January, 1948.

Ferrite-Tuned Resonant Cavities*

CLIFFORD E. FAY†, FELLOW, IRE

Summary—**The case of a dominant-mode rectangular cavity with a slab of ferrite against one side wall is treated. Use is made of the change in effective rf permeability of the ferrite in response to changes in the applied static magnetic field. Experimental results on an *X*-band cavity show a 10 per cent tuning range with an unloaded *Q* of 1,000 or more at 9,000 megacycles. Calculation of the *Q* of the cavity from the loss tangents of the ferrite material is outlined.**

Introduction

THE nonreciprocal properties of ferrites at microwave frequencies have made possible many useful devices such as gyrators, circulators, isolators, and modulators. The reciprocal properties are also useful and one of the important applications is the tuning of cavities in response to an applied magnetic field. Cacheris, Jones, and Van Wolfe[1] have reported obtaining a tuning range of 160 megacycles in an *X*-band cavity. With a somewhat different approach described in the following discussion, a considerably greater tuning range has been obtained.

The problem treated in this paper is the simple case of a rectangular dominant-mode cavity containing a slab of ferrite against one end wall. The magnetic field is applied to the ferrite in a direction parallel to that of the electric field vector in the cavity. Use is made of the change in effective permeability of the ferrite for a wave traveling in a direction perpendicular to that in which it is magnetized. The treatment of the problem is only approximate in that the exact field configurations in the ferrite are not developed. The wave is assumed to be traveling in a direction normal to the broad face of the ferrite, that is, the ferrite is assumed to be in one "end" of the cavity.

Theoretical Considerations

Since use is being made of the magnetic properties of the ferrite, it seems logical that the material be placed in the position of highest magnetic field in the cavity, *i.e.*, along the side walls. Also, since the ferrite has some dielectric loss it seems desirable to keep it in a position of minimum electric field which is also along the side walls. The effective permeability of the ferrite is given by the relation

$$\mu_e = \frac{\mu'^2 - k'^2}{\mu'} \tag{1}$$

where μ' and k' are the components of the Polder tensor which describes the permeability of the ferrite. μ_e here is the effective rf permeability for a plane wave propagating in a direction perpendicular to the direction of magnetization of the ferrite.[2] The use of the plane wave concept seems reasonable since dominant-mode propagation in a rectangular waveguide can be thought of as consisting of a plane wave propagating diagonally and being reflected from the side-walls.

When the applied magnetic field is zero, μ_e is nearly 1 (cgs units). The combination of the internal fields arising from anisotropy and from demagnetizing effects due to the shape of the crystallities and/or domains within the material will result in μ_e being somewhat less than unity. Fig. 1 shows a plot of the permeability components of a representative ferrite as functions of the applied magnetic field. As the applied field increases, μ_e decreases and a point may be reached where $\mu_e = 0$, $(\mu'^2 = k'^2)$. Here the intrinsic impedance of the ferrite, $\sqrt{\mu_e/\epsilon}$, becomes zero and the effect on the cavity resonance is the same as if the metallic wall had been moved to the inside edge of the ferrite. As the applied field is further increased, μ_e can become negative but in this region the magnetic losses in the material are increasing rapidly as the condition of gyromagnetic resonance is approached. It will be seen that beyond gyromagnetic resonance there is a region where μ_e changes rapidly

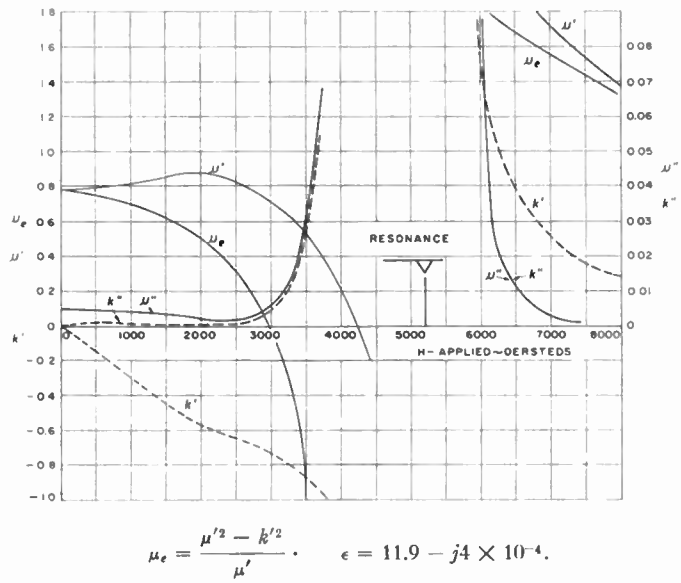

$$\mu_e = \frac{\mu'^2 - k'^2}{\mu'}. \qquad \epsilon = 11.9 - j4 \times 10^{-4}.$$

Fig. 1—Permeability components of Ferramic *R1* measured on a thin disk sample at 9,000 megacycles. μ' and k' are permeabilities. μ'' and k'' are loss components.

* Original manuscript received by the IRE, July 3, 1956.
† Bell Telephone Labs., Inc., Murray Hill, N.J.
[1] J. Cacheris, G. Jones, and R. Van Wolfe, "Topics in the Microwave Application of Ferrites," Diamond Ordnance Fuze Labs., Rep. No. TR-188; July 28, 1955.

[2] H. Suhl and L. R. Walker, "Topics in guided wave propagation, through gyromagnetic media," *Bell Sys. Tech. J.*, vol. 33, pp. 939–986; July, 1954.

with applied field, but this is still too near resonance to be attractive because of the loss situation. Therefore the low field region appears to be most attractive for tuning purposes from both the loss and required field standpoint.

In Fig. 2, a rectangular cavity is illustrated which has dimensions a, b, l. A slab of ferrite of dimensions a, b, l_2 is placed against one wall of the cavity. We assume the cavity is excited in the dominant mode, TE_{101}, with the E vector parallel to the b dimension.

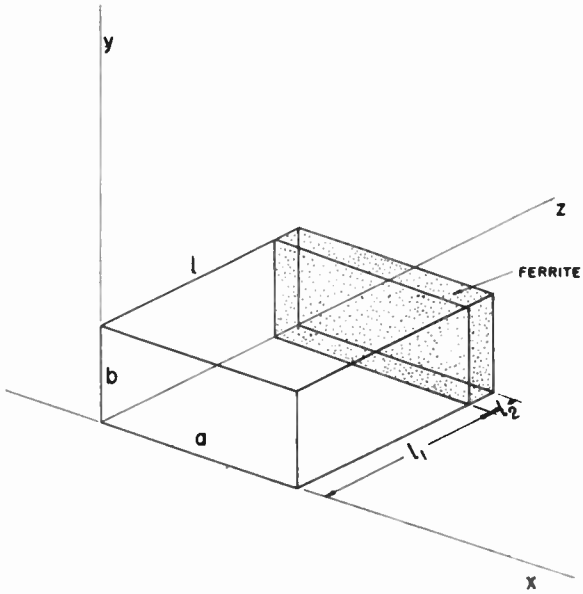

Fig. 2—Rectangular dominant-mode cavity containing a ferrite slab.

We may consider the cavity to be a piece of waveguide short-circuited at both ends. If the cavity is resonant at the assumed frequency of operation, the reactance at the ferrite-air boundary looking into the air section must equal the negative of the reactance seen at the same point looking into the ferrite-filled section. From transmission line equations we then obtain relation

$$\text{Tan } \beta_1 l_1 = -\sqrt{\frac{\mu_e}{\epsilon}}\,\frac{K_1}{K_2}\,\text{Tan } \beta_2 l_2 \qquad (2)$$

where:

μ_e = effective permeability of the ferrite

ϵ = dielectric constant of the ferrite

$\beta_1 = \dfrac{2\pi}{\lambda_g} = \dfrac{2\pi K_1}{\lambda_0}$ for the air region

$\beta_2 = \dfrac{2\pi K_2 \sqrt{\mu_e \epsilon}}{\lambda_0}$ for the ferrite region

$K_1 = \sqrt{1 - \dfrac{(\lambda_0)^2}{(2a)^2}}$

$K_2 = \sqrt{1 - \dfrac{(\lambda_0)^2}{(2a\sqrt{\mu_e \epsilon})^2}}$

λ_0 = free space wavelength.

Eq. (2) above is based on the assumption that the ferrite is an isotropic medium having permeability μ_e and dielectric constant ϵ. It is a transcendental equation which can be solved numerically by assuming values for μ_e, ϵ, λ_0, and a length. The point $\mu_e = 0$ is a good one to choose for the high frequency point. There l_1 is merely $\lambda_g/2$ for this frequency. l_2 can then be determined by assuming a value for μ_e at the low frequency. This value of μ_e will be somewhere between the value for no applied field and the value for maximum μ' in a curve similar to Fig. 1 for the material used.

Experimental Results

Data on a ferrite-tuned cavity obtained experimentally are shown in Fig. 3, where we have plotted frequency of resonance and unloaded Q of the cavity as functions of magnetic field applied in the y direction of Fig. 2. The cavity used was a section of X-band waveguide 0.4 inch × 0.9 inch having an effective length of 0.95 inch. It was coupled to the exciting waveguide by means of a circular iris in one end wall. The resonance frequency of this cavity with no ferrite in it was 9,025 megacycles and its unloaded Q, 4,400. The piece of ferrite inserted against one end wall was 0.395 inch × 0.895 inch × 0.101 inch. The point $\mu_e = 0$ indicated on the curve is merely that frequency for which $l_1 = \lambda_g/2$. At the low frequency point, where no external field is applied, the μ_e was calculated to be 0.77.

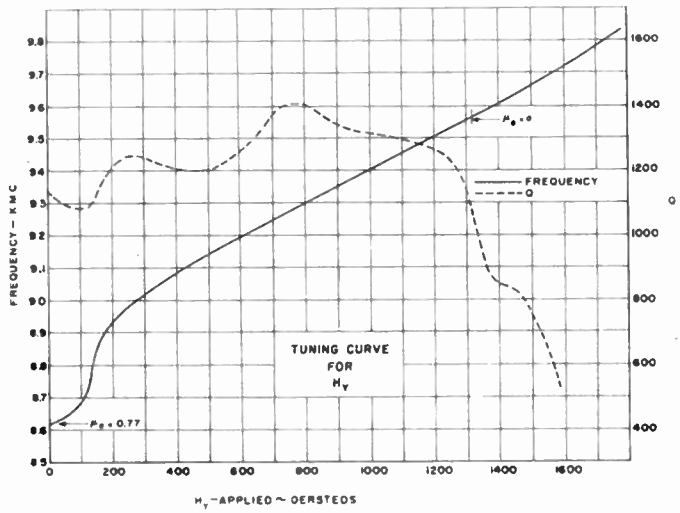

Fig. 3—Tuning curve of cavity. Frequency and unloaded Q are given as functions of magnetic field applied in the y direction of Fig. 2.

It was found that if a field was applied to the ferrite in the x direction, the frequency of resonance decreased. The principal rf field in the ferrite as positioned in Fig. 2, is h_x which is a maximum at the wall of the cavity. When a dc field is applied along the x direction it tends to line up the electron spins in this direction. When all the spins are so aligned or in other words when the material is saturated, then the effective μ in the x direction is μ_0 or 1. However there is also an h_z component

in the ferrite and when the material is saturated in the x direction, h_z fields will produce a precession of the spins and the μ effective for h_z components will be less than unity so the over-all effective μ of the ferrite can never be equal to unity for magnetization in the x direction. Fig. 4 shows the tuning effect of a field applied in the x direction. Here we see that applying a field in the x direction decreases the frequency of resonance at first, a minimum is reached and then the frequency increases with applied field. Before much increase in frequency is obtained however the losses have increased greatly as indicated by the drop in Q. The effective μ corresponding to the minimum frequency was calculated to be approximately 0.9 from (2).

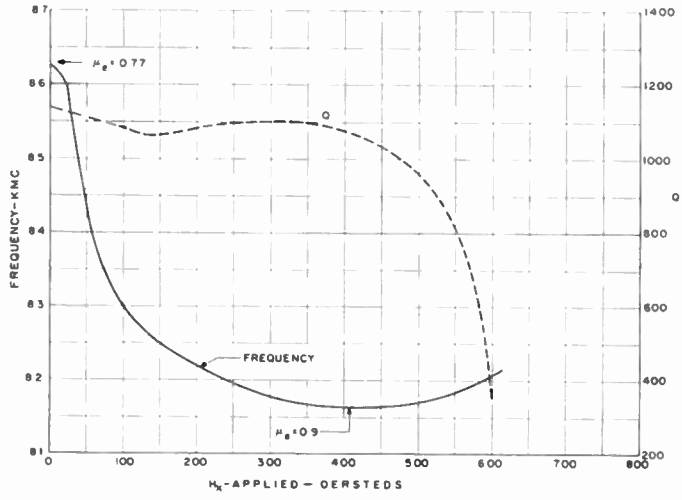

Fig. 4—Tuning curve of cavity. Frequency and unloaded Q are given as functions of magnetic field applied in the x direction of Fig. 2.

The use of thicker slabs of ferrite results in increased tuning range with a corresponding decrease in Q. However if the ferrite slab exceeds about 12 per cent of the cavity length it was found that other resonances occur at points in the tuning range. These have not been investigated.

Calculation of Q

It would be useful to be able to calculate what the approximate Q of the cavity would be if various ferrite materials were used for tuning. If data similar to those of Fig. 1 were available for each material, a simplified calculation of Q for the condition $\mu_e=0$ could be made. At this condition, from (1), $|\mu'|=|k'|$, the intrinsic impedance of the ferrite medium, $\sqrt{\mu_e/\epsilon}$ is zero and no E field can exist in the ferrite. As previously pointed out, this is equivalent to moving the metallic wall of the cavity to the surface of the ferrite insofar as the effect on tuning is concerned. This also represents a point near the high frequency end of the useful tuning range since losses are increasing rapidly beyond this point in most cases. At this point the tangential h field, h_z, has its maximum value at the surface of the ferrite. Since the ferrite is a good insulator, practically no conduction current is flowing on the surface of the ferrite at the ferrite-air boundary so tangential h must be continuous across the boundary.

Maxwell's equations give us Curl $E=-(\partial b/\partial t)$. If $E=0$ in the ferrite, then $\partial b/\partial t=0$, and this is possible only if $b=0$ inside the ferrite. From Polder's relations we have

$$\left.\begin{aligned} b_x &= \mu' h_x - jk' h_z \\ b_z &= \mu' h_z + jk' h_x \end{aligned}\right\} H_{dc} \text{ applied in the } y \text{ direction.} \quad (3)$$

Thus if $b_x=b_z=0$ in the ferrite, $\mu' h_x=jk' h_z$, $\mu' h_z=-jk' h_x$, but $|\mu'|=|k'|$ and hence $h_x=h_z$ but they are apart 90° in phase. For the simplified calculation we will assume that h_x (and hence h_z) varies sinusoidally with x and has no variation with z. This can be shown to be a reasonably accurate assumption where the thickness of the ferrite slab is small compared to the length of the cavity.

The magnetic energy in the ferrite is then

$$U_{HF}=\tfrac{1}{2}\int_{\text{ferrite}} \mu' h_x \cdot h_x^* dv. \quad (4)$$

In terms of H_x, the maximum value of h_x, we have

$$U_{HF}=\frac{\mu' H_x^2}{2}\int_0^a\int_0^b\int_0^{l_2} \sin^2\frac{\pi x}{a}\,dx\,dy\,dz. \quad (5)$$

H_x is related to E_0, the maximum electric field in the cavity by

$$H_x=\frac{\lambda_0}{2l_1}E_0=K_1E_0.$$

Making this substitution and integrating we get

$$U_{HF}=\frac{\mu' E_0^2 K_1^2 abl_2}{4}. \quad (6)$$

The energy stored in the air portion of the cavity is

$$U_{EA}=\frac{E_0^2 abl_1}{8}=U_{HA}. \quad (7)$$

Then the total energy stored in the cavity is

$$U_T=U_{HF}+U_{HA}=E_0^2 ab\left(\frac{\mu' K_1^2 l^2}{4}+\frac{l_1}{8}\right). \quad (8)$$

From the data of Fig. 1, the magnetic loss tangents, μ''/μ' and k''/k' can be found for the point $\mu_e=0$. These are equivalent to $1/Q$ of the material where

$$\frac{1}{Q}=\frac{\text{power lost}}{\omega\cdot\text{energy stored}}.$$

We may assume that half of the time the magnetic energy in the ferrite is due to k' and half of the time to μ' so that if $\mu'' \neq k''$ we can write for the power lost in the ferrite

$$W_F = \frac{\omega E_0^2 K_1^2 abl_2(k'' + \mu'')}{4} \tag{9}$$

and the Q of the cavity would be

$$Q_c = \frac{\omega U_T}{W_F} = \frac{\mu' K_1^2 l_2 + \frac{l_1}{2}}{K_1^2 l_2(\mu'' + k'')} \tag{10}$$

assuming all losses are in the ferrite. If it is necessary to include ohmic losses in the walls, it should be sufficiently accurate to measure or calculate the Q_0 of the cavity before adding ferrite, whence

$$\frac{1}{Q_c'} = \frac{1}{Q_0} + \frac{W_F}{\omega U_T}. \tag{11}$$

The value of Q_c' at $\mu_s = 0$ from the data of Fig. 1, calculated by the method outlined above is 720. The measured value is 1,060.

Conclusion

The tuning of a ferrite-loaded cavity over a 10 per cent frequency band at 9,000 megacycles and at low power levels has been accomplished using a typical ferrite. Unloaded Q of the order of 1,000 was obtained. This may be improved if less lossy ferrites are made available. A simple theory has been developed which predicts the results obtained with reasonable accuracy.

Ferrite-Tunable Microwave Cavities and the Introduction of a New Reflectionless, Tunable Microwave Filter*

CONRAD E. NELSON†, ASSOCIATE MEMBER, IRE

Summary—**Large ferrite samples are placed in microwave cavities with the object of achieving tunable microwave cavities. Experimental data, at *X* band frequencies, on ferrite tuning of conventional band-pass and band elimination cavities are presented. Curves of applied dc magnetic field vs cavity resonant frequency, bandwidth, loss, cavity *Q*, and window coupling coefficients are included.**

Of particular interest are the results obtained with a new type cavity filter. With a single circularly polarized cavity, a *reflectionless* filter is achieved which couples nearly 100 per cent of the energy from the main waveguide at the cavity resonant frequency. Experimental results, on the ferrite loading of these circularly polarized cavities, are presented, and a number of practical microwave applications are discussed.

Introduction

MANY USEFUL microwave devices, such as isolators, switches, and gyrators, have been built using ferrites in waveguide systems. The properties of these ferrites have usually been determined by placing small ferrite samples in a microwave cavity and then measuring the change in the cavity loss and resonant frequency. If large pieces of ferrite are placed in cavities, the application of a dc magnetic field to the ferrite will cause an appreciable shift in cavity resonant frequency. Hence, ferrite-loaded cavities may be tuned electronically. This method of tuning opens a new field in the application of ferrites at microwave frequencies. The new microwave components which will be made available are 1) tunable band-pass and band elimination filters, and 2) reflectionless, nonreciprocal, tunable filters. One of the latter components may be used as a passive duplexer for a single frequency radar. Very little data have been published on ferrite tunable filters.[1] It is the purpose of this paper to present experimental data on the ferrite tuning of conventional band-pass and band elimination cavities and to present information on a new reflectionless, nonreciprocal, tunable filter.

For the past several years, many articles have been published which present theoretical and experimental information on the tensor properties of the magnetic permeability of ferrites in the microwave region.[2,3] Several articles have appeared which present information on the cavity technique of measuring the complex

* Original manuscript received by the IRE, July 3, 1956.
† Research Labs., Hughes Aircraft Co., Culver City, Calif.

[1] J. C. Cacheris and G. Jones, "Magnetic tuning of klystron cavities," PROC. IRE, vol. 43, p. 1017; August, 1955.
[2] D. Ponder, "On the theory of ferromagnetic resonance," *Phil. Mag.*, vol. 40, pp. 99–115; January, 1949.
[3] C. L. Hogan, "The ferromagnetic Faraday effect at microwave frequencies and its applications—the microwave gyrator," *Bell Sys. Tech. J.*, vol. 31, pp. 1–31; January, 1952.

permeability of ferrites.[4,5] Usually, the ferrite is placed in a region of linear polarized magnetic field in the cavity. Then the complex ferrite permeability will be found in rectangular coordinates. Recently ferrites have been placed in a circularly polarized magnetic field in the cavity, and the complex positive and negative circularly polarized permeabilities have been found.[6,7] The ratio of ferrite volume to cavity volume for these permeability measurements is near 0.005 per cent. However, when the ferrite is used to tune the cavity for filter purposes, the ratio of ferrite volume to cavity volume is near 0.5 per cent.

Ferrite-Loaded Conventional Band-Pass Cavities

In general, there are three main considerations in ferrite loading a cavity. The first consideration is that the ferrite be placed in a high rf magnetic field in the cavity. A band-pass filter, using the circularly cylindrical TE_{111} cavity mode, is illustrated in Fig. 1(a). The ferrite is in the shape of a disk and is placed in the position of maximum cavity magnetic field. A thin rectangular-shaped ferrite would do just as well. The second factor to consider is that for a given applied dc magnetic field it would be desirable to have a high internal field in the ferrite. Fig. 1(a) illustrates two possible orientations of applied dc field. For a dc field applied in the No. 1 direction, the ferrite internal magnetic field intensity is much greater than for the No. 2 orientation of field. Therefore, the former orientation of dc applied magnetic field will have the greater effect on the ferrite rf permeability and cause greater resonant frequency shifts. The rf cavity fields at the ferrite are normal to the dc applied field. In these conventional cavity filters the cavity rf magnetic fields are linearly polarized. Therefore, if the applied dc magnetic fields are reversed, the same magnitude and direction of frequency shift should result. The third consideration is that the ferrite should be placed in the cavity to produce a minimum loss without greatly reducing the frequency shift. Further investigation is being made on this last point.

A series of experimental curves are shown in Fig. 1(b) for the TE_{111} cavity mode band-pass filter. The X band cavity resonant frequency is varied 150 mc with an applied field of 750 oersteds. The larger pieces of ferrite cause large frequency shifts and greater losses. Without a ferrite, cavity loss is 1.25 db and bandwidth is 5.9 mc. The filter bandwidth, with different ferrites, is reasonably constant. These curves are intended only to give general information on the subject since further development is required to produce the optimum cavity mode, cavity dimensions, and ferrite shape and position.

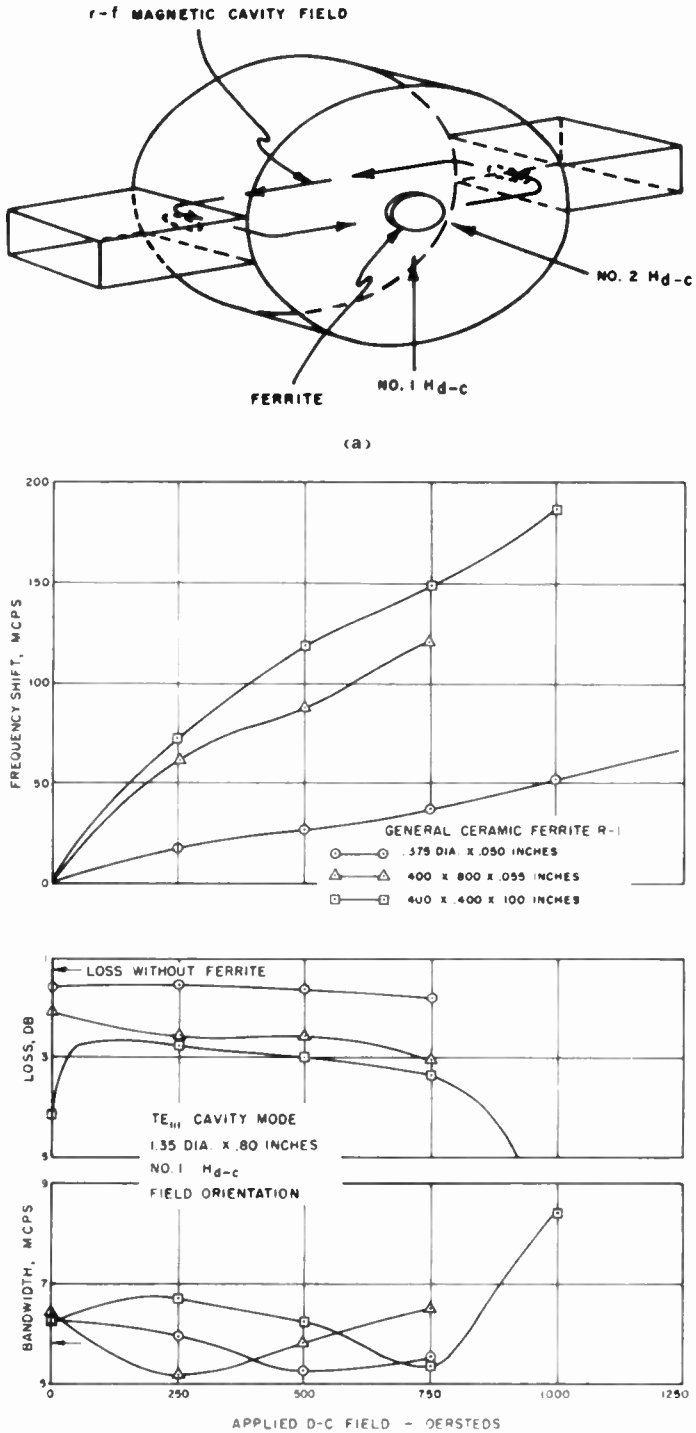

Fig. 1—(a) Ferrite-loaded band-pass filter, TE_{111} cavity mode. (b) Experimental data, ferrite-loaded band-pass filter, TE_{111} cavity mode.

Fig. 2(a) shows a lower loss band-pass filter using the circularly cylindrical TE_{011} cavity mode. The cavity size

[4] A. D. Berk and B. Lax, "Cavities with complex media," 1953 IRE Convention Record, part 10, pp. 65–73.

[5] A. D. Berk and B. A. Lengyel, "Magnetic fields in small ferrite bodies with applications to microwave cavities containing such bodies," Proc. IRE, vol. 43, pp. 1587–1591; November, 1955.

[6] E. G. Spencer, R. C. LeCraw, and F. Reggia, "Measurement of microwave dielectric constants and tensor permeabilities of ferrite spheres," 1955 IRE Convention Record, part 8, pp. 113–121.

[7] Other circularly polarized cavity techniques have been developed at the Gen. Elec. Co., Electronics Div., Syracuse, N.Y. (Internal Reports).

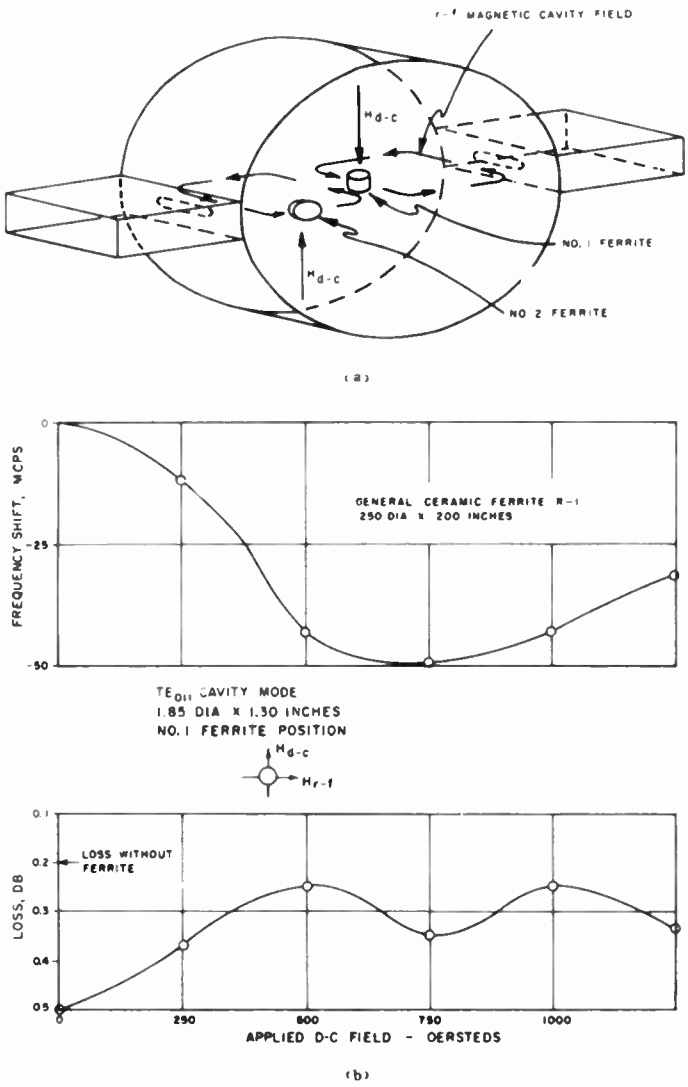

Fig. 2—(a) Ferrite-loaded band-pass filter, TE_{011} cavity mode. (b) Experimental data, ferrite-loaded band-pass filter, TE_{011} cavity mode.

is larger but this mode has a very low cavity wall loss. Ferrites could either be placed in the center of cavity (No. 1 position) or against cavity wall (No. 2 position). Without a ferrite, the filter has a 0.2-db loss and a 16–20-mc bandwidth. The large bandwidth also helps in reducing loss. A small ferrite in position No. 1 caused a −50 mc frequency shift at 750 oersteds [Fig. 2(b)]. The added ferrite loss is low. Larger pieces of ferrite in the cavity caused a dual mode effect which might be due to the TM_{111} cavity mode, that has the same resonant frequency as the TE_{011} mode. The coupling slots do not couple to the TM_{111} mode but the ferrite could, especially if the ferrite were in position No. 2.

Ferrites in a Conventional Band Elimination Cavity

A rectangular TE_{101} cavity mode is used as a side wall coupled band elimination filter. [See Fig. 3(a) on the next page.] The cavity is elongated to produce a high concentration of cavity rf magnetic fields near the ferrite. The cavity rf magnetic fields near the coupling slot are low, due to the elongated cavity, which produces only a small amount of coupling to the waveguide. At the cavity resonant frequency, the cavity reflects the input energy and causes a null in the output power. The magnitude of the output null at resonance is dependent upon the cavity-waveguide coupling and the cavity Q or cavity losses.

Fig. 3(b) illustrates the effect of various size ferrites. Frequency shifts greater than 200 mc are attainable. The 3-db output power bandwidths vary slightly. The output power null is small, but this fact is not discouraging because the null without a ferrite is only −11.5 db. The null can be increased by increasing the window size, which also increases the bandwidth. The increased cavity loss due to the ferrite loss reduces the null. This added ferrite loss can be seen more clearly from a curve of cavity loss or cavity Q, Q_c. The measured quantities are bandwidth or loaded Q, Q_L, and the output power null, "n." The theoretical relationships between the measured quantities and the cavity Q and window coupling factor, Q_w are

$$Q_c = Q_L \sqrt{\frac{1}{n} - 2}$$

$$Q_w = \frac{Q_L}{2} \frac{\sqrt{1-2n}}{1-\sqrt{n}}$$

where

$$n = \frac{P_{out}}{P_{inc}} \text{ at resonant frequency}$$

$$Q_L = \frac{f_0}{BW}.$$

The reciprocal of Q_w is a measure of the coupling to the cavity. A low value of Q_w indicates large coupling and a large bandwidth. Fig. 3(c) illustrates this window coupling factor. The resulting curve of cavity Q illustrates the increased ferrite losses over the cavity wall losses. For this cavity mode, the wall losses are high. The ferrite losses can arbitrarily be separated from the wall losses by assuming the wall losses are the same as those without the ferrite. Since the cavity Q is 7620 without the ferrite, then the so-called ferrite Q is

$$\frac{1}{Q_f} = \frac{1}{7620} - \frac{1}{Q_c}.$$

Fig. 3(c) illustrates that the ferrite Q is reasonably high and the reason the curves of Q_c are so low is due to the combination of wall and ferrite losses. If a different cavity mode were used, with lower wall losses, the resulting total cavity losses might be acceptable.

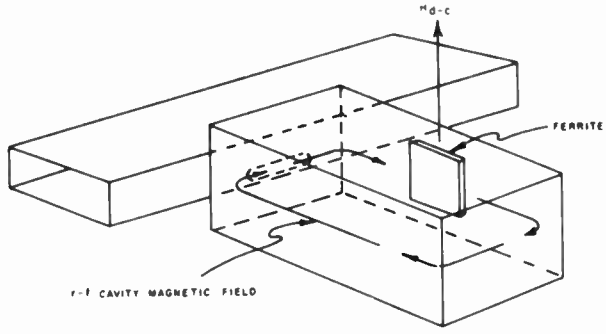

(a)

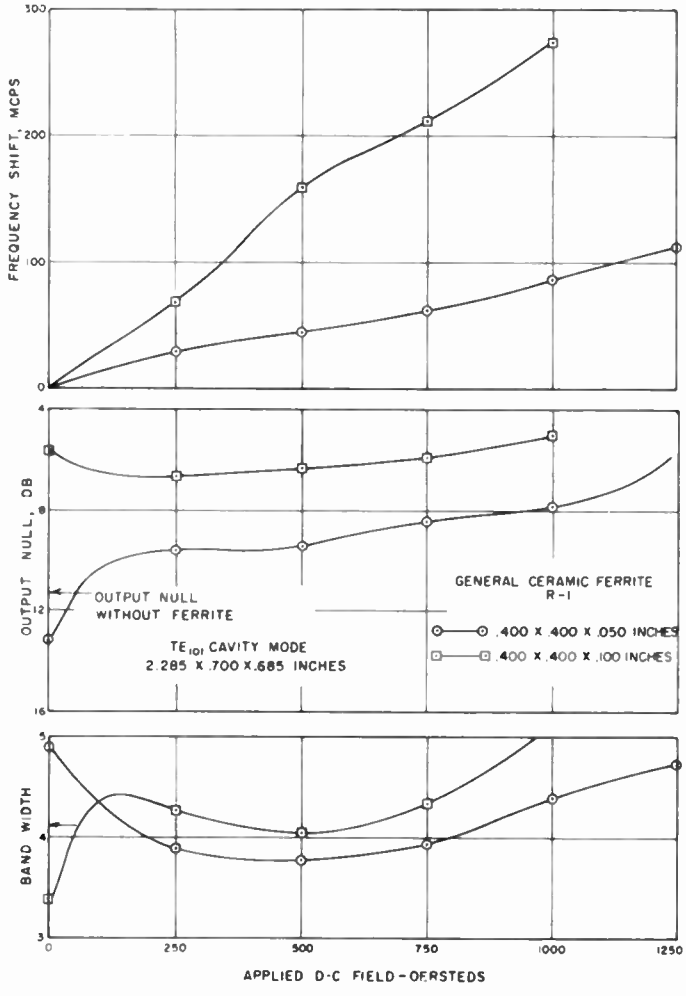

(b)

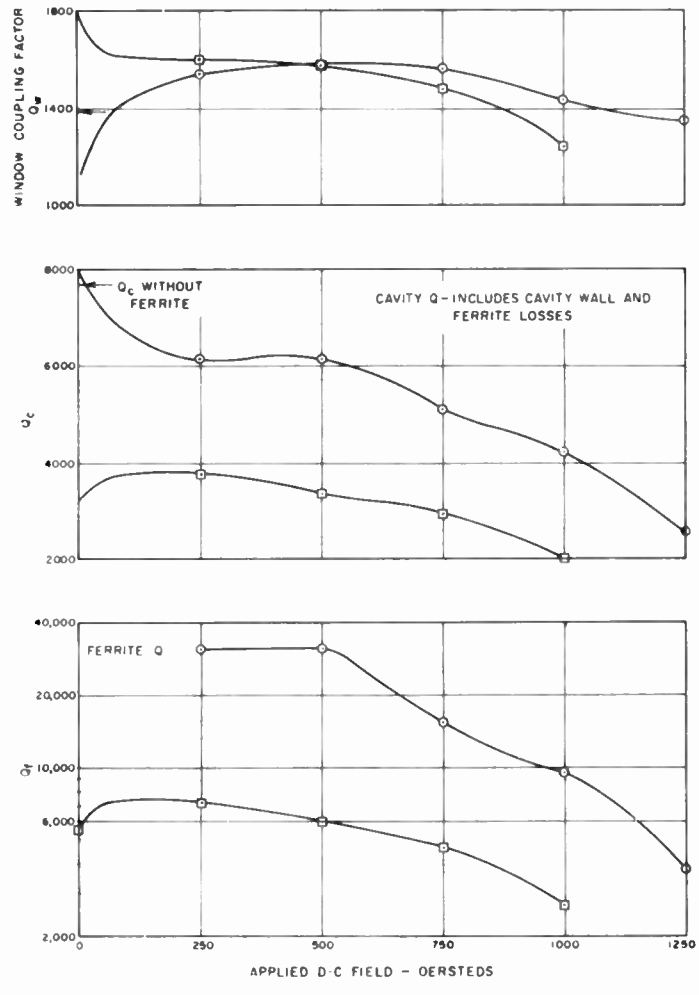

(c)

Fig. 3—(a) Ferrite-loaded band elimination filter, TE_{101} cavity mode, (b) Experimental data, ferrite-loaded band elimination filter, and (c) TE_{101} cavity mode.

A New Reflectionless, Tunable Microwave Filter

A new type of cavity filter has been utilized which is reflectionless and will couple nearly 100 per cent of the energy from the main waveguide. Only one cavity is used. The filter uses a circularly polarized cavity mode, and the addition of a ferrite results in a reflectionless, nonreciprocal, tunable filter. Fig. 4 illustrates this cavity, waveguide, and ferrite arrangement. The filter has four waveguide ports and only one cavity. The cavity is designed to operate with two orthogonal, degenerate, TE_{112} modes. Two circular coupling holes

are centered at each end of the cavity but are offset from the waveguide centerline. Fig. 4(b) shows the cavity rf magnetic fields. These cavity rf magnetic fields are coupled to the waveguide transverse (H_x) and longitudinal (H_z) magnetic fields. The circular coupling holes are placed in the waveguides at the point of circular polarization of the waveguide magnetic fields.

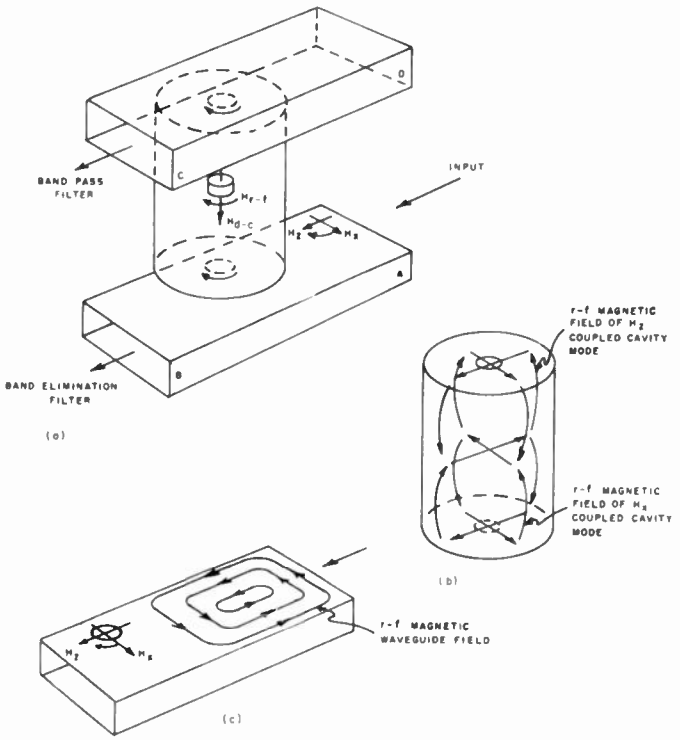

Fig. 4—Ferrite-loaded, circularly polarized microwave filter, TE_{112} cavity mode. (a) Cavity-waveguide configuration. (b) Two orthogonal TE_{112} cavity modes. (c) Rectangular waveguide, TE_{10} mode.

The operation of the filter is described as follows: energy enters the waveguide at port A and excites the cavity in a circularly polarized TE_{112} mode. The excited cavity radiates into waveguides A-B and C-D. However, due to the direction of circulation of the cavity modes, the cavity will radiate only toward waveguide ports B and C. Therefore, with an input signal at port A, there will not be any reflection back to port A, and the output energy will divide between ports B and C.

The fact that the filter is reflectionless is important, but a more important characteristic is that nearly 100 per cent of the energy entering port A can be coupled into arm C at the cavity resonant frequency (neglecting cavity wall losses). Normally a single mode cavity must divide the input energy with the load in arm B since the two are in series. However, with the dual mode cavity, each cavity mode couples out one half of the incident energy which produces a null in arm B. A more detailed analysis will be given at a later date since this subject is beyond the scope of this study. Off resonance, the cavity will not couple to the waveguide, and all the energy entering port A will leave port B. The result is a single cavity, reflectionless filter which is band elimination between ports A-B and band-pass between ports A-C. For maximum power transfer between ports A and C, the two coupling holes should be made the same size. However, due to the cavity wall losses, the maximum isolation between ports A and B at resonance is achieved if the coupling hole in arm C-D is slightly smaller than the coupling hole in the main waveguide. Two small cavity mode tuning screws are required to adjust both modes to the same resonant frequency and to produce a minimum reflection back to port A.

This circularly polarized microwave filter can be made tunable and nonreciprocal by inserting a ferrite in the cavity at the position of circularly polarized rf magnetic field, as illustrated in Fig. 4. A dc magnetic field is applied perpendicular to the two rf magnetic fields. Energy entering port A will see a shift in resonant frequency since the dc magnetic field causes a change in rf permeability of the ferrite. However, energy entering port B will see a shift in resonant frequency in the opposite direction because the direction of rotation of cavity magnetic field has been reversed. This nonreciprocal filter can be used as a passive duplexer for a single frequency radar. For example, if the radar operating frequency is 9000 mc, then design the cavity, with a permanent magnet and ferrite, to have a resonant frequency of 9000 mc from port A to B and 8800 mc from port B to A. The transmitter, antenna, and receiver are attached to arms B, A, and C respectively. When transmitting from arm B at 9000 mc, the cavity is off resonance, and all the energy reaches the antenna in arm A without loss. Target reflections entering arm A will be completely coupled to the receiver in arm C since the cavity is resonant in this direction of propagation at 9000 mc. The system acts as a duplexer and band-pass filter. The only loss in the system is in the receive channel. There is high isolation between the transmitter and the receiver due to a cavity 200 mc off resonance and the added directivity between ports B and C. The duplexer will operate at high power since only the low power echo signal travels through the cavity.

Experimental curves of resonant frequency shift, insertion loss between A-C, bandwidth between A-C, and isolation between A-B at resonance are given in Fig. 5(a) and Fig. 5(b) for the ferrite-loaded reflectionless filter illustrated in Fig. 4. The smaller ferrite causes an added loss of about 0.7 db. The coupling hole in waveguide A-B is 0.360-inch diameter, and the other coupling hole is 0.350 inch. Without a ferrite, the filter has a 30-db isolation between arms A-B at resonance. The difference in hole sizes is not optimum for maximum isolation. The smaller ferrite produces at 21 and 24-db isolation between arms A-B depending upon the direction of applied dc field. These isolations are reason-

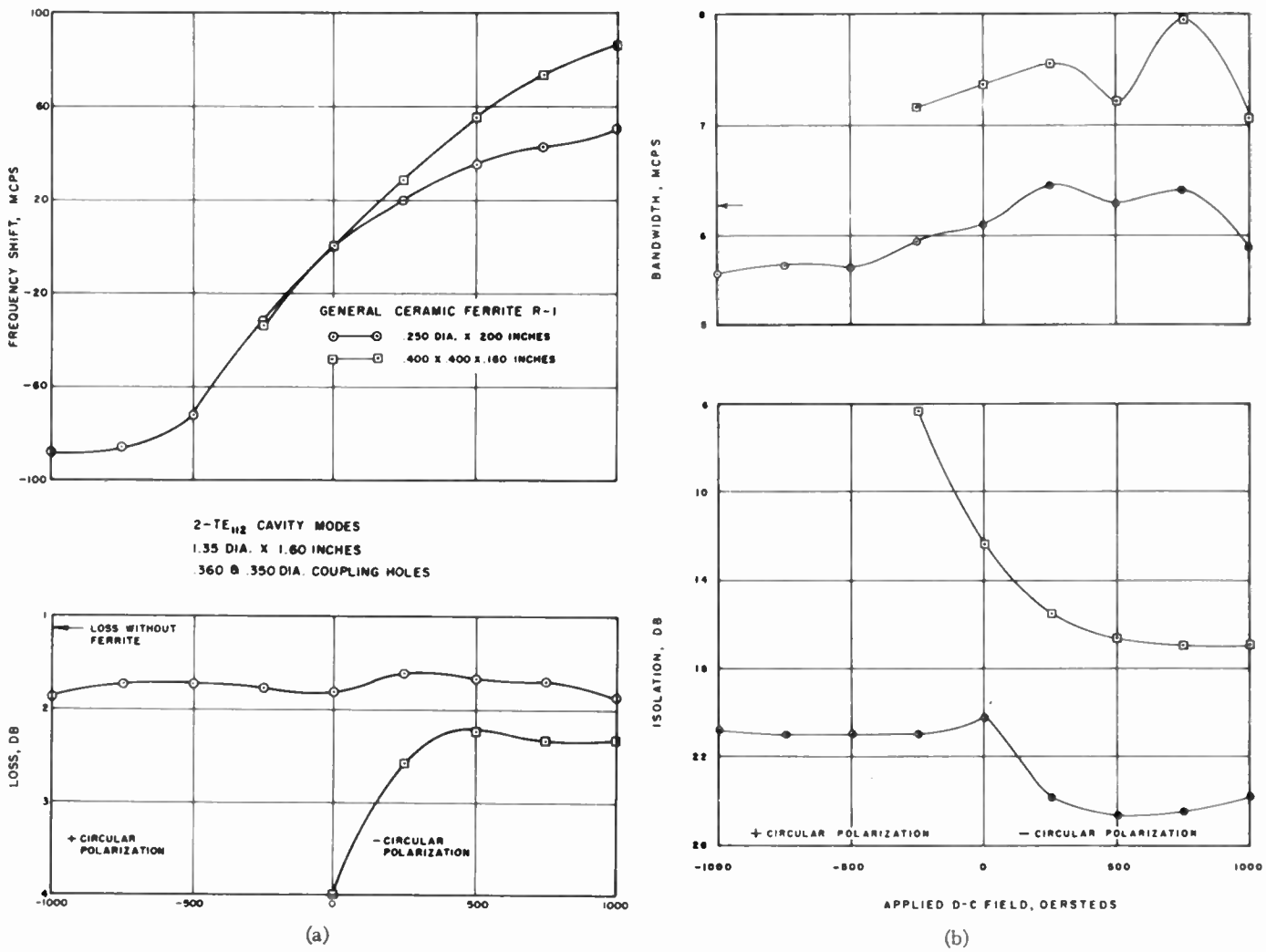

Fig. 5—Experimental data, ferrite-loaded, circularly polarized microwave filter, TE_{112} cavity mode.

ably constant, so that a change in one hole dimension should greatly increase the isolation over the range of dc fields. The larger ferrite caused considerable loss with positive circular polarization in the cavity.

Other cavity modes are being investigated to produce a better cavity-ferrite arrangement. As an example, Fig. 6 illustrates a TM_{110} degenerate cavity mode which uses off-center coupling to the waveguide. Two orthogonal TM_{110} modes, 90° in time phase, produce several points where circular polarization of the magnetic fields occurs. The coupling holes are positioned at these off-center circular polarization points. This arrangement leaves the other cavity end free for placing a ferrite against the end plate in a circularly polarized field. The advantage of this arrangement is that it permits a permanent magnet to be placed close to the ferrite.

In the arrangement shown in Fig. 7(a) opposite, only a single waveguide is used with the circularly polarized cavity, which at resonance without ferrite loading could be made to absorb nearly 100 per cent of the energy in the waveguide by introducing an absorbing material

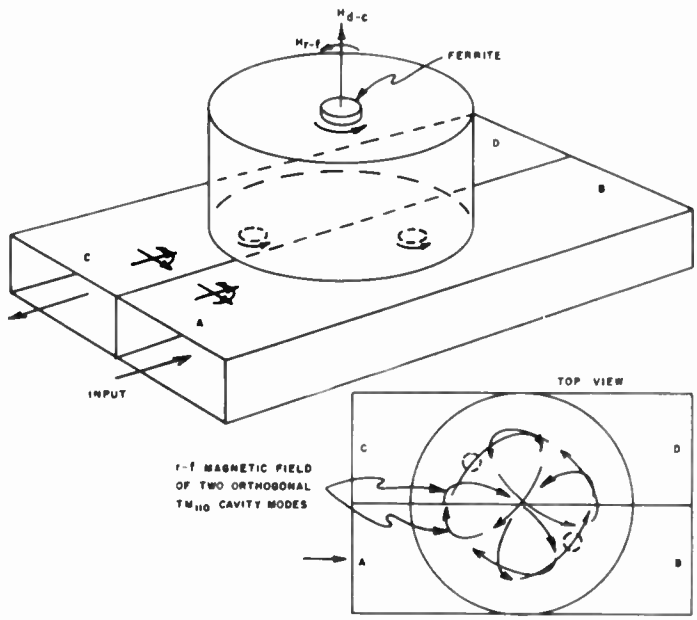

Fig. 6—Ferrite-loaded, circularly polarized microwave filter, TM_{110} cavity mode.

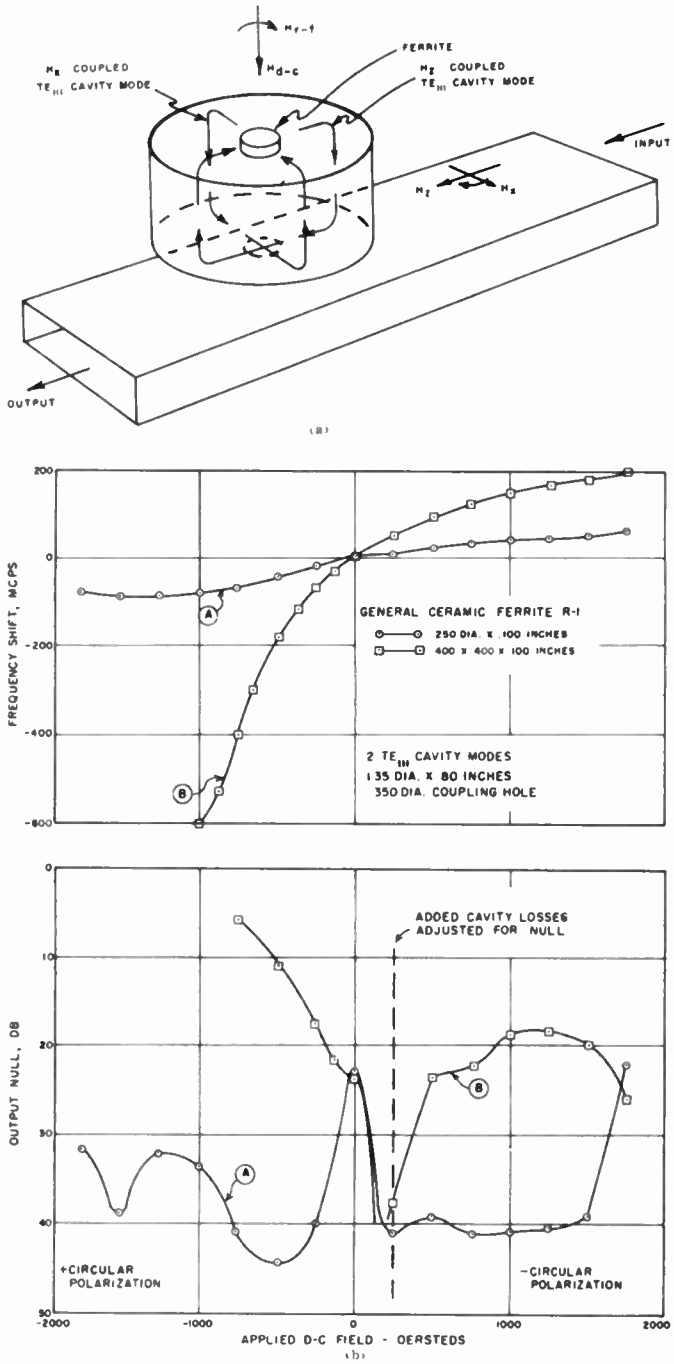

Fig. 7—(a) Ferrite-loaded, circularly polarized band elimination filter, TE_{111} cavity mode. (b) Experimental data, ferrite-loaded, circularly polarized band elimination filter, TE_{111} cavity mode.

into the cavity. The total cavity losses must be adjusted to a critical value for high absorption at resonance. Cavity losses greater or less than the critical loss will reduce the null at resonance. Again, it might be added that an analysis of this problem has been made and will be published at a later date.

With a ferrite in this filter, the device is tunable and nonreciprocal. For a given dc magnetic field, energy entering each end of the waveguide will see a different resonant frequency at which energy is absorbed. For this system, the ferrite losses are not a disadvantage since it is desirable to have a lossy cavity. The only requirement is that, for a given bandwidth, the ferrite losses are below a critical value. The requirement for a zero null in output at resonance is

$$Q_c = 2Q_w$$

then

$$Q_w = Q_L = \frac{f_0}{BW} \cdot$$

or

$$Q_c = \frac{2f_0}{BW} \cdot$$

Therefore the larger the bandwidth (and coupling hole size), the larger are the required cavity losses for zero output null.

Experimental results for the ferrite loaded cavity are illustrated in Fig. 7(b). For both ferrite sizes, the added cavity losses (in the form of lossy dielectric screws) were adjusted for a zero null at +250 oersteds. At the same time, metal tuning screws were adjusted for zero reflected power. With the smaller ferrite, values of cavity loss and bandwidth varied slightly, but the output null at resonance was kept between 30 and 40 db except at zero dc field. The effect of the larger ferrite was different. The ferrite loss was almost to the crictical value, so only a little additional cavity loss was required. For high positive dc fields (negative circular polarization), the loss decreased or the bandwidth increased so that the right-hand portion of curve B, Fig. 7(b), is a region of too little loss. In the left-hand region, the loss is too large. If the added cavity losses (lossy dielectric screws) were increased, the dip in curve B would move toward the right and produce greater isolation at higher positive dc fields. If the lossy screws were removed, the dip in curve B would probably only move to the −250 oersted field position because of the high ferrite losses for this large ferrite.

Three New Ferrite Phase Shifters*

HOWARD SCHARFMAN†, ASSOCIATE MEMBER, IRE

Summary—**Three new devices for the electrical control of microwave phase shift are discussed. The first of these, the bucking rotator phase shifter, is a reciprocal unit. It employs two series ferrite rotators, the field coils of which are connected so as to produce opposing longitudinal magnetic fields. It is shown that the total rotation is zero independent of coil current, whereas the phase shift is a function of the current. The operation and limitations of the device are discussed. Curves of phase shift vs coil current for several configurations are presented.**

The other two devices are based on the use of a circular polarized phase shifter between quarter wave plates. In the new types, a reflection technique is described wherein only one quarter wave plate is required and the phase shift section is used twice. A nonreciprocal phase shifter and an electrically controllable short circuit based on this technique are described. The principles of operation are discussed, and the devices are compared with other types as to performance, size, and bandwidth.

Introduction

A NUMBER of techniques employing ferrites for obtaining essentially lossless microwave phase shift have recently been devised. Several varieties of phase shifters, based on the use of a transversely magnetized slab of ferrite located either in a region of local circular polarization or along the longitudinal axis in rectangular guide, have been successfully constructed.[1-4] A number of articles on the theory and application of such phase shifters may be found in the literature, and specific devices are available commercially. Another type of ferrite phase shifter which has received considerable attention uses a longitudinally magnetized ferrite rod in square or circular guide preceded and followed by circular polarizers. Detailed reports on this type may also be found in the literature.[4] Each type has advantages and disadvantages which suit it best for specific applications.

In this paper three new phase shift devices are presented. Their individual characteristics are described and compared with each other as well as with other devices previously investigated.

The Bucking-Rotator Phase Shifter

As has been shown by Sakiotis and Chait, both the rotation of the plane of polarization and the transmission phase shift through a ferrite rotator are functions of the left- and right-hand circular polarized phase constants. These phase constants are in turn functions of the applied longitudinal magnetic field. The rotation, θ, and phase shift, ϕ, can be expressed in terms of the phase constants by:

$$\theta = \frac{(\beta_- - \beta_+)L}{2} \tag{1}$$

$$\phi = \frac{(\beta_- + \beta_+)L}{2} \tag{2}$$

where

β_+ = phase constant of the circularly polarized wave rotating in the same sense as current causing the magnetic field.

β_- = phase constant of the circularly polarized wave rotating in the opposite sense of B_+.

L = length of ferrite rod.

The variation of the phase constants as functions of applied field for X-band rotators have been investigated previously. Experimental curves taken in our laboratories are shown in Fig. 1. Plotted in the same figure

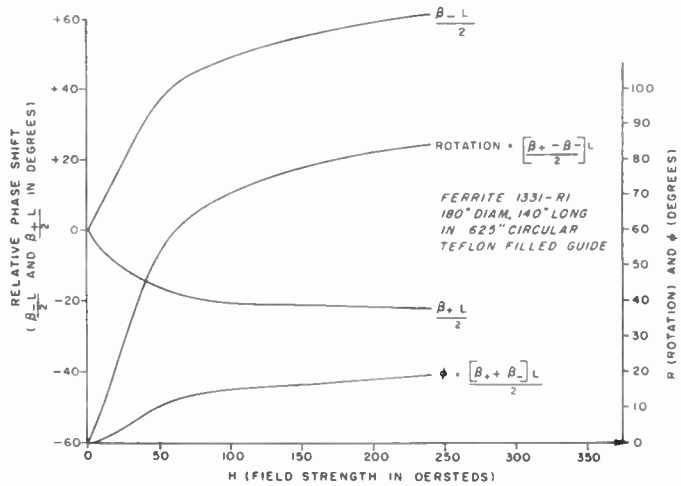

Fig. 1—Phase shift and rotation as functions of field strength.

are the calculated rotation and phase shift curves. The familiar rotation curve has been widely used as a basis for several ferrite devices in recent years, but the phase shift curve has evidently not been exploited. Whereas

$$\lim_{H \to 0} \frac{d\theta}{dH} \gg 1,$$

$$\lim_{H \to 0} \frac{d\phi}{dH} = 0.$$

As the field is increased, the phase shift increases slowly,

* Original manuscript received by the IRE, July 31, 1956.

† Raytheon Mfg. Co., Bedford, Mass.

[1] N. G. Sakiotis and H. N. Chait, "Ferrite at microwaves," PROC. IRE, vol. 41, pp. 87-93; January, 1953.

[2] H. N. Chait, "Nonreciprocal microwave components," 1934 IRE CONVENTION RECORD, part 8, pp. 82-87.

[3] B. Lax, K. J. Button, and L. M. Roth, "Ferrite phase shifters in rectangular waveguide," *J. Appl. Phys.*, vol. 25, pp. 1413-1421; November, 1954.

[4] A. G. Fox, S. E. Miller, and M. T. Weiss, "Behavior and applications of ferrites in the microwave region," *Bell Syst. Tech. J.*, vol. 34, pp. 5-103; January, 1955.

then passes through an approximately linear region, and finally saturates. The linear region is of considerable interest, for it can be used to obtain linear, reciprocal phase shift proportional to the magnetic field. By using a dc biasing field sufficient to reach the center of the linear region, phase advance or delay may be achieved.

In order to use the phase shift phenomenon described above in a worth-while device, some arrangement must be made for the ouput waveguide to rotate (either mechanically or electrically) with the applied field. This can be done most easily by means of a second rotator, similar to the first but rotating the polarization in the opposite sense. If the coils of the two rotators are connected in series, the total rotation through the two rotators will be zero independent of current, but the phase shift will be twice that for each rotator.

This type of phase shifter is illustrated in Figs. 2, 3, and 4. As a two-port microwave device, it has reciprocal

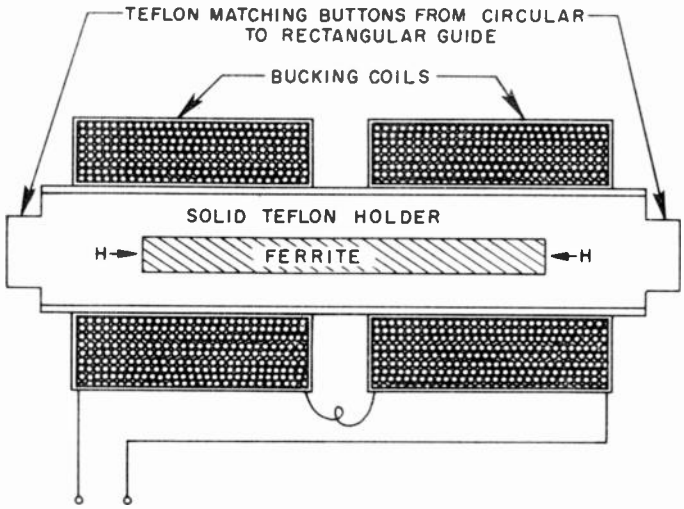

Fig. 2—Bucking rotator phase shifter.

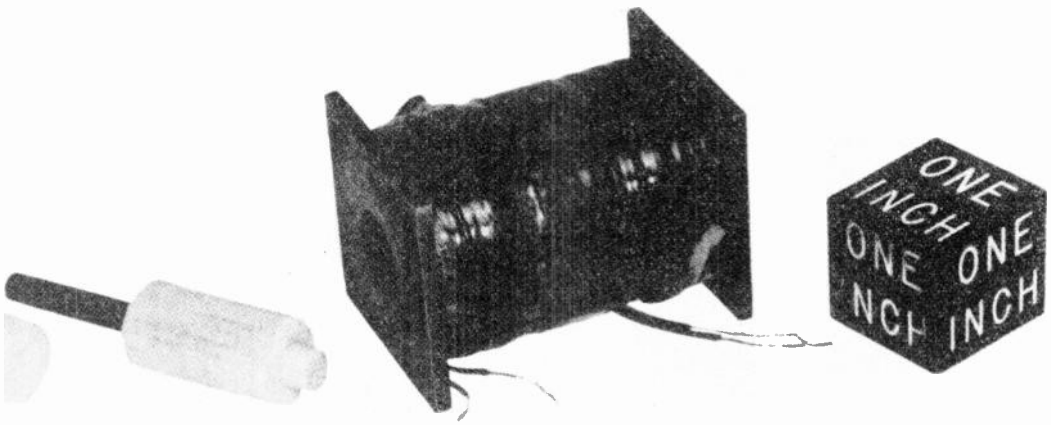

Fig. 3—Bucking rotator phase shifter, disassembled.

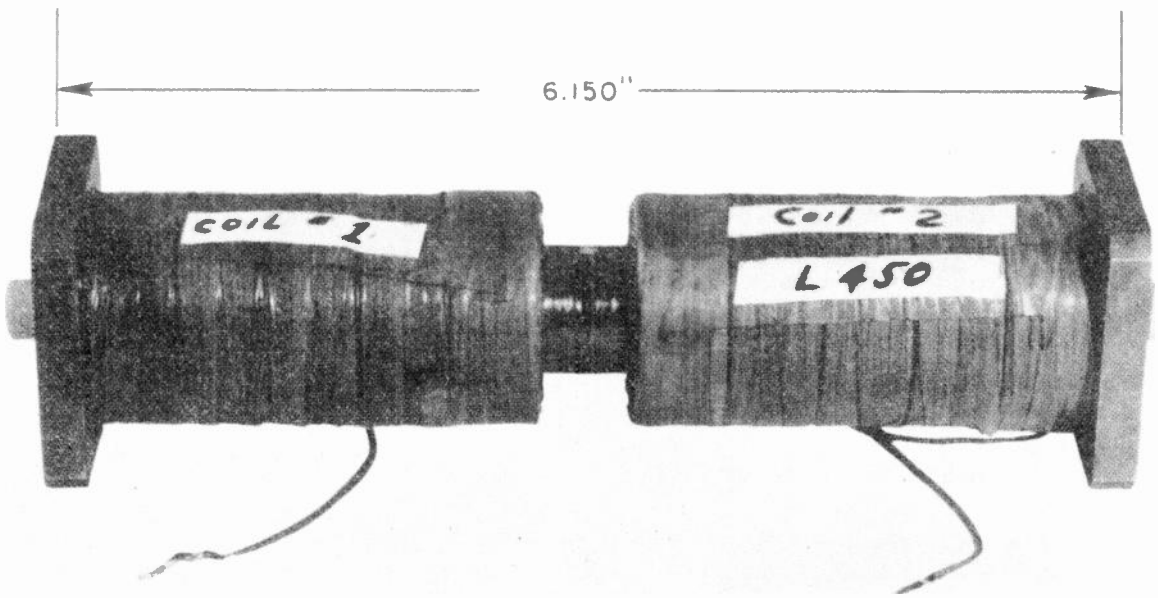

Fig. 4—Bucking rotator phase shifter.

properties for any value of current. With an appropriate dc biasing current applied, it can be operated to produce a microwave phase shift (either positive or negative) that is approximately linear with coil current. In addition, the insertion loss of the device is independent of applied coil current. Figs. 5, 6, and 7 show curves of phase shift vs applied field for three bucking-rotator phase shifters of different lengths and ferrite sizes. In each case the device operated over $2\frac{1}{2}$ per cent of the X band. A vswr of less than 1.1 was maintained when connected to 1 inch $\times \frac{1}{2}$ inch input and output waveguides.

As can be seen from the curves of Figs. 1, 5, 6, and 7 the maximum variation of phase shift of a bucking-rotator phase shifter is a function of ferrite length, diameter, and saturation magnetization. In principle, any arbitrarily large electrically variable phase shift could be obtained by increasing the length of the device. However, the practical difficulties inherent in maintaining precise symmetry in the two rotator sections become severe as the diameter and length of the ferrite rod is increased. In the latter case the rotations and rates of change of rotation of the plane of polarization in the individual rotator sections become quite large for small changes in applied coil current (*i.e.*, magnetic field). Consequently slight asymmetries may cause the rotations in each rotator section to be appreciably different with a resulting net rotation through the device. This results in the "capture" and eventual dissipation of some of the input energy with a corresponding spike of insertion loss. By the same token, any stray magnetic fields in the region of the device can cause asymmetries leading to similar effects. As a result, the device appears limited to phase variations up to ± 90 degrees unless special precautions are taken. The device is particularly well suited for applications requiring small linear phase variations with low constant insertion loss. It is simple in construction and small in size and weight. The longitudinal fields required can be applied from a low power driver over a wide frequency range provided proper precautions are taken to circumvent the shorted turn effect of the circular waveguide.

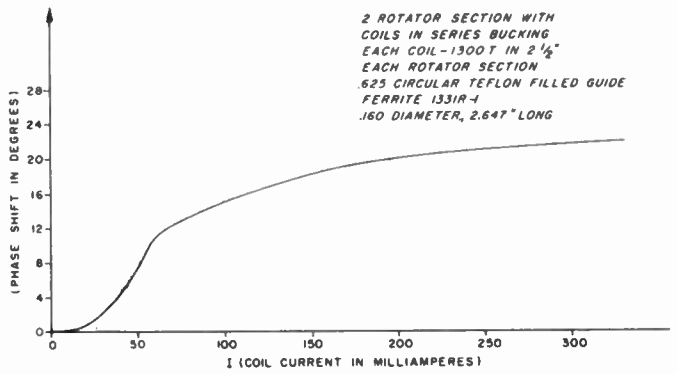

Fig. 5—Phase shift vs coil current.

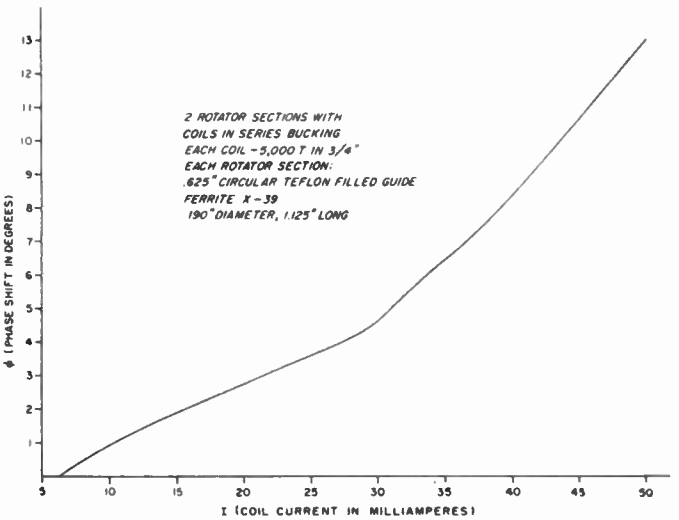

Fig. 6—Phase shift vs coil current.

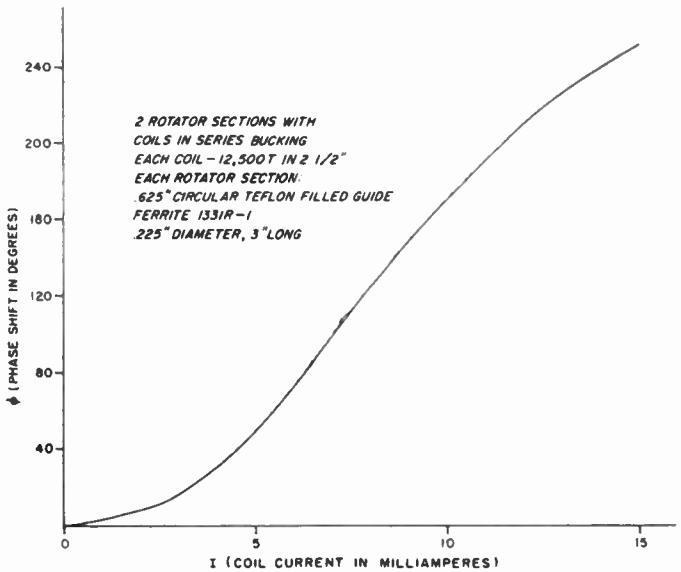

Fig. 7—Phase shift vs coil current.

The Cross-Polarized Phase Shifter

As mentioned earlier in this paper, a longitudinally magnetized ferrite rod preceded and followed by circular polarizers has been used as a variable phase shifter.[4] such a device is illustrated schematically in Fig. 8 opposite. The energy is converted from linearly polarized to circular polarized in the first polarizer, is phase shifted in the ferrite section proportional to the applied longitudinal field, and converted back to linear polarization in the output polarizer. The resultant phase shift is proportional to the applied field (up to saturation of the ferrite).

Two improvements have been made on this device. Fig. 9 illustrates a method of doubling the phase shift for a given applied field (or doubling the maximum phase shift before saturation), Energy is fed through a two-mode transducer (thruplexer) in either round or square waveguide into a circular polarizer. The resultant circularly polarized field is phase shifted proportional to the applied longitudinal field in the ferrite section and hits the shorting plate. The reflected wave moving back through the ferrite experiences a second phase shift

Fig. 8—Circular polarized phase shifter.

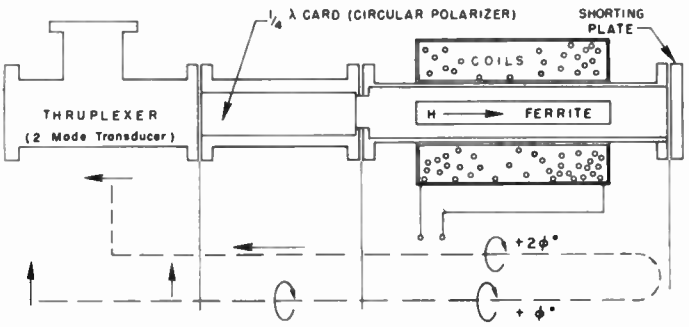

Fig. 9—Cross-polarized phase shifter.

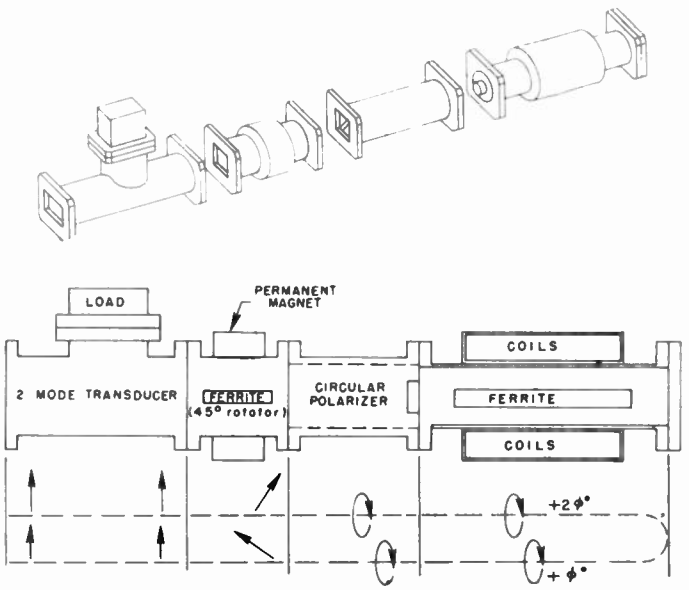

Fig. 10—Electrically controllable short circuit.

of the same sign as the first. Consequently the phase shift is doubled on the second trip through the ferrite. The action of the polarizer is to convert the circularly polarized reflected wave back to linear in a plane cross-polarized to the input field. The side arm of the thruplexer may therefore be used as the output of the device. It should be noted that this device, as the one from which it was derived, is also nonreciprocal in the sense that a phase advance is realized for one direction of propagation and a delay is obtained for the other direction. The cross-polarized phase shifter is capable of producing very large phase variations. It is considerably larger and more complex than the bucking-rotator type because of the required thruplexer and circular polarizer. These two types are supplementary rather than competitive. In contrast to the slab type and the original circularly-polarized type described above, the cross-polarized phase shifter produces greater phase variation per unit length. Another point to be considered, depending on system application and packaging, is the location of the output port close to the input port.

Electrically Controllable Short Circuit

As shown in Fig. 10 on the left, a modification of the cross-polarized phase shifter may be made for certain applications. In place of the thruplexer, a fixed 45 degree rotator (or isolator) is used preceding the polarizer. In this manner the input and output linearly polarized fields are in the same plane. The device is thus an electrically controllable short circuit.

Broad-band Considerations

Although the three new devices introduced above were not specifically designed for broad-band operation, their limitations are readily apparent. The bucking-rotator phase shifter is completely symmetrical. Its satisfactory operation over any band is thus only a function of how well one can match the input and output guides into the ferrite rod section. The phase shift for a particular applied field will, of course, vary with frequency, but from a microwave viewpoint it appears that this device could be made very broad-band (*i.e.*, approximately 25 per cent bandwidth).

The broad-band limitations of the cross-polarized phase shifters and controllable short is a function of the broad-band properties of several components (polarizers, rotators, thruplexers, and 45 degree isolators). From this standpoint one would expect a gradual degradation in performance for bandwidths in excess of 10 per cent.

Conclusion

Three new types of electrically controllable ferrite phase shift devices have been presented. Their characteristics are supplementary to each other and in a general sense to other types which have been previously reported. The bucking-rotator type is particularly suitable for applications requiring small phase changes in a small space. The cross-polarized phase shifter and controllable short circuits have very high possible phase variation and in some applications can be more easily packaged in a system than other high phase variation types.

In order to obtain the necessary difference between β_+ and β_- at other than dc conditions, the longitudinal field devices require less driving power than the transverse field types. Therefore, all of the new types discussed herein employ a longitudinal magnetic field and have been successfully modulated using miniature tube drivers.

Acknowledgment

It is a pleasure to acknowledge the help of Dr. Ernest Wantuch and Dr. Peter Rizzi whose many suggestions and ideas contributed greatly to this work. Thanks are due also to C. G. Shaw for making many of the measurements.

Ferrite-Tunable Filter for Use in S Band*

JAMES H. BURGESS†

Summary—**Using recently developed low magnetization ferrite materials, it is possible to extend the application of ferromagnetic resonance absorption down through S band. An electronically tunable image rejection filter designed to operate with a 2 to 4 kmc receiver has been constructed in coaxial transmission line. Image suppression considerably greater than 50 db with signal attenuation only 1.5 db is attained for an intermediate frequency of 500 mc.**

Introduction

PRIOR TO 1954, the application of ferrites to microwave problems was primarily confined to frequencies above 5 kmc. This limitation was due mainly to the inherent properties of the ferrite. The low frequency problem has been discussed by several workers[1–3] and solutions described in the case of low-loss applications. On the other hand, another class of applications makes direct use of the resonance losses. Low frequency operation in this case requires low magnetization ferrites. The recent development of materials having magnetizations as low as 500 gauss makes it possible to construct resonance absorption devices for use at frequencies down to 2 kmc. A device is described here which is designed specifically to solve the image rejection problem in microwave receivers in the 2- to 4-kmc band.

In this application the resonance absorption line is positioned by magnetic field adjustment to provide a small allowable loss at the signal frequency while strongly attenuating the image (see Fig. 1). An advantage incidental to this technique is the local oscillator attenuation also provided. The amount of image suppression for a given insertion loss and given intermediate frequency will depend inversely on the width of the absorption line. Hence, it is important to use materials having narrow linewidth as well as low magnetization.

Several techniques have been employed to produce low magnetization ferrites. The addition of a nonmagnetic divalent metal such as zinc causes an initial increase in the saturation magnetization but at sufficiently high concentrations the exchange couplings become diluted so that a reduction in magnetization occurs. However, the Curie temperature is likewise reduced to values close to normal operating temperatures, a condition which results in unstable operation. On the other hand, the addition of trivalent aluminum to form ferrite-aluminates results in an immediate reduction of the magnetization. Moreover, a narrowing of the absorption line occurs. Further additions of small amounts of manganese produce higher density ferrites and result in higher Curie temperatures.

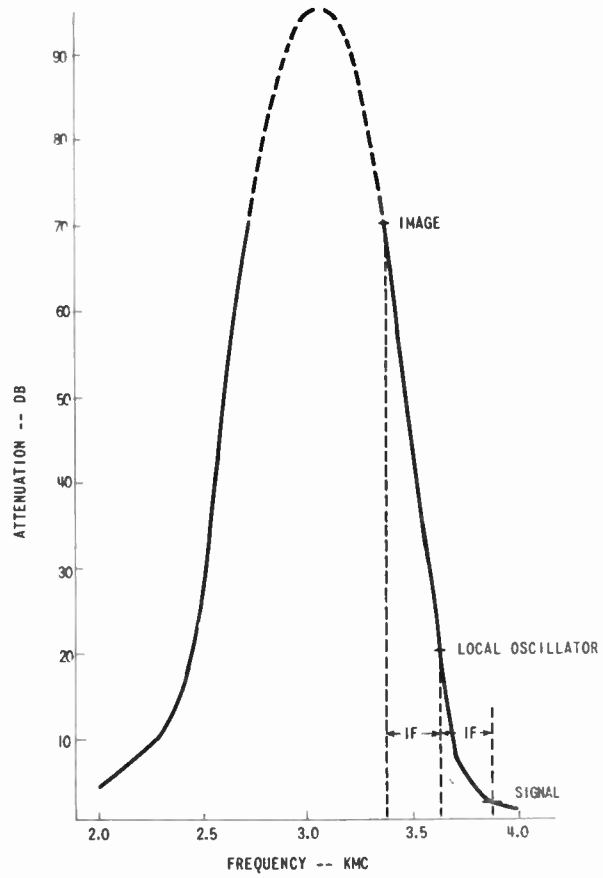

Fig. 1—Ferrite resonance absorption curve showing application to receiver image rejection.

Other factors also influence the absorption characteristics of a ferrite as measured in an rf structure. In the first place, the high dielectric constant of ferrites necessitates some form of matching to the transmission line. Otherwise multiple reflections from the ends of the ferrite element result in undesirable bumps or spikes in the absorption line. Over the 2-to-1 frequency range required in this application, tapering the ferrite was considered to be the most convenient solution. Line-

* Original manuscript received by the IRE, July 31, 1956. This work was performed under Signal Corps Contract No. DA-36-039-sc-31435.

† Electronic Defense Lab., Sylvania Electric Prods. Inc., Mountain View, Calif.

[1] L. G. Van Uitert, J. P. Shafer, and C. L. Hogan, "Low loss ferrites for applications at 4000 megacycles per second," *J. Appl. Phys.*, vol. 25, pp. 925–926; July, 1954.

[2] R. H. Fox, "Extension of nonreciprocal ferrite devices to the 500–3000 megacycle frequency range," *J. Appl. Phys.*, vol. 26, p. 128; January, 1955.

[3] B. Lax, Lincoln Lab. Quart. Progress Rep., Group 37, p. 67; February 1, 1955.

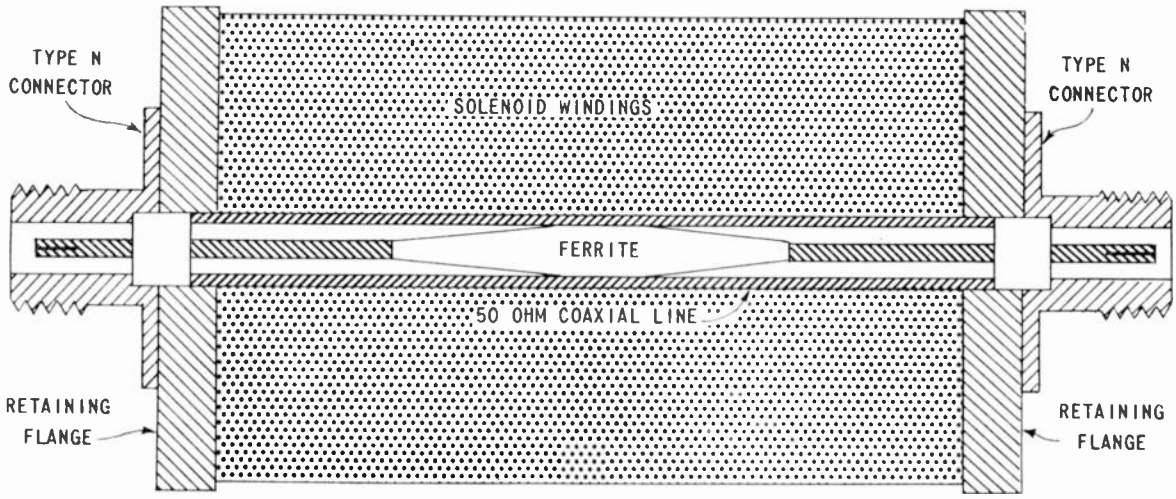

Fig. 2—Cross sectional view of ferrite tunable filter.

width problems are encountered in most matching schemes, however, because sample shapes usually are not ellipsoidal; consequently the magnetization is not uniform. This nonuniform magnetization produces a spread in resonance frequencies and results in a broadening of the absorption characteristic. In the second place, dynamic demagnetizing effects depending on sample shape and size may cause distortion of the absorption curve.

Two broad band wave-guiding structures were tried in this work, coaxial line and stripline. These configurations require respectively sleeves and thin plates of ferrite. The use of disks in a coaxial line was not considered because of the serious rf matching problem. Tests of both arrangements in transverse and longitudinal applied magnetic fields indicated that the coaxial configuration in a longitudinal field is superior. Not only is the high frequency edge of the absorption curve steep but in addition very high attenuations are possible with small amounts of ferrite.

Description

Fig. 2 shows a cross sectional sketch of the tunable filter element. A length of $\frac{3}{8}$-inch brass tubing and a piece of $\frac{1}{8}$-inch brass rod form a 50-ohm coaxial line. At each end are fastened brass flanges which are machined to recieve modified Type *N* receptacles. The flanges also serve to hold the magnetic field solenoid windings in place.

The ferrite was machined in three pieces from a length of $\frac{1}{4}$-inch rod. A total of about four inches of ferrite was used with tapers accounting for nearly two-thirds of this length. The material used was a magnesium-aluminum-manganese ferrite supplied by the Bureau of Mines. This ferrite has a saturation magnetization of 600 gauss and exhibits very low dielectric losses.

The device requires a magnetic field variable from 200 to 1200 oersteds and uniform to within 10 per cent; however, specific design of a solenoid depends critically upon the intended application. The element shown is designed to operate with a 6-inch solenoid about $2\frac{1}{4}$ inches in diameter which will provide a maximum field of 1200 oersteds (drawing $\frac{1}{2}$ ampere at 200 volts.) The data were taken using a large laboratory solenoid. A photograph of the complete filter is shown in Fig. 3.

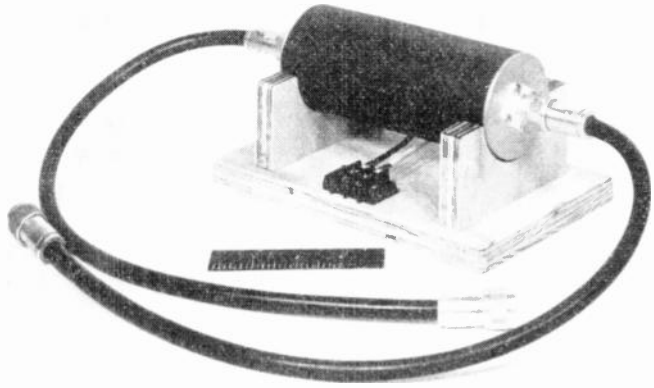

Fig. 3—Ferrite tunable filter.

Operation

Absorption characteristics were obtained using the arrangement shown in Fig. 4. Data were taken as a function of frequency: 1) without test element, 2) with test element and no magnetic field, 3) with test element and magnetic field. In this way both insertion loss and absorption could be determined.

A typical absorption curve is shown in Fig. 1. The dotted portion was not measured because of limited incident power. Fig. 5 gives a family of curves for various magnetic field strengths. Only the high frequency edges are shown. Examination of these curves shows that the following filter characteristics may be obtained for local oscillator frequencies in the range from 2 to 4

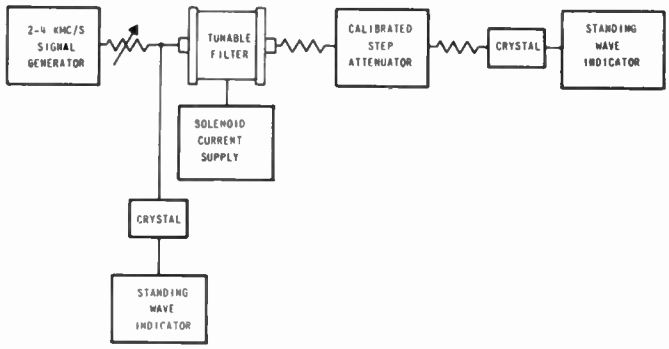

Fig. 4—Block diagram of apparatus for measurement of ferrite filter characteristics.

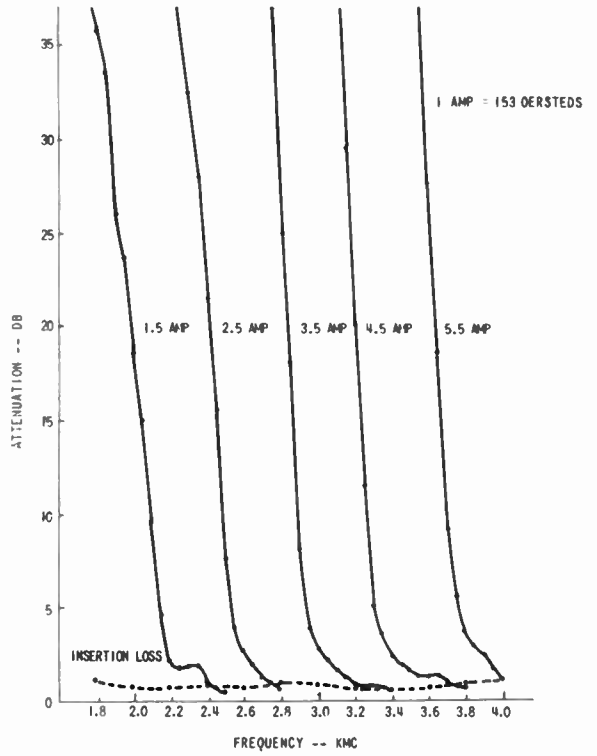

Fig. 5—Attenuation characteristics of ferrite tunable filter.

kmc. (See Table I.) Greater image suppression may be obtained in most cases at the expense of signal strength. However, no advantage results by increasing the IF above 500 mc because the image frequency then falls below the frequency of peak attenuation. Above 2.5 kmc the straight line portion of the curves has a slope greater than 16 db per 100 mc. These curves also yield the magnetic field tuning-relation which does not depart greatly from linearity. Additional measurements have shown that the insertion loss remains below 1 db and the vswr in the case of no magnetic field remains below 1.4 from 1.8 to 4.8 kmc.

TABLE I

IF (mc)	Absorption (db)		
	Sig.	L.O.	Image (lower side band)
200	1.5	2	20
300	1.5	9	35
400	1.5	20	>35
500	1.5	26	>50

Conclusion

Through the use of low magnetization aluminum-addition ferrites it has been possible to construct a tunable resonance absorption filter operating in the 2 to 4 kmc range. It appears feasible to extend the application of resonance absorption to even lower frequencies by continued reduction of saturation magnetization. However, the following factors should be considered. In the first place, a decreased magnetization and a lower frequency will result in a considerable weakening of the interaction of the ferrite with the rf magnetic field. Hence a much larger amount of ferrite will be required to obtain the same attenuations. In the second place, unless anisotropy can be reduced as well as magnetization the magnetic field strength necessary for saturation may exceed that required for resonance at the operating frequency. Finally, and most importantly, the reduction in Curie temperature brought about by high dilution will lead to an undesirable temperature sensitivity of the absorption characteristics.

Other applications of this device which are of interest include amplitude modulation, electronically programmed variable attenuation, fm discrimination, and variable phase shifting.

Acknowledgment

The author is indebted to Dr. A. L. Aden, Dr. W. P. Ayres, Dr. J. L. Melchor, and Dr. P. H. Vartanian for many helpful discussions of this problem and to A. B. Howard for making many of the measurements.

Radiation from Ferrite-Filled Apertures*

D. J. ANGELAKOS† AND M. M. KORMAN†

Summary—**The properties of ferrites at microwave may be used in antennas to produce some interesting effects.**

A rectangular waveguide termininating in the plane of an infinite ground screen and radiating into a half space has a ferrite slab located at the aperture. With a TE_{10} mode of 9365 mc sent through the waveguide the far-zone radiation pattern in the *H* plane has been measured as a function of a transversely applied static magnetic field. It was discovered that for certain thicknesses of the ferrite slab the radiation lobe deviated considerably from the normal to the infinite screen with only small changes in the applied magnetic field. For some of these resonance points and their neighborhoods more detailed investigations were carried out in order to determine: a) the amplitude and phase distributions of the electric field in the aperture; b) reciprocity relationships.

Small holes backed with a ferrite slab also exhibit a pattern shift with applied magnetic field.

When an axial magnetic field is applied to a ferrite rod protruding from an open circular guide, the radiation pattern of the rod antenna may be shifted considerably. This effect has cylindrical symmetry.

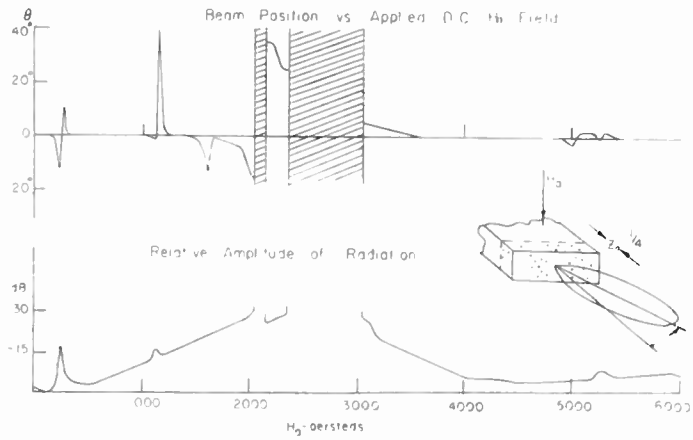

Fig. 1

Ferrite-Filled Slot Antenna

A FERRITE slab was inserted at the open end of a radiating waveguide and a transverse magnetic field applied.

The radiation patterns taken indicate the relative electric field strengths in the far-zone *H* plane due to the radiation from the aperture of the waveguide. Patterns up to 2,500 oersteds (as measured by the probe) at intervals of not more than 50 oersteds were taken for many ferrite slabs. At field strengths, where noticeable changes in the pattern occurred, measurements were taken at much closer intervals, sometimes at 5-oersted intervals. The possibility of having overlooked phenomena occurring in the intervals between taken field strengths points is therefore rather small. No matching device was used for the transmitting system. For each field strength the vswr in the transmitting waveguide was recorded. Fig. 1 shows the effect of a large variation of applied magnetic field on the beam position and on the amplitude of the radiated field.

With a sample of thickness $\frac{1}{4}$ inch, the radiation beam shifts gradually to a negative θ and reaches a minimum of $-10°$ at 240 oersteds. Then it shifts, apparently continuously, to $+10°$ with a change of only 20 oersteds. From about 260 oersteds it shifts gradually back to normal. At 1150 oersteds a new phenomenon occurs. The lobe position changes from 0 to 40° with a very small change of the magnetic field, possibly only about 10 oersteds. This change is accompanied by a slight broadening of the beam. It is suggested that here an interchange of lobes occurs, but not of two symmetrically opposite lobes as is the case to be illustrated later but one lobe located at 40°, the other at 0°. When the field strength is further raised the lobe comes back to normal while undergoing a certain broadening. At 1600 oersteds the beam reaches $-10°$ and then comes back to normal.

With negative magnetic fields the signs of θ interchange. For changes of vswr attenuation with H_a see the middle portion of Fig. 2.

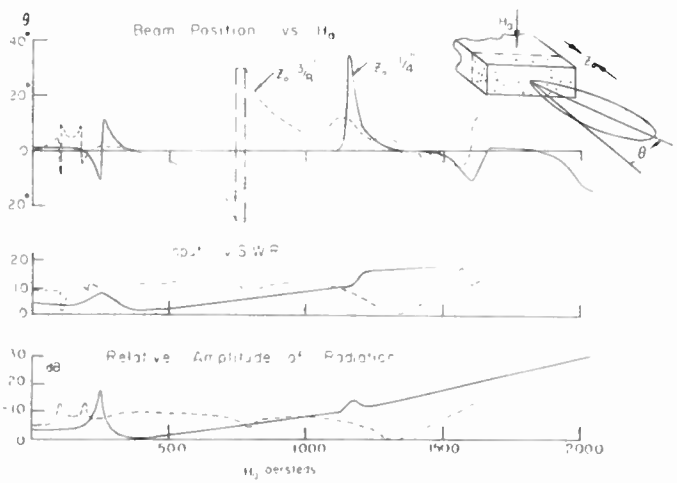

Fig. 2

Fig. 2 compares the effects for a ferrite sample 3/8 of an inch thick with those of the $\frac{1}{4}$-inch sample. It is noticed that for the thicker sample some unusual results are obtained. To emphasize this effect, a $\frac{1}{2}$-inch sample was then used. Fig. 3 indicates the general results.

The sample of thickness, $z_0 = \frac{1}{2}$ inch exhibits the most diversified behavior. From $H_a = 0$ to 300 oersteds the direction of the radiation beam, θ, remained constant. From $H_a = 300$ oersteds on, the beam begins to shift

* Original manuscript received by the IRE, July 3, 1956. This work was supported by contract N7 onr-29529.

† Electronics Res. Lab., Div. of Elec. Eng., University of California, Berkeley, Calif.

continuously to negative θ's with increasing fields reaching a minimum of $\theta = -22°$ at 480 oersteds. Immediately after having reached a minimal θ value another lobe appears at $\theta = 30°$. This lobe is rather sharp. Between 480 to 510 oersteds the lobe grows while the original lobe diminishes and completely disappears at 510 oersteds This interchange of lobes is accompanied by a sharp attenuation in amplitude. From 510 oersteds on, the right-hand lobe shifts back continuously to smaller θ's while gradually losing its sharp shape. At 970 oersteds, θ has reached a minimum angle of $-28°$ and between 970 and 990 oersteds, an interchange of lobes occurs, as before. Around 1330 oersteds θ again changes rather sharply from 15° to −15°. This change is accompanied by a broadening of the beam, which may be interpreted as an overlapping of two lobes, one at $\theta = 15°$, the other at $\theta = -15°$. It seems, then, that the interchange of lobes phenomenon is repeated

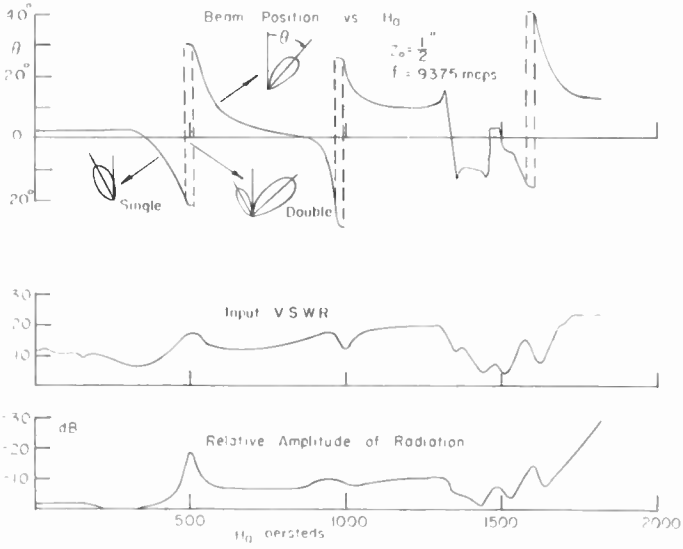

Fig. 3—Thick sample.

here; however with smaller extreme angles. Smaller changes in θ occur next. At 1600 oersteds another interchange of lobes occurs. Again the right-hand side beam is icicle shaped. Here, however, it is certain that the two extreme angles are not of the same magnitude. At 1825 oersteds the attenuation of the signal became so large that the signal was overshadowed by noise. When the field H_a was reversed the same phenomena repeated themselves with an interchange of signs in front of the angle θ. For the variation of the vswr and attenuation with H_a see Fig. 3.

Mode Control

Referring to Fig. 4(a) the mechanism by which the pattern shift occurs is due to conversion in the ferrite of some of the incident power into higher order modes which may propagate in the filled portion of the waveguide due to its high value of $\mu\epsilon$ product. In particular, previous experiments at this laboratory have shown that

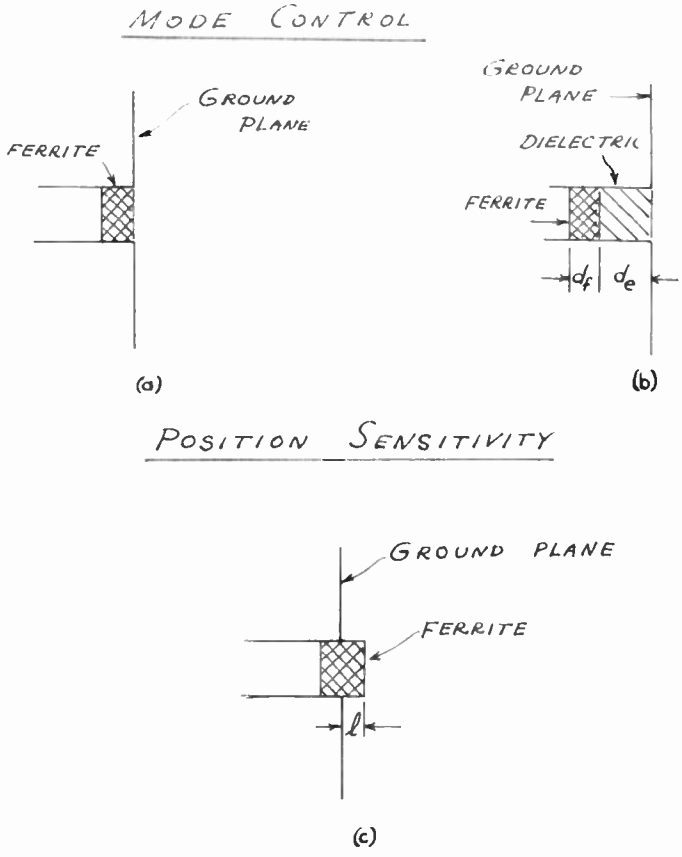

Fig. 4—(a), (b) Mode control. (c) Position sensitivity.

a combination of TE_{10} and TE_{20} modes applied to a similar aperture in the proper amplitude and phase relations can produce radiation patterns very similar to those observed in this apparatus. Since the various modes propagate at different velocities, their relative phases at the aperture can be adjusted by changing the length of the ferrite. Thus an experimental adjustment of length can be used to optimize performance.

If the ferrite is moved back from the aperture into the waveguide, it is found that the pattern shifting effect disappears due to the fact that the higher order modes generated cannot propagate in the unfilled section of the guide. However, one may fill the guide between the ferrite and the aperture with a dielectric material, as suggested in Fig. 4(b), and by adjusting the characteristics of this material select modes up to the highest order desired. Adjustment of the length can be used to adjust relative phases at the aperture for optimum performance, as before.

An experiment of this type was carried out, using Lucite ($\epsilon_r = 2.6$) for the dielectric. The ferrite sample chosen was one-fourth inch in thickness (dimension d_f is Fig. 4(b), a dimension which had been found to give favorable results when used at the aperture. The dielectric constant of the lucite was high enough to pass the TE_{20} mode, but no higher ones. The length of the dielectric material was chosen so that the phases of the TE_{10} and TE_{20} modes would be the same at the aperture as at the outer surface of the ferrite. This is accom-

plished by setting

$$\beta_1 d_e = \beta_2 d_e + 2n\pi \cdot$$

Here β_1, and β_2 are the propagation constants for the first and second modes, respectively. Solving for d_e in terms of the guide wavelengths one obtains:

$$d_e = \frac{n\lambda_2\lambda_1}{\lambda_2 - \lambda_1} \cdot$$

Taking $n=1$ to obtain the shortest test section and using known values of the λg's, the required length of the dielectric section d_e becomes approximately 1.75 inches at 9375 mc.

Using this setup one group of field values was found at which total pattern shifts of about 35° were obtained, verifying the assumptions of the experiment. The behavior, as expected, was somewhat different from that obtained with the ferrite placed in the aperture. In particular, only one set of field values was found at which pattern shifts occurred, rather than several, and the dependence, or sensitivity to the static magnetic field was much decreased.

One interesting fact was that to a first order the pattern shift appeared to be independent of frequency over a limited range (about 150 mc) whereas previous measurements with ferrite at the aperture had shown a rather steep linear dependence on frequency.

Position Sensitivity

Some investigation was made of the sensitivity of the system to exact positioning of the ferrite in the aperture. Thus, in one experiment the ferrite was permitted to protrude from the aperture by a small value l, as in Fig. 4(c). Very pronounced effects were noted in one case for $l=0.040$ inch. Lobe splitting and other unusual effects were observed. It is possible that some of these effects were caused by nonuniformity of the static magnetic field in front of the ground plane, since the pole pieces must of necessity be behind the plane and no shaping expedients were used to maintain the field uniform in the region in front of the aperture. However, it seems more likely that the effects observed were due to modifications of the boundary restrictions along the ferrite so that more complicated fields are permitted to exist. It appears that precise position of the ferrite in the aperture is very important.

A photograph of the experimental arrangement is shown in Fig. 5. The receiving horn antenna is located 43 inches from the radiating slot. The microwave absorbing screen placed in a semicircle about the setup and 50 inches from the slot reduces the reflections to a practical minimum.

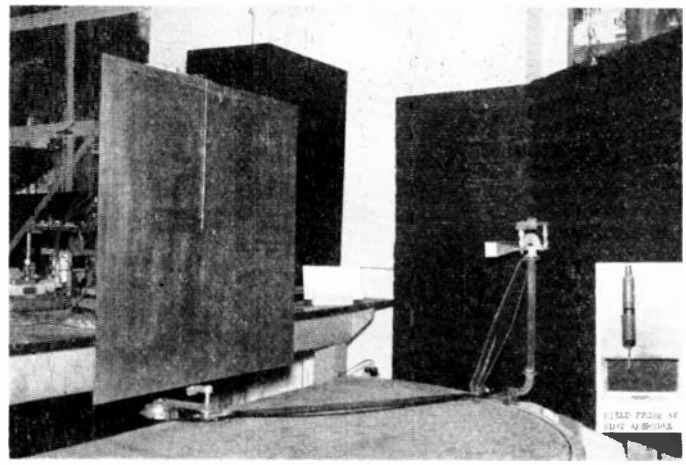

Fig. 5—Pattern measurement arrangement.

Aperture Field Distribution

Since the radiation patterns are entirely determined by the field distributions at the aperture of the transmitting waveguide, it was found appropriate to investigate the electric field distribution at the waveguide aperture. Only the E vector in the upper half of the aperture cross section was measured. The introduction of the measuring probe distorted the field distribution to a very slight extent. For comparison the amplitude and phase shift distributions are presented for the empty waveguide (see Fig. 6), a distribution that coincided closely with that of the sample with no applied magnetic field.

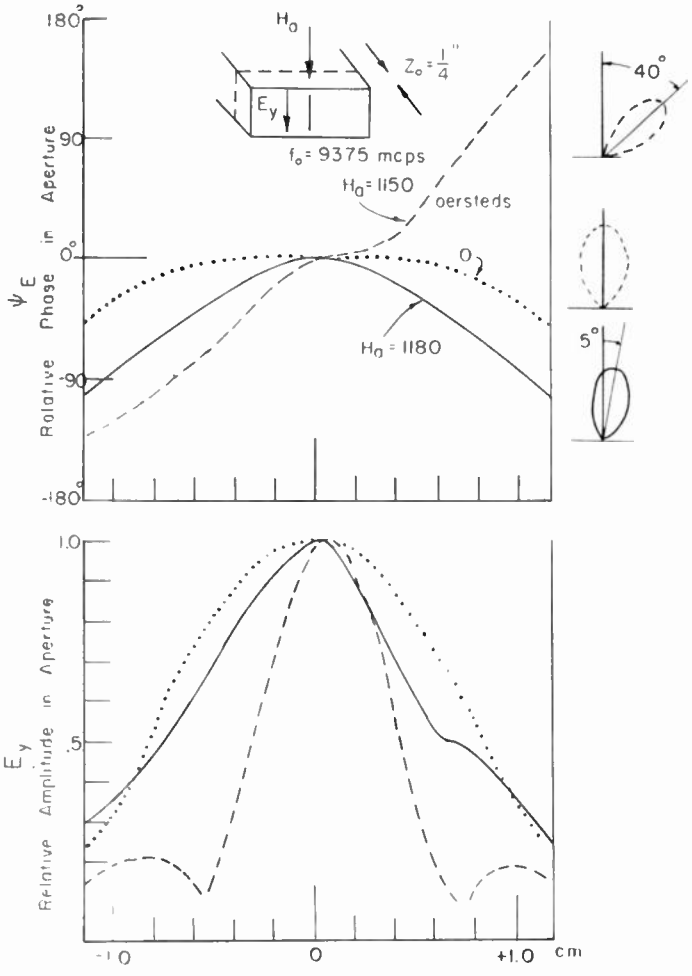

Fig. 6—Aperture distribution.

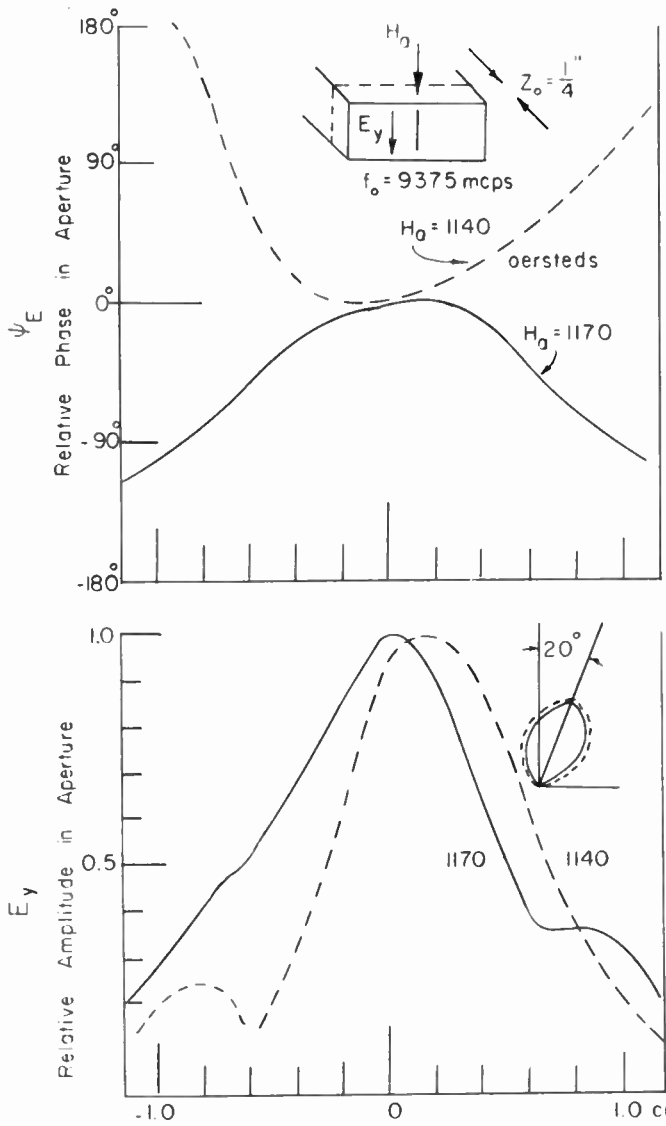

Fig. 7—Aperture distribution.

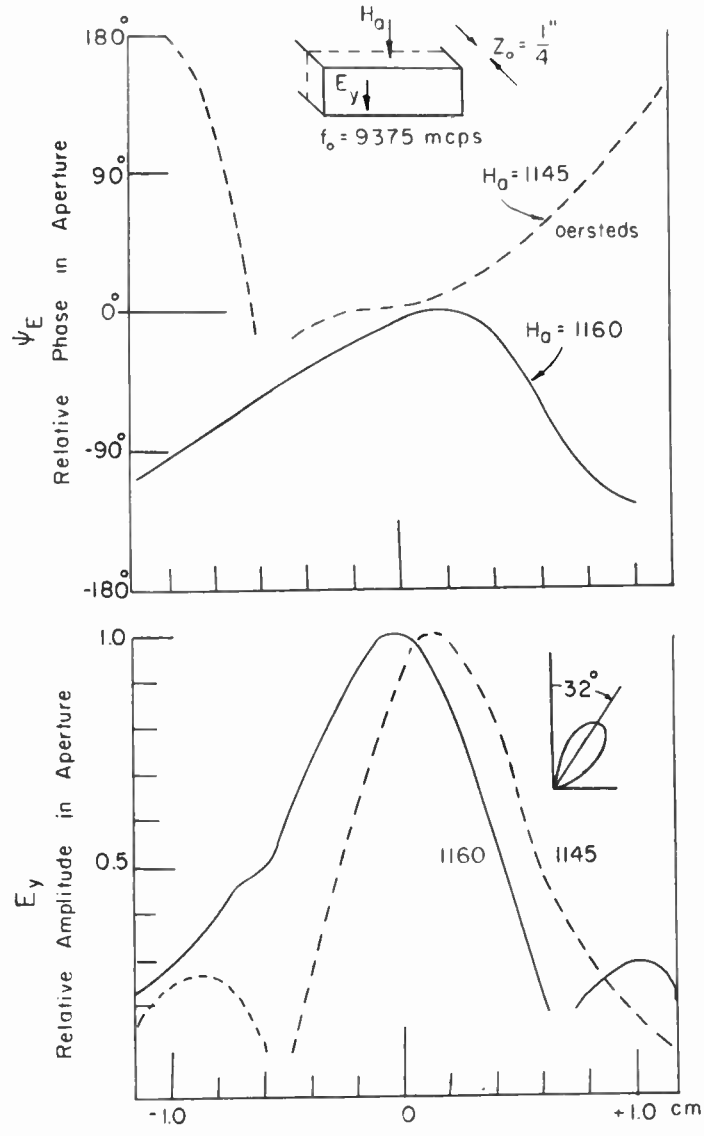

Fig. 8—Aperture distribution.

The aperture field distribution was recorded for the sample of $\frac{1}{4}$-inch thickness for three different magnetic field values in the vicinity of the lobe interchange at $H_a = 1150$ oersteds and for $H_a = 1180$ oersteds where $\theta = 5°$. It was observed that the amplitude of the electric vector retained a large peak at the center of the waveguide with a small peak at the left side (negative x) for fields smaller than $H_a = 1150$ oersteds which switched to the right side for fields larger than $H_a = 1150$ oersteds. At $H_a = 1150$ oersteds both small peaks were in evidence. The phase too exhibited some symmetry about $H_a = 1150$ oersteds. For equal θ's on opposite sides of $H_a = 1150$ oersteds the phase distributions are the same if the signs of both the phase shift angle and of x are reversed. The abrupt change in phase shift angle at the low amplitude points is a possible phase reversal. Other electric field distributions for several values of applied magnetic field are shown in Fig. 7 and Fig. 8. The patterns so obtained were similar although the electric field and phase distributions were not.

Variation of Parameters with Applied Field

The variation of the orientation of the radiation pattern with applied field is shown in Fig. 9, for two regions of the applied magnetic field scale. In addition, the input impedance of the slot antenna was measured as a function of the applied magnetic field; in one case the antenna was tuned by means of a slide-screw transformer for unity vswr at 1150 oersted and in the other case for unity vswr at 245 oersteds. It is noticed that for the stronger field region, the device is relatively quite insensitive to changes in the applied magnetic field. This is also indicated by the lower portion of the figure. The radiated energy is fairly constant for small changes in the applied magnetic field of value 1150 oersteds. Fig. 10 indicates the polarization of the E-vector as a function of the applied magnetic field.

Variations with Frequency

A limited investigation of the effect of change of frequency is summarized in Fig. 11. A sample ($\frac{1}{4}$ inch) was

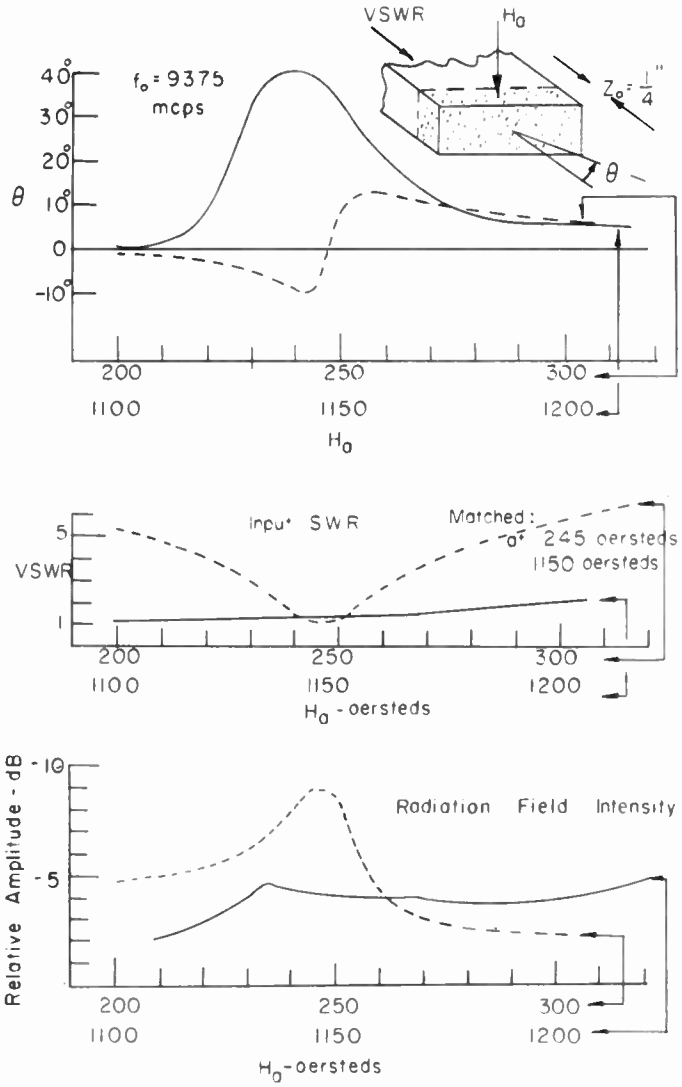

Fig. 9—Effect of applied field.

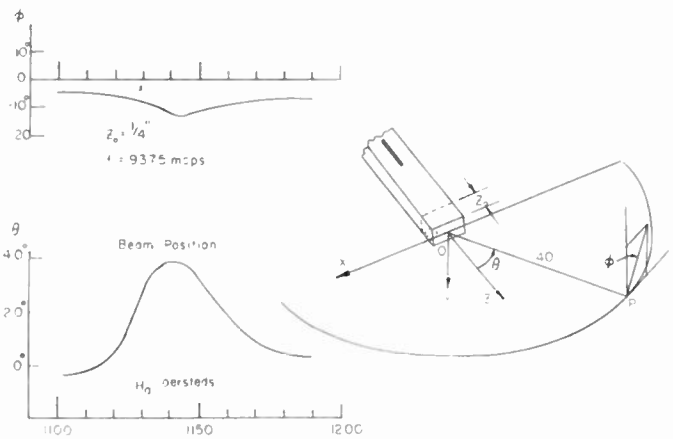

Fig. 10—Field vector polarization.

chosen to illustrate the frequency dependence. For 9365 mc the magnetic field was set at $H_a = 1150$ oersteds to give a θ of 40°. Then the frequency was varied and the H_a adjusted so as to keep θ at its maximum value which was 40°. Over the limited frequency range investigated

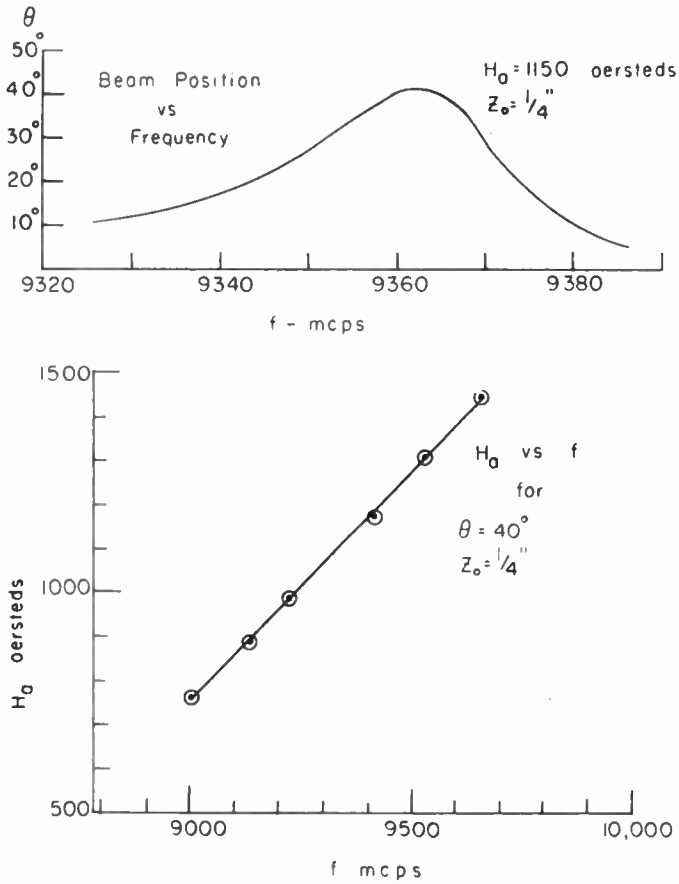

Fig. 11—Variations with frequency.

a straight line relationship resulted between H_a and frequency (lower portion of Fig. 11). This phenomena was not investigated past the limited frequency range.

Using θ as the independent variable with a constant magnetic field the frequency was again varied starting from an initial setting of 9365 mc, H_a of 1550 oersteds, θ or 40°. The results are recorded in the upper portion of Fig. 11 and illustrate the interrelationship between frequency and the radiation pattern shift.

Nonreciprocity

In all the preceding experiments the ferrite-filled slot antenna fulfilled the transmitting function and the horn antenna acted as the receiver. Let us call this setup the transmitting setup and the resulting pattern the transmitting pattern.

With the functions reversed, *i.e.*, the horn acting as the transmitter and the ferrite-filled slot antenna as the receiver the setup will be called the receiving setup and the resulting pattern the receiving pattern. It was observed that the transmitting and receiving patterns were images of each other with $\theta = 0°$ being the axis of symmetry (see Fig. 12).

This is called a nonreciprocal system, since by definition a reciprocal system would result in the transmitting and receiving patterns coinciding. This nonreciprocal system can be explained by the reciprocity of the Cotton-Mouton effect.

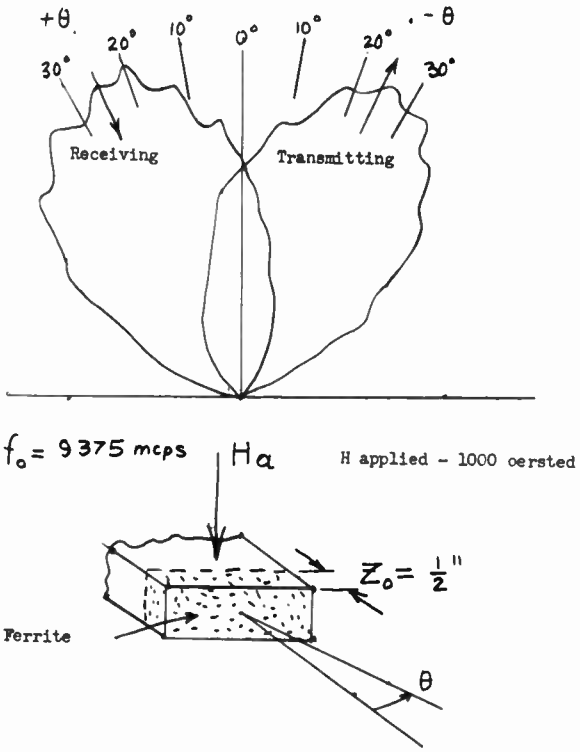

Fig. 12—Nonreciprocity.

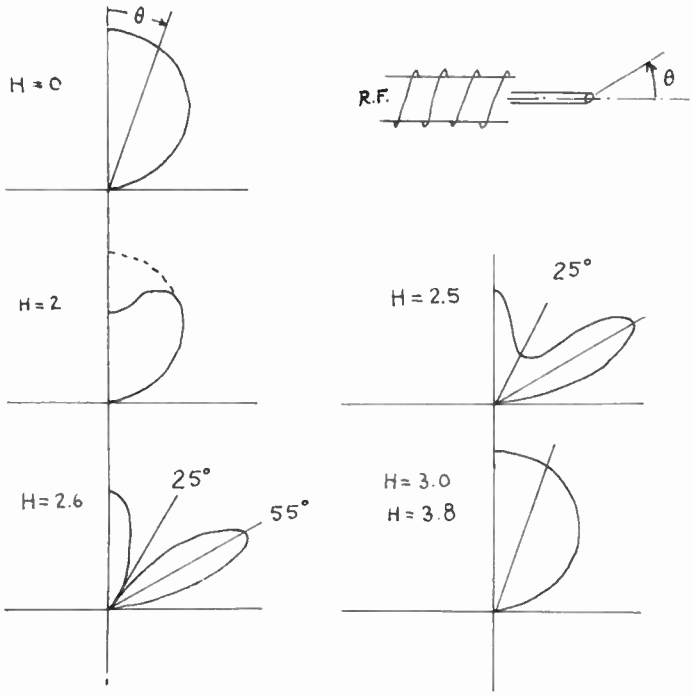

Fig. 13

When we have the transmitting setup there is a change in direction $\theta°$ counterclockwise with respect to the direction of propagation as the wave passes the ferrite resulting in the radiation lobe centering at $+\theta$. When we have the receiving setup, then, as we pass the ferrite, there will again be a change in direction of $\theta°$ counterclockwise with respect to the direction of propagation, because of the reciprocity of the Cotton-Mouton effect. This, however, will result in the receiving lobe centering at $-\theta$.

Radiation from Circular Apertures

For the case in which the large rectangular apertures is reduced to a small circular aperture (0.1 inch) located at the center of the face of the guide, the only effect that the applied magnetic field can produce is to change the level of the radiated power. On the other hand, two holes placed symmetrically a quarter of the guide width from the walls do have a radiation pattern which can be controlled through the applied transverse field. The ferrite thickness was maintained at $\frac{1}{4}$ inch.

Radiation from a Ferrite Rod

A circular cylindrical waveguide with a ferrite rod extending on passed the mouth of the guide and having a longitudinal magnetic field has a radiation pattern which can be controlled. The variable permeability and resulting field within and at the boundary of the ferrite produce a radiating pattern as shown in Fig. 13. The magnetic field applied is expressed in relative units.

Correction

The following correction to "Some Aspects of Mixer Crystal Performance," by Peter D. Strum, which appeared on pages 875–889 of the July, 1953 issue of Proceedings of the IRE, has been brought to the attention of the author by Harry J. Thomas.

On page 878, (17) should read:

$$\gamma_n = \frac{\left(\frac{x-1}{2}!\right)^2}{\left(\frac{x+n-1}{2}!\ \frac{x-n-1}{2}!\right)(1+\gamma_b)} \qquad (17)$$

The difference is in the $(1+\gamma_b)$ term. The curves of Fig. 3 were computed from this correct version of (17).

Correspondence

The Radiation Patterns and Conductances of Slots Cut on Rectangular Metal Plates*

Radiation Patterns

It is easy to predict the form of the principal E-plane radiation pattern obtained from a radiating slot cut on a long metal plate. Consider, for example, the plate of width W, shown in Fig. 1. Let S represent

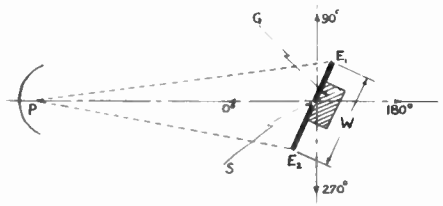

Fig. 1

the slot (whose axis is perpendicular to the plane of the paper) and let G represent the waveguide feeding power to the slot. Very far away from the waveguide and plate is a receiving antenna P.

When the slot is pointing toward P, *i.e.*, in the 0° direction, a large field strength results, but if the slot points away from P (in the 180° direction) the field strength is small, its actual value being determined by the fraction of the total power radiated which is diffracted behind the sheet to P. In the intermediate directions 90° and 270° the field strength at P would lie between the values obtained for the 0° and 180° directions. Thus, in the absence of further complications, the radiation pattern of the metal sheet antenna would resemble the dashed line of Fig. 2(a). Actually one important feature has been overlooked in this development.

It will be appreciated that the edges E_1 and E_2 of the metal sheet form a discontinuity to the field traveling outward from the slot and along the sheet. Radiating line sources will, therefore, be induced near the edges E_1 and E_2 of the sheet and these will come in and out of phase with each other as the antenna is rotated. Thus, instead of the radiation pattern looking like the dashed line of Fig. 2(a), it will resemble the full line of the same figure. The number of interference fringes in a complete rotation of the plate will be greater for wide sheets than for narrow ones since a smaller incremental rotation is required to form a given path difference for a wide sheet. The amplitude of the fringes will be smaller for wide sheets than for narrow ones, however, since the strength of the induced line sources decreases as the sheet width is increased.

From what has been said, the radiation patterns for narrow, moderately wide, wide, and infinitely wide sheets will be like the full lines of Figs. 2(a), 2(b), 2(c), and 2(d), respectively.

* Received by the IRE, June 20, 1956.

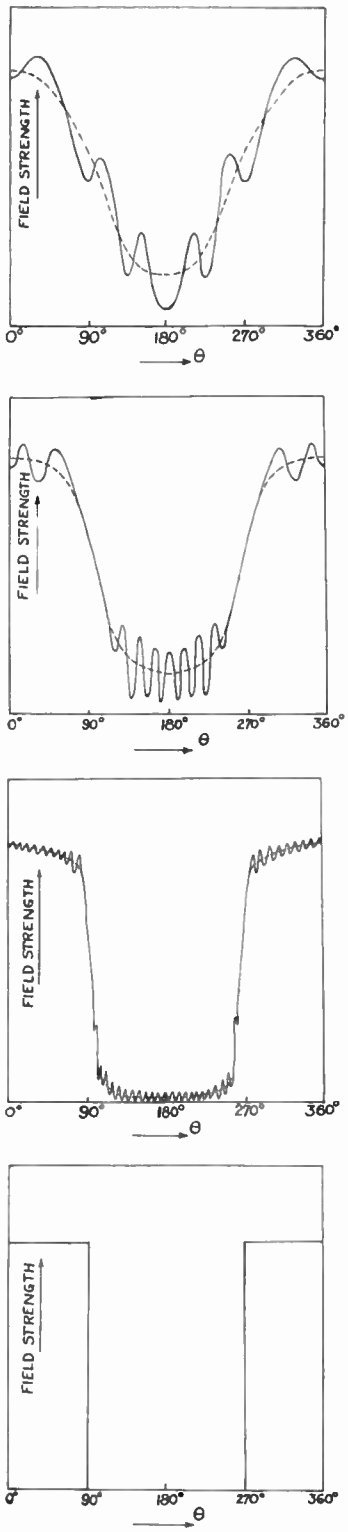

Fig. 2—Azimuth or E-plane radiation patterns for plate width, w, of about 2, 4, 15, and ∞ in wavelength.

Experimentally it was found that the radiation pattern of a plate of given width (W) was independent of its length (L) if:

$$L/W \geqq 1.$$

For sufficiently long plates the calculated and measured radiation patterns agreed very closely, but for narrow plates there was some asymmetry in the patterns due to diffraction effects caused by the waveguide behind the plate. For widths greater than two or three free space wavelengths, this effect was negligible, however.

Conductance

Applying simple physical arguments, such as were used to predict the radiation patterns, it can be shown that the conductance (g) of a resonant slot in a flat metal plate is a damped oscillating function of plate width (W) with a period of about one free space wavelength, λ_0, (Fig. 3).

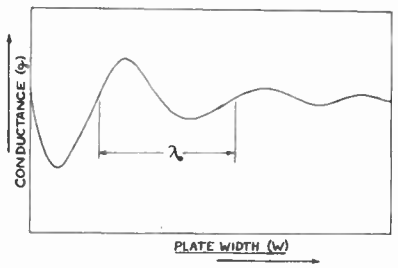

Fig. 3

It was found that the measured and calculated slot conductances, as a function of plate width, agreed very closely except that the measured conductances were always about 10 per cent lower than theoretical ones. This discrepancy may have been due to the fact that theory requires the slot length (l) and slot width (w) to be such that

$$\log_{10}\left(\frac{l}{w}\right) \gg 1.$$

Clearly, this condition is very hard to fulfill in practice.

After the preparation of this paper, further research was done on the method of measuring slot properties. It was found that the technique used above (the quarterwave method) is not, in general, as good as a new method which is independent of the vswr and any reflections from the probe in the slotted line. The essentials of this work will be published shortly. The full mathematical and experimental details of the flat plate antenna discussed here have been given.[1,2]

J. R. Wait,
Central Radio Propagation Lab.,
National Bureau of Standards,
Boulder, Colo.

D. G. Frood,
Physics Dept.,
University of Liverpool,
Liverpool, England.

[1] J. R. Wait and R. E. Walpole, "Calculated radiation characteristics of slots cut in metal sheets," Part I, *Can. J. Tech.*, vol. 33, pp. 211–227; May, 1955 and part II, vol. 34, pp. 60–70; January, 1956.
[2] D. G. Frood and J. R. Wait, "An investigation of slot radiators in rectangular metal plates," *Proc. IEE*, vol. 103, pp. 103–110; January, 1956.

Standard Frequencies and Time Signals WWV and WWVH*

The National Bureau of Standards' Radio Stations WWV (in operation since 1923) and WWVH (since 1949) broadcast six widely used technical services: 1) Standard Radio Frequencies, 2) Standard Audio Frequencies, 3) Standard Time Intervals, 4) Standard Musical Pitch, 5) Time Signals, 6) Radio Propagation Forecasts. All inquiries concerning the technical radio broadcast services should be addressed to: National Bureau of Standards Boulder Laboratories, Boulder, Colorado.

The radio bands in which the foregoing services are broadcast are: 2500 ± 5 kc (2500 ± 2 kc in Region 1); 5000 ± 5 kc; $10{,}000 \pm 5$ kc; $15{,}000 \pm 10$ kc; $20{,}000 \pm 10$ kc; $25{,}000 \pm 10$ kc. These bands were allotted by international agreement, in 1947, for exclusive standard-frequency-broadcast use.

standard of frequency and time interval and making it readily available throughout the United States and over much of the world. The broadcast program is shown schematically in Fig. 1.

Standard Radio Frequencies

Station WWV broadcasts on standard radio frequencies of 2.5, 5, 10, 15, 20, and 25 mc. The broadcasts are continuous, night and day, except WWV is off the air for approximately 4 minutes each hour. The silent period commences at 45 minutes, plus 0 to 15 seconds, after each hour.

Station WWVH broadcasts on standard radio frequencies of 5, 10, and 15 mc. The WWVH broadcast is interrupted for 4 minutes following each hour and half hour and for periods of 34 minutes each day beginning at 1900 UT (Universal Time, UT is the same as GMT and GCT.)

too low for audibility on ordinary radio receivers.

The accuracy of each of the radio frequencies as transmitted is better than 1 part in 100,000,000. The stability (quality of remaining fixed or unvarying) at the transmitter is normally within 1 part in 10^9 at WWV and 5 parts in 10^9 at WWVH. Deviations at WWV are about 2 in 10^{10} each day; frequency adjustments are made each day if necessary at 1900 UT. Deviations at WWVH are about 4 in 10^{10} each day; frequency adjustments are made each day if necessary during the interval 1900 to 1935 UT. If received accuracies better than 3 parts in 10^7 are desired it is necessary to make measurements over a long interval, *e.g.*, 24 hours, to obtain an accuracy of 1 part in 10^8. Such long-interval measurements should preferably be of the type that result in a strip chart record of frequency or phase changes (local oscillator vs WWV or

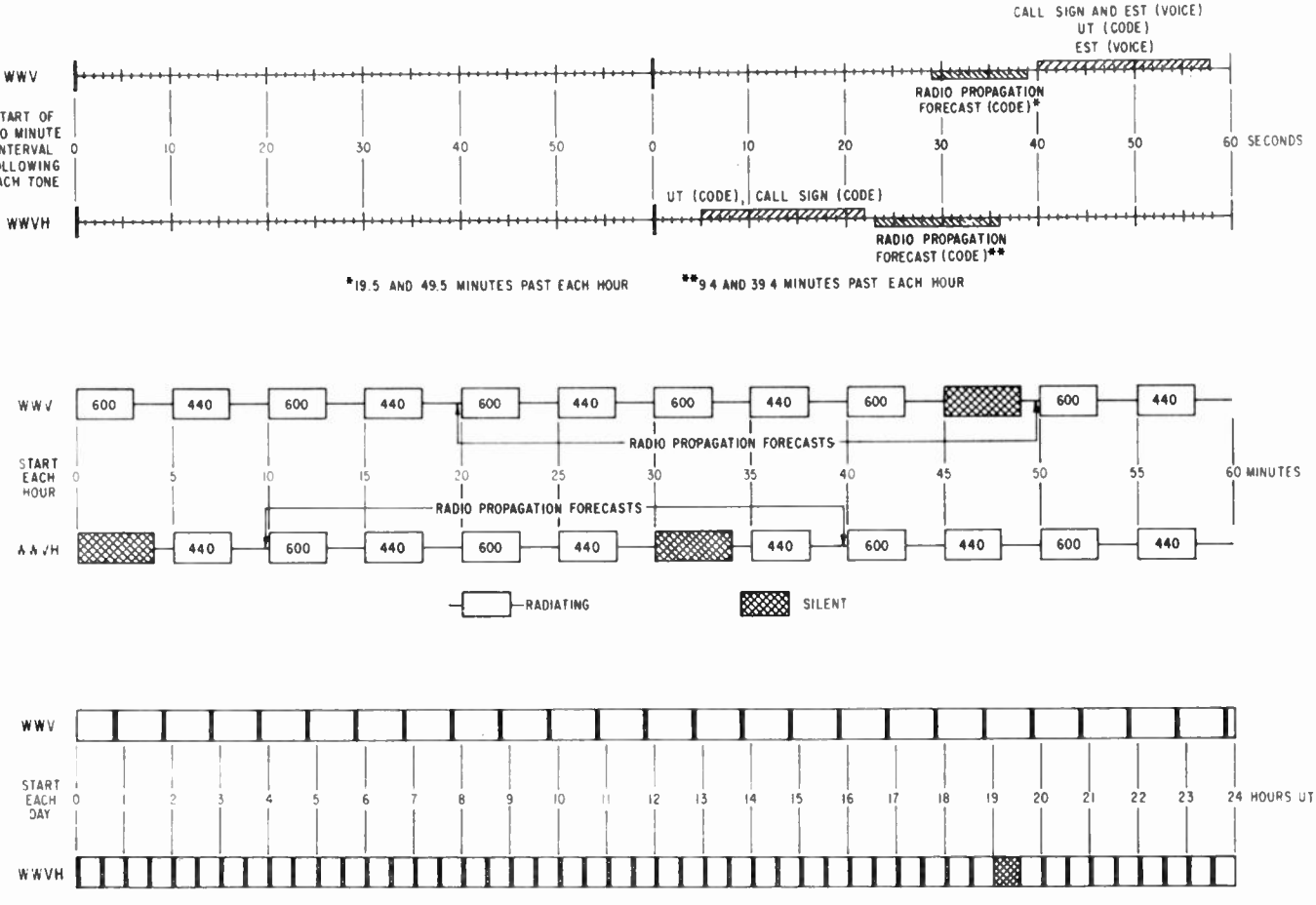

Fig. 1

The National Bureau of Standards' radio stations are located as follows: WWV, Beltsville, Maryland (Box 182, Route 2, Lanham, Maryland); WWVH, Maui, Territory of Hawaii (Box 901, Puunene, Maui, T. H.). Coordinates of the stations are: WWV (lat. 38°59′33″ N., long. 76°50′52″ W.); WWVH (lat. 20°46′02″ N., long. 156°27′42″ W.).

The WWV-WWVH broadcasts are a convenient means of transferring the national

The standard radio frequencies are widely used, *e.g.*, by the communications and electronics industry, research laboratories, and government. A local oscillator may be set vs the received frequency, and any desired radio frequency, including microwave frequencies, may be accurately measured in terms of the standard. The beat frequency method, or variations of it, is generally used. With a very narrow band receiver the standard radio frequency can be used when the received field strength is

WWVH) during the measurement interval. During intervals of about 10 hours or less, one may obtain highest accuracy when ionospheric conditions are normal and when measurements are made at the optimum time of day which is when sunrise or sunset does not occur over the radio propagation path.

Final corrections to the broadcast frequencies are available on a quarterly basis from the National Bureau of Standards Boulder Laboratories, Boulder, Colorado.

* Received by the IRE, July 23, 1956.

Standard Audio Frequencies

Two standard audio frequencies, 440 cps and 600 cps, are broadcast on each radio carrier frequency. The audio frequencies are given alternately starting with 600c on the hour for three minutes, interrupted two minutes, followed by 440c for three minutes and interrupted two minutes. Each 10-minute period is the same except for transmitter interruptions [see 1, p. 1470].

Standard Time Intervals

Seconds pulses at intervals of precisely one second are given as double sideband amplitude modulation on each radio carrier frequency. The pulse duration is 0.005 second. The pulse wave form is shown in Fig. 2. At WWV each pulse consists of five cycles of a 1000c frequency. At WWVH each pulse consists of six cycles of a 1200c frequency. The pulse spectrum is composed of discrete frequency components at intervals of 1.0c. The components have maximum amplitudes at approximately 995c and 1194c for the WWV and WWVH pulses respectively. At WWV the tone is interrupted 0.040 second for the seconds pulse. The pulse commences 0.010 second after commencement of the interruption.

The seconds pulses provide a useful standard time interval for quick and accurate measurement or calibration of time and frequency standards and timing devices. For example, a watch rate recorder may be checked by recording the seconds pulses. Intervals of one minute are marked by omitting the pulse at the beginning of the last second of every minute and by commencing each minute with two pulses spaced by 0.1 second. The two-minute, three-minute, and five-minute intervals are synchronized with the seconds pulses and are marked by the beginning or ending of the periods when the audio frequencies are off.

A time interval as broadcast from WWV is accurate to 1 part in 10^8 plus or minus 1 microsecond. Received pulses have random phase shifts or jitter because of changes in the propagating medium. The magnitudes of these changes range from practically zero for the direct or ground wave to about 1000 microseconds when received via a changing ionosphere. Multiple pulses and echoes are sometimes received because of propagation around the world and reflection from objects

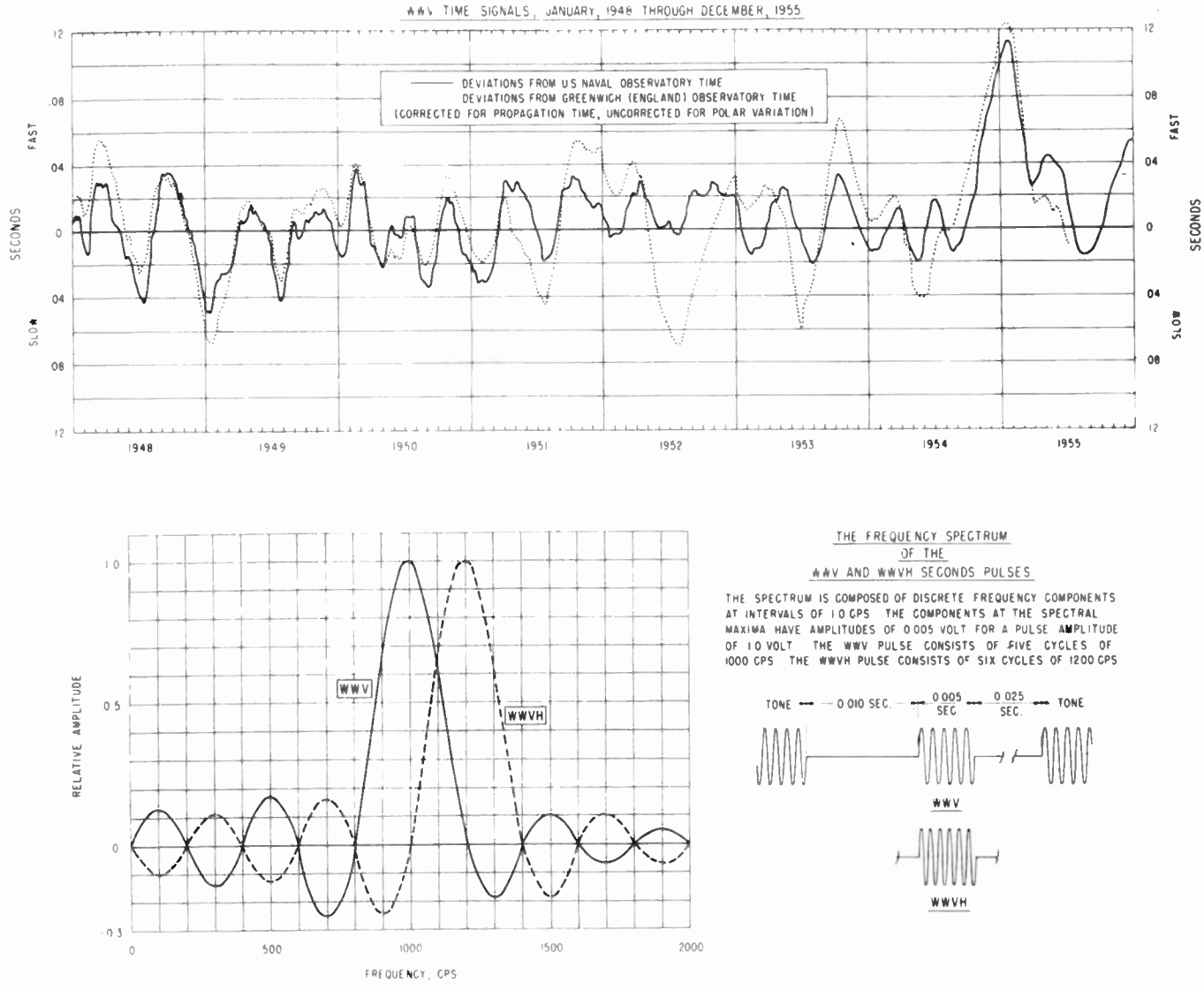

Fig. 2

on the earth's surface. The beginning of the first pulse received, *i.e.*, the part having least delay, is most accurate and should be used. When ionospheric conditions are normal and the correct time of day is chosen, a frequency standard can be checked in a few hours vs WWV with a precision of about 1 part in 10^9; however, it is best to use intervals of 24 hours when comparing with this precision.

In using the time interval markers for high precision work it is necessary to remember that step adjustments of precisely ± 20 milliseconds may be made at the transmitter on Wednesdays at 1900 UT; this is explained under the section on Time Signals.

The seconds pulses from WWVH are adjusted if necessary each day during the interval 1900 to 1935 UT so as to commence simultaneously with those from WWV, within plus or minus 500 microseconds.

Standard Musical Pitch

The frequency 440 cps for note A above middle C has been the standard in the music industry in the United States since 1925. The radio broadcast of this standard was commenced by the National Bureau of Standards in 1937. It is now given six times per hour, 18 minutes per hour, from WWV and WWVH as shown in Fig. 1. With this broadcast the standard pitch is maintained and musical instruments are manufactured and adjusted vs an unvarying standard. Listeners of music are benefited because there are fewer instruments not in tune and practically no instruments are manufactured which cannot be tuned to 440c.

A high frequency or short-wave radio receiver is the only equipment needed to effectively use the musical pitch standard.

Time Signals

The audio frequencies are interrupted at precisely two minutes before each hour. They are resumed precisely on the hour and each five minutes thereafter; they mark accurately the hour and the successive 5-minute periods (see Fig. 1).

Time signals from WWV are maintained in close agreement with uniform time, called UT 2, determined by the U. S. Naval Observatory. This is done by occasional step adjustments in time, when necessary, of precisely plus or minus twenty milliseconds. These adjustments may be necessary several times per year. When required, they are made on Wednesdays at 1900 UT simultaneously at WWV and WWVH.

Universal Time is announced in telegraphic code each five minutes from WWV and WWVH. This provides a quick reference to correct time where a timepiece may be in error by a few minutes. The zero- to twenty-four-hour system is used starting with 0000 at midnight. The first two figures give the hour and the last two figures give the number of minutes past the hour when the tone returns. For example, at 1655 UT, or 11:55 A.M., Eastern Standard Time, four figures (1, 6, 5, and 5) are broadcast in code. The time announcement refers to the end of an announcement interval, *i.e.*, when the audio frequencies are resumed.

At Station WWV a voice announcement of *Eastern* Standard Time is given before and after each telegraphic code announcement. For example, at 9:10 A.M., EST, the voice announcement in English is: "National Bureau of Standards, WWV; when the tone returns, Eastern Standard Time is 9:10 A.M."

Final corrections to the time signals, as broadcast, are determined and published, on a weekly basis, by the U. S. Naval Observatory, Washington 25, D. C.

Radio Propagation Forecasts

A forecast of radio propagation conditions is broadcast in telegraphic code on each of the standard radio carrier frequencies: from WWV at approximately 19.5 and 49.5 minutes past each hour, and from WWVH at approximately 9.4 and 39.4 minutes past each hour, as shown in Fig. 1. Propagation notices were first broadcast from WWV in 1946; the present type of announcement has been broadcast from WWV since July, 1952, and from WWVH since January, 1954.

The forecast announcement tells users the condition of the ionosphere at the regular time the forecast is made and how good or bad communication conditions are expected to be in the succeeding 6 or more hours. The NBS forecasts are based on information obtained from a world-wide network of geophysical and solar observatories, including radio soundings of the upper atmosphere, short-wave reception data, and similar information. Trained forecasters digest the information and formulate the predictions.

From WWV the forecasts refer only to North Atlantic radio paths, such as Washington to London or New York to Berlin. The times of issue are 0500, 1200 (1100 in summer), 1700, 2300 UT. These are the short-term forecasts prepared by NBS-CRPL North Atlantic Radio Warning Service, Box 178, Fort Belvoir, Va.

From WWVH the forecasts are for North Pacific radio paths, such as Seattle to Tokyo or Anchorage to San Francisco. The times of issue are 0200 and 1800 UT, with these forecasts first broadcast at 0239 and 1839 UT respectively. These are short-term forecasts prepared by NBS-CRPL North Pacific Radio Warning Service, Box 1119, Anchorage, Alaska. (Another short-term forecast at 0900 UT may be broadcast at a later date.)

The forecasters assume that the most suitable radio freqencies for communications are available and in use for the typical paths. Because of this assumption, their notices must be interpreted on a relative scale in terms of experience on each radio circuit in use. It is impossible to rate conditions on an absolute scale since the varied effects of transmitter power, type of communications traffic and procedure, antennas and receivers, prevent an evaluation which will be valid for all circuits. One purpose of broadcasting both a description and a forecast is to show more clearly whether propagation conditions are expected to deteriorate or improve in the coming period.

The forecasts broadcast by WWV and WWVH apply only to short-wave radio transmissions over paths which are near the auroral zone for a considerable part of their length. In this zone the ionospheric layers are very likely to be disturbed, and because short-wave, long-range radio transmissions are dependent on the condition of the ionosphere, communications may be disrupted. Often the ionospheric disturbance accompanies intense magnetic field variations and a brilliant aurora. The resulting propagation effects range from severe fading to a complete break in the communications link.

The forecast is broadcast as a letter and a digit. The letter portion of the announcement identifies the radio quality at the time the forecast is made. The letters denoting quality are "N," "U," and "W," signifying that radio propagation conditions are normal, unsettled, and disturbed. The digit portion is the forecast of the radio propagation quality on a typical North Atlantic (from WWV) or a typical North Pacific (from WWVH) transmission path during the 6 or more hours after the forecast is made. Quality is graded in steps ranging from 1 (useless) to 9 (excellent) as follows in Table I. If, for example, propagation conditions at the time the forecast is made are normal but are expected to be only "poor-to-fair" within the next 6 or more hours, the announcement would be broadcast as N4 in international Morse code.

TABLE I

Disturbed Grades (W)	Unsettled Grade (U)	Normal Grades (N)
1—useless 2—very poor 3—poor 4—poor-to-fair	5—fair	6—fair-to-good 7—good 8—very good 9—excellent

Radiated Power, Transmitting Antennas, Modulation

Radiated power is shown in Table II below.

TABLE II

Frequency, mc	Power, kw WWV	Power, kw WWVH
2.5	1	
5	8	2
10	9	2
15	9	2
20	1	
25	0.1	

The broadcast on 2.5 mc is from a vertical quarter-wave antenna. The broadcasts on all other frequencies are from vertical half-wave dipoles. The radiation is omnidirectional.

The per cent amplitude modulation, double sideband, is:

audio frequencies 440 or 600 cps — 75 per cent
voice and seconds pulses, peak, — 100 per cent.

At WWV, the tone frequency 440 or 600 cps, except on 25 mc, is experimentally operated as a single upper sideband with full carrier. Power output from the sideband transmitter is about one-third the carrier power. Single sideband tone on 25 mc may be added at a later date. Other signals (announcements and seconds pulses) are double sideband, 100 per cent amplitude modulation.

Accuracy

Frequencies from WWV and WWVH are accurate to within 1 part in 10^8 as broadcast; this is with reference to the U. S. Naval Observatory time and is limited by uncertainties in the immediate determination of astronomical time.

The radio frequencies may be consistently received with accuracies equal to those transmitted for several hours per day during total light or total darkness over the transmission path at locations in the service range. This was described in the first section.

Large errors are caused by motion of the radio receiver relative to the transmitting stations or by motions of the reflecting ionospheric layers on which long-distance radio propagation depends. For example, on a vehicle moving 60 miles per hour relative to a fixed station, the received frequency would be in error by about 1 part in 10^7. Measurements made at NBS Boulder Laboratories and at WWVH have shown that during the course of the day errors in the received frequencies vary approximately -3 to $+3$ parts in 10^7.

Daily deviations in frequency and time of stations WWV and WWVH are tabulated on a quarterly basis. These data are available on request. In Fig. 2 are plotted time signal deviations extending back 7 years. The deviations may be considerably less commencing in 1956.

Distance Range of Reception

Of the standard radio frequencies (2.5, 5, 10, 15, 20, and 25 mc), the lowest provide service to short distances, and the highest to great distances. Reliable reception is in general possible throughout the United States and the North Atlantic and Pacific Oceans, and reception at times throughout the world. One should select the frequency that gives best reception at any particular place and time. This can be done by two methods:

1) By tuning to the different frequencies and selecting the one most suitable at that time.

2) By making use of techniques of prediction of usable frequencies. NBS publications useful for this purpose are the reports of the CRPL-D series, "Basic Radio Propagation Predictions," which are issued monthly, three months in advance of the month of prediction, and Circular 465 of the National Bureau of Standards, "Instructions for the Use of Basic Radio Propagation Predictions." These two publications may be obtained from the Superintendent of Documents, U. S. Government Printing Office, Washington 25, D. C., price in U. S. $1.00 per year (12 issues) and 30 cents per copy, respectively (foreign, $1.25, and 40 cents).

Other Standard Frequency and Radio Time Signal Services

The U. S. Naval Observatory, Department of the Navy, broadcasts time signals at regular intervals from NSS (Annapolis, Md.), NPG (Mare Island, Calif.), NPM (Pearl Harbor, Hawaii), NBA (Balboa, Canal Zone). Detailed information may be obtained from the U. S. Naval Observatory, Washington 25, D. C.

The Dominion Observatory, Ottawa, Canada, broadcasts time signals continuously over Station CHU on frequencies of 3330, 7335 and 14670 kc. Information may be obtained by writing the Dominion Observatory.

A comprehensive list of United States and foreign radio time signals is given in chapter 3 of "Radio Navigational Aids," Hydrographic Office publication No. 205, for sale by the Hydrographic Office, Washington 25, D. C., price $2.00, U. S. or foreign.

Standard frequencies and time signals are broadcast by other stations as indicated in Table III above.

TABLE III

Call Sign	Location	Carrier Frequency Mc	Modulation cps	Carrier Power kw
LOL	Buenos Aires, Argentina	2.5, 5, 10, 15, 20, and 25	1, 440, 1000	2
ZUO	Johannesburg, South Africa	5	1	0.1
ZLFS	Lower Hutt, New Zealand	2.5	—	0.035
—	Moscow, USSR	10 and 15	1	—
MSF	Rugby, England	2.5, 5, and 10	1, 1000	0.5
JJY	Tokyo, Japan	2.5, 5, 10, and 15	1, 1000	1
IBF	Torino, Italy	5	1, 440, 1000	0.3
—	Uccle, Belgium	2.5	—	0.02

National Bureau of Standards,
Boulder Laboratories,
Boulder, Colo.

Analog Computer Amplifier Circuits*

Operational amplifiers most frequently found in electronic analog computers have a general connection shown in the block diagram of Fig. 1(a). Here, A is a dc amplifier whose gain is real and negative over the range of operating frequencies, and N_I and N_F are the input and the feedback networks, respectively. If the gain of A is sufficiently high, the transfer function is determined only by N_I and N_F. In this case the terminals b and c are essentially at the ground potential.[1] Then it can be said that, so long as the reciprocity theorem holds with these networks, the terminal connections of the networks may be reversed with no change in the transfer function. In other words, the operational amplifiers of Fig. 1(b), 1(c), and 1(d) give the same transfer function.

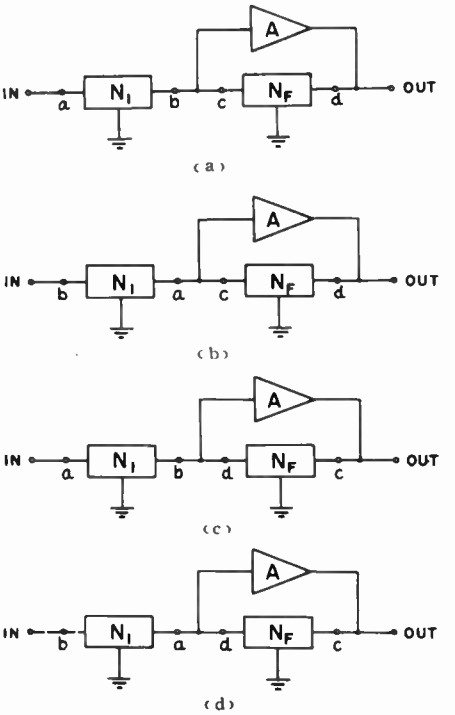

Fig. 1—Operational amplifiers.

An example follows: Fig. 2(a) is a constant coefficient multiplier commonly found in analog computers, whereas Fig. 2(b) is a new constant coefficient multiplier derived from Fig. 2(a) using the principle described above. These multipliers have the identical transfer function when the gain A is very high. When the gain A is limited, the transfer function is affected by A. The amount of error due to this effect depends on the circuit connection. The circuit of Fig. 2(a) is superior, in this respect, to that of Fig. 2(b). However, the latter has a higher input impedance than the former, because R_1 is usually made much higher than R to reduce the error resulting from potentiometer loading.

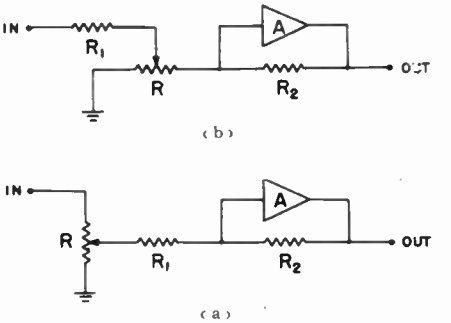

Fig. 2—Constant coefficient multipliers.

Hiroshi Amemiya,
Showa Denshi, Ltd.,
Totsuka-ku,
Yokohama City, Japan.

* Received by the IRE, June 20, 1956.

[1] G. A. Korn and T. M. Korn, "Electronic Analog Computers," McGraw-Hill Book Co., Inc., New York, N. Y., 1952; Ch. 4.

Spurious Modulation in Q-Band Magnetrons*

This note is concerned with further evidence of spurious modulation of electron streams and should be read in conjunction with a recent paper by C. C. Cutler.[1]

In the course of the development of a Q-band magnetron designed to operate in the minimum voltage regime[2] at a wavelength of around 8–9 mm, strong spurious modulation of the output has been observed. The experimental setup is shown in Fig. 1.

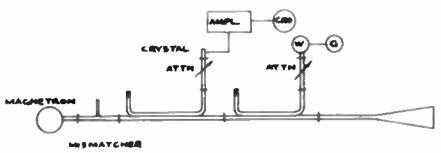

Fig. 1

It consists of a magnetron feeding through a mismatcher and two directional couplers a matched load in the form of a rectangular horn. The first directional coupler is terminated by a crystal of approximately square law characteristic; the output from the crystal is taken to the deflecting plates of a cro via a 50 cps–5 mc amplifier. The second directional coupler is used for providing a wavemeter reading.

It was observed that for certain positions of the mismatcher spurious modulation approximately of the form shown in Fig. 2 would appear in the output of most tubes.

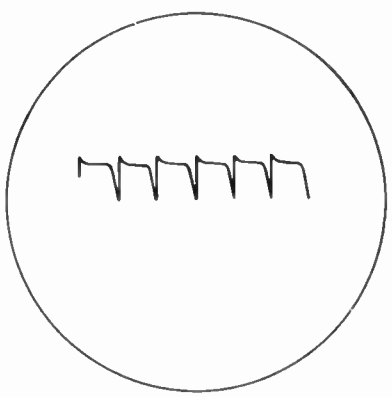

Fig. 2

Fig. 3 shows frequency, relative power, and the spurious modulation plotted against the position of the mismatcher for a typical tube.

The modulation in most cases was markedly of the relaxation type; its frequency for all tubes would vary from 1 kc to 2 mc. For any given tube the range of frequency variation was considerably smaller, the amplitude and frequency depending strongly on the position of the mismatcher. The frequency was always lowest just before the modulating oscillations would disappear, usually at the point opposite to the frequency jump. The oscillations always depended on all the parameters of the tube which themselves showed a large degree of interdependency. The oscillations could be partly locked for observations on a cathode-ray tube. The amplitude of the modulation was always at least 1000 times greater than the mean amplitude of the accompanying noise generated by the tube.

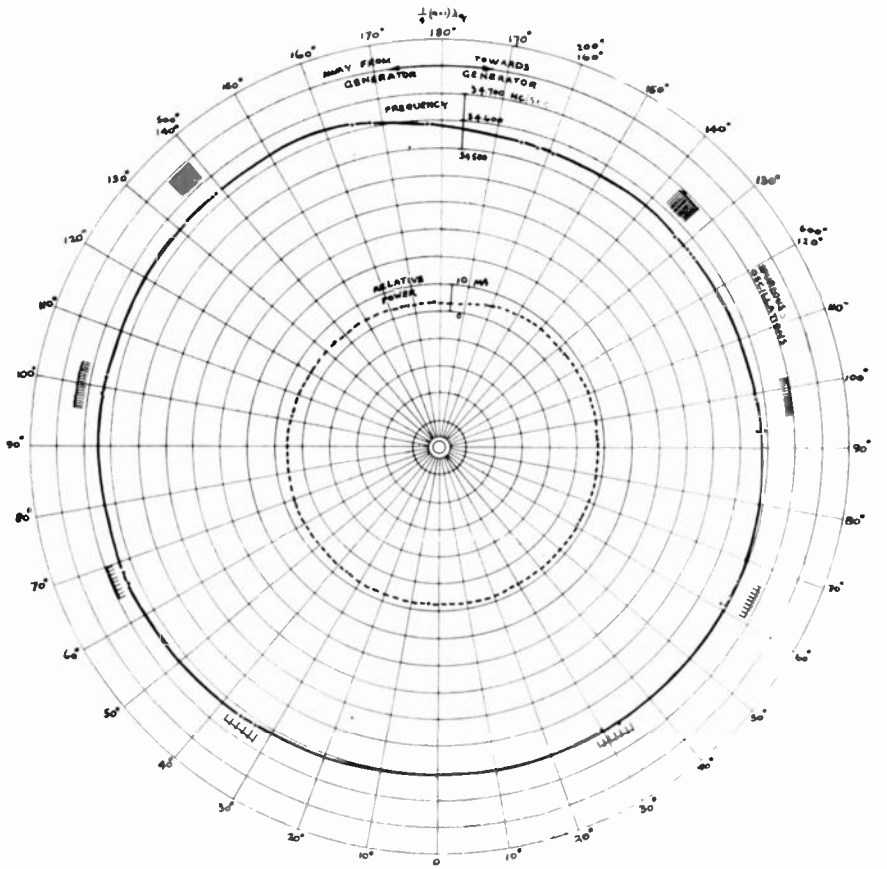

Fig. 3—Tube 215, hob 31, block 538. Ia=30 ma; Va=5.3 kv.

It was discovered eventually that a judicious adjustment of the position of the cathode while the tube was running provided the only way of reducing, or even altogether eliminating the modulation. Often the position of the cathode for minimum spurious modulation would not necessarily coincide with the position of the cathode for the sharpest cut-off. The modulation would appear equally when the tubes were run continuously or under interrupted cw conditions, although individual tubes would normally show a preference either for one or the other mode of operation.

It seems that the spurious modulation observed in our case was caused by the "ion plasma" oscillations together with some "ionization relaxation" effects, as described by Cutler in his paper. Our range of frequencies (1 kc–2mc) agrees with the range of frequencies of 100 kc–2 mc for "ion oscillations" and 10–100 kc of "relaxation oscillations" given by Cutler, both types of oscillations occurring quite readily at pressures of 10^{-6} mm Hg and finally disappearing at about 10^{-7} mm Hg. In our case the pressure was thought to be between 5.10^{-6} and 5.10^{-4} mm Hg in most tubes. When the tube was pulsed (2 kc, 1:1 duty ratio) in many cases the oscillations would take time to develop; a time lag of 50–100 μsec was quite common in such cases. It is of some interest that the oscillations could be excited in many cases by tapping the tube and inducing microphony in the cathode assembly.

The mechanism of oscillations suggested by Cutler seems possible in our case for the following reasons. It is known that the cathodes of magnetrons are nearly always subjected to strong back bombardment. The tube in question was actually relying on the back bombardment to keep the cathode temperature sufficiently high, once the initial filament current was switched off. It seems reasonable to assume that this type of powerful back bombardment of the cathode would almost certainly let loose large numbers of secondary electrons into the interaction space. According to Cutler these secondaries, in his case obtained from the collector, are essential to the generation of "ion oscillations." Our own experience of reducing the oscillations by centering the cathode seems to favor this conclusion. It might be of interest to add that the change from tantalum to thoria emitter, both having fairly similar coefficients of secondary emission, did not seem to affect these spurious oscillations in any appreciable way. Cooling of the anode block would, however, in many cases, reduce them. Further, since the tube was operated in the minimum voltage regime, large spread of the space charge would favor the creation of areas of low field strength where the mechanism of "ionization relaxation" suggested by Cut-

* Received by the IRE, July 13, 1956.

[1] C. C. Cutler, "Spurious modulation of electron beams," PROC. IRE, vol. 44, pp. 61–64; January, 1956.

[2] W. E. Willshaw and R. G. Robertshaw, "The behaviour of multiple circuit magnetrons in the neighbourhood of the critical anode voltage," *Proc. Phys. Soc. B*, vol. 63, pp. 41–45; January, 1950.

ler could operate. This would explain the admixture of low frequency (1–100 kc) components in the spectrum of the spurious oscillations, although at the time it was unfortunately impossible to embark on the direct investigation of the dependence of those oscillations on the pressure within the tube.

Summing up, it seems reasonable to assume that the validity of Cutler's work is much wider than would be generally inferred from the simple boundary conditions of his experiments.

ACKNOWLEDGMENT

Acknowledgment is made to the Admiralty for permission to publish this letter.

T. M. GOSS AND P. A. LINDSAY,
Res. Labs.,
The Gen. Elec. Co. Ltd.,
Wembley, England.

Inductive AC Admittance of Junction Transistor*

It has been customary to take the small signal ac admittance of the transistor as capacitive. An experimental study reveals, however, that both the collector and the emitter admittances become inductive under certain conditions.

A typical plot of grounded-base open-circuit collector admittance against collector current for a *p-n-p* alloy junction

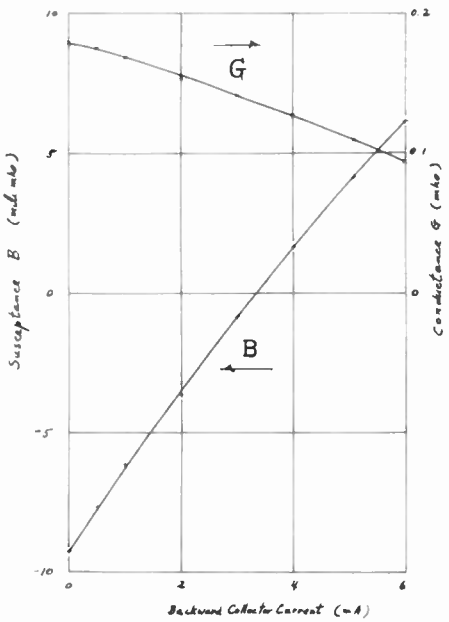

Fig. 1—Collector conductance (G) and susceptance (B) vs backward collector current for *p-n-p* alloy junction transistor, for emitter current of 10 ma.

transistor is shown in Fig. 1. It should be noted that the emitter current is held constant to a high value of 10 ma. It was measured at angular frequency of 3×10^8 radians/sec (47.7 kc) using a bridge specially designed to cover a wide range of variation of admittance. The amplitude of the ac signal across the transistor was held below 10 mv. It can be seen that, besides the variation of conductance with collector current, there is a remarkable variation of susceptance. At high collector current the susceptance is capacitive as usual, but it decreases almost linearly with the collector current until it becomes inductive. A change of emitter current shifts the intercept, where the susceptance is zero, but does not modify the slope greatly.

Fig. 2 shows the relation between the collector and the emitter currents at which the collector admittance (curve C) or the emitter admittance (curve E) have zero susceptance. To avoid confusion we call the junction of the larger area *collector*, and another *emitter*, regardless of bias direction.

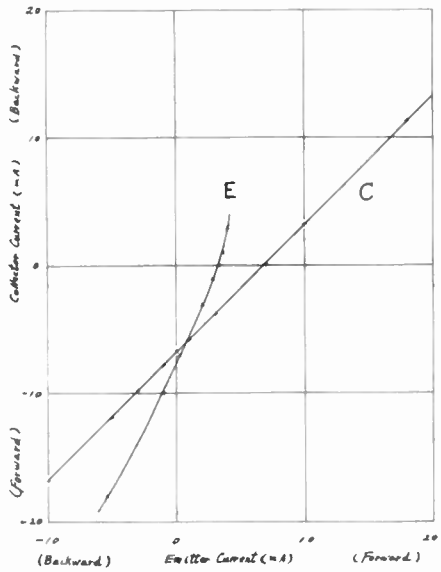

Fig. 2—Relation between the collector and the emitter currents at which the collector admittance (curve C) or the emitter admittance (curve E) have zero susceptance for *p-n-p* alloy junction transistor.

In the first quadrant of Fig. 2 the transistor is biased as in the ordinary operation, while in the third quadrant, as in the inverted operation, the collector is forward-biased and the emitter is backward-biased. It can be seen that both junctions may have inductive admittance in both operations when the forward-biased current is high. In the fourth quadrant both junctions are forward-biased.

Fig. 3 is a plot similar to Fig. 2 for a *n-p-n* grown junction transistor. A marked difference from Fig. 2 is that inductive admittance does not occur for the backward-biased junction, though it does for the forward-biased junction.

Measurements of other parameters reveal that grounded-base short-circuit admittances may become inductive as well as open-circuit admittances. However, no change of sign of imaginary part has been observed for the current amplification factors when the bias currents vary.

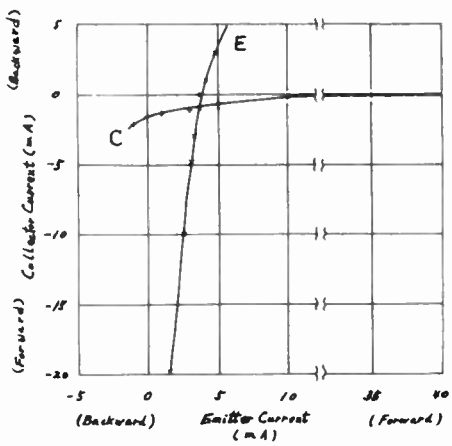

Fig. 3—Plot similar to Fig. 2 for *n-p-n* grown junction transistor.

We are indebted to Profs. N. Takagi, M. Imaoka, and Y. Adachi for many stimulating suggestions.

M. ONOE AND A. USHIROKAWA,
Institute of Industrial Science,
University of Tokyo,
Chiba City, Japan.

Note on "The Variation of Junction Transistor Current Amplification Factor with Emitter Current"*

In 1954, W. M. Webster in the above paper[1] and E. S. Rittner[2] published theories describing the variation of α with emitter current for junction transistors. While the assumptions made were approximately equivalent, the limiting forms of the current dependence at high currents given by the two treatments differed by a factor of two. This disagreement has been noted[3] but it seems worthwhile to point out its source in detail and to show how rectification of an error in Webster's treatment brings the two theories into concord. This is the more necessary since Webster's treatment is that usually referred to by transistor engineers. We shall use Webster's notation throughout and refer to his paper for definition of the symbols used.

Webster's (15) describes the variation of emitter efficiency with current by

$$\frac{\partial I_{Ee}}{\partial I_{Ep}} \approx \frac{\sigma_b W}{\sigma_e L_e}(1+Z) \qquad (1)$$

whereas Rittner's (70) can be manipulated to give, in Webster's notation,

$$\frac{\partial I_{Ee}}{\partial I_{Ep}} \sim \frac{\sigma_b W}{\sigma_e L_e}\cdot\frac{Z}{2} \qquad (2)$$

for $Z \gg 1$ and $1-\gamma \ll 1$.

* Received by the IRE, July 2, 1956.

* Received by the IRE, June 11, 1956.

[1] PROC. IRE, vol. 42, pp. 914–920; June, 1954.

[2] E. S. Rittner, "Extension of the theory of the junction transistor," *Phys. Rev.*, vol. 94, pp. 1161–1171; June, 1954.

[3] Toshio Misawa, "Emitter efficiency of junction transistor," *J. Phys. Soc. Japan*, vol. 10, pp. 362–367; May, 1955.

Webster's error lies in ignoring his own warning[4] and simply substituting

$$\sigma_b\left(1+\frac{Z}{2}\right)$$

for σ_b in his (6). While the majority carrier density in the base near the emitter is modified by this factor, or more properly by $(1+hZ)$, where

$$h(Z)=\frac{1}{Z}\int_0^Z g(Z)dZ=\frac{1}{Z}\cdot\frac{p_e}{N_d} \qquad (3)$$

with a consequent increase in I_{Ee}, there is also an increase in I_{Ep} due to the increase in the effective diffusion coefficient of holes in the base region because of the potential gradient. This is described[5] by writing $D_p/h(Z)$ for D_p in the equations from which Webster's (6) is derived. The result is then

$$\frac{I_{Ee}}{I_{Ep}}=\frac{\sigma_b W}{\sigma_e L_e}(1+hZ)h. \qquad (4)$$

Now, following Webster, we find

$$\frac{\partial I_{Ee}}{\partial I_{Ep}}=\frac{\sigma_b W}{\sigma_e L_e}(1+2hZ)g \qquad (5)$$

which, since both $g(Z)$ and $h(Z)$ approach $\frac{1}{2}$ for large Z, is seen to agree with Rittner's result (2).

[4] Webster, *op. cit.*, footnote 4.
[5] To an approximation similar to that used in other parts of Webster's treatment.

A similar disagreement occurs in the two treatments of volume recombination. Rittner's treatment neglects variation of τ with injection level, but his (74) shows that if transport loss only is considered, then

$$1-\alpha\approx\frac{1}{2}\left(\frac{W}{L_b}\right)^2 \quad \text{for} \quad Z\to 0 \qquad (6)$$

and

$$1-\alpha\approx\frac{1}{4}\left(\frac{W}{L_b}\right)^2 \quad \text{for} \quad Z\to\infty. \qquad (7)$$

This is a consequence of the doubling of the effective diffusion coefficient of minority carriers in the base region at high currents.

Webster has again neglected this effect in deriving his (16) which states

$$\frac{\partial I_{VR}}{\partial I_{Ep}}=\frac{1}{2}\left(\frac{W}{L_b}\right)^2(1+Z). \qquad (8)$$

Since the $(1+Z)$ factor relates only to variation of τ,[6] which was neglected by Rittner, (8) is clearly at variance with (6) and (7).

When this effect is included in Webster's treatment, we find, in place of (8),

$$\frac{\partial I_{VR}}{\partial I_{Ep}}=\frac{1}{2}\left(\frac{W}{L_b}\right)^2(1+2hZ)g. \qquad (9)$$

Webster's result for surface recombination loss is correct (on the basis of the assumption that s does not depend on injection level) and gives

$$\frac{\partial I_{SR}}{\partial I_{Ep}}=\frac{sWA_s}{D_pA}g(Z). \qquad (10)$$

The final result is thus

$$\frac{1}{\alpha_{cb}}\approx\frac{sWA_s}{D_pA}g(Z)+\left[\frac{\sigma_b W}{\sigma_e L_e}+\frac{1}{2}\left(\frac{W}{L_b}\right)^2\right](1+2hZ)g(Z) \qquad (11)$$

and differs from Webster's original result in that the "fall-off factor" is now

$$(1+2hZ)g\approx\tfrac{1}{2}(1+Z) \qquad (12)$$

rather than

$$f(Z)=1+(g+h)Z\approx 1+Z. \qquad (13)$$

This correction to the theory alters in a corresponding way (by the introduction of a factor $\frac{1}{2}$ into the fall-off factor at high levels) the results of other derivations based upon it.[7] It does not affect the observed agreement of Webster's expression with experiment, since comparisons have generally been made[1,8] by choosing values of s and $\sigma_e L_e$ yielding best fit.

N. H. Fletcher,
Div. of Radiophysics,
C.S.I.R.O.,
Sydney, Australia.

[6] Recent work indicates that the variation of τ with injection level may be more complicated than this assumed linear variation (private communication from Webster), as also does the Hall-Shockley-Read recombination theory. A different fall-off factor may therefore prove necessary for the volume recombination term.

[7] N. H. Fletcher, "Self-bias cut-off effect in power transistors," PROC. IRE, vol. 43, p. 1669; November, 1955.
[8] L. J. Giacoletto, "Variation of junction transistor current amplification factor with emitter current," PROC. IRE, vol. 43, p. 1529; October, 1955.

Contributors

Dodge J. Angelakos (A'45–S'48–A'49–SM'52) received the B.S.E.E. degree from Notre Dame in 1942, and the M.S. and Ph.D. degrees from Harvard in 1946 and 1950.

D. J. Angelakos

He was employed by the Westinghouse Electric Company from 1942 to 1943. From 1943 to 1946 he was an instructor at Notre Dame. He was a teaching fellow at Harvard's Cruft Laboratories during 1947 and 1949, and an electronics research engineer during 1949–1950. In 1950 he returned to Notre Dame as an assistant professor. Since 1951 he has been with the Electrical Engineering Division of the University of California at Berkeley. He became associate professor in 1954, and conducts research in microwaves and ferrites. He is a member of Sigma Xi.

Joseph O. Artman was born in New York, N. Y., on April 22, 1926. He received the B.S. degree in physics from the College of the City of New York in 1944. From 1944 to 1946 he served in the U. S. Navy. In 1948 and 1953 respectively, he received the M.A. and the Ph.D. degrees in physics from Columbia University in New York, N.Y. From 1952 to 1955 he was a staff member at Lincoln Laboratory, Massachusetts Institute of Technology, Cambridge, Mass., engaged in studies on the microwave properties of ferrites. Since October 1, 1955 he has been continuing this work as a research fellow at Harvard University.

J. O. Artman

Dr. Artman is a member of the American Physical Society and Sigma Xi.

Leonard A. Ault was born October 28 1933 in Chicago Heights, Ill. He received the B.S. degree in physics from Roanoke College, Salem, Va., in June, 1955. He then joined the Microwave Development Section of the Diamond Ordnance Fuze Laboratories, where he is engaged in developing techniques for the precise measurements of the microwave properties of ferrites. He is also a graduate student in physics at the University of Maryland.

L. A. Ault

❖

For a photograph and biography of A. D. Berk, see page 1672 of the November, 1955 issue of PROCEEDINGS OF THE IRE.

N. Bloembergen was born in 1920, in the Netherlands. He studied physics at the University of Utrecht. After the war he came to Harvard and did research in nuclear magnetic resonance with Purcell. He obtained the Ph.D. degree in 1948 at the University of Leiden where he was a research associate. In 1949, he returned to Harvard as a member of the Society of Fellows and was appointed associate professor of applied physics at Harvard in 1951. His research work lies in the field of solid state physics with particular emphasis on magnetic resonance experiments.

N. BLOEMBERGEN

He is a fellow of the American Physical Society, associate editor of the *Physical Review*, member of the Netherlands Physical Society, corresponding member of the Koninklijke Nederlandse Akademie van Wetenschappen, and member of the American Academy of Arts and Sciences.

❖

James H. Burgess was born in Portland, Ore., on May 11, 1929. He attended the State College of Washington and received the B.S. degree in chemistry in 1949 and the M.S. degree in physics in 1951. Subsequently Dr. Burgess studied at Washington University in St. Louis where he received the Ph.D. degree in physics in 1955. His research was in the fields of nuclear and paramagnetic resonance.

J. H. BURGESS

Since 1955 he has been employed by the Electronic Defense Laboratory of Sylvania Electric Products, Inc. where he has worked on the applications of ferrites at microwave frequencies.

Dr. Burgess is a member of the American Physical Society and Sigma Xi.

❖

John C. Cacheris (M'48–SM'56) was born on May 18, 1916, in Chicago, Ill. He graduated from the Capitol Radio Engineering Institute in 1941. He received the B.S. degree in electrical engineering from Carnegie Institute of Technology in 1946, and the M.S. degree from Maryland University in 1953.

J. C. CACHERIS

From 1941 to 1946 Mr. Cacheris was employed as a radio engineer in the test department of Radio Division of the Westinghouse Electric Corporation, Baltimore, Md. From 1946 until 1949, as an electronic scientist with the Naval Ordnance Laboratory in White Oak, Md., he designed circuits and instruments for ultra high and microwave frequency ranges.

He joined the staff of the Ordnance Development Division of the National Bureau of Standards, Washington, D. C. in 1949, where he engaged in microwave antenna and diffraction studies, and in investigations of the microwave properties of ferrites. He is continuing the latter investigations at the Diamond Ordnance Fuze Laboratories, Department of the Army, to which the functions and staff of the Ordnance Development Division were transferred on September 27, 1953. He is chief of the Ferrite Research Section of the Supporting Research Laboratory.

Mr. Cacheris is a member of the American Physical Society and Eta Kappa Nu, and is a registered professional engineer in the District of Columbia.

❖

Ernest R. Carlson (S'49–A'50–M'55–SM'56) was born August 3, 1923, at Tacoma, Wash. Following Military Service in the Army Signal Corps, he attended Washington State College, receiving the B.S.E.E. degree in 1949.

E. R. CARLSON

Mr. Carlson joined the General Electric Company in 1949, and following graduation from the test engineering program, he joined the High-Frequency Transmission and Radiation unit of the General Electric Electronics Laboratory.

Since July 1955, he has been with the Heavy Military Electronics Equipment Department of General Electric.

❖

Bengt N. Enander (A'55) was born in Lund, Sweden, on December 9, 1928. He attended the Royal Institute of Technology in Stockholm, where he received the M.S. degree in physics in 1952. He also did postgraduate work in nuclear physics at the same school.

B. N. ENANDER

Since 1952, Mr. Enander has been employed by the Svenska Elektronror in Stockholm, where he has been working on the development of microwave tubes. During 1955 he was with the RCA Laboratories in Princeton, N. J., as an American-Scandinavian Foundation Fellow. While there he was engaged in microwave applications of ferrites.

❖

Clifford E. Fay (A'26–SM'45–F'55) was born December 2, 1903, in St. Louis, Mo. He attended Washington University in St. Louis and received the B.S. degree in 1925 and the M.S. degree in 1927.

C. E. Fay

In 1927, he joined the Bell Telephone Laboratories, Murray Hill, N. J., where he was engaged in electron tube development. Since 1955, he has been in ferrite device development work. He is a member of Sigma Xi and Tau Beta Pi.

❖

Donald L. Fresh was born in Wheeling, W. Va. in 1927. He served as an electronics technician in the United States Navy during the years 1945 and 1946. Mr. Fresh received the B.S. degree in chemistry from the University of Maryland in 1951. In 1956, he received the Ph.D. degree in physical chemistry from the Catholic University of America in Washington, D.C. for a study of the solid state reaction kinetics of the formation of magnesium ferrite. He was employed in the Ceramic Section of the Eastern Experiment Station of the Bureau of Mines, at College Park, Md. from 1949 to 1956. Mr. Fresh is now Vice-President of Research and Development at Trans-Tech, Inc., Rockville, Md.

D. L. FRESH

He is a member of the American Chemical Society, Alpha Chi Sigma, and Sigma Xi. He is also a consulting member of the ASTM Committee C-21 Ferrites Section.

❖

Gerald S. Heller was born on September 5, 1920, in Detroit, Mich. He received the Sc.B. degree in physics in January, 1942, from Wayne University.

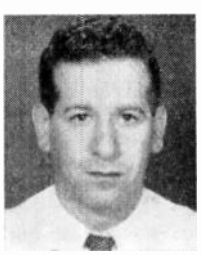

G. S. HELLER

From 1942 to 1945 he was a staff member of the Radiation Laboratory at Massachusetts Institute of Technology. For one year during this period he was a member of the Australian Group of the Radiation Labora-

tory at the Radio Physics Laboratory in Sydney.

After leaving M.I.T. he was a Fellow in applied mathematics at Brown University, where he received the Sc.M. degree in applied mathematics in 1946, and the Ph.D. degree in physics in 1948. Dr. Heller remained at Brown until 1954 as Assistant Professor of physics, and worked in theoretical acoustics.

Since 1954 he has been a member of the Microwave Section of the Solid-State Group at the Lincoln Laboratory, M.I.T.

❖

C. Lester Hogan (SM'54) was born on February 8, 1920, in Great Falls, Mont.

In 1942, he received the B.S. degree from Montana State College; in 1947, the M.S. degree from Lehigh University, and in 1950, the Ph.D. degree in physics. Harvard University conferred an honorary M.A. degree upon him in 1954.

C. L. Hogan

Following his graduation from Montana State, Mr. Hogan became a research engineer with the Anaconda Copper Mining Company. From 1943 to 1946 he served as a lieutenant (jg) with the U. S. Naval Reserves.

Mr. Hogan became an instructor in physics at Lehigh University in 1947. He left that position in 1950 to join the technical staff at Bell Telephone Laboratories, and in 1953, he was named a subdepartment head.

In 1954, he became associate professor of applied physics at Harvard University, Cambridge, Mass.

His research interest is the application of ferrites and semiconductors to microwave transmission systems.

He is a member of the American Physical Society, Sigma Xi, Phi Kappa Phi, and Tau Beta Pi.

❖

George R. Jones (A'54) was born August 16, 1930, at Los Angeles, Calif. He attended Western Maryland College on a Maryland state scholarship award. In 1951 he received the B.S. degree there, with a double major in mathematics and physics, and in 1953, received the M.S. degree in physics from the Catholic University of America.

G. R. Jones

In 1951 he joined the engineering staff at the Davies Laboratories, Incorporated, where he performed research and design of computer circuits, vhf antenna systems, and precision measurements and frequency control methods in vhf region.

He has been in the Supporting Research Laboratory of the Diamond Ordnance Fuze Laboratories since 1954, where he is investigating microwave and solid state phenomena.

❖

Morris L. Kales (M'51) was born on August 26, 1910, in New York, N. Y. He received the B.S. and M.S. degrees in mathematics from Massachusetts Institute of Technology in 1933 and 1934, and the Ph.D. in mathematics from Brown University in 1936.

M. L. Kales

From 1936 to 1944 Dr. Kales taught mathematics at Brown University, the University of Michigan, Tulane University, and the University of Maine, successively. In April, 1944, he joined the Radiation Laboratory at M.I.T. At present he is a member of the Microwave Antennas and Components Branch at the Naval Research Laboratory, in Washington, D. C.

Dr. Kales is a member of the American Mathematical Society and Sigma Xi.

❖

Nicholas Karayianis was born on August 17, 1931 in Washington, D. C. He majored in physics at George Washington University, where he received the B.S. degree in February, 1954. He was awarded a Sanders Fellowship for graduate studies and joined the University faculty for a year as a physics laboratory instructor, receiving the M.S. degree in February, 1956.

N. Karayianis

Since 1954, he has been employed by the Supporting Research Laboratory of the Diamond Ordnance Fuze Laboratories, where he has been investigating the microwave properties of ferrites. Mr. Karayianis is a member of Sigma Pi Sigma and an associate member of Sigma Xi.

❖

Mordechai M. Korman (A'52) was born in Frankfort on the Main, Germany, on February 20, 1923. He studied in Israel, spending several years at the Hebrew University, and obtained the B.S. degree by examination from London University in 1946. He also attended the University of California, receiving the B.S. degree in engineering in 1952 and the M.S. degree in 1955. From September, 1953 until late in 1955, Mr. Korman was a faculty member of the University of California, serving first as a teaching assistant and later as an associate. He returned to Israel early in 1956.

M. M. Korman

He is an associate member of Sigma Xi.

❖

Benjamin Lax was born in Hungary, on December 29, 1915. He received the B.M.E. degree from Cooper Union in 1941 and the Ph.D. degree in physics from M.I.T. in 1949.

B. Lax

From 1942 to 1946 he served with the Signal Corps and then with the Air Force. He attended the Army Electronics and Radar courses at Harvard and M.I.T. in 1943. Through 1944 and 1946 he was stationed at the M.I.T. Radiation Laboratory carrying on radar development. In 1946 he became a radar consultant for the Sylvania Electric Products Company, Boston, Mass. In the fall of 1946 he joined the staff of the Air Force Cambridge Research Center and at the same time enrolled as a graduate student in physics at M.I.T. He carried on research in microwave gas discharges until November, 1949. At this time Dr. Lax became a member of the Solid State Group at the Lincoln Laboratory and became involved in research of semiconductors and microwave aspects of ferrites. In May, 1953 he became the head of the Ferrites Group which carried on research in the field of ferrites and semiconductors at microwave frequencies. Since 1955, he has been leader of the Solid State Group which carries on fundamental and applied work on semiconductors and ferrites.

Dr. Lax is a member of the American Physical Society and of Sigma Xi.

❖

For a photograph and biography of R. C. LeCraw, see page 821 of the June, 1956 issue of PROCEEDINGS OF THE IRE.

❖

Clyde A. Morrison was born in Lachine, Mich., on July 17, 1926. He attended Michigan State College, receiving the B.S. degree in physics in 1950 and the M.S.

degree in 1951. From 1951 to 1953 he was a research associate in the digital computer group at the Willow Run Research Center of the University of Michigan. In 1953 he was employed by the digital computer group at National Bureau of Standards, Washington, D. C.

C. A. MORRISON

Since 1954 Mr. Morrison has been employed by the mathematics group and the ferrite research group of the Supporting Research Laboratory, Diamond Ordnance Fuze Laboratories, Washington, D. C.

❖

Earle B. Mullen was born March 3, 1925, in Toronto, Can. He received the B.A. and the M.A. degrees in physics in 1946 and 1948 from the University of Toronto.

E. B. MULLEN

In 1948, he joined the Newmont Mining Company in Jerome, Ariz., where he was associated with a gravimetric survey for six months. From late 1948 to 1952, he taught physics and mathematics at the University of Scranton. In 1952, he joined the Electronics Laboratory at the General Electric Company in Syracuse, N. Y., where he has worked on a variety of problems at microwave frequencies, in particular on measurements of ferrite characteristics.

❖

Conrad E. Nelson (A'52) was born on December 4, 1927, at Long Island, N. Y. He received the B.S. degree in electrical engineering from the University of California at Los Angeles in 1949. From 1949 to 1955, Mr. Nelson was employed by the General Electric Company. He graduated from the three-year Advanced Engineering Program at GE in Schenectady, N. Y., in 1952 and was then located for the following three years in Syracuse, N. Y., doing advanced development of microwave components. In 1955 Mr. Nelson became a registered professional engineer in New York. Since August, 1955, he has been a member of the Technical Staff in the Electronics Department of the Microwave Laboratory, Hughes Research Laboratories, Culver City, Calif. He has been engaged in microwave component development.

C. E. NELSON

He is a member of Eta Kappa Nu.

❖

C. Dale Owens (M'51–SM'51) was born in Wadesville, Ind., on May 15, 1906. He graduated from Indiana University in 1928 with the A.B. degree in physics and immediately joined Bell Telephone Laboratories. He spent two years in the development of capacitors, then became interested in the development and applications of magnetic materials, on which he has specialized since that time. He worked on molybdenum permalloy powder cores for loading coils and inductors and on iron powder cores for special applications. From 1940 to 1945, Mr. Owens designed inductors for high powered radar. Since that time he has studied the characteristics and applications of new magnetic materials, particularly the ferrites.

C. D. OWENS

Mr. Owens carried on graduate work at Columbia University and received the M.A. degree in physics in 1936.

He is a member of Phi Beta Kappa, the American Physical Society, the American Ordnance Association, and a Fellow of the American Association for the Advancement of Science.

❖

Howard Scharfman (S'47–A'50) was born in New York, N.Y., December 27, 1924. He entered the U. S. Signal Corps in 1943 where he worked on radar and pulse modulation equipment. He left the service in 1946. In 1947 he received the B.S.E.E. degree from New York University, and in 1948 was awarded the M.S.E.E. degree from Northwestern University.

H. SCHARFMAN

After working at the Kew Gardens, Long Island, Sylvania Electric Company plant over the summer of 1948, Dr. Scharfman joined the teaching staff of the Polytechnic Institute of Brooklyn. He taught undergraduate electrical engineering and continued his graduate studies there until 1950. He then joined the Antenna Section of the Seattle division of Boeing Airplane Company where he did research and development on receivers, antenna pattern ranges, and aircraft antennas.

From 1951–1954, Dr. Scharfman worked at the Radiation Laboratory of The Johns Hopkins University, Institute for Cooperate Research on vhf and uhf circuits and microwave scattering problems while completing graduate studies for the Ph.D. degree in electrical engineering. In June, 1954 he joined the staff of the Missile and Radar Division of the Raytheon Manufacturing Company as head of the microwave ferrite section. He is a member of Eta Kappa Nu and Sigma Xi.

❖

Marden H. Seavey, Jr. was born in Preston, Cuba, on January 12, 1929. He attended Worcester Polytechnic Institute and received the A.B. degree in physics in 1952 at Harvard College. In June, 1956 he received the M.S. degree in mathematics-physics from Northeastern University, Evening Graduate School of Engineering.

M. H. SEAVEY, JR.

From 1952 to 1955 Mr. Seavey was employed as a physicist for the Air Force Cambridge Research Center, Geophysics Division, where he was engaged in infrared radiation studies. Since September, 1955, he has been with the Solid State Group of Lincoln Laboratory where he has studied ferromagnetic resonance phenomena in ferrites and in metals.

❖

Harold Seidel (A'47) received the B.E.E. degree from the College of the City of New York in 1943, and the M.E.E. and D.E.E. degrees from the Polytechnic Institute of Brooklyn in 1947 and 1954. After employment with the Microwave Research Institute of Polytechnic Institute of Brooklyn, Arma Corporation, and the Federal Telecommunications Laboratory, he joined Bell Telephone Laboratories in 1953. His work there has generally been concerned with microwave problems, and he is presently engaged in the analysis of ferrite devices.

H. SEIDEL

Dr. Seidel is a member of Sigma Xi, and the American Association for the Advancement of Science.

❖

Samuel Sensiper (S'39–A'42–SM'47) was born in Elmira, N.Y., on April 26, 1919. He received the B.S. in electrical engineering from the Massachusetts Institute of Technology in 1939, the E.E. degree from Stanford University in 1941, and the Sc.D. in electrical engineering from the Massachusetts Institute of Technology in 1951. From 1939 to 1941 he was a Research and Teaching

SAMUEL SENSIPER

Assistant at Stanford. From 1941 to 1948 he was employed by the Sperry Gyroscope Company. From 1949 to 1951 he was a staff member of the Research Laboratory of Electronics at the Massachusetts Institute of Technology. Since 1951 Dr. Sensiper has been at the Hughes Aircraft Company, formerly in the Microwave Laboratory, and now in the Electron Tube Laboratory.

Dr. Sensiper received a World War II Certificate of Commendation from the Bureau of Ships and was an Industrial Electronics Fellow at M.I.T. from 1947 to 1948.

He is a member of Sigma Xi, RESA, and Eta Kappa Nu.

❖

For a photograph and biography of E. G. Spencer, see page 822 of the June, 1956 issue of PROCEEDINGS OF THE IRE.

❖

Eric Strumwasser (M'53) was born in Vienna, Austria on November 4, 1920. He received the B.S. degree in mechanical engineering from Stevens Institute of Technology in 1943 and the M.S. degree in electrical engineering from the University of Southern California in 1951. From 1943 to 1946, he served with the U. S. Navy.

E. STRUMWASSER

Between 1946 and 1949 he worked as a mechanical and electro-mechanical design engineer for M. W. Kellogg in New York, and De-Morney Budd in Los Angeles. In 1949, he joined the Hughes Research and Development Laboratories, where he has been active in antenna and microwave development. Currently, Mr. Strumwasser is head of the Microwave Components Section and a senior member of the Technical Staff.

❖

Harry Suhl was born on October 18, 1922 in Leipzig, Germany. He received the B.Sc. degree from the University of Wales in 1943, and the Ph.D. degree in theoretical physics from Oriel College, Oxford, in 1948. From 1943 to 1946 he worked on radar at the Admiralty Signal Establishment. In 1948 he joined Bell Telephone Laboratories where he has worked on electron-dynamics, physical properties of germanium, electromagnetic wave propagation, and ferromagnetic resonance. He is currently concerned with solid state theory.

H. SUHL

Dr. Suhl is a member of the American Institute of Physics, and a Fellow of the American Physical Society.

❖

Peter E. Tannenwald was born in Kiel, Germany, on March 30, 1926. He received his undergraduate and graduate training at the University of California, culminating in the Ph.D. degree in physics in 1952. From 1947 to 1950 he was a teaching assistant in physics at Berkeley and between 1950 and 1952 did research in high-energy nuclear physics at the University of California Radiation Laboratory. He joined the M.I.T. Lincoln Laboratory in 1952 and became engaged in the study of magnetic and microwave properties of matter. His current activities involve magnetic resonance at microwave frequencies, particularly in ferrite single crystals.

P. E. TANNENWALD

Dr. Tannenwald is a member of the American Physical Society, Sigma Xi, and Phi Beta Kappa.

❖

Milton A. Treuhaft (S'38–A'39–SM'52) was born on February 27, 1916, in Union City, N. J. He received the B.S. and M.S. degrees in electrical engineering from Columbia University in 1937 and 1938.

M. A. TREUHAFT

In 1940, he held the position of design engineer at the Westinghouse Industrial Electronics Division in Baltimore, and in 1945, became a research engineer at National Union Radio Corporation, Newark, N.J.

He joined Bendix Aviation Corporation, Teterboro, N.J., as a development engineer in 1946, and a year later became a senior partner in the Hudson Electrochemical Co., Union City.

From 1951 to the present, he has been a research supervisor at the Microwave Research Institute of the Polytechnic Institute of Brooklyn, working on data transmission equipment, uhf antennas, and network properties of ferrite devices.

Mr. Treuhaft, a registered professional engineer in New York and New Jersey, holds patents in the field of dynamic balancing and electropolishing.

He is a member of Sigma Xi and the Electrochemical Society.

LeGrand G. Van Uitert was born in Salt Lake City, Utah, on May 6, 1922. He was graduated from George Washington University in 1949 with the B.S. degree. He received the M.S. degree in 1951 and the Ph.D. degree in 1952 from the Pennsylvania State University.

L. G. VAN UITERT

Mr. Van Uitert served in the United States Navy from 1940 to 1946. He was employed at the Naval Research Laboratory in Washington, D. C., during the years 1948 and 1949.

He did his graduate work in the field of coordination chemistry. Since joining the Bell Telephone Laboratories in 1952, he has worked on magnetic oxides. He is the author of a number of published articles in both fields.

Mr. Van Uitert is a member of the American Chemical Society, Sigma Xi, and Alpha Chi Sigma.

❖

J. H. Van Vleck was born March 13, 1899, in Middletown, Conn. He received the A.B. degree from the University of Wisconsin in 1920, and the Ph.D. degree from Harvard University in 1922. He holds honorary degrees from Wesleyan, Wisconsin, Grenoble, and Maryland. He was at the University of Minnesota from 1923 as assistant professor and became full professor there in 1927. From 1928–1934 he was professor of theoretical physics at the University of Wisconsin. Since 1934 he has been at Harvard University, where he is at present Dean of Engineering and Applied Physics, and holds the Hollis Professorship of Mathematics and Natural Philosophy, the oldest endowed scientific chair in North America.

J. H. VAN VLECK

During World War II he was head of the theory group at Radio Research Laboratory at Harvard, as well as consultant to the Radiation Laboratory at M. I. T.

Professor Van Vleck is author of "The Theory of Electric and Magnetic Susceptibilities" (Oxford University Press), and has contributed various scientific papers on magnetism, quantum mechanics, etc., as well as a few articles on microwave detection or propagation written during the war.

He is a member of the National Academy of Science, the American Philosophical Society, the American Academy of Arts and Sciences, and several other scientific societies. He was president of the American Physical Society in 1952. He is a foreign member of the Royal Netherlands Academy of Arts and Sciences, and honorary member of the Societé Française de Physique.

IRE News and Radio Notes

National Bureau of Standards Will Relocate in Maryland

A tract of approximately five hundred fifty acres of land near Gaithersburg, Maryland has been selected for relocation of the Washington laboratories of the National Bureau of Standards. The move will permit the Bureau to plan new buildings to replace present research facilities in the physical sciences and engineering, which over the past fifty years have become inadequate for current needs.

Congress had appropriated funds for site acquisition and preliminary planning early in June after details about the proposed site had been presented to House and Senate Appropriations Committees. Plans for the site have been given to the National Capital Planning Commission and to the Regional Planning Council, and it is expected that these groups will work with the Bureau in utilizing the land. The General Services Administration will participate in planning and will supervise construction. Transfer of operations to the new location will be completed in about five years. It is expected that the rural location will remove the Bureau's work from the variety of mechanical, electrical, and atmospheric disturbances present in a city and will reduce the effect of these forces upon precise scientific measurements.

The Bureau occupied its present site on Connecticut Avenue in Washington in 1903.

In addition to its Washington laboratories, the Bureau maintains a major research center in Boulder, Colorado, and twenty widely scattered field stations. The Boulder Laboratories are concerned with radio propagation research, radio standards, and cryogenic engineering. Most of the field stations are engaged in gathering data on radio propagation.

Soviet Automation Journal Is Now Available in English

The first (January, 1956) issue of the English translation of the Soviet monthly journal *Avtomatika i Telemekhanika* has recently been published by Consultants Bureau, Inc., 227 West 17th Street, New York 11, N. Y. The title of the English translation is *Automation and Remote Control*. Subsequent issues, translated, will appear as regular monthly issues, and will be mailed to subscribers immediately upon publication. A subscription to the entire journal in translation will cost $185.00 per year.

The translation of the Consultants Bureau includes all diagrams, photographs and tabular material integrated with the text. The translation is reproduced by the multilith process, from typewritten copy. Each issue is provided with a sturdy paper cover, and staple-bound.

Individual articles, exactly as they appear in the published translation, may be purchased for $12.50. Tables of contents of each issue of *Automation and Remote Control* will be mailed without charge to scientific laboratories and libraries upon request.

IRE Welcomes New Subsection

On August 21, the IRE Executive Committee approved the formation of the Hampton Roads Subsection, a Subsection of the North Carolina-Virginia Section.

Final Call for Papers

IRE National Convention, March 18–21, 1957

Prospective authors are requested to submit all of the following information:
(1) 100-word abstract in triplicate with title, name and address of author.
(2) 500-word summary in triplicate with title, name and address of author.
(3) Indicate the technical field in which your paper falls:

Aeronautical & Navigational Electronics
Antennas & Propagation
Audio
Automatic Control
Broadcast & Television Receivers
Broadcast Transmission Systems
Circuit Theory
Communications Systems
Component Parts
Electron Devices
Electronic Computers
Engineering Management
Industrial Electronics
Information Theory
Instrumentation
Medical Electronics
Microwave Theory & Techniques
Military Electronics
Nuclear Science
Production Techniques
Reliability and Quality Control
Telemetry & Remote Control
Ultrasonics Engineering
Vehicular Communications

Deadline for acceptance of papers: November 2, 1956

Address all material to: Ben Warriner
1957 Technical Program Committee
Institute of Radio Engineers, Inc.
1 East 79 Street, New York 21, N. Y.

Calendar of Coming Events

National Electronics Conference, Hotel Sherman, Chicago, Ill., Oct. 1–3
Canadian IRE Convention & Exposition, Automotive Bldg., Exhibition Park, Toronto, Can., Oct. 1–3
AIEE Fall General Meeting, Morrison Hotel, Chicago, Ill., Oct. 1–5
Second Annual Symposium on Aeronautical Communications, Hotel Utica, Utica, N. Y., Oct. 8–10
SMPTE Eightieth Convention, Ambassador Hotel, Los Angeles, Calif., Oct. 8–12
Computer Applications Symposium, Morrison Hotel, Chicago, Ill., Oct. 9–10
URSI Fall Meeting, Univ. of Calif., Berkeley, Calif., Oct. 11–12
IRE-RETMA Radio Fall Meeting, Hotel Syracuse, Syracuse, N. Y., Oct. 15–17
Conference on Magnetism & Magnetic Materials, Hotel Statler, Boston, Mass., Oct. 16–18
PGED Annual Technical Meeting, Shoreham Hotel, Washington, D. C., Oct. 25–26
East Coast Conference on Aeronautical & Navigational Electronics, Fifth Regiment Armory, Baltimore, Md., Oct. 29–30
Convention on Ferrites, Institute of Electrical Engineers, London, England, Oct. 29–Nov. 2
Conference on Electrical Techniques in Medicine and Biology, McAlpin Hotel, N. Y., Nov. 7–9
Kansas City IRE Technical Conference, Town House Hotel, Kansas City, Kan., Nov. 8–9
Symposium on Applications of Optical Principles to Microwaves, Washington, D. C., Nov. 14–16
New England Radio Engineering Meeting, Bradford Hotel, Boston, Mass., Nov. 15–16
Office Automation & Human Engineering Conferences of the International Automation Exposition, Trade Show Bldg., N. Y., N. Y., Nov. 26–30
PGVC Eighth National Meeting, Fort Shelby Hotel, Detroit, Mich., Nov. 29–30
Midwest Symposium on Circuit Theory, Michigan State University, E. Lansing, Mich., Dec. 3–4
Second Instrumentation Conference & Exhibit, Biltmore Hotel, Atlanta, Ga., Dec. 5–7
IRE-AIEE-ACM Eastern Joint Computer Conference, Hotel New Yorker, New York City, Dec. 10–12
Symposium on Communication Theory and Antenna Design, Hillel House, Boston Univ., Boston, Mass., Jan. 9–11
Winter Meeting of Amer. Nuclear Society, Sheraton-Park Hotel, Washington, D. C., Dec. 10–12
RETMA Symposium on Applied Reliability, Bovard Hall, Univ. of So. Calif., Los Angeles, Calif., Dec. 19–20
Symposium on Reliability & Quality Control in Elec., Statler Hotel, Wash., D. C., Jan. 14–15, 1957
Symposium on VLF Waves, Boulder Labs., Boulder, Colo., Jan. 23–25

Highlights of PGED Meeting on Oct. 25–26 Are Revealed

A session of invited papers on recent developments in electron devices will be a feature of the Second Annual Technical Meeting of the IRE Professional Group on Electron Devices, to be held at the Shoreham Hotel, Washington, D. C., October 25–26, 1956.

Four papers are scheduled for this session, which takes place on Thursday morning, October 25, according to R. L. Pritchard, Chairman, Technical Program Committee.

They are: *Display and Storage Devices*, D. W. Epstein, RCA Laboratories; *Ferroelectric and Ferromagnetic Devices*, C. L. Hogan, Harvard University; *Microwave Tubes*, R. Kompfner, Bell Telephone Laboratories; and *Transistors*, H. L. Owens, Texas Instruments.

Traveling-wave tubes and magnetrons will be among other devices covered at this session.

A special program of social events has been scheduled for the opening day of the PGED Meeting by the Local Arrangements Committee. A luncheon at the Shoreham for those attending the meeting, and, in the afternoon, a get-together tea for the ladies are planned. In the evening, there will be an informal dinner preceded by a cocktail hour.

For those who wish to visit the many places of interest in the capital and its surroundings, tours of almost any desired duration for any size group can be arranged through the Hospitality Desk set up by the Local Arrangements Committee for the convenience of PGED delegates and guests.

Human Engineering and Data Processing Will Be Discussed

A Human Engineering Conference, which will be jointly sponsored by Manhattan College and the Third International Automation Exposition, will be held in New York City November 26–30. The conference, directed by industrial consultant Douglas Courtney, will cover such topics as machine design for human use, man-machine placement, research requirements for complex industrial operations, and economic, social and cultural implications of automation in eight sessions.

Nearly two hundred exhibits at the International Automation Exposition, Trade Show Building, 500 Eighth Ave., New York City, will be available to the administrative, engineering and research executives attending this conference.

The Office Automation Conference, which will be jointly sponsored by the Fordham University School of Business and the Exposition, will also be held in New York City November 26–27. G. L. Mattson, management consultant and director of the conference, stated that the conference aims to serve the needs of executives who contemplate office automation projects or who already have such projects started.

Complete information concerning registration and schedules of the two conferences and exposition may be obtained from Richard Rimbach Associates, Inc., Room 359, 525 Lexington Ave., New York 17, N. Y.

Southwestern Conference Convenes at Houston in April

The Ninth Southwestern IRE Conference and Electronics Show, sponsored by the Houston Section, will be held at the Shamrock-Hilton Hotel, Houston, Tex., April 11–13, 1957.

One of the three simultaneous sessions planned for conference attendees will be held by the National Simulation Council under the aegis of the IRE Professional Group on Electronic Computers. There will also be a meeting of the national IRE Board of Directors, papers on the earth satellite program and the International Geophysical Year, and over a hundred booths available for exhibits.

Members of the conference committee are as follows: R. L. Ransome, Section Chairman; Harvey Wheeler, Conference Chairman; W. J. Greer, Vice-Chairman; P. E. Franklin, Business Manager; L. H. Gollwitzer, Secretary; F. C. Smith, Jr., Program; K. O. Heintz, Exhibits; J. K. Hallenburg, Tours and Banquet; R. A. Arnett, Technical Chairman; E. F. Neuenschwander, Arrangements; M. A. Arthur, Publicity; Mrs. K. H. Woehst, Ladies' Program.

Illinois Institute of Technology Holds Fall Meetings

The Armour Research Foundation of the Illinois Institute of Technology will sponsor a symposium on computer applications of medium scale machines at the Morrison Hotel, Chicago, Oct. 9–10.

H. H. Kanter, program chairman, stated that first-day sessions would be devoted to papers on business and management applications of such machines as the IBM 650 and Datatron. The following day's program would cover engineering and research applications of these machines. The two-day symposium will center around discussions of problems encountered in computer installation, revision of programs to give effect to changes in procedures, use of computers on problems which cannot be solved otherwise, and methods of approach and type of personnel required.

Inquiries concerning the symposium should be directed to J. J. Kowal, Conference Secretary, Armour Research Foundation, Illinois Institute of Technology, 10 W. 35 St., Chicago 16, Ill.

Another conference is sponsored by Illinois Institute of Technology in cooperation with Northwestern University, University of Illinois, and the Illinois chapters of the American Society of Tool Engineers. This is the sixth annual Tool Engineering Conference, which is to be held on the campus of the Illinois Institute of Technology Nov. 2–3.

The opening session of the conference will feature an exchange of views on the industrial progress in technology by representatives of labor and management. Harry Osborn, Ohio Crankshaft Company, and P. L. Siemiller, International Association of Machinists, will be the speakers.

The morning program on the second day of the conference will be devoted to panel discussions on new cutting tool materials, and economic analyses of machine tool and equipment replacement. Panel discussions on new developments in extrusion methods, and automation in the metal-working industry are scheduled for the afternoon.

Inquiries concerning the conference should be addressed to S. E. Rusinoff, Mechanical Engineering Dept., Illinois Institute of Technology, Technology Center, Chicago 16, Ill.

IRE and AIEE of Philadelphia Set Creative Engrg. Sessions

The Philadelphia Sections of IRE and AIEE will jointly sponsor a Creative Engineering Symposium consisting of six lectures. The first five lectures will be on consecutive Thursday evenings, October 11 through November 8, 1956, and the sixth lecture will be on Tuesday, November 13, 1956. All lectures will be held in the University Museum's auditorium, University of Pennsylvania, Philadelphia, Pa.

This will be a series of talks designed to stimulate engineering imagination and thinking. Speakers in the fields of research, design, product development, psychology, promotion and advertising are included on the program. Among these speakers will be K. E. Brigham, S. O. English, D. G. Fink, A. N. Goldsmith, G. F. Metcalf, J. A. Morton, J. J. Newman, C. M. Sinnett, W. F. G. Swann, H. J. Woll and William Wills.

Advance registration for IRE and AIEE members is $3.00 and for non-members, $4.00. There will be a $1.00 additional fee for all registrations received after October 4, 1956. Single session fees will cost $1.50 each. Checks should be made payable to F. Jones, Treasurer, Creative Engineering Symposium.

Advance registrations should be forwarded to: AIEE-IRE Creative Engineering Symposium, Earl Masterson, Remington Rand Univac, P.O. Box 5616, Philadelphia 29, Pennsylvania.

Second School for Nuclear Training Opens at Brookhaven

A second school, to supplement the facilities of the summer school at Argonne National Laboratory, is being established by the Atomic Energy Commission, National Science Foundation and American Society for Engineering Education at the Brookhaven National Laboratory, Upton, Long Island, New York. It will accommodate thirty students.

The basic aim of both schools is to expand the number and scope of engineering course offerings in atomic and nuclear fields. Teaching services and facilities are provided by the Atomic Energy Commission and the two laboratories. Partial travel and minimum matching funds for stipends from the candidates' colleges are supplied by the National Science Foundation. The American Society for Engineering Education provides overall supervision of the program and makes the final selections of candidates for admission to the schools. Local administration of each school's program is provided by Northwestern University at Argonne, and by Associated Universities, Inc. at Brookhaven.

Israel IRE Section Co-Sponsors First National Electronics Convention in Israel

The year-old Israel IRE Section, and the Association of Engineers and Architects were joint sponsors of a convention held in Haifa, Israel, May 9–10. The convention was held in conjunction with the Israel Industrial Fair.

Franz Ollendorff of the Israel Institute of Technology, who is chairman of the Israel Section, gave the welcoming address to an audience of 250 engineers and scientists who had gathered to hear twenty papers presented during four sessions.

The first session, presided over by Professor Ollendorff, dealt with electronic computers. Z. Risel and A. Frenkel of the Weizman Institute presented a paper on the problems encountered in constructing a large digital computer at the Weizman Institute. A. Fuchs of the Scientific Department of the Ministry of Defense described the department's analog computer and its applications. A. Nathan of the Israel Institute of Technology spoke on the effective error in linear analog computers, and A. Freedman of the Scientific Department of the Ministry of Defense presented his work on an analog-digital multiplier for use in analog computers.

The second session centered around the subjects of communication and military electronics. G. Finer of the Israel police force discussed police communication systems, and U. Galil of the Israel Navy dealt with specific problems of naval electronic equipment. A. Berman delivered a talk entitled *Radio Equipment in the Service of the Post Office*, while his colleague, J. Sussman, described the post office's project on an automatic radio telephone network for the Negev. K. May of the Palestine Electric Corporation outlined his firm's radio communication installations for the supervision of power lines.

Chairman of the third session was Y. Shamir, head of the electronics laboratory at the Scientific Department of the Ministry of Defense. The first paper in this session was Professor Ollendorff's *Noise Problems in the Movement of Electrons in Vacuum Tubes*. New devices using the effects of magnetic fields on resistance of wires were then described by D. Reves of the Weizman Institute. The Scientific Department of the Ministry of Defense was represented by two papers, one by J. Mass on correlation filters and the other by S. Amarel on transient analysis by X-transforms. S. Zohar of the Signals Branch gave a paper on measurements in quartz crystals. S. Wollstein and E. H. Frei of the Weizman Institute delivered the final paper of this session on an electromagnetic instrument for flow measurement.

Mr. Frei presided over the last session of the convention, which was concerned with the various applications of electronics to the radio industry. A. Fischman of the Scientific Department of the Ministry of Defense described the design of a radar operator trainer. D. Itzkovitsch of the Voice of Israel discussed the problems peculiar to installations of high-power transmitters. Electronic instrumentation problems in nuclear medicine were discussed by Dr. Tcherniak. A talk by C. Dobkin of Galim then followed, in which the necessity of appropriate standards for the radio receiver industry was stressed. R. Gamzon of the Amron factory closed the convention with a speech on the production problems of electronic components in Israel.

J. Mass lectures on correlation filters while (*left to right*) Franz Ollendorff, Israel Section chairman, Y. Shamir, U. Galil, and G. Finer listen.

K. May was chairman of the executive committee for the convention. J. Mass, Y. Shamir, and U. Galil headed the convention committees on the program, papers, and publicity, respectively.

Complete abstracts in Hebrew of the papers presented at the convention are available to IRE members upon request from the Israel Section Secretary, A. Wulkan, P.O. Box 1, Kiryat Motzkin, Israel.

MISCELLANEOUS PUBLICATIONS OF THE IRE

The following publications have recently been published, and are now available from the Institute of Radio Engineers, Inc., 1 East 79th Street, New York, N. Y. at the following prices. The contents of each publication are given below.

Electronic Computer Conferences	
Review of Electronic Digital Computers, Joint IRE-AIEE Computer Conferences, December 10–12, 1951, Philadelphia, Pennsylvania.	$3.50
Input and Output Equipment Used in Computing Systems, Joint IRE-AIEE-ACM Computer Conference, December 10–12, 1952, New York, N. Y.	4.00
Proceedings of the Joint IRE-AIEE-ACM Western Computer Conference, February 11–12, 1954, Los Angeles, California.	3.00
Proceedings of the Joint IRE-AIEE-ACM Western Computer Conference, March 1–3, 1955, Los Angeles, California.	3.00
Proceedings of the Joint IRE-AIEE-ACM Western Computer Conference, February 7–9, 1956, San Francisco, California.	3.00
Proceedings of the Joint IRE-AIEE-ACM Eastern Computer Conference, December 8–10, 1954, Philadelphia, Pennsylvania.	3.00
Proceedings of the Joint IRE-AIEE-ACM Eastern Computer Conference, November 7–9, 1955, Boston, Massachusetts.	3.00
Telemetering Conferences	
1953 National Telemetering Conference, May 20–22, 1953, Chicago, Illinois.	2.00
1954 National Telemetering Conference, May 24–26, 1954, Chicago, Illinois.	2.00
1955 National Telemetering Conference, May 18–20, 1955, Chicago, Illinois.	3.50
Component Symposiums	
Proceedings of the 1954 Electronic Components Symposium, May 4–6, 1954, Washington, D. C.	4.50
Proceedings of the 1955 Electronic Components Symposium, May 26–27, 1955, Los Angeles, California.	4.50
Reliability & Quality Control Symposiums	
Proceedings of the National Symposium on Quality Control and Reliability in Electronics, November 12–13, 1954, New York, N. Y.	5.00
Proceedings of the Second National Symposium on Quality Control and Reliability in Electronics, January 9–10, 1956, Washington, D. C.	5.00*

* IRE member price—$3.00.

Nat'l Elec. Conference Held Three Tutorial Sessions

Twenty-four technical sessions and three luncheon addresses of general interest highlighted the 1956 National Electronics Conference in Chicago Oct. 1–3.

The NEC is sponsored annually by the IRE American Institute of Electrical Engineers, Illinois Institute of Technology, University of Illinois, and Northwestern Univ.

Also participating in the conference are Michigan State, Purdue, Michigan, and Wisconsin Universities, as well as the Radio-Electronics-Television Manufacturer's Association, and Society of Motion Picture and Television Engineers.

R. R. Jenness, 1956 NEC President

More than 10,000 persons attended the three-day technical meeting and exhibition. "Fifty Years of Progress Through Electronics" was the theme of this year's conference. A record 240 commercial exhibits were displayed at the conference, stated G. J. Argall, Exhibits Chairman.

A feature of the conference was the staging of three half-day educational sessions dealing with information theory, radio isotopes, and solid state.

Presiding over the educational sessions were: R. M. Fano, Massachusetts Institute of Technology, Cambridge, Mass., Information Theory; Leonard Reiffel, Armour Research Foundation of Illinois Institute of Technology, Chicago, Radio Isotopes; and J. P. Jordan, General Electric Co., Syracuse, N. Y., Solid State.

Luncheon addresses were given by J. P. Hagen, Director of the Vanguard project at the Naval Research Laboratory, Washington; F. L. Hovde, President of Purdue University, Lafayette, Ind., and Herbert Scoville, Jr., Assistant Director of the U. S. Central Intelligence Agency, Washington.

Dr. Hagen discussed earth satellites and space travel; Dr. Scoville compared U. S. and Russian technical educational policies.

Approximately one hundred papers on electronic research, development, and application, were presented during the conference according to L. T. De Vore, Prog. Ch.

The opening day's technical sessions concerned components and materials, instrumentation, measurements, receiver techniques, data storage systems, servomechanism theory and applications.

On Oct. 2, the technical program dealt with information theory applications, magnetic amplifiers, solid state devices and applications, network and filter theory, data processing systems, microwaves, and radio isotopes.

The conference concluded on Oct. 3 with sessions relating to solid state, high power audio systems, network synthesis, antennas, quality control and reliability, automation techniques, medical electronics, and pulse techniques.

The Midwestern Simulation Council held a concurrent session on simulation of hydraulic systems during the afternoon of Oct. 3 for those specializing in this field.

Communication Theory and Antenna Design to Be Topics

The Air Force Cambridge Research Center and Boston University are sponsoring a symposium on communication theory and antenna design January 9–11, 1957, at Hillel House, Boston University, Boston, Mass. The purpose of the symposium is to acquaint antenna designers with communication theory techniques by outlining the mathematics of the theory, and then applying them to the fields of electronics, optics and microwaves.

Further information may be obtained from Miss Alice Cahill, Attention: CRRD, Air Force Cambridge Research Center, Air Research and Development Command, Laurence G. Hanscom Field, Bedford, Mass.

AIEE Celebrates Tesla Centennial and Honors Kettering

The American Institute of Electrical Engineering celebrated the Nikola Tesla Centennial at its Fall General Meeting held at the Morrison Hotel, Chicago, October 1–5. Dr. C. F. Kettering was also honored by a luncheon marking his eightieth birthday.

In addition to the many technical sessions, a panel discussion was held by several young graduate engineers on educational and vocational opportunities. Tours of Acme Steel Company, the Ridgeland Station of the Commonwealth Edison Company, Zenith Radio Company, Swift & Company, WNBQ-TV, Prudential Building, and the Kellogg Switchboard Company were also scheduled.

Call for Papers

1957 IRE-AIEE-U. of Pa. Conference on Transistor & Solid-State Circuits
Feb. 14–15, 1957,
Philadelphia, Pa.

Papers on transistor and solid-state circuits are solicited. Deadline for submission of 100-word abstracts is Nov. 5, 1956. Please send abstracts to G. H. Royer, Westinghouse Electric Corp., 356 Collins Ave., Pittsburgh 6, Pa.

Papers are Being Solicited for EJC Nuclear Congress

The IRE Professional Group on Nuclear Science is cooperating with the EJC Second Annual Nuclear Science and Engineering Congress which has been scheduled for March 11–14, 1957 in Philadelphia. Anyone wishing to submit papers of broad interest is invited to do so. The Engineers' Joint Council will prepare preprints only, which will indicate the author's society affiliation; publication rights remain with the parent society and, therefore, the Editor of the Transactions must review and accept papers in accordance with IRE standards before forwarding them to the EJC to meet the following deadlines: October 1—titles and abstracts (100 words minimum); December 1—final manuscript (based on not more than 20 minutes presentation).

Please submit papers to: Sidney Krasik, Editor, IRE—PGNS Transactions, 5621 Wilkins Avenue, Pittsburgh 17, Pennsylvania.

Ferrite Specifications Group was Recently Formed

At the annual meeting of the American Ceramic Society in April, 1956, a group was formed under the ASTM C-21 Committee to set up testing specifications for ferrites.

The next meeting of the group is scheduled for October 15 at the Massachusetts Institute of Technology. Persons interested in this group's activities are invited to write to S. Blum, Correspondence Secretary, Research Division, Raytheon Manufacturing Co., Waltham, Mass., for further details.

Vacuum Technology Symposium Is Planned for Oct. 10–12

The Committee on Vacuum Techniques, Inc. has announced that the Third National Symposium on Vacuum Technology will be held on October 10–12, 1956, at Hotel Sheraton, Chicago.

Papers will be presented with particular emphasis on the following categories: fundamental developments in vacuum technology; methods and techniques for obtaining high vacuum; instrumentation and control of high vacuum equipment; vacuum distillation and evaporation; metallurgical and chemical applications; and vacuum technology as related to atomic energy and extra-terrestial problems.

Further information may be obtained from A. H. Peterson, Chairman of the Committee on Publications and Publicity, 4400 Fifth Ave., Pittsburgh 13, Pa.

Obituaries

M. Barry Carlton (SM'54), Director of the Government Division of the Magnavox Company, was killed in an air collision in

the Grand Canyon, Ariz., on June 30, at the age of 37.

Mr. Carlton received his bachelor's degree from Brooklyn College in 1942, and took his graduate work at Northeastern University and Massachusetts Institute of Technology.

M. B. CARLTON

He served the United States as a scientist from the start of World War II to 1954 with the Brooklyn Navy Yard in New York; Scott Field at Belleville, Ill.; MIT Radiation Laboratory in Cambridge, Mass.; Naval Research Laboratory and Office of Naval Research, Washington, D. C.; and the Office of the Assistant Secretary of Defense in research and development, and applied engineering in Washington, D. C.

In 1954 Mr. Carlton joined the Magnavox Company, Fort Wayne, Indiana, as Director of its Government Division. He held this position until his death.

He was a member of RETMA, and a registered professional engineer in the District of Columbia. He was moderator at the Second National Symposium on Reliability and Quality Control held in Washington, D. C. last January, and a member of the administrative committee of the Professional Group on Military Electronics.

❖

Carl R. Englund (A'17–F'28), an expert in radiotelephony, formerly on the staff of Bell Telephone Laboratories, Holmdel, N. J., died recently. His age was 71.

C. R. ENGLUND

Mr. Englund had retired from Bell Laboratories in 1944, after thirty years of service with the Bell System. Throughout his telephone career, he had specialized in radio research and contributed to the development of such services as ship-to-shore and long-wave transatlantic radiotelephony. A pioneer in the radio field, he pointed out as early as 1914 the existence of "sidebands" in radio transmission. He made fundamental contributions in the technique of radio field strength measurements and in the propagation of ultra-short waves.

During World War II he was engaged in a military project undertaken by Bell Laboratories for the National Defense Research Committee.

Mr. Englund was born in Sioux City, Iowa. He received his B.S. degree in chemical engineering from the University of South Dakota in 1909 and then entered the University of Chicago for two years of graduate study. Before joining the Bell System in 1914 he had served on the staffs of Western Maryland College and the University of Michigan.

He was the author of many technical articles on radio research.

❖

Scott Helt (A'47–M'48), patent administrator at Allen B. Du Mont Laboratories, Inc., Clifton, New Jersey died recently. He was 49 years old.

Mr. Helt was a veteran in the radio and television industry. He had been active in radio broadcasting and television for a period of 32 years. Prior to his position as patent administrator at Du Mont, he had been in charge of professional relations for the company and before that was chief engineer of the Du Mont television network. He joined the Du Mont organization in 1944.

Before his association with Du Mont Mr. Helt served as engineer and chief engineer in a number of radio stations in the South and Mid-West, including stations in Columbia, South Carolina; Lexington, Kentucky; Mobile, Alabama; and Indianapolis, Indiana.

Mr. Helt was an authority on television engineering practices and served as a lecturer in electrical engineering and as an instructor in principles and practice of television at Columbia University. He was the author of the television engineering book *Practical Television Engineering*, and was also the author of a number of technical papers published in electrical journals.

Mr. Helt was a member of the following organizations: American Institute of Electrical Engineers; Society of Motion Picture and Television Engineers; American Association for the Advancement of Science and the Radio Society of Great Britain. He was Vice-Chairman of the IRE Professional Group on Broadcast Transmission Systems in 1955, and chairman of its papers review committee in 1956.

❖

John P. Shanklin (M'47) died recently. Since 1947 he had been in charge of antenna design at the Research and Development Division of Collins Radio Company in Cedar Rapids, Iowa.

J. P. SHANKLIN

Born in 1907 at Glendale, Ohio, Mr. Shanklin received the B.S. degree in electrical engineering from Virginia Polytechnic Institute in 1929. He was employed by RCA Communications, Inc. and Bendix Radio before joining the staff of Collins Radio Company.

Mr. Shanklin was responsible for the design of a number of antennas currently in use by the civil airlines and the military services. He is probably best known for his design of the vhf navigation "deerhorn" antenna now in almost universal service in the air transport field. Among his military antenna designs are the AS-505, AS-555 and AT-197 uhf ground station communication antennas. At the time of his death he was active in the design of antennas for transhorizon and long-range hf communication systems.

Mr. Shanklin had been issued a number of patents on antennas.

❖

TECHNICAL COMMITTEE NOTES

There were no technical committee meetings to report for the month of July due to the relative inactivity of the committees during the summer. The Technical Secretary, L. G. Cumming, would, therefore, like to take this opportunity to discuss the proposed standards that will be considered during the coming year.

The **Antennas and Waveguides** Committee, under the chairmanship of Henry Jasik, is presently working on the Proposed Standards on Antennas and Waveguides: Methods of Measurements of Waveguides and Waveguide Components.

The **Audio-Techniques** Committee, under the chairmanship of Iden Kerney, is preparing a Proposed Standard on Audio Techniques. Definitions of Terms.

The **Circuits** Committee, under the chairmanship of W. A. Lynch, is preparing a list of definitions for linear active circuits.

The **Electron Tubes** Committee, with P. A. Redhead as chairman, is nearing completion of a definition standard to cover all phases of electron tubes. Work is beginning on a similar standard to cover all methods of measurement.

The **Facsimile** Committee, under the chairmanship of K. R. McConnell, is actively working on test standards.

J. E. Eiselin, chairman of the **Industrial Electronics** Committee, has reported that two subcommittees are presently working on definitions, instrumentation and control.

The **Information Theory and Modulations Systems** Committee under the chairmanship of J. G. Kreer, Jr., is giving consideration to a Proposed Standard on Information Theory and Modulation Systems: Definitions of Terms.

P. S. Christaldi, chairman of the **Measurements and Instrumentation** Committee, has reported that his Subcommittee on Oscillography is preparing a summary of terms.

The **Navigation Aids** Committee, under the chairmanship of H. R. Mimno, is nearing completion of the Proposed Standards on Radio Aids to Navigation: Methods of Testing the VHF Omni-Directional Radio Range (VOR).

The **Nuclear Techniques** Committee under the chairmanship of G. A. Morton, is preparing a proposed standard on scintillation counter definitions.

Hans Jaffe, chairman of the **Piezoelectric Crystals** Committee, has submitted for review the Proposed Standards on Piezoelectric Crystals: The Piezoelectric Vibrator: Definitions and Methods of Measurement.

The **Radio Frequency Interference** Committee, under the chairmanship of R. M. Showers, has two subcommittees actively working on the interference problem.

The **Radio Receivers** Committee, with D. E. Harnett as chairman, is presently reviewing a revision of the Standards on Television: Methods of Testing Monochrome Television Receivers, prepared by his Subcommittee on Television Receivers.

H. Goldberg, chairman of the **Radio Transmitters** Committee, has reported that his subcommittees are presently working on definitions and measurements standards.

The **Recording and Reproducing** Committee, under the chairmanship of D. E. Maxwell, is presently reviewing the Proposed Standards on Sound Recording and Reproducing: Methods of Calibration of Mechanically Recorded Frequency Records.

The **Solid State Devices** Committee, under the chairmanship of H. L. Owens, has numerous subcommittees actively working on definitions and methods of measurement to cover all phases of semi-conductors.

H. R. Terhune, chairman of the **Symbols** Committee, has reported that his committee is working jointly with ASA on a proposed standard on reference designations.

The **Television Systems** Committee, under the chairmanship of W. T. Wintringham, has a Subcommittee on Picture Element that is presently working on definitions of terms.

The **Video Techniques** Committee under the chairmanship of J. L. Jones, has subcommittees working on both definitions and methods of measurement in this field.

This brief report on our Technical Committees will give a general idea of the standards that may be approved within the next year.

L. G. Cumming
Technical Secretary

Books

Electronics and Electron Devices by A. L. Albert

Published (1956) by the Macmillan Co., 60 Fifth Ave., N. Y. 11, N. Y. 572 pages+10 index pages+xi pages. Illus. 9¼×6¼. $8.00.

This book is the third edition of the author's *Fundamental Electronics and Vacuum Tubes*, the title having been modified to conform with present usage. The objectives of the book remain as for preceding editions, and as stated in the preface, are "to provide a textbook for junior and senior college and university courses on basic electronics and electron devices; a book that is well balanced between theory and illustrative applications. . . ." The chapter titles give an idea of topics which receive some attention: Basic Electronic Theory; Emission of Electrons; Two-Electrode Electron Tubes; Three-Electrode Electron Tubes; Multielectrode Electron Tubes; Electron-Tube Rectifiers; Vacuum-Tube Voltage Amplifiers; Vacuum-Tube Power Amplifiers; Vacuum-Tube Oscillators; Semiconductor Electron Devices; Transistor Amplifiers and Oscillators; Modulators; Demodulators; Wave-Shaping and Control Circuits; Magnetic Amplifiers; Photoelectric Devices; Cathode-Ray Tubes.

The chapter titles and the section headings provide a far more impressive outline than the resulting subsequent development. If one is interested in a book which has something to say in a general way about most important topics in electronics, this book will meet this need. If one is interested in a text that includes some mathematical substance to support the skeleton of words, this volume will fail to meet such a need. Perhaps it would satisfy the nonspecialist, but for an engineer or student who wishes a complete story of the behavior of electronics devices, the book is completely inadequate. Chapter 11 on transistor amplifiers and oscillators includes some theory, but the only chapter which does a reasonably adequate job is Chapter 15, Magnetic Amplifiers, which was written by a former colleague of the author.

The book seems to be quite correct technically, although several incorrect statements were noted in reading through the text. For example, on page 76 it is stated that "the heating of a rectifier tube is influenced by the average anode current." It is proportional to this figure in the gas rectifier tube, that while it is influenced, in the vacuum rectifier tube, the influence is not defined in terms of the average tube current. Chapter 4 proceeds with a discussion of three-electrode electron tubes as a circuit element, but the failure to define a complete set of reference conditions results in equations which are ambiguous. Equation (4-21), which defines the voltage amplificator factor of an amplifier, is not unique, owing to the failure to show the reference polarity for potential of the output; that is, phase information is lacking. The statement on page 128 that the "equivalent plate circuit theorem" is an application of Thevenin's theorem is incorrect. On page 304 it is stated that the cathode-follower is a current feedback amplifier. This is in error; this is a potential feedback circuit.

As to its use, those who found the prior two editions suitable for their courses will find the present edition equally suitable. For those who wish a text that includes the mathematical details of the theory being discussed, this text will not meet their needs.

Samuel Seely
Case Institute of Technology
Cleveland, Ohio

A Study of the Double Modulated FM Radar by Mohamed Ismail

Published (1955) by Verlag Leeman, Zurich, Switzerland. 112 pages. 43 figures. 8¼×6¼. 10.40 F.

This is a treatise on frequency-modulated radar. A refreshingly lucid coverage is given for three types of system. These are identified as "The Usual System," "The Double Modulated System," and "A New System."

"The Usual System" involves single frequency modulation of a transmitter, with cycle counter techniques used for determination of range and range rate. The inherent limitations are quantitatively defined. "The Double Modulated FM Radar (Witmer's System)" involves a transmitter which is frequency modulated by two different modulation frequencies, with a discriminator followed by narrow band-pass and low pass filters for deriving range and range-rate information respectively. Measurement errors arising from imperfect receiver adjustment, and sensitivity limitations imposed by thermal noise and by self-generated low-frequency interference are quantitatively evaluated.

The "New System" is presented as the author's invention to overcome the identified rather serious limitations of the other two methods. This is accomplished by frequency modulation of the transmitter with a single, low frequency sine wave, stabilization of intermediate frequency in the receiver by direct generation at IF, elimination of unwanted mixer products by successive reductions of frequency in several stages, and derivation of range and range rate information by means of a discriminator and filters as in the double modulated case. Experiments with the double modulated and the new systems are reported not only as having validated the theoretical work but as having demonstrated rather convincingly the attainment of the objective in the new system.

Anyone attempting to follow the analysis in detail may have some difficulty in keeping up with the nomenclature. For instance, the small letter c is used variously to represent cycles, an arbitrary constant, the velocity of light, and capacitance, while capacitance is also represented by capital C. Such evidences of inexperience are easily forgiven, however, in the light of the clarity of presentation of rather complex concepts achieved by the author. Most of the mathematics is simple enough to be understood by the average radio engineer who wants to follow it through. However, the text and figures are complete enough to give the idea clearly to those who prefer to "skip" the math. It is a book that could be well justified in the library of every engineer engaged in radar research and development. It should also be available, at least as a reference, to students in the field of radar systems engineering.

R. M. Page
Naval Research Laboratory
Washington 25, D. C.

Electronic Computers and Management Control by George Kozmetsky and Paul Kircher

Published (1956) by McGraw-Hill Book Co., 330 W. 42 St., N. Y. 36, N. Y. 243 pages+5 index pages+38 appendix pages+5 pages of bibliography+vii pages. 6 figures. 9¼×6¼. $5.00.

The field of computer engineering is so very new that a relatively small number of books on the subject have appeared. Further, the reviewer has not seen any before which give an adequate explanation of how computer systems might be used in industry, the problems faced in introducing them, and how they are related to management planning and control.

The authors state in the preface that "this book is written primarily for the business executive." An engineer may then ask of what value the book is to him. Insofar as the reviewer is concerned, the authors have written a book that will show the engineer some of the basic uses and decisions underlying use of computer equipment.

Since as stated above, the book is written for the businessman, the first chapter shows him why he may be interested in computers which (1) increase transmission, processing and reproducing speeds, (2) reduce the need for manpower, (3) reduce storage-space requirements, and/or (4) automatically handle intermediate steps in data processing. The engineer will find this interesting.

The next two chapters deal with computer fundamentals and a rather sketchy survey of electronic methods of data processing. This information will seem "old hat" to any engineer already in the field but will prove useful to those who although not working with computers wish to obtain some idea as to what has been done.

Chapter IV entitled "Studies and Applications of Electronic Systems" is the first one in which the authors begin to explore their subject. It covers many of the present commercial applications and many of the businessmen now using computers are quoted directly. Such applications as the General Electric payroll, Commonwealth Edison billing, AMA system, and the du-Pont general accounting approach are briefly described.

Chapter V describes the administrative problems created by the introduction of electronic systems. Included are the replacement of old equipment, retraining, regrouping and relieving of personnel, the hiring and orientation of experts, and the review of data-gathering, -processing, and -reporting methods. Much of the discussion is based on the experience with General Electric's Univac installation at Louisville which company according to the authors "has been the first in America to experiment with the installation of a large-scale general-purpose business computer."

The next two chapters covering management and the scientific approach, and management planning and control were read with great interest by the reviewer. They are quite general in nature and discuss among other things the technical and administrative problems executives face when beginning to study a possible computer application, the scientific method, mathematical tools and models, and the difficulty in the attainment of planning and control objectives.

Chapter VIII is concerned with programming, scheduling, and feedback. "Programming" is defined as the selection of the best plan or budget for a company which recognizes alternative combinations of the basic planning factors. Determination of the timing, the specific methods to be employed, and the specific resources to be used in carrying out the program in a coordinated and consistent manner is called "scheduling." Communication of current information to the proper organizational level for analysis, action-taking, and decision-making with regard to both programming and scheduling is termed "feedback."

Chapter IX entitled "Integrated Business Systems" combines the concepts covered in the preceding chapters. Because of the complexity of this subject, the authors are limited in how much they can cover. They do, however, present the basic ideas and indicate the utility of models in making systems studies.

Chapter X is concerned with automation and scientific computation and the authors attempt in this chapter to discuss the subjects in enough detail to indicate the significant relationships between them and the topics discussed in earlier chapters.

Chapters XI and XII are concerned with the role of the executive in the selection of the electronic system and the challenge to the executive. The reviewer does not believe that these chapters will be of interest to engineers.

The authors have also provided the reader with a summary at the end of each chapter which serves a useful purpose in firmly fixing in the reader's mind the important points covered. Their writing style makes for easy reading and the subject matter is fascinating. In many cases the reviewer was personally familiar with the applications presented and commends the authors on the pains to which they have gone to gather facts. It could not have been an easy task. Needless to say, the book will be read with interest by engineers and is the first of a number of excellent texts on the subject.

J. R. WEINER
Remington Rand Univac
Sperry Rand Corp.
Philadelphia 29, Pa.

Random Processes in Automatic Control by J. H. Laning, Jr. and R. H. Battin

Published (1956) by McGraw-Hill Book Co., 330 W. 42 St., N. Y. 36, N. Y. 358 pages+64 pages of appendix+6 pages of bibliography+4 index pages+ix pages. Illus. 9¼×6¼. $10.00.

The broad objective of this book is a quantitative study of errors in control systems. In general the problem is to distinguish between a wanted signal representing the true information upon which the system should act and the ever-present disturbances which tend to falsify the data. The latter may be lumped together under the term "noise" and constitute a random process intimately associated with the performance of the system. The response of physical systems to noise excitation and to signals in the presence of noise is thus of fundamental importance.

Almost all of the first half of the book is devoted to a review of the relevant statistical background. This preliminary development is necessary for a unified treatment because of the scattered status of the source material in present-day literature. The preparation is thorough, beginning with elementary probability theory and carrying well into sophisticated techniques based on correlation, spectral density, characteristic functions, and Gaussian processes. Illustrative problems are generously furnished all along the way. The reader can take as much as he wants from this part of the book, and even those who may not need the exposition should be grateful for the collected results available for ready reference in the remainder of the book.

The actual applications to control systems include a comprehensive treatment of what now may be called the classical theory of linear time-invariant systems excited by stationary random processes. There is a brave assault on the more difficult and less extensively explored domains of linear time-varying systems and non-stationary processes, and a quite pertinent chapter on operations with finite data. The lucid treatment of mean-square-error minimization in smoothing and predicting by both the time and frequency-domain approaches should do much to dispel the mystery which has often seemed to envelop these procedures.

Results on the non-stationary and linear time-varying problems in the most general cases amount principally to prescriptions for programming the solutions on analogue computers, which are concisely described in a helpful appendix. The quantities dealt with are natural generalizations of those studied in the time-invariant case. The impulse response becomes a function of both time of application and elapsed time, while the correlation functions depend on both running time and lag time. Mean-square errors vary with time and the frequency-response function depends on both frequency and time. The spectral density is however averaged over time to yield a function of frequency only. It is a question whether this might be an over-simplification which would sometimes throw away valuable information. A special case treated in more comprehensive detail is that of the transient response of a linear constant-constant coefficient system to random processes. This system becomes time-varying by virtue of the starting switch.

The analytic procedures are carefully and accurately described. There are very few typographical errors, and in fact, none of any consequence was noted. The nearest grounds for a quibble was found in the definition (3.6-23) on page 126 for power spectral density. For his own information the present reviewer would like to see just one non-trivial example of a random process for which the indicated limit exists. In the illustrative example 3.6-2 it was found necessary to evaluate an ensemble average in order to obtain a limit.

In summary, the book is timely and informative. In a broad engineering field, it should be helpful to both the student and educator, and to the practical engineer as well as the researcher.

W. R. BENNETT
Bell Telephone Labs.
Murray Hill, N. J.

Transistors I by RCA Laboratories

Published (1956) by *RCA Review*, David Sarnoff Research Center, Princeton, N. J. 676 pages+46 abstracts of papers+vi pages. Illus. 9¼×6¼. $4.50.

This book is a collection of articles dealing with various aspects of semiconductors and their applications. The volume contains 41 papers (31 heretofore unpublished in print and 10 having already been published elsewhere) grouped into six sections: general, materials and techniques, devices, fluctuation noise, test and measurement equipment, and applications.

The first paper is a summary of basic transistor device concepts which will serve as useful and enjoyable reading not only to those unfamiliar with transistors but also to those who may feel that device theory transcends the comprehension of circuit engineers. A paper on "new advances in junction transistors" containing much useful but rather heterogeneous material (from junction geometry to automatic gain control of a transistor receiver) completes the introductory section.

The section on materials and techniques includes papers on methods and apparatus for germanium purification, single-crystal growing and surface treatment of silicon. Microscopic examination of crystals as well as considerations and techniques related to alloy-junction and melt-quench transistors are also treated.

The section on devices contains papers dealing with silicon n-p-n and high emitter efficiency p-n-p alloy transistors, power and high-frequency transistors. An interesting paper discusses junction transistors designed for iterative operation (approximately equal input and output impedances) and is followed by a study of drift-transistors. A variable-capacitance diode applicable to automatic frequency control at uhf is also described.

The (1/f)-noise is studied in a first article devoted to noise. This is followed by two papers on noise containing theoretical and experimental results.

The section on test equipment will be welcome to engineers who devote their time to the design of transistor measuring equipment. A test set for 455 kc IF transistors, equipment for measuring power gain and small-signal parameters up to 50 mc and measuring equipments for junction temperature and class-*B* properties are also described.

Almost half of the volume is devoted to the section on applications. The subjects treated are: temperature effects in transistor circuits, stability of tuned amplifiers, cross-modulation in rf amplifiers, behavior of rf transistors, automobile and portable receivers, complementary symmetry circuits, audio amplifiers, modulated oscillators, TV receiver sync, deflection and automatic frequency control circuits, switching characteristics, and counting circuits.

The book certainly does present an impressive number of valuable individual contributions. One of its principal merits is to make available for the record several papers which have been read at various conferences and have attracted the attention of the profession. It is, of course, very difficult to present a balanced picture of the transistor art in the form of a collection of articles (by authors whose principal common denominator is their affiliation with the Radio Corporation of America) and, consequently, it is not surprising that such a volume should contain contributions having not only widely differing subject material but also very different significance and level of treatment. However, by including review-type articles and articles available elsewhere, the publishers have succeeded in maintaining a certain unity of presentation and scope. The book will be useful to transistor specialists and also to circuit engineers who have only a rudimentary knowledge of transistors.

A. P. STERN
General Electric Co.
Syracuse, New York

Electronic Engineering by Samuel Seely

Published (1956) by McGraw-Hill Book Co., Inc., 330 W. 42 St., N. Y. 36, N. Y. 484 pages+28 page appendix+vii pages. Illus. 9¼×6¼. $8.00.

Dr. Seely is now the author or coauthor of books entitled *Electronics*, *Electronics Engineering*, and *Radio Electronics*. He hasn't yet covered the entire field of electronics and the reviewer judges it unfortunate that such comprehensive titles should be used. The book under review here, *Electronic Engineering*, is one-half of the revision and enlargement of the author's *Electron-Tube Circuits*, the other half being *Radio Electronics*.

Electron-Tube Circuits appeared at an excellent time. Its topics were well chosen and the book lent itself to the education of undergraduate electronic engineers in the subject given by its title. On the other hand the book was apparently written with great rapidity and printed under a somewhat similar condition. The result was a mixture of satisfaction and disappointment. To some extent it represented an opportunity seized because of its timeliness, but from another viewpoint it represented an opportunity lost because of the cracks in its quality which resulted from the speed of its production.

Electronic Engineering seems to this reviewer to show many of the same faults as its predecessor. There has been some rewriting, some rearrangement, some addition of material, as for example, the chapters on solid-state theory, and transistors as circuit elements, and much elimination of which the chapters on untuned power amplifiers, tuned voltage amplifiers, tuned power amplifiers, amplitude modulation, demodulation, and frequency modulation and detection, are examples. The reader can get an idea of the contents of the companion volume, *Radio Electronics*, by noting these omissions. On the other hand, both *Electron-Tube Circuits* and *Electronic Engineering* are more than 500 pages long, which will give an idea of the expansion.

In some respects the book under review and its companion volume seem to be approaching handbook exhaustiveness. The dust cover states "emphasis is placed on the physical and mathematical analyses." There is a good bit of descriptive material, the mathematics is mostly algebra, and there seems to be an avoidance of basic analysis which would require mathematics beyond algebra.

The use of bold face type for complex numbers is excellent, and the author is to be congragulated on this and on other items such as improvement of some of the figures. On the other hand the reviewer expresses a purely personal opinion that there is carelessness in the use of English, and lack of preciseness, which indicate the same hurried preparation as was mentioned above. To illustrate three cases from the many which the reviewer has noted:

"e_c = instantaneous signal that appears between grid and cathode of tube
e_g = instantaneous signal component that appears between grid and cathode of tube"

in which the distinction between e_c and e_g is difficult for a student to determine (if it exists), and

"It should be emphasized that the bel or the decibel denotes a power ratio" in contrast, with which the first use of db is in connection with a voltage ratio where the db's do not indicate a power ratio. The sentences—"Suppose that an unsymmetrical waveform is passed through a capacitor or a transformer. The average ordinate of the output waveform must assume a zero potential, since neither the capacitor nor the transformer will pass a d-c current."—give about as confused a picture as possible.

The totality of instances such as those cited above makes the book a somewhat dangerous one to place in the hands of students whom an instructor would like to have think along rigorous lines. In the reviewer's opinion this is a serious subtraction from the good qualities of the text and should be given careful consideration by instructors who might consider adopting it.

Incidentally, the author avoids almost completely the use of the word *voltage* and does not hesitate to add "potentials" (not even differences of potentials) to be a total "potential."

J. G. BRAINERD
The Moore School of Electrical Engineering
University of Pennsylvania

Radio Electronics by Samuel Seely

Published (1956) by McGraw-Hill Book Co., 330 W. 42 St., N. Y. 36, N. Y. 442 pages+12 index pages +30 pages of appendix+vii pages. Illus. 9¼×6¼. $7.00.

This book gives an excellent coverage of the performance of vacuum tubes in the various applications found in radio circuits, such as amplifiers, oscillators, modulators, etc. The author has presented this material in his usual clear, straight-forward style, with adequate mathematical treatment. He has carefully distinguished complex quantities and phasors by the use of bold-face roman type (although one might prefer the use of bold-face italics, to conform to recently established standards, wherein bold-face roman type is used for space vectors.) Mathematics used includes calculus, both differential and integral, but at elementary levels only. The number of problems included is impressive, averaging over twenty per chapter; thus giving students ample opportunity to apply the information provided in the text. The level of treatment seems to be that of college juniors, or possibly, second-term sophomores.

The book starts out with a general introduction to communication systems, with block diagrams used to indicate the general make-up of radio receivers and transmitters. This chapter is followed by a brief coverage of vacuum tube characteristics, including emission, tube parameters, and static characteristics. The balance of the book gives in reasonable detail basic circuits and the mathematical treatment of the performance of the vacuum tube as a rectifier; as an amplifier, tuned and untuned, power and voltage with and without feedback; as an oscillator; as a modulator and demodulator. The book concludes with a very brief chapter on information theory.

The only serious criticism which this reviewer has of this otherwise excellent book is that it includes but little material which is not also found in a number of other well-known texts and fails to include some material which should not be left out. There is nothing on transistors or other semiconductor devices, and no book on radio electronics seems complete which does not contain considerable material on the operation and application of these new devices. A better title for this book as it is written might be

Vacuum Tubes in Radio Electronics. Nevertheless, this book should meet with at least as enthusiastic a reception as did its predecessor, *Electron-Tube Circuits*.

A. V. EASTMAN
University of Washington
Seattle, Washington

Solid State Physics, Vol. I, ed. by Frederick Seitz and David Turnbull

Published (1955) by Academic Press Inc., Publishers, 125 E. 23 St., N. Y. 10, N. Y. 450 pages+18 index pages+xii pages. Illus. 9¼×6¼. $10.00.

Through an interesting coincidence this reviewer in a recent review of *Advances in Electronics and Electron Physics* expressed the view that a similar volume was needed to cover the growing field of solid state physics. It was with satisfaction and surprise, therefore, that the present volume was received.

This series will consist of compact and authoritative reviews of important areas of the field of solid state physics. It is hoped in this way to provide a broad and balanced picture to the specialist of the entire field as well as presenting specialized articles describing important new techniques.

It seems to this reviewer that a good beginning has been made in Volume One. Chapters are presented on the following topics: Methods of the One Electron Theory of Solids, Qualitative Analysis of the Cohesion in Metals, Quantum Defect Method, Theory of Order Disorder Transitions in Alloys, Valence Semiconductors, Germanium and Silicon, and Electron Interaction in Metals. As is evident from the titles above, the emphasis in this volume is largely theoretical. Treatments while complete and authoritative are sufficiently self-contained that they should serve as a useful and unified text for the experimentalist interested in broadening his understanding of theory and as a useful reference to the theorist.

The emphasis in this series is heavily on the side of fundamental physics Many engineers may therefore find the subject matter difficult and given to less than direct application. For the engineer interested in delving into the quantum theoretic foundations of the growing field of solid state engineering, it is, however, recommended.

In view of the coincidence mentioned above, the reviewer would like hopefully to point out that yet another series with particular emphasis on the advances in solid state *device* physics and engineering would fill a deeply felt need.

G. C. DACEY
Bell Telephone Laboratories, Inc.
Murray Hill, New Jersey

RECENT BOOKS

1955 Vacuum Symposium Transactions. Compiled by the Committee on Vacuum Techniques, Inc., Box 1282, Boston 9, Mass. $10.00.

Criteria for Professional Employment of Engineers. Published by the National Society of Professional Engineers, 2029 K St., N.W., Washington 6, D. C. $0.25 for single copies.

Deane, L. D., and Young, C. C., Jr., *TV Servicing Guide*. Howard W. Sams and Co., Inc., 2201 E. 46 St., Indianapolis 5, Ind. $2.00.

Giet, A., *Abacs or Nomograms*, Philosophical Library, Inc., 15 E. 40 St., N. Y. 16, N. Y. $12.00.

Lieberman, Myron, *Education as a Profession*. Prentice-Hall Inc., 70 Fifth Ave., N. Y. 11, N. Y. $8.00.

Schure, A., *Inverse Feedback*, John F. Rider, Inc., 480 Canal St., N. Y. 13, N. Y. $.90.

Television Factbook, 23rd edition. Published by Television Digest, Wyatt Building, Washington 5, D. C. $4.50.

Tranter, C. J., *Integral Transforms in Mathematical Physics*, 2nd ed. John Wiley & Sons, Inc., 440 Fourth Ave. N. Y. 16, N. Y. $2.00.

Radio Fall Meeting

SPONSORED BY THE IRE AND THE RETMA ENGINEERING DEPARTMENT
OCTOBER 15–17, 1956—HOTEL SYRACUSE, SYRACUSE, N. Y.

Registration is required for admission to all morning and afternoon technical sessions. The registration fee is $3.00. There will be no advance registration.

MONDAY, OCTOBER 15

9:30 a.m.

AUTOMATION

F. C. Collings, presiding.

High Production Method of Etching Printed Wiring Boards, E. F. Altens, Philco Corporation.

Basic Considerations in Foil Transformer Production, W. A. Brackman, R. Levinsohn, and D. McCarthy, American Machine and Foundry Company.

Automatic Manufacture of a Small Choke Coil, D. H. Esperson, General Electric Company.

Effect of Printed Circuits on the Television Industry, J. Toyzer, Radio Corporation of America.

2:00 p.m.

SEMICONDUCTOR APPLICATIONS AND RELIABILITY

J. R. Steen, presiding.

Review of Applications Status for Semiconductors, D. B. Krett, RCA.

Naval Material Laboratory Transistor Reliability Study, R. E. Martin, Naval Material Laboratory.

Factors Determining Reliability of a Germanium Power Transistor, A. B. Jacobsen, Motorola Inc.

Success Story—Transistor Reliability—1956, C. M. Zierdt, Jr., Gen. Elec. Co.

8:00 p.m.

SESSION WITH SYRACUSE IRE SECTION

Management of Military Engineering Programs, J. M. Bridges, Director of Electronics, O.A.S.D.

8:30 p.m.

Stag Party

TUESDAY, OCTOBER 16

9:00 a.m.

TELEVISION RECEIVERS I

L. R. Fink, presiding.

An Ultrasonic Remote Control for Home Receivers, Robert Adler, Peter Desmares and J. G. Stracklen, Zenith Radio Corporation.

Portable TV Design Considerations, F. R. Wellner and M. E. Jones, General Electric Company.

Determination of Transistor Performance Characteristics at VHF, G. E. Theriault and H. M. Mason, Radio Corp. of America.

Transistorized Television Vertical Deflection Systems, W. F. Palmer and George Schiess, Sylvania Electric Products, Inc.

Transistor Feedback Preamplifiers, R. P. Burr, Burr-Brown Research Corporation.

2:00 p.m.

TELEVISION RECEIVERS II

W. E. Good, presiding.

A New Noise-Gate AGC and Sync System for TV Receivers, G. C. Wood, General Electric Company, and J. G. Spracklen and Walter Stroh, Zenith Radio Corporation.

The Measurement of CRT Beam Apertures, E. J. Quinlan, Philco Corporation.

Color-Hold Considerations in Color Receivers, J. R. Banker, Westinghouse Electric Corporation.

An One-Tube Crystal Filter Reference Generator for Color TV Receivers, R. H. Rausch and T. T. True, Gen. Elec. Co.

Technique of Color Purity Adjustment in a Receiver Employing the "Apple CRT," R. C. Moore, A. Hopengarten, P. G. Wolfe and W. F. Simon, Philco Corporation.

6:15 p.m.

Cocktail party

6:45 p.m.

Dinner

Toastmaster: A. V. Loughren.

Speaker: W. R. G. Baker, on "The Outlook for TV."

WEDNESDAY, OCTOBER 17

9:00 a.m.

ELECTRON DEVICES

T. M. Liimatainen, presiding.

Receiving Tubes Operating at 12 Volts Anode Potential, C. E. Atkins, Tung-Sol Electric Inc.

Tube Design Considerations for Low Voltage Operation in Hybrid Circuitry, R. J. Bisso, Sylvania Electric Products.

Electron Tube and Circuit Considerations for Series-String Applications, R. G. Rauth, Radio Corporation of America.

Effects of the Earth's Magnetic Field on Color Purity in the Shadow-Mask Color Kinescope, H. N. Hillegass and J. L. Hudson, Radio Corporation of America.

A Horizontal Deflection Circuit with Miniature Tubes, R. E. Schwab, Sylvania Electric Products.

Voltage Tuneable Magnetrons and Their Applications, G. C. Griffin, General Electric Company.

2:00 p.m.

SEMICONDUCTOR DEVICES

W. H. Forster, presiding.

High Frequency Germanium NPN Tetrode, D. W. Baker, Gen. Elec. Co.

PNP Transistors with High Current Amplification—Forward and Reverse—at High Collector Current, A. P. Kordalewski, General Electric Company.

High Frequency Silicon Transistors, C. Thornton, J. Roschen and T. Miles, Philco Corporation.

Application of Power Transistors to Audio Output Stages, R. Minton, Radio Corporation of America.

A New Device for Transistor Stabilization, C. F. Wheatley and R. E. Kleppinger, Radio Corporation of America.

Transistor Symbology, C. D. Todd and L. F. Leinweber, General Electric Company

Ninth Annual Conference on Electrical Techniques in Medicine and Biology

NOVEMBER 7–8–9, 1956

MCALPIN HOTEL, NEW YORK CITY

The purpose of this annual conference is to bring together electrical engineers, medical doctors, biologists, electronic instrumentologists, radiation physicists, and radiologists, to discuss the latest electrical and electronic techniques in biology and medicine, and to arrange symposia on current problems. The conference is sponsored jointly by the IRE, American Institute of Electrical Engineers, and the Instrument Society of America. The coming conference will be held November 7–9 at the McAlpin Hotel in New York City. All persons having a professional medical, physical, or biological interest in electrical therapeutic, diagnostic or investigative techniques are invited to attend. There will be two days of technical sessions with an evening symposium on the first day, and a one-day field trip to Brookhaven National Laboratory.

The General Chairman is E. Dale Trout of the General Electric Co., Milwaukee, Wisconsin. Other committee members are: Program Chairman, D. A. Holaday, Presbyterian Medical Center, New York; Publicity Chairman, Carl Berkley, Allen B. DuMont Laboratories, Inc.; Arrangements, R. S. Gardner, AIEE Headquarters, New York.

NOVEMBER 7

Morning Session

Panel discussion on "Instrumentation for Cardiology."

Chairman: L. B. Lusted, Clinical Center, National Institute of Health.

A Cathode-Ray Cardiograph, C. E. Webb, Allen B. DuMont Laboratories, Inc.

High Voltage Condenser Discharge as a Means of Cardiac Resuscitation in Ventricular Fibrillation, G. S. Shields, Ridgewood, New Jersey.

Afternoon Session

Panel on, "Methods and Standards for Measurement of Electron Beams."

Chairman: John Laughlin, Memorial Hospital, New York City.

Evening Session

Lecture and succeeding discussion on "The Philosophy Underlying Radiation Protection," by L. S. Taylor, Chief, Division of Atomic and Radiation Physics of the National Bureau of Standards.

NOVEMBER 8

Field trip to Brookhaven National Laboratory, Upton, Long Island.

NOVEMBER 9

Morning Session

Panel Discussion on "Design of Instruments for Research in Artificial Respiration."

Afternoon Session

Session on "Instrumentation in Medicine and Biology."

Artificial Respiration Control, L. H. Montgomery, Vanderbilt University.

A New Type Electroencephalograph Wave Analyser, R. J. Levine, Edin Corporation.

Kansas City IRE Section Technical Conference

NOVEMBER 8–9, 1956

TOWN HOUSE HOTEL, KANSAS CITY, KANSAS

Thursday morning, November 8

OPENING SESSION

Moderator: R. W. Butler, Chairman, Kansas City IRE Section, Bendix Aviation Corporation.

Welcome to the Conference: C. V. Miller, Conference Chairman, Bendix Aviation Corporation.

Opening Address: To be announced.

Thursday afternoon, November 8

SESSION I

Moderator: C. F. Wood, Westinghouse Electric Corporation.

A Transistor Negative Immitance Converter, M. A. Karp, Johns Hopkins Univ.

The Analysis and Design of a Transistor Phase Shift Oscillator, speaker from University of Kansas.

Magnetic Amplifier Stability, speaker from Communications Accessories Co.

SESSION II

Moderator: J. B. Heffelfinger, Consulting Radio Engineer, Kansas City, Missouri.

Electron Tube Reliability, W. H. Hailey, Bendix Aviation Corporation.

Ferrites in Switching Circuits, Jack Moon, Kansas State College.

Thursday evening, November 8

Banquet

Toastmaster: C. N. Kimball, President Midwest Research Institute.

Speaker: S. F. Singer, University of Maryland, on earth satellites.

Friday morning, November 9

SESSION I

Moderator: R. R. Hancox, Director of Research, Great Lakes Pipe Line Company.

Measurement of Plating Thicknesses Using Pulsed and Sinusoidal Eddy Currents, D. L. Waidelich, Engineering Experiment Station, University of Missouri.

The Use of Photoconduction in Image Display Devices, J. E. Jacobs, Advanced Development Laboratory, General Electric Company.

SESSION II

Moderator: To be announced.

A System for General-Purpose Analog-Digital Computation, G. P. West, Computer Systems Division, The Ramo-Wooldridge Corporation.

Analysis of Servo Systems, A. C. Cotts, Midwest Research Institute.

A Design Application of Graphical Statistics, D. J. Nigg, Bendix Aviation Corporation.

Friday afternoon, November 9

MANAGEMENT SYMPOSIUM

Moderator: Martin Goland, Southwest Research Institute.

Industrial Management, C. D. Moore, General Electric Company.

Pure Relations and Problems with Engineers, Walter Anderson, Westinghouse Electric Corporation.

Science of Research Management, F. N. Stephens, Midwest Research Institute.

Industrial Psychology, R. W. Ogan, industrial psychologist.

Operations Research, An Integrated Science of Management; R. L. Ackoff, Case Institute of Technology.

For additional information regarding registration and exhibits write Technical Conference, Inc., Kansas City I.R.E. Section, P.O. Box 9201, Kansas City 15, Mo.

Abstracts of IRE Transactions

The following issues of "Transactions" have recently been published, and are now available from the Institute of Radio Engineers, Inc., 1 East 79th Street, New York 21, N. Y. at the following prices. The contents of each issue and, where available, abstracts of technical papers are given below.

Sponsoring Group	Publication	Group Members	IRE Members	Non-Members*
Circuit Theory	Vol. CT-3, No. 2	$1.60	$2.40	$4.80
Engineering Management	Vol. EM-3, No. 3	.90	1.35	2.70
Medical Electronics	PGME-5	1.75	2.60	5.25
Ultrasonics Engineering	PGUE-4	1.50	2.25	4.50

*** Public libraries and colleges may purchase copies at IRE Member rates**

Circuit Theory

VOL. CT-3, NO. 2, JUNE, 1956

Abstracts of Papers in This Issue

The Scattering Matrix in Network Theory

—H. J. Carlin

This paper gives an introductory treatment of the concept and uses of scattering methods in network problems. The scattering parameter description for linear networks is defined and the utility of this formalism for problems involving power flow in terminated networks is discussed. Examples of scattering computations for transformer 4-ports, transformerless impedance matching networks and transducers with parasitic capacitance are given. The physical realizability requirements for linear lumped networks in the frequency domain are presented in scattering terms, and some exten-

sions to the realizability of distributed networks are briefly discussed.

Elementary Applications of the Scattering Formalism to Network Design—V. Bélévitch

The purpose of this paper is to show the considerable simplification introduced by the scattering formalism in the derivation of many theorems of elementary network theory, and to illustrate how often this concept discloses new aspects of known results, or new connections between apparently unrelated properties. The examples chosen are somewhat unrelated, but they have been selected to emphasize the fertility of the scattering concept; for the sake of simplicity, the examples are limited to calculations at a single frequency, or deal with properties of frequency independent networks, so that the complex frequency plane is never used.

Four-Dimensional Transformations of 4-Pole Matrices with Application to the Synthesis of Reactance 4-Poles—Vitold Bélévitch

The various matrices (impedance, admittance chain, scattering) commonly used in 4-pole theory are shown to originate from 4-dimensional transformations on the vector formed by the input and output voltages and currents. Several particular transformations are studied and lead naturally to a matrix (the transfer matrix) already introduced by Bauer, Dicke, and Watson. This is applied to the synthesis of reactance 4-poles: in particular, their decomposition into a tandem connection of two 4-poles of lower degree, studied by Talbot, is considerably simplified.

Application of Scattering Matrices to the Synthesis of n-Ports—Yosiro Oono

Scattering matrices are applied to the synthesis of finite passive n-ports (n-terminal pair networks) with frequency dependence. A realizability theorem for scattering matrices is shown and an n-port is synthesized as a nondissipative network terminated in resistances. By considering the various numbers of resistance terminations and introducing the notion of generalized minimum phase shift, the relation among all the equivalent networks with a prescribed scattering matrix is studied. Reciprocal or nonreciprocal networks containing the minimum number of reactances or the minimum number of reactances and resistances are generally treated.

Scattering Equivalent Circuits for Common Symmetrical Junctions—W. H. Kahn

A novel form of equivalent circuit is presented for the symmetric two-port, the shunt-T junction, the hybrid-T junction, and certain directional couplers. These circuits are derived from symmetry properties of the scattering matrix and represent simplifications in that one and two-ports interconnected by ideal hybrid junctions replace the corresponding multiport junctions. The term "scattering equivalent circuit" is employed principally because it is possible to trace incident and reflected waves through this internal structure. The circuit form is based on symmetry considerations and therefore essentially independent of the frequency.

The equivalent circuits are conveniently tabulated, and their properties discussed in sections independent of those dealing with their derivation. Examples of application are given.

Network Properties of Circulators Based on the Scattering Concept—M. A. Treuhaft

By treating the scattering matrix as an operator, it is possible to relate the properties of circulators to the cyclic substitutions of group theory and the oriented 1-circuits of topology. The body of knowledge made available by these two branches of mathematics is shown to yield precise definitions of circulator performance. Useful results in treating the symmetries, interconnections, and cascade combinations of circulators are found by further application of group theory and topology.

A Metric Representation of the Geometrically Tapered Chain of Four Terminal Networks—H. L. Armstrong

The geometrically tapered chain of two-terminal pairs is defined as a chain whose individual sections have transmission matrices, whose diagonal elements are the same for all sections, while the antidiagonal elements for successive sections differ by a multiplicative factor which is independent of position along the chain. The transmission matrix of the chain is then expressed in terms of Tchebycheff functions. It is shown how, in special cases, the results reduce to previously known formulas. The phase shift network used in phase shift oscillators is considered briefly as a particular case of the geometrically tapered network.

A Treatment of Cascaded Active Four-Terminal Networks with Application to Transistor Circuits—H. L. Armstrong

A formula previously given for the transmission matrix of n identical passive four-terminal networks connected in cascade, in terms of the modified Tchebycheff functions of the second kind, is extended to active networks. The formula is found to differ chiefly in that the determinant of the matrix (which is now not identically unity), enters explicitly into it. Applications to cascaded transistor circuits are discussed.

Frequency Transformations in Filter Design—A. Papoulis

The problem of determining the possible functions $\omega=\phi(y)$, that will transform the amplitude characteristic $A(\omega)$ of a given network to the amplitude characteristic $A[\phi(y)]$ of another network, is considered. It is shown that the general form of these transformations is given by $\omega=\sqrt{F(y^2)}$, where $F(y^2)$ is a positive rational function of y^2.

The network function whose amplitude characteristic is $A[\phi(y)]$ is determined from the original network and the function $F(y^2)$. The concept of frequency transformations is used in filter design and network analysis; the Butterworth and Tchebycheff filters result as special forms of such transformations.

Design of Feedback Amplifiers for Prescribed Closed-Loop Characteristics—J. L. Stewart

Feedback amplifiers having real feedback are analyzed in general terms in order to express the open-loop transfer function uniquely in terms of a prescribed closed-loop transfer function. Then, the proper amplifier interstage compensating networks can readily be designed. It is shown that bandwidth degradation of the open-loop transfer function is required. Specific numerical functional examples are given for open- and closed-loop functions having 2, 3, and 4 poles. The 4-pole function, which in the example yields a 4-pole maximally flat closed-loop transfer function, is applied to the design of a three-stage feedback amplifier with transformer output. The design procedure, although general, is described by means of specific examples.

All-pole functions must be degraded with a pole near the origin. It is shown that the bandwidth degradation may also be accomplished with functions having both poles and zeros, with the number of poles exceeding the number of zeros by unity. A numerical example is given which shows that the open-loop bandwidth of the degraded system can be made considerably larger by using zeros as well as poles.

The design method for all-pole functions is precise in that it results in a system which, with feedback, has the transfer function specified beforehand. When zeros are added, the method is not quite precise, although the error may be entirely negligible.

A discussion of low-frequency stabilization problems, as introduced by coupling and bypass networks, is given. Although it does not appear practical to employ precision methods, certain optimization procedures are nevertheless applicable.

From the numerical examples, it is evident that the procedure described here not only leads to an unique solution, but in many instances is considerably easier and quicker to apply than classic methods which make use of Nyquist and log-frequency plots. Also, the various stages of an amplifying system can more easily be associated with particular parts of the required open-loop transfer function.

Reviews of Current Literature—Elementary Operations Which Generate Network Matrices—R. J. Duffin . . . Reviewed by E. S. Kuh

Transient Phenomena in Amplitude and Frequency Modulation for Certain Special Networks—Ernst Henze (in German)

Graphic Determination of the Geometric Characteristics of Lossless Linear Four-Terminal Networks—Johann de Buhr (in German)

Determination of the Two-Pole Function Whose Complex Values are Given within a Partial Range of Real Frequencies—Werner Krageloh (in German)

A Derivation Method for Determining Two- and Three-Element Filter Structures—J. E. Colin (in French)

On a Practically-Time and Frequency-Limited Signal Type—J. Ville and J. Bouzitat (in French)

Correspondence

PGCT News

Engineering Management

Vol. EM-3, No. 3, July, 1956

Engineering Managerial Control—E. S. White

Engineering Personnel, Requirements for Research and Development Laboratories—W. J. Schoenberger

Management Problems of the Business Computer Installation—F. P. Brooks, Jr.

Systems Engineering—Key to Modern Development—K. J. Schlager

Weapon System Cost Analysis—David Novick

Management Viewed by an Engineer—R. W. Johnson

Electronics Looks at the Future—H. L. Hoffman

Medical Electronics

PGME-5, July, 1956

Introduction

Recent Developments in Color Translating Ultraviolet Microscopy—H. P. Hovnanian and R. B. Holt

Some Theoretical and Practical Aspects of Microscanning—W. E. Tolles and R. C. Bostrom

Instrumentation for Spectral Phonocardiography—G. N. Webb and V. A. McKusick

The development stages of the instrumentation system for displaying the three dimensions of heart sounds, time, frequency and intensity are described. The heart sounds and physiological data are recorded on magnetic tape. The tape information is repetitively played back, filtered and presented as intensity modulation on cathode-ray tubes having a slow TV type raster where the horizontal sweep represents time in the cardiac cycle and the vertical represents frequency. The resulting patterns which are photographed and visually monitored are used for research, teaching and diagnosis.

Effects of Electric Shock on Man—C. F. Dalziel

The Electrocardiophone—A Surgical Tool—A. J. Morris and J. P. Swanson

Ultrasonics Engineering

PGUE-4, August, 1956

Our First Three Years—A Message from the Chairman—M. D. Fagen

Low-Loss 1000 Microsecond Ultrasonic Delay Lines—J. E. May, Jr.

This paper describes the application of barium titanate ceramic transducers to multiple reflection polygon type 1000 μsec delay lines in order to reduce the loss to around 20 db. This compares with a 50 db loss for the same delay line using quartz crystal transducers. Since the ceramic transducers generate longitudinal waves, mode conversion has been used in order that a shear wave can be propagated through the polygon reflection pattern. The low-loss delay lines have a 6 mc bandwidth centered at 15 mc and an impedance of 50 ohms. Unwanted responses for a 1250 μsec design are about 43 db down from the main response, which is comparable to the best results obtained using quartz transducers.

Analysis and Application of Magnetostriction Delay Lines—T. B. Thompson and J. A. M. Lyon

Uniformly variable sonic delay lines are discussed, with particular attention to the factors affecting the formation of the mechanical signal of transmitting transducer and the electrical signal of the receiving transducer. Examples of pulse shapes for different conditions are calculated and sketched. For comparison with these, some experimental results are described and illustrated. Consideration is given to variation of delay, use of multiple transducers and the control of the polarity of the response. Several devices in which magnetostriction delay lines may be used are briefly described.

Magnetostriction Frequency-Control Units and Oscillator Circuits—E. A. Roberts

Magnetostriction oscillators and associated circuits have been investigated as a means of frequency control in the 50 to 5000 kc frequency range. Factors that affect stability are discussed. It is shown that the temperature coefficient of frequency of the resonator can be controlled by special heat treatment of a commercially available alloy, Ni-Span C. Frequency stabilities of ±0.01 per cent over the temperature range from −55° to +90°C have been achieved for resonators oscillating in the width-extensional and width-shear modes at frequencies between 250 and 2000 kc. Maximum power capability of magnetostriction resonators is discussed and it is shown that these units may be limited either by heating or by exceeding the maximum strain of the material. Magnetostriction resonator units have been developed that cover the frequency range from 250 to 2000 kc. For frequencies below 1000 kc the units fit into a FT249 holder. The high frequency unit is $\frac{7}{8}$ inch in diameter and 1 inch high and covers the frequency range above 1 mc per second. These units all use resonator elements made from 0.010 inch flat stock material, have two coil coupling systems and contain an Alnico VI magnet to supply the required magnetizing field.

Detection of Ultrasound with Phosphorescent Materials—L. A. Petermann and P. B. Oncley

The subject of ultrasonoscopy has been studied by many authors, and several methods have been worked out by which an ultrasonic beam pattern can be visualized. Thermosensitive phosphors of the type CaS-SrS, doubly activated, are found very suitable for the detection of ultrasound around room temperature in the megacycle range; an ultrasonic beam intensity pattern can be converted into a light and dark picture on a phosphorescent screen. A photographic recording of this picture shows a great power of resolution (a few tenths of a millimeter) and a useful sensitivity down to 0.1 to 0.05 watt/cm² at 3 mc. A brief theory of the effect is presented with a discussion of the advantages and disadvantages of this method.

Recent Developments in Ferroelectric Transducer Materials—Don Berlincourt

Ultrasonic Cutting of Quartz Wafers—N. E. Gibbs

Apparatus has been designed and built which simultaneously cuts 20 or more quartz wafers, each of which may be $1\frac{1}{4}$ by $\frac{3}{4}$ by $\frac{1}{64}$ inches in dimension, by ultrasonic methods.

The problems involved in the development of this equipment covered a wide range. Adequate amplitude of motion of the tool assembly was a prime requisite. One of the most stubborn problems lay in achieving stability in the cutting tool itself. The high acceleration involved created difficult bonding problems as well.

Quartz bars must be cut into thin wafers, the surface of which must lie within close limits, measured in minutes, of specified angles with the atomic planes of the quartz crystal. Basic elements of this problem are presented with a brief statement of the limitations and possibilities of the equipment as a tool.

Biographical Notes on the Authors

IRE COMMITTEES—1956

Executive

A. V. Loughren, *Chairman*
W. R. G. Baker, *Vice-Chairman*
Haraden Pratt, *Secretary*

D. G. Fink
J. T. Henderson
A. G. Jensen
J. D. Ryder

Admissions

G. M. Rose, Jr., *Chairman*

H. S. Bennett
*T. M. Bloomer
*E. W. Borden
*H. A. Brown
C. M. Burrill
L. A. Byam, Jr.
L. J. Castriota
*W. E. Darnell
*E. T. Dickey
*J. S. Donal
E. E. Ecklund
*A. D. Emurian
*N. S. Freedman
*Jerome Fox
L. O. Goldstone
J. A. Hansen
F. S. Mabry
G. P. McCouch
*Andrew Mercier
H. G. Miller
*O. D. Perkins
*Harold Rapaport
W. L. Rehm
N. B. Ritchey

* Alternates.

L. M. Rodgers
O. J. Sather
J. L. Sheldon
*W. B. Sullinger
*Richard Talpey
*Eugene Torgow
*J. G. Weissman

Appointments

W. R. Hewlett, *Chairman*

C. R. Burrows
J. N. Dyer
J. J. Gershon
J. T. Henderson
A. V. Loughren
J. D. Ryder
D. J. Tucker

Awards

E. B. Ferrell, *Chairman*

Henri Busignies
R. M. Fano
L. R. Fink
D. E. Foster
A. V. Haeff
A. E. Harrison
H. E. Hartig
C. J. Hirsch
D. R. Hull
J. F. Jordan
J. E. Keto
C. N. Kimball
Urner Liddle
Garrard Mountjoy
A. B. Oxley
L. R. Quarles
George Sinclair
A. W. Straiton
W. L. Webb
H. W. Wells
E. M. Williams
Irving Wolff
H. A. Zahl

Awards Coordination

W. M. Rust, Jr., *Chairman*

F. B. Llewellyn
A. V. Loughren

Constitution and Laws

A. W. Graf, *Chairman*

S. L. Bailey
I. S. Coggeshall
R. A. Heising
W. R. Hewlett

Editorial Board

D. G. Fink, *Chairman*
W. N. Tuttle, *Vice-Chairman*
E. K. Gannett, *Managing Editor*

Ferdinand Hamburger, Jr.
E. W. Herold
T. A. Hunter
J. D. Ryder

Editorial Reviewers

W. R. Abbott
M. A. Acheson
R. B. Adler
Robert Adler
H. A. Affel
H. A. Affel, Jr.
W. J. Albersheim
B. H. Alexander
A. E. Anderson
J. A. Aseltine
W. S. Bachman
H. G. Baerwald
E. M. Baldwin
J. T. Bangert
W. L. Barrow
J. M. Barstow
B. L. Basore
B. B. Bauer
W. R. Beam
L. L. Beranek
P. P. Beroza
F. J. Bingley
H. S. Black
J. T. Bolljahn
H. G. Booker
J. L. Bower
W. E. Bradley
J. G. Brainerd
D. R. Brown
J. H. Bryant
Werner Buchholz
Kenneth Bullington
J. G. Burnett
R. P. Burr
C. R. Burrows
W. E. Caldes
H. J. Carlin
T. J. Carroll
J. A. Chambers
H. A. Chinn
Marvin Chodorow
J. W. Christensen
L. J. Chu
J. K. Clapp
E. L. Clarke
L. E. Closson
J. D. Cobine
R. E. Colander
J. W. Coltman
P. W. Crapuchettes
M. G. Crosby
C. C. Cutler
Sidney Darlington
B. J. Dasher
W. B. Davenport, Jr.
A. R. D'Heedene
A. C. Dickieson
Milton Dishal
Wellesley Dodds
Melvin Doelz
R. B. Dome
H. D. Doolittle
J. O. Edson
W. A. Edson
D. W. Epstein
Jess Epstein
W. L. Everitt
R. M. Fano
L. M. Field
J. W. Forrester
W. H. Forster
G. A. Fowler
R. W. Frank
G. L. Fredendall
H. B. Frost
E. G. Fubini
I. A. Getting
L. J. Giacoletto
E. N. Gilbert
Bernard Gold
W. M. Goodall
A. W. Graf
J. V. N. Granger
V. H. Grinich
A. J. Grossman
R. A. Gudmundsen
E. A. Guillemin
A. V. Haeff
N. I. Hall
W. W. Harman
D. B. Harris
A. E. Harrison
L. B. Headrick
P. J. Herbst
J. K. Hilliard
C. J. Hirsch
Gunnar Hok
J. L. Hollis
W. H. Huggins
J. F. Hull
R. G. E. Hutter
D. D. Israel
E. T. Jaynes
A. G. Jensen
R. L. Jepsen
Harwick Johnson
E. C. Jordan
Robert Kahal
Martin Katzin
W. H. Kautz
R. D. Kell
C. R. Knight
W. E. Kock
Rudolph Kompfner
J. B. H. Kuper
A. E. Laemmel
H. B. Law
R. R. Law
Vincent Learned
M. T. Lebenbaum
W. R. Lepage
F. H. Lewis
W. D. Lewis
J. G. Linvill
F. B. Llewellyn
S. P. Lloyd
A. W. Lo
J. R. MacDonald
Nathan Marchand
Nathan Marcuvitz
F. L. Marx
W. P. Mason
G. L. Matthaei
W. J. Mayo-Wells
E. D. McArthur
D. O. McCoy
Knox McIlwain
Brockway McMillan
R. E. Meagher
T. H. Meisling
Pierre Mertz
H. R. Mimno
S. E. Miller
A. R. Moore
Norman Moore
G. E. Mueller
E. J. Nalos
H. Q. North
K. A. Norton
W. B. Nottingham
B. M. Oliver
H. F. Olson
G. D. O'Neill
P. F. Ordung
C. H. Page
R. M. Page
R. C. Palmer
C. H. Papas
M. C. Pease, III
R. W. Peter
H. O. Peterson
W. H. Pickering
J. A. Pierce
W. J. Poch
A. J. Pote
R. L. Pritchard
C. F. Quate
W. H. Radford
J. R. Ragazzini
J. A. Rajchman
H. J. Riblet
D. H. Ring
Stanley Rogers
T. A. Rogers
H. E. Roys
V. H. Rumsey
J. D. Ryder
R. M. Ryder
Vincent Salmon
A. L. Samuel
H. A. Samulon
O. H. Schade
S. W. Seeley
Samuel Seely
O. G. Selfridge
Samuel Sensiper
R. F. Shea
R. E. Shelby
Donald Shuster
W. M. Siebert
D. B. Sinclair
George Sinclair
David Slepian
R. W. Slinkman
C. E. Smith
O. J. M. Smith
L. D. Smullin
R. A. Soderman
A. H. Sommer
R. C. Spencer
J. R. Steen
Leo Storch
A. W. Straiton
D. E. Sunstein
Charles Susskind
G. C. Sziklai
G. K. Teal
J. C. Tellier
E. R. Thomas
H. P. Thomas
H. E. Tompkins
J. G. Truxal
D. F. Tuttle, Jr.
L. C. Van Atta
K. S. Van Dyke
E. K. Van Tassel
S. N. Van Voorhis
O. G. Villard, Jr.
R. L. Wallace, Jr.
L. G. Walters
C. C. Wang
D. A. Watkins
D. K. Weaver, Jr.
S. E. Webber
W. M. Webster
P. K. Weimer
Louis Weinberg
J. R. Weiner
H. G. Weiss
J. O. Weldon
J. M. West
G. W. Wheeler
H. A. Wheeler
J. R. Whinnery
W. D. White
J. B. Wiesner
Irving Wolff
G. O. Young
L. A. Zadeh

Education

J. M. Pettit, *Chairman*

V. A. Babits
A. B. Bereskin
E. M. Boone
C. C. Britton
W. L. Cassell
J. N. Dyer
I. O. Ebert
W. A. Edson
R. M. Fano
C. L. Foster
Ferdinand Hamburger, Jr.
A. E. Harrison
H. E. Hartig
G. B. Hoadley
F. S. Howes
T. A. Hunter
S. B. Ingram
T. F. Jones
Glenn Koehler
Jerome Kurshan
H. A. Moench
A. D. Moore
P. H. Nelson
R. E. Nolte
J. L. Potter
L. R. Quarles
G. A. Richardson
J. D. Ryder
Samuel Seely
George Sinclair
A. W. Straiton
O. I. Thompson
W. N. Tuttle
David Vitrogan
D. L. Waidelich
J. R. Whinnery
D. G. Wilson
A. L. Winn
M. E. Zaret

Finance

W. R. G. Baker, *Chairman*

A. V. Loughren
Haraden Pratt
J. D. Ryder

History

Haraden Pratt, *Chairman*

Melville Eastham
Keith Henney
Lloyd Espenschied
H. W. Houck
L. E. Whittemore

Nominations

W. R. Hewlett, *Chairman*

S. L. Bailey
E. M. Boone
J. N. Dyer
J. J. Gershon
F. H. R. Pounsett
Haraden Pratt
J. D. Ryder
C. F. Wolcott

Policy Advisory

J. N. Dyer, *Chairman*

J. F. Byrne
A. W. Graf
J. T. Henderson
E. W. Herold
A. G. Jensen
Ernst Weber
C. F. Wolcott

Professional Groups

W. R. G. Baker, *Chairman*
A. W. Graf, *Vice-Chairman (Central Div.)*
M. E. Kennedy, *Vice-Chairman (Western Div.)*
Ernst Weber, *Vice-Chairman (Eastern Div.)*

M. C. Batsel
M. S. Corrington
R. M. Emberson
George Espersen
J. H. Felker
D. G. Fink
R. A. Heising
J. T. Henderson
F. S. Hird
W. W. Mumford
Leon Podolsky
E. A. Post
W. M. Rust, Jr.
J. D. Ryder
L. C. Van Atta

Tellers

W. M. Baston, *Chairman*

P. S. Christaldi
P. G. Hansel
John Hessel
G. P. McCouch
David Sillman
N. A. Spencer
B. F. Tyson

Special Committees

Armed Forces Liaison Committee

G. W. Bailey, *Chairman*

IRE-IEE International Liaison Committee

F. S. Barton
Ralph Bown
R. H. Davies
Willis Jackson
F. B. Llewellyn
C. G. Mayer
R. L. Smith-Rose
J. A. Stratton

Professional Recognition

G. B. Hoadley, *Chairman*

C. C. Chambers
H. F. Dart
W. E. Donovan
C. M. Edwards

Technical Committees

20. Standards Committee

M. W. Baldwin, Jr., *Chairman*
C. H. Page, *Vice-Chairman*
R. F. Shea, *Vice-Chairman*
L. G. Cumming, *Vice-Chairman*

W. R. Bennett
J. G. Brainerd
P. S. Carter
P. S. Christaldi
A. G. Clavier
J. E. Eiselein

H. Goldberg
V. M. Graham
R. A. Hackbusch
H. C. Hardy
D. E. Harnett
Hans Jaffe
Henry Jasik
A. G. Jensen
J. L. Jones
I. M. Kerney
L. G. Kreer, Jr.
E. A. Laport
W. A. Lynch
A. A. Macdonald
Wayne Mason
D. E. Maxwell
K. R. McConnell
H. R. Mimno
M. G. Morgan
G. A. Morton
H. L. Owens
P. A. Redhead
R. Serrell
R. M. Showers
H. R. Terhune
W. E. Tolles
J. E. Ward
E. Weber
W. T. Wintringham

20.5 Definitions Coordinating

C. H. Page, *Chairman*
P. S. Carter
J. G. Kreer, Jr.
E. A. Laport

20.8 Basic Terms

J. G. Brainerd, *Chairman*
M. W. Baldwin, Jr.
C. H. Page

2. Antennas and Waveguides

Henry Jasik, *Chairman*
G. E. Deschamps, *Vice-Chairman*
R. L. Mattingly, *Secretary*
P. S. Carter
H. A. Finke
W. C. Jakes, Jr.
P. A. Loth
A. A. Oliner
K. S. Packard, Jr.
D. C. Ports
W. Sichak
G. Sinclair
P. H. Smith
K. Tomiyasu
W. E. Waller
M. S. Wheeler

2.2 Waveguide and Transmission Line Definitions

G. Deschamps, *Chairman*
W. Sichak

2.4 Waveguide and Waveguide Component Measurements

A. A. Oliner, *Chairman*
P. A. Loth
K. Packard
W. E. Waller

3. Audio Techniques

Iden Kerney, *Chairman*
C. A. Cady
R. H. Edmondson
A. P. Evans
L. H. Good
F. K. Harvey
F. L. Hopper
D. E. Maxwell
R. C. Moody
F. W. Roberts
F. H. Slaymaker
H. O. Saunders
R. E. Yaeger

3.1 Audio Definitions

R. E. Yaeger, *Chairman*
W. E. Darnell
D. S. Dewire
W. F. Dunklee
A. A. McGee
C. W. Frank

3.3 Methods of Measurement of Distortion

R. C. Moody, *Chairman*
L. H. Bowman
F. Coker
J. French
L. D. Grignon
F. Ireland
E. King
J. J. Noble
E. Schreiber
R. Scoville
K. Singer
A. E. Tilley
P. Vlahos
P. Whister

3.4 Methods of Measurement of Noise

H. O. Saunders, *Chairman*
C. A. Cady
B. M. Oliver
J. P. Smith

4. Circuits

W. A. Lynch, *Chairman*
J. T. Bangert, *Vice-Chairman*
W. R. Bennett
J. G. Brainerd
A. R. D'Heedene
T. R. Finch
R. M. Foster
W. H. Huggins
R. Kahal
H. L. Krauss
J. G. Linvill
J. C. Logue
C. H. Page
E. H. Perkins
E. J. Robb
W. N. Tuttle
L. Weinberg

4.1 Transistor Circuitry

T. R. Finch, *Chairman*
R. H. Baker
R. L. Bright
E. Gonzales
F. P. Keiper, Jr.
J. G. Linvill
A. W. Lo
J. C. Logue
G. H. Roger (Alt. for Bright)
J. J. Suran

4.2 Linear Lumped-Constant Passive Circuits

L. Weinberg, *Chairman*
J. A. Aseltine
R. Kahal
G. L. Matthaei
J. G. Truxal

4.3 Circuit Topology

R. M. Foster, *Chairman*
R. L. Dietzold
S. Goldman
E. A. Guillemin
J. Riordan

4.4 Linear Varying-Parameter and Nonlinear Circuits

W. R. Bennett, *Chairman*
J. G. Kreer, Jr.
C. H. Page
J. R. Weiner

4.5 Time-Domain Network Analysis and Synthesis

W. H. Huggins, *Chairman*
S. Goldman
W. H. Kautz
J. G. Linvill
S. J. Mason
D. F. Tuttle, Jr.

4.7 Linear Active Circuits Including Networks with Feedback Servomechanism

E. H. Perkins, *Chairman*
E. J. Angelo, Jr.
W. A. Lynch
J. M. Manley
C. F. Rehberg

4.8 Circuit Components

A. R. D'Heedene, *Chairman*

4.9 Fundamental Quantities

H. L. Krauss, *Chairman*
P. F. Ordung
J. D. Ryder

6. Electroacoustics

H. C. Hardy, *Chairman*
H. S. Knowles, *Vice-Chairman*
B. B. Bauer
M. Copel
W. D. Goodale, Jr.
C. J. LeBel
H. F. Olson
V. Salmon
F. M. Wiener
A. M. Wiggins
P. B. Williams

7. Electron Tubes

P. A. Redhead, *Chairman*
G. A. Espersen, *Vice-Chairman*
J. R. Adams
E. M. Boone
A. W. Coolidge
P. A. Fleming
K. Garoff
E. O. Johnson
W. J. Kleen
P. M. Lapostolle
R. M. Matheson
L. S. Nergaard
G. D. O'Neill
H. J. Reich
A. C. Rockwood
H. Rothe
W. G. Shepherd
R. W. Slinkman
R. G. Stoudenheimer
B. H. Vine
R. R. Warnecke

7.1 Tubes in Which Transit-Time Is not Essential

R. W. Slinkman, *Chairman*
T. A. Elder
W. T. Millis
R. E. Spitzer
A. K. Wing
A. H. Young

7.2 Cathode-Ray and Television Tubes

J. R. Adams, *Chairman*
R. Dressler
H. J. Evans
L. T. Jansen
R. Koppelon
J. C. Nonnekens
G. W. Pratt
D. Van Ormer

7.2.2 Storage Tubes

A. S. Luftman, *Chairman*
J. A. Buckbee, *Secretary*
A. Bramley
A. E. Beckers
Joseph Burns
G. Chafaris
C. L. Corderman
M. Crost
D. Davis
H. J. Evans
Frances Darne
M. D. Harsh
B. Kazan
M. Knoll
C. C. Larson
W. E. Mutter
D. S. Peck
D. L. Schaefer
R. W. Sears
H. M. Smith
W. O. Unruh
P. Youtz

7.3 Gas Tubes

A. W. Coolidge, *Chairman*
J. H. Burnett
E. J. Handley
R. A. Herring
D. E. Marshall
G. G. Riska
W. W. Watrous
H. H. Wittenberg

7.3.1 Methods of Test for TR and ATR Tubes

K. Garoff, *Chairman*
A. Marchetti, *Secretary*
N. Cooper
H. Heins
F. Klawsnik
F. McCarthy
L. W. Roberts
R. Scudder
R. Walker

7.4 Camera Tubes, Phototubes, and Storage Tubes in Which Photo-Emission is Essential

R. G. Stoudenheimer, *Chairman*
B. R. Linden
B. H. Vine

7.5 High-Vacuum Microwave Tubes

E. M. Boone, *Chairman*
J. H. Bryant
R. L. Cohoon
H. W. Cole
G. A. Espersen
M. S. Glass
P. M. Lally
R. A. LaPlante
H. L. McDowell
A. W. McEwan
R. R. Moats
M. Nowogrodzki
S. E. Webber

7.5.1 Non-Operating Characteristics of Microwave Tubes

M. Nowogrodzki, *Chairman*
R. L. Cohoon, *Secretary*

M. S. Glass — E. D. Reed
R. C. Hergenrother — F. E. Vacarro

7.5.2. Operating Measurements of Microwave Oscillator Tubes

R. R. Moats, *Chairman*
R. A. LaPlante, *Secretary*

T. P. Curtis — G. I. Klein
C. Dodd — M. Siegman
W. Ghen — W. W. Teich

Consultants

J. S. Needle — A. E. Harrisan
E. C. Okress — J. F. Hull
T. Moreno — W. G. Shepherd

7.5.3 Operating Measurements of Microwave Amplifier Tubes

S. E. Webber, *Chairman*
P. M. Lally, *Secretary*

J. Berlin — H. L. McDowell
H. W. Cole — A. W. McEwan
H. J. Hersh — R. W. Peter
G. Weibel

7.6 Physical Electronics

R. M. Matheson, *Chairman*

R. W. Atkinson — H. B. Frost
J. G. Buck — P. N. Hamblenton
L. Cronin — J. M. Lafferty
J. E. White

7.6.2 Noise

H. A. Haus, *Chairman*

W. B. Davenport — S. W. Harrison
W. A. Harris — T. E. Tapley

7.8 Camera Tubes

B. H. Vine, *Chairman*

B. R. Linden — D. H. Schaeffer

8. Electronic Computers

R. Serrell, *Chairman*
D. R. Brown, *Vice-Chairman*

S. N. Alexander — G. W. Patterson
W. T. Clary — J. A. Rajchman
R. D. Elbourn — Q. W. Simkins
M. K. Haynes — R. L. Snyder, Jr.
L. C. Hobbs — W. H. Ware
J. R. Johnson — C. R. Wayne
M. Middleton, Jr. — J. R. Weiner
C. D. Morrill — C. F. West
Way Dong Woo

8.3 Static Storage Elements

M. K. Haynes, *Chairman*

A. O. Black — W. M. Papian
T. H. Bonn — J. Rajchman
H. R. Brownell — E. A. Sands
T. G. Chen — R. Stuart-Williams
E. Gelbard — D. H. Toth

8.4 Definitions (Eastern Division)

L. C. Hobbs, *Chairman*

R. D. Elbourn — R. P. Mayer
J. R. Johnson — G. W. Patterson

8.5 Definitions (Western Division)

W. H. Ware, *Chairman*

H. T. Larson — W. S. Speer
W. E. Smith — R. Thorensen

8.6 Magnetic Recording for Computing Purposes

S. N. Alexander, *Chairman*

8.7 Computer Block Diagrams and Logical Symbols

G. W. Patterson, *Chairman*
J. S. Murphy, *Vice-Chairman*

C. F. Lee — R. J. Nelson
M. P. Marcus — A. J. Neumann
R. P. Mayer — J. J. O'Farrell
G. E. Poorte

8.8 Analog Computers—Definitions and Symbols

C. D. Morrill, *Chairman*

9. Facsimile

K. R. McConnell, *Chairman*
D. Frezzolini, *Vice-Chairman*

H. F. Burkhard — P. Mertz
C. K. Clauer — M. P. Rehm
A. G. Cooley — H. C. Ressler
J. A. Doremus — R. B. Shanck
J. Hackenberg — G. S. Thompson
J. V. Hogan — P. Turkheimer
B. H. Klyce — R. J. Wise
L. R. Lankes — K. Woloschak

26. Feedback Control Systems

J. E. Ward, *Chairman*
E. A. Sabin, *Vice-Chairman*

M. R. Aaron — J. C. Lozier
G. S. Axelby — T. Kemp Maples
V. B. Haas, Jr. — W. M. Pease
R. J. Kochenburger — P. Travers
D. P. Lindorff — R. B. Wilcox
W. K Linvill — S. B. Williams
D. L. Lippitt — F. R. Zatlin

26.1 Terminology for Feedback Control Systems

F. Zweig, *Chairman*

G. R. Arthur — J. S. Mayo
C. F. Rehberg

26.2 Methods of Measurement and Test of Feedback Control Systems

V. Azgapetian, *Chairman*

R. Gordon — M. Matthews
A. F. Stuart

10. Industrial Electronics

J. E. Eiselein, *Chairman*
E. Mittelmann, *Vice-Chairman*

W. H. Brearley, Jr. — H. R. Meahl
G. P. Bosomworth — J. H. Mennie
R. I. Brown — W. D. Novak
Cledo Brunetti — H. W. Parker
J. M. Cage — S. I. Rambo
E. W. Chapin — E. A. Roberts
R. D. Chipp — R. J. Roman
D. Cottle — W. Richter
C. W. Frick — C. E. Smith
R. A. Gerhold — C. F. Spitzer
H. C. Gillespie — L. W. Thomas
A. A. Hauser, Jr. — W. R. Thurston
E. A. Keller — M. P. Vore
T. P. Kinn — J. Weinberger
E. W. Leaver — S. L. Yarbrough

10.1 Definitions

R. J. Roman, *Chairman*

W. H. Brearley, Jr. — C. W. Frick
D. W. Cottle — W. Hausz
J. E. Eiselein — E. Mittelmann
C. F. Spitzer

10.3 Industrial Electronics Instrumentation and Control

E. Mittelmann, *Chairman*
W. H. Brearley, Jr., *Vice-Chairman*

C. F. Bagwell — E. A. Keller
S. F. Bartles — D. Krett
R. I. Brown — J. Niles
H. Chestnut — W. D. Novak
D. Esperson — C. F. Spitzer
C. E. Jones — L. W. Thomas
N. P. Kalmus — W. A. Wildhack

11. Information Theory and Modulation Systems

J. G. Kreer, Jr., *Chairman*
M. J. E. Golay, *Vice-Chairman*

P. L. Bargellini — S. Goldman
N. M. Blachman — H. W. Kohler
W. R. Bennett — E. R. Kretzmer
T. P. Cheatham, Jr. — N. Marchand
L. A. DeRosa — L. Meacham
P. Elias — J. F. Peters
D. Pollack

11.1 Modulation Systems

D. Pollack, *Chairman*

11.2 East Coast Information Theory

P. Elias, *Chairman*

11.3 West Coast Information Theory

N. M. Blachman, *Chairman*

25. Measurements and Instrumentation

P. S. Christaldi, *Chairman*
J. H. Mulligan, Jr., *Vice-Chairman*

M. J. Ackerman — G. A. Morton
J. L. Dalke — C. D. Owens
W. D. George — A. P. G. Peterson
G. B. Hoadley — J. G. Reid, Jr.
W. J. Mayo-Wells — R. M. Showers

25.1 Basic Standards and Calibration Methods

W. D. George, *Chairman*

S. L. Bailey — G. L. Davies
F. J. Gaffney

25.2 Dielectric Measurements

J. L. Dalke, *Chairman*

C. A. Bieling — F. A. Muller

25.3 Magnetic Measurements

C. D. Owens, *Chairman*

W. E. Cairnes — R. C. Powell
D. I. Gordon — J. H. Rowen
P. H. Haas — E. J. Smith

25.4 Audio-Frequency Measurements

A. P. G. Peterson, *Chairman*

R. Grim — R. A. Long

25.5 Video Frequency Measurements

G. L. Fredendall, *Chairman*

J. F. Fisher
H. A. Samulon
C. O. Marsh
W. R. Thurston

25.6 High Frequency Measurements

R. V. Lowman, *Chairman, Joint AIEE-IRE Committee High Frequency Measurements*
G. B. Hoadley, *Chairman, IRE Subcommittee 25.6*

R. A. Braden
I. G. Easton
F. J. Gaffney
E. W. Houghton
D. Keim
B. M. Oliver
B. Parzen

25.8 Interference Measurements

R. M. Showers, *Chairman*

H. E. Dinger
C. W. Frick
F. M. Greene
A. W. Sullivan

25.9 Measurement of Radio Activity

G. A. Morton, *Chairman*

25.10 Oscillography

M. J. Ackerman, *Chairman*

F. J. Bloom
W. G. Fockler
C. F. Fredericks
H. M. Joseph
G. R. Mezger (alternate)
M. S. Rose
A. L. Stillwell
H. Vollum

25.13 Telemetering

W. J. Mayo-Wells, *Chairman*

J. L. Blackburn
J. F. Brinster
R. E. Colander
A. P. Gruer
T. L. Harding
C. H. Hoeppner
M. R. Kiebert
F. W. Lehan
E. E. Lynch
M. G. Pawley
W. E. Phillips
G. M. Thynell
F. L. Verwiebe
G. F. C. Weedon
W. A. Wildhack

25.14 Electronic Components

J. G. Reid, Jr., *Chairman*

M. B. Carlton
G. B. Devey
J. W. Gruol
J. N. Hall
W. G. James
A. E. Javitz
J. H. Muncy
F. A. Paul
F. E. Wenger

29. Medical Electronics

W. E. Tolles, *Chairman*

A. M. Grass
J. P. Jervey
T. F. Hueter
L. H. Montgomery, Jr.
H. M. Rozendaal

16. Mobile Communication Systems

A. A. Macdonald, *Chairman*
W. A. Shipman, *Vice-Chairman*

N. Caplan
D. B. Harris
N. Monk
J. C. O'Brien
N. H. Shepherd
D. Talley
T. W. Tuttle
A. Whitney

12. Navigation Aids

H. R. Mimno, *Chairman*
W. Palmer, *Vice-Chairman*

A. M. Casabona
C. M. Jansky, Jr.
H. I. Metz
A. G. Richardson
L. M. Sherer

12.2 Standard DF Measurements

E. D. Blodgett, *Chairman*
J. Kaplan, *Vice-Chairman*
R. Silberstein, *Secretary*

A. D. Bailey
H. I. Butler
J. J. Kelleher
F. M. Kratokvil
A. A. Kunze
J. T. Lawrence
H. R. Mimno
W. M. Richardson
J. A. Solga
J. O. Spriggs
C. A. Strom, Jr.
S. R. Thrift
J. H. Trexler
H. W. von Dohlen

12.3 Measurement Standards for Navigation Systems

F. Moskowitz, *Chairman*
S. B. Fishbein, *Secretary*

P. Adams
R. Alexander
S. Anderson
R. Battle
S. D. Gurian
P. Hansel
G. Litchford
J. T. MacLemore
G. E. Merer
J. S. Pritchard
P. Ricketts
Abe Tatz
V. Weihe

13. Nuclear Techniques

G. A. Morton, *Chairman*

R. L. Butenhoff
D. L. Collins
D. C. Cook
Louis Costrell
T. R. Kohler
W. W. Managan
M. A. Schultz

14. Piezoelectric Crystals

H. Jaffe, *Chairman*
P. L. Smith, *Vice-Chairman*

J. R. Anderson
J. H. Armstrong
H. G. Baerwald
R. Bechmann
W. G. Cady
A. I. Dranetz
W. A. Edson
I. E. Fair
W. D. George
E. Gerber
R. L. Harvey
W. P. Mason
C. F. Pulvari
K. S. VanDyke

14.1 Ferroelectric Memory Material and Devices

J. R. Anderson, *Chairman*

J. H. Armstrong
E. J. Hurbregtse
E. D. Kennedy
Walter Merz
C. Pulvari

27. Radio Frequency Interference

R. M. Showers, *Chairman*
S. J. Burruano, *Vice-Chairman*

C. C. Chambers
J. F. Chappell
E. W. Chapin
K. A. Chittick
L. E. Coffey
M. S. Corrington
H. E. Dinger
E. C. Freeland
A. B. Glenn
J. A. Hansen
S. D. Hathaway
W. Mason
J. B. Minter
W. E. Pakala
D. W. Pugsley
D. Talley
H. G. Towlson
W. A. Shipman

27.1 Basic Measurements

M. S. Corrington, *Chairman*

S. J. Burruano
E. W. Chapin
H. E. Dinger
C. W. Frick
A. B. Glenn
F. M. Greene
W. R. Koch

Task Group

E. O. Johnson, *Chairman*

E. W. Chapin
F. M. Greene
I. K. Munson

27.2 Definitions

W. Mason, *Chairman*
C. W. Frick

27.3 Radio and TV Receivers

A. B. Glenn, *Chairman*

Z. Atlas
A. Augustine
D. L. Carpenter
E. W. Chapin
M. S. Corrington
T. Cuniff
R. J. Farber
R. F. Foster
A. M. Intrator
E. O. Johnson
W. R. Koch
W. A. Needs
P. Pan
W. E. Scull
C. G. Seright
P. Simpson
W. S. Skidmore
M. Soja
J. W. Stratman
D. Thomas
R. S. Yoder

27.4 Radio Transmitters

27.5 Industrial Electronics

S. J. Burruano, *Chairman*

27.6 Recording Equipment

M. S. Corrington, *Acting Chairman*

27.7 Mobile Communications Equipment

W. Shipman, *Chairman*

27.8 Carrier Current Equipment

27.9 Community Antennas

27.10 Test Equipment

J. B. Minter, *Chairman*

27.11 Atmospherics

H. E. Dinger, *Chairman*

E. W. Chapin
W. O. Critchlow
F. H. Dickson
M. M. Newman
A. W. Sullivan

17. Radio Receivers

D. E. Harnett, *Chairman*
W. O. Swinyard, *Vice-Chairman*

K. A. Chittick
L. E. Closson
D. J. Healey III
K. W. Jarvis
J. K. Johnson
W. R. Koch
I. J. Melman
G. Mountjoy
L. Riebman
J. D. Reid
L. M. Rodgers
S. W. Seeley
F. B. Uphoff
R. S. Yoder

17.8 Television Receivers

W. O. Swinyard, *Chairman*

W. R. Alexander
J. Avins
J. Bell
C. E. Dean
E. Floyd
E. C. Freeland
W. J. Gruen
W. R. Koch
C. O. Marsh
I. J. Melman
B. S. Parmet
E. Pufahl
G. F. Rogers
S. P. Ronzheimer

17.10 Automatic Frequency and Phase Control

F. B. Uphoff, *Chairman*

R. Davies
K. Farr
W. J. Gruen
W. R. Koch
R. N. Rhodes
D. Richman
L. Riebman

15. RADIO TRANSMITTERS

H. Goldberg, *Chairman*
A. E. Kerwien, *Vice-Chairman*

J. H. Battison — P. J. Herbst
M. R. Briggs — L. A. Looney
A. Brown — J. F. McDonald
H. R. Butler — S. M. Morrison
T. Clark — J. Ruston
W. R. Donsbach — G. W. Sellers
L. K. Findley — B. Sheffield
H. E. Goldstine — B. D. Smith
F. B. Gunter — M. G. Staton
R. N. Harmon — V. E. Trouant
J. B. Heffelfinger — I. R. Weir
V. Ziemelis

15.1 FM TRANSMITTERS

J. Ruston, *Chairman*

J. Bose — N. Marchand
J. R. Boykin — P. Osborne
H. P. Thomas

15.2 RADIO-TELEGRAPH TRANSMITTERS UP TO 50 MC

H. R. Butler, *Chairman*

J. L. Finch — F. D. Webster
J. F. McDonald — I. R. Weir

15.3 DOUBLE SIDEBAND AM TRANSMITTERS

J. B. Heffelfinger, *Chairman*

R. B. Beetham — D. H. Hax
W. T. Bishop, Jr. — L. A. Looney
L. K. Findley — E. J. Martin, Jr.

15.4 PULSE-MODULATED TRANSMITTERS

B. D. Smith, *Chairman*

R. Bateman — H. Goldberg
L. V. Blake — G. F. Montgomery
L. L. Bonham — W. K. Roberts

15.5 SINGLE SIDEBAND RADIO COMMUNICATION TRANSMITTERS

Adamant Brown, *Chairman*

W. B. Bruene — L. Kahn
J. P. Costas — A. E. Kerwien
H. E. Goldstine — E. A. Laport
J. B. Singel

15.6 TELEVISION BROADCAST TRANSMITTERS

R. N. Harmon, *Chairman*

E. Bradburd — L. A. Looney
W. F. Goetter — J. Ruston
F. E. Talmage

19. RADIO AND REPRODUCING

D. E. Maxwell, *Chairman*

S. J. Begun — R. C. Moyer
M. Camras — C. B. Pear
F. A. Comerci — H. E. Roys
E. W. D'Arcy — W. E. Stewart
S. M. Fairchild — L. Thompson
R. M. Fraser — T. G. Veal
A. W. Friend — R. A. VonBehren
C. J. LeBel — C. F. West

19.1 MAGNETIC RECORDING

R. C. Moyer, *Chairman*

J. S. Boyers — E. W. D'Arcy
M. Camras — W. H. Ericson
F. A. Comerci — O. Kornei
K. I. Lichti — E. Schmidt
C. B. Pear — W. T. Selsted
R. A. VonBehren

19.2 MECHANICAL RECORDING

L. Thompson, *Chairman*

W. S. Bachman — F. W. Roberts
S. M. Fairchild — M. F. Royston
A. R. Morgan — R. A. Schlegel
R. C. Moyer — A. S. R. Tobey

19.3 OPTICAL RECORDING

T. G. Veal, *Chairman*

P. Fish — J. A. Maurer
R. M. Fraser — E. Miller
C. Townsend

19.5 FLUTTER

H. E. Roys, *Chairman*

F. A. Comerci — U. Furst
S. M. Fairchild — C. J. LeBel

CCIR LIAISON GROUP OF IRE COMMITTEE 19

H. E. Roys, *Chairman (Representative)*
A. W. Friend, *Alternate*

W. S. Bachman — R. C. Moyer
R. M. Fraser — L. Thompson

28. SOLID STATE DEVICES

H. L. Owens, *Chairman*
R. R. Law, *Vice-Chairman*
V. P. Mathis, *Secretary*

A. E. Anderson — L. T. MacGill
J. B. Angell — W. J. Mayo-Wells
S. J. Angello — C. W. Mueller
Abraham Coblenz — W. J. Pietenpol
L. Davis, Jr. — R. L. Pritchard
J. M. Early — R. H. Rediker
J. J. Ebers — J. R. Roeder
H. Epstein — C. A. Rosen
H. Goldberg — B. J. Rothlein
J. R. Hyneman — R. M. Ryder
J. P. Jordan — J. Saby
N. R. Kornfield — B. R. Shepard
A. W. Lampe — S. Sherr
J. R. Macdonald — C. F. Spitzer
W. M. Webster

28.4 SEMI-CONDUCTOR DEVICES

S. J. Angello, *Chairman (AIEE)*
J. M. Early, *Chairman (IRE)*

J. B. Angell — H. T. Mooers
R. L. Bright — C. W. Mueller
A. C. Clarke — R. L. Pritchard
A. Coblenz — K. A. Pullen, Jr.
S. K. Ghandi — B. J. Rothlein
J. D. Johnson — S. Saby
W. H. Lapham — H. N. Sachar
R. M. LeLacheur — A. C. Scheckler
B. R. Lester — A. P. Stern
L. T. MacGill — W. J. Mayo-Wells

28.4.1 DIODES

A. C. Scheckler, *Chairman*

L. D. Armstrong — B. Seddon
J. D. Johnson — K. D. Smith
R. P. Lyon — E. L. Steele

28.4.2 METHODS OF TEST FOR TRANSISTORS FOR LINEAR CW TRANSMISSION SERVICE

A. Coblenz, *Chairman*

28.4.3 DEFINITIONS OF SEMICONDUCTORS

B. J. Rothlein, *Chairman*

28.4.4 METHODS OF TEST FOR SEMICONDUCTOR DEVICES FOR LARGE-SIGNAL APPLICATIONS

W. H. Lapham, *Chairman*

A. W. Berger — R. M. LeLacheur
C. Huang — R. L. Trent
R. L. Wooley

28.4.5 METHODS OF TEST FOR BULK SEMICONDUCTORS

B. J. Rothlein, *Chairman*

E. N. Clarke — J. R. Haynes
D. C. Cronemeyer — A. Kestenbaum
I. Drukaroff — M. F. Lamorte
K. W. Uhler

28.4.6 PHOTO DEVICES

28.4.7 TRANSISTOR INTERNAL PARAMETERS

R. L. Pritchard, *Chairman*

R. B. Adler — J. M. Early
J. B. Angell — W. M. Webster

28.5 DIELECTRIC DEVICES

H. Epstein, *Co-Chairman (AIEE)*
C. A. Rosen, *Co-Chairman (IRE)*

J. H. Armstrong — E. E. Loebner
W. D. Bolton — E. F. Mayer
R. B. Delano, Jr. — A. Myerhoff
H. Diamond — H. I. Oshry
D. P. Faulk — C. F. Pulvari
L. A. Finzi — N. Rudnick
F. P. Hall — E. A. Sack
S. R. Hoh — F. A. Schwartz
H. F. Ivey — G. Shaw
B. Jaffee — B. R. Shepard
N. R. Kornfield — C. F. Spitzer
L. E. Walkup

28.6 MAGNETIC DEVICES

J. A. Hornbeck, *Chairman (IRE)*
H. W. Welch, Jr., *Chairman (AIEE)*

A. Applebaum — J. A. Rajchman
D. R. Brown — J. B. Russell
T. H. Crowley — H. F. Storm
R. L. Harvey — V. C. Wilson
M. L. Kales — G. F. Pittman
C. A. Maynard — M. Sirvetz
T. R. McGuire — C. L. Hogan
J. A. Osborn — H. W. Katz

21. SYMBOLS

H. R. Terhune, *Chairman*
R. T. Haviland, *Vice-Chairman*

E. W. Borden — M. B. Reed
D. C. Bowen — A. C. Reynolds, Jr.
M. C. Cisler — R. V. Rice
W. A. Ford — M. P. Robinson
I. L. Marin — M. S. Smith
C. D. Mitchell — R. M. Stern
C. Neitzert — H. P. Westman

21.3 FUNCTIONAL REPRESENTATION OF CONTROL, COMPUTING AND SWITCHING EQUIPMENT

A. C. Reynolds, Jr., *Chairman*

T. G. Cober — H. P. Kraatz
C. W. Frank — F. T. Meyer
H. F. Herbig — E. W. Olcott
W. S. Humphrey, Jr. — J. S. Osborne
T. J. Reilly

21.5 New Proposals and Special Assignments

M. P. Robinson, *Chairman*

21.7 Letter Symbols

C. Neitzert, *Chairman*

M. C. Cisler
G. A. Deschamps
D. C. Livingston
R. M. Stern
C. F. Rehberg

22. Television Systems

W. T. Wintringham, *Chairman*
W. F. Bailey, *Vice-Chairman*

M. W. Baldwin, Jr.
J. E. Brown
K. A. Chittick
C. G. Fick
D. G. Fink
P. C. Goldmark
R. N. Harmon
J. E. Hayes
A. G. Jensen
I. J. Kaar
R. D. Kell
D. C. Livingston
H. T. Lyman
L. Mautner
J. Minter
A. F. Murray
D. W. Pugsley
D. B. Smith
M. E. Strieby
A. J. Talamini

22.2 Television Picture Element

D. C. Livingston, *Chairman*

J. B. Chatten
A. V. Bedford (Alternate for O. H. Schade)
P. W. Howells
P. Mertz
O. H. Schade

23. Video Techniques

J. L. Jones, *Chairman*
S. Doba, Jr., *Vice-Chairman*

S. W. Athey
A. J. Baracket
J. M. Barstow
J. H. Battison
E. E. Benham
K. B. Benson
E. M. Coan
J. R. DeBaun
V. J. Duke
G. L. Fredendall
J. R. Hefele
R. T. Petruzzelli
C. G. Pierce
W. J. Poch
H. O. Saunders

23.1 Definitions

G. L. Fredendall, *Chairman*

I. C. Abraham
R. F. Cotellessa
S. Deutsch
W. C. Espenlaub

23.2 Utilization, Including Video Recording: Methods of Measurement

S. W. Athey, *Chairman*

K. B. Benson
J. M. Brumbaugh
V. J. Duke
G. Gordon

23.3 Video Systems and Components Methods of Measurement

J. R. Hefele, *Chairman*

I. C. Abrahams
G. M. Glassford
A. Lind
N. E. Sprecher
E. Stein
W. B. Whalley

23.4 Video Signal Transmission: Methods of Measurement

J. M. Barstow, *Chairman*

K. B. Benson
R. I. Brown
R. D. Chipp (Alternate for R. I. Brown)
M. H. Diehl
E. E. Gloystein
H. P. Kelly
R. S. O'Brien (Alternate for K. B. Benson)
H. Mate
R. M. Morris
J. R. Popkin-Clurman
E. B. Pores
E. H. Schreiber
L. Staschover
J. W. Wentworth

24. Wave Propagation

M. G. Morgan, *Chairman*

E. W. Allen, Jr.
H. G. Booker
K. Bullington
C. R. Burrows
T. J. Carroll
J. T. deBettencourt
J. H. Dellinger
F. H. Dickson
H. E. Dinger
I. H. Gerks
M. Katzin
R. C. Kirby
M. Kline
L. A. Manning
H. R. Mimno
R. K. Moore
K. A. Norton
H. O. Peterson
J. A. Pierce
G. Sinclair
J. C. W. Scott
R. J. Slutz
N. Smith
R. L. Smith-Rose
J. B. Smyth
H. Staras
A. W. Straiton
A. H. Waynick

24.1 Standard Practices

H. O. Peterson, *Chairman*

24.2 Theory and Application of Tropospheric Propagation

T. Carroll, *Chairman*

24.3 Theory and Application of Ionospheric Propagation

M. G. Morgan, *Chairman*

24.4 Definitions and Publications

H. Staras, *Chairman*

24.6 Radio Astronomy

C. R. Burrows, *Chairman*

A. E. Covington
F. T. Haddock, Jr.
J. P. Hagen

24.7 Terrestrial Radio Noise

H. Dinger, *Chairman*

IRE REPRESENTATIVES ON OTHER BODIES

American Association for the Advancement of Science: J. G. Brainerd

ASA Conference of Executives of Organization Members: G. W. Bailey, L. G. Cumming, alternate

ASA Standards Council: E. Weber, A. G. Jensen, alternate, L. G. Cumming, alternate

ASA Electrical Standards Board: E. Weber, A. G. Jensen, L. G. Cumming

ASA Acoustical Standards Board: E. Weber, L. G. Cumming, alternate

ASA Graphic Standards Board: H. R. Terhune, R. T. Haviland, alternate

ASA Nuclear Standards Board: G. A. Morton, W. E. Shoupp, alternate, L. G. Cumming, alternate

ASA Sectional Committee (C16) on Radio: A. G. Jensen, Chairman, D. E. Harnett, M. W. Baldwin, Jr., L. G. Cumming, Secretary

ASA Sectional Committee (C39) on Electrical Measuring Instruments: P. S. Christaldi, J. E. Mulligan, alternate

ASA Sectional Committee (C42) on Definitions of Electrical Terms: M. W. Baldwin, Jr., J. G. Brainerd, A. G. Jensen, J. G. Kreer

ASA Subcommittee (C42.1) on General Terms: J. G. Brainerd

ASA Subcommittee (C42.6) on Electrical Instruments: R. F. Shea

ASA Subcommittee (C42.13) on Communications: J. C. Schelleng

ASA Subcommittee (C42.14) on Electron Tubes: P. A. Redhead

ASA Sectional Committee (C60) on Standardization on Electron Tubes: L. S. Nergaard, P. A. Redhead

ASA Sectional Committee (C61) on Electric and Magnetic Magnitudes and Units: S. A. Schelkunoff, J. W. Horton, E. S. Purington

ASA Sectional Committee (C63) on Radio-Electrical Coordination: C. C. Chambers, R. M. Showers

ASA Sectional Committee (C67) on Standardization of Voltages—Preferred Volt-

ages—100 Volts and Under: No IRE Voting Representative; Liaison: J. R. Steen
ASA Sectional Committee (C83) on Components for Electronic Equipment: P. K. McElroy
ASA Sectional Committee (C85) on Terminology for Automatic Controls: J. E. Ward, E. A. Sabin
ASA Sectional Committee (Y1) on Abbreviations: H. R. Terhune, R. T. Haviland, alternate
ASA Sectional Committee (Y10) on Letter Symbols: H. R. Terhune, R. T. Haviland, alternate
ASA Subcommittee (Y10.9) on Letter Symbols for Radio: C. Netizert, Chairman
ASA Subcommittee (Y10.14) on Nomenclature for Feedback Control Systems: J. E. Ward, W. A. Lynch, G. Biernson
ASA Sectional Committee (Y14) on Standards for Drawing and Drafting Room Practices: Austin Bailey, K. E. Anspach, alternate
ASA Sectional Committee (Y15) on Preferred Practice for the Preparation of Graphs, Charts and other Technical Illustrations: C. R. Muller, M. P. Robinson, alternate
ASA Sectional Committee (Y32) on Graphical Symbols and Designations: Austin Bailey, A. G. Clavier, A. F. Pomeroy, alternate
ASA Sectional Committee (Z17) on Preferred Numbers: H. R. Terhune
ASA Sectional Committee (Z24) on Acoustical Measurements and Terminology: H. S. Knowles, H. F. Olson, alternate
ASA Sectional Committee (Z57) on Sound Recording: A. G. Jensen, Acting Chairman, H. E. Roys, Representative, A. W. Friend, Alternate, L. G. Cumming, Secretary
ASA Sectional Committee (Z58) on Standardization of Optics: T. Gentry Veal, E. Dudley Goodale, alternate
International Radio Consultative Committee. Executive Committee of U. S. Delegation: A. G. Jensen, Ernst Weber, L. G. Cumming, alternate
International Scientific Radio Union (URSI) Executive Committee: S. L. Bailey, Ernst Weber, alternate
Joint IRE-AIEE Committee on High Frequency Measurements: G. B. Hoadley. IRE Chairman, R. A Braden, I. G. Easton, W. H. Fenn, F. J. Gaffney, E. W. Houghton, J. W. Kearney, D. Y. Keim, B. M. Oliver, B. Parzen, P. S. Christaldi
Joint IRE-RETMA-SMPTE-NARTB Committee for Inter-Society Coordination (Television) (JCIC): W. J. Poch, M. W. Baldwin, Jr., L. G. Cumming, alternate
National Electronics Conference: A. W. Graf
National Research Council—Division of Engineering and Industrial Research: F. B. Llewellyn
U. S. National Committee of the International Electrotechnical Commission: A. G. Jensen, E. Weber, L. G. Cumming

IRE REPRESENTATIVES IN COLLEGES

*Agricultural and Mechanical College of Texas: H. C. Dillingham
*Akron, Univ. of: P. C. Smith
*Alabama Polytechnic Institute: H. E. O'Kelley
Alabama, Univ. of: P. H. Nelson
Alaska, Univ. of: R. P. Merritt
*Alberta, Univ. of: J. W. Porteous
Arizona State College: C. H. Merritt
*Arizona, Univ. of: H. E. Stewart
*Arkansas, Univ. of: W. W. Cannon
Augustana College: V. R. Nelson
Brigham Young University: D. Bartholomew
*British Columbia, Univ. of: A. D. Moore
*Polytech. Inst. of Bklyn. (Day Div.): M. V. Joyce
*Polytech. Inst. of Bklyn. (Eve. Div): G. J. Kent
Brooklyn College: E. H. Green
*Brown University: C. M. Angulo
*Bucknell University: G. A. Irland
Buffalo, Univ. of: W. Greatbach
*Calif. Institute of Technology: H. C. Martel
*Calif. State Polytech. College: H. Hendriks
*Calif. University of: H. J. Scott
California, Univ. of at L. A.: W. L. Flock
Capitol Radio Eng'g. Institute: L. M. Upchurch, Jr.
*Carnegie Institute of Technology: J. B. Woodford, Jr.
*Case Institute of Technology: J. R. Martin
Catholic University of America: G. E. McDuffie, Jr.
Central Technical Institute: J. E. Lovan
*Cincinnati, Univ. of: A. B. Bereskin
*Clarkson College of Tech.: Appointment later
*Clemson Agricultural College: L. C. Adams
*Colorado Agri. and Mech. College: C. C. Britton
*Colorado, Univ. of: C. T. Johnk
*Columbia University: P. Mauzey
*Connecticut, Univ. of: H. W. Lucal
*Cooper Union School of Eng'g.: J. B. Sherman
*Cornell University: T. McLean
Dartmouth College: M. G. Morgan
*Dayton, Univ. of: L. H. Rose
*Delaware, Univ. of: H. S. Bueche
*Denver, Univ. of: C. A. Hedberg
*Detroit, Univ. of: G. M. Chute
DeVry Technical Institute: W. B. McClelland
*Drexel Inst. of Technology: R. T. Zern
Duke University: H. A. Owen, Jr.
*Fenn College: K. S. Sherman
*Florida, Univ. of: M. H. Latour
*George Washington Univ.: G. Abraham
*Georgia Institute of Technology: B. J. Dasher
Gonzaga University: H. J. Webb
Harvard University: C. L. Hogan
Hofstra College: B. Zeines
Houston, Univ. of: W. L. Anderson
Idaho, Univ. of: Appointment later
*Illinois Inst. of Technology: G. T. Flesher
*Illinois, Univ. of: P. F. Schwarzlose
Institute Technologico De Aeronautica: D. K. Reynolds
*Iowa State College: G. A. Richardson
*Iowa, State Univ. of: J. E. Fankhauser
*John Carroll University: Appointment later
*John Hopkins University: W. H. Huggins
*Kansas State College: K. W. Reister
*Kansas, Univ. of: D. Rummer
*Kentucky, Univ. of: N. B. Allison
*Lafayette College: F. W. Smith
Lamar State College of Tech.: L. Cherry
*Laval University: J. E. Dumas
*Lehigh University: L. G. McCracken
Louisiana Polytechnic Inst.: D. L. Johnson
*Louisiana State Univ.: L. V. McLean
*Louisville, Univ. of: S. T. Fife
Lowell Technological Institute: C. A. Stevens
Loyola University: J. H. Battocletti
McGill University: F. S. Howes
*Maine, Univ. of: C. Blake
*Manhattan College: C. J. Nisteruk
Manitoba, Univ. of: H. Haakonsen
*Marquette University: E. W. Kane
*Maryland, Univ. of: H. W. Price
*Mass. Institute of Technology: J. F. Reintjes
*Mass., Univ. of: J. W. Langford
*Miami, Univ. of: F. B. Lucas
*Michigan College of Mining and Tech.: R. R. Jones
*Michigan State University: I. O. Ebert
*Michigan, Univ. of: J. F. Cline

* Colleges with approved student branches.

Milwaukee School of Eng'g.: W. A. Van Zeeland
*Minnesota, Univ. of: L. T. Anderson
*Mississippi State College: Appointment later
*Missouri School of Mines & Metallurgy, Univ. of: R. E. Nolte
*Missouri, Univ. of: J. C. Hogan
*Montana State College: R. C. Seibel
Montreal, Univ. of: Appointment later
Multnoman College: A. B. Tyle
*Nebraska, Univ. of: C W. Rook
*Nevada, Univ. of: W. L. Garrott
*Newark College of Eng'g.: D. W. Dickey
*New Hampshire, Univ. of: F. A. Blanchard
*New Mexico College of Agriculture & Mechanical Arts: H. A. Brown
*New Mexico, Univ. of: R. K. Moore
*New York, College of the City: H. Wolf
*New York University (Day Div.): L. J. Hollander
*New York University (Eve. Div.): L. J. Hollander
*North Carolina State College: E. G. Manning
*North Dakota Agric. College: E. M. Anderson
*North Dakota, Univ. of: C. Thomforde
*Northeastern University: J. S. Rochefort
*Northwestern University: C. W. McMullen
*Norwich University: R. F. Marsh
*Notre Dame, Univ. of: C. Hoffman
Oberlin College: C. E. Howe
*Ohio State University: C. E. Warren
*Ohio University: D. B. Green
*Oklahoma Agri. and Mech. College: H. T. Fristoe
Oklahoma Inst. of Technology: H. T. Fristoe
*Oklahoma, Univ. of: C. E. Harp
*Oregon State College: A. L. Albert
Ottawa, University of: L. A. Beauchesne
Pacific Union College: I. R. Neilsen
*Pennsylvania State University: H. J. Nearhoof
*Pennsylvania, University of: R. Berkowitz
*Pittsburgh, Univ. of: J. Brinda, Jr.
*Pratt Institute: D. Vitrogan
*Princeton University: J. B. Thomas
Puerto Rico, Universidad De: Appointment later
*Purdue University: W. H. Hayt, Jr.
Queen's University: H. H. Stewart
RCA Institutes, Inc.: P. J. Clinton
*Rensselaer Polytechnic Institute: H. D. Harris
*Rhode Island, Univ. of: R. S. Haas
*Rice Institute: C. R. Wischmeyer
*Rose Polytechnic Institute: P. D. Smith
Royal Tech. University of Denmark: G. Bruun
*Rutgers University: C. V. Longo
*Saint Louis University: G. E. Dreifke
*San Diego State College: C. R. Moe
*San Jose State College: H. Engwicht
Santa Clara, Univ. of: H. P. Nettesheim
*Seattle University: F. P. Wood
*South Carolina University: R. G. Fellers
South Dakota State College of Agriculture and Mechanical Arts: J. N. Cheadle
*South Dakota School of Mines & Technology: D. R. Macken
*Southern Calif., Univ. of: G. W. Reynolds
*Southern Methodist University: P. Harton
Southern Technical Institute: R. C. Carter
*Stanford University: J. Linvill
*Stevens Institute of Technology: E. Peskin
*Swarthmore College: C. Barus
*Syracuse University: H. Hellerman
Tennessee A. & I. State University: F. W. Bright
*Tennessee, University of: J. R. Eckel, Jr.
*Texas College of Arts and Industries: J. R. Guinn
*Texas Technological College: C. Houston
*Texas, University of: W. H. Hartwig
*Toledo, University of: D. J. Ewing
*Toronto, University of: G. Sinclair
*Tufts University: A. L. Pike
*Tulane University: J. A. Cronvich
Union College: R. B. Russ
*U. S. N. Postgraduate School: G. R. Giet
*Utah State Agricultural College: W. L. Jones
*Utah, University of: D. K. Gehmlich
Valparaiso Technical Institute: E. E. Bullis
*Vanderbilt University: P. E. Dicker
*Vermont, University of: P. R. Low
*Villanova University: J. A. Klekotka
*Virginia Polytechnic Institute: R. R. Wright
*Virginia, University of: O. R. Harris
*Washington State College of: R. D. Harbour
*Washington University: H. A. Crosby
*Washington, University of: F. D. Robbins
Washington & Lee University: R. E. Alley
*Wayne University: D. V. Stocker
Wentworth Institute: T. A. Verrechhia
Wesleyan University: K. S. Van Dyke
Western Ontario, Univ. of: E. H. Tull
*West Virginia University: C. B. Seibert
*Wisconsin, Univ. of: G. Koehler
*Wichita, Univ. of: A. T. Murphy
*Worcester Polytechnic Institute: H. H. Newell
*Wyoming, Univ. of: E. M. Lonsdale
*Yale University: J. G. Skalnik

Abstracts and References

Compiled by the Radio Research Organization of the Department of Scientific and Industrial Research, London, England, and Published by Arrangement with that Department and the *Wireless Engineer*, London, England

NOTE: The Institute of Radio Engineers does not have available copies of the publications mentioned in these pages, nor does it have reprints of the articles abstracted. Correspondence regarding these articles and requests for their procurement should be addressed to the individual publications, not to the IRE.

Acoustics and Audio Frequencies..... 1502
Antennas and Transmission Lines..... 1502
Automatic Computers..... 1503
Circuits and Circuit Elements..... 1504
General Physics..... 1505
Geophysical and Extraterrestrial Phenomena..... 1506
Location and Aids to Navigation..... 1508
Materials and Subsidiary Techniques... 1508
Mathematics..... 1512
Measurements and Test Gear..... 1512
Other Applications of Radio and Electronics..... 1513
Propagation of Waves..... 1513
Reception..... 1514
Stations and Communication Systems... 1514
Subsidiary Apparatus..... 1514
Television and Phototelegraphy..... 1514
Transmission..... 1515
Tubes and Thermionics..... 1515
Miscellaneous..... 1516

The Index to the Abstracts and References published in the PROC. IRE from February, 1955 through January, 1956 is published by the PROC. IRE, April, 1956, Part II. It is also published by *Wireless Engineer* and included in the March, 1956 issue of that journal. Included with the Index is a selected list of journals scanned for abstracting with publishers' addresses.

The number in heavy type at the upper left of each Abstract is its Universal Decimal Classification number and is not to be confused with the Decimal Classification used by the United States National Bureau of Standards. The number in heavy type at the top right is the serial number of the Abstract. DC numbers marked with a dagger (†) must be regarded as provisional.

ACOUSTICS AND AUDIO FREQUENCIES

534.01 2597

Group Theory of Vibrations of Symmetric Molecules, Membranes, and Plates—M. A. Melvin and S. Edwards, Jr. (*J. Acoust. Soc. Amer.*, vol. 28, pp. 201–216; March, 1956.) "It is shown that the detailed group-theoretical analysis of molecular vibrations can be extended to continuous bodies of various shapes by regarding them as the limits of discrete systems with the number of particles becoming indefinitely large."

534.121.2 2598

On the Vibrations of Triangular Membranes—S. K. L. Rao. (*J. Indian Inst. Sci.*, Section B, vol. 38, pp. 1–3; January, 1956.) Analysis is presented for the free-edge case.

534.2 2599

The Propagation and Reflection of Sound Pulses of Finite Amplitude—T. F. W. Embleton. (*Proc. Phys. Soc.*, vol. 69, pp. 382–395; March 1, 1956.) "Experimental results are discussed covering many aspects of the propagation and reflection of finite amplitude sound pulses and weak shock fronts. These are compared with theory and show amongst other features a) that an *N*-shaped wave form tends to shorten on reflection and b) that a shock front disappears on reflection at an open-ended tube."

534.23 2600

Determination of the Amplitude Distribution on Plane Surfaces from the Directional Distribution of the Radiation Fields—K. Fehér. (*Arch. Elekt. Übertragung*, vol. 10, pp. 125–131; March, 1956.) Theory based on Fourier analysis of the radiation pattern is supported by results of measurements on vibrating plates.

534.232–8 2601

Experimental Characteristics of Continuously-Variable-Resonant-Frequency Crystal Systems—F. Dunn, F. J. Fry, and W. J. Fry. (*J. Acoust. Soc. Amer.*, vol. 28, pp. 275–280; March, 1956.) The characteristics of the transducer described in 2813 of 1955 (Fry *et al.*) are presented graphically and are discussed.

534.24+[538.566:535.42 2602

Variational Method for the Calculation of the Distribution of Energy Reflected from a Periodic Surface: Part 1—W. C. Meecham. (*J. Appl. Phys.*, vol. 27, pp. 361–367; April 1956.)

534.612 2603

Anomalous Behavior of Rayleigh Disk for High-Frequency Waves—J. Awatani. (*J. Acoust. Soc. Amer.*, vol. 28, pp. 297–301; March, 1956.)

534.75:533.723 2604

How Loud is Silence?—C. E. White. (*Audio*, vol. 40, pp. 17–19, 68; March, 1956.) A quantitative discussion of the relation between thermal noise level and hearing threshold.

534.78:621.39 2605

Speech Bandwidth Compression—W. E. Kock. (*Bell Lab. Rec.*, vol. 34, pp. 81–85; March, 1956.) The basic principles of operation of three systems, the "Vocoder," "Audrey," and "Vobanc," are described.

534.845 2606

Measurements on Resonant Absorbent Acoustic Structures—E. Brosio. (*Alta Frequenza*, vol. 25, pp. 32–37; February, 1956.) Laboratory measurements on plastic membranes are reported. Curves show the variation of absorption coefficient with frequency for different distances of the membrane from the wall and for different materials, etc.

534.85/.86:534.76 2607

Two-Channel Stereophonic Sound Systems—F. H. Brittain and D. M. Leakey. (*Wireless World*, vol. 62, pp. 331–334; July, 1956.) Continuation of paper abstracted in July, of 1946, giving practical details of the equipment used.

534.86:061–3(47) 2608

Scientific Symposium on Electroacoustics—B. D. Tartakovski. (*Uspekhi Fiz. Nauk*, vol. 58, pp. 347–358; February, 1956.) Summaries are given of the 17 papers read at the symposium held at Kiev, July 1–5, 1955.

621.395.623.7+621.395.625.3 +621.375.029.3]:061.4 2609

Developments in Sound Reproduction—(*Wireless World*, vol. 62, pp. 335–339; July, 1956.) Equipment shown at the London Audio Fair, the British Sound Recording Association's exhibition, and the Radio Components Show is described.

621.395.625.3 2610

New 16-mm Magnetic Signal-Level Test Film—(*J. Soc. Mot. Pict. Telev. Engrs.*, vol. 65, p. 110; February, 1956.) A film providing a reference level for measurements based on work by Schwartz *et al.* (1864 of 1955).

621.395.625.3 2611

Field Strength and Gap Distribution Function in the [magnetic] Reproducing Head with and without Tape—J. Greiner. (*Nachr Tech.*, vol. 6, pp. 63–70; February, 1956.) Analysis is presented for six different types of gap. The field distribution is closest to ideal for the ring head, the longitudinal component having a nearly rectangular waveform and the transverse component being largely suppressed.

621.395.625.3:538.221 2612

The Process of the Magnetization of Magnetic Tape—W. Guckenburg. (*J. Soc. Mot. Pict. Telev. Engrs.*, vol. 65, pp. 69–72; February, 1956.) A method for making visible a magnetic recording on tape involves softening the agent binding the magnetic particles so that the magnetic forces between the particles can produce mechanical displacement. It is possible to examine recordings of wavelengths <0.4 mil. The azimuth angles of the recording head can be measured to within ± 1 foot of arc.

ANTENNAS AND TRANSMISSION LINES

621.372 2613

Electromagnetic Properties of a Medium comprising Thin Layers—S. M. Rytov. (*Zh. Eksp. Teor. Phys.*, vol. 29, pp. 605–616; November, 1955.) A medium comprising alternate thin layers of two different isotropic materials behaves effectively as a uniform but anisotropic medium. The tensors of the effective permittivity and permeability are derived as functions of the parameters of the materials and of the frequency. The losses and boundary conditions at the surface of the medium are also considered. The theory is relevant to laminated lines of the general type described by Clogston (*e.g.*, 2908 of 1951).

621.372.2 2614

Line Transmission Circuits—E. D. Fitton and R. E. Howland. (*Wireless Engr.*, vol. 33, pp. 143–150; June, 1956.) An examination is made of effects in transmission-line pairs and associated apparatus due to longitudinal currents and voltages which may be introduced by either em or es coupling. Complex waveforms transmitted along a line in the presence of such currents or voltages will suffer undesired modi-

fication. To keep this effect as small as possible, not only should the line pairs be screened and twisted, but the terminal-to-earth impedances should be accurately balanced. Details of suitable techniques are discussed, with numerical illustrations.

621.372.2 2615
Investigation of the Energy Exchange and the Field Distribution for Parallel Surface-Wave Transmission Lines—D. Marcuse. (*Arch. Elekt. Übertragung*, vol. 10, pp. 117–124; March, 1956.) The coupling between two parallel surface-wave lines is calculated by considering them as a two-wire system, different initial conditions being represented by the superposition of cophase and opposed-phase waves on the two lines. With identical lines, the whole of the current fed into one of them is coupled into the other at a distance along the line termed the "exchange length." The presence of a dissimilar conductor near a surface-wave line is shown to impair the field concentration.

621.372.2:621.396.677.75 2616
Diffraction of Surface Electromagnetic Waves. Application to the Theory of the Dielectric Aerial—G. Weill. (*Ann. Radioélect.*, vol. 10, pp. 228–255; July, 1955.) Radiation losses from dielectric-coated single conductors are analyzed and related to the operation of dielectric antennas. Diffraction of the surface wave at discontinuities of the dielectric permittivity or surface impedance is particularly considered. Methods used and results obtained in measurements of phase along a line with variable characteristics are discussed; phase-velocity anomalies have been observed on rhombic antennas. The characteristics of some end-fire antennas 80 λ long are described.

621.372.22 2617
Bibliography of Nonuniform Transmission Lines—H. Kaufman. (IRE TRANS., vol. AP-3, pp. 218–220; October, 1955.)

621.372.8:538.221:538.6 2618
Calculation of the Faraday Effect in a Gyroparamagnetic Medium—J. Soutif-Guicherd. (*Compt. Rend. Acad. Sci., Paris*, vol. 242, pp. 1868–1871; April 9, 1956.) Continuation of work reported previously (2289 of 1955) on propagation in waveguides conatining a gyromagnetic medium. Formulas are derived for the absorption and the rotation of the plane of polarization.

621.372.8:621.316.726 2619
Propagation of Electromagnetic Waves in Circular Waveguides with Finite Wall Conductivity, at Frequencies near Cutoff—W. Schaffeld and H. Bayer. (*Arch. Elekt. Übertragung*, vol. 10, pp. 89–97; March, 1956.) Analysis is presented applicable to all possible E and H modes. Calculations of the propagation constants are based on the assumption of an infinitely thick wall, this approximation being satisfactory for all actual thicknesses >0.1 mm. The results were verified experimentally for H_{11} mode propagation. The high slope of the attenuation/frequency characteristic near cutoff is used as the basis of a method for stabilizing klystron oscillators; the effectiveness of the method is improved by introducing a suitable gas filling in the waveguide.

621.372.8:621.385.029.6 2620
Nonlinear Phenomena in a Waveguide in the Presence of an Electron Beam with Nearly Equal Electron and Wave Velocities—Loshakov. (See 2914.)

621.396.67 2621
On an Error in the Use of the Method of Integral Equations in the Theory of Aerials—B. V. Braude. (*Zh. Tekh. Fiz.*, vol. 25, pp. 1819–1824; September, 1955.)

621.396.674.3 2622
Some Comments on Wide-Band and Folded Aerials—E. O. Willoughby. (*Proc. IRE, Aust.*, vol. 17, pp. 79–87; March, 1956.) "The impedance-frequency characteristic of simple cylindrical antennas is discussed and it is shown that the bandwidth may be considerably improved by the use of appropriate correcting networks. The folded type of antenna automatically makes use of some of these principles. Folded antennas with equal and unequal legs are considered and experimenatl results illustrating the analysis are given."

621.396.676:621.398 2623
A Multiple Telemetering Antenna System for Supersonic Aircraft—R. E. Anderson, C. J. Dorrenbacher, R. Krausz, and D. L. Margerum. (IRE TRANS., vol. AP-3, pp. 173–176; October, 1955.) A system comprising three independent antennas for three separate telemetering transmitters operating in the frequency band 216–235 mc makes use of the existing angle-of-attack indicator and ram-pressure tubes.

621.396.676.029.6:621.3.012.12 2624
Patterns of Stub Antennas on Cylindrical Structures—J. R. Wait and K. Okashimo. (*Canad. J. Phys.*, vol. 34, pp. 190–202; February, 1956.) A theoretical investigation relevant to microwave antennas for aircraft is reported. Radiation patterns are presented for radial electric dipoles located on an insulated cylinder and on a cylindrically tipped half-plane. The patterns are in reasonable agreement with those obtained experimentally by Bain (*Stanford Research Inst. Tech. Rep. No.* 42, April, 1953).

621.396.676.2 2625
Current Distribution on Wing-Cap and Tail-Cap Antennas—I. Carswell. (IRE TRANS., vol. AP-3, pp. 207–212; October, 1955.)

621.396.677 2626
A New Antenna Feed having Equal E- and H-Plane Patterns—A. C.[h]lavin. (IRE TRANS., vol. AP-2, pp. 113–119; July, 1954. *Proc. IRE, Aust.*, vol. 17, pp. 88–93; March, 1956. Abstract, PROC. IRE, vol. 42, p. 1197; July, 1954.) The design of feeds for circular paraboloids is discussed.

621.396.677.3 2627
Cross Section of Colinear Arrays at Normal Incidence—J. M. Minkowski and E. S. Cassedy. (*J. Appl. Phys.*, vol. 27, pp. 313–317; April, 1956.) The back-scattering cross section of colinear arrays of thin dipoles is derived by the variational method, for normally incident waves. The case of the two-dipole array is investigated particularly. Measurements made using the method described by Scharfman and King (2310 of 1954) confirm the validity of the theory.

621.396.677.7/.8 2628
Horn-Parabola Aerials for Wide-Band Directional Radio Systems—H. Laub and W. Stöhr. (*Frequenz.*, vol. 10, pp. 33–44; February, 1956.) Detailed discussion is presented of the radiation properties of antennas comprising parabolic sectors illuminated at high angle and formed as integral structures with the primary radiator. A particular antenna designed for operation at 4 kmc center frequency can be adapted to operate at 6 kmc by suitably modifying the waveguide-to-horn transition in the primary radiator. Two channels can be provided by radiating waves polarized at right angles to one another. Another type of antenna suitable for television transmissions is a paraboloid of revolution excited axially; this can be provided with extensions to reduce the intensity of side lobes.

621.396.677.71 2629
Radiation Patterns of Slotted-Elliptic Cylinder Antennas—J. Y. Wong. (IRE TRANS., vol. AP-3, pp. 200–203; October, 1955.) Continuation of theoretical work reported previously (3482 of 1953). The results can be applied to determine the patterns radiated by very thin slotted cylinders such as wing and tail surfaces of aircraft.

621.396.677.71 2630
The Application of Mathieu Functions in computing the Field Distribution of an Aerial from its Directional Characteristic—A. A. Pistol'kors. (*NachrTech.*, vol. 6, pp. 128–129; March, 1956.) German version of paper abstracted previously from the Russian (3468 of 1954).

621.396.677.833 2631
The Curved Passive Reflector—E. Bedrosian. (IRE TRANS., vol. AP-3, pp. 168–173; October, 1955.) Analysis for antenna reflectors with slightly curved surfaces indicates that with appropriate illumination the gain can be increased indefinitely by increasing the size. In systems in which the reflector is at the top of a tower and the illuminating antena at the foot, the effect of reducing tower height is to widen the main lobe of the radiated pattern and to reduce the level of side lobes.

AUTOMATIC COMPUTERS

681.142 2632
A New Serial Digital Decoder—S. V. Soanes. (*Electronic Engng.*, vol. 28, pp. 247–249; June, 1956.) Intermediate storage and an amplifier feedback loop are used, making the decoder practically independent of clock timing pulses. It can also be used in an analog system to solve certain types of polynomial equation.

681.142 2633
Interconnection of Electronic Computers—(*Tech. News Bull. Nat. Bur. Stand.*, vol. 40, pp. 33–35; March, 1956.) Brief account of experiments on the joint operation of the SEAC and DYSEAC machines on business data-processing work; the former machine transmits control signals to the latter via a cable.

681.142 2634
Design and Construction of Small Automatic Computers with Programming Arrangement, at the Higher Technical School in Dresden—I. Lemann. (*Avtomatika i Telemekhanika* vol. 17, pp. 3–18; January, 1956.) Illustrated description of a computer which includes about 600 tubes and measures 290×180×60 cm; the control desk is separate. A magnetic-drum store is used.

681.142 2635
Principles and Application of Electronic Analogue Computers—P. Heggs. (*Electronic Engng.*, vol. 28, pp. 120–122, 168–170, 212–215, and 257–259; March/June, 1956.) Typical examples of electrical analogs and the equipment for producing them are discussed and general design considerations are presented. The Saunders-Roe general-purpose analog computer is described.

681.142 2636
New Electronic Analogue Apparatus of the Institute of Automatics and Telemechanics of the U.S.S.R. Academy of Sciences—V. V. Gurov, B. Ya. Kogan, A. D. Talantsev, and V. A. Trapeznikov. (*Avtomatika i Telemekhanika*, vol. 17, pp. 19–35; January, 1956.) An illustrated description, including block and circuit diagrams, of the EMU-5 comprising a unit for solving linear differential equations of up to the sixth order, a unit for solving nonlinear differential equations and a power supply unit as well as additional special-purpose units.

681.142 2637
Design of a Timing Device and Nonlinear Units for an Electronic Differential Analyser—V. C. Rideout, N. S. Nagaraja, S. Sampath, V. N. Chiplunkar, and L. S. Manavalan. (*J. Indian Inst. Sci.*, Section B, vol. 38, pp. 66–79; January, 1956.)

681.142:621.3 2638
Basic Circuits used in Digital Automation—M. L. Klein, F. K. Williams, and H. C. Morgan. (*Instrum. and Automation*, vol. 29, pp. 271–279; February, 1956.) Commonly used circuits are described from a practical point of view, with circuit diagrams and details of components.

681.142:621.374.32 2639
An Economical Relay-Operated Accumulator—J. K. Wood. (*Electronic Engng.*, vol. 28, pp. 250–253; June, 1956.) Design details are given of a binary adder with a maximum capacity of about 2^{24}.

681.142:621.385.832 2640
The Hyperbolic-Field Tube, an Electron Beam Tube for Multiplication in Analogue Computers—Schmidt. (See 2924.)

CIRCUITS AND CIRCUIT ELEMENTS

621.3.012.1:621.372.4 2641
Impedance and Admittance Surfaces—R. Merten. (*Arch. Elektrotech.*, vol. 42, pp. 205–216; February 3, 1956.) Three-dimensional locus diagrams are used to investigate the variation of impedance (or admittance) and phase displacement in two-pole circuits in response to variations of frequency, resistance, inductance, or capacitance. The impedance and admittance surfaces include straight lines corresponding to the important special case of zero phase displacement, when the impedance is independent of the damping or detuning.

621.3.066.6 2642
Bridge and Short-Arc Erosion of Copper, Silver, and Palladium Contacts on Break—W. B. Ittner, III. (*J. Appl. Phys.*, vol. 27, pp. 382–388; April, 1956.)

621.314.22.029.3:621.375.23 2643
Transformer Design for "Zero" Impedance Amplifiers—N. R. Grossner. (*Audio*, vol. 40, pp. 27–30, 69; March, 1956.) Lamination-weight reductions of up to 42 per cent may be obtained without increased distortion in a transformer designed for an af "zero-impedance" output stage [*e.g.* 1390 of 1950 (Miller)]. Design formulas are given.

621.316.726:621.396.6 2644
The Stabilidyne—M. Colas. (*Onde Élect.*, vol. 36, pp. 83–93; February, 1956.) A method for applying the harmonics of a quartz crystal oscillator to control the frequency of a receiver or transmitter is described. For reception, the signal frequency and a suitable harmonic of the crystal oscillator are separately mixed with oscillations from a common local oscillator and the two products are then mixed to obtain a frequency which is the difference between that of the signal and the crystal harmonic. Stability of the order of ±50 cps with a signal frequency of 30 mc is readily obtained. The characteristics of several industrial equipments are described.

621.316.727 2645
A 90°-Phase-Shift Circuit for a Wide Frequency Range—O. Limann. (*Elektronik*, vol. 5, p. 46; February, 1956.) A *CR* and a *RC* network are combined in such a way that the undesired phase changes at the outputs of the individual networks due to a frequency change cancel one another in the combined output.

621.318.424 2646
Calculations for Ferroxcube-Pot-Cored Coils—J. Arrazau. (*Onde. Élect.*, vol. 36, pp. 252–267; March, 1956.) A method of calculating core dimensions and windings is presented, giving results accurate to within 10–15 per cent.

621.318.5 2647
Ferroresonant Computing Circuits—R. S. Arbon and G. Phylip-Jones. (*Wireless World*, vol. 62, pp. 324–330; July, 1956.) The basic ferroresonant circuit and applications to switching and counting devices are described.

621.318.57 2648
The Equilibrium States of a Bistable Flip-Flop from the Point of View of Reliable and Stable Operation—M. Bataille. (*Onde Élect.* vol. 36, pp. 94–103; February, 1956.) The influence of individual components on the functioning of the Eccles-Jordan circuit is discussed and permissible tolerances for given performance are determined.

621.319.4:621.375.5 2649
Influence of an Alternating Voltage and a Direct Voltage on a Nonlinear Capacitor—J. C. Hoffmann. (*Compt. Rend. Acad. Sci., Paris*, vol. 242, pp. 2122–2124; April 23, 1956.) Families of curves are presented showing measured variations of capacitance and tan δ as functions of a direct voltage and a 2-kmc voltage, applied simultaneously, for a capacitor with $BaTiO_3$ dielectric. The curves facilitate determination of optimum working point for dielectric amplifiers.

621.372.41:534.01 2650
Linear Systems—B. Gross. (*Nuovo Cim.*, Supplement to vol. 3, pp. 235–296; 1956. In German.) The method of analysis presented previously (2245 of 1953) is developed; the treatment is applicable to all linear passive resonator systems, whether damped or undamped.

621.372.41:534.01 2651
Possibility of Free Oscillations in a Variable-Parameter Resonant System—E. Cambi. (*Nuovo Cim.*, Supplement to vol. 3, pp. 137–181; 1956. In English.) Comprehensive general analysis is presented for time-variable linear systems.

621.372.412+621.373.421.13+537.227/228.1 2652
Papers presented at the 2nd Conference on Piezoelectricity (Moscow, 26th–29th April, 1955)—(See 2770.)

621.372.412:621.372.5 2653
The Equivalent Network of a Piezoelectric Crystal with Divided Electrodes—B. van der Veen. (*Philips Res. Rep.*, vol. 11, pp. 66–79; February, 1956.) A general equivalent circuit is worked out for the crystal treated as a quadripole, for frequencies close to that of mechanical resonance.

621.372.413 2654
Spherical-Frustum Cavities—G. Boudouris. (*Onde Élect.*, vol. 36, pp. 104–121; February, 1956.) Symmetrical spherical-frustum cavities are studied as intermediate cases between the sphere and the cylinder. Resonance wavelengths and Q factors are determined by Abele's method (3823 of 1947). A wavemeter using a hemispherical cavity partly filled with Hg is proposed. Curves are presented showing the variation of Q with cavity size, for $\lambda \sim 3$ cm and 10 cm.

621.372.413 2655
Theory of Coupled Endovibrators [cavity resonators]: Part 2—A. I. Akhiezer and G. Ya. Lyubarski. (*Zh. Tekh. Fiz.*, vol. 25, pp. 1597–1603; September, 1955.) Continuation of work noted previously (658 of 1955). A mathematical analysis is given of the propagation of waves in a chain of cavity resonators coupled by long narrow slots.

621.372.413 2656
Electromagnetic Oscillations in a Parabolic Tube as a Particular Case of the Interaction of Two Cavities through a Throat—E. R. Mustel'. (*Zh. Tekh. Fiz.*, vol. 25, pp. 1788–1799; September, 1955.) Free oscillations in a tube of parabolic profile and rectangular cross section are considered. The tube is regarded as consisting of two cavities interacting through the throat. The wave equation is derived and solutions are found for the cases where the two cavities are a) identical and b) not identical. Experimental results are in good agreement with the theoretical conclusions.

621.372.413:621.317.335.3 2657
Calculation of the Natural Frequency of a w-type [single re-entrant] Cavity Partly Filled with an Absorbing Dielectric—V. L. Patrushev. (*Compt. Rend. Acad. Sci. U.R.S.S.*, vol. 107, pp. 409–412; March 21, 1956. In Russian.) The system considered comprises a reentrant cylindrical cavity resonator with a solid dielectric specimen in the form of a truncated cone placed between the base of the cylinder and the butt-end of the inner conductor. Formulas derived for the natural frequency and the damping can be used also to determine the components of the complex dielectric constant of the specimen; this analysis also provides the theoretical basis of the measurement method described by Works (173 of 1948) and others.

621.372.413:621.318.134 2658
Ferrites in Resonant Cavities—R. A. Waldron. (*Brit. J. Appl. Phys.*, vol. 7, p. 114; March, 1956.) A formula is derived for the frequency shift produced by introducing a sphere of ferrite into a resonant cavity.

621.372.5 2659
Parallel-T *RC* Network—G. V. Buckley. (*Wireless Engr.*, vol. 33, pp. 168–173; July, 1956.) A simplified design method is presented based on finding an equivalent network which is more amenable to mathematical treatment.

621.372.5.01 2660
A Note on Bandwidth—A. Nathan. PROC. IRE, vol. 44, Part 1, pp. 788–790; June, 1956.) The concept of bandwidth is examined in relation to networks such as integrators, which are not designed to provide faithful transmission of a waveform. The bandwidth of such a network is defined as the maximum bandwidth of the input signal for which the output does not differ from that of an ideal network by more than a prescribed amount.

621.372.54 2661
Resistance-Capacitance Filter Networks with Single-Component Frequency Control—W. K. Clothier. IRE TRANS., vol. CT-2, pp. 97–102; March, 1955. Abstract, PROC. IRE, vol. 43, p. 641; May, 1955.)

621.372.54.029.42:621.375 2662
A Practical Method of designing *RC* Active Filters—R. P. Sallen and E. L. Key. (IRE TRANS., vol. CT-2, pp. 74–85; March, 1955.) A method for 30 cps, with sharp cutoff, is based on consideration of five basic variables, namely two resistances, two capacitances, and the gain; from these, further practical parameters are derived by taking the products of resistance and capacitance, the ratio of resistances, and the ratio of capacitances. The active elements can in many cases be simple cathode-follower circuits. Design data for a number of different cases are tabulated.

621.372.542.3.029.4:621.375.23 2663
The Design of Low-Frequency High-Pass *RC* Filters—D. D. Crombie. (*Electronic Engng.*, vol. 28, pp. 254–256; June, 1956.) The design of a twin-T network incorporated in a feedback amplifier circuit is discussed and details are given relating frequency response to phase

shift in the amplifier. The use of compensating sections for securing a flat pass-band characteristic is considered and a practical example is worked out.

621.372.543.3 2664
New Rejector Circuit: Bifilar-T Trap—H. J. Orchard: W. P. Wilson. (*Wireless Engr.*, vol. 33, pp. 175–177; July, 1956.) Comments on 1993 of 1956 (Cocking).

621.372.57 2665
Theory of Noisy Four-Poles—H. Rothe and W. Dahlke. (PROC. IRE, vol. 44, part 1, pp. 811–818; June, 1956.) English version of paper originally published in German (2568 of 1955).

621. 373.4 2666
Nonlinear Coupled Systems—L. Sideriades. (*Compt. Rend. Acad. Sci., Paris*, vol. 242, pp. 1784–1787; April 4, 1956.) Analysis applicable to tube oscillator circuits generally is presented. Different types of oscillator are distinguished topologically.

621.373.421.1 2667
Amplitude Limitation in *LC*-Oscillators—Z. Akçasu. (*Wireless Engr.*, vol. 33, pp. 151–155; June, 1956.) "An *LC*-oscillator which includes two biased diodes in the grid circuit to limit oscillation amplitude is analyzed. Amplitude of oscillation and harmonic distortion are calculated and represented by curves. From these curves it is observed that oscillations can be modulated linearly; no frequency modulation occurs during amplitude modulation and harmonic distortion is very low. Also the circuit is found to be adequate for high frequency stability. The distinctive feature of the circuit is shown to be that the static conditions of the tube, such as bias voltage and direct anode current, are independent of the oscillation amplitude. A practical circuit is described."

621.375.029.3+621.395.623.7+621.395.625.3]
:061.4 2668
Developments in Sound Reproduction—(See 2609.)

621.375.13 2669
Docile Behavior of Feedback Amplifiers—S. J. Mason. (PROC. IRE, vol. 44, part 1, pp. 781–787; June, 1956.) "A docile amplifier is one that remains stable when connected to any passive network of a specified class. A simplified geometrical approach is used to derive the docility criteria for passive-end-loading, ideal-transformer feedback, bilateral passive feedback, and arbitrary passive feedback."

621.375.221.2 2670
Notes on the Design of Distributed Amplifiers—G. Fidecaro and A. M. Wetherell. (*Nuovo Cim.*, vol. 3, pp. 359–370; February 1, 1956. In English.) The treatment used takes account of the self-capacity of the coils and the effect of using anode and grid lines with different propagation speeds; the latter effect can be useful in avoiding the large increase in gain of the *m*-derived filter-type amplifier at the upper end of the band.

621.375.232.9 2671
Differential Amplifiers with Asymmetrical Output—E. Giua. (*Alta Frequenza*, vol. 25, pp. 4–14; February, 1956.) The basic circuit discussed comprises a pair of similar triodes with equal resistances in anode and cathode leads; when equal-phase voltages are applied to the two grids, voltages in phase opposition are produced at the cathode of one tube and the anode of the other; the output is taken from the midpoint of the circuit connecting these two points. Theory of operation is presented and two experimental models are described.

621.375.3 2672
Design of Push-Pull Magnetic Power Amplifiers—N. P. Vasil'eva. (*Avtomatika i Telemekhanika*, vol. 17, pp. 53–65; January, 1956. Addendum, *ibid.*, vol. 17, p. 361; April, 1956.) The method is described in detail and is illustrated by discussion of a 120-w amplifier with a power amplification of 500 and internal feedback.

621.375.3 2673
Principles of Construction of Magnetic Amplifiers with a Low Sensitivity Threshold—M. A. Rozenblat. (*Avtomatika i Telemekhanika*, vol. 17, pp. 66–77; January, 1956.)

621.375.3 2674
High-Frequency Operation of Magnetic Amplifiers—H. W. Collins. (*Elect. Engng., N.Y.*, vol. 75, p. 53; January, 1956. Digest of paper published in *Trans. AIEE, Part I, Communication and Electronics*, vol. 74, pp. 500–505; September, 1955.) Operation at high frequency (*e.g.*, 200 kc) makes possible power gains and bandwidths unattainable at power frequencies, since a given power can be controlled with a smaller core.

621.375.4:621.314.7 2675
[The design of circuits using] Junction Transistors at High Frequencies—J. Vasseur. (*Onde Élect.*, vol. 36, pp. 230–251; March, 1956.) Methods of stabilizing transistor amplifiers are discussed and formulas are presented for calculating the characteristics of a linear amplifier at any frequency, and for determining the principal parameters of junction transistors with common-emitter, common-base, or common-collector connections. Curves are given of maximum gain as a function of frequency.

GENERAL PHYSICS

53.05 2676
The Successive Derivation of Experimental Laws—P. Vernotte. (*Compt. Rend. Acad. Sci., Paris*, vol. 242, pp. 1966–1968; April 16, 1956.) Refinement of the method of smoothing experimental curves described previously (2345 of 1955).

530.162:519.2 2677
On the Use of Gram-Charlier Series to represent Noise—C. W. Horton. (*J. Appl. Phys.*, vol. 27, pp. 350–355; April, 1956.) The stochastic time series produced by the random occurrence of identical events is considered. If the waveforms corresponding to the individual events and to the resulting autocorrelation function and power spectrum are each represented by a Gram-Charlier series, relatively simple relations exist between the different sequences of coefficients. If the noise bandwidth is not too great, the number of terms in the series is small enough to permit computation. The formulas are applied to the analysis of experimental data for noise associated with reverse current in a Si diode.

534.2-16:537.21 2678
On the Theory of the Acousto-Electric Effect—A. Van Den Beukel. (*Appl. Sci. Res.*, vol. B5, pp. 459–468; 1956.) When an acoustic wave passes through an insulated solid it gives rise to an electric field in the direction of propagation. The influence on this phenomenon of thermal lattice vibrations at temperatures above the Debye temperature is investigated theoretically. The calculations indicate that the field is proportional to both the intensity and frequency of the acoustic wave. The effect is so small that it would not generally be observable in Cu, but is larger by several orders of magnitude in Ge.

535.37:061.3(47) 2679
4th Symposium on Luminescence (Molecular Luminescence and Luminescence Analysis)—B. S. Neporent and P. P. Feofilov. (*Uspekhi Fiz. Nauk*, vol. 58, pp. 151–164; January, 1956.) Brief summaries are given of about 50 papers read at the symposium held at Minsk, June 20–25, 1955.

535.515 2680
Birefringence resulting from the Application of an Intense Beam of Light to an Isotropic Medium—A. D. Buckingham. (*Proc. Phys. Soc.*, vol. 69, pp. 344–349; March 1, 1956.)

537/538 2681
A New Model of Classical Electron—P. Caldirola. (*Nuovo Cim.*, Supplement to vol. 3, pp. 297–343; 1956. In English.)

537.122 2682
Electron Physics Tables—L. Marton, C. Marton, and W. G. Hall. (*Nat. Bur. Stand. Circulars*, 83 pp.; March 30, 1956.) Eight parameters are tabulated relating to the energy and motion of electrons accelerated by a potential difference.

537.122 2683
Magnetic Moment of the Electron—P. Kusch. (*Science*, vol. 123, pp. 207–211; February 10, 1956.) A survey of experimental and theoretical work, indicating evidence of anomalies.

537.22:621.315.616 2684
Electrostatic Charges in Plastics—S. M. Skinner. J. Gaynor, and G. W. Sohl. (*Mod. Plast.*, vol. 33, pp. 127–136, 246; February, 1956.) "Experimental evidence is presented that the "static" charge on plastics is a volume charge distribution rather than a surface distribution. The charge contained in a plastic that has been in contact with metal is found to drain out of the plastic by a flow process which depends both upon the resistivity of the plastic and upon the possibility of neutralization of surface charges by opposite charges external to the plastic such as in air."

537.312.8 2685
Field Dependence of Magnetoconductivity—J. W. McClure. (*Phys. Rev.*, vol. 101, pp. 1642–1646; March 15, 1956.) A theoretical calculation is made of the dependence of the elements of the conductivity tensor on the magnetic field for the case of a crystal with arbitrary energy-band structure. The results are the same as would be given by a superposition of electron gases whose cyclotron frequencies are related harmonically. The strengths of the harmonics depend on the band structure. The diagonal elements of the conductivity tensor are monotonically decreasing functions of the magnetic field strength.

537.5 2686
The Characteristics of a Discharge at a Probe at a Positive Potential and the Measurement of the Associated Gas Density—B. N. Klyarfel'd, A. A. Timofeev, N. A. Neretina, and L. G. Guseva. (*Zh. Tekh. Fiz.*, vol. 25, pp. 1581–1596; September, 1955.)

537.5 2687
On the Floating Probe Method for the Measurement of Ionized Gas—K. Yamamoto and T. Okuda. (*J. Phys. Soc. Japan*, vol. 11, pp. 57–68; January, 1956.) Revised expressions are obtained for the positive-ion current and electron temperature for the usual double-probe method. A triple-probe method is proposed for measurement of energy distribution in electrodeless or hf discharges and the applicability of the techniques is discussed.

537.5:538.566 2688
Formulae for the Mean Losses of Energy in Collisions of Slow Electrons moving in Diatomic Gases—L. G. H. Huxley. (*Aust. J. Phys.*, vol. 9, pp. 44–53; March, 1956.) Approximate formulas are derived which correspond closely with results of experiments for electrons of low energy. The formulas are relevant to the theory of interaction of radio waves.

537.52:538.561 2689
Two-Electrode High-Frequency Discharge at Pressures from 100 mm Hg to Atmospheric—G. S. Solntsev and M. M. Dmitrieva. (*Zh. Eksp. Teor. Phys.*, vol. 29, pp. 651–657; November, 1955.) An experimental investigation is reported of discharges in nitrogen and argon at frequencies of 35 to 36 mc and 1.5 mc. Variation of running-voltage with electrode separation and variation of electric field with pressure are shown graphically and photographs of discharges are reproduced.

537.533 2690
Theoretical Interpretation of Field Emission Experiments—T. J. Lewis. (*Phys. Rev.*, vol. 101, pp. 1694–1698; March 15, 1956.) Experimental results obtained by various workers on field emission from tungsten and barium-on-tungsten surfaces are discussed in relation to theories regarding the nature of the surface potential barrier and the distortion of the field by space charge.

537.56:538.56 2691
Kinetic Theory of the Lorentz Gas: Case of "Maxwellian" Molecules—M. Bayet. (*J. Phys. Radium*, vol. 17, pp. 167–168; February, 1956.) Discussion of differences between the views and results of the author (*e.g.* 2925 of 1954) and those of Jancel and Kahan (1366 of 1956, 2196 of 1954 etc.)

537.56:538.6 2692
Use of the Boltzmann Equation for the Study of Ionized Gases of Low Density—(*Phys. Rev.*, vol. 102, pp. 12–27; April 1, 1956.) part 1—K. M. Watson (pp. 12–19). part 2—K. A. Brueckner and K. M. Watson (pp. 19–27).

The behavior of the gas in a strong magnetic field is discussed.

537.562:538.56 2693
On the Dipole Resonant Mode of an Ionized Gas Column—G. H. Keitel. (*Aust. J. Phys.*, vol. 9, pp. 144–147; March, 1956.) Calculations show that the multiple resonances found by Makinson and Slade (3532 of 1954) were created by the discontinuities in their approximation to the Gaussian function, and that the actual Gaussian distribution exhibits only one resonance. See also PROC. IRE, vol. 43, pp. 1481–1487; October, 1955.)

538.3 2694
Fundamental Equations of a Classical Nonconservative Electromagnetism—É. Durand. (*Compt. Rend. Acad. Sci., Paris*, vol. 242, pp. 1862–1865; April 9, 1956.)

538.311:621.318.4 2695
The Computation of Coils for producing Uniform Magnetic Fields and Constant Field Gradients—W. Berger and H. J. Butterweck. (*Arch. Elektrotech.*, vol. 42, pp. 216–222; February 3, 1956.) Calculations for Helmholtz-coil systems are presented. For the field at the midpoint on the axis to be uniform, the second derivative of the field in the axial direction must be zero at that point; for the field gradient to be constant, the third derivative must vanish. Families of curves suitable for design purposes are derived.

538.566 2696
Incidence of Electromagnetic Waves on Double Infinite Grids—Ya. N. Fel'd. (*Compt. Rend. Acad. Sci. U.R.S.S.*, vol. 107, pp. 71–74; March 1, 1956. In Russian.) The system considered comprises a double grid of parallel metal rods; the grids are spaced a apart and the rods in each grid are spaced l apart, the rods in one grid being staggered by an amount d relative to the rods in the other grid; the radius of the rods is r_0. Calculations are made of the reflection coefficient $|R|$ and the refractive index $|Q|$ corresponding to three values of a/λ, for $l=0.2\lambda$, $d=0.1\lambda$ and $r_0=0.01\lambda$, for normal incidence; with $a/\lambda=0.25$, $|R|=0.994$ and $|Q|=0.110$.

538.566:535.13 2697
A Method for integrating Maxwell's Equations—R. Valée. (*Onde Élect.*, vol. 36, pp. 122–133; February, 1956.) Maxwell's equations for propagation of em waves are integrated for the case where the functions representing the wave contours are separable. Applications are discussed showing the relation between the em theory and geometrical optics.

538.566:535.42]+534.24 2698
Variational Method for the Calculation of the Distribution of Energy Reflected from a Periodic Surface: Part 1—W. C. Meecham. (*J. Appl. Phys.*, vol. 27, pp. 361–367; April, 1956.)

538.566:535.42 2699
Experimental Study of the Diffraction of Microwaves by Rotationally Symmetrical Apertures—A. Boivin, A. Dion, and H. P. Koenig. (*Canad. J. Phys.*, vol. 34, pp. 166–178; February, 1956. In French.) Measurements at 1.25 cm λ have been made using circular and annular apertures. The results indicate that diffraction calculations based on Kirchhoff's approximation are accurate to within 5 per cent at planes as close as twice the diameter of the aperture, the accuracy improving as the distance increases.

538.566:535.42 2700
Rigorous Solution of a Particular Diffraction Phenomenon—P. Poincelot. (*Ann. Télécommun.*, vol. 11, pp. 50–56; March, 1956.) Diffraction of a plane em wave by a perfectly conducting infinitely thin screen is analyzed, using an infinite system of algebraic equations and an infinite number of unknowns, for the case of the electric vector parallel to the screen edges. The procedure is to calculate the vector potential for the surface assuming a sinusoidal distribution of parallel straight-line currents. Extension of the method to the more general case of arbitrary direction of electric vector would be feasible using electronic computers.

538.566:537.56 2701
Structure of a Magnetohydrodynamic Shock Wave in a Plasma of Infinite Conductivity—H. K. Sen. (*Phys. Rev.*, vol. 102, pp. 5–11; April 1, 1956.) The analysis presented is relevant to problems of solar rf radiation, the ionosphere, and cosmic rays.

538.566:537.56:621.385.029.6 2702
Growing Electric Space-Charge Waves—J. H. Piddington. (*Aust. J. Phys.*, vol. 9, pp. 31–43; March, 1956.) Theory presented previously, purporting to explain the operation of the electron-wave tube and the origin of solar rf emission, is shown to be unsound; alternative theory is given. See also 2258 of 1956.

538.569.4:547.556 2703
Some Measurements on the Spectral Line Shape and Width of a Paramagnetic Resonance Absorption Line—F. Bruin and M. Bruin. (*Physica*, vol. 22, pp. 129–140; February, 1956.) Measurementa on $\alpha\alpha$-diphenyl-β-picryl hydrazyl at a frequency of about 20 mc are reported.

538.691 2704
The Motion of Charged Particles in Weakly Variable Magnetic Fields—G. Hellwig. (*Z. Naturf.*, vol. 10a, pp. 508–516; July, 1955.) Analysis is simplified by considering in place of the actual particle, which follows a helical path, an equivalent particle following a mean path and having a magnetic moment.

548.0:539.11 2705
Interaction of Excitons with Lattice Vibrations in Polar Crystals: Part 1—H. J. G. Meyer. (*Physica*, vol. 22, pp. 109–120; February, 1956.)

GEOPHYSICAL AND EXTRATERRESTRIAL PHENOMENA

523.16 2706
Early History of Radio Astronomy—G. C. Southworth. (*Sci. Mon.*, vol. 82, pp. 55–66; February, 1956.)

523.16 2707
Cosmic Radio Sources Observed at 600 Mc/s—J. H. Piddington and G. H. Trent. (*Aust. J. Phys.*, vol. 9, pp. 74–83; March, 1956.) A survey has been made over most of the celestial sphere between declinations 90° S and 51° N, using a narrow pencil beam. 49 discrete sources giving flux densities of about 10^{-24} W/m² per cps were identified, including 18 which may not have been previously reported. Nearly all the discrete sources are associated with irregularities of the background radiation.

523.16 2708
Radio Emission from Novae and Supernovae—B. Y. Mills, A. G. Little, and K. V. Sheridan. (*Aust. J. Phys.*, vol. 9, pp. 84–89; March, 1956.) "Attempts have been made to observe the radio emission at 3.5 m from two supernovas and ten novas. Kepler's star was the only reasonably certain identification. A comparison with radio observations of other supernova remnants suggests a constant ratio between the present radio emission and the maximum emissions of light. It is concluded that for common novas, which are not detectable as radio sources, this ratio must be smaller than for supernovas. The galactic radio emission near the plane of the Milky Way could be largely the integrated emission of supernova remnants but common novas could not contribute appreciably."

523.16 2709
The Masses of the Magellanic Clouds from Radio Observations—F. J. Kerr and G. de Vaucouleurs. (*Aust. J. Phys.*, vol. 9, pp. 90–111; March, 1956.)

523.16:523.4 2710
18.3-Mc/s Radiation from Jupiter—C. A. Shain. (*Aust. J. Phys.*, vol. 9, pp. 61–73; March, 1956.) An examination of records at Sydney shows that bursts at 18.3 mc observed in 1950–1951 and previously ascribed to a terrestrial cause were in fact due to radiation from Jupiter; this confirms the observations of Burke and Franklin (2933 of 1955). Some new observations are also mentioned. The usefulness of Jupiter radiation for studying propagation conditions near the sun is pointed out. See also 406 of 1956.

523.16:523.991 2711
Observation of an Eclipse of the Crab Nebula—A. Boischot, E. J. Blum, M. Ginat, and E. Le Roux. (*Compt. Rend. Acad. Sci., Paris*, vol. 242, pp. 1849–1852; April 9, 1956.) Report of observations at frequencies of 169 and 900 mc during the occultation of the Crab nebula by the moon, on January 24, 1956. The radio source corresponds closely to the visible structure of the nebula; it is deduced from this result that the electron density in the lunar atmosphere is $<10^4$/cm³.

523.165:523.746 2712
The Daily Variation of the Cosmic Ray Intensity Measured near the 1954 Sunspot Minimum—M. Possener and I. J. van Heerden. (*Phil. Mag.*, vol. 1, pp. 253–260; March, 1956.)

523.5:551.510.535 2713
A Note on the Interpretation of Transient Echoes from the Ionosphere—A. C. B. Lovell. (*J. Atmos. Terr. Phys.*, vol. 8, pp. 293–294; May, 1956.) Comment on a note by Shain and Kerr (3075 of 1955). Recent radio-echo work on meteors shows that a midday maximum is often observed in the rate of occurrence of meteors. Observations with narrow-beam antennas on 70 mc show that a tendency during the months

October to March for the main peak to occur at 0600 is completely reversed from April to September, when the major peak occurs during the daytime.

523.7:538.12 2714
The Sun's General Magnetic Field—H. Alfvén. (*Tellus*, vol. 8, pp. 1–12; February, 1956.)

523.75:551.594.6 2715
The Solar Outburst, 23 February 1956. Observations by the Royal Greenwich Observatory—T. Gold and D. R. Palmer. (*J. Atmos. Terr. Phys.*, vol. 8, pp. 287–291; May, 1956.) Cosmic-ray, photographic, and magnetic observations are presented; records of the intensity of atmospherics on a frequency of 27 kc show a very substantial decrease in received signal level at 0345 UT, which appears to be attributable to the cosmic-ray increase associated with the flare.

523.75:551.594.6 2716
A Long-Wave Anomaly associated with the Arrival of Cosmic-Ray Particles of Solar Origin on 23 February 1956—M. A. Ellison and J. H. Reid. (*J. Atmos. Terr. Phys.*, vol. 8, pp. 291–293; May, 1956.) Records of atmospherics received on a frequency of 24 kc at the Royal Observatory, Edinburgh, show a sudden decrease coinciding with the time of arrival of solar cosmic-ray particles in the dark hemisphere of the earth.

523.75:621.396.11:551.510.535 2717
Some Unusual Radio Observations made on 23 February 1956—J. S. Belrose, M. H. Devenport, and K. Weekes. (*J. Atmos. Terr. Phys.*, vol. 8, pp. 281–286; May, 1956.) Records of sky-wave signals obtained at Cambridge, England, on frequencies 70–300 kc showed very strong absorption during the occurrence of the solar flare of this date; on 16 kc the main effect was a decrease of 7–8 km in the reflection height. On frequencies 1.5–8 mc at Upsala, almost complete absorption occurred from sunrise until the late afternoon.

55:621.396.934 2718
Symposium on the U.S. Earth Satellite Program—Vanguard of Outer Space—(PROC. IRE, vol. 44, part 1, pp. 741–767; June, 1956.) The text is given of seven papers presented at a symposium held in New York in March, 1956, dealing with various aspects of the USA plans for launching earth satellites during the International Geophysical Year, 1957–1958.

550.384 2719
The Crust as the Possible Seat of Earth's Magnetism—J. S. Chatterjee. (*J. Atmos. Terr. Phys.*, vol. 8, pp. 233–239; May, 1956.) Magnetic material in the earth's crust, to a depth of 20 km, will be highly permeable as a result of temperature and pressure conditions. Interaction between solar corpuscular streams and a very weak initial magnetic field in the crust will magnetize it to saturation; the estimated magnetic moment of the shell agrees with the observed magnetic moment of the earth.

550.385.24:523.746.5 2720
Long-Period Variations in Geomagnetic Activity—E. J. Chernosky. (*Trans. Amer. Geophys. Union*, vol. 36, pp. 591–595; August, 1955.) Analysis of data shows that correlation between the sunspot number R and the magnetic a figure is markedly improved by taking means for the 11-year sunspot-number cycle and for the 22-year sunspot-magnetism cycle in place of annual means.

551.510.53:534.22 2721
Theory of the Rocket-Grenade Method of determining Upper-Atmospheric Properties by Sound Propagation—G. V. Groves. (*J. Atmos. Terr. Phys.*, vol. 8, pp. 189–203; May, 1956.) Theory applicable to projected experiments is developed from earlier work (2046 of 1956); a knowledge of the composition of the atmosphere and of the velocity of the sound of the explosions is assumed.

551.510.535 2722
Electron Distribution in the Ionosphere—G. A. M. King and C. H. Cummack. (*J. Atmos. Terr. Phys.*, vol. 8, pp. 270–273; May, 1956.) Analysis of $h'f$ records by the method described earlier [117 of 1955 (King)] suggests that the ionosphere consists of three Chapman layers, E, F_1, and F_2, and that the temperature is uniform.

551.510.535 2723
Effective Tilts of the Ionosphere at Places about 1000 km apart—H. A. Whale. (*Proc. Phys. Soc.*, vol. 69, pp. 301–310; March 1, 1956.) Fuller account of work described previously (1978 of 1955).

551.510.535 2724
The Rates of Production and Loss of Electrons in the F Region of the Ionosphere—J. A. Ratcliffe, E. R. Schmerling, C. S. G. K. Setty, and J. O. Thomas. (*Phil. Trans. A*, vol. 248, pp. 621–642; March 1, 1956.) From the results of Schmerling and Thomas (2726 below) the rates of production and loss of electrons in the region are deduced. Bradbury's theory of the formation of the F layers (1757 and 2184 of 1938) is shown to be self-consistent; it gives a scale height of 45 km for the ionizable constituent of the atmosphere between 180 and 350 km. This result agrees better with the atmospheric R model deduced by Bates from rocket experiments (*Rocket Exploration of the Upper Atmosphere*, pp. 347–356; 1954) than with the G model deduced from experiments made on the ground. Limits are deduced for the movements caused by electron diffusion under gravity.

551.510.535 2725
The Formation of the Ionospheric Layers F_1 and F_2—J. A. Ratcliffe. (*J. Atmos. Terr. Phys.*, vol. 8, pp. 260–269; May, 1956.) It is shown that an electron loss coefficient varying with height in the manner suggested previously (2724 above) would explain the known facts about the splitting of the F layer and might also be a factor in determining the height of the peak of electron density in the F_2 layer.

551.510.535 2726
The Distribution of Electrons in the Undisturbed F_2 Layer of the Ionosphere—E. R. Schmerling and J. O. Thomas. (*Phil. Trans. A*, vol. 248, pp. 609–620; March 1, 1956.) The variation of electron density with height is deduced from $h'(f)$ records obtained at Watheroo, Huancayo, and Slough, and the form of the typical F layer for magnetically quiet days is described in a series of curves; detailed tabulated results are available at the Cavendish Laboratory, Cambridge, England.

551.510.535 2727
Processes controlling Ionization Distribution in the F_2 region of the Ionosphere—D. F. Martyn. (*Aust. J. Phys.*, vol. 9, pp. 161–165; March, 1956.) Rocket measurements at heights approaching 200 km suggest that the atmospheric density in the F_2 region may be some 30 times less than previously deduced from radio experiments. If the new value were correct, diffusion of F_2 ionization under the forces of gravity and of its own pressure gradient would be likely to affect the shape and height of the region notably. An investigation was made of the possible effects of diffusion processes at such levels. The results indicate that a region with arbitrary height distribution of ionization will by diffusion assume the form of a Chapman region after a time which, for F_2 levels, is a few hours if the radio determinations of density are correct, but only a few minutes if the rocket determinations are correct. It is suggested that there must be a systematic error in the rocket observations.

551.510.535 2728
Observations and Analysis of Ionospheric Drift—D. G. Yerg. (*J. Atmos. Terr. Phys.*, vol. 8, pp. 247–259; May, 1956.) Spaced-receiver fading observations made at Puerto Rico during 1954–1955 on 2.33 and 4.57 mc indicate average drift speeds of 19 mps and 12 mps respectively. The 2.33-mc data are thought to apply to the E layer, and the 4.57-mc data to the F_1 layer. Owing to random changes, the method of similar fades is less reliable than the correlation method of evaluation.

551.510.535 2729
Automatic Recording of Ionospheric Characteristics—K. Bibl. (*J. Atmos. Terr. Phys.*, vol. 8, p. 295; May, 1956.) Following the proposals of Nakata *et al.* (2937 of 1954) a device is proposed which gives a direct record of muf.

551.510.535 2730
Ionospheric Recorders and Sporadic E—J. A. Thomas, A. C. Svenson, and H. E. Brown. (*Aust. J. Phys.*, vol. 9, pp. 159–161; March, 1956.) Brief report of tests made at Brisbane, disproving the statement, which has been made by various workers, that the observed frequency characteristics of the E_s region vary rapidly with the overall sensitivity of the recording $P'f$ equipment.

551.510.535:523.16:550.385 2731
Spread F-Layer Echoes and Radio-Star Scintillation—R. W. Wright, J. R. Koster, and N. J. Skinner. (*J. Atmos. Terr. Phys.*, vol. 8, pp. 240–246; May, 1956.) Correlation is noted between observations of radio-star scintillations at one station in equatorial W. Africa and of spread F layers at another, 510 km distant. Disturbed magnetic conditions, in winter, cause decreased F-layer spread.

551.510.535:523.78 2732
Ionospheric Observations during the Solar Eclipse of June 20, 1955—A. K. Saha, S. Ray, S. Datta, and R. K. Mitra. (*Sci. and Cult.*, vol. 21, pp. 475–477; February, 1956.) Observations made at Haringhata, 28 miles NE of Calcutta, are described. The recorder used provided a frequency sweep from 1 to 13 mc in 1 min 55 seconds. The observed variation of f_0E shows that the disappearance and reappearance of the ionizing radiation source for the E layer was not symmetrical with respect to the time of the eclipse maximum. The ionization of the F_1 layer also showed a marked drop during the eclipse. An observed drop in the ionization of the F_2 layer may or may not have been an eclipse effect.

551.510.535:525.624 2733
Lunar Variations in the Ionosphere—R A. Duncan. (*Aust. J. Phys.*, vol. 9, pp. 112–132; March, 1956.) The global pattern of the observed lunar variations of the height and electron density of the F_2 region is summarized, new analyses being presented for Canberra (f_0F_2), Brisbane ($h'F_2$), and Washington ($h'F_2$ and f_0F_2). The height variation has an amplitude of 1–3 km; maximum height occurs at 06 lunar hours at moderate latitudes and at 09 lunar hours at the geomagnetic equator. The variation of f_0F_2 has an amplitude of 2–4 per cent; the maximum occurs at about 09 lunar hours at moderate geomagnetic latitudes and at 04 lunar hours near the geomagnetic equator. Theory is developed on the basis of a current system at a height of about 100 km. The tidal winds needed to drive the current, the potential distribution in the dynamo layer, and the resulting periodic vertical drifts of ionization in the higher layers are calculated. The lunar variations in f_0F_2 are calculated taking into account probable height variations of recombination coefficient and ionization production

rate; the results are in good agreement with observations. It is concluded that the amplitude of the lunar tidal wind near the E layer is about 45 times greater than that on the ground.

551.510.535:551.557 2734
Influence of Variable Flow of Positive Solar Particles on the Wind in the Ionosphere—V. V. Shuleikin and L. A. Korneva. (*Compt. Rend. Acad. Sci. U.R.S.S.*, vol. 107, pp. 59–62; March 1, 1956. In Russian.) Qualitative results of a calculation of the interaction of electrodynamic and hydrodynamic forces in the ionosphere, at a height where the two forces are of the same order of magnitude, indicate a distribution of wind velocity and direction [Fig. 2(a)] similar to that observed by Hoffmeister (1932 of 1949) and shown in Fig. 2(b). Fig. 1 shows the variation of the E-W and N-S components and of the resultant of the wind velocity over a 27-day period

551.510.535:621.396.11 2735
Oblique Transmission by the Meteoric E-Layer—Naismith. (See 2871.)

551.576/.578:621.396.969.36 2736
The Nature and Detectability of Clouds and Precipitation as determined by 1.25-cm Radar—Plank, Atlas, and Paulsen. (See 2749.)

551.59:538.566.029.6:523.72 2737
Measurement of Atmospheric Absorption on 9350 Mc/s, using Solar R. F. Radiation—P. André, I. Kazes, and J. L. Steinberg. (*Compt. Rend. Acad. Sci., Paris*, vol. 242, pp. 2099–2101; April 23, 1956.) Measurements were made at various times of day, using a radiotelescope described previously [1636 of 1955 (Kazes and Steinberg)]. Only a part of the attenuation observed during sunset can be attributed to absorption by oxygen and water vapor; the remainder, about 35 per cent is so far unexplained.

551.593 2738
The Height of Emission of the 5577 Line of the Air-Glow as observed on the Jungfraujoch—H. Elsässer and H. Siedentopf. (*J. Atmos. Terr. Phys.*, vol. 8, pp. 222–232; May, 1956. In German.) A mean altitude of 90 ± 10 km is deduced.

551.594.5:621.396.11.029.62 2739
A Theory of Scattering by Nonisotropic Irregularities with Application to Radar Reflections from the Aurora—H. G. Booker. (*J. Atmos. Terr. Phys.*, vol. 8, pp. 204–221; May, 1956.) The existence and aspect sensitivity of auroral vhf echoes can be explained as back scatter from nonisotropic columns of ionization parallel to the earth's magnetic field, of length about 40 m and diameter 1 m, caused by turbulence in an E region having a maximum electron density about 100 times the normal value; but the theory fails to explain the rapid fading rates associated with auroral echoes.

551.594.6:621.396.933 2740
Low-Frequency Atmospheric Noise Levels in Southern and Central Africa—D. Hogg. (*Trans. S. Afr. IEE*, vol. 46, part 12, pp. 341–348; December, 1955.) Detailed report of measurements made to determine the interfering effect of atmospherics on radio navigation aids. Results are presented graphically and discussed with reference to local thunder conditions. See also 2305 of 1955.

523.5:061.3 2741
Meteors [Book review]—T. R. Kaiser (Ed.). Publishers: Pergamon Press, London and New York, 204 pp.; 1955. (*J. Franklin Inst.*, vol. 261, p. 275; February, 1956.) The text is given of the papers presented at the symposium reported previously (1016 of 1955).

LOCATION AND AIDS TO NAVIGATION

534.88–14 2742
Underwater Echo-Ranging—D. G. Tucker. (*J. Brit. IRE*, vol. 16, pp. 243–269; May, 1956.) A review covering basic principles, engineering aspects, and various applications. 66 references.

621.396.93 2743
D.F. Plotting Aid—H. G. Hopkins. (*Wireless Engr.*, vol. 33, pp. 173–175; July, 1956.) The simple aid described is in the form of a transparent graticule which is placed on the map over the most probable position of the transmitter to facilitate the determination of the area within which the transmitter lies with a given probability.

621.396.93:621.396.11.029.55 2744
An Automatic Direction Finder for recording Rapid Fluctuations of the Bearing of Short Waves—H. A. Whale and W. J. Ross. (*Proc. Phys. Soc.*, vol. 69, pp. 311–320; March 1, 1956.) The signals in two pairs of antennas placed at the corners of a rectangle $10\text{ m} \times 5\text{ m}$ are combined so that a required 90° phase shift is automatically maintained at all frequencies up to about 17 mc; sense is determined manually. The accuracy of the system is discussed; the effective aperture must be small if it is to follow bearing fluctuations when there is an appreciable spread of the component waves in the incoming signal.

621.396.933:551.594.6 2745
Low-Frequency Atmospheric Noise Levels in Southern and Central Africa—Hogg. (See 2740.)

621.396.969.13 2746
The Radar Measurement of Low Angles of Elevation—J. S. Hey and S. J. Parsons. (*Proc. Phys. Soc.*, vol. 69, pp. 321–328; March 1, 1956.) "The errors which occur in the measurement of low angles of elevation by centimetric radar on a flat ground site are estimated theoretically and compared with experimental measurements. It is demonstrated that a very considerable improvement in angular accuracy is obtained by erecting a screen to intercept the ground-reflected wave. The diffraction effects due to the screen are discussed."

621.396.969.3 2747
The Effect of A.G.C. on Radar Tracking Noise—R. H. Delano and I. Pfeffer. (PROC. IRE, vol. 44, part 1, pp. 801–810; June, 1956.) Low-frequency components of the noise arising from the fluctuating properties of the target echo are enhanced by the agc action. This disadvantage could be avoided by slowing down the agc response, but such a solution might be unsatisfactory for other reasons, *e.g.*, in the case of a radar system closing rapidly on a target. The solution presented is to place a nonlinear filter in the agc path, providing a fast response to rising signals and a slow response to decaying signals.

621.396.969.35 2748
Multipath Phase Errors in C.W.-F.M. Tracking Systems—T. E. Sollenberger. IRE TRANS. vol. AP-3, pp. 185–192, October, 1955.) Errors in missile-tracking systems due to reflections from the ground and from neighboring objects are discussed. Use of frequency modulation permits discrimination against the relatively weak interfering signals. The phase error can be reduced indefinitely by increasing the bandwidth used.

621.396.969.36:551.576/.578 2749
The Nature and Detectability of Clouds and Precipitation as determined by 1.25-cm Radar—V. G. Plank, D. Atlas, and W. H. Paulsen. (*J. Met.*, vol. 12, pp. 358–378; August, 1955.) Results are presented of a survey of the frequency of occurrence of various cloud types from their echo characteristics. With most types, temperature is the most important factor affecting detectability; the presence of ice crystals increases detectability. The 1.25-cm radar equipment used would detect only about 15 per cent of clouds of common types at ranges up to 1 mile. The characteristic features of stratiform precipitation are discussed.

MATERIALS AND SUBSIDIARY TECHNIQUES

531.788.7:621.311.6 2750
Stabilized Power Supply for an Ionization Gauge for Industrial Use—R. P. Henry. (*Le Vide*, vol. 11, pp. 28–33; January/February, 1956.) Neon stabilizers are used for the (positive) grid potential. A triode stabilizing circuit in the filament supply compensates for variations in the grid current of the gauge.

533.5 2751
Some Particular Features of the Ionization Method of producing a Very High Vacuum—N. D. Morgulis. (*Zh. Tekh. Fiz.*, vol. 25, pp. 1667–1670; September, 1955.) Experiments made to investigate the nature of the method are briefly reported and a number of practical suggestions are offered.

533.56 2752
Experimental Study of a Rotary Molecular Pump—G. Mongodin and F. Prevot. (*Le Vide*, vol. 11, pp. 3–13; January/February, 1956.)

535.215 2753
Spectral Distribution of Photoconductivity—H. B. DeVore. (*Phys. Rev.*, vol. 102, pp. 86–91; April 1, 1956.) "A theoretical analysis of the shape of photoconductivity spectral distribution curves is presented, based upon the effects of surface and volume recombination of the charge carriers liberated by the light. Representative curves of photoconductivity vs absorption are computed and compared with experimental observations. As an application of this analysis, experimental data for antimony sulfide are compared with a theoretical curve, and the difference is found to be resolvable into two bands representing nonphotoconductive transitions."

535.215:537.311.33:546.289 2754
The Energy Distribution of Electrons in the External Photoeffect of Germanium containing Impurities—A. N. Arsen'eva-Geil.' (*Zh. Tekh. Fiz.*, vol. 25, pp. 1544–1546; September, 1955.) Experimental V/I characteristics are plotted indicating that photo-electrons are emitted from two energy regions. When the Ge layer is heated to 60°–100° C, an irreversible change in the contact-potential difference between the collector and the emitter takes place, and the number of photo-electrons is considerably increased.

535.215:537.311.33:546.482.21 2755
Comparison of Surface-Excited and Volume-Excited Photoconduction in Cadmium Sulfide Crystals—R. H. Bube. (*Phys. Rev.*, vol. 101, pp. 1668–1676; March 15, 1956.) Measurements have been made of the spectral response, the variation of the photocurrent with illumination intensity, the quenching effect of infrared radiation, the decay time of the photocurrent, and the effect of thermal stimulation. The results can be largely explained by assuming that the surface is inherently less sensitive than the interior of the crystals, the surface sensitivity being highly dependent on the surrounding atmosphere.

535.215:537.311.33:546.482.21:537.312.8 2756
Change of Photocurrent of CdS Single Crystal in a Magnetic Field—S. Tanaka., T. Masumi, and S. Iijima. (*J. Phys. Soc. Japan*, vol. 11, pp. 90–91; January, 1956.) Experiments indicate that the photocurrent increases or decreases, depending on the direction of the magnetic field.

535.215:546.57 2757
Photoemission from Silver into Sodium Chloride, Thallium Chloride and Thallium

Bromide—W. J. Turner. (*Phys. Rev.*, vol. 101, pp. 1653–1660; March 15, 1956.) Experiments yielding negative results are reported.

535.37:546.472.21 2758

Investigation of the Origin of Electron Localization Levels in Zinc Sulphide [ZnS-Cu] Phosphors—N. V. Zhukova. (*Zh. Eksp. Teor. Phys.*, vol. 29, pp. 680–692; November, 1955.) Three thermoluminescence intensity maxima were observed; these occurred at a) −120°C, due to excess Zn in the ZnS lattice, at b) −60°C., and at c) +20°C., due to Cu luminescence centers. The shape of the curve over different temperature ranges is related to the composition. The quenching effect of Fe, Ni, and Co was investigated at temperatures from −180° to +60°C. Results are presented graphically.

535.37:546.472.21 2759

Conductivity Measurements and Spectrographic and X-Ray Investigations on Zinc Sulphide Crystals—J. Krumbiegel, and K. H. Jost. (*Z. Naturf.*, vol. 10a, pp. 526–529; July, 1955.) The conductivity measurements indicate that the photosensitivity maximum occurs at a wavelength of 3520 Å. The spectrographic investigation indicates that crystals with different colored luminescence do not necessarily contain different impurities.

535.376 2760

Contribution to the Study of Quenching and Sensitizing Effects of Electric Fields—H. E. Gumlich. (*J. Phys. Radium*, vol. 17, pp. 117–121; February, 1956.) The luminescence of ZnS-CdS mixtures activated by Mn and excited by ultraviolet or X-rays was investigated experimentally. With ultraviolet excitation an applied field has a quenching effect, with X-ray excitation it produces permanent enhancement of the luminescence. See also 2081 of July (Destriau *et al.*).

535.376 2761

The Temperature Dependence of Brightness Waves in Electroluminescence—D. Hahn and F. W. Seemann. (*Z. Naturf.*, vol. 10a, pp. 586–587; July, 1955.) A number of phosphors have been studied. Oscillograms are reproduced showing the change in the form of the brightness waves of two phosphors at temperatures between −95° and +110°C in a 500-cps field.

535.376:[546.472.21+546.48.47.221 2762

Spectral Energy Distribution Curves of ZnS:Ag and ZnCdS:Ag after Thermal Vacuum Treatment—C. H. Bachman, M. L. Sawner, and W. Allen. (*J. Electrochem. Soc.*, vol. 103, pp. 117–122; February, 1956.) Phosphor screens of thickness comparable to that used in cr tubes were maintained at temperatures between 300° and 800°C. for 5–30 minutes in vacuum; measurements were then made of the spectral energy distribution under bombardment by a diffuse 1000-v electron beam. The heating produces both general reductions and spectral redistributions of emission. The results are discussed in relation to the ion-burn effect in cr tubes.

535.376:546.472.21 2763

Electrophotoluminescence Effects—F. Matossi and S. Nudelman. (*J. Electrochem. Soc.*, vol. 103, pp. 122–127; February, 1956.) A study is reported of the frequency and field-strength dependence of the intensity quenching and the intensity ripple occurring on application of an electric field to a phosphor; 28 different ultraviolet excited ZnS phosphors of cubic and hexagonal structure were investigated.

535.376:546.472.21 2764

Electroluminescence in Zinc Sulfide—W. A. Thornton. (*Phys. Rev.*, vol. 102, pp. 38–46; April 1, 1956.) Simple theory based on single-level electron trapping and a field-controlled thermal release process is developed to explain the observed dependence of the electroluminescence waveform and the integrated light output on voltage, frequency, and temperature.

537.226/.228:546.431.824–31 2765

Role of Domain Processes in Polycrystalline Barium Titanate—M. McQuarrie. (*J. Amer. Ceram. Soc.*, vol 39, pp. 54–59; February 1, 1956.) Discussion of results obtained by various workers indicates that while the high initial dielectric constant of polycrystalline $BaTiO_3$, and possibly also the frequency variation of the initial dielectric constant, can be accounted for without making assumptions regarding domain-wall motion, effects associated with the "poling" and aging processes can be explained more satisfactorily in terms of movements of both 90° and 180° walls.

537.226/.227:546.431.824–31 2766

Retarded Polarization Phenomena in $BaTiO_3$ Crystals—H. H. Wieder. (*J. Appl. Phys.*, vol. 27, pp. 413–416; April, 1956.) An investigation was made of the relation between the applied electric field and the resulting polarization of *c*-domain $BaTiO_3$ crystals in the tetragonal crystal phase for field strengths <1 kv/cm. The results indicate that the processes involved are the same as for greater field strengths. No threshold value of field strength was found for the propagation of antiparallel nuclei.

537.226.31 2767

Dielectric Losses in Ionic Dielectrics in Strong Electric Fields—L. E. Gurevich and V. N. Gribov. (*Zh. Eksp. Teor. Phys.*, vol. 29, pp. 629–636; November, 1955.) Dielectrics in which the ions in the crystal lattice exist in two nearly equal energy states are considered theoretically. Polarization, low-frequency and high-frequency losses are calculated.

537.226.31:549.514.51 2768

Electric Polarizability of Colour Centres in Quartz Crystals and Glasses—J. Volger and J. M. Stevels. (*Philips Res. Rep.*, vol. 11, pp. 79–80; February, 1956.) Relaxation losses induced in clear crystals by irradiation at low temperatures are attributed to orientational polarizability of color centers generated by impurities, such that transitions occur between equivalent positions of trapped electrons or holes. The effect has not been observed in glasses.

537.226.8 2769

Effects of Pressure on the Complex Dielectric Constant of Liquids—P. Caillon and E. Groubert. (*Compt. Rend. Acad. Sci., Paris*, vol. 242, pp. 1855–1856; April 9, 1956.) Measurements on chlorodiphenyl at a frequency of 127 kc indicate that the characteristic variation of dielectric constant with pressure at normal temperature is similar to that with temperature at normal pressure.

537.227/228.1+621.372.412+621.373.421.13 2770

Papers presented at the 2nd Conference on Piezoelectricity (Moscow, 26th–29th April 1955—(*Bull. Acad. Sci. U.R.S.S., Sér. Phys.*, vol. 20, pp. 163–272; February, 1956. In Russian.) The following 15 papers are collected in this issue:

New Ferroelectrics and Antiferroelectrics of the Oxygen-Octahedral Type—G. A. Smolenski (pp. 163–177).

X-Ray Structural Investigation of Solid Solutions of Ferroelectrics with Perovskite-Type Structure—Yu. N. Venevtsev and G. S. Zhdanov (pp. 178–184).

Nonlinear Properties of Ferroelectrics—T. N. Verbitskaya (pp. 185–194).

Stability of the Piezoelectric Effect in Polycrystalline Barium Titanate—I. P. Kozlobaev (pp. 195–198).

Effect of Pressure on the Dielectric Properties of Ferroelectric Ceramics—I. A. Izhak (pp. 199–205).

Fusion of Barium Titanate by Conduction Currents—N. S. Novosil'tsev, O. I. Prokopalo, and A. F. Yatsenko (pp. 206–210).

Some Physical Properties of Ferroelectric-Salt Crystals exposed to Radioactive Irradiation—I. S. Zheludev and V. A. Yurin (pp. 211–214).

Some Physical Properties of Ferroelectric-Salt Crystals—I. Ya Eisner (pp. 215–218).

Investigation of New Piezoelectric Crystals—V. A. Koptsik (pp. 219–225).

Piezoelectric Properties of Wood and Cellulose Materials—V. A. Bazhenov (pp. 226–230).

Thermal Mechanical Oscillations (Fluctuations) of Piezoelectric Crystals—K. V. Goncharov and V. A. Krasil'nikov (pp. 231–236).

New Quartz Parameters and Engineering Method of Quartz Oscillator Design—E. I. Kamenski (pp. 237–250).

Parasitic Oscillations of Piezoelectric Plates with Fundamental Longitudinal Oscillations—E. G. Bronnikova (pp. 251–260).

Theory of the Compound Piezoelectric Vibrator—V. A. Solov'ev and I. G. Mikhailov (pp. 261–267).

Piezoelectric Resonators with Crystals having Structural Defects—M. I. Yaroslavski (pp. 268–272).

537.227 2771

X-ray and Neutron Diffraction Study of Ferroelectric $PbTiO_3$—G. Shirane, R. Pepinsky, and B. C. Frazer. (*Acta Cryst.*, vol. 9, part 2, p. 131–140; February 10, 1956.) Detailed account of work noted previously from shorter paper (2312 of 1955).

537.227 2772

Guanidine Vanadium Sulfate Hexahydrate: a New Ferroelectric Material—J. P. Remeika and W. J. Merz. (*Phys. Rev.*, vol. 102, p. 295; April 1, 1956.) A brief note on the preparation and properties of this material; the shape of the 60-cps hysteresis loop is more nearly rectangular than that of the corresponding compound with aluminum in place of the vanadium [2415 of August (Holden *et al.*)].

537.227:[546.431.824–31+546.824–3]:548.0 2773

An Explanation of the Structures of Hexagonal Barium Tittanate and Titanium Dioxide—P. Vousden. (*Acta Cryst.*, vol. 9, part 2, pp. 141–142; February 10, 1956.)

537.227:647.476.3 2774

On Ferroelectric Barkhausen Pulses of Rochelle Salt—R. Abe. (*J. Phys. Soc. Japan*, vol. 11, pp. 104–111; February, 1956.) Experiments are described in which Barkhausen pulses were observed on applying an electric field to the crystal. The volumes whose polarization reversal corresponds to single pulses are estimated to be of the order of 10^{-9} cm³. From the field-strength threshold values it is inferred that the pulses occur when a domain wall passes across a hollow in a crystal.

537.311.33 2775

The Voltage/Current Characteristic of the *n-p* Junction for a Weak Signal—E. I. Rashba. (*Zh. Tekh. Fiz.*, vol. 25, pp. 1663–1667. September, 1955.) Published literature on the subject is reviewed and inaccuracies in a paper by Shockley (379 of 1950) are pointed out. A statistical system of equations (1) determining the dynamic characteristic of a *p-n* junction is quoted and applied to the case of small alternating voltages, of the order of a few hundred mV, superimposed on a constant reverse bias. Methods are indicated for an approximate solution of these equations for various conditions, and formulas are derived for determining the capacitance of the junction.

537.311.33 2776
Theoretical Study of the Current/Voltage Characteristic of a Semiconductor *p-i-p* Structure, taking Account of Ionization of the medium due to Carriers—A. Leblond. (*Compt. Rend. Acad. Sci., Paris*, vol. 242, pp. 1856–1859; April 9, 1956.) In the structure considered, the major part of an applied voltage is across the intrinsic middle region, since the adjacent *p* regions have much higher conductivity. Theory is developed affording an explanation of the negative region of the *I/V* characteristic which has been observed experimentally; this negative characteristic is a consequence of ionization which occurs in the vicinity of the two junctions, where very strong fields develop at high current values.

537.311.33 2777
Diffusion Effects in Drift-Mobility Measurements in Semiconductors—J. P. McKelvey. (*J. Appl. Phys.*, vol. 27, pp. 341–343; April, 1956.) A simple method of measurement, using low-strength steady fields between the emitter and collector, gives results of satisfactory accuracy if an appropriate correction is made for diffusion effects.

537.311.33:061.3 2778
Research in Semiconductors: Symposium at Ottawa—T. H. K. Barron. (*Nature, Lond.*, vol. 177, p. 833; May 5, 1956.) Brief report of a symposium held in February, 1956.

537.311.33:535.215 2779
The Photoelectric Properties of some Compounds with Zinc-Blende Structure—N. A. Goryunova, V. S. Grigor'eva, B. M. Konovalenko, and S. M. Ryvkin. (*Zh. Tekh. Fiz.*, vol. 25, pp. 1675–1682; September, 1955.) Experiments were conducted with compounds of indium and gallium having the same crystal structure as zinc blende. All these materials are semiconductors and sensitive to light. Spectral characteristics are shown, together with tables of experimental data.

537.311.33:535.215:538.63 2780
Theory of the Photomagnetoelectric [PME] Effect in Semiconductors—W. van Roosbroeck. (*Phys. Rev.*, vol. 101, pp. 1713–1725; March 15, 1956.) "Through an ambipolar treatment, the underlying general theory for current carrier transport with magnetic field, which can provide . . . unrestricted results for the Hall, Suhl, and magnetic rectifier effects, is first developed. The PME effect is considered in detail for the infinite slab with strongly absorbed steady radiation on one surface and parallel, steady, uniform magnetic field. Small Hall angles and constant surface recombination velocities and lifetime are assumed. Small-signal theory is given as well as nonlinear theory for arbitrary light intensity. The latter provides methods for determining lifetime that require only negligible dark-surface concentration of added carriers, as well as a method for determining surface recombination velocity; curves for these are given for germanium."

537.311.33:541.57 2781
Chemical Bond in Semiconductors—E. Mooser and W. B. Pearson. (*Phys. Rev.*, vol. 101, pp. 1608–1609; March 1, 1956.) Semiconductivity results from the existence in a solid of essentially covalent bonds, with filled *s* and *p* sub-shells occurring in at least one of any two atoms connected by a bond. This property allows a sharp distinction to be made between semiconductors and metals. A simple rule is given for predicting whether a given compound will be semiconducting from a knowledge of the stoichiometric formula and the valencies of the constituent atoms. The formation of a continuous network of bonds distinguishes semiconductors from molecular crystals.

537.311.33:546.23 2782
Conductivity Measurements on Highly Purified Selenium—F. Eckart. (*Ann. Phys., Lpz.*, vol. 17, pp. 84–93; February 1, 1956.) A continuation of earlier work (3582 fo 1954) is reported. The activation energy, determined in the temperature range 18°–40°C., was 1.2–1.6ev for a specimen remelted several times in vacuum. After heat treatment in air the activation energy dropped to 0.14–0.19ev and the conductivity increased by a factor of 10^6.

537.311.33:546.26 2783
Thermoelectric Power, Electrical Resistance, and Crystalline Structure of Carbons—E. E. Loebner. (*Phys. Rev.*, vol. 102, pp. 46–57; April 1, 1956.) Report of measurements on soft and hard carbons; the influence of heat-treatment temperature was investigated.

537.311.33:546.26–1 2784
Electrical and Optical Properties of a Semiconducting Diamond—I. G. Austin and R. Wolfe. (*Proc. Phys. Soc.*, vol. 69, pp. 329–338; March 1, 1956.) The resistivity, Hall coefficient and infrared absorption spectrum of a type-IIb diamond have been investigated over a wide range of temperatures. The material behaves like a normal *p*-type semiconductor. Photoconductivity was detected at −155°C. over the wavelength range 0.9–3.6 μ. A model energy-band structure is proposed.

537.311.33:546.26–1 2785
Electrical Measurements on Type-IIb Diamonds—H. B. Dyer and P. T. Wedepohl. (*Proc. Phys. Soc.*, vol. 69, pp. 410–412; March 1, 1956.) The rectification characteristics, resistance linearity, temperature dependence of conductivity, and Hall coefficient of type-IIb diamonds have been determined. Conductivity at room temperature is found to be related to the strength of infrared absorption bands.

537.311.33:546.26–1 2786
Some Physical Consequences of Elementary Defects in Diamonds—F. C. Champion. (*Proc. Roy. Soc. A*, vol. 234, pp. 541–556; March 6, 1956.) Using the concept of the defect bond, a qualitative theory is developed of the physical properties of pure diamond, including the electrical properties and the electronic energy levels.

537.311.33:[546.28+546.289 2787
Influence of Holes and Electrons on the Solubility of Lithium in Boron-Doped Silicon—H. Reiss and C. S. Fuller. (*J. Metals, N.Y.*, vol. 8, pp. 276–282; February, 1956.) Fuller details are given of work reported previously (2011 of 1955). Experimental results support the theoretical prediction that increase of acceptor (boron) content leads to increased solubility of donor (lithium) in the boron-doped Si; the expected temperature variation is observed. Qualitative results for Ge indicate that doping with a donor decreases the solubility of another donor.

537.311.33:546.28 2788
Spiral Etch Pits in Silicon—W. Bardsley and B. W. Straughan. (*J. Electronics*, vol. 1, pp. 561–562; March, 1956.)

537.311.33:546.28 2789
Radiation resulting from Recombination of Holes and Electrons in Silicon—J. R. Haynes and W. C. Westphal. (*Phys. Rev.*, vol. 101, pp. 1676–1678; March 15, 1956.) Recombination radiation produced following application of current pulses to Si *p-n* junctions has been investigated using a PbS cell. The results indicate that the radiation at room temperature is a property of the intrinsic material; additional radiation observed at 77°K is associated with the presence of impurities.

537.311.33:546.28 2790
Drift and Conductivity Mobility in Silicon—G. W. Ludwig and R. L. Watters. (*Phys. Rev.*, vol. 101, pp. 1699–1701; March 15, 1956.) The drift mobility of minority carriers has been measured at temperatures between 120° and 400°K for *p*-type specimens and between 78° and 400°K for *n*-type specimens, using a pulsed-field method. Formulas are derived for the temperature variation of the mobilities; the validity of these formulas is confirmed by the results of conductivity measurements over the same temperature range.

537.311.33:546.281.26 2791
Energy-Band Structure of the Carborundum SiC Crystal—S. Kobayasi. (*J. Phys. Soc. Japan*, vol. 11, pp. 175–176; February, 1956.) Brief preliminary report of computations.

537.311.33:546.289 2792
On the Impurity Conduction in Germanium—Y. Kanai and R. Nii. (*J. Phys. Soc. Japan*, vol. 11, pp. 83–84; January, 1956.) The work of Hung and Gliessmann (1696 of 1955) and of Firtzsche and Lark-Horovitz (2018 of 1955) is confirmed by an investigation of Ni-doped Ge, in which impurity-type conduction is shown to occur at higher temperatures than with normal Ge.

537.311.33:546.289 2793
Thermally Induced Acceptors in Germanium—R. A. Logan. (*Phys. Rev.*, vol. 101, pp. 1455–1459; March 1, 1956.) Previous investigations (*e.g.*, 170 of 1954) are extended. Results indicate that acceptor centers formed by rapid quenching from high temperatures are either vacant lattice sites or a chemical impurity with atomic radius smaller than that of Ge. The annealing process depends on both the density of dislocations and the concentration of Cu; no mechanism has yet been proposed capable of explaining the observed characteristics of the annealing process.

537.311.33:546.289 2794
The Effect of Heat Treatment on the Lifetime of Minority Current Carriers in Germanium (the Kinetics of the Formation of Defects during Heat Treatment)—T. V. Mashovets and S. M. Ryvkin. (*Zh. Tekh. Fiz.*, vol. 25, pp. 1530–1534; September, 1955.) If Ge is heated to relatively low temperatures (400°–550° C.) the lifetime of the minority carriers is decreased when the temperature and duration of heating are increased. This is explained by the formation of defects which act as recombination centers. From a study of the process of appearance of the defects, data have been obtained on their energy structure. For the temperature range investigated, this process is different from that involved in the formation of thermal defects in Ge at higher temperatures.

537.311.33:546.289:537.533 2795
Temperature Variations of the Work Functions of *n*-Type and *p*-Type Germanium—A. R. Shul'man and A. N. Pisarevski. (*Zh. Tekh. Fiz.*, vol. 25, pp. 1547–1555; September, 1955.) Results of an experimental investigation indicate that there is a definite temperature dependence of the work function and of the position of the chemical potential level and that in each case it is different for *n*-type and *p*-type Ge. The experiments are described, and a number of curves are plotted. A theoretical interpretation of the results is given.

537.311.33:546.289:538.63 2796
The Resistance Variation of Ge Single Crystals in a Magnetic Field at 10°-300°K—G. Lautz and W. Ruppel. (*Z. Naturf.*, vol. 10a, pp. 521–526; July, 1955.) Measurements of the variation of transverse resistance have been made on *p*- and *n*-type specimens in magnetic fields of strengths up to 24 kG. The results are not in agreement with theories based on semiconductor isotropy, such as that of Appel (450 of 1955); measured values are much higher than calculated ones. For a particularly pure

n-type specimen at 11°K a variation of 1200 per cent was observed without any indication of saturation. The mechanism giving rise to this variation is not yet understood, but quantization of the electron paths at low temperatures may be the explanation.

537.311.33:546.289.05 2797
Electrolytic Stream Etching of Germanium—M. V. Sullivan and J. H. Eigler. (*J. Electrochem. Soc.*, vol. 103, pp. 132–134; February, 1956.) The stream of 0.1 per cent KOH solution used for the etching is restricted to a junction area by means of a special jig. The technique and results obtained are described.

537.311.33:546.3–1:541.5 2798
On the Valence and Atomic Size of Silicon, Germanium, Arsenic, Antimony, and Bismuth in Alloys—L. Pauling and P. Pauling. (*Acta Cryst.*, vol. 9, part 2, pp. 127–130; February 10, 1956.)

537.311.33:546.461–31 2799
The Mechanism of Growth of Cuprous Oxide Crystals at High Temperature—A. I. Andrievski and M. T. Mishchenko. (*Compt. Rend. Acad. Sci. U.R.S.S.*, vol. 107, pp. 81–83; March 1, 1956. In Russian.) Photographs of Cu_2O surfaces after heating at a temperature of 1020°C. for 90 and 157 hours are presented and discussed.

537.311.33:546.471.95 2800
The Semiconductor Properties of $ZnAs_2$—C. Fritzsche. (*Ann. Phys., Lpz.*, vol. 17, pp. 94–101; February 1, 1956.) The preparation of $ZNAs_2$ and similar compounds is briefly described and the results of conductivity and rectification measurements are presented graphically. The highest observed forward/reverse current ratio in a $ZnAs_2$ point-contact diode was 3000:1 at 3v. This ratio depends on the orientation of the crystal, the best results being obtained when the current flow is in the direction of the highest resistance.

537.311.33:546.57.241.1 2801
Electrical and Optical Properties of Silver Telluride Ag_2Te—J. Appel. (*Z. Naturf.*, vol. 10a, pp. 530–541; July, 1955.) An extensive experimental investigation of the semiconductor properties of Ag_2Te is reported. A phase transition occurs at 150°C., associated with marked variation of the electrical properties. From the temperature variation of the properties of stoichiometric n-type specimens a covalent metallic bond is inferred for the low-temperature (β) phase. Impurities such as Ge, Sn, and Sb have a strong effect on carrier concentration and mobility. Temperature variation of the properties in the high-temperature (α) phase indicates that Ag ions as well as electrons participate in the participate in the conduction. Discussion of the mobility values in the light of Howarth and Sondheimer's theory (381 of 1954) leads to a value of 0.4 m for the apparent mass of the carriers. A value of 0.67 ev is obtained for the energy gap of the β phase from optical absorption measurements.

537.311.33:546.682.86 2802
Elastic Constants of Indium Antimonide—L. H. DeVaux and F. A. Pizzarello. (*Phys. Rev.*, vol. 102, p. 85; April 1, 1956.) Values of the elastic constants derived from sound-velocity measurements are given.

537.311.33:546.682.86 2803
The Conductivity of Indium Antimonide at Low Temperature—J. Bok. (*Compt. Rend. Acad. Sci., Paris*, vol. 242, pp. 2114–2117; April 23, 1956.) Measurements were made of the electric field strength as a function of current strength at a temperature of 20°K using two specimens with different resistivities. In each case the curve obtained first rises in accordance with Ohm's law, then turns horizontal, and finally rises sharply again. The significance of this characteristic is discussed with reference to theory advanced by Conwell (3328 of 1953) in relation to Ge.

537.311.33:546.682.86 2804
Effects at High-Angle Grain Boundaries in Indium Antimonide—I. M. Mackintosh. (*J. Electronics*, vol. 1, pp. 554–558; March, 1956.) Experiments on n- and p-type filament specimens at room temperature and lower temperatures are reported.

537.311.33:546.682.86 2805
Low Temperature Magnetoresistance Anomalies in Indium Antimonide—I. M. Mackintosh. (*Proc. Phys. Soc.*, vol. 69, pp. 403–406; March 1, 1956.) The observation of Fritzsche and Lark-Horovitz (160 of 1956), that the magnetoresistive ratio of InSb becomes negative below about 8°K, may be explained by changes in the concentration of charge carriers which occur when the impurity levels supplying these carriers are split in a magnetic field, although serious quantitative discrepancies are found on attempting to verify the theory.

537.311.33:546.682.86 2806
Population Changes with Magnetic Field—K. W. H. Stevens. (*Proc. Phys. Soc.*, vol. 69, pp. 406–407; March 1, 1956.) The relative change in the number of conduction electrons on application of a magnetic field is determined by an alternative method to that of Mackintosh (2805 above). The possibility of a reversal in the sign of the magnetoresistance at low temperature is confirmed.

537.311.33:546.682.86:535.215 2807
Recombination Radiation from InSb—T. S. Moss and T. H. Hawkins. (*Phys. Rev.*, vol. 101, pp. 1609–1610; March 1, 1956.) Radiation produced by the recombination of optically produced execss carriers has been detected in the wavelength region near the absorption edge. From the magnitude of the effect it is deduced that the fraction of total recombinations which are radiative approaches 100 per cent.

537.331.33:546.682.86.05:669.054 2808
Effect of Zone-Refining Variables on the Segreation of Impurities in Indium-Antimonide—T. C. Harman. (*J. Electrochem. Soc.*, vol. 103, pp. 128–132; February, 1956.) Zinc and tellurium can be removed from the indium used in the preparation of InSb by electrolytic refining and zone-refining, respectively. The compound is further purified by zone-refining.

537.311.33:548.1 2809
Junction Rectification as a Function of Crystal Orientation—W. Kossel, E. Menzel, and G. Naumann. (*Z. Naturf.*, vol. 10a, pp. 590–592; July, 1955.) Experiments with junctions of Cu and Cu_2O single crystals are described and discussed. Forward current is greater and reverse current is smaller for an octahedral crystal surface than for a dodecahedral surface, and the forward/reverse current ratio is better for the octahedral surface.

537.311.33:669.046.54/.55 2810
Zone-Melting Processes for Pure Compounds AB with a Negligible Vapour Pressure—J. van den Boomgaard. (*Philips Res. Rep.*, vol. 11, pp 27–44; February, 1956.) Expressions are derived for deviations from the stoichiometric composition as a function of position along a rod of a binary semiconductor subjected to zone melting.

537.311.33.07 2811
Micromanipulators—W. L. Bond. (*Bell Lab. Rec.*, vol. 34, pp. 90–92; March, 1956.) An illustrated note on two devices for controlling and locating metal contacts on a semiconductor surface in research.

538.22+537.311.3 2812
Magnetic and Electrical Properties of Manganese Telluride—E. Uchida, H. Kondoh, and N. Fukuoka. (*J. Phys. Soc. Japan*, vol. 11, pp. 27–32; January, 1956.) The temperature variation of susceptibility may be explained by assuming the presence of two phases corresponding to MnTe and $MnTe_2$, possessing different susceptibilities. The electrical properties show anomalies at the Néel point; at higher temperatures the material behaves as a semiconductor, at lower temperatures as a metal. A change in crystalline structure at about 130°C. is indicated.

538.22 2813
Magnetic Properties of Nickel Telluride—E. Uchida and H. Kondoh. (*J. Phys. Soc. Japan*, vol. 11, pp. 21–27; January, 1956.) $Ni\ Te_x$ is ferromagnetic in the range $0.1 \leqq c \leqq 0.65$. There is a transition at $x=0.33$ from a heterogeneous phase beginning at $x=0$ to a homogeneous phase. In the range $0.7 \leqq c \leqq 2.0$ the material is paramagnetic, but its behavior is anomalous at high temperatures.

538.22 2814
Condition for Resonance in a Nearly Compensated Ferrimagnetic—K. F. Niessen. (*Philips Res. Rep.*, vol. 11, pp. 57–65; February, 1956.) The resonance condition is calculated for a ferrimagnetic with two sublattices having slightly different properties. The theory is applicable to an antiferromagnetic in whose sublattice a relatively small number of magnetic ions have been replaced by nonmagnetic ones.

538.22 2815
Domain Walls in Antiferromagnets and the Weak Ferromagnetism of α-Fe_2O_3—Y. Y. Li. (*Phys. Rev.*, vol. 101, pp. 1450–1454; March 1, 1956.)

538.22:538.652 2816
Magnetostrictive Effects in an Antiferromagnetic Hematite Crystal—H. M. A. Urquhart and J. E. Goldman. (*Phys. Rev.*, vol. 101, pp. 1443–1450; March 1, 1956.) "Magnetostrictive distortions in an antiferromagnetic natural single crystal of hematite have been studied in the region of the transition near −25°C., where the antiferromagnetic axis spontaneously shifts its crystallographic direction by 90°. The magnetostriction is shown to be closely related to the parasitic magnetization and is interpreted in terms of the existence of domain walls separating antiferromagnetic domains."

538.221 2817
Ferromagnetic Relaxation and Gyromagnetic Anomalies in Metals—C. Kittel and A. H. Mitchell. (*Phys. Rev.*, vol. 101, pp. 1611–1612; March 1, 1956.) A new mechanism is proposed which may contribute to relaxation to account for both the apparent frequency dependence of the observed g values and the apparent inaccuracy of the theoretical connection between microwave and magnetomechanical studies.

538.221:538.569.4 2818
Ferromagnetic Resonance Absorption in a Nickel Single Crystal at Low Temperatures—K. H. Reich. (*Phys. Rev.*, vol. 101, pp. 1647–1648; March 15, 1956.) Measurements have been made at 9 kmc and at 24.3 kmc. Values are derived for the spectroscopic splitting factor, the resonance line width, and the anisotropy contents and for their variation over a range of low temperatures.

538.221:538.632 2819
Hall Effect and Magnetic properties of Armco Iron—S. Foner. (*Phys. Rev.*, vol. 101, pp. 1648–1652; March 15, 1956.) Experimental results presented previously [3652 of 1953 (Foner and Pugh)] are analyzed in detail. Over a wide range of values of the magnetizing field, the Hall effect in armco iron is given by the sum of the ordinary and extraordinary

effects, the extraordinary Hall constant being independent of the magnetizing field strength.

538.221:548.0 2820
Deformations in Perovskites composed of Rare Earths and Trivalent Transition Elements—F. Bertaut and F. Forrat. (*J. Phys. Radium*, vol. 17, pp. 129–131; February, 1956.) A crystallographic study of bodies represented by the general formula A_2O_3, B_2O_3, where A is a rare earth and B one of the transition elements. The subject is important in relation to the magnetic properties of ferrites.

538.221:621.318.134 2821
Magnetic Properties of Gadolinium Ferrites—R. Pauthenet. (*Compt. Rend. Acad. Sci., Paris*, vol. 242, pp. 1859–1862; April 9, 1956.) Measurements on $Fe_2O_3 \cdot Gd_2O_3$, and $5Fe_2O_3 \cdot 3Gd_2O_3$ are reported and discussed.

538.221:621.318.134 2822
On the Magnetism of the Ferrites (La, Sr) FeO_x with Perovskite Structure—H. Watanabe. (*Sci. Rep. Res. Inst. Tohoku Univ., Ser. A*, vol. 8, pp. 14–23; February, 1956.) Thermomagnetic studies are reported; the magnetic properties of this system of solid solutions are strongly dependent on preliminary heat treatment.

538.221:621.318.2 2823
The Definition and Determination of the Coercive Force of Permanent Magnets taking Account of Irreversible After-Effect—A. Kussmann and O. Yamada. (*Arch. Elektrotech.*, vol. 42, pp. 237–244; February 3, 1956.) Calculations and measurements indicate that as a consequence of the irreversible after-effect the static coercive force of ferromagnetic materials varies with time; for alni and alnico permanent magnets the variation may amount to several per cent. A more precise definition of coercive force is required, including reference to the measuring time and an index characterizing the after-effect. The appropriate commutation rate for taking hysteresis curves is discussed.

538.224:546.3–1–56 2824
The Magnetic Susceptibilities of some Diamagnetic Alloys: the Primary Solid Solutions of Zinc, Gallium, Germanium and Arsenic in Copper—W. G. Henry and J. L. Rogers. (*Phil. Mag.*, vol. 1, pp. 237–252; March, 1956.) A method of alloy preparation is described. Results of measurements, by a modified Gouy method, of the rate of change of diamagnetic susceptibility with concentration of the solid solutions are presented. Conclusions are drawn regarding the states occupied by the electrons.

538.652:546.3–1–72–621 2825
Dynamic Magnetostrictive Properties of Alfenol—C. M. Davis and S. F. Ferebee. (*J. Acoust. Soc. Amer.*, vol. 28, pp. 286–290; March, 1956.) Report of an experimental investigation of a cold-rolled Al-Fe alloy containing between 11 per cent and 16 per cent Al. The electromechanical coupling coefficient is comparable to that of N.

549.514.51 2826
Dislocations, Relaxations, and Anelasticity of Crystal Quartz—H. E. Bömmel, W. P. Mason, and A. W. Warner. (*Phys. Rev.*, vol. 102, pp. 64–71; April 1, 1956.) Experimental evidence indicates that the Q of quartz crystals varies as an inverse function of frequency between 1 and 100 mc at room temperature; this variation is consistent with the existence of two relaxation processes, with time constants of 10^{-13} and 7.7×10^{-10} sec respectively; the first of these is probably associated with lattice distortion due to impurities, and the second with dislocation loops. An observed long-term aging effect may be due to closer pinning of dislocations by impurity atoms. A frequency standard of improved time stability might be obtained by maintaining the crystal at the temperature of liquid helium.

621.315.612 2827
Fundamental Factors controlling Electrical Resistivity in Vitreous Ternary Lead Silicates—S. W. Strauss, D. G. Moore, W. N. Harrison, and L. E. Richards. (*J. Res. Nat. Bur. Stand.*, vol. 56, pp. 135–142; March, 1956.) Resistivity measurements were made on a number of vitreous ternary lead silicates of widely varied compositions, as well as on vitreous silica and quartz, over the temperature range 200°–500°C., with an applied direct field of 525 V/cm. The results are presented as log-resistivity/ composition curves for specimens containing alkali and alkaline-earth ions, and as log-resistivity/temperature curves for specimens containing other ions.

621.315.616 2828
Materials used in Radio and Electronic Engineering: Part 4—Plastics—(*J. Brit. IRE*, vol. 16, pp. 283–294; May, 1956.) A survey including information about the physical properties and commercial availability of numerous plastics, together with British Standards and more than 50 references.

621.315.616:621.3.002.2 2829
Casting Resins insulate and protect Electronic Components—H. L. Loucks. (*Mater. and Math.*, vol. 43, pp. 90–94; February, 1956.) Polyester and and epoxy resins, foam-type resins such as polyisocyanates and polystyrenes, and elastomeric resins such as polysulphides and silicone rubber compounds are discussed; factors to be considered in choosing the appropriate resin for a particular application are indicated; methods of embedment are outlined.

MATHEMATICS

512.3 2830
On Generalized Tchebycheff Polynomials—J. L. Walsh and M. Zedek. (*Proc. Nat. Acad. Sci., Wash.*, vol. 42, pp. 99–104; February, 1956.)

517 2831
The Method of Comparison Equations in the Solution of Linear Second-Order Differential Equations (Generalized W.K.B. Method)—R. B. Dingle. (*Appl. Sci. Res.*, vol. B5, pp. 345–367; 1956.)

519.272 2832
A Simple Interpretation of the Complex Correlation Coefficient—H. J. Linn and K. Poschl. (*Arch. Elekt. Übertragung*, vol. 10, pp. 105–106; March, 1956.)

51 2833
Mathematische Methoden in der Hochfrequenztechnik [Book Review]—K. Poschl. Publishers: Springer, Berlin, 331 pp., (*Wireless Engr.*, vol. 33, p. 156; June, 1956.) The first ten chapters develop the mathematics and the last five deal with its application to field problems, cavity resonators, waveguides, antennas, magnetrons, space-charge waves, etc.

MEASUREMENTS AND TEST GEAR

531.711+531.761 2834
The Standard of Length and the Standard of Time—A. Perard. (*Nature, Lond.*, vol. 177, pp. 850–851; May 5, 1956.) Critical comments on the arguments advanced by Clemence (1153 of 1956).

531.765:621.374.3 2835
Time-to-Pulse-Height Converter for Measurement of Millimicrosecond Time Intervals—W. Weber, C. W. Johnstone, and L. Cranberg. (*Rev. Sci. Instrum.*, vol. 27, pp. 166–170; March, 1956.) Details are given of a circuit designed to measure the time between a neutron-detector signal and the next subsequent pulse of a reference series.

538.56:535.51.088.2 2836
Errors in Measurements of an Elliptically Polarized Electromagnetic Field—O. M. Barsukov. (*Bull. Acad. Sci. U.R.S.S., Sér. Géophys.*, pp. 226–231; In Russian. February, 1956.) The ratio of the principal axes and the orientation of the polarization ellipse relative to a given direction can be calculated, using the set of (4), from the measured ratio of the components of field strength in two known directions and the phase difference between them. The effect of an error in the orientation of the pickup loop is considered theoretically and results of calculations are presented graphically. The graphs should be useful for finding the conditions for minimizing the effect of an error.

621.3.011.4 (0.83.74) 2837
A New Theorem in Electrostatics and its Application to Calculable Standards of Capacitance—A. M. Thompson and D. G. Lampard. (*Nature, Lond.*, vol. 177, p. 888; May 12, 1956.) It is shown that, for the class of cylindrical capacitors whose cross section has at least one axis of symmetry and is bounded by a closed curve, the capacitance can be calculated from only one length determination. A preliminary study is made of a capacitance standard constituted by the space between four parallel circular cylinders whose cross sections are arranged in a square.

621.3.018.41(083.74)+621.396.91 2838
Improvements in Standard Frequencies broadcast by Radio Stations WWV and WWVH (*Tech. News Bull. Nat. Bur. Stand.*, vol. 40, pp. 37–38; March, 1956.) The accuracy of standard frequencies and time signals has been increased; a new uniform time, designated UT2, is used for reference.

2839
621.3.018.41(083.74)+621.396.91]:529.786
MSF Standard Frequencies expressed in Terms of the Caesium Resonance—L. Essen. (*Wireless Engr.*, vol. 33, p. 178; July, 1956.) A note explaining a modification of the basis of the reports of standard-frequency transmissions published monthly in *Wireless Engineer*.

621.317.2:621.3 2840
Testing of Components and Valves at the Laboratoire Central des Industries Électriques—M. A. Dauphin. (*Onde Élect.*, vol. 36, pp. 176–185; March, 1956.) An account of equipment used for electrical and life testing and quality control and of methods used for checking the climatic and mechanical endurance of finishes.

621.317.2:621.373.4.029.5/.64 2841
The Signal Generator and its Uses in Modern Telecommunications—J. F. Golding. (*Brit. Commun. Electronics*, vol. 3, pp. 75–81; February, 1956.) A general discussion of the signal generator as a piece of receiver test equipment. The principal characteristics of representative British-made apparatus for frequencies up to 4 kmc are tabulated.

621.317.3:621.314.7:546.289 2842
Measurements on Alloy-Type Germanium Transistors and their Relation to Theory—Evans. (See 2903.)

621.317.32 2843
Measurement of Electric Field Distributions—R. Justice and V. H. Rumsey. (IRE TRANS., vol. AP-3, pp. 177–180; October, 1956.) A method which eliminates the need for a transmission line between observation point and detecting apparatus is based on introducing a thin straight conductor to act as a reflector of the field. Applications mentioned include measurements on slot antennas.

621.317.326 2844
Voltage Calibration System for Pulse-Height Measurement—W. A. Rhinehart and D. J. Zaffarano. (*Nucleonics*, vol. 14, pp. 54, 56; February, 1956.) Description of a cro method of measuring pulse height by compari-

son of the pulse waveform with a direct voltage, the two displays alternating at mains frequency on a long-persistence screen.

621.317.335.3+621.317.411 2845
Extension of the "Thin-Sample Method" for the Measurement of Initial Complex Permeability and Permittivity—E. E. Conrad, C. S. Porter, N. J. Doctor, and P. J. Franklin. (*J. Appl. Phys.*, vol. 27, pp. 346–350; April, 1956.) The method described *e.g.*, by Birks (2807 of 1948) is adapted for use with a commercial dielectric-filled slotted line. The frequency range is 5 mc–1 kmc. Errors and corrections are discussed.

621.317.335.3+621.317.411]:621.318.134
:621.372.413 2846
Measurement of Microwave Dielectric Constants and Tensor Permeabilities of Ferrite Spheres—E. G. Spencer, R. C. LeCraw, and F. Reggia. (PROC. IRE, vol. 44, part 1, pp. 790–800; June, 1956.) Detailed account of a cavity-perturbation method using circularly polarized waves. Experimental results obtained with a polycrystalline MgMn ferrite are presented. (See also 2366 of 1955.)

621.317.335.3:621.372.413 2847
Calculation of the Natural Frequency of a π-type [single re-entrant] Cavity Partly Filled with an Absorbing Dielectric—Gatrushev. (See 2657.)

621.317.411:621.372.413 2848
A Re-entrant Cavity for Measurement of Complex Permeability in the Very-High-Frequency Region—R. D. Harrington, R. C. Powell, and P. H. Haas. (*J. Res. Nat. Bur. Stand.*, vol. 56, pp. 129–134; March, 1956.) The equipment described is suitable for measurements on toroidal cores at frequencies from 60 to 180 mc. Design problems are discussed, calibration techniques described, and some measurement results presented.

621.317.44:621.384.612 2849
A Magnetic Differential Probe. Its Employment for the Determination of the Static Median Magnetic Surface in the Gap of a Synchrotron—G. D. Palazzi. (*Nuovo Cim.*, vol. 3, pp. 336–349; February 1, 1956. In English.) The probe comprises two thin ferromagnetic wires subjected to opposing magnetic fields at a frequency of 1 kc. The position of the probe is determined for which the components of the magnetic field along the two wires, parallel to the radius of the synchrotron and lying in a vertical plane, are equal and opposite. The technique used for preparing the wires is explained in some detail.

621.317.725.029.6:621.372.55 2850
Stable Radiofrequency Voltmeters—(*Tech. News Bull. Nat. Bur. Stand.*, vol. 40, pp. 29–30; February, 1956.) The voltmeter described, developed by Selby and Behrent at the NBS, comprises a waveguide piston attenuator together with a frequency-insensitive thermoelement and dc millivoltmeter. The piston houses the thermoelement and a built-in probe for calibrating one rf voltage level. The voltage range is from 0.1 v to several hundred volts, at frequencies up to about 1 kmc.

621.317.729 2851
Determination of the Intensity of the Electron Current in a Vacuum by the Use of a Rubber Membrane—V. M. Kel'man and I. F. Krasnov. (*Zh. Tekh. Fiz.*, vol. 25, pp. 1714–1725; September, 1955.) The rubber-membrane method of investigating electron trajectories is modified so that, for the case of a cathode operating with space-charge limitation, all parameters of a two-dimensional electron beam in a two-dimensional electric field can be determined if the shapes and potentials of the electrodes are known.

621.317.729:621.385.2 2852
The Solution of the Problem of a Planar Diode with a Limited-Width Emitting Surface by Use of a Rubber Membrane—I. F. Krasnov and V. M. Kel'man. (*Zh. Tekh. Fiz.*, vol. 25, pp. 1726–1734; September, 1955.) A description is given of the apparatus used for determining the density distribution of the current at the cathode of a diode consisting of two long parallel electrodes, with emission only from a narrow middle strip of the cathode. A number of experimental curves are shown.

621.317.729.087.6:621.396.62 2853
Instruments for Recording and Automatic Analysis of Field-Strength Measurements—H. J. Griese and E. Haberkant. (*Elektronische Rundschau*, vol. 10, pp. 43–46; February, 1956.) Modern technique is reviewed and a null instrument for field-strength measurements is described. It includes a standard signal generator and an automatically operated piston-type attenuator. The field strength is recorded by cutting a continuously moving metal foil, and this record is analyzed by a simple scanning device.

621.317.733:621.317.33 2854
Bridge for Measurement of the Differential Resistance of Nonlinear Elements—M. Mancianti. (*Alta Frequenza*, vol. 25, pp. 15–31; February, 1956.) The variation of the unbalanced bridge voltage as a function of the input voltage is shown on an oscillograph. By observing the disappearance of the derivative of the unbalanced voltage, the relation between the unknown differential resistance and the three known bridge resistances can be established. Results of measurements on a triode tube are presented.

621.317.75.029.42:621.396.822 2855
Low-Frequency Power Spectrum Analyzer—T. E. Firle. (*Rev. Sci. Instrum.*, vol. 27, pp. 140–143; March, 1956.) A system devised for measurements of semiconductor noise in the frequency range 0.00006–0.02 cps [3426 of 1955 (Firle and Winston)] involves making a variable-area film recording of the noise, reproducing this at a speed increased up to 500,000-fold, and picking up the signal with a photocell whose output is fed to an af analyzer.

621.317.755 2856
A Cathode-Ray Oscillograph for the Measurement of Very Short, Aperiodic, Single, High-Voltage Phenomena—F. Brüninghaus. (*Arch. Elektrotech.*, vol. 42, pp. 245–256; February 3, 1956.) A comparison of various beam-forming systems indicates that a gun with a thermionic cathode designed on the Steigerwald principle (*Optik, Stuttgart*, vol. 5, p. 469; 1949) gives the best results in respect of small spot size and beam aperture. The signal deflection is effected by means of a parallel-wire system and the time-base deflection by a pair of plates. A time-base and blanking circuit is described giving a fixed response delay and a linear timebase adjustable between 10^{-7} and 10^{-9} second with an oscillogram size of 6×9 cm.

621.317.794 2857
A Simple Theory for Solid-Backed Bolometers—L. M. Roberts and S. J. Fray. (*J. Sci. Instrum.*, vol. 33, pp. 115–119; March, 1956.) A theory of the speed of response of solid-backed bolometers is developed and is applied to measurements on Nb_4N_3 superconducting bolometers. Constructional details of the bolometers used in the experimental part of the investigation are given and their characteristics are tabulated.

OTHER APPLICATIONS OF RADIO AND ELECTRONICS

621.384.612 2858
The Acceleration of Protons to Energies above 10 GeV—M. L. Oliphant. (*Proc. Roy. Soc. A*, vol. 234, pp. 441–456; March 6, 1956.) Text of Bakerian Lecture. Methods of accelerating protons are reviewed with particular reference to proton synchrotrons. The new 10-GeV, 15-ft-radius proton synchrotron at Canberra will use magnetic fields of up to 80,000 G produced by passing currents of the order of 10^6A in opposite directions through two suitably arranged field coils. The homopolar generator is also described.

621.384.612 2859
The Nonlinear Theory of Betatron Oscillations in the Strong-Focusing Synchrotron: Part 1—Y. Orlov. (*Nuovo Cim.*, vol. 3, pp. 252–259; February 1, 1956. In English.) Resonances due to errors in the field gradient are examined analytically.

621.384.612 2860
An Analysis of Injection Phenomena in the Birmingham Proton Synchrotron—C. A. Ramm, R. F. Coe, and T. B. Vaughan. (*J. Sci. Instrum.*, vol. 33, pp. 102–106; March,1956.)

621.385.833 2861
Electron-Optical Image of an Atomic Beam—L. Marton, D. C. Schubert, and S. R. Mielczarek. (*J. Appl. Phys.*, vol. 27, p. 419; April, 1956.) The shadow technique (see *e.g.*, 199 of 1950) is used to demonstrate the scattering of an electron beam by an atomic beam projected across its path.

621.385.833 2862
The Aperture Error of Magnetic Electron Lenses—W. Glasser. (*Optik, Stuttgart*, vol. 13, 1956.) Discussion indicates that lower limits previously published for the aperture errors of rotationally symmetrical lenses cannot be confirmed.

621.385.833 2863
Pulsed T-F [temperature-and-field] Emission Electron Projection Microscopy—W. P. Dyke and J. P. Barbour. (*J. Appl. Phys.*, vol. 27, pp. 356–360; April, 1956.)

621.386.8:621.397.611.2:620.179.1 2864
Large-Area Photoconductive X-Ray Pickup-Tube Performance—J. Jacobs and H. Berger. (*Elect. Engng., N.Y.*, vol. 75, pp. 158–161; February, 1956.) Discussion of the general characteristics and the detection sensitivity of a low-velocity-scan vidicon tube and of some of its industrial applications. The advantages and disadvantages of film, direct fluoroscopy, direct-image intensifying tube, and scanned-image pickup tube for observing X-ray images are listed.

621.387.424 2865
Double Pulses in Rare-Gas/Halogen Geiger Counters—D. van Zoonen. (*Appl. Sci. Res.*, vol. B5, pp. 368–386; 1956.)

621.396.934:55 2866
Symposium on the U. S. Earth Satellite Program—**Vanguard of Outer Space**—(See 2718).

642.6:681.142 2867
Machine Translation of Languages: Fourteen Essays [Book Review]—W. N. Locke and A. D. Booth (Eds). Publishers: Chapman and Hall, London, (*Engineering, Lond.*, vol. 181, p. 136; February 10, 1956.) This book includes papers given at a conference held in 1952 at the Massachusetts Institute of Technology, revised and supplemented, with a bibliography of 40 other papers. Both engineering and linguistic problems are discussed. The central engineering problem is the development of a large, cheap storage unit to hold the stem dictionary, conjunction with a rudimentary computer.

PROPAGATION OF WAVES

538.566 2868
The Frequency Dependence of the Propagation of Electromagnetic Waves in Conducting Media—J. G. Smit. (*NachrTech.*, vol. 6,

pp. 71–75; February and pp. 121–125; March, 1956.) Theory is presented based on Maxwell's equations of the critical wavelength in the medium, the phase velocity in the nondispersive frequency range, and the reference frequency for the normalized representation. The reduced curves are constituted, to a first approximation, by two straight lines in a double-logarithmic coordinate system, intersecting at the point corresponding to unity normalized group delay time and unity normalized frequency. Formulas are derived for attenuation, refractive index and delay time for both dispersive and nondispersive ranges. Values of important parameters are tabulated for salt water, fresh water, and various types of ground.

621.396.11 2869
Amplitude and Phase Pulsations of a Wave propagated in a Slightly Inhomogeneous Atmosphere—V. I. Tatarski. (*Compt. Rend. Acad. Sci. U.R.S.S.*, vol. 107, pp. 245–248; March 11, 1956. In Russian.) The modification of the distant field by an atmosphere in which the scale of the refractive-index inhomogeneities is large compared with the wavelength is considered by a statistical method. The expressions obtained are simpler than those derived earlier by Obukhov (*Bull. Acad. Sci. U.R.S.S.*, No. 2, pp. 155–165; 1953. in Russian). See also 2024 of 1949 (Krasil'nikov.)

621.396.11:551.510.52 2870
Tropospheric Scatter Propagation and a Theoretical Study of the Transmission Loss—J. A. Fejer. (*Trans. S. Afr. IEE*, vol. 46, part 12, pp. 348–363; December, 1955. Discussion, pp. 364–367.) The internal-reflection theory of usw propagation beyond the horizon [240 of 1956 (Carroll and Ring)] is critically examined; it is concluded that reflections from a smoothly varying atmosphere are too weak to account for observed field strengths. The transmission loss for propagation beyond the horizon is calculated on the assumption of scattering by turbulent fluctuations, for the case of identical transmitting and receiving antennas. For given values of distance and antenna aperture, there is a minimum value of transmission loss; this value is calculated for both the Booker-Gordon (1757 of 1950) and Villars-Weisskopf (244 of 1956) theories. Some applications of tropospheric scattering to communications are discussed briefly.

621.396.11:551.510.535 2871
Oblique Transmission by the Meteoric E-Layer—R. Naismith. (*Wireless Engr.*, vol. 33, pp. 159–162; July, 1956.) A report is presented on transmissions effected during the winter of 1951 and the summer of 1952 over distances of 900–1900 km between England and Norway, on frequencies of 22.7, 25 and 27 mc. The observations indicate that propagation took place by way of the meteoric E layer (2666 of 1954). The results confirm that this layer may enable long-distance communication to be maintained at frequencies higher than those normally propagated by way of the E and F layers.

621.396.11:551.510.535 2872
Focusing on a "Rippled" Ionosphere—K. Rawer. (*J. Atmos. Terr. Phys.*, vol. 8, p. 296; May, 1956.) Exact formulas are given for the field strength produced by echoes of orders 1–4, assuming reflection by spherically shaped ripples in the ionosphere.

621.396.11:551.510.535:523.75 2873
Some Unusual Radio Observations made on 23 February 1956—Belrose, Devenport, and Weekes. (See 2717).

621.396.11.029.55:621.396.93 2874
An Automatic Direction Finder for recording Rapid Fluctuations of the Bearing of Short Radio Waves—Whale and Ross. (See 2744.)

621.396.11.029.6:535.42 2875
A Simple Theory of Diffraction of Radio Waves beyond the Optical Horizon—H. Poeverlein. (*Z. Angew. Phys.*, vol. 8, pp. 90–95; February, 1956.) The propagation of waves of wavelength less than about 10 m is treated by repeated application of Huygens' principle. Reflection from the earth's surface is taken into account.

621.396.11.029.6:621.396.96 2876
Prediction of Oceanic Duct Propagation from Climatological Data—L. J. Anderson and E. E. Gossard. (IRE TRANS., vol. AP-3, pp. 163–167; October, 1955.) Procedure is indicated whereby data obtained from routine shipboard observations of sea and air temperature, humidity, and wind speed are combined to permit prediction of the coverage of low-sited microwave radar systems. Maps are presented for an area in the NW Pacific showing the probability of extended coverage for the radar X-bands in July and December.

621.396.11.029.62:551.594.5 2877
A Theory of Scattering by Nonisotropic Irregularities with Application to Radar Reflections from the Aurora—Booker. (See 2739.)

621.396.11.029.6 2878
UKW-Fernempfangsbeobachtungen, ihre Bedeutung für Meteorologie und Funktechnik [Book Review]—L. Klinker. Publishers: Akademie-Verlag, Berlin, 68 pp., 1955. (*Frequenz*, vol. 10, pp. 60–61; February, 1956.) Theory of usw radio propagation is presented and observations over 200-km paths with different weather conditions are analyzed. Diurnal and annual field-strength variations are discussed. The common occurrence of high field strengths at distances of several hundred kilometers with m-λ transmissions is considsidered in relation to the planning of broadcasting services.

RECEPTION

621.376.33:621.372.5 2879
Response of Nonlinear Circuits to Oscillations modulated in Amplitude and Frequency according to an Arbitrary Law—E. De Castro. (*Ricerca Sci.*, vol. 26, pp. 470–481; February, 1956.) Fourier-series analysis is presented relevant to the operation of limiter circuits; idealized characteristics are assumed, with different properties in the positive and negative regions.

621.396.621:621.376.3 2880
Crystal-Controlled F.M. Receiver—D. N. Corfield. (*Wireless World*, vol. 62, pp. 312–316; July, 1956.) Circuit and constructional details are given of a fixed-tuned receiver for the three British fm broadcast frequencies. Three overtone crystals are used generating the local-oscillator frequencies directly, with manually operated selection switch.

621.396.621:621.396.812.3 2881
Improvement of Reception by Diversity Operation—R. Heidester and E. Henze. (*Arch. Elekt. Übertragung*, vol. 10, pp. 107–116; March, 1956.) Calculations are made of the time averages of the signal/noise ratio for space-diversity and frequency-diversity systems; a value is derived for the average error figure in frequency-shift telegraphy. The probabilities of the signal/noise ratio exceeding or falling below a given value are determined. A practical diversity circuit is described.

STATIONS AND COMMUNICATION SYSTEMS

621.396:621.376.3 2882
Spain and Frequency Modulation—F. Moyano Reina. (*Rev. Española Electrónica*, vol. 3, Nos. 15 & 16, pp. 54–57, 79; February, and pp. 51–53, 57; March, 1956.) Frequency allocations and coverage problems are discussed with special reference to Spain, and the advantages, both for peacetime and wartime, of vhf operation with fm are indicated. An appropriate development plan has been laid before the Government by the First Congress of Telecommunication Engineers.

621.396.41:621.396.822.1 2883
Spectral Density of Cross-Modulation Noise—R. Codelupi. (*Alta Frequenza*, vol. 25, pp. 38–64; February, 1956.) Detailed analysis is presented for a multichannel transmission system considered as a cascaded series of alternate nonlinear and phase-distorting quadripoles, and assuming that the probability distribution at the input is Gaussian.

SUBSIDIARY APPARATUS

621.314.1:621.373.52:621.314.7 2884
The Design and Operation of Transistor D.C. Converters—(*Mullard Tech. Commun.*, vol. 2, pp. 157–204; February, 1956.) Circuits are discussed in which a junction transistor is made to oscillate and thus to chop the current from a battery; the chopped current is fed to a transformer or ringing choke, and the stepped-up-voltage output is rectified and smoothed. Design procedures are described in detail. See See also 573 of 1956.

621.314.63:[546.28+546.289 2885
Germanium and Silicon Power Rectifiers—T. H. Kinman, G. A. Carnick, R. G. Hibberd, and A. J. Blundell. (PROC. IRE, part A, vol. 103, pp. 89–107; April, 1956. Discussion, pp. 107–111.) The development of *p-n* junction power rectifiers is reviewed and the special features of a unit rated up to 2 kw are described. For a shortened version, see *IEE*, vol. 2, pp. 144–151; March, 1956.

621.314.63:546.289 2886
Germanium Power Rectifiers—M. Sassier. (*Onde Élect.*, vol. 36, pp. 224–229; March, 1956.) The production and characteristics of Ge junction rectifiers capable of handling current densities of the order of 100 A/cm² at an ambient temperature of 60°C. are described and compared with those of other rectifiers. Some suitable circuits are indicated.

621.316.722.1 2887
An A.C. Voltage Stabilizer—F. A. Benson and M. S. Seaman. (*Electronic Engng.*, vol. 28, pp. 260–265; June, 1956.) A temperature-limited diode placed in one arm of a resistance bridge controls the output voltage through a saturable reactor and autotransformer.

621.352.3 2888
Wafer Cells—R. W. Hallows. (*Wireless World*, vol. 62, pp. 341–343; July, 1956.) The Burgess (U.S.A.) dry battery is described and discharge characteristics are given. The cells are of sandwich construction, hermetically sealed, and the construction affords substantial savings in size and weight as compared with earlier types of dry battery.

TELEVISION AND PHOTOTELEGRAPHY

621.397(083.7) 2889
IRE Standards on Facsimile: Definitions of Terms, 1956—(PROC. IRE, vol. 44, part 1, pp. 776–781; June, 1956.) Standard 56 IRE 9. S1.

621.397.26:396.65.029.63 2890
The Microwave System between London and Windsor in Canada—A. D. Hodgson and G. M. B. Wills. (*G.E.C. Telecommun*, pp. 4–24; February, 1956.) The television link described provides two one-way reversible channels and includes four repeater stations separated by up to 26.4 miles; the fm transmitters operate in the 1.7–2.3-kmc bandwith output power of about 2w.

621.397.5:535.623 2891
Colour Television—H. Anglès d'Auriac. (*Onde Élect.*, vol. 36, pp. 134–144; February

and pp. 277–282; March, 1956.) The development and present practice of color television in the U.S.A. are reviewed, in order to point the way for development of a European service. Differences in economic and technical factors between the two continents are emphasized.

621.397.62 2892

Some Remarks on the Radio-Frequency Phase and Amplitude Characteristics of Television Receivers—A. van Weel. (*J. Brit. IRE*, vol. 16, pp. 271–280; May, 1956.) "The influence on the picture of the steady state characteristics of the radio frequency part of a television receiver is considered especially for the frequencies close to the carrier frequency (the so-called Nyquist flank). It follows from numerical calculations that the shape of the amplitude characteristics of this Nyquist flank has but little influence on the picture quality. The performance of a receiver will be substantially the same in combination with a double-sideband transmitter as with a vestigial-sideband transmitter, provided the lattter has been compensated for its own phase errors. The performance of a vestigial-sideband transmitter should be monitored with a phase-linear receiver, of which the exact shape of the Nyquist flank is not very critical."

621.397.62:621.373.43 2893

Television Sweep Generation with Resonant Networks and Lines—K. Schlesinger. (Proc. IRE, vol. 44, part 1, pp. 768–775; June, 1956.) Circuits for producing horizontal-deflection current waveforms with economical use of power are discussed. Such waveforms can be obtained by synthesis from a limited number of harmonics of a sinusoidal oscillation. Satisfactory linearity can be obtained using only four harmonics, if their relative amplitudes are slightly adjusted, but to achieve a retrace time not greater than 15 per cent eight harmonics must be used. Various circuits using shock excitation of multiresonators have been tried. The best multiresonator found was a delay line just under $\lambda/2$ long; a construction which minimizes dispersion is described.

621.397.62:621.397.8 2894

Television Pattern Eliminator—(*Wireless World*, vol. 62, p. 307; July, 1956.) Band-I interference experienced when receiving band III with a band-I set and converter is balanced out by an equal, oppositely phased signal.

621.397.7 2895

Südwestfunk Television Studio Technique—(*Tech. Hausmitt. NordwDtsch. Rdfunks*, vol. 8, pp. 1–39; 1956.) Eight individual papers are presented, dealing with various aspects of the Baden-Baden television center; these include the general plan, the program handling equipment, the lighting and back-projection, the transmission chain, and the use of 16-mm film.

621.397.7 2896

The New B.B.C. Television Station at the Crystal Palace—(*J. Telev. Soc.*, vol. 8, pp. 35–36, 40; January/March, 1956.) A brief description of this station, which took over the srevice from Alexandra Palace in March, 1956. The station transmits on 45 mc (vision) and 41.5 mc (sound) with a vestigial-upper-sideband characteristic.

621.397.8 2897

Definition of the Signal/Noise Ratio due to Statistical Fluctuations in Television—R. Theile and H. Fix. (*Arch. Elekt. Übertragung*, vol. 10, pp. 98–104; March, 1956.) The amplitude distribution of fluctuations in television signals is discussed; oscillograms obtained with different pickup systems are compared. Experiments to determine the disturbing effect of fluctuations at different brightness levels are reported. A new method is proposed for defining signal/noise ratio based on measurements at three signal levels, corresponding respectively to black, white, and a selected grey.

621.397.8:535.623 2898

Television Picture Quality—W. T. Cocking. (*Wireless Engr.*, vol. 33, pp. 157–158; July, 1956.) A brief discussion of factors affecting vertical and horizontal picture definition, in relation to the decision yet to be made regarding the line standard to be adopted for color television in Great Britain.

621.397.82 2899

Interference with Television Reception: some Causes and Cures—R. A. Dilworth. (*J. Telev. Soc.*, vol. 8, pp. 3–15; January/March, 1956.) Complaints of interference received by the British Post Office in 1954–1955 were attributed to commutator motors, contact devices, power lines, filament lamps, discharge lamps, receiver oscillators, ignition, transmitters, industrial and medical equipment, and faulty electric wiring, in descending order of frequency of occurrence. No serious difficulty is foreseen in suppressing interference generated by motor-driven machines, but other sources still present many practical problems.

TRANSMISSION

621.396.61:621.376.22 2900

Anode Self-Modulation, a High-Frequency-Engineering Paradox—F. H. Lange. (*Nachr-Tech.*, vol. 6, pp. 58–62; February, 1956.) Anode self-modulation is a term applied to an AM process for a transmitter output stage in which af and hf control are effected in the grid circuit. The arrangement is equivalent to a reflex type of constant-current anode-voltage using af choke. Features distinguishing the operation of this circuit from the ordinary grid modulator are indicated.

TUBES AND THERMIONICS

621.314.63:546.28 2901

The Blocking Properties of Alloyed Si-Junction Rectifiers—A. Herlet and H. Patalong. (*Z. Naturf.*, vol. 10a, pp. 584–586; July, 1955.) Rectifiers of this type generally have a *p-n-s* structure [2776 of 1955 (Herlet and Spenke)]. The relation between the breakdown voltage and resistivity has been investigated for specimens with high-resistivity *p*-type middle zones; the relation is not linear. It is deduced that the critical field strength depends markedly on the resistivity.

621.314.7 2902

The Determination of Base Thickness in Alloy-Junction Transistors by Etching—J. Rolfe. (*Brit. J. Appl. Phys.*, vol. 7, pp. 109, 112; March, 1956.) The geometry of In *p-n* junctions in Ge is investigated by using a short duration (20 or 30 s) C.P.4 etch [Haynes and Shockley (1928 of 1951)]. The method is described and photographs of junctions are shown.

621.314.7:546.289:621.317.3 2903

Measurements on Alloy-Type Germanium Transistors and their Relation to Theory—D. M. Evans. (*J. Electronics*, vol. 1, pp. 461–476; March, 1956.) Two methods of determining the current amplification α are described. On the basis of an injection ratio of unity, the frequency dependence of α is compared with the theoretical variation of the base transport factor β obtained from the equations of the one-dimensional minority-carrier-diffusion theory. The comparison confirms the applicability of this theory, and further confirmation is obtained by consideration of the variation of emitter-base impedance with emitter current. The results are applied to show that the mobility of holes in *n*-type Ge varies as $T^{-2.2}$ and that the effective diffusion constant is doubled in going from small to large emitter currents. Three methods for estimating the effective base thickness are described.

621.314.7.012.8 2904

Transistor Equivalent Circuits—J. Gaschi. (*Onde. Élect.*, vol. 36, pp. 268–276; March, 1956.) Equivalent circuits representing the behavior of fused-junction *p-n-p* transistors at high frequencies are discussed based on the solution of the diffusion equation; eight elements are involved. Practical formulas for the principal parameters are derived.

621.383.2 2905

The Time Lag and other Undesirable Phenomena observed in Vacuum Photo-tubes at Weak Illumination: Part 1—M. Sugawara. (*J. Phys. Soc. Japan*, vol. 11, pp. 169–175; February, 1956.) Experiments have been made to determine the causes of nonlinearity and time-varying response in photoemissive cells. Abnormal effects are mainly due to photoemissive materials such as Cs adhering to parts of the cell wall in poor contact with the photocathode.

621.385 2906

Origin and Analysis of Gas in Electron Tubes—S. J. Stoll. (*Brit. J. Appl. Phys.*, vol. 7, p. 94–96; March, 1956.) The gas liberated during electron bombardment of the anode is mainly CO which is probably produced by a reaction between the CO_2 and the Ba adsorbed during cathode conversion. By keeping the anode at 600°C. or higher temperatures during conversion and removing the CO_2 by pumping, tubes have been made which were relatively free of gas and required no aging.

621.385 2907

Axially Symmetrical Electron Beams of Given Shape—V. T. Ovcharov. (*Compt. Rend. Acad. Sci., U.R.S.S.*, vol. 107, pp. 47–50; March 1, 1956. In Russian.) Equations are derived for the field required to produce a beam of given shape. Space charge effects are taken into account.

621.385.012 2908

An Analysis of Grid Current—W. Knappe. (*Frequenz*, vol. 10. pp. 44–50; February, 1956.) The dc and first three harmonic components grid current are calculated as functions of the fraction of the cycle during which grid current flows. The over-all rms. value and the separate rms values for even and odd harmonics are also determined for various V_0/I_0 characteristics. Results are shown graphically.

621.385.029.6 2909

Space-Charge Effects in Dense, Velocity-Modulated Electron Beams—M. Weinstein and H. M. Von Foerster. (*J. Appl. Phys.*, vol. 27, pp. 344–346; April, 1956.) The motion of electrons in the drift space of a klystron is examined; the debunching effect is analyzed using a coordinate system moving at a speed equal to the initial speed of the electrons, space-periodic rather than time-periodic distributions being considered. A discrete spectrum of beam oscillations is deduced, with the plasma frequency as limiting frequency. The results are supported by observations with a beam analyzer [*e.g.*, 2379 of 1955 (Purl and Von Foerster)].

621.385.029.6 2910

Calculation of the Performance Chart of Magnetrons—W. Praxmarer. (*Nachr Tech.* vol. 6, pp. 97–104; March, 1956.) From consideration of limiting conditions and estimates of mean values, analytical relations are derived between anode voltage, anode current, over-all efficiency, and power of a magnetron, thus permitting advance calculation of the characteristics. Predictions have been checked by measurements on various types of magnetron at wavelengths between 1.21 and 33.5 cm with pulsed and continuous operation. No large errors result from space charge, but the effect of the load on the efficiency is difficult to predict; the theoretical results are however sufficiently accurate for practical purposes.

621.385.029.6 2911
Design Information on Large-Signal Traveling-Wave Amplifiers—J. E. Rowe. (PROC. IRE, vol. 44, part 1, pp. 818–819; June, 1956.) Addendum to 1589 of 1956.

621.385.029.6:537.533 2912
Excitation of Space-Charge Waves in Drift Tubes—M. Scotto and P. Parzen. (*J. Appl. Phys.*, vol. 27, pp. 375–381; April, 1956.) "An analysis has been made of the effect of initial conditions on the excitation of electromagnetic waves in a drift tube. The method employs the Laplace transform which directly includes the initial quantities. Field quantities which have been transformed with respect to the longitudinal coordinate are solved for and the results then inverted. Explicit expressions are then obtained for the velocity, charge density, and current density modulations as a series of modes."

621.385.029.6:538.566:537.56 2913
Growing Electric Space-Charge Waves—Piddington. (See 2702.)

621.385.029.6:621.372.8 2914
Nonlinear Phenomena in a Waveguide in the Presence of an Electron Beam with Nearly Equal Electron and Wave Velocities—N. L. Loshakov. (*Zh. Tekh. Fiz.*, vol. 25, pp. 1768–1787; September, 1955.) By considering a model consisting of a waveguide with a dielectric in which free movement of electrons is postulated, theory based on the method of successive approximations is developed. The theory is used to estimate nonlinear phenomena characterizing the interacting of the beam with the field of the traveling wave for nearly equal velocities of the electrons and waves.

621.385.029.6:621.374.4 2915
The Frequency-Multiplier Klystron—V. J. Norris. (*J. Electronics*, vol. 1, pp. 477–486; March, 1956.) "The factors controlling design and performance of frequency-multiplier klystrons are examined and the conclusions drawn are checked against the performance of the VX 8175, a tube driven at 937.5 mc and delivering about 100 mw of cw power at 9375 mc. Good agreement between theory and practice is found despite limitations of the former."

621.385.032.213 2916
Measurement of the Cathode Temperature in Triodes by the Method of Initial Current—A. E. Gershberg. (*Zh. Tekh. Fiz.*, vol. 25, pp. 1703–1713; September, 1955.) Development of a method described *e.g.*, by Ikehara (3405 of 1954).

621.385.032.216 2917
Current/Voltage Characteristics of the Oxide Coated Cathode at Low Activation Energies—R. E. J. King. (*Research, Lond.*, vol. 9, pp. S9–S10; March, 1956.) The I/V characteristics in the temperature range 300°–600° K have been determined by applying a sinusoidal voltage across the coating and a small series resistance, and observing the variation of the voltage across the latter. Assuming the characteristic to be represented by an equation of the form $I=aV+bV^2+\ldots$, the coefficients of the power series can be evaluated from the harmonics in the observed variation. The deviation from linearity decreases with increasing temperature over the range examined. Possible mechanisms giving rise to the observed results are briefly discussed.

621.385.032.216 2918
Impregnated Barium Dispenser Cathodes containing Strontium or Calcium Oxide—I. Brodie and R. O. Jenkins. (*J. Appl. Phys.*, vol. 27, pp. 417–418; April, 1956.) Tests have been made on cathodes of the type described by Levi (3125 of 1955) modified by addition of CaO or SrO to the barium silicate or barium aluminate impregnant. Emission/temperature characteristics are shown; the additions lead to increased emission in all cases.

621.385.15 2919
The Secondary Emission Valve and its Application—A. H. Atherton. (*J. Telev. Soc.*, vol. 8, pp. 23–29; January/March, 1956.) Consideration is confined to tubes with a single stage of multiplication. By comparison with the conventional tube, the secondary-emission tube has the advantage that a high-gain-bandwidth product can be obtained more easily in practice, and that an output in phase with the input is obtained from the dynode. Difficulties in achieving stability of characteristics over the lifetime are discussed and two commercially available stable types are briefly described. The required operating voltages and the noise are both high compared with the values for conventional tubes. The use of secondary-emission tubes merits consideration when designing for bandwidths >10 mc.

621.385.2:621.317.729 2920
The Solution of the Problem of a Planar Diode with a Limited-Width Emitting Surface by use of a Rubber Membrane—Krasnov and Kel'man. (See 2852.)

621.385.4/.5 2921
Non-additivity in Selenium Photocells with Barrier Layers under the Influence of an External Voltage—Z. A. Gol'dman. (*Zh. Tekh. Fiz.*, vol. 25, pp. 1689–1695; September, 1955.) If a Se photocell is simultaneously illuminated by light waves of different wavelengths, the resulting photocurrent may greatly exceed the sum of the currents obtained with separate illuminations. Experiments have shown that short-wave illumination removes the barrier layer and the resistance due to it, so that the decrease in the resistance of the Se caused by long-wave illumination results in an amplification of the photocurrent.

621.385.832 2922
Deposition and Removal of Electric Charges on Insulators by Secondary Emission: Part 2—M. Barbier. (*Ann. Radioélect.*, vol. 10, pp. 303–323; July, 1955.) Experiments are reported providing the basis for the theory presented previously (2262 of 1956). Special cr tubes were used to facilitate observations of the electron movements with different field distributions. Results indicate that a high-voltage beam should be used for writing and a low-voltage beam for reading, in conjunction with a perfect insulator.

621.385.832:681.142 2923
Coplanar-Mesh Storage—G. R. Hoffman. (*Brit. J. Appl. Phys.*, vol. 7, pp. 102–108; March, 1956.) A storage system is described using a cr tube with a target consisting of a sheet of mica on to which a conducting mesh has been evaporated. In this system the writing is controlled by the bright-up pulses alone and transient voltages on the mesh are eliminated.

621.385.832:681.142 2924
The Hyperbolic-Field Tube, an Electron Beam Tube for Multiplication in Analogue Computers—W. Schmidt. (*Z. angew Phys.*, vol. 8, pp. 69–75; February, 1956.) The tube comprises three deflector systems and a pair of target anodes. The first and third deflectors are pairs of X and Y plates, respectively, the second comprises four cross-connected plates with hyperbolic section in the xy plane, oriented with the asymptotes along the axes. The deflection of the electron beam in the y direction in the second deflector is proportional to the x displacement produced by the first deflector. A control voltage depending on the difference between the currents collected by the two target anodes is fed back to the third deflector to produce equal currents in the target anodes; its value is then proportional to the required product of the voltages applied to the first and second deflectors.

621.387 2925
Experiments with Gas-Filled Triodes—J. A. Kok. (*Appl. Sci. Res.*, vol. B5, pp. 445–453; 1956.) "In this paper experiments are described showing the different types of electrical discharges in a gas-filled triode. The determining parameters are the following: the cathode emission, the spacing of cathode, grid and anode, the diameter of the meshes of the grid, the potentials of the grid and the anode, the gas pressure and the differential ionization function of the gas. The anode voltage may be concentrated in a space charge sheath. If this space charge sheath is located at the grid, the anode current may be modulated with moderate grid potentials. If not, much larger voltages are required for modulation."

621.387 2926
The Hydrogen Thyratron—D. Charles and R. J. Warnecke. (*Ann. Radioélect.*, vol. 10, pp. 256–302; July, 1955.) A detailed study is reported of the pulsed operation of the medium-power thyratron Type-T.G.200. The variations of grid and anode currents and voltages were measured both during the passage of the pulses and during the intervals. An estimate was made of the power required to control the tube with positive grid. The curve showing dissipated power as a function of time is characterized by a peak corresponding to the initiation of ionization. Bombardment of the anode by ions in the period immediately after the pulse must be taken into account in developing new tubes. 49 references.

621.387 2927
Investigation of a New Continuously Controllable Gas Discharge using a Cold Cathode—C. H. Hertz. (*Ark. Fys.*, vol. 10, part 3, pp. 213–245; February 7, 1956. In German.) An account is given of the design and operation of a corona tube developed as a result of experiments described previously (*e.g.*, 1938 of 1955). A negative point corona serves as cathode, and the anode system comprises an array of fine tungsten wires arranged in parallel grooves cut in a brass plate serving as control grid; the operation depends on the provision of a very strong electric field in the neighborhood of the anode wires. When such a discharge is operated in hydrogen at a pressure of 150 mm Hg its characteristics resemble those of a vacuum tube, the amplification factor being 50–100. The internal resistance is negative. Use of the tube as an amplifier may be restricted by considerations of noise and frequency range, but it should be useful for stabilization.

MISCELLANEOUS

621.3.002.2:68 2928
Dip Soldering—H. G. Manfield. (*Wireless World*, vol. 62, pp. 304–306; July, 1956.) A simple method evolved at the British Radar Research Station for use with printed circuits is described.

621.3:537 2929
Advances in Electronics and Electron Physics, Vol. VII [Book Review]—L. Marton (Ed.). Publishers: Academic Press, New York, 503 pp., 1956. (PROC. IRE, vol 44, part 1, pp. 828–829; June, 1956.) Review articles are presented on the physics of semiconductor materials, theory of electrical properties of Ge and Si, energy losses of electrons in solids, sputtering by ion bombardment, observational radio astronomy, analog computers, and electrical discharge in gases and modern electronics.